BEILSTEIN JOURNAL OF ORGANIC CHEMISTRY

Chemistry in flow systems II

Edited by Andreas Kirschning

Imprint

Beilstein Journal of Organic Chemistry
www.bjoc.org
ISSN 1860-5397
Email: journals-support@beilstein-institut.de

The *Beilstein Journal of Organic Chemistry* is published by the Beilstein-Institut zur Förderung der Chemischen Wissenschaften.

Beilstein-Institut zur Förderung der Chemischen Wissenschaften
Trakehner Straße 7–9
60487 Frankfurt am Main
Germany
www.beilstein-institut.de

Beilstein Journal of Organic Chemistry

Chemistry in flow systems II

Andreas Kirschning

Editorial

Open Access

Address:
Leibniz University of Hannover, Schneiderberg 1B, 30167 Hannover, Germany

Email:
Andreas Kirschning - andreas.kirschning@oci.uni-hannover.de

Beilstein J. Org. Chem. **2011,** *7,* 1046–1047.
doi:10.3762/bjoc.7.119

Received: 11 July 2011
Accepted: 21 July 2011
Published: 02 August 2011

This article is part of the Thematic Series "Chemistry in flow systems II".

Guest Editor: A. Kirschning

This is the second Thematic Series on chemistry in flow systems that I have edited for the Beilstein Journal of Organic Chemistry. Is this perhaps too much of a tribute to an enabling technology that will probably never move beyond the status of a trend or a fashion? Have we not already seen this kind of fashionable topic initially promise so much and subsequently not quite meet expectations? For example the impact of "combinatorial chemistry" has turned out to be important, but the field did not live up to the original hype.

No one can predict the future impact of flow chemistry, but it is an enabling technology that was introduced to the laboratories of synthetic organic chemists around ten years ago and has flourished for about half a decade now. We can draw a parallel with microwave-assisted synthesis, for which almost two decades passed until it became a broadly accepted enabling heating technology, and which will continue to have a strong impact on practical organic chemistry. Flow systems have already been implemented in various areas in organic chemistry with very promising results, and the lasting effects will certainly become apparent in the years to come.

I am very pleased to say that this series contains representative examples of fields in organic synthesis where continuous flow conditions have already made a significant impact. In particular I would like to highlight three areas. First of all, we have the application to photochemistry, which has the chance of experiencing a renaissance particularly in an industrial environment. Second, flow chemistry lends itself naturally to the synthesis and direct application of reactive intermediates or reactive reagents, which are difficult to handle in a batch reactor. And third, new heating concepts, including inductive heating, are rendered possible, allowing us to carry out accelerated synthesis under pressure, up to supercritical conditions, but whereby only a small volume of the reaction mixture inside the flow reactor is exposed to these extreme conditions.

You are invited to explore this Thematic Series and you will see contributions from some of the most prominent and creative groups in the world working in the field of flow chemistry. Not surprisingly this series has significantly increased in size since the first Thematic Series "Chemistry in flow systems" published in 2009 [1]. Particularly, I would like to draw your attention to the review on enzyme-mediated synthesis under flow conditions, a topic that has not been covered for a long time in an organic chemistry context. This review clearly illustrates the scope of this enabling technology with far reaching implications even for industrial biotechnology.

I am thankful to all my colleagues who have helped to create this diverse and state of the art flow series. Finally, special thanks are dedicated to the staff of the Beilstein-Institut for their support and professional realization.

Hannover, July 2011

Andreas Kirschning

Reference

1. Kirschning, A. *Beilstein J. Org. Chem.* **2009,** *5,* No. 15. doi:10.3762/bjoc.5.15

License and Terms

Beilstein Journal of Organic Chemistry

Unusual behavior in the reactivity of 5-substituted-1*H*-tetrazoles in a resistively heated microreactor

Bernhard Gutmann[1], Toma N. Glasnov[1], Tahseen Razzaq[1], Walter Goessler[2], Dominique M. Roberge[3] and C. Oliver Kappe[*1]

Full Research Paper

Open Access

Address:
[1]Christian Doppler Laboratory for Microwave Chemistry (CDLMC) and Institute of Chemistry, Karl-Franzens-University Graz, Heinrichstrasse 28, A-8010 Graz, Austria, [2]Institute of Chemistry, Analytical Chemistry, Karl-Franzens-University Graz, Universitätsplatz 1, A-8010 Graz, Austria and [3]Continuous Flow/Microreactor Technologies, Lonza AG, CH-3930 Visp, Switzerland

Email:
C. Oliver Kappe[*] - oliver.kappe@uni-graz.at

* Corresponding author

Keywords:
flow chemistry; heterogeneous catalysis; microreactors; palladium; process intensification

Beilstein J. Org. Chem. **2011,** *7,* 503–517.
doi:10.3762/bjoc.7.59

Received: 02 February 2011
Accepted: 31 March 2011
Published: 21 April 2011

This article is part of the Thematic Series "Chemistry in flow systems II".

Guest Editor: A. Kirschning

Abstract

The decomposition of 5-benzhydryl-1*H*-tetrazole in an *N*-methyl-2-pyrrolidone/acetic acid/water mixture was investigated under a variety of high-temperature reaction conditions. Employing a sealed Pyrex glass vial and batch microwave conditions at 240 °C, the tetrazole is comparatively stable and complete decomposition to diphenylmethane requires more than 8 h. Similar kinetic data were obtained in conductively heated flow devices with either stainless steel or Hastelloy coils in the same temperature region. In contrast, in a flow instrument that utilizes direct electric resistance heating of the reactor coil, tetrazole decomposition was dramatically accelerated with rate constants increased by two orders of magnitude. When 5-benzhydryl-1*H*-tetrazole was exposed to 220 °C in this type of flow reactor, decomposition to diphenylmethane was complete within 10 min. The mechanism and kinetic parameters of tetrazole decomposition under a variety of reaction conditions were investigated. A number of possible explanations for these highly unusual rate accelerations are presented. In addition, general aspects of reactor degradation, corrosion and contamination effects of importance to continuous flow chemistry are discussed.

Introduction

Microreactor technology has opened up new avenues for synthetic organic chemistry [1-6] and the chemical manufacturing industry [7,8]. Traditionally, most synthetic transformations performed in microreactors have involved ambient or even low-temperature conditions in order to conduct highly exothermic reactions safely [1-9]. More recently, following the concepts of "Process Intensification" and "Novel Process Windows" [10-12], flow chemistry executed in high-temperature and/or high-

pressure regimes have become increasingly popular [13]. High-temperature processing offers many distinct advantages as demonstrated by the recent success of microwave-assisted organic synthesis [14-18]. In microwave chemistry, reaction times can often be reduced from hours to minutes by efficient and rapid direct dielectric heating of the reaction mixture in a sealed vessel to temperatures far above the boiling point of the solvent under atmospheric conditions. Since batch microwave chemistry is inherently difficult to scale up to production quantities [14-16], translating high-speed, high-temperature microwave chemistry to scalable continuous flow processes is becoming increasingly important. In the past few years our research group [19-25] has reported a number of successful case studies where initial reaction optimization for a variety of synthetic transformations was performed under batch microwave conditions, followed by translation to high-temperature/high-pressure scalable continuous flow processes ("microwave-to-flow" paradigm) [26-28].

A recent example involves the synthesis of 5-substituted-1*H*-tetrazoles via an azide–nitrile cycloaddition pathway, using sodium azide (NaN_3) as an inexpensive azide source and acetic acid (AcOH) as the reagent/catalyst in a NMP/H_2O solvent mixture [25]. These 1,3-dipolar cycloadditions which involve in situ generated free hydrazoic acid (HN_3) were performed on small scale (≈1 mL) at 220 °C in a microwave batch reactor with reaction times of 4–15 min, depending on the reactivity of the nitrile [25]. Despite the comparatively high reaction temperatures, virtually no side products were observed in these transformations and the desired tetrazole products were isolated in high yield and purity after a simple work-up procedure [25]. Since HN_3 is not only extremely toxic but also highly explosive, a scale-up of this batch protocol is clearly not possible. A key advantage of using microreactors compared to conventional batch reactors is the ability to process potentially hazardous compounds or reagents safely [1-9,29-32]. In a continuous flow system, synthetic intermediates can be generated and consumed in situ, which eliminates the need to store toxic, reactive or explosive intermediates and thus makes the synthetic protocol safer. However, initial attempts to convert the azide–nitrile cycloaddition protocols to a high-temperature continuous flow process using a stainless steel microtubular flow reactor have failed. Instead of the desired tetrazole products, formation of a number of decomposition products was observed.

In this paper the mechanistic details and kinetic profiles of high-temperature tetrazole decompositions in both microwave batch and metal-based microreactors are investigated. A number of possible explanations for the unusual failure to convert batch to flow conditions for this specific transformation are presented. In addition, often ignored aspects of reactor degradation, corrosion and contamination effects in flow chemistry are also discussed.

Results and Discussion

Flow degradation of 5-benzhydryl-1*H*-tetrazole

As a model system for tetrazole formation the microwave-assisted cycloaddition of diphenylacetonitrile (**1**) with NaN_3 was studied (Scheme 1). After considerable experimentation [25] an optimum set of conditions that fulfilled both the requirement of reaction homogeneity and reaction rate whilst at the same time providing clean and complete nitrile to tetrazole conversion involved the use of NMP as solvent, AcOH as Brønsted acid and H_2O as co-solvent. Thus, 2.5 equiv of NaN_3 and a 5:3:2 ratio of NMP/AcOH/H_2O at 220 °C (≈15 bar) led to full conversion of the reactants to the desired 5-benzhydryl-1*H*-tetrazole (**2**) at a 0.69 M nitrile concentration within 15 min, and furnished the product in 81% isolated yield.

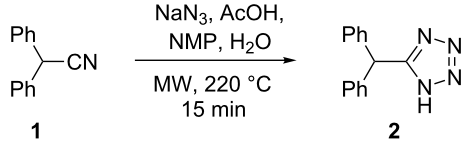

Scheme 1: Azide–nitrile cycloaddition under batch microwave conditions.

To our surprise, however, we were initially unable to translate these high-temperature batch conditions obtained in sealed Pyrex glass reaction vessel (using either conventional or microwave heating) [25] to a continuous flow format. The microreactor system used for these studies was a high-temperature, high-pressure microtubular flow unit that can be used for processing homogeneous reaction mixtures [24]. This reactor uses stainless steel coils of variable length (4, 8 or 16 mL internal volume) that can be directly heated across their full length (5–20 m) by electric resistance heating to temperatures up to 350 °C. Thermocouples are attached to the outer surface of the stainless steel tubing at two different points along the length of the coil to measure the temperature of the coils. In the actual cycloaddition experiment, the reaction mixture was introduced to the reactor block containing a 8 mL stainless steel coil (SX 316L, i.d. 1 mm) heated to 220 °C via a standard HPLC pump at a flow rate of 0.5 mL/min. This translates to a residence time of 16 min inside the heated coil, comparable to the reaction time in the batch microwave experiment (Scheme 1). However, instead of the anticipated tetrazole **2** the only major product observed by HPLC-UV monitoring was diphenylmethane (**3**) (Figure 1). This very unusual behavior was in stark

contrast to our previous experience in converting microwave to flow conditions with the same instrument [19-24], and was not limited to nitrile **1** but was also observed for other nitrile building blocks.

We initially speculated that the observed disintegration of the tetrazole nucleus could somehow be connected to the metal surface of the steel reactor. The particularly high surface-to-volume ratio in a micro structured reactor (the inner surface area of a 16 mL coil with an inner diameter of 1 mm is 640 cm^2) may entail pronounced reactor wall effects and unexpected/undesired side and degradative reactions [33]. The stainless steel reactor contains a variety of metals and the reactor walls could possibly act as heterogeneous catalysts (surface catalysis) [34]. Furthermore, the surface can potentially be considered as a metal oxide which usually forms surface hydroxyl groups in contact with water. Depending on the pH of the processed mixture, the surface hydroxides are protonated or deprotonated and, hence, the surface is uncharged at the isoelectric point or positively (negatively) charged at lower (higher) pH values [35]. In this regard, the surface area, the material of construction and the reactor use history have to be considered. In addition, the stainless steel components of the flow reactor are prone to corrosion if harsh conditions, such as concentrated acids are used [36]. Hydrazoic acid itself (pK_a 4.7) is both a strong oxidant ($E°$ = 1.96 V) and, in the presence of oxidants, a strong reducing agent ($E°$ = −3.09V). It also dissolves metals such as Fe, Zn, Mn and Cu. Thus, HN_3 should in principle be considered as incompatible with the use of steel reactors [37]. Furthermore, iron nitrides are readily formed from HN_3 and Fe metal at temperatures around 100 °C which represents a serious safety hazard [38].

On the other hand, it has been reported that the decomposition of tetrazoles can be catalyzed by a whole range of metals. For example, Cu powder was found to lower the decomposition temperature of 1,5-diphenyltetrazole by about 60 °C [39]. However, in case of the parent tetrazole (CN_4H_2) itself, differential scanning calorimetry (DSC) experiments suggest that the decomposition onset temperature does not change significantly when the material is contaminated with either Fe or 316 stainless steel [40].

Whatever the reason for the inability to translate microwave batch conditions optimized in Pyrex glass to a continuous flow regime with a stainless steel coil, the problem was ultimately solved by employing a passivated silica coated stainless steel coil (Sulfinert®) mimicking a glass environment [41], in combination with the use of a flow reactor that employed a standard Al heating block as a coil heater [25]. Using this set-up, a

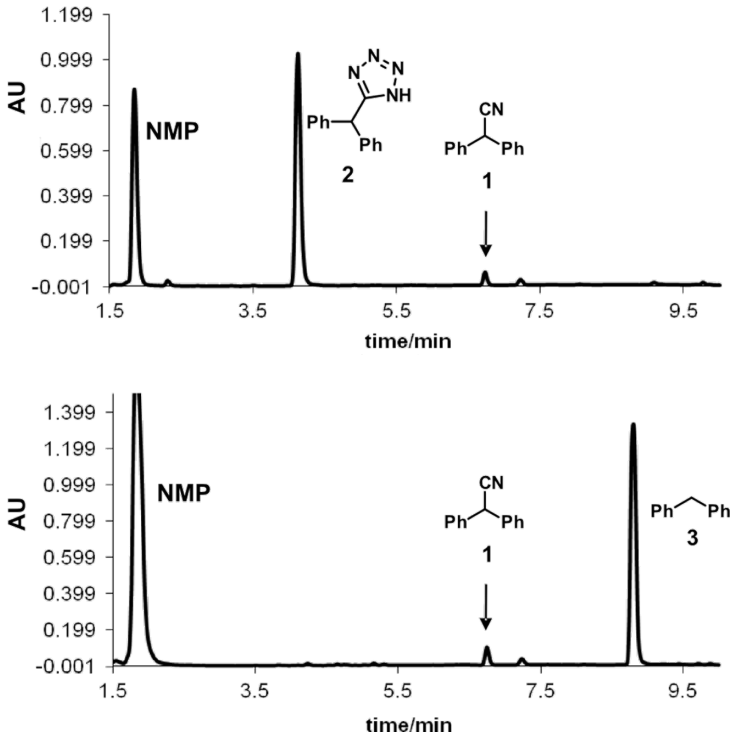

Figure 1: HPLC-UV chromatograms (215 nm) of crude reaction mixtures from the cycloaddition of diphenylacetonitrile (**1**) with NaN_3 (Scheme 1) comparing microwave batch (top) and continuous flow conditions (bottom). Reaction parameters: 220 °C, ≈16 min, 2.5 equiv NaN_3, NMP/AcOH/H_2O 5:3:2.

general and scalable method for the continuous flow synthesis of 5-substituted-1*H*-tetrazoles via the addition of HN_3 to organic nitriles was developed [25]. For specific substrates the coil temperature could be raised up to 260 °C (2.5 min residence time) without any significant amounts of decomposition products being detected in the crude reaction mixture [25].

Control experiments subjecting the isolated pure tetrazole **2** to a NMP/AcOH/H_2O solvent mixture quickly revealed that indeed the very low stability of the tetrazole nucleus in the resistively heated stainless steel flow reactor was responsible for the observed decomposition of the product. The pure tetrazole **2** in NMP/AcOH/H_2O (5:3:2) started to decompose at temperatures as low as 150 °C after a only few min residence time under flow conditions and the HPLC-UV traces of the crude reaction mixtures became fairly complicated (Figure 2). On increasing the reactor temperature or applying longer residence times, however, all peaks except the diphenylmethane (**3**) signal vanished. At 220 °C, the temperature contemplated for the tetrazole synthesis, diphenylmethane (**3**) was the only detectable product after ≈10 min of residence time.

Apparently, the degradation of tetrazole **2** in the NMP/AcOH/H_2O solvent mixture involves various consecutive reactions and/or parallel pathways that finally channel to diphenylmethane (**3**). We have identified virtually all the peaks in the HPLC chromatograms and therefore have a rather complete picture of the complex degradation processes (Scheme 2, Figure S1 in Supporting Information File 1). The main degradation path starts with the *N*-acetylation of the tetrazole nucleus at position 2. The resulting *N*-acetyltetrazole **4** looses nitrogen to form nitrilimine **5**. Interception of the nitrilimine dipolar intermediate by water produces *N'*-acetyl-diphenylacetohydrazide (**7**) (the first detectable intermediate in this sequence), while intramolecular interception leads to the oxadiazole **6**. This mechanism for the degradative acylation of tetrazoles as shown in Scheme 2 was suggested by Huisgen and coworkers in 1958 [42,43]. An alternative mechanism, whereby the 5-substituted-1*H*-tetrazole is acetylated at position N1 followed by ring opening at the 1,2-position, elimination of nitrogen from the resulting azido group and a subsequent 1,2-migration of the acylimido group from carbon to nitrogen to give the same nitrilimine intermediate was ruled out by Herbst via ^{15}N labeling studies [44]. The degradative acylation of 5-substituted-1*H*-tetrazoles with acyl halides is in fact an elegant method for the synthesis of 1,3,4-oxadiazoles [45,46]. In the NMP/AcOH/H_2O solvent mixture, however, the formation of the oxadiazole **6** can scarcely compete with the intermolecular addition of water and oxadiazole **6** was therefore detectable only in minor amounts. Using NMP/AcOH as the solvent system, 2-benzhydryl-5-methyl-1,3,4-oxadiazole (**6**) became one of the major products in the flow reactor under these reaction conditions. The resulting hydrazide **7** can be expected to have a weak N–N bond, however, the products obtained from the decomposition of diacylhydrazides are generally considered to arise via polar pathways rather than via a radical path [47]. Under the employed reaction conditions the hydrazide apparently hydrolyzes to diphenylacetic acid (**8**) which finally decarboxylates to yield diphenylmethane (**3**). Decarboxylation may proceed via an intramolecular, concerted mechanism as proposed for β,γ-unsaturated acids [48].

In addition to these structures, a different set of intermediates resulting from a second decomposition pathway were identified, although in much smaller quantities. The second path possibly involves cyclo-reversion of the tetrazole to the nitrile **1**, hydrolysis of the nitrile to the amide **9** and then further to the carboxylic acid **8**, which again finally decarboxylates to

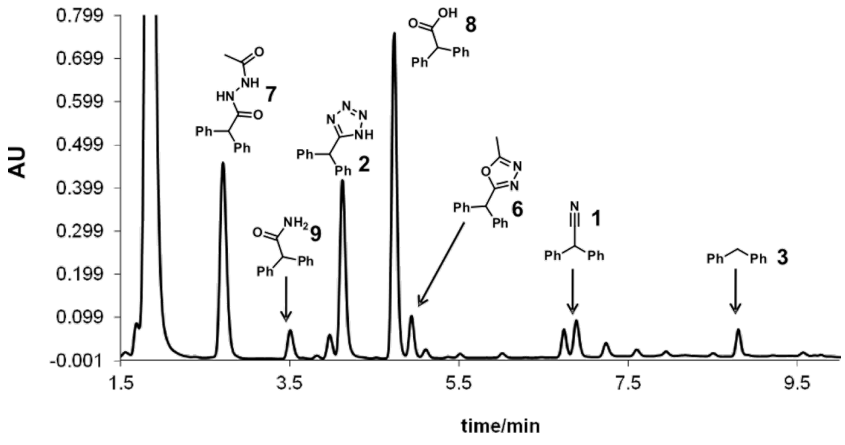

Figure 2: HPLC-UV chromatogram (215 nm) showing the decomposition of tetrazole **2** in NMP/AcOH/H_2O 5:3:2 (0.125 M) after heating in a stainless steel flow coil at 180 °C for 5.3 min.

produce diphenylmethane (**3**) (Scheme 2) [49]. Further details and control experiments supporting the proposed decomposition pathways are discussed in the Supporting Information File 1.

Notably, exactly the same decomposition pathway involving the identical set of intermediates as in the stainless steel reactor were indeed also observed in a microwave batch reactor using a Pyrex glass vessel, but the reactions were nowhere near as fast. In the microwave reactor equipped with an accurate internal fiber-optic temperature probe [50] there was no appreciable disintegration of tetrazole **2** in the NMP/AcOH/H_2O system at 220 °C after 30 min. In order to obtain reasonable decomposition rates for a kinetic analysis, the reaction temperature had to be increased to 240 °C, but even at 240 °C the decomposition process required many hours. The intermediates from the "second path" (Scheme 2) were hardly detectable and the resulting experimental data could be fitted nicely with the rate law shown in Scheme 3 with each step assumed to be (pseudo) first order. A least square fit revealed $k_1 = 1.11 \times 10^{-3}$, $k_2 = 0.432 \times 10^{-3}$ and $k_3 = 0.0832 \times 10^{-3}$ s^{-1} at 240 °C (Figure 3). Control experiments in a microwave reaction vial constructed from strongly microwave absorbing silicon carbide (SiC), which shields the vessel contents from the electromagnetic field and therefore mimics a conventionally heated autoclave experiment, provided identical results and demonstrates that the observed decomposition in the microwave reactor was the result of purely thermal effects [51,52].

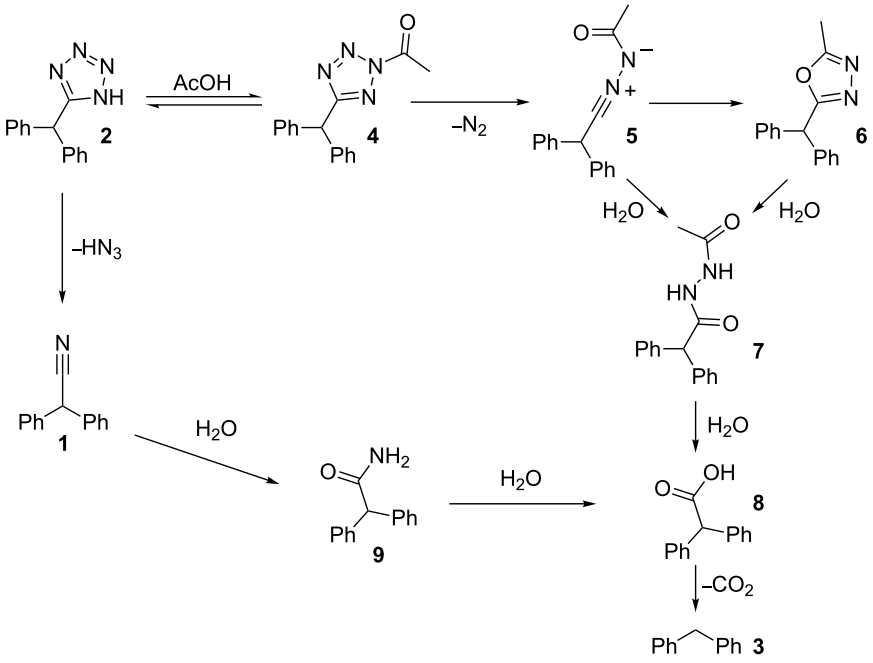

Scheme 2: Possible decomposition mechanisms for tetrazole **2** in NMP/AcOH/H_2O.

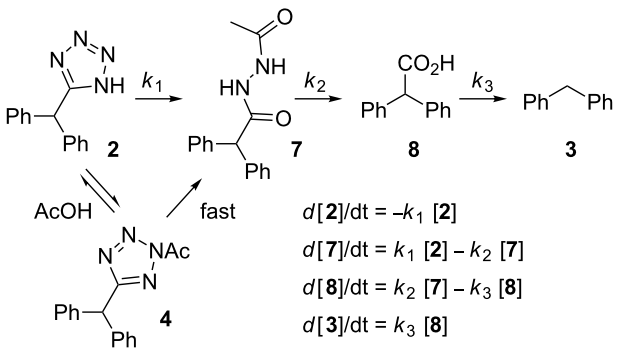

Scheme 3: Reaction steps for the degradation of tetrazole **2** and the corresponding rate equations.

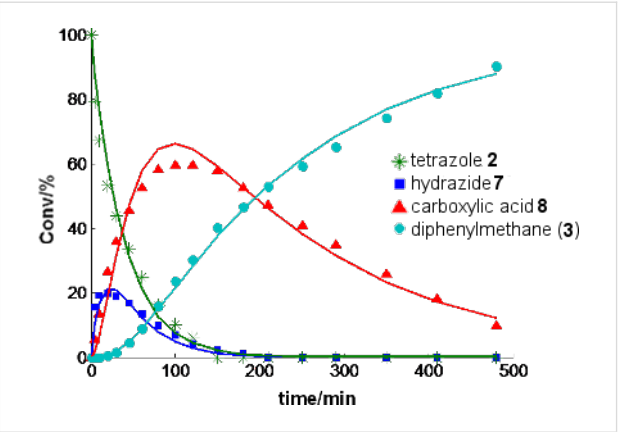

Figure 3: Decomposition of tetrazole **2** at 240 °C in a NMP/AcOH/H_2O 5:3:2 mixture (0.125 M) (points: experimental results; solid lines: predicted with a rate law according Scheme 3 with k_1 = 1.11 × 10^{-3}, k_2 = 0.432 × 10^{-3} and k_3 = 0.0832 × 10^{-3} s^{-1}). Conversions in percent were derived from HPLC-UV (215 nm) peak area integration without correction for response factors. The corresponding conversions for 250 °C and 260 °C and additional data are shown in the Supporting Information File 1 (Figures S2–S4).

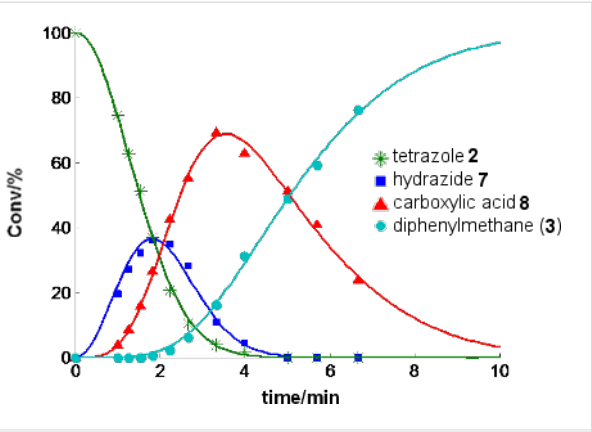

Figure 4: Decomposition of tetrazole **2** in a 4 mL resistance heated stainless steel coil at a nominal temperature of 220 °C in a NMP/AcOH/H_2O 5:3:2 mixture (0.125 M) (points: experimental results; solid lines: predicted with a rate law according Scheme 3 on the assumption that the rate constants are proportional to the residence time k_i = $a_i \cdot t$ (i.e., inversely proportional to the flow rate $k_i = a_i \cdot V \cdot v^{-1}$, t = residence time, V = reactor volume, v = flow rate) with a_1 = 0.169 × 10^{-3}, a_2 = 0.166 × 10^{-3} and a_3 = 0.0207 × 10^{-3} s^{-2}). Conversions in percent were derived from HPLC-UV (215 nm) peak area integration without correction for response factors. Similar curves for different coils are shown in Figure S5 in the Supporting Information File 1.

A comparison of the batch and flow data presented above shows that the tetrazole decomposition in the stainless steel flow coil is ≈100 times faster than decomposition in the Pyrex vial at the same temperature. The rate constants for the decomposition process in the resistively heated flow reactor are apparently not simple first order and appear to depend on the flow rate/residence time and show decreasing rate constants with increasing flow rates/decreasing residence times. For example, the experimental data obtained in a 4 mL stainless steel coil can be fitted nicely with the rate law shown in Scheme 3 assuming that the rate constants are inversely proportional to the flow rate ($k \sim v^{-1}$) (Figure 4). Although some differences in the rate of decomposition between individual coils (4, 8, 16 mL internal volume, different age and history) were noticeable (Figure S5, Supporting Information File 1), in all cases the disintegration of the tetrazoles was dramatically faster compared to the microwave batch conditions.

In order to investigate if the enhanced tetrazole decomposition in the stainless steel coils is connected to metal contamination as a result of steel corrosion phenomena, a series of inductively coupled plasma mass spectrometry (ICPMS) experiments were performed. ICPMS analysis of a NMP/AcOH/H_2O (5:3:2) mixture pumped through the continuous flow reactor at 220 °C (residence time 5 min) revealed that a range of metals are released from the coil under these conditions. Especially Fe (up to 113 ± 6 mg/L) but also Ni (up to 21.0 ± 1.0 mg/L), Cr (up to 32.3 ± 1.5 mg/L) and Mn (up to 4.9 ± 0.3 mg/L) were found in the processed solvent (Table S1, Supporting Information File 1). We hypothesized that several of these metals liberated from the stainless steel capillary may catalyze some of the decomposition steps in solution. Indeed, for example, deliberately added stoichiometric amounts of Fe_2O_3 markedly accelerated the decarboxylation of diphenylacetic acid (**8**) under batch microwave conditions, so that the acid no longer accumulated. The other degradation steps, however, remained virtually unaffected (Figure S6, Supporting Information File 1).

The detected individual amounts of metals in the solvent mixture after treatment in coils of different length varied significantly and correlated somewhat with the age and history of the coils. The decomposition rates, on the other hand, did not show a correlation with the detected quantity of any of the released metals (Figure S5, Supporting Information File 1). Furthermore, decomposition of tetrazole **2** under batch microwave conditions in Pyrex using a NMP/AcOH/H_2O mixture pre-treated as described in the stainless steel reactor was not appreciably faster compared to the decomposition in "fresh" NMP/AcOH/H_2O (Figure S7, Supporting Information File 1). It thus appears that the surprisingly fast degradation of tetrazole **2** in the resistively heated steel reactor compared to the microwave batch experiment at the same temperature is not the result of homogenous catalysis by some of the released metals.

In order to obtain further insights into this remarkable enhancement of tetrazole decomposition, the same reaction was subsequently carried out in flow devices using metal coils made from different materials heated either in an oil bath or with an Al heating block. Remarkably, the stability of tetrazole **2** in a 5.21 mL Hastelloy C-4 coil (i.d. 2.0 mm) at 240 °C was very

close to the stability observed in the microwave batch experiment (Figure S8, Supporting Information File 1). The superior resistance of the Hastelloy material toward the NMP/AcOH/H_2O mixture at high temperature was also evident from an ICPMS analysis of the solvent mixture processed in the Hastelloy C-4 capillary at 220 °C (5 min residence time, 1.0 mL/min flow rate). Hastelloy is a high-performance Ni-Cr-Mo alloy with enhanced corrosion stability compared to standard steel materials under high temperature conditions [53]. Therefore, only comparatively small amounts of released Ni (5.3 ± 1.1 mg/L), W (2.4 ± 0.6 mg/L) and Mo (2.0 ± 0.4 mg/L) were detected in the processed solvent mixture. The amounts of other metals, including Fe, were negligible compared to the background values (Table S1, Supporting Information File 1).

In an additional experiment, we demonstrated that the decomposition of the pure tetrazole **2** in a stainless steel capillary heated on an Al heating block was only marginally faster than the decomposition in the microwave reactor at the same measured reaction temperature. A least square fit of the obtained experimental data with the kinetic model depicted in Scheme 3 gave $k_1 = 2.52 \times 10^{-3}$, $k_2 = 1.15 \times 10^{-3}$ and $k_3 = 0.184 \times 10^{-3}$ s^{-1}. All reaction steps are hence about two times faster than under microwave conditions (Figure S9, Supporting Information File 1). This rather small difference in the decomposition rate (compared to the factor 100 found in the resistively heated coils) can be explained by an inaccurate temperature calibration of the Al block coil heating system used for heating the stainless steel capillary. If metal/surface catalysis would be involved it could be expected that the individual reaction steps of the decomposition pathway would be affected to different extents. However, the rate constants for all consecutive reactions in the flow reactor at a measured temperature of 240 °C were very close to those found under microwave batch conditions at 250 °C (Figure S10, Supporting Information File 1). These results strongly suggest that the degradation process for tetrazoles of type **2** is indeed not influenced by the stainless steel material and thus does not involve heterogeneous/surface catalysis phenomena.

Ultimate proof that the enhanced tetrazole decomposition in the resistively heated coils is related to the method of heating and not to the coil material itself was obtained from a control experiment where the very same 8 mL stainless steel coil initially used in the dedicated flow reactor employing electric resistance heating [24] was subsequently used in a conductively heated experiment. This was achieved by immersing the complete reactor block containing the steel coil and accessories into a well agitated silicone oil bath. Remarkably, with a 10 min residence time for both types of flow experiments, the conductively heated flow run at 192 °C showed no sign of tetrazole decomposition, whilst with electric resistance heating, complete disintegration of the tetrazole occurred at even lower temperatures (Figure S11, Supporting Information File 1).

At the moment we have no compelling explanation for the dramatic discrepancies observed in tetrazole decomposition rates comparing different heating principles. One possible reason for the exceptionally fast disintegration of the tetrazoles in flow reactors utilizing direct electrical resistance heating would be the occurrence of extreme hot spots or uneven temperature distributions along the capillary. To explain the observed degradation rates, however, average temperatures well above 300 °C in the resistively heated reactor have to be assumed (Figure S10, Supporting Information File 1). This appears unlikely taking our previous experience in microwave-to-flow translations into account, where the same instrument and coils were used, but inconsistencies as seen in the tetrazole decomposition have never been observed [19,24]. As the experiments in the resistively heated flow reactor were typically performed at a higher pressure (140 bar) than the corresponding experiments in a conductively heated flow instrument (34 bar), the influence of reaction pressure on tetrazole decomposition was also investigated. Although some differences could be observed performing flow decomposition experiments at 50 and 140 bar in the resistively heated flow reactor, respectively (Figure S12, Supporting Information File 1), these differences were not large enough to suggest a genuine pressure effect. Finally, the possibility of electrochemical phenomena, as a result of the electric current passing through the steel coil interacting with the reaction mixture, were considered (Figure S13, Supporting Information File 1) [54]. Comparative experiments for the tetrazole decomposition carried out in batch mode at 220 °C for 10 min in a short stainless steel loop (≈300 μL) heated either by direct electrical resistance heating with a DC-switching power supply (Figure S14, Supporting Information File 1), or by immersion into an oil bath, support the notion that the enhanced decomposition is somehow related to the electric current. While the batch experiment in the conductively heated coil showed little to no tetrazole decomposition, diphenylmethane (**3**) and diphenylacetic acid (**8**) were the main products in the resistively heated run (Figure S15, Supporting Information File 1).

Corrosion effects influencing flow chemistry in steel reactors

Extreme care is required in the selection of the reactor materials when solutions containing even relatively dilute concentrations of HCl or other Brønsted acids are handled in a flow environment [36]. The corrosion results described earlier involving comparatively benign mixtures of NMP/AcOH/H_2O (5:3:2) passed through stainless steel coils at 220 °C provide

testimony to the fact that even mild acids (the pK_a of AcOH is 4.75) can act as corrosive reagents on stainless steel in an elevated temperature regime. Aqueous HCl is a much stronger acid and lacks the oxidizing properties that stainless steel requires to maintain its "passive" corrosion resistant surface layer [55]. Furthermore, chloride containing acidic solutions will in many situations show a corrosive nature similar to HCl itself. The corrosion attack of HCl, as with most acids, is highly dependent on the temperature but all common stainless steel types should be considered non-resistant to HCl at any concentration and temperature [36]. Hastelloy type reactor materials in turn are known to offer better corrosion resistance in both reducing and oxidizing environments [53].

In order to evaluate the relative corrosiveness of HCl at different concentrations and in different reactor environments, a test reaction was developed that can readily reflect the level of corrosion. For this purpose a 0.5 M solution of nitrobenzene (**10**) in EtOH containing varying amounts of aqueous conc. HCl (0–1.0 M) was flowed through reactor coils made out of PTFE, SX 316L stainless steel or Hastelloy C-4 at 150 °C (≈20 min residence time) (Table 1). The "nascent" hydrogen formed in the corrosion process causes unwanted reduction reactions when susceptible groups, e.g., nitro groups, are in the molecule. The reduction of nitro compounds with Fe in the presence of HCl is known as the Bechamp reduction and large amounts of aniline from nitrobenzene are produced by this reaction [56]. As expected, the reduction of nitrobenzene (**10**) to aniline (**11**) in metal coils increased steadily with increasing HCl concentration. With $R–NO_2 + 6\ H^+ + 6\ e^- \rightarrow R–NH_2 + 2\ H_2O$, the reactions were more or less quantitative with respect to HCl after 20 min at 150 °C in a stainless steel coil. Significant reduction to aniline was, however, also observed in a Hastelloy coil under these conditions. As expected, no reduction was experienced in reactor coils made out of chemically inert PTFE, which unfortunately lacks the temperature and pressure resistance to perform genuine high-temperature/high-pressure flow chemistry (the autogenic pressure in the Bechamp reduction at 150 °C was ≈9 bar) [13]. The corrosion in steel and Hastelloy coils was also clearly evident as strongly colored solutions, probably due to dissolved $Fe^{II/III}$, exited the coil (Figure S16, Supporting Information File 1).

Table 1: Conversion of nitrobenzene (**10**) to aniline (**11**) in different flow environments.[a]

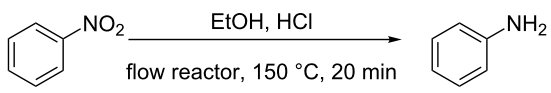

10 **11**

HCl equiv[b]	Conversion (%)[c]		
	Stainless steel	Hastelloy	PTFE
0.0	0	0	0
0.5	5	2	0
1.0	14	7	0
2.0	31	19	0

[a]Reaction conditions: conductively heated (150 °C, 20 min) stainless steel (20 mL, flow rate 1.0 mL/min), Hastelloy (5.21 mL, flow rate 0.26 mL/min) and high-temperature PTFE (14 mL, flow rate 0.7 mL/min) coils. [b]HCl equiv with respect to nitrobenzene (**10**). [c]Conversions were obtained by GC-FID monitoring.

Reactor contamination by catalytically active transition metals

Another critical issue in flow chemistry that is often overlooked is reactor contamination (fouling) as a result of substrate, solvent, reagent or catalyst degradation inside the flow device. In high-temperature flow chemistry, the problem is particularly serious as the sometimes rather extreme temperatures on the reactor walls may lead to the decomposition of otherwise quite stable materials. The potential disintegration may be further enhanced by material and/or surface phenomena resulting from the high surface-to-volume ratio in a microreactor environment. Since, in most cases, microreactors or related flow devices (coils, tubular reactors) for high-temperature/high-pressure applications are made out of non-transparent materials (i.e., stainless steel, alloys, ceramics) [13], the problem is further aggravated since reactor contamination may not be immediately obvious. As flow devices are generally designed for long-term use, the inadvertent accumulation of chemical contaminants inside of these reactors must always be taken into account when interpreting the results from flow chemistry experiments. In the case of the tetrazole decomposition discussed above (Scheme 2), a careful inspection of the individual kinetic profiles obtained in stainless steel coils that had been exposed to different chemistries over several months of usage (Figure 4 and Figure S5 in Supporting Information File 1) clearly reveals that the age/history of the reactor can have an influence on the chemical transformations occurring inside these flow devices.

The use of transition metal catalysts for carbon–carbon or carbon–heteroatom bond formation under continuous flow conditions represents an interesting opportunity for studying the effects of metal contaminations inside of microreactors, as many of these coupling reactions proceed in the presence of extremely small quantities of transition metal catalysts in so-called "homoeopathic" doses [57,58]. In a recent publication we reported the Mizoroki–Heck coupling of 4-iodobenzonitrile (**12**) with *n*-butyl acrylate (**13**) under high-temperature continuous flow conditions (150–190 °C) employing $Pd(OAc)_2$ as a

homogeneous pre-catalyst and a stainless steel-based coil flow system (Scheme 4) [59]. With only 0.01 mol % of $Pd(OAc)_2$ as catalyst, MeCN as solvent and triethylamine as base gave cinnamic ester **14** in very high yield (≈95%) and good selectivity. It can be assumed that at the comparatively high reaction temperatures applied in the high-temperature flow reactor, the homogeneous Pd pre-catalyst will be rapidly converted into Pd colloids/nanoparticles with high catalytic activity [57,58].

In the course of these investigations, we noticed that catalytically active Pd species were apparently retained inside the steel reactor coil on performing these Pd-catalyzed high-temperature coupling transformations, despite an extensive washing regime with pure solvent. This became very obvious, since running the Mizoroki–Heck coupling shown in Scheme 4 without any added Pd catalyst still led to complete conversion in subsequent flow experiments utilizing the same coil. Control experiments in batch mode confirmed that the untreated steel material itself (SX 316L) cannot catalyze Mizoroki–Heck couplings of this type, despite of the fact that Ni and even Fe-catalyzed carbon–carbon bond forming reactions are well known in the literature [60,61]. Furthermore, very low levels of conversion were obtained in this coupling when using a pristine, unused stainless steel coil in the flow reactor without the addition of a Pd catalyst.

In order to investigate these phenomena in more detail, a new set of experiments involving "palladated" steel coils was designed. For this purpose, a 16 mL internal volume stainless steel coil (≈20 m of 1.0 mm i.d. coil) was "loaded" with Pd by processing ≈2 mL of the Mizoroki–Heck reaction mixture through the coil under reaction conditions (180 °C, 1.6 mL/min flow rate) with 1 mol % of the $Pd(OAc)_2$ as pre-catalyst. As expected, the desired product **14** was obtained in 94% isolated yield after chromatographic purification. To clean the instrument extensive washing at 170 °C for 20 min with MeCN was performed. The so conditioned steel coil was then used for processing a new portion of the reaction mixture that did not contain any Pd catalyst. Remarkably, analysis of the reaction mixture by GC-MS demonstrated full conversion to cinnamic ester **14** in the initial product fractions exiting the flow reactor. To establish for how long this "palladated" steel coil could be used without additional amounts of catalyst being added, 15 mL of reaction mixture containing 1.125 g of aryl iodide **12** (8.45 mmol) were processed through the coil under the same reaction conditions (180 °C, 1.6 mL/min flow rate). The analytical results clearly demonstrated that after processing ≈7 mL of reaction mixture conversions started to decrease and ultimately reached almost 0% after 12 mL.

With the purpose of investigating the nature of the Pd leaching from the coil in more detail a freshly "palladated" coil was subjected to a similar series of experiments, measuring the amount of leached Pd by ICPMS analysis (Table 2). While the background leaching for pure solvent at room temperature and at the reaction temperature was relatively low (Table 2, entries 1 and 2), significantly higher levels of Pd were found in samples derived from the Mizoroki–Heck reaction mixture (Table 2, entry 3). These results, both in terms of decreasing conversion and Pd leaching are therefore analogous to the experiments using Pd/C as a heterogeneous pre-catalyst in continuous flow Mizoroki–Heck chemistry [59]. Catalysis essentially proceeds via dissolution/re-adsorption of Pd from the support (here from the steel coil). The mechanism is quasi-homogeneous with small Pd^0 species (colloids/nanoparticles) in solution acting as the catalytically active species. Presumably, the heterogeneous "Pd-on-steel" pre-catalyst is initially solubilized by oxidative addition of the aryl iodide and enters the catalytic cycle in the form of a soluble Pd species. Therefore, significant levels of Pd leaching are observed for the reaction mixture, not for pure solvent [59].

Table 2: Leaching of Pd from a "palladated" steel coil for the Mizoroki–Heck coupling of aryl iodide **12** with *n*-butyl acrylate (**13**) (Scheme 4).[a]

Entry	Reaction mixture composition	Leaching [µg Pd][b]
1	MeCN at rt	4.9
2	MeCN at 180 °C	10.9
3	Reaction mixture at 180 °C	52.9

[a]Complete reaction mixture composition: 0.65 mmol aryl iodide **12**, 1.5 equiv *n*-butyl acrylate (**13**), 1.5 equiv Et_3N, 2 mL MeCN. Conditions: 16 mL stainless steel coil, 180 °C, 1.6 mL/min flow rate. bDetermined by ICPMS analysis of the product contained in a 10 mL fraction.

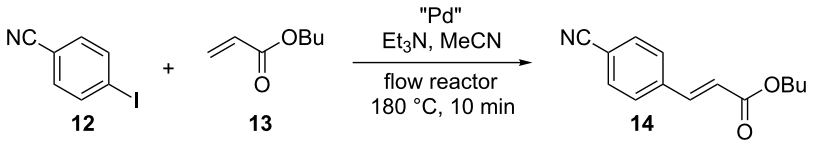

Scheme 4: Mizoroki–Heck coupling under continuous flow conditions.

We suspect that the Pd metal inside the steel coil is present in the form of a thin film of nanometer-sized Pd crystallites, very similar to the highly porous and catalytically active Pd films that can be generated very easily inside glass capillaries by the decomposition of $Pd(OAc)_2$ under somewhat similar elevated temperature conditions [62]. Work by Organ and coworkers has demonstrated, that these Pd-on-glass films (and other metal-coated glass capillaries) can be used for a variety of synthetically important flow chemistry applications in an elevated temperature regime [63,64], including Mizoroki–Heck chemistry [62]. It should be emphasized that our interest in this steel-based immobilized catalytic Pd system was mainly to demonstrate reactor contamination/fouling and not of a preparative nature. After all, only 1.5 mg of $Pd(OAc)_2$ were used to load a 20 m long stainless steel coil, a procedure clearly not suitable to sustain catalytic activity of the "palladated" reactor coil for an extended time [65-67].

Since the "Pd-on-steel" catalyst cannot be easily removed by washing with pure solvent and steel coils for most flow instruments are designed for multiple usage, a cleansing procedure was developed. After considerable experimentation, we found that the use of a KCN/*m*-nitrobenzenesulfinic acid sodium salt mixture in water [68] at 80 °C effectively removes all Pd from the surface of the steel coils as these coils were not catalytically active in subsequent Mizoroki–Heck chemistry. Only renewed loading of the coil by running a Mizoroki–Heck reaction with $Pd(OAc)_2$ or by simply processing a $Pd(OAc)_2$ solution through the coil at elevated temperature regenerated the "palladated" stainless steel coils.

Influence of pressure on reaction rate in flow reactors

In the resistively heated flow reactor used in this work, the pressure during a flow experiment can be set in a range of 50–180 bar with the help of a back-pressure valve [24]. This allows the influence of pressure on the rate of chemical transformations under continuous flow conditions to be studied. While in the tetrazole decomposition described earlier, reaction pressure apparently had no significant influence, there are some transformations that can potentially be influenced by reaction pressure under these flow conditions. In general, the rate and equilibrium of many chemical reactions can be influenced when pressures in the range of 1–20 kbar are applied. Typically, reactions that are accompanied by a decrease in molar volume can be accelerated by increasing pressure ($\Delta V^{\neq} < 0$) and the equilibria are shifted towards the side of the products (reaction volume $\Delta V < 0$) [69,70]. A variety of high-pressure flow chemistry examples have been reported in the literature, but the number of cases where a pressure influence is seen in the medium pressure range (50–200 bar) accessible in standard flow reactors is rather limited [69,70]. One transformation where pressure-dependent rate enhancements (1–600 bar) have been observed in a 3 μL fused-silica capillary, albeit not under continuous flow conditions, is the nucleophilic aromatic substitution reaction of 4-fluoro-1-nitrobenzene (**15**) with pyrrolidine (**16**) in THF ($\Delta V^{\neq} = -58$ cm^3/mol) (Scheme 5) [71]. In order to confirm that these pressure enhancements can also be experienced in a stainless steel mesofluidic flow reactor, the nucleophilic substitution was repeated in an X-Cube Flash instrument. Employing an 8 mL steel coil and an overall flow rate of 1 mL/min (two individual reagent streams at 0.5 mL/min each, residence time = 8 min), the conversion of the substitution reaction at 40 °C was determined at 60, 120 and 180 bar pressure. Indeed, for this transformation a higher reaction pressure increases the reaction rate as previously observed in a fused-silica capillary (Figure 5) [71]. Since the mesofluidic reactor not only allows variation of pressure but also temperature, a series of experiments was designed in which temperature and pressure were increased at the same time. As the data presented in Figure 5 demonstrate, a significant influence of reaction pressure on reaction rate is no longer observable at a temperature of 70 °C.

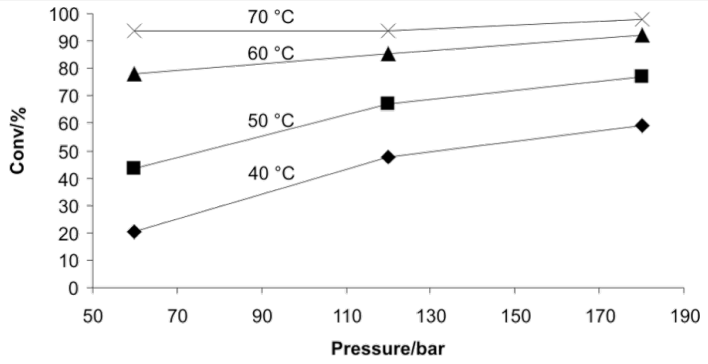

Figure 5: Nucleophilic aromatic substitution reaction of 1-fluoro-4-nitrobenzene (**15**) with pyrrolidine (**16**) in THF (Scheme 5) at different temperatures and three different pressures performed in a 8 mL stainless steel coil at a flow rate of 1 mL/min.

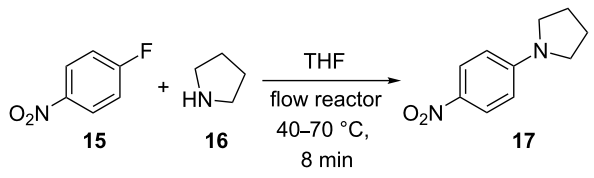

Scheme 5: Nucleophilic aromatic substitution of 4-fluoro-1-nitrobenzene (**15**) with pyrrolidine (**16**) under continuous flow conditions.

Conclusion

In summary, we have demonstrated that the high-temperature decomposition of 5-benzhydryl-1*H*-tetrazole (**2**) in a NMP/AcOH/H_2O 5:3:2 mixture is remarkably accelerated when performed in a resistively heated stainless steel coil as compared to either microwave batch experiments using Pyrex vessels or flow experiments where stainless steel or Hastelloy coils are heated by conductive techniques. Through a series of control experiments, effects of homogeneous metal catalysis as a result of reactor corrosion, and heterogeneous catalytic effects derived from the large metal surface area in the microreactor environment (wall effects) were excluded from being responsible for these unusual phenomena. Although no obvious explanation for these dramatic enhancements in reaction rates can be offered at this time, the results presented herein clearly demonstrate that the conversion of batch to flow chemistry can sometimes be a non-trivial affair and great care must therefore be taken in the interpretation of results.

In this context, we have also presented results of microreactor fouling studies that highlight the fact that reactor contamination, for example, by deposition of catalytically active transition metals inside a microreactor, must also be carefully considered in executing flow chemistry. In the case of a Mizoroki–Heck coupling, we have demonstrated that small amounts of Pd metal retained inside a stainless steel reactor can exhibit catalytic activity in subsequent chemical transformations. As most microreactors for high-temperature applications are made out of non-transparent materials, reactor contamination may not be immediately obvious.

Finally, the fact that stainless steel or Hastelloy-based flow reactors are sensitive to acids, even in small quantities, is sometimes disregarded. In particular at high temperatures, significant corrosion of the reactor material can result, leading to unwanted side reactions. In addition, in specific cases reaction pressure can influence reaction rates as evidenced by the nucleophilic aromatic substitution reaction of 1-fluoro-4-nitrobenzene with pyrrolidine in the 60–180 bar pressure range.

Experimental

General remarks: ^{1}H NMR spectra were recorded on a Bruker 300 MHz instrument. Melting points were determined on a Stuart™ SMP3 melting point apparatus. Low resolution mass spectra were obtained on an Agilent 1100 LC/MS instrument using atmospheric pressure chemical ionization (APCI) in positive or negative mode. Analytical HPLC analysis was carried out on a Shimadzu LC-20 system with a LiChrospher 100 C18 reversed–phase analytical column (119 × 3 mm, 5 µm particle size) at 25 °C, using mobile phase A (water/MeCN 9:1 (v/v) + 0.1% TFA) and phase B (MeCN + 0.1% TFA), with linear gradient from 30% B to 100% B in 8 min and 2 min with 100% phase B. GC-FID analysis was performed on a Trace-GC (ThermoFisher) with a flame ionization detector with an HP5 column (30 m × 0.250 mm × 0.025 µm). After 1 min at 50 °C the temperature was increased in 25 °C/min steps up to 300 °C and kept at 300 °C for 4 min. The detector gas for the flame ionization was H_2 and compressed air (5.0 quality). GC–MS conditions were as follows: injection temperature 250 °C, HP-5 MS column (30 m × 0.250 mm ID, 0.25 µm film); carrier gas helium 5.0, flow 1 mL min^{-1}, temperature gradient programmed from 60 to 300 °C at 20 °C min^{-1} after an initial time of 6 min.

The MS conditions were as follows: positive EI ionization, ionization energy 70 eV, ionization source temperature 280 °C, emission current 100 µA. Flash chromatography separations were performed on a Biotage SP1 instrument with petroleum ether/ethyl acetate mixtures as eluent. Microwave irradiation experiments were carried out in an Anton Paar Monowave 300 instrument with appropriate internal fiber-optic temperature control [50-52]. All products synthesized in this study are known in the literature and have been characterized by ^{1}H NMR and MS analysis. All solvents and chemicals were obtained from standard commercial vendors and were used without any further purification.

Pd concentrations from the leaching experiments of a "palladated" steel coil and the metal screening of the "NMP/AcOH/H_2O mixtures" were determined after microwave assisted acid digestion in an MLS UltraClave III. The temperature was ramped up in 30 min to 250 °C and kept at this temperature for a further 30 min. Pd was quantitatively determined at *m*/*z* 105 with an Agilent 7500ce inductively coupled plasma mass spectrometer. A calibration was performed with an external calibration curve established from 1.000 g Pd/L standard (CPI International). Indium was used as the internal standard. The element screening in the digests of the "NMP/AcOH/H_2O mixtures" was performed in the semi-quantitative analysis mode using the Merck VI ICPMS standard for calibration. For both measurements, the samples were dispatched from the

autosampler via an integrated sample introduction system (ISIS) from Agilent Technologies to an Ari Mist HP nebulizer (Burgener Research International) and further into the ICPMS.

Continuous flow experiments

The flow experiments described herein were performed in a Thales X-Cube Flash reactor (electric resistance heating) [24], a Uniqsis FlowSyn instrument (conductive heating) [25] or in a self-made flow device constructed by immersing the corresponding coil material – connected to a HPLC pump and back-pressure regulator – into a pre-heated oil bath. The flow reactors were equipped with coils made from different materials (SX 316L steel, Hastelloy C-4 or PTFE), of variable lengths and inner diameters. A system pressure of 140 bar was applied for all experiments in the X-Cube Flash reactor while a pressure of ≈34 bar was selected for all experiments in the FlowSyn instrument and in the self-made device. Experiments in PTFE coils were limited to system pressures of ≤ 14bar.

Tetrazole decomposition in flow

The reactor was heated to the selected temperature while the solvent mixture (e.g., NMP/AcOH/H_2O 5:3:2) was pumped through the reactor at the desired flow rate. After the temperature was stable, the feed was switched from pure solvent to reagent (e.g., 0.125 M solution of tetrazole **2** in NMP/AcOH/H_2O 5:3:2). A defined volume (≈1 mL) of the reagent solution was introduced into the reactor and the feed was then changed back to pure solvent. The outcoming processed reagent solution was collected. For the kinetic analysis of the decomposition process (Figure 4 and Figure S5, Supporting Information File 1), the flow rate was varied and, after equilibration, the feed was switched back from pure solvent to reagent. The processed mixture was collected and the procedure repeated until enough data points were collected. For reaction monitoring and kinetic analysis, 100 µL samples were taken from the collected mixtures, diluted with 0.9 mL MeCN and analyzed by HPLC-UV at 215 nm. A detailed description of the isolation and characterization of decomposition products (Scheme 2) is given in the Supporting Information File 1.

Tetrazole synthesis in flow (Scheme 1)

The first attempts to synthesize tetrazole **2** (Figure 1) were performed in a resistively heated 8 mL coil at 220 °C with a residence time of 16 min (0.5 mL/min flow rate). The reagent mixture was a 0.67 M solution of diphenylacetonitrile (**1**) with 2.5 equiv of NaN_3 in NMP/AcOH/H_2O 5:3:2.

Tetrazole decomposition using microwave conditions

A 2.5 mL sample of a 0.125 M solution of tetrazole **2** in NMP/AcOH/H_2O (5:3:2) in a 10 mL microwave process vial with a stirrer bar was heated in the microwave reactor (Monowave 300) at the indicated temperature (Figure 3 and Figures S1–S4, Supporting Information File 1). For reaction monitoring the vial was cooled to 60 °C. After a defined time, 40 µL samples were taken with a transfer pipette, the sample diluted with 1.0 mL of MeCN and analyzed by HPLC at 215 nm. The experiments were carried out either in a standard 10 mL Pyrex tube or a vessel made from sintered silicon carbide and gave identical results.

Bechamp reduction (Table 1)

A 0 M, 0.25 M, 0.5 M and 1 M aqueous HCl solution in ethanol was prepared from conc. HCl and ethanol. A sample of 1 mmol (123.1 mg) of nitrobenzene (**10**) was added in a graduated cylinder and the volume was made up to 2 mL with the respective HCl solution to obtain a 0.5 M solution of nitrobenzene. The flow experiments were performed at 150 °C in coils made from stainless steel, Hastelloy or PTFE. The flow rates for the different coils were selected in order that the residence time was 20 min in every coil. The feed was switched between pure ethanol and reagent solutions.

Heck–Mizoroki coupling using palladated steel coils. Loading procedure

4-Iodobenzonitrile (150 mg, 0.65 mmol), *n*-butyl acrylate (126 mg, 142 mL, 0.98 mmol, 1.5 equiv), $Pd(OAc)_2$ (1.5 mg, 0.0065 mmol, 1 mol %) and triethylamine (100 mg, 137 mL, 0.98 mmol, 1.5 equiv) were mixed together with MeCN (2 mL) into a 5 mL glass vial and stirred for 2 min. The X-Cube Flash instrument was equipped with a stainless steel reaction coil (16 mL volume, 10 min residence time at 1.6 mL/min flow rate). The reaction parameters – temperature (180 °C), flow rate (1.6 mL/min), and pressure (55 bar) – were selected on the flow reactor and processing was started, whereby only pure solvent was pumped through the system until the instrument had achieved the desired reaction parameters and stable processing was assured. At that point, the inlet tube was switched to the vial containing the freshly prepared reaction mixture. After processing through the flow reactor, the inlet tubing was dipped back into a vial with pure solvent and processed for further 10 min, thus washing the system from any remaining reaction mixture. The processed reaction mixture was then combined with the washings and the solvent was removed under vacuum. The residue was dissolved in acetone (2 mL) and transferred to a silica-samplet, dried for 2 h at 70 °C in a drying oven, and then subjected to automated flash chromatography with petroleum ether/ethyl acetate (0 to 45% gradient) as eluent to provide 141 mg (94%) of cinnamic ester **14**, identical in all respects with a previously prepared sample in our laboratories [20].

Pd leaching studies

An identical experiment was performed in the loading procedure, but in the absence of the Pd catalyst employing the "palladated" coil described earlier. After complete processing through the flow reactor, the inlet tubing was dipped back into a vial with pure solvent and processed for further 10 min, thus washing any remaining reaction mixture from the system. A 10 mL sample was collected and the solvent removed under vacuum before submission for ICPMS analysis. Conversion was determined by the means of GC-MS. In a similar manner 10 mL fractions of solvent were collected at room temperature and at 180 °C, the solvent evaporated and the residues submitted to ICPMS analysis.

Pd cleaning procedure

The X-Cube Flash instrument was equipped with a "palladated" stainless steel reaction coil (16 mL volume, 10 min residence time at 1.6 mL/min flow rate). The reaction parameters – temperature (80 °C), flow rate (1.6 mL/min), and pressure (55 bar) – were selected on the flow reactor and processing was started, whereby only distilled water was pumped through the system until the instrument had achieved the desired reaction parameters and stable processing was assured. At that point, the inlet tube was switched to the vial containing 100 mL freshly prepared mixture of KCN (10 g/L) and *m*-nitrobenzenesulfinic acid sodium salt (10 g/L) in water. After processing of the 100 mL through the flow reactor (ca. 60 min), the inlet tubing was dipped back into a vial with distilled water and processed for a further 10 min. The process was repeated two more times with fresh 100 mL portions of KCN/*m*-nitrobenzenesulfinic acid sodium salt in water mixture before the reactor was finally washed with distilled water for 30 min to remove any remaining residues of the KCN/*m*-nitrobenzenesulfinic acid sodium salt in water mixture.

Pressure dependence of nucleophilic aromatic substitution (Scheme 5)

The reaction parameters – temperature (40 °C), flow rate (0.5 mL/min), and pressure (60 bar) – were selected on the X-Cube Flash flow reactor, equipped with an 8 mL stainless steel reaction coil and processing was started with pure THF. After the instrument had achieved the desired reaction parameters and stable processing was assured, freshly prepared solutions of 1-fluoro-4-nitrobenzene (**15**) (904 mg, 680 µL, 6.41 mmol) in 25 mL of THF and pyrrolidine (**16**) (4.56 g, 5.35 mL, 64.1 mmol) in 25 mL THF were introduced separately into the coil at flow rates of 0.5 mL min^{-1} utilizing two pumps to give a total flow rate of 1 mL/min (8 min residence time). After processing 5 mL of the reaction mixture through the flow reactor, the inlet tubings were dipped back into the vials with pure solvent and a sample was collected after an appropriate time. To a 100 µL portion of this collected sample, 500 µL of 2 M HCl were immediately added to quench the reaction. Then 500 µL of water and 600 µL DCM were added to extract the product and unreacted nitrobenzene**.** After vigorous shaking and settling, 100 µL of the organic layer was then diluted with 1 mL of MeCN before injecting into the HPLC for an offline analysis. The pressure was increased to 120 bar and then to 180 bar to collect two more samples at 40 °C. Similarly, the above steps were repeated to collected data for temperatures of 50, 60 and 70 °C (Figure 5).

Supporting Information

Supporting Information File 1

Details of experimental procedures, kinetic analysis and spectral data.
[http://www.beilstein-journals.org/bjoc/content/supplementary/1860-5397-7-59-S1.pdf]

Acknowledgements

This work was supported by a grant from the Christian Doppler Research Society (CDG). We thank J.-P. Roduit (Lonza) for helpful comments. T. R. thanks the Higher Education Commission of Pakistan for a Ph. D. scholarship.

References

1. Geyer, K.; Gustafson, T.; Seeberger, P. H. *Synlett* **2009,** 2382–2391. doi:10.1055/s-0029-1217828
2. Hartman, R. L.; Jensen, K. F. *Lab Chip* **2009,** *9,* 2495–2507. doi:10.1039/b906343a
3. Wirth, T., Ed. *Microreactors in Organic Synthesis and Catalysis;* Wiley-VCH: Weinheim, Germany, 2008.
4. Hessel, V.; Schouten, J. C.; Renken, A.; Wang, Y.; Yoshida, J.-i., Eds. *Handbook of Micro Reactors;* Wiley-VCH: Weinheim, Germany, 2009.
5. Yoshida, J.-i. *Flash Chemistry - Fast Organic Synthesis in Microsystems;* Wiley-VCH: Weinheim, Germany, 2008.
6. Luis, S. V.; Garcia-Verdugo, E., Eds. *Chemical Reactions and Processes under Flow Conditions;* Royal Society of Chemistry: Cambridge, U.K., 2010.
7. Roberge, D. M.; Gottsponer, M.; Eyholzer, M.; Kockmann, N. *Chim. Oggi* **2009,** *27,* 8–11.
8. Roberge, D. M.; Zimmermann, B.; Rainone, F.; Gottsponer, M.; Eyholzer, M.; Kockmann, N. *Org. Process Res. Dev.* **2008,** *12,* 905–910. doi:10.1021/op8001273
9. Yoshida, J.-i.; Nagaki, A.; Yamada, T. *Chem.–Eur. J.* **2008,** *14,* 7450–7459. doi:10.1002/chem.200800582
10. Hessel, V. *Chem. Eng. Technol.* **2009,** *32,* 1641. doi:10.1002/ceat.200990054
11. Hessel, V.; Kralisch, D.; Krtschil, U. *Energy Environ. Sci.* **2008,** *1,* 467–478. doi:10.1039/B810396H
12. Van Gerven, T.; Stankiewicz, A. *Ind. Eng. Chem. Res.* **2009,** *48,* 2465–2474. doi:10.1021/ie801501y
13. Razzaq, T.; Kappe, C. O. *Chem.–Asian J.* **2010,** *5,* 1274–1289. doi:10.1002/asia.201000010

14. Leadbeater, N. E., Ed. *Microwave Heating as a Tool for Sustainable Chemistry;* CRC Press: Boca Raton, 2010.
15. Kappe, C. O.; Dallinger, D.; Murphree, S. S. *Practical Microwave Synthesis for Organic Chemists - Strategies, Instruments, and Protocols;* Wiley-VCH: Weinheim, Germany, 2009.
16. Loupy, A., Ed. *Microwaves in Organic Synthesis,* 2nd ed.; Wiley-VCH: Weinheim, Germany, 2006.
17. Caddick, S.; Fitzmaurice, R. *Tetrahedron* **2009,** *65,* 3325–3355. doi:10.1016/j.tet.2009.01.105
18. Kappe, C. O.; Dallinger, D. *Mol. Diversity* **2009,** *13,* 71–193. doi:10.1007/s11030-009-9138-8
19. Razzaq, T.; Glasnov, T. N.; Kappe, C. O. *Eur. J. Org. Chem.* **2009,** 1321–1325. doi:10.1002/ejoc.200900077
20. Glasnov, T. N.; Findenig, S.; Kappe, C. O. *Chem.–Eur. J.* **2009,** *15,* 1001–1010. doi:10.1002/chem.200802200
21. Fuchs, M.; Goessler, W.; Pilger, C.; Kappe, C. O. *Adv. Synth. Catal.* **2010,** *352,* 323–328. doi:10.1002/adsc.200900726
22. Damm, M.; Glasnov, T. N.; Kappe, C. O. *Org. Process Res. Dev.* **2010,** *14,* 215–224. doi:10.1021/op900297e
23. Glasnov, T. N.; Kappe, C. O. *Adv. Synth. Catal.* **2010,** *352,* 3089–3097. doi:10.1002/adsc.201000646
24. Razzaq, T.; Glasnov, T. N.; Kappe, C. O. *Chem. Eng. Technol.* **2009,** *32,* 1702–1716. doi:10.1002/ceat.200900272
25. Gutmann, B.; Roduit, J.-P.; Roberge, D.; Kappe, C. O. *Angew. Chem.* **2010,** *122,* 7255–7259. doi:10.1002/ange.201003733
Angew. Chem., Int. Ed. **2010,** *49,* 7101–7105. doi:10.1002/anie.201003733
26. Gustafsson, T.; Pontén, F.; Seeberger, P. H. *Chem. Commun.* **2008,** 1100–1102. doi:10.1039/b719603b
27. Bedore, M. W.; Zaborenko, N.; Jensen, K. F.; Jamison, T. F. *Org. Process Res. Dev.* **2010,** *14,* 432–440. doi:10.1021/op9003136
28. Ulbrich, K.; Kreitmeier, P.; Reiser, O. *Synlett* **2010,** 2037–2040. doi:10.1055/s-0030-1258534
29. Sahoo, H. R.; Kralj, J. G.; Jensen, K. F. *Angew. Chem.* **2007,** *119,* 5806–5810. doi:10.1002/ange.200701434
Angew. Chem. Int. Ed. **2007,** *46,* 5704–5708. doi:10.1002/anie.200701434
30. Bogdan, A. R.; Sach, N. W. *Adv. Synth. Catal.* **2009,** *351,* 849–854. doi:10.1002/adsc.200800758
31. Brandt, J. C.; Wirth, T. *Beilstein J. Org. Chem.* **2009,** *5,* No. 30. doi:10.3762/bjoc.5.30
32. Kopach, M. E.; Murray, M. M.; Braden, T. M.; Kobierski, M. E.; Williams, O. L. *Org. Process Res. Dev.* **2009,** *13,* 152–160. doi:10.1021/op800265e
33. Reactor wall, aging, and temperature history effects etc. on reaction rate and/or selectivity are not uncommon in high temperature (usually gas-phase) continuous flow processes. For some recently reported surface effects on solution phase organic reactions in micro-structured devices at moderate or low temperatures [72-74].
34. Hao, J.; Cheng, H.; Wang, H.; Cai, S.; Zhao, F. *J. Mol. Catal. A: Chem.* **2007,** *271,* 42–45. doi:10.1016/j.molcata.2007.02.031
35. Kittaka, S. J. *Colloid and Interface Sci.* **1974,** *48,* 327–333. doi:10.1016/0021-9797(74)90167-2
36. Dillon, C. P. *Corrosion Resistance of Stainless Steel;* CRC Press: Boca Raton, 2010.
37. HN_3 dissolves some metals (M = Zn, Fe, Mn, and Cu) without evolution of dihydrogen: $M + 3\ HN_3 + H^+ \rightarrow M(N_3)_2 + N_2 + NH_4^+$ [75].
38. Muetterties, E. L.; Evans, W. J.; Sauer, J. C. *J. Chem. Soc., Chem. Commun.* **1974,** 939–940. doi:10.1039/C39740000939
39. Vaughan, J.; Smith, P. A. S. *J. Org. Chem.* **1958,** *23,* 1909–1912. doi:10.1021/jo01106a023
40. Chervin, S.; Bodman, G. T.; Barnhart, R. W. *J. Hazard. Mater.* **2006,** *130,* 48–52. doi:10.1016/j.jhazmat.2005.07.062
41. Sulfinert® is a Siltek® treated stainless steel coil (i.e., chemical vapor-deposited multilayer silica coating) that has the advantages of Teflon® coatings or glass/fused silica coils without the problems with gas permeability and temperature limitations associated with polymeric coatings such as Teflon® coatings, and with far higher flexibility and durability than glass/fused silica coils. The temperature limit of these coils is 600 °C.
42. Huisgen, R.; Sauer, J.; Sturm, H. J. *Angew. Chem.* **1958,** *70,* 272–273. doi:10.1002/ange.19580700918
43. Huisgen, R.; Sauer, J.; Seidel, M. *Chem. Ber.* **1961,** *94,* 2503–2509. doi:10.1002/cber.19610940926
44. Herbst, R. M. *J. Org. Chem.* **1961,** *26,* 2372–2373. doi:10.1021/jo01351a055
45. Huisgen, R.; Sauer, J.; Sturm, H. J.; Markgaf, J. H. *Chem. Ber.* **1960,** *93,* 2106–2124. doi:10.1002/cber.19600930932
46. Sauer, J.; Huisgen, R.; Sturm, H. J. *Tetrahedron* **1960,** *11,* 241–251. doi:10.1016/S0040-4020(01)93173-4
47. Walling, C.; Naglieri, A. N. *J. Am. Chem. Soc.* **1960,** *82,* 1820–1825. doi:10.1021/ja01492a065
48. Arnold, R. T.; Elmer, O. C.; Dodson, R. M. *J. Am. Chem. Soc.* **1950,** *72,* 4359–4361. doi:10.1021/ja01166a007
49. In principle, the nitrile/amide may also arise from a Lossen rearrangement of *N'*-acetyl-diphenylacetohydrazide (**7**). This, however, would require the migration of the methyl group rather than of the benzhydryl group. The small amounts of *N*-benzhydrylacetamide detected in the reaction mixture by GC-MS are possibly formed via this rearrangement and subsequent acylation of the formed amine with acetic acid (see also [47]).
50. Obermayer, D.; Kappe, C. O. *Org. Biomol. Chem.* **2010,** *8,* 114–121. doi:10.1039/b918407d
51. Obermayer, D.; Gutmann, B.; Kappe, C. O. *Angew. Chem.* **2009,** *121,* 8471–8474. doi:10.1002/ange.200904185
Angew. Chem., Int. Ed. 2**009,** *48,* 8321–8324. doi:10.1002/anie.200904185
52. Gutmann, B.; Obermayer, D.; Reichart, B.; Prekodravac, B.; Irfan, M.; Kremsner, J. M.; Kappe, C. O. *Chem.–Eur. J.* **2010,** *16,* 12182–12194. doi:10.1002/chem.201001703
53. Hastelloy is the registered trademark name of Haynes International, Inc. for Ni-based high performance alloys.
54. Kunz, U.; Turek, T. *Beilstein J. Org. Chem.* **2009,** *5,* No. 70. doi:10.3762/bjoc.5.70
For a similar continuous flow device using direct electric resistance heating of stainless steel coils.
55. Kreysa, G.; Schütze, M., Eds. *Corrosion Handbook - Corrosive Agents and Their Interaction with Materials,* 2nd ed.; Wiley-VCH: Weinheim, Germany, 2009; Vol. 2.
56. Béchamp, A. J. *Ann. Chim. Phys.* **1854,** *42,* 186–196.
57. Reetz, M. T.; de Vries, J. G. *Chem. Commun.* **2004,** 1559–1563. doi:10.1039/b406719n
58. Phan, N. T. S.; Van der Sluys, M.; Jones, C. W. *Adv. Synth. Catal.* **2006,** *348,* 609–679. doi:10.1002/adsc.200505473
59. The preparative and mechanistic aspects of this Mizoroki–Heck coupling using both heterogeneous and homogeneous Pd sources under microwave batch and continuous flow conditions are described in detail in [20].

60. Ackermann, L.; Born, R. Mizoroki–Heck Reactions with Metals Other than Palladium. In *The Mizoroki-Heck Reaction;* Oestreich, M., Ed.; John Wiley & Sons Ltd.: Chichester, U. K., 2009; pp 383–403. doi:10.1002/9780470716076.ch10
61. Loska, R.; Volla, C. M. R.; Vogel, P. *Adv. Synth. Catal.* **2008,** *350,* 2859–2864. doi:10.1002/adsc.200800662
62. Shore, G.; Morin, S.; Organ, M. G. *Angew. Chem.* **2006,** *118,* 2827–2832. doi:10.1002/ange.200503600
Angew. Chem., Int. Ed. **2006,** *45,* 2761–2766. doi:10.1002/anie.200503600
63. Shore, G.; Yoo, W. J.; Li, C. J.; Organ, M. G. *Chem.–Eur. J.* **2010,** *16,* 126–133. doi:10.1002/chem.200902396
64. MacQuarrie, S.; Horton, J. H.; Barnes, J.; McEleney, K.; Loock, H.-P.; Crudden, C. M. *Angew. Chem.* **2008,** *120,* 3112–3115. doi:10.1002/ange.200890074
Angew. Chem., Int. Ed. **2008,** *47,* 3279–3282. doi:10.1002/anie.200800153. For recent mechanistic studies on Pd-catalyzed cross-coupling reactions using Pd foil.
65. Hornung, C. H.; Hallmark, B.; Mackley, M. R.; Baxandale, I. R.; Ley, S. V. *Adv. Synth. Catal.* **2010,** *352,* 1736–1745. doi:10.1002/adsc.201000139
66. Costantini, F.; Benetti, E. M.; Tiggelaar, R. M.; Gardeniers, H. J. G. E.; Reinhoudt, D. N.; Huskens, J.; Vancso, G. J.; Verboom, W. *Chem.–Eur. J.* **2010,** *16,* 12406–12411. doi:10.1002/chem.201000948
67. Rebrov, E. V.; Klinger, E. A.; Berenguer-Murcia, A.; Sulman, E. M.; Schouten, J. C. *Org. Process Res. Dev.* **2010,** *13,* 991–998. doi:10.1021/op900085b
68. Herrmann, S.; Landau, U. Method for Recovering Precious Metals. WO/2000/001863, Jan 13, 2000.
69. Benito-López, F.; Egberink, R. J. M.; Reinhoudt, D. N.; Verboom, W. *Tetrahedron* **2008,** *64,* 10023–10040. doi:10.1016/j.tet.2008.07.108
70. Verboom, W. *Chem. Eng. Techn.* **2009,** *32,* 1695–1701. doi:10.1002/ceat.200900369
71. Benito-López, F.; Verboom, W.; Kakuta, M.; Gardeniers, J. H. G. E.; Egberink, R. J. M.; Oosterbroek, E. R.; van den Berg, A.; Reinhoudt, D. N. *Chem. Commun.* **2005,** 2857–2859. doi:10.1039/b500429b
72. Brivio, M.; Oosterbroek, R. E.; Verboom, W.; Goedbloed, M. H.; van den Berg, A.; Reinhoudt, D. N. *Chem. Commun.* **2003,** 1924–1925. doi:10.1039/b305226p
73. Benito-López, F.; Tiggelaar, R. M.; Salbut, K.; Huskens, J.; Egberink, R. J. M.; Reinhoudt, D. N.; Gardeniers, H. J. G. E.; Verboom, W. *Lab Chip* **2007,** *7,* 1345–1351. doi:10.1039/b703394j
74. Yao, X.; Yao, J.; Zhang, L.; Xu, N. *Catal. Lett.* **2009,** *132,* 147–152. doi:10.1007/s10562-009-0072-2
75. King, R. B., Ed. *Encyclopedia of Inorganic Chemistry,* 2nd ed.; Wiley-VCH: Weinheim, Germany, 2005.

License and Terms

Beilstein Journal of Organic Chemistry

Continuous flow hydrogenation using polysilane-supported palladium/alumina hybrid catalysts

Hidekazu Oyamada, Takeshi Naito and Shū Kobayashi*

Letter

Open Access

Address:
Department of Chemistry, School of Science and Graduate School of Pharmaceutical Sciences, The University of Tokyo, Hongo, Bunkyo-ku, Tokyo 113-0033, Japan

Email:
Shū Kobayashi* - shu_kobayashi@chem.s.u-tokyo.ac.jp

* Corresponding author

Keywords:
flow chemistry; hydrogenation; polysilane; palladium; reduction

Beilstein J. Org. Chem. **2011,** *7,* 735–739.
doi:10.3762/bjoc.7.83

Received: 24 March 2011
Accepted: 04 May 2011
Published: 31 May 2011

This article is part of the Thematic Series "Chemistry in flow systems II".

Guest Editor: A. Kirschning

Abstract

Continuous flow systems for hydrogenation using polysilane-supported palladium/alumina (Pd/(PSi–Al_2O_3)) hybrid catalysts were developed. Our original Pd/(PSi–Al_2O_3) catalysts were used successfully in these systems and the hydrogenation of unsaturated C–C bonds and a nitro group, deprotection of a carbobenzyloxy (Cbz) group, and a dehalogenation reaction proceeded smoothly. The catalyst retained high activity for at least 8 h under neat conditions.

Findings

Catalytic hydrogenation is one of the most important methods for the reduction of C–C double and triple bonds, and other functional groups. Heterogeneous catalysts including Pd/C, Pt/C and Pd/SiO_2 are commonly used in reduction reactions both in research and industrial environments because of the ease of separation of the catalysts and products. However, the contamination of products as a result of leaching of metals from supports as well as the decreased catalytic activity, are both serious problems with the use of conventional heterogeneous catalysts. To address these problems, we recently developed novel methods for the immobilization of metal and non-metal catalysts on supports. This involved the development of microencapsulated (MC) and polymer-incarcerated (PI) catalysts, which have high catalytic activity without causing metal leaching [1].

Heterogeneous catalytic hydrogenation in a batch system has recently been applied to continuous flow hydrogenation systems for high-throughput synthesis [2-10]. There are several problems associated with conducting heterogeneous catalytic hydrogenation in a batch system. These include the necessity for filtration of hydrogen-saturated pyrophoric catalysts from flammable solvents, the possible requirement to use hydrogen gas under high pressure, difficulties in the re-use of catalysts (or inability for their re-use), the need for vigorous stirring to achieve catalytic activity, and the possible necessity for longer reaction times, which may lead to undesirable side reactions or harsh reaction conditions. Continuous flow systems have the potential to overcome these problems and disadvantages. In our laboratory, PI catalysts were applied to tri-phase hydrogenation

reactions in a microreactor system and led to markedly shorter reaction times [11]. While the productivity of a single microreactor is low, increasing the number of reactors ("numbering up") could readily and substantially increase production.

We also recently reported novel transition metal catalysis involving the immobilization of Pd or Pt onto polysilane supports by the microencapsulation method [12]. The Pd catalyst (Pd/PSi) had high activity with no or very little leaching of Pd, and it could be recovered and re-used in hydrogenation reactions in batch systems. We then developed polysilane-supported Pd/metal oxide hybrid catalysts [13] using the PI method (microencapsulation and cross-linking), which were then applied in these microreactor systems [14]. The hybrid catalysts were insoluble, did not swell in any solvent, and were predicted to be applicable to continuous flow reactors. In this study, we investigated hydrogenation reactions of C–C double and triple bonds as well as various other functional groups using continuous flow systems with Pd/(PSi–Al_2O_3) catalysts.

A schematic diagram of the continuous flow reactor and an image of the top of the column are shown in Figure 1. A high performance liquid chromatography (HPLC) pump was used to feed the substrate into the central hole in the top of the column, which was filled with the Pd/(PSi–Al_2O_3) catalyst. Hydrogen gas was introduced into the six holes surrounding the central hole using a mass flow controller. The column was heated in a water bath as required. The substrate reacted with the H_2 gas inside the column, and the product was collected downstream of the column.

We initially examined the hydrogenation reaction of ethyl cinnamate (Scheme 1) and collected the product for 8 h without contamination of the starting material. This demonstrated that the catalyst retained high activity for at least 8 h, and the turnover number (TON) reached 8700.

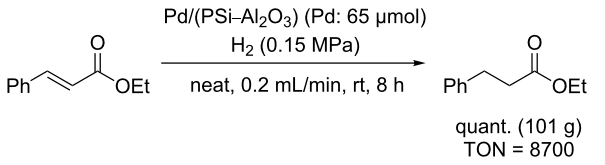

Scheme 1: Hydrogenation of ethyl cinnamate.

We then investigated the hydrogenation of other substrates. The hydrogenation reactions of C–C double and triple bonds in various substrates are shown in Table 1; these proceeded quantitatively at room temperature under neat conditions. The products were obtained at approximately 10 g/h through the 4 cm^3 column.

The hydrogenation reactions of *trans*-stilbene and *trans*-chalcone, as representative solid substrates (Scheme 2), were also examined. The substrates were dissolved in toluene or ethyl acetate. The reduction of *trans*-stilbene proceeded quantitatively, but an overreaction product was obtained (7% yield) in the reduction of *trans*-chalcone.

We then investigated the hydrogenation of a nitro group (nitrobenzene) and the deprotection of a carbobenzyloxy (Cbz) group (Scheme 3). The hydrogenation reaction of nitrobenzene proceeded quantitatively under neat conditions, and the deprotection of Cbz–Ser also proceeded quantitatively in a mixed solvent system (EtOH/H_2O 1:4).

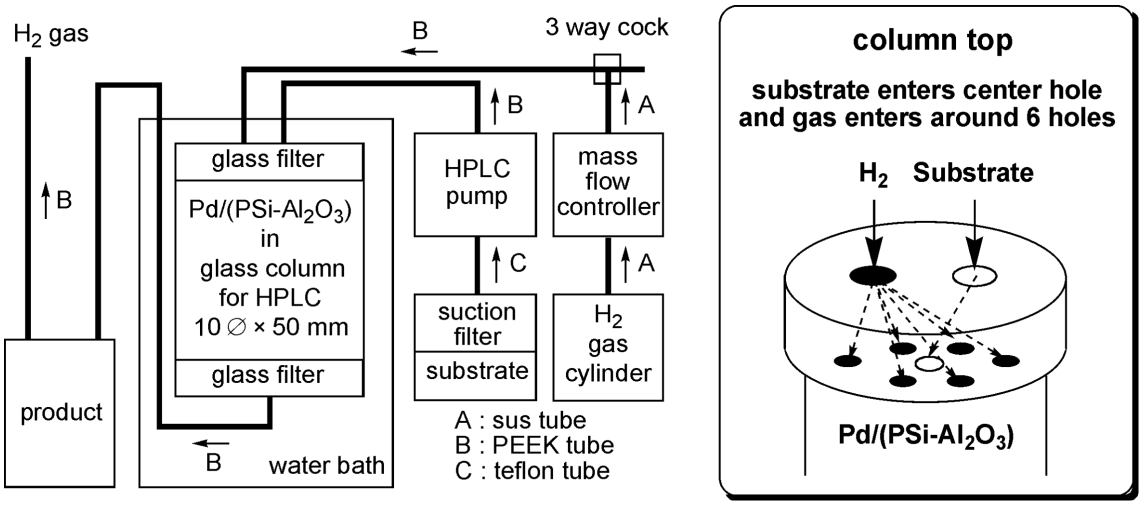

Figure 1: Schematic diagram of the continuous flow reactor (left) and the column top (right).

Table 1: Hydrogenation of C–C double and triple bonds.

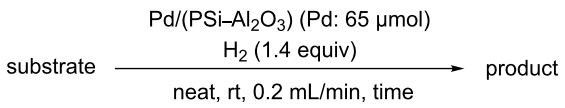

Entry	Substrate	Time (h)	Product	Yield (TON)
1	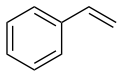	1.5	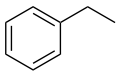	14.9 g (2200)
2		1.5		13.9 g (2400)
3	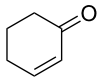	1.5		18.0 g (2700)
4		1.5		16.3 g (2100)
5	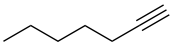	1.7	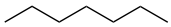	14.9 g (2300)
6	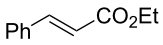	1.5	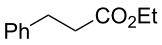	19.4 g (1700)

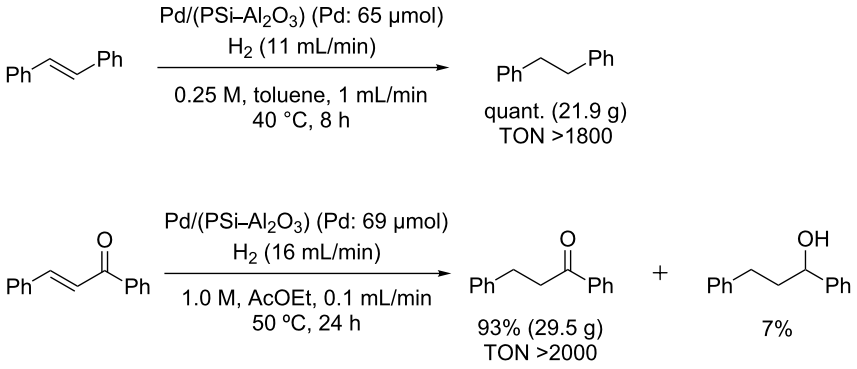

Scheme 2: Hydrogenation of *trans*-stilbene and *trans*-chalcone.

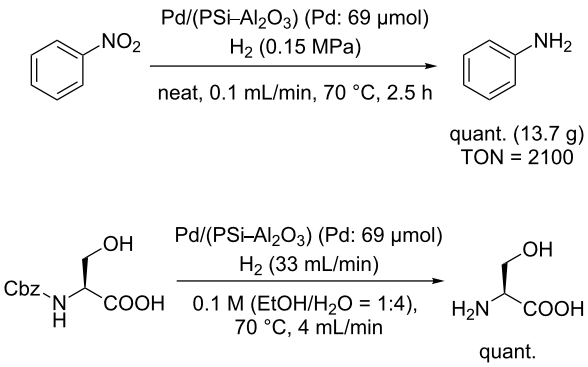

Scheme 3: Hydrogenation of nitrobenzene and deprotection of the Cbz group.

Hydrogenation reactions could also be carried out successfully in water (Scheme 4). The reduction of aqueous maleic acid proceeded quantitatively. Dehalogenation of *p*-chlorobenzoic acid in basic aqueous solution also proceeded smoothly and benzoic acid was obtained after acid treatment. In the case of *p*-chlorophenol, the conversion was complete; however, in this case some by-product (5%) was also obtained.

In summary, we developed continuous flow systems for hydrogenation using a Pd/(PSi–Al_2O_3) catalyst. Our original Pd/(PSi–Al_2O_3) catalysts were successfully used in these systems. In the hydrogenation reactions studied, i.e., the reduction of unsaturated C–C bonds and a nitro group, deprotection of a Cbz group, and a dehalogenation reaction, all proceeded

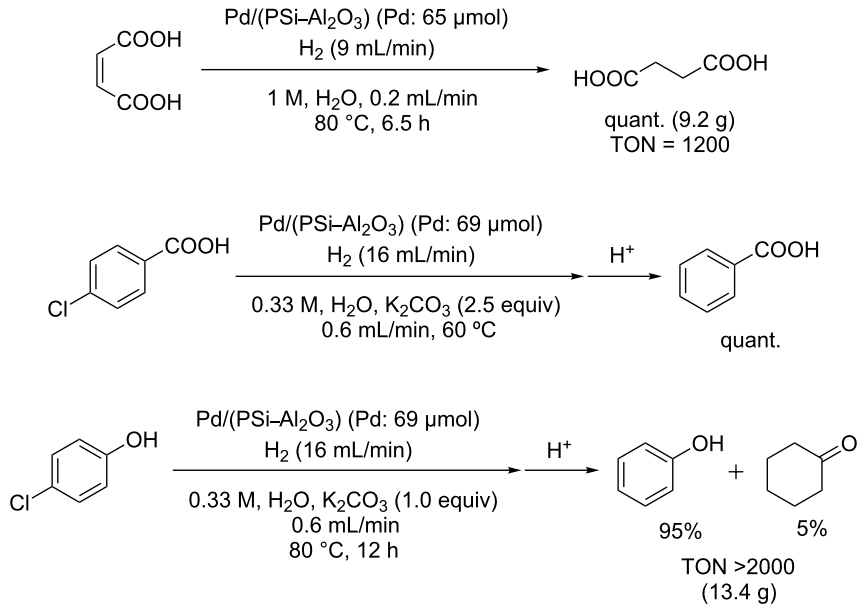

Scheme 4: Hydrogenation in water.

smoothly. The catalysts could be used for a long time, with high activity being retained for at least 8 h under neat conditions. It is noted that in all cases no Pd leaching was detected (ICP). Further studies of the application of these systems to large-scale production are now in progress.

Experimental

The continuous flow reactor system comprised the following devices (Figure 1): HPLC pump: Shimadzu LC-6AD or Eyela 301. Mass flow controller: Lyntec MC-3000E and RP-300. Column: 10∅ × 50 mm Eyela glass column filled with 4 g of Pd/(PSi–Al_2O_3) and equipped on the top with a glass filter (pore size 10 μm), a 7-hole plate (polychlorotrifluoroethylene; PCTFE) and a screw cap, and on the bottom with a glass filter (pore size 10 μm), a 1-hole plate (PCTFE) and a screw cap. Line: A sus tube (outside diameter: 1/16 inch) was used for line A, a PEEK tube (outside diameter: 1/16 inch) was used for line B and a Teflon tube (outside diameter: 3 mm) was used for line C.

Typical procedure for hydrogenation reactions (Table 1, entry 1): Styrene was fed into the column using the HPLC pump, and H_2 gas was introduced into the column using the mass flow controller. The system was left to stabilize for 30 min, and the product was then sampled over 1.5 h. The sample was analyzed by ^{1}H NMR, and the complete conversion of styrene to ethyl benzene was confirmed. ^{1}H NMR (500 MHz, $CDCl_3$) δ 1.24 (t, *J* = 7.7 Hz, 3H), 2.65 (q, *J* = 7.7 Hz, 2H), 7.15–7.23 (m, 3H), 7.26–7.30 (m, 2H).

Hydrogenation reaction of *trans*-stilbene (Scheme 2): *trans*-Stilbene (Aldrich) in toluene (0.25 M) was fed into the column (maintained at 40 °C in a water bath) using the HPLC pump (1.0 mL/min), and H_2 gas was introduced into the column using the mass flow controller (11 mL/min). The system was left to stabilize for 30 min. The product was then sampled over 8 h and dried in vacuo. The sample was analyzed by ^{1}H NMR, and the full conversion of *trans*-stilbene to 1,2-diphenylethane was confirmed. ^{1}H NMR (500 MHz, $CDCl_3$) δ 2.92 (s, 4H), 7.17–7.21 (m, 6H), 7.26–7.30 (m, 4H).

Hydrogenation reaction of nitrobenzene (Scheme 3): Nitrobenzene was fed into the column (maintained at 70 °C in a water bath) using the HPLC pump (0.1 mL/min), and H_2 gas was introduced into the column at a pressure of 0.15 MPa. The system was left to stabilize for 30 min and the product then sampled for 2.5 h. The sample (18.9 g as a mixture of aniline and H_2O; calculated quantity of aniline = 13.7 g) was analyzed by GC, and the complete conversion of nitrobenzene to aniline was confirmed.

Hydrogenation reaction of *p*-chlorobenzoic acid (Scheme 4): *p*-Chlorobenzoic acid in H_2O (0.33 M, including 2.5 equiv of K_2CO_3) was fed into the column (maintained at 60 °C in a water bath) using the HPLC pump (0.6 mL/min) and H_2 gas was introduced into the column using the mass flow controller (16 mL/min). The system was left to stabilize for 30 min and the product was then sampled for 8 min. Aqueous HCl (1 N) was added to the mixture, which was then extracted twice with

AcOEt. The combined organic layers were dried in vacuo. The sample was analyzed by ^{1}H NMR, and complete dehalogenation of the Cl group was confirmed. ^{1}H NMR (500 MHz, $CDCl_3$) δ 7.46–7.50 (m, 2H), 7.60–7.63 (m, 1H), 8.12–8.14 (m, 2H).

Acknowledgements

This work was partially supported by a Grant-in-Aid for Scientific Research from the Japan Society for the Promotion of Science (JSPS), Global COE Program, The University of Tokyo, MEXT, Japan, and NEDO.

References

1. Akiyama, R.; Kobayashi, S. *J. Am. Chem. Soc.* **2003,** *125,* 3412–3413. doi:10.1021/ja029146j
2. Solodenko, W.; Wen, H.; Leue, S.; Stuhlmann, F.; Sourkouni-Argirusi, G.; Jas, G.; Schönfeld, H.; Kunz, U.; Kirschning, A. *Eur. J. Org. Chem.* **2004,** 3601–3610. doi:10.1002/ejoc.200400194
3. Yoswathananont, N.; Nitta, K.; Nishiuchi, Y.; Sato, M. *Chem. Commun.* **2005,** 40–42. doi:10.1039/b410014j
4. Jones, R.; Gödörházy, L.; Szalay, D.; Gerencsér, J.; Dormán, G.; Ürge, L.; Darvas, F. *QSAR Comb. Sci.* **2005,** *24,* 722–727. doi:10.1002/qsar.200540006
5. Jones, R. V.; Godorhazy, L.; Varga, N.; Szalay, D.; Urge, L.; Darvas, F. *J. Comb. Chem.* **2006,** *8,* 110–116. doi:10.1021/cc050107o
6. Desai, B.; Kappe, C. O. *J. Comb. Chem.* **2005,** *7,* 641–643. doi:10.1021/cc050076x
7. Saaby, S.; Knudsen, K. R.; Ladlow, M.; Ley, S. V. *Chem. Commun.* **2005,** 2909–2911. doi:10.1039/b504854k
8. Mennecke, K.; Cecilia, R.; Glasnov, T. N.; Gruhl, S.; Vogt, C.; Feldhoff, A.; Larrubia Vargas, M. A.; Kappe, C. O.; Kunz, U.; Kirschning, A. *Adv. Synth. Catal.* **2008,** *350,* 717–730. doi:10.1002/adsc.200700510
9. Irfan, M.; Petricci, E.; Glasnov, T. N.; Taddei, M.; Kappe, C. O. *Eur. J. Org. Chem.* **2009,** *9,* 1327–1334. doi:10.1002/ejoc.200801131
10. Ceylan, S.; Coutable, L.; Wegner, J.; Kirschning, A. *Chem.–Eur. J.* **2011,** *17,* 1884–1893. doi:10.1002/chem.201002291
11. Kobayashi, J.; Mori, Y.; Okamoto, K.; Akiyama, R.; Ueno, M.; Kitamori, T.; Kobayashi, S. *Science* **2004,** *304,* 1305–1308. doi:10.1126/science.1096956
12. Oyamada, H.; Akiyama, R.; Hagio, H.; Naito, T.; Kobayashi, S. *Chem. Commun.* **2006,** 4297–4299. doi:10.1039/b610241g
13. Oyamada, H.; Naito, T.; Miyamoto, S.; Akiyama, R.; Hagio, H.; Kobayashi, S. *Org. Biomol. Chem.* **2008,** *6,* 61–65. doi:10.1039/b715220e
14. Ueno, M.; Suzuki, T.; Naito, T.; Oyamada, H.; Kobayashi, S. *Chem. Commun.* **2008,** 1647–1649. doi:10.1039/b715259k

License and Terms

Beilstein Journal of Organic Chemistry

Continuous gas/liquid–liquid/liquid flow synthesis of 4-fluoropyrazole derivatives by selective direct fluorination

Jessica R. Breen[1], Graham Sandford[*1], Dmitrii S. Yufit[2], Judith A. K. Howard[2], Jonathan Fray[3] and Bhairavi Patel[3]

Full Research Paper

Open Access

Address:
[1]Department of Chemistry, Durham University, South Road, Durham, DH1 3LE, UK, [2]Chemical Crystallography Group, Department of Chemistry, Durham University, South Road, Durham, DH1 3LE, UK and [3]Pfizer Global Research & Development, Ramsgate Road, Sandwich, Kent, CT13 9NJ, UK

Email:
Graham Sandford[*] - Graham.Sandford@durham.ac.uk

* Corresponding author

Keywords:
continuous flow reactions; fluorine; fluoropyrazole; gas-liquid flow reactor; selective direct fluorination

Beilstein J. Org. Chem. **2011,** *7,* 1048–1054.
doi:10.3762/bjoc.7.120

Received: 16 May 2011
Accepted: 04 July 2011
Published: 02 August 2011

This article is part of the Thematic Series "Chemistry in flow systems II".

Guest Editor: A. Kirschning

Abstract

4-Fluoropyrazole systems may be prepared by a single, sequential telescoped two-step continuous gas/liquid–liquid/liquid flow process from diketone, fluorine gas and hydrazine starting materials.

Introduction

Organic systems which bear fluorine atoms are used in an ever widening range of applications in the life sciences. Many commercially significant pharmaceutical and agrochemical products [1-3] owe their biological activity to the presence of fluorinated groups within their structure. Since carbon–fluorine bonds are rare in naturally occurring organic molecules [4], an efficient, selective and economically viable methodology for the synthesis of fluoroorganic derivatives is required to exploit fully the use of fluorinated systems in life science applications. In general, there are two complimentary approaches to the synthesis of fluoroorganic products [5,6], which involve either carbon–fluorine bond formation, requiring functional group interconversion utilising an appropriate nucleophilic or electrophilic fluorinating agent [6], or syntheses based on the reactions of appropriate fluorine containing building blocks [7]. Of course, whichever methodology is used for the synthesis of a specific fluorinated organic molecule, a carbon–fluorine bond must be formed at some stage of the synthetic process, and various fluorinating agents have been developed over many years in attempts to meet synthetic requirements, with varying degrees of success [5].

In an on-going research programme at Durham, aimed at developing widely applicable an effective, selective, direct fluorin-

ation methodology, we have been exploring the use of elemental fluorine, a previously underused reagent in organic chemistry, for the synthesis of fluoroorganic systems [8-10]. Methodologies for the preparation of, for example, a range of fluorinated aliphatic [11], carbonyl [12-14], aromatic [15] and heterocyclic [16,17] systems have been established and scaled-up by our industrial collaborators for use in the synthesis of commercially important pharmaceutical intermediates [18]. As part of our studies, aimed at further control of the direct fluorination procedures for larger scale manufacturing, we developed continuous flow microreactor systems that enabled gas/liquid fluorination reactions between fluorine and various substrates to occur in very efficient processes [19-21].

Fluoro-carbonyl derivatives can, in principle, be utilised as building blocks for the preparation of more complex systems such as fluorinated terpenoids, steroids and a range of heterocyclic systems, upon appropriate synthetic elaboration [7], and, consequently, there is much interest in the development of a synthetic methodology for the preparation of such useful fluorinated intermediates. It has been established that, in both batch and continuous flow processes, 1,3-dicarbonyl derivatives are not equally reactive towards fluorine gas [12] and that the ease of selective direct fluorination depends on the nature and proximity of other functional groups. Substrates that have a high initial equilibrium enol concentration in the reaction media that are used for fluorination reactions, such as formic acid or acetonitrile, and/or rapidly convert from the keto to the enol form, will react rapidly and selectively with fluorine to give monofluorinated products in high yield. Conversely, substrates that have low enol concentrations at equilibrium and/or slow keto-enol exchange rates give low yields of the desired monofluorinated dicarbonyl products [12]. Indeed, for carbonyl systems with low enol equilibrium contents and/or low keto-enol exchange rates, direct fluorination must be carried out in conditions that enhance enol formation by base catalysis, by metal catalysis or by fluorination of appropriate pre-formed enol derivatives, such as trimethylsilyl enols or enol acetate derivatives [13,14].

Dicarbonyl systems are, of course, widely used for the construction of heterocyclic ring systems such a pyrimidine, pyridazine and pyrazole derivatives [22,23]. Of relevance to this paper, pyrazole and its derivatives constitute an important class of compounds, which exhibit various biological and pharmaceutical activities ranging from antitumor to anti-inflammatory, antipsychotic, antimicrobial, antiviral and antifungal activities. Pyrazoles are also useful intermediates for many industrial products and it is, therefore, not surprising that many synthetic methods have been developed for the preparation of such heterocyclic systems, for example, through 1,3-dipolar cycloadditions of diazo compounds and the direct condensation of 1,3-diketones and hydrazines [23].

However, the synthetic methodology for the preparation of the corresponding fluoropyrazole derivatives has not been developed to any great extent despite the potential use of such systems in life science applications. Recently, we explored direct fluorination of various pyrazole substrates using elemental fluorine and, in many cases, obtained low yields of the desired fluoropyrazole products due to significant tar formation [24], while the corresponding fluorination of a limited number of pyrazole systems by Selectfluor™ has been described by other researchers [25]. Various building block strategies that yield fluoropyrazole derivatives from, for example, reactions of appropriate fluorodicarbonyl [26] and fluorocyano-ketones [27], have also been reported.

Consequently, we aimed to develop an effective, selective continuous flow methodology for the efficient synthesis of fluoropyrazole systems and, in this paper, we demonstrate that fluorination of diketones to corresponding fluorodiketones, followed by sequential cyclization to the appropriate fluoropyrazoles upon reaction with a hydrazine derivative, can be accomplished in a single, two-step, telescoped, gas/liquid–liquid/liquid continuous flow process. No examples of gas/liquid–liquid/liquid processes involving direct fluorination as the first stage of a continuous flow procedure have been reported previously.

Results and Discussion

After some development work, a continuous flow reactor for sequential gas/liquid–liquid/liquid synthesis of fluoropyrazoles from fluorine, hydrazine and diketone starting materials was constructed from nickel metal and narrow bore PTFE tubing as described previously [28,29] (Figure 1).

Briefly, fluorine gas, diluted to 10% v/v solution in nitrogen was added via a mass flow controller to the microchannel through Input A, the diketone substrate dissolved in acetonitrile was added by a syringe pump into the microchannel via Input B and was made to react with fluorine while both these starting materials passed down the reactor channel in a ‘pipe flow’ regime, as observed in previous direct fluorination reactions using this reactor design. The hydrazine solution was added by a syringe pump, via a T-piece at Input C, into the liquid flow, which was carried along the flow reaction channel by the pressure of the accompanying nitrogen gas. The crude reaction mixture was then passed into a vessel containing water to quench the reaction and neutralise any excess HF. Work-up by extraction of the crude reaction mixture with dichloromethane, drying and evaporation of the organic solvent gave a crude product

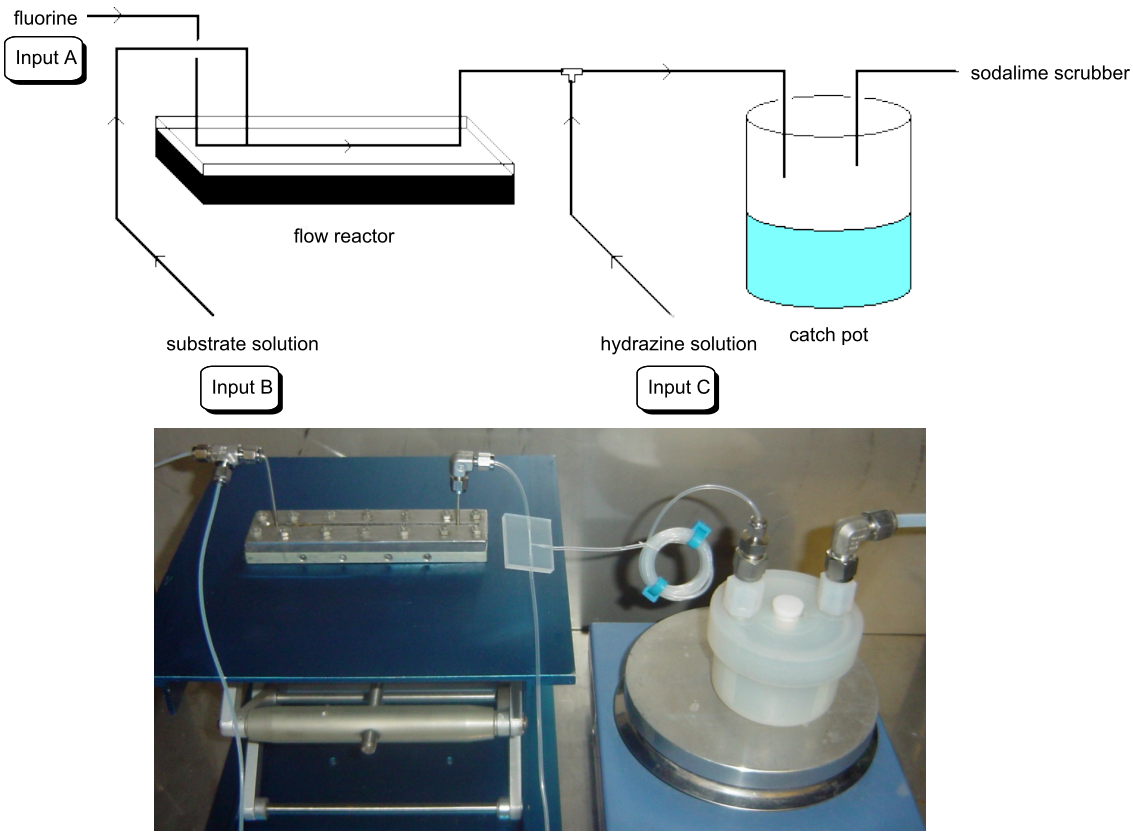

Figure 1: Sequential gas/liquid–liquid/liquid flow reactor for the synthesis of 4-fluoropyrazole derivatives.

which was further purified by column chromatography or recrystallisation if required.

In our initial exploratory reactions, pentane-2,4-dione (**1a**) was used as the substrate, because this system has a high initial enol content at equilibrium and rapidly enolises in acetonitrile solution [12]. By varying the flow rate of fluorine gas we were able to achieve reaction conditions that would convert all of the diketone substrate to a fluorodiketone in the first stage of the continuous process. Subsequent separation of fluoropyrazole (**4a**) from the corresponding non-fluorinated pyrazole, formed by the coupling of not reacted pentane-2,4-dione and hydrazine, was difficult to achieve. Any remaining difluorinated diketone formed by excess fluorination of the substrate was not involved in the second cyclization process and remained in aqueous solution in the collection vessel.

In initial experiments, 1 mmol of the pentane-2,4-dione (**1a**) was diluted in 4 mL of acetonitrile, and 1.2 mmol of hydrazine hydrate (**3a**) was also dissolved in 4 mL of solvent (either acetonitrile, ethanol or water). Both were added concurrently to the flow reactor at the rate of 2 mL/min into Inputs B and C, respectively, using accurate syringe pumps. Excess 10% F_2/N_2 gas mixture was passed into the flow channel at a rate of 18 mL/min to achieve full conversion of pentane-2,4-dione to the corresponding 3-fluoropentane-2,4-dione, and subsequent formation of the fluoropyrazole product **4a** occurred with no non-fluorinated pyrazole by-product observed. Early investigations showed that some of the 3-fluoropentane-2,4-dione remained unchanged when only 1.2 mmol of the hydrazine was used and, therefore, in subsequent reactions excess hydrazine (1.5 mmol) was added to ensure complete conversion of the 3-fluoropentane-2,4-dione to the 4-fluoropyrazole **4a** (Table 1).

In all reactions, acetonitrile was used as the solvent for the fluorination stage as this reaction medium has been found to be very effective for direct fluorination reactions of dicarbonyl systems [12]. The hydrazine was added to the continuous flow process dissolved in either acetonitrile, water or ethanol depending on the solubility of the hydrazine derivative. Water and ethanol are miscible with acetonitrile, thus enabling the cyclisation process to occur by efficient mixing of the two flow streams within the reactor channel.

Similarly, fluoropyrazole derivatives **4b** and **4c** were prepared by reaction of **1a** with fluorine and methyl hydrazine **3b** and

Table 1: Synthesis of 4-fluoro-3,5-dimethylpyrazole derivatives.

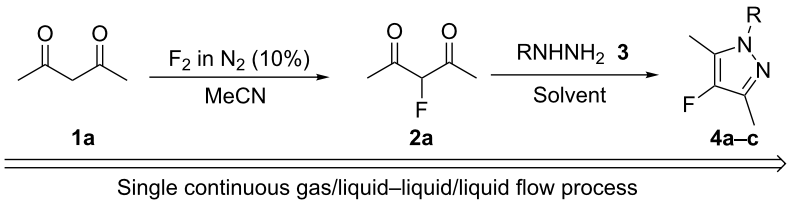

Diketone **1**	Hydrazine **3**	Solvent	4-Fluoropyrazole **4** Yield
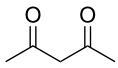			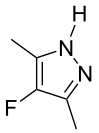
1a	NH_2–NH_2·H_2O, **3a**	H_2O	**4a**, 74%
1a	**3a**	EtOH	**4a**, 66%
1a	**3a**	MeCN	**4a**, 77%
			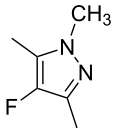
1a	MeNH–NH_2, **3b**	H_2O	**4b**, 83%
1a	**3b**	EtOH	**4b**, 73%
1a	**3b**	MeCN	**4b**, 68%
			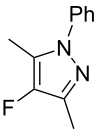
1a	PhNH–NH_2, **3c**	EtOH	**4c**, 72%
1a	**3c**	MeCN	**4c**, 67%

phenyl hydrazine **3c**, respectively, and these results are included in Table 1.

With the conditions for gas/liquid–liquid/liquid processes established from reactions involving pentane-2,4-dione (**1a**), several other fluoropyrazole systems **4d**–**h** were synthesised from a series of related diketone starting materials **1b**–**f** in one continuous flow process from hydrazine **3a** and these are collated in Table 2.

All fluoropyrazole products **4a**–**h** were isolated and purified, and then characterised by NMR spectroscopy and mass spectrometry techniques; results were compared to literature data where available. ^{19}F NMR spectra of all 4-fluoropyrazole products show singlets at ~ −175 to −185 ppm, consistent with literature values.

Furthermore, the structures of **4a** and **4f** were confirmed by X-ray crystallography (Figure 2). In both cases, the 5-membered rings are planar and the pyrazole hydrogen atoms are disordered over two positions. The molecules of both compounds in the crystals are linked together in H-bonded cycles. In the case of **4a**, the cycles are $R^3_3(9)$ trimers [30], while the presence of bulky *t*-Bu groups in **4f** results in the formation of $R^2_2(6)$ dimers (Figure 2).

Conclusion

4-Fluoropyrazole derivatives were synthesised by sequential direct fluorination of appropriate 1,3-diketones and subsequent cyclisation of the in situ generated fluorodiketone with a hydrazine derivative. This represents the first example of a sequential, continuous flow gas/liquid–liquid/liquid process involving direct fluorination in the first stage of a multi-step,

Table 2: Synthesis of 4-fluoropyrazole derivatives.

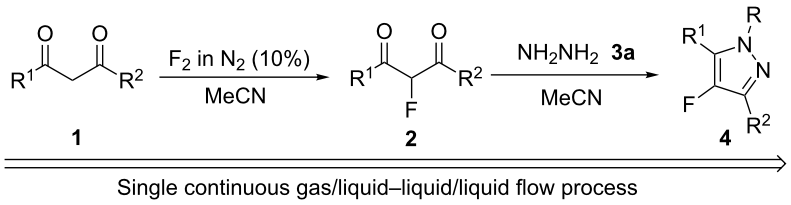

Diketone **1**	4-Fluoropyrazole **4** Yield
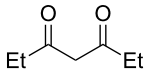 **1b**	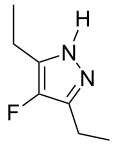 **4d** 72%
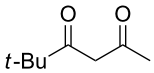 **1c**	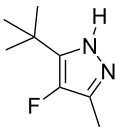 **4e** 71%
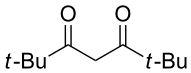 **1d**	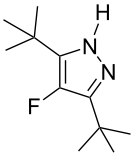 **4f** 74%
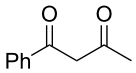 **1e**	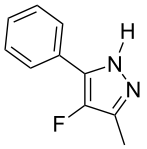 **4g** 69%
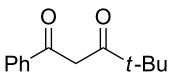 **1f**	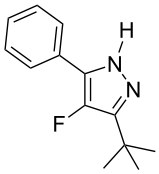 **4h** 80%

telescoped, continuous flow process. Thus, continuous flow methodology was used for successful sequential carbon-fluorine bond formation and subsequent fluorine-containing building block reactions in a single continuous high yielding, efficient and regioselective process.

Experimental

Synthetic procedures for the preparation of all the 4-fluoropyrazole compounds described in this paper are given either below or in Supporting Information File 1. Supporting Information File 2 contains copies of the NMR spectra.

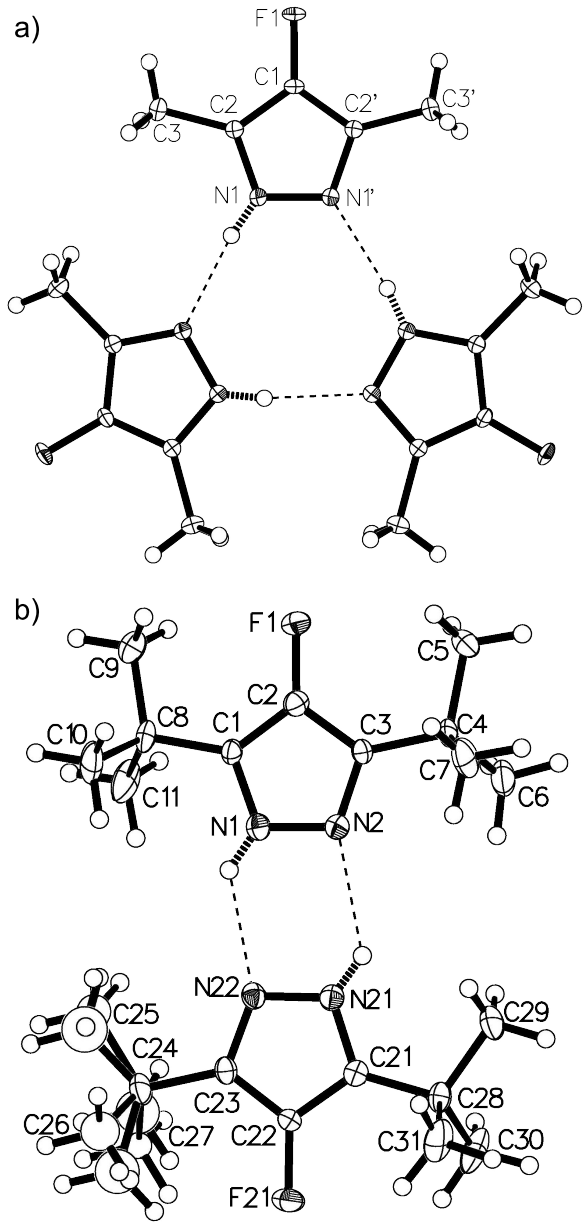

Figure 2: H-bonded cycles in structures **4a** (a) and **4f** (b) (only one disordered pyrazole hydrogen atom is shown in each case).

Two step process – general procedure

After purging the continuous flow reactor apparatus [29] (Figure 1) with nitrogen, a 10% mixture of fluorine in nitrogen (v:v) was passed through the flow reactor via Input A at a prescribed flow rate that was controlled by a gas mass flow controller (Brooks Instruments). The flow reactor was cooled by an external cryostat to 5–10 °C. The diketone solution was injected by a mechanised syringe pump into the flow reactor channel at a prescribed flow rate through the substrate Input B. At the same time, the hydrazine mixture was injected by a mechanised syringe pump at Input C, into the flow reactor via a T-piece, at a prescribed flow rate. All flow streams were passed through the reactor and the product mixture was collected in a vessel containing water. The collected mixture was then extracted from DCM (3 × 30 mL) and washed with sodium bicarbonate (30 mL) and water (30 mL). The combined extracts were then dried ($MgSO_4$), filtered and the solvent evaporated to give a solid residue, which was purified by recrystallisation or column chromatography on silica gel to give the desired 4-fluoropyrazole product.

4-Fluoro-3,5-dimethyl-1*H*-pyrazole (4a)

Pentane-2,4-dione (**1a**) (0.10 g, 1.0 mmol) in MeCN (4 mL, 2 mL/h), fluorine (8 mL/min), and hydrazine hydrate (**3a**, 0.07 g, 1.5 mmol) in ethanol (4 mL, 2 mL/h), after purification by column chromatography on silica gel with hexane and ethyl acetate (1:1) as the eluent, gave 4-fluoro-3,5-dimethyl-1*H*-pyrazole (**4a**) (0.075 g, 66%) as pale yellow crystals; mp 107–109 °C (lit. [31]: mp 108–110 °C); ^{1}H NMR (400 MHz, $CDCl_3$) δ 2.26 (s, 6H, CH_3), 8.61 (br s, 1H, NH); ^{13}C NMR (126 MHz, $CDCl_3$) δ 9.1 (d, $^3J_{CF}$ 2.9 Hz, CH_3), 129.6 (br s, C-3), 143.5 (d, $^1J_{CF}$ 239.8 Hz, C-4); ^{19}F NMR (376 MHz, $CDCl_3$) δ −183.4 (s); MS (EI^+) *m/z:* 114.1 ($[M]^+$, 100%), 113.0 (82), 41.9 (79); HRMS (*m/z*): $[M + H]^+$ calcd for $C_5H_7FN_2$, 115.0672; found, 115.0667.

Supporting Information

Supporting Information File 1

Experimental data.
[http://www.beilstein-journals.org/bjoc/content/supplementary/1860-5397-7-120-S1.pdf]

Supporting Information File 2

NMR spectra.
[http://www.beilstein-journals.org/bjoc/content/supplementary/1860-5397-7-120-S2.pdf]

Acknowledgements

We thank EPSRC (Durham University DTA) and Pfizer R&D for funding.

References

1. Hagmann, W. K. *J. Med. Chem.* **2008,** *51,* 4359–4369. doi:10.1021/jm800219f
2. Müller, K.; Faeh, C.; Diederich, F. *Science* **2007,** *317,* 1881–1886. doi:10.1126/science.1131943
3. Banks, R. E.; Smart, B. E.; Tatlow, J. C. *Organofluorine Chemistry. Principles and Commercial Applications;* Plenum: New York, 1994.

4. Harper, D. B.; O'Hagan, D.; Murphy, C. B. *Fluorinated Natural Products: Occurrence and Biosynthesis*. *Natural Production of Organohalogen Compounds; Handbook of Environmental Chemistry*, Vol. 3P; Springer: Berlin, Heidelberg, 2003; pp 141–149.
5. Baasner, B.; Hagemann, H.; Tatlow, J. C. *Houben-Weyl Organofluorine Compounds;* Thieme: Stuttgart, Germany, 2000; Vol. E10a.
6. Chambers, R. D. *Fluorine in Organic Chemistry;* Blackwell: Oxford, 2004. doi:10.1002/9781444305371
7. Percy, J. M. *Top. Curr. Chem.* **1997,** *193,* 131–196. doi:10.1007/3-540-69197-9_4
8. Hutchinson, J.; Sandford, G. *Top. Curr. Chem.* **1997,** *193,* 1–43. doi:10.1007/3-540-69197-9_1
9. Chambers, R. D.; Hutchinson, J.; Sandford, G. *J. Fluorine Chem.* **1999,** *100,* 63–73. doi:10.1016/S0022-1139(99)00202-X
10. Sandford, G. *J. Fluorine Chem.* **2007,** *128,* 90–104. doi:10.1016/j.jfluchem.2006.10.019
11. Chambers, R. D.; Kenwright, A. M.; Parsons, M.; Sandford, G.; Moilliet, J. S. *J. Chem. Soc., Perkin Trans. 1* **2002,** 2190–2197. doi:10.1039/B204776B
12. Chambers, R. D.; Greenhall, M. P.; Hutchinson, J. *Tetrahedron* **1996,** *52,* 1–8. doi:10.1016/0040-4020(95)00883-A
13. Chambers, R. D.; Hutchinson, J. *J. Fluorine Chem.* **1998,** *89,* 229–232. doi:10.1016/S0022-1139(98)00132-8
14. Chambers, R. D.; Hutchinson, J. *J. Fluorine Chem.* **1998,** *92,* 45–52. doi:10.1016/S0022-1139(98)00254-1
15. Chambers, R. D.; Hutchinson, J.; Sparrowhawk, M. E.; Sandford, G.; Moilliet, J. S.; Thomson, J. *J. Fluorine Chem.* **2000,** *102,* 169–173. doi:10.1016/S0022-1139(99)00238-9
16. Chambers, R. D.; Parsons, M.; Sandford, G.; Skinner, C. J.; Atherton, M. J.; Moilliet, J. S. *J. Chem. Soc., Perkin Trans. 1* **1999,** 803–810. doi:10.1039/A809838G
17. Chambers, R. D.; Holling, D.; Sandford, G.; Batsanov, A. S.; Howard, J. A. K. *J. Fluorine Chem.* **2004,** *125,* 661–671. doi:10.1016/j.jfluchem.2003.11.012
18. Butters, M.; Ebbs, J.; Green, S. P.; MacRae, J.; Morland, M. C.; Murtiashaw, C. W.; Pettman, A. J. *Org. Process Res. Dev.* **2001,** *5,* 28–36. doi:10.1021/op0000879
19. Chambers, R. D.; Fox, M. A.; Holling, D.; Nakano, T.; Okazoe, T.; Sandford, G. *Lab Chip* **2005,** *5,* 191–198. doi:10.1039/b416400h
20. Chambers, R. D.; Fox, M. A.; Holling, D.; Nakano, T.; Okazoe, T.; Sandford, G. *Chem. Eng. Technol.* **2005,** *28,* 344–352. doi:10.1002/ceat.200407123
21. Chambers, R. D.; Fox, M. A.; Sandford, G. *Lab Chip* **2005,** *5,* 1132–1139. doi:10.1039/b504675k
22. Katritzky, A. R.; Rees, C. W. *Comprehensive Heterocyclic Chemistry;* Pergamon Press: Oxford, 1984; Vol. 1-8.
23. Joule, J. A.; Mills, K. *Heterocyclic Chemistry;* Blackwell: Chichester, 2010.
24. Breen, J. R.; Sandford, G. unpublished results.
25. Sloop, J. C.; Jackson, J. L.; Schmidt, R. D. *Heteroat. Chem.* **2009,** *20,* 341–345. doi:10.1002/hc.20556
26. Sloop, J. C.; Bumgardner, C. L. *J. Fluorine Chem.* **2002,** *118,* 135–147. doi:10.1016/S0022-1139(02)00221-X
27. Surmont, R.; Verniest, G.; De Kimpe, N. *Org. Lett.* **2010,** *12,* 4648–4651. doi:10.1021/ol1019713
28. Chambers, R. D.; Spink, R. C. H. *Chem. Commun.* **1999,** 883–884. doi:10.1039/a901473j
29. McPake, C. B.; Murray, C. B.; Sandford, G. *Tetrahedron Lett.* **2009,** *50,* 1674–1676. doi:10.1016/j.tetlet.2008.12.073
30. Etter, M. C.; MacDonald, J. C.; Bernstein, J. *Acta Crystallogr.* **1990,** *B46,* 256–262. doi:10.1107/S0108768189012929
31. Vilarrasa, J.; Galvez, G.; Calafell, M. *An. Quim.* **1975,** *71,* 631–636.

License and Terms

Beilstein Journal of Organic Chemistry

Microphotochemistry: 4,4'-Dimethoxybenzophenone mediated photodecarboxylation reactions involving phthalimides

Oksana Shvydkiv[1], Kieran Nolan[1] and Michael Oelgemöller[*2]

Full Research Paper

Open Access

Address:
[1]School of Chemical Sciences, Dublin City University, Dublin 9, Ireland and [2]School of Pharmacy and Molecular Sciences, James Cook University, Townsville, QLD 4811, Australia

Email:
Michael Oelgemöller[*] - michael.oelgemoeller@jcu.edu.au

* Corresponding author

Keywords:
microflow; microreactor; photochemistry; photodecarboxylation; phthalimide

Beilstein J. Org. Chem. **2011,** *7,* 1055–1063.
doi:10.3762/bjoc.7.121

Received: 16 May 2011
Accepted: 12 July 2011
Published: 02 August 2011

This article is part of the Thematic Series "Chemistry in flow systems II".

Guest Editor: A. Kirschning

Abstract

A series of 4,4'-dimethoxybenzophenone mediated intra- and intermolecular photodecarboxylation reactions involving phthalimides have been examined under microflow conditions. Conversion rates, isolated yields and chemoselectivities were compared to analogous reactions in a batch photoreactor. In all cases investigated, the microreactions gave superior results thus proving the superiority of microphotochemistry over conventional technologies.

Introduction

Organic photochemistry is a highly successful synthesis method that allows the construction of complex molecules with a "flick of a switch" [1-4]. Light is furthermore considered a clean "reagent" and consequently, photochemistry has contributed extensively to the growing field of Green Chemistry [5-7]. It is therefore surprising that synthetic organic photochemistry has been widely neglected by the chemical industry. In fact, most photochemical production processes in industry were developed and realized decades ago [8-11]. A major drawback of photochemistry as a modern research and development (R&D) tool has been the usage of specialized reactors and lamps, which are often considered "exotic" by synthetic chemists [12]. Over the last decade, microflow chemistry has emerged as a new tool in preparative organic chemistry [13-16]. Microflow reactors (μ-reactors) offer a number of advantages for photochemical transformations. In particular, their narrow reaction channels enable extensive penetration of light even at high chromophore concentrations. In addition, products are removed from the irradiated area thus preventing light-induced follow-up reactions or decompositions [17-19]. Recently, a number of photoreactions in microreactors have therefore been described [20-23] and specialized micro-photoreactors for laboratory- to technical-scale synthesis have been developed [24-26]. We have recently reported on acetone-sensitized photodecarboxylation (PDC) reactions of phthalimides in a commercially available microreactor [27]. The photochemistry of phthalimides and its

analogues has been intensively studied over the last decades [28-32]. Among the various transformations developed, photodecarboxylation reactions have emerged as efficient and powerful alkylation procedures with high quantum yields of up to 60% [33,34]. Selected transformations have also been realized on a semi-technical scale using an advanced falling-film batch reactor equipped with a 308 nm excimer light source [35,36]. However, the established PDC protocol utilizes UVB light for the activation step (direct or acetone sensitized), thus limiting the desired future application of LEDs [37]. We have therefore investigated the usage of 4,4'-dimethoxybenzophenone (DMBP) as a photocatalyst that absorbs readily in the UVA region. In this publication we present preliminary results of five DMBP mediated model transformations (Scheme 1). All reactions were previously studied under acetone-sensitized conditions using UVB light [27].

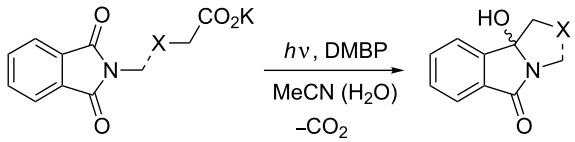

Scheme 1: General photodecarboxylation involving phthalimides (the broken line indicates intra- as well as intermolecular reactions).

Results and Discussion

Experimental setups

The reaction setup is shown in Figure 1. A commercially available dwell device (mikroglas chemtech) was placed under a UV panel (Luzchem) fitted with five 8 W UVA lamps (λ = 350 ± 25 nm). The reactor itself was fabricated from Foturan™ glass, which has a transmission of approximately 30% at 300 nm, and consisted of a heat-exchanging channel on the top and a serpentine reaction channel on the bottom. The reaction channel had a total path length of 1.15 m with 20 turns, a depth of 0.5 mm, a width of 2 mm and a total volume of 1.68 mL. The reaction mixture was loaded into a programmable syringe pump, degassed with nitrogen, pumped through the microreactor (flow rate: 0.028 mL/min) and collected in a flask outside the irradiated area. In a parallel series of experiments, a conventional Rayonet chamber reactor (RPR-200) equipped with sixteen 8 W UVA lamps in a circular arrangement was used for batch reactions. A Pyrex Schlenk flask, with a transmission of approximately 30% at 300 nm, of 32 mm inner diameter and equipped with a cold finger of 24 mm diameter, thus creating an effective path length of 4 mm, was inserted into the chamber. After a fixed irradiation time of 1 h, which was not optimized, and work-up the crude reaction products were analyzed by ^{1}H NMR spectroscopy and conversions and selectivities were determined. In represented cases the pure products were isolated for characterization purposes from the batch processes. Due to the small amounts used under microflow conditions, purification and isolation of products was not attempted. Previous work has, however, demonstrated that isolated yields typically match conversion rates [38].

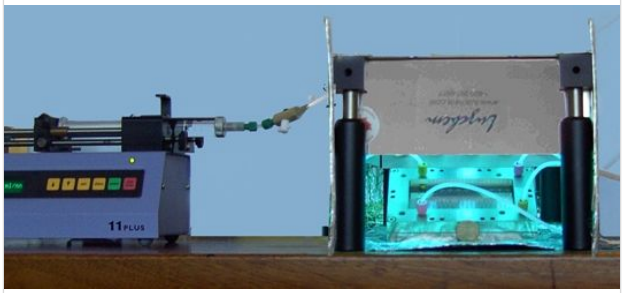

Figure 1: Microreactor (dwell device, mikroglas chemtech) under a UV exposure panel (Luzchem) and connected to a syringe pump.

Wavelength matching and light penetration

When the absorption spectrum of DMBP in acetonitrile was compared to the emission spectrum of the chosen UVA lamp (Figure 2), its important n→π* absorption matched well with the emission maximum of the light source. At 350 nm, an extinction coefficient ($\varepsilon_{350\ nm}$) for DMBP of 496 L mol^{-1} cm^{-1} was determined. In contrast, the crucial n→π* absorption maximum of *N*-alkylated phthalimides in acetonitrile lies around 290 nm and consequently, photoprocesses induced by direct excitation may be neglected [39].

The light transmission for a 1.5 mM DMBP solution in acetonitrile (Figure 3) was subsequently calculated using the Beer–Lambert law [8]. As indicated by vertical lines, both setups guaranteed complete penetration of light at 350 nm. As would be expected from its much smaller path length, the light transmission in the microchannel was superior at 92%, compared to 50% in the batch system.

α-Photodecarboxylation of *N*-phthaloylglycine

The photodecarboxylation of phthaloyl amino acids results in a formal exchange of –CO_2H by –H and offers a convenient pathway to primary amines [40]. The reaction of *N*-phthaloylglycine (**1**) in acetonitrile using 0.1 equivalents of DMBP as a mediator was thus investigated as an early model transformation (Scheme 2). After 1 hour, complete conversions of **1** to *N*-methylphthalimide (**2**) were achieved in the batch and microreactor, as demonstrated by ^{1}H NMR spectroscopy. In acetone-d_6, the N–CH_3 group in **2** showed a singlet at 3.11 ppm. DMBP remained unchanged and neither photoreduction nor photopinacolization products were detectable in the crude reaction mixture [41]. An attempt was made to isolate pure **2** by column chromatography but it eluted together with DMBP. The

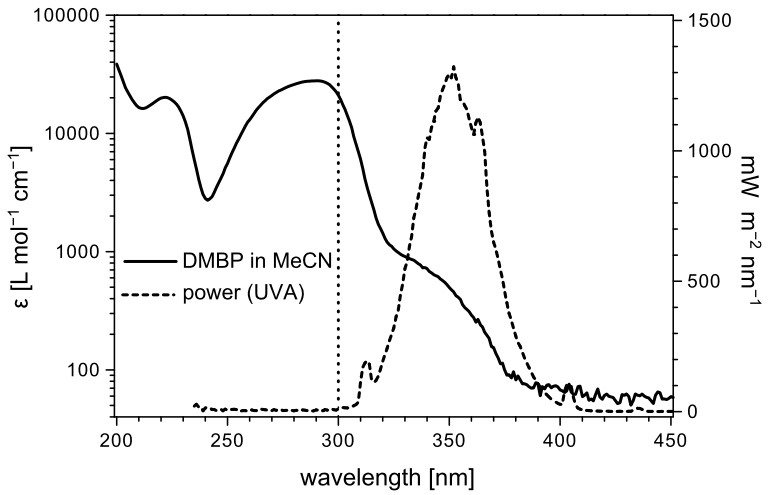

Figure 2: UV-spectrum of DMBP (in MeCN) versus emission spectrum of the UVA lamp. The vertical dotted line represents the cut-off wavelength of Foturan™ and Pyrex at 300 nm (approx. 30% transmission).

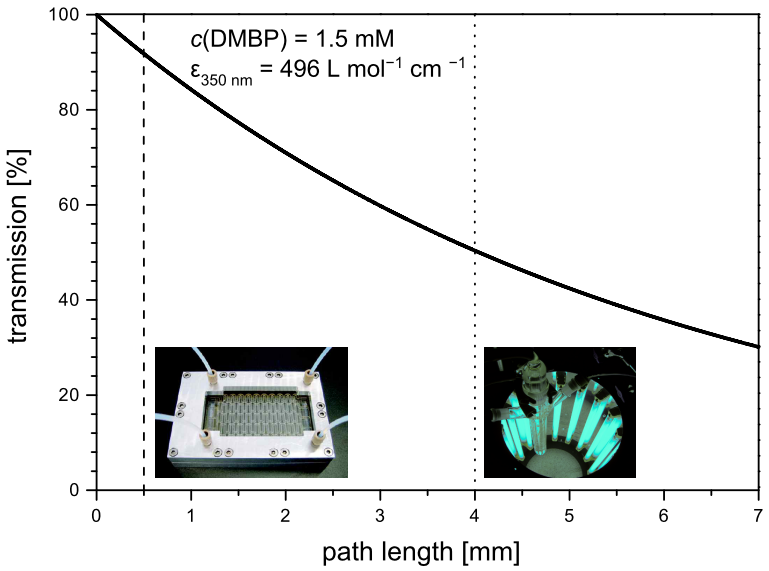

Figure 3: Light-penetration profile for a 1.5 mM solution of DMBP at 350 nm. The vertical lines represent the path length in the dwell device (vertical dashed line) versus the effective path length in the Schlenk flask (vertical dotted line).

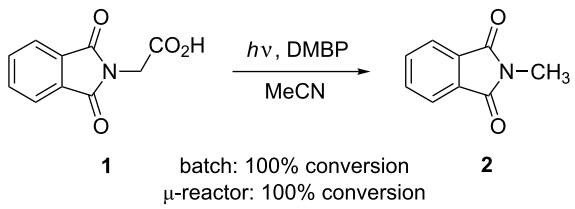

Scheme 2: DMBP mediated α-photodecarboxylation of *N*-phthaloylglycine (**1**).

α-photodecarboxylation is, however, known to proceed with high selectivity [40].

Photodecarboxylative cyclizations

Two photodecarboxylative cyclization reactions were investigated with potassium phthaloyl-γ-aminobutyrate (**3**) and potassium phthalimidomethylsulfanylacetate (**6**) as starting materials [42]. A main advantage of these transformations is the ease of removal of the unreacted starting material by simple extraction. In contrast to acetone-sensitized reactions [43], DMBP-mediated irradiations of **3** furnished mixtures of the desired cycliza-

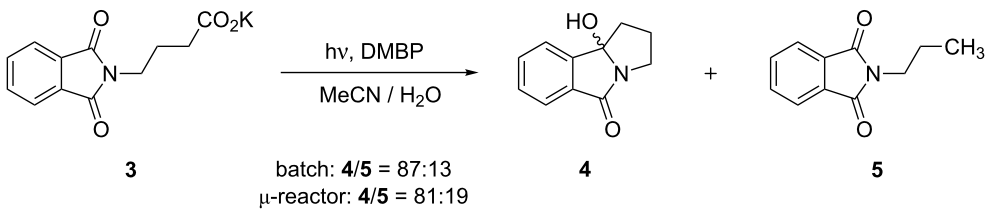

Scheme 3: Photodecarboxylation of potassium phthaloyl-γ-aminobutyrate (**3**).

tion product **4** and the simple decarboxylation product **5** (Scheme 3; Table 1). When conducted in the batch system, **4** and **5** were obtained in a ratio of 87:13. Careful column chromatographic purification gave the polycyclic product **4** in an isolated yield of 29%. In the ^{13}C NMR in acetone-d_6, the C–OH group in **4** gave a characteristic singlet at 96.9 ppm. The simple decarboxylation product **5** eluted together with DMBP and could not be obtained in pure form. Its identity was thus confirmed by comparison with literature data. In acetone-d_6, the terminal –CH_3 group in **5** furnished a triplet at 0.90 ppm with a coupling constant of 7.4 Hz. Using the microreactor setup, a **4**/**5** mixture of 81:19 was isolated after 1 h of exposure. Despite the slightly lower selectivity, the cyclization product **4** was isolated in an improved yield of 47%. In both cases, DMBP showed no signs of decomposition suggesting that the reactions had not reached completion. Possible unreacted starting material was removed by extraction and no recovery attempts were made.

Table 1: Experimental results for the photodecarboxylation of **3**.

	batch	μ-reactor
time [h]	1	1
4/**5** ratio[a]	87/13	81/19
yield **4** [%][b]	29	47

[a]Determined by ^{1}H NMR analysis of the crude product. [b]Isolated yield after column chromatography.

When potassium phthalimidomethylsulfanylacetate (**6**) was used as the starting material, only the polycyclic thiazolidine derivative **7** could be isolated (Scheme 4). After purification by column chromatography, **7** was obtained in yields of 57% for the batch system and 56% for the microreactor. In acetone-d_6, the methylene protons in the thiazolidine ring gave two sets of doublets at 2.97/3.39 ppm and 4.36/4.93 ppm. The increased yield of **7** compared to its carbon-analogue **3** suggests that the sulfur-atom in α-position to the carboxylate group in **6** accelerates photodecarboxylation [44,45]. In addition to the high chemoselectivity, DMBP remained photostable and could be reisolated almost quantitatively during chromatography.

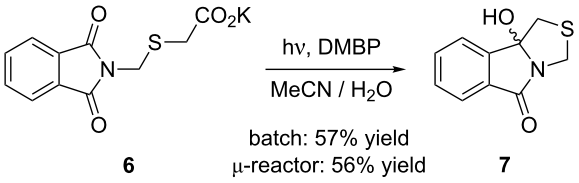

Scheme 4: Photodecarboxylative cyclization of potassium phthalimidomethylsulfanylacetate (**6**).

Photodecarboxylative additions

Phthalimides can be efficiently alkylated by photodecarboxylation of carboxylates and this methodology has emerged as a powerful alternative to Grignard additions [46-48]. In contrast to the acetone-sensitized procedure, the DMBP mediated reaction of *N*-methylphthalimide (**2**) and potassium phenylacetate (**8**) furnished the corresponding phenylmethyleneisoindolinone **10** with high *E*-selectivity (Scheme 5; Table 2), as determined by comparison with literature data. In acetone-d_6, the olefinic

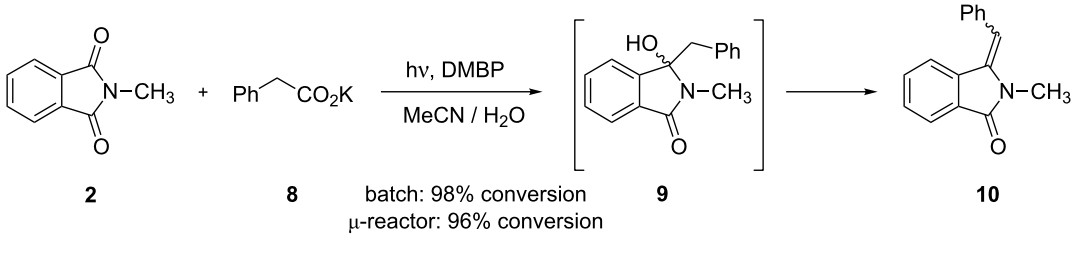

Scheme 5: Photodecarboxylative benzylation of **2**.

proton gave a clear singlet at 6.70 ppm. The formation of **10** can be explained by subsequent dehydration of the initially formed benzylated hydroxyphthalimidine **9**, a process favored by the extensive conjugation in **10** [49]. Under batch conditions, an almost complete conversion of **2** to **10** of 98% was achieved after 1 h of irradiation. Partial photoreduction of DMBP (ca. 10%) was furthermore observed. Using the same residence time, the transformation under microflow condition furnished a conversion to **10** of 96% but showed no decomposition of the mediator DMBP. Compound **10** could not be isolated in pure form but its NMR data was identical to that of an independently synthesized sample [49].

Table 2: Experimental results for the photobenzylation of **2**.

	batch	μ-reactor
time [h]	1	1
conversion [%][a]	98	96
(*E*/*Z*)-**10** ratio[a]	>10/1	>10/1

[a]Determined by ^{1}H NMR analysis of the crude product.

Likewise, the addition of potassium 2-(methylthio)acetate (**11**) to *N*-methylphthalimide (**2**) was investigated [50]. In the larger Rayonet (batch) reactor, the photoreduction product of *N*-methylphthalimide, i.e., compound **13**, was identified next to the expected addition product **12** (Scheme 6; Table 3). In its ^{1}H NMR spectrum in acetone-d_6, the addition product **12** showed a pair of doublets for the –CH_2S group at 3.20 and 3.27 ppm with a ^2J coupling constant of 14.0 Hz. In contrast, the reduction product **13** gave a doublet for its –CH group at 5.78 ppm, which changed into a singlet upon addition of D_2O due to H/D exchange at the adjacent –OH group. Under batch conditions, the reaction had reached completion after 1 h and a 9:1 mixture of **12**/**13** was isolated. In addition, a large proportion of DMBP underwent photoreduction processes [41]. Column chromatography gave pure **12** and **13** in yields of 41% and 9%, respectively. When performed in the microreactor, the conversion was lower with 90%, but the transformation was highly selective. Neither the photoreduction product **13** nor any decomposition products of DMBP were identified by NMR analysis of the crude reaction mixture.

Table 3: Experimental results for the photodecarboxylative addition of **11** to **2**.

	batch	μ-reactor
time [h]	1	1
conversion [%][a]	100	90
12/**13** ratio[a]	90/10	100/0
yield **12** [%][b]	41	n.d.[c]

[a]Determined by ^{1}H NMR analysis of the crude product. [b]Isolated yield after column chromatography. [c]Yield not determined.

To investigate the role of DMBP, the reaction was repeated under batch conditions, but in the absence of *N*-methylphthalimide (**2**). After one hour, DMBP was completely consumed and its corresponding addition product **14** was obtained next to the expected benzpinacol **15** (Scheme 7). In acetone-d_6, **14** gave singlets at 1.96 ppm for its –SCH_3- and at 3.41 ppm for its –CH_2S group, respectively. These values closely match those for the related benzophenone adduct [51]. The product ratio of **14**/**15** was determined to be 55:45.

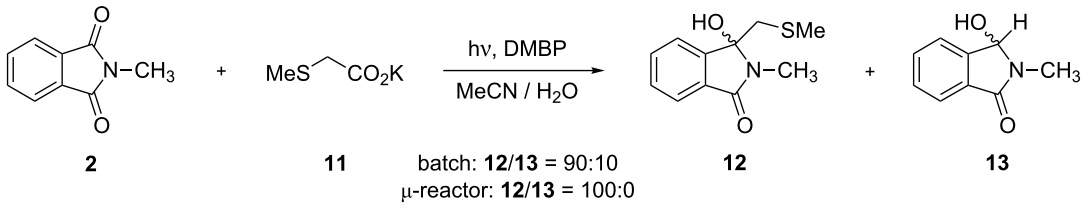

Scheme 6: Photodecarboxylative addition of **11** to **2**.

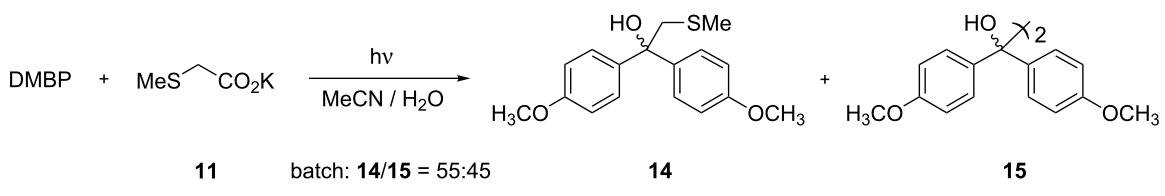

Scheme 7: Photodecarboxylative addition of **11** to DMBP.

Reactor comparison

Based on the conversions or yields achieved, the two reactor systems showed very similar performances. Judged by the amounts of by-products, however, the product quality was somewhat superior for the microsystem. This finding is primarily attributed to the flow design of the dwell device which removes the product mixture from the irradiated area and consequently prevents follow-up reactions. The key parameters for the batch and microreactor are compiled in Table 4. Compared to the Schlenk tubes (50 mL and 100 mL), the irradiated area-to-volume (surface-to-volume) ratio of the dwell device was five to eight times larger with 1369 m^2/m^3. The dwell setup also gave the largest lamp power to irradiated area ratio of 1.74 W/cm^2. The batch reactor incorporating the 50 mL Schlenk flask achieved a slightly lower value of 1.50 W/cm^2, whereas the larger 100 mL Schlenk vessel gave the smallest ratio of 0.47 W/cm^2.

Table 4: Technical details of the two reactor types.

Parameter	batch[a]	μ-reactor
aperture [cm^2][b]	85 / 274	86.1
irradiated area [cm^2]	85 / 274	23.0
irradiated volume [cm^3]	50 / 100	1.7
irradiated area/volume ratio [m^2/m^3]	171 / 274	1369
lamp power [W]	16 × 8	5 × 8
lamp power/aperture [W/cm^2]	1.5 / 0.5	0.46
lamp power/irradiated area [W/cm^2]	1.5 / 0.5	1.74

[a]Values given for 50 mL and 100 mL flask volumes. [b]Assuming a cylindrical geometry for the Schlenk flask.

The conversion/yield per watt-hour (Wh), and the conversion/yield per Wh per irradiated area were furthermore determined for all transformations studied (Table 5) [38]. In all cases, the dwell device showed significantly larger energy efficiencies than the batch reactor. The values obtained for experiments with complete conversions represent the minimum energy efficiencies due to possible contributions from "over-irradiation". Once all phthalimide is consumed, photoreduction of DMBP becomes the dominant reaction due to its continuing excitation [41]. The degree of these decomposition processes can thus be used as an indicator for "over-irradiation".

Mechanistic scenario

For ketone-sensitized photodecarboxylations involving phthalimides, energy transfer and electron transfer processes have both been proposed [44,52]. A similar, simplified scenario is depicted in Scheme 8. Due to the comparable triplet energies of DMBP (T_1 = 69.4 kcal/mol or 290 kJ/mol [53]) and phthalimides (**2**: T_1 = 71 kcal/mol or 297 kJ/mol [39]), energy transfer (Scheme 8, path A) is not very efficient but has been confirmed spectroscopically for a related *N*-phthalimidocarboxylate/benzophenone pair [52]. Subsequent electron transfer (ET) from the carboxylate function to the triplet excited phthalimide furnishes an unstable carboxy radical, which undergoes rapid decarboxylation to the corresponding carbon radical. Protonation and C–C bond formation yields compounds **4** and **9**, and the latter undergoes further dehydration to **10**. Alternatively, back electron transfer (BET) and protonation generates the simple decarboxylation products **2** and **5**. Path A thus mirrors the mechanism proposed for acetone sensitization [43]. In contrast to carboxylates (for $MeCO_2^-$ calc. E_{Ox} = 1.54 V in MeCN versus SCE), thioethers (for Me_2S: E_{Ox} = 1.23 V versus SCE) are more readily oxidized [23]. As a result, electron transfer to the triplet excited DMBP becomes energetically feasible (Scheme 8, path B) [52]. Similar electron transfer scenarios have been established for photoreactions of *N*-methylphthalimide or benzophenone with either thioethers [54,55] or alkyl- and arylthioacetic acids [48,56], respectively. With compound **6** or in the presence of **2**, successive electron transfer generates the corresponding phthalimide radical anion. Subsequent decarboxylation, protonation and C–C bond formation furnish products **7** and **12**. In the absence of *N*-methylphthalimide **2**, protonation and C–C bond formation to **14** or photopinacolization to **15** operate instead (not shown).

Table 5: Energy efficiencies of the two reactor types.

Reaction	batch[a]		μ-reactor[a]	
	[% Wh^{-1}]	[% Wh^{-1} cm^{-2}]	[% Wh^{-1}]	[% Wh^{-1} cm^{-2}]
1 → **2**	≥0.78[b]	≥0.0028[b]	≥2.5[b]	≥0.11[b]
3 → **4**[c]	0.23	0.0027	1.18	0.05
6 → **7**[c]	0.45	0.0052	1.40	0.06
2 → **10**	0.77	0.0028	2.40	0.10
2 → **12**	≥0.78[b]	≥0.0028[b]	2.25	0.09

[a]Batch: 128 Wh; microreactor: 40 Wh. [b]Minimum values due to possible "over-irradiation". [c]Based on isolated yield of **4** or **7**.

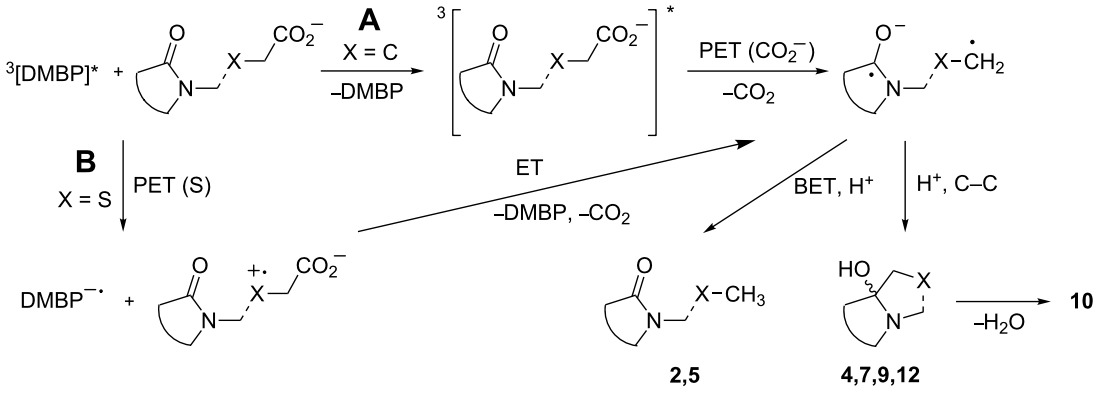

Scheme 8: Mechanistic scenario (the broken line indicates intra- and intermolecular reactions).

Conclusion

DMBP mediated photodecarboxylation reactions involving phthalimides can be successfully transferred from batch to microflow conditions. While DMBP allows for the application of UVA light, its removal from the product remains challenging. Compared to their acetone-sensitized counterparts [27], however, selectivities and yields were reduced. We are therefore currently investigating water soluble or solid-supported photocatalysts that absorb in the UVA region. The results from this study nevertheless confirm the benefits of microflow reactors over batch systems in terms of energy efficiencies and selectivities. It is hoped that micro(flow)photochemistry will find future applications in chemical and pharmaceutical R&D processes [14,57].

Supporting Information

Supporting Information contains full experimental procedures and NMR data of all photoproducts.

Supporting Information File 1

Full experimental details and NMR data.
[http://www.beilstein-journals.org/bjoc/content/supplementary/1860-5397-7-121-S1.pdf]

Acknowledgements

This work was financially supported by Science Foundation Ireland (SFI, 07/RFP/CHEF817), the Environmental Protection Agency (EPA, 2008-ET-MS-2-S2) and the Department of Environment, Heritage and Local Government (DEHLG, 2008-S-ET-2). The authors thank Dr. Thomas Dietrich (mikroglas chemtech) and Dr. J. C. Scaiano (Luzchem) for technical advice and support.

References

1. Bach, T.; Hehn, J. P. *Angew. Chem., Int. Ed.* **2011,** *50,* 1000–1045. doi:10.1002/anie.201002845
2. Hoffmann, N. *Chem. Rev.* **2008,** *108,* 1052–1103. doi:10.1021/cr0680336
3. Demuth, M.; Mikhail, G. *Synthesis* **1989,** 145–162. doi:10.1055/s-1989-27181
4. Margaretha, P. *Preparative Organic Photochemistry;* Lehn, J.-M., Ed.; Topics in Current Chemistry, Vol. 103; Springer: Berlin, Germany, 1982; pp 1–72. doi:10.1007/BFb0022837
5. Albini, A.; Fagnoni, M. In *Green Chemical Reactions (NATO Science for Peace and Security Series, Series C: Environmental Security);* Tundo, P.; Esposito, V., Eds.; Springer: Dordrecht, 2008; pp 173–189.
6. Hoffmann, N. *Pure Appl. Chem.* **2007,** *79,* 1949–1958. doi:10.1351/pac200779111949
7. Oelgemöller, M.; Jung, C.; Mattay, J. *Pure Appl. Chem.* **2007,** *79,* 1939–1947. doi:10.1351/pac200779111939
8. Braun, A. M.; Maurette, M.; Oliveros, E. *Photochemical Technology;* Wiley: Chichester, 1991.
9. Gollnick, K. *Chim. Ind. (Milan)* **1982,** *63,* 156–166.
10. Fischer, M. *Angew. Chem., Int. Ed. Engl.* **1978,** *17,* 16–26. doi:10.1002/anie.197800161
11. Pape, M. *Pure Appl. Chem.* **1975,** *41,* 535–558. doi:10.1351/pac197541040535
12. Ciana, C.-L.; Bochet, C. G. *Chimia* **2007,** *61,* 650–654. doi:10.2533/chimia.2007.650
13. Wegner, J.; Ceylan, S.; Kirschning, A. *Chem. Commun.* **2011,** *47,* 4583–4592. doi:10.1039/c0cc05060a
14. Chin, P.; Barney, W. S.; Pindzola, B. A. *Curr. Opin. Drug Discovery Dev.* **2009,** *12,* 848–861.
15. Fukuyama, T.; Rahman, M. T.; Sato, M.; Ryu, I. *Synlett* **2008,** 151–163. doi:10.1055/s-2007-1000884
16. Jähnisch, K.; Hessel, V.; Löwe, H.; Baerns, M. *Angew. Chem., Int. Ed.* **2004,** *43,* 406–446. doi:10.1002/anie.200300577
17. Coyle, E. E.; Oelgemöller, M. *Photochem. Photobiol. Sci.* **2008,** *7,* 1313–1322. doi:10.1039/b808778d
18. Matsushita, Y.; Ichimura, T.; Ohba, N.; Kumada, S.; Sakeda, K.; Suzuki, T.; Tanibata, H.; Murata, T. *Pure Appl. Chem.* **2007,** *79,* 1959–1968. doi:10.1351/pac200779111959

19. Ichimura, T.; Matsushita, Y.; Sakeda, K.; Suzuki, T. In *Microchemical Engineering in Practice;* Dietrich, T. R., Ed.; Wiley: Hoboken, 2009; pp 385–402.
20. Matsubara, H.; Hino, Y.; Tokizane, M.; Ryu, I. *Chem. Eng. J.* **2011,** *167,* 567–571. doi:10.1016/j.cej.2010.08.086
21. Fuse, S.; Tanabe, N.; Yoshida, M.; Yoshida, H.; Doi, T.; Takahashi, T. *Chem. Commun.* **2010,** *46,* 8722–8724. doi:10.1039/c0cc02239j
22. Tsutsumi, K.; Terao, K.; Yamaguchi, H.; Yoshimura, S.; Morimoto, T.; Kakiuchi, K.; Fukuyama, T.; Ryu, I. *Chem. Lett.* **2010,** *39,* 828–829. doi:10.1246/cl.2010.828
23. Tan, S. B.; Shvydkiv, O.; Fiedler, J.; Hatoum, F.; Nolan, K.; Oelgemöller, M. *Synlett* **2010,** 2240–2243. doi:10.1055/s-0030-1258032
24. Vasudevan, A.; Villamil, C.; Trumbull, J.; Olson, J.; Sutherland, D.; Pan, J.; Djuric, S. *Tetrahedron Lett.* **2010,** *51,* 4007–4009. doi:10.1016/j.tetlet.2010.05.119
25. Werner, S.; Seliger, R.; Rauter, H.; Wissmann, F. Quarzglas-Mikrophotoreaktor und Synthese von 10-Hydroxycamptothecin und 7-Alkyl-10-hydroxycamptothecin. Eur. Pat. 2065387A2, June 3, 2009. *Chem. Abstr.*, **2009**, *150,* 376721.
26. Sugimoto, A.; Sumino, Y.; Takagi, M.; Fukuyama, T.; Ryu, I. *Tetrahedron Lett.* **2006,** *47,* 6197–6200. doi:10.1016/j.tetlet.2006.06.153
27. Shvydkiv, O.; Gallagher, S.; Nolan, K.; Oelgemöller, M. *Org. Lett.* **2010,** *12,* 5170–5173. doi:10.1021/ol102184u
28. McDermott, G.; Yoo, D. J.; Oelgemöller, M. *Heterocycles* **2005,** *65,* 2221–2257. doi:10.3987/REV-05-601
29. Hovart, M.; Mlinarić-Majerski, K.; Basarić, N. *Croat. Chem. Acta* **2010,** *83,* 179–188.
30. Oelgemöller, M.; Kramer, W. H. *J. Photochem. Photobiol., C: Photochem. Rev.* **2010,** *11,* 210–244. doi:10.1016/j.jphotochemrev.2011.02.002
31. Oelgemöller, M.; Griesbeck, A. G. *J. Photochem. Photobiol., C: Photochem. Rev.* **2002,** *3,* 109–127. doi:10.1016/S1389-5567(02)00022-9
32. Mazzocchi, P. H. *Org. Photochem.* **1981,** *5,* 421–471.
33. Griesbeck, A. G.; Kramer, W.; Oelgemöller, M. *Synlett* **1999,** 1169–1178. doi:10.1055/s-1999-3159
34. Kramer, W.; Griesbeck, A. G.; Nerowski, F.; Oelgemöller, M. *J. Inf. Rec.* **1998,** *24,* 81–85.
35. Griesbeck, A. G.; Maptue, N.; Bondock, S.; Oelgemöller, M. *Photochem. Photobiol. Sci.* **2003,** *2,* 450–451. doi:10.1039/b212357f
36. Griesbeck, A. G.; Kramer, W.; Oelgemöller, M. *Green Chem.* **1999,** *1,* 205–207. doi:10.1039/a905076k
37. Shvydkiv, O.; Yavorskyy, A.; Nolan, K.; Youssef, A.; Riguet, E.; Hoffmann, N.; Oelgemöller, M. *Photochem. Photobiol. Sci.* **2010,** *9,* 1601–1603. doi:10.1039/c0pp00223b
38. Shvydkiv, O.; Yavorskyy, A.; Tan, S. B.; Nolan, K.; Hoffmann, N.; Youssef, A.; Oelgemöller, M. *Photochem. Photobiol. Sci.*, in press. doi:10.1039/C1PP05024A
39. Wintgens, V.; Valat, P.; Kossanyi, J.; Biczok, L.; Demeter, A.; Bérces, T. *J. Chem. Soc., Faraday Trans.* **1994,** *90,* 411–421. doi:10.1039/ft9949000411
40. Griesbeck, A. G.; Henz, A. *Synlett* **1994,** 931–932. doi:10.1055/s-1994-23052
41. Pitts, N. J., Jr.; Letsinger, R. L.; Taylor, R. P.; Patterson, J. M.; Recktenwald, G.; Martin, R. B. *J. Am. Chem. Soc.* **1959,** *81,* 1068–1077. doi:10.1021/ja01514a014
42. Oelgemöller, M.; Griesbeck, A. G.; Kramer, W.; Nerowski, F. *J. Inf. Rec.* **1998,** *24,* 87–94.
43. Griesbeck, A. G.; Henz, A.; Kramer, W.; Lex, J.; Nerowski, F.; Oelgemöller, M.; Peters, K.; Peters, E.-M. *Helv. Chim. Acta* **1997,** *80,* 912–933. doi:10.1002/hlca.19970800324
44. Görner, H.; Oelgemöller, M.; Griesbeck, A. G. *J. Phys. Chem. A* **2002,** *106,* 1458–1464. doi:10.1021/jp011090c
45. Griesbeck, A. G.; Oelgemöller, M.; Lex, J.; Haeuseler, A.; Schmittel, M. *Eur. J. Org. Chem.* **2001,** 1831–1843. doi:10.1002/1099-0690(200105)2001:10<1831::AID-EJOC1831>3.0.CO;2-7
46. Hatoum, F.; Gallagher, S.; Baragwanath, L.; Lex, J.; Oelgemöller, M. *Tetrahedron Lett.* **2009,** *50,* 6335–6338. doi:10.1016/j.tetlet.2009.08.115
47. Oelgemöller, M.; Cygon, P.; Lex, J.; Griesbeck, A. G. *Heterocycles* **2003,** *59,* 669–684. doi:10.3987/COM-02-S77
48. Griesbeck, A. G.; Oelgemöller, M. *Synlett* **1999,** 492–494. doi:10.1055/s-1999-2622
49. Belluau, V.; Noeureuil, P.; Ratzke, E.; Skvortsov, A.; Gallagher, S.; Motti, C. A.; Oelgemöller, M. *Tetrahedron Lett.* **2010,** *51,* 4738–4741. doi:10.1016/j.tetlet.2010.07.017
50. Griesbeck, A. G.; Oelgemöller, M. *Synlett* **2000,** 71–72. doi:10.1055/s-2000-6443
51. Barluenga, J.; Fernández-Simón, J. L.; Concellón, J. M.; Yus, M. *J. Chem. Soc., Perkin Trans. 1* **1988,** 3339–3343. doi:10.1039/P19880003339
52. Görner, H.; Griesbeck, A. G.; Heinrich, T.; Kramer, W.; Oelgemöller, M. *Chem.–Eur. J.* **2001,** *7,* 1530–1538. doi:10.1002/1521-3765(20010401)7:7<1530::AID-CHEM1530>3.0.CO;2-L
53. Bertrand, S.; Hoffmann, N.; Pete, J.-M. *Eur. J. Org. Chem.* **2000,** 2227–2238. doi:10.1002/1099-0690(200006)2000:12<2227::AID-EJOC2227>3.0.CO;2-8
54. Hatanaka, Y.; Sato, Y.; Nakai, H.; Wada, M.; Mizoguchi, T.; Kanaoka, Y. *Liebigs Ann. Chem.* **1992,** 1113–1123. doi:10.1002/jlac.1992199201184
55. Ando, W.; Suzuki, J.; Migita, T. *Bull. Chem. Soc. Jpn.* **1971,** *44,* 1987–1989. doi:10.1246/bcsj.44.1987
56. Davidson, R. S.; Steiner, P. R. *J. Chem. Soc., Perkin Trans. 2* **1972,** 1357–1362. doi:10.1039/p29720001357
57. Rubin, A. E.; Tummala, S.; Both, D. A.; Wang, C.; Delaney, E. J. *Chem. Rev.* **2006,** *106,* 2794–2810. doi:10.1021/cr040674i

Beilstein Journal of Organic Chemistry

Homocoupling of aryl halides in flow: Space integration of lithiation and $FeCl_3$ promoted homocoupling

Aiichiro Nagaki, Yuki Uesugi, Yutaka Tomida and Jun-ichi Yoshida*

Full Research Paper

Open Access

Address:
Department of Synthetic Chemistry and Biological Chemistry, Graduate School of Engineering, Kyoto University, Kyotodaigakukatsura, Nishikyo-ku, Kyoto, 615-8510, Japan

Email:
Aiichiro Nagaki - anagaki@sbchem.kyoto-u.ac.jp; Jun-ichi Yoshida* - yoshida@sbchem.kyoto-u.ac.jp

* Corresponding author

Keywords:
homocoupling; iron salts; microreactor; organolithiums

Beilstein J. Org. Chem. **2011,** *7,* 1064–1069.
doi:10.3762/bjoc.7.122

Received: 15 April 2011
Accepted: 29 June 2011
Published: 02 August 2011

This article is part of the Thematic Series "Chemistry in flow systems II".

Guest Editor: A. Kirschning

Abstract

The use of $FeCl_3$ resulted in a fast homocoupling of aryllithiums, and this enabled its integration with the halogen–lithium exchange reaction of aryl halides in a flow microreactor. This system allows the homocoupling of two aryl halides bearing electrophilic functional groups, such as CN and NO_2, in under a minute.

Introduction

Biaryl structures often occur in various organic compounds including natural products, bioactive compounds, functional polymers, ligands in catalysts and theoretically interesting molecules, and the oxidative homocoupling of arylmetals is one of the most useful methods for the construction of biaryl frameworks [1]. Stoichiometric amounts of transition metal salts such as $TiCl_4$ [2], TlCl [3], $VO(OEt)Cl_2$ [4], $CoCl_2$ [5], $CuCl_2$ [6] and $Pd(OAc)_2$ [7] have been used for homocoupling of arylmetals. In some cases catalytic processes in the presence of a reoxidant, such as oxygen or other organic oxidants, are effective. Recently, iron salts have been also used because of their low costs and lack of toxicity [8-18]. For example, Hayashi et al. reported the iron-catalyzed oxidative homocoupling of Grignard reagents, using 1,2-dihalogenoethanes as an oxidant [19]. Cahiez et al. have also reported the $FeCl_3$-catalyzed homocoupling reaction of Grignard reagents bearing functional groups, using atmospheric oxygen [20]. The use of aryllithium compounds instead of Grignard reagents is very interesting, because they are easily generated by halogen–lithium exchange under homogeneous conditions, thus enabling the generation in a flow. However, to the best of our knowledge, oxidative homocoupling of aryllithiums using iron salts has not been reported so far. One of the major reasons for this seems to be the instability of aryllithiums, especially of those bearing electrophilic functional groups such as cyano and nitro groups [21], making the subsequent homocoupling difficult or impossible.

Recently, we have reported that flow microreactor systems [22-85] are quite effective for the generation and reaction of highly reactive organolithiums such as functionalized aryllithiums,

oxiranyllithums, aziridinyllithiums, and allenyllithiums [86-98]. Herein we report that integration [99,100] of the generation of aryllithiums, especially those bearing electrophilic functional groups, by halogen–lithium exchange and $FeCl_3$ promoted homocoupling has been effectively accomplished in an integrated flow microreactor system.

Results and Discussion

First, we focused on the generation of *p*-methoxyphenyllithium from *p*-bromoanisole (Scheme 1). A flow microreactor system, consisting of two T-shaped micromixers (**M1** and **M2**) and two microtube reactors (**R1** and **R2**) shown in Figure 1, was used. A solution of *p*-bromoanisole (Ar–X) (0.10 M in THF, flow rate: 6.0 mL/min) and a solution of *n*-butyllithium (0.40 M in hexane, flow rate: 1.5 mL/min) were introduced to **M1** (∅ = 250 μm) by syringe pumps. The resulting mixture was passed through **R1** to conduct the bromine–lithium exchange reaction. Methanol (neat, flow rate: 3.0 mL/min) was added in **M2** (∅ = 500 μm) and the mixture was passed through **R2** (∅ = 1000 μm, L = 50 cm) to protonate *p*-methoxyphenyllithium. The reactions were carried out with varying residence time in **R1** (t^{R1}: 0.2–6.3 s) and varying temperature (T: −78 to 24 °C). The temperature (T) was controlled by adjusting the bath temperature. The residence time (t^{R1}) was adjusted by changing the inner diameter and the length in the microtube reactor **R1** with a fixed flow rate. After a steady state was reached, the product solution was collected for 30 s. As shown in Figure 2, the yield of the protonated product, anisole, depends on both T and t^{R1}. The reaction at low temperatures (T < −48 °C) with short residence times (t^{R1} < 0.79 s) resulted in very low yields, because the Br–Li exchange reaction was not complete. The increase in T and t^{R1} caused an increase in the yield, and high yields (>85%) were obtained through the appropriate choice of T and t^{R1}.

Next, we examined the integration of the halogen–lithium exchange reaction with $FeCl_3$ promoted homocoupling (Scheme 2). Integrated flow microreactor systems consisting of three micromixers (**M1**, **M2**, and **M3**) and three microtube reac-

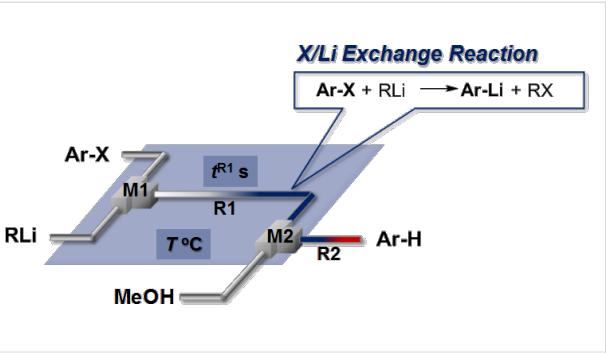

Figure 1: Flow microreactor system for halogen–lithium exchange of aryl halide followed by reaction with methanol. T-shaped micromixer: **M1** (inner diameter: 250 μm), and **M2** (inner diameter: 500 μm), microtube reactor: **R1** and **R2** (∅ = 1000 μm, length = 50 cm), a solution of aryl halides: 0.10 M in THF (6.0 mL/min), a solution of lithium reagent: 0.40 M or 0.42 M in hexane (*n*-BuLi) or Et_2O (PhLi) (1.5 mL/min), a solution of methanol: Neat (3.0 mL/min).

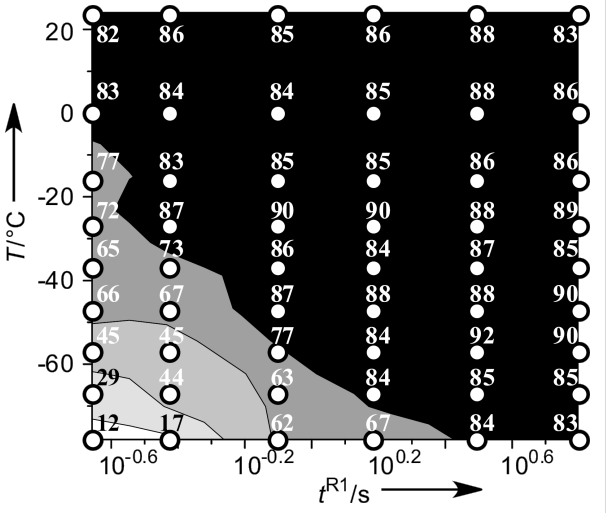

Figure 2: Effects of the temperature (T) and the residence time in **R1** (t^{R1}) on the yield of anisole in the Br–Li exchange reaction of *p*-bromoanisole followed by reaction with methanol in the flow microreactor system. The contour plot with scatter overlay shows the yields of anisole (%), which are indicated by small circles.

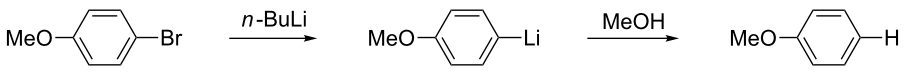

Scheme 1: Halogen–lithium exchange of *p*-bromoanisole followed by reaction with methanol.

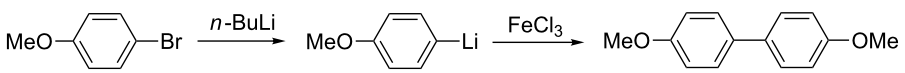

Scheme 2: Halogen-lithium exchange of *p*-bromoanisole followed by oxidative homocoupling with $FeCl_3$.

tors (**R1**, **R2**, and **R3**) were used, as shown in Figure 3. A solution of *p*-bromoanisole (Ar–X) (0.10 M in THF, flow rate: 6.0 mL/min) and a solution of *n*-butyllithium (0.42 M in hexane, flow rate: 1.5 mL/min) were introduced to **M1** (∅ = 250 μm) by syringe pumps. The resulting mixture was passed through **R1** (t^{R1} = 13 s (−78 °C), t^{R1} = 13 s (−48 °C), t^{R1} = 3.1 s (−28 °C), t^{R1} = 3.1 s (0 °C), t^{R1} = 3.1 s (24 °C)) at the corresponding temperatures and was mixed with a solution of $FeCl_3$ (0.10 M in THF, flow rate: 6.0 mL/min) in **M2** (∅ = 500 μm). The resulting mixture was passed through **R2** and was then mixed with methanol (neat, flow rate: 1.5 mL/min) in **M3** (∅ = 500 μm) to protonate the unchanged *p*-methoxyphenyllithium. The resulting solution was passed through **R3** (∅ = 1000 μm, L = 50 cm). The temperature (*T*) was controlled by adjusting the bath temperature, and the residence time in **R2** (t^{R2}) by changing the inner diameter and the length in **R2** with the fixed flow rate. After a steady state was reached, the product solution was collected for 30 s. The results obtained from varying t^{R2} and *T* are summarized in Figure 4, in which the yield of 4,4'-dimethoxybiphenyl is plotted against *T* and t^{R2} as a contour map with scattered overlay (see Supporting Information File 1 for details). The yield depends on both *T* and t^{R2}. At −78 °C, the yield increased with t^{R2} because of the progress of the homocoupling. At 0 °C, the homocoupling product was obtained in reasonable yields for a wide range of t^{R2}. The productivity of the present system is acceptable for large scale laboratory synthesis (6.2 g/h). It is noteworthy that the integrated reactions were complete within the overall residence time of 14.7 s, even at low temperatures such as −48 °C. Thus, we envisaged that the reaction could also be applied to less stable aryllithium compounds that decompose very quickly.

One of the major benefits of flow microreactor synthesis is the ability to use highly unstable reactive intermediates. Such intermediates can be rapidly generated and transferred to another location to be used in a subsequent reaction before they decompose. We have already reported the generation and reactions of unstable aryllithium species such as *o*-bromophenyllithiums, and aryllithiums bearing alkoxycarbonyl, cyano, nitro, and ketone carbonyl groups [86,87,93,95,96,98], which are difficult to use in conventional macro batch reactors. As shown in Table 1, reactions of aryllithiums bearing cyano and nitro groups proceeded successfully to give the corresponding homocoupling products, where in contrast it is very difficult to achieve such reactions using conventional batch reactors. A mechanism involving transmetalation of the aryl group from lithium to iron followed by reductive elimination of the homocoupling product seems to be plausible, while a similar mechanism is proposed for homo-coupling of organomagnesium compounds with $FeCl_3$ [19,20]. The regiospecificity of the coupling is consistent with this mechanism. Radical coupling seems to be less likely.

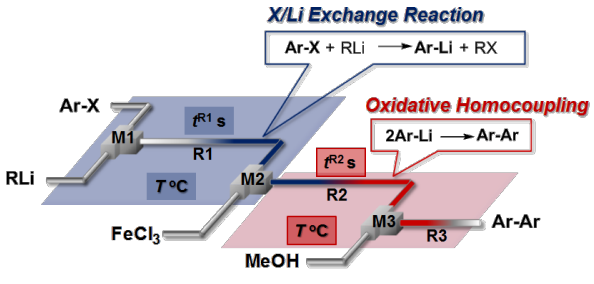

Figure 3: Integrated flow microreactor system for oxidative homocoupling reaction of aryllithium with $FeCl_3$. T-shaped micromixer: **M1** (inner diameter: 250 μm), **M2** (inner diameter: 500 μm), and **M3** (inner diameter: 500 μm), microtube reactor: **R1**, **R2** and **R3** (∅ = 1000 μm, length = 50 cm), a solution of aryl halides: 0.10 M in THF (6.0 mL/min), a solution of lithium reagent: 0.42 M in hexane (*n*-BuLi) or Et_2O (PhLi) (1.5 mL/min), a solution of $FeCl_3$: 0.10 M in THF (6 mL/min), a solution of methanol: Neat (1.5 mL/min).

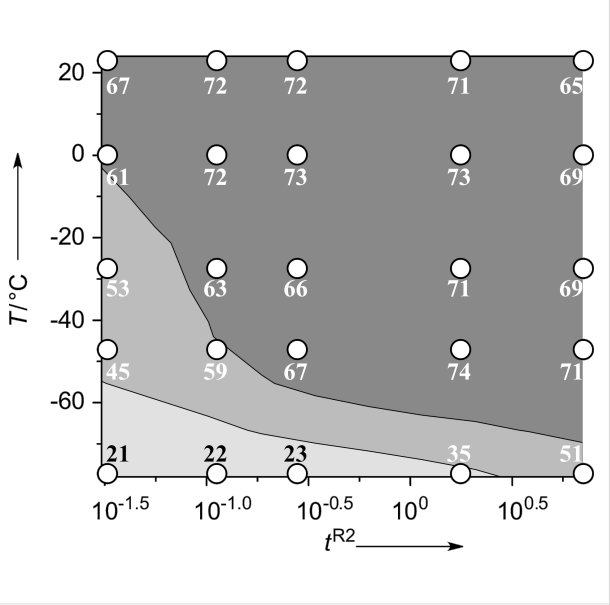

Figure 4: Effects of the temperature (*T*) and the residence time in **R2** (t^{R2}) on the yield of 4,4'-dimethoxybiphenyl in the oxidative homocoupling of *p*-methoxyphenyllithium with $FeCl_3$ in the integrated flow microreactor system. Contour plot with scatter overlay of the yields of 4,4'-dimethoxybiphenyl (%), which are indicated by small circles.

Conclusion

In conclusion, we found that the use of $FeCl_3$ results in fast oxidative homocoupling of aryllithiums, which enables its integration with the halogen–lithium exchange of aryl halides. Various aryl halides, including those bearing electrophilic functional groups, can be used for this transformation in the integrated flow microreactor system. Hence, the method greatly enhances the synthetic utility of aryllithium compounds and adds a new dimension to the chemistry of coupling reactions.

Table 1: Homocoupling of aryl halides using the integrated flow microreactor system.

Ar–X	*T* (°C)	t^{R1} (s)	Ar–Ar	Yield (%)
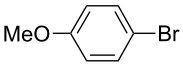	24	3.100	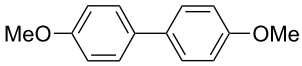	72
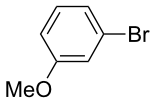	24	3.100	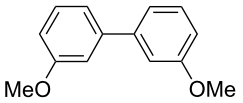	69
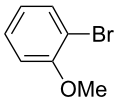	0	3.100	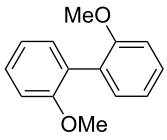	76
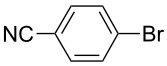	−28	0.055	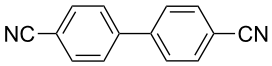	75
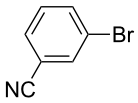	0	0.055	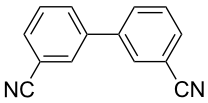	66
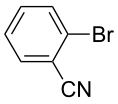	24	0.055	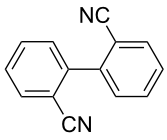	76
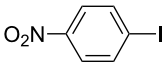	−48	0.014	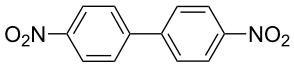	53[a]
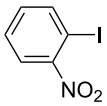	−48	0.014	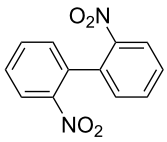	63[a]

[a]PhLi instead of *n*-BuLi was used as lithiating reagent.

Supporting Information

Supporting Information features experimental procedures and full spectroscopic data for all new compounds.

Supporting Information File 1

Experimental details.
[http://www.beilstein-journals.org/bjoc/content/supplementary/1860-5397-7-122-S1.pdf]

Acknowledgements

This work was financially supported in part by a Grant-in-Aid for Scientific Research from the Japan Society for the Promotion of Science and NEDO projects.

References

1. Cepanec, I. *Synthesis of Biaryls;* Elsevier: Amsterdam, Boston, 2004.
2. Inoue, A.; Kitagawa, K.; Shinokubo, H.; Oshima, K. *Tetrahedron* **2000,** *56,* 9601–9605. doi:10.1016/S0040-4020(00)00929-7
3. McKillop, A.; Elsom, L. F.; Taylor, E. C. *J. Am. Chem. Soc.* **1968,** *90,* 2423–2424. doi:10.1021/ja01011a041
4. Ishikawa, T.; Ogawa, A.; Hirao, T. *Organometallics* **1998,** *17,* 5713–5716. doi:10.1021/om980607c
5. Kharasch, M. S.; Fields, E. K. *J. Am. Chem. Soc.* **1941,** *63,* 2316–2320. doi:10.1021/ja01854a006
6. Sakellarios, E.; Kyrimis, T. *Ber. Dtsch. Chem. Ges.* **1924,** *57,* 322–326. doi:10.1002/cber.19240570233
7. Lei, A.; Srivastava, M.; Zhang, X. *J. Org. Chem.* **2002,** *67,* 1969–1971. doi:10.1021/jo011098i
8. Cahiez, G.; Marquais, S. *Pure Appl. Chem.* **1996,** *68,* 53–60. doi:10.1351/pac199668010053
9. Cahiez, G.; Marquais, S. *Tetrahedron Lett.* **1996,** *37,* 1773–1776. doi:10.1016/0040-4039(96)00116-5

10. Cahiez, G.; Avedissian, H. *Synthesis* **1998,** 1199–1205. doi:10.1055/s-1998-2135
11. Dohle, W.; Kopp, F.; Cahiez, G.; Knochel, P. *Synlett* **2001,** 1901–1904. doi:10.1055/s-2001-18748
12. Fürstner, A.; Leitner, A.; Méndez, M.; Krause, H. *J. Am. Chem. Soc.* **2002,** *124,* 13856–13863. doi:10.1021/ja027190t
13. Fürstner, A.; Leitner, A. *Angew. Chem., Int. Ed.* **2002,** *41,* 609–612. doi:10.1002/1521-3773(20020215)41:4<609::AID-ANIE609>3.0.CO;2-M
14. Quintin, J.; Franck, X.; Hocquemiller, R.; Figadère, B. *Tetrahedron Lett.* **2002,** *43,* 3547–3549. doi:10.1016/S0040-4039(02)00568-3
15. Martin, R.; Fürstner, A. *Angew. Chem., Int. Ed.* **2004,** *43,* 3955–3957. doi:10.1002/anie.200460504
16. Scheiper, B.; Bonnekessel, M.; Krause, H.; Fürstner, A. *J. Org. Chem.* **2004,** *69,* 3943–3949. doi:10.1021/jo0498866
17. Nakamura, M.; Matsuo, K.; Ito, S.; Nakamura, E. *J. Am. Chem. Soc.* **2004,** *126,* 3686–3687. doi:10.1021/ja049744t
18. Nagano, T.; Hayashi, T. *Org. Lett.* **2004,** *6,* 1297–1299. doi:10.1021/ol049779y
19. Nagano, T.; Hayashi, T. *Org. Lett.* **2005,** *7,* 491–493. doi:10.1021/ol047509+
20. Cahiez, G.; Chaboche, C.; Mahuteau-Betzer, F.; Ahr, M. *Org. Lett.* **2005,** *7,* 1943–1946. doi:10.1021/ol050340v
21. Knochel, P., Ed. *Handbook of Functionalized Organometallics;* Wiley-VCH: Weinheim, Germany, 2005. doi:10.1002/9783527619467
22. Yoshida, J. *Flash Chemistry: Fast Organic Synthesis in Microsystems;* Wiley: Hoboken, N.J., 2008.
23. Fletcher, P. D. I.; Haswell, S. J.; Pombo-Villar, E.; Warrington, B. H.; Watts, P.; Wong, S. Y. F.; Zhang, X. *Tetrahedron* **2002,** *58,* 4735–4757. doi:10.1016/S0040-4020(02)00432-5
24. Jähnisch, K.; Hessel, V.; Löwe, H.; Baerns, M. *Angew. Chem., Int. Ed.* **2004,** *43,* 406–446. doi:10.1002/anie.200300577
25. Yoshida, J. *Chem. Commun.* **2005,** 4509–4516. doi:10.1039/b508341a
26. Doku, G. N.; Verboom, W.; Reinhoudt, D. N.; van den Berg, A. *Tetrahedron* **2005,** *61,* 2733–2742. doi:10.1016/j.tet.2005.01.028
27. Yoshida, J.; Nagaki, A.; Iwasaki, T.; Suga, S. *Chem. Eng. Technol.* **2005,** *28,* 259–266. doi:10.1002/ceat.200407127
28. Geyer, K.; Codee, J. D. C.; Seeberger, P. H. *Chem.–Eur. J.* **2006,** *12,* 8434–8442. doi:10.1002/chem.200600596
29. Whitesides, G. *Nature* **2006,** *442,* 368–373. doi:10.1038/nature05058
30. deMello, A. J. *Nature* **2006,** *442,* 394–402. doi:10.1038/nature05062
31. Song, H.; Chen, D. L.; Ismagilov, R. F. *Angew. Chem., Int. Ed.* **2006,** *45,* 7336–7356. doi:10.1002/anie.200601554
32. Kobayashi, J.; Mori, Y.; Kobayashi, S. *Chem.–Asian J.* **2006,** *1,* 22–35. doi:10.1002/asia.200600058
33. Mason, B. P.; Price, K. E.; Steinbacher, J. L.; Bogdan, A. R.; McQuade, D. T. *Chem. Rev.* **2007,** *107,* 2300–2318. doi:10.1021/cr050944c
34. Ahmed-Omer, B.; Brandtand, J. C.; Wirth, T. *Org. Biomol. Chem.* **2007,** *5,* 733–740. doi:10.1039/b615072a
35. Watts, P.; Wiles, C. *Chem. Commun.* **2007,** 443–467. doi:10.1039/b609428g
36. Yoshida, J.; Nagaki, A.; Yamada, T. *Chem.–Eur. J.* **2008,** *14,* 7450–7459. doi:10.1002/chem.200800582
37. Fukuyama, T.; Rahman, M. T.; Sato, M.; Ryu, I. *Synlett* **2008,** 151–163. doi:10.1055/s-2007-1000884
38. McMullen, J. P.; Jensen, K. F. *Annu. Rev. Anal. Chem.* **2010,** *3,* 19–42. doi:10.1146/annurev.anchem.111808.073718
39. Yoshida, J. *Chem. Rec.* **2010,** *10,* 332–341. doi:10.1002/tcr.201000020
40. Yoshida, J.; Kim, H.; Nagaki, A. *ChemSusChem* **2011,** *4,* 331–340. doi:10.1002/cssc.201000271
41. Watts, P.; Wiles, C.; Haswell, S. J.; Pombo-Villar, E.; Styring, P. *Chem. Commun.* **2001,** 990–991. doi:10.1039/b102125g
42. Suga, S.; Okajima, M.; Fujiwara, K.; Yoshida, J. *J. Am. Chem. Soc.* **2001,** *123,* 7941–7942. doi:10.1021/ja015823i
43. Fukuyama, T.; Shinmen, M.; Nishitani, S.; Sato, M.; Ryu, I. *Org. Lett.* **2002,** *4,* 1691–1694. doi:10.1021/ol0257732
44. Ueno, M.; Hisamoto, H.; Kitamori, T.; Kobayashi, S. *Chem. Commun.* **2003,** 936–937. doi:10.1039/b301638b
45. Garcia-Egido, E.; Spikmans, V.; Wong, S. Y. F.; Warrington, B. H. *Lab Chip* **2003,** *3,* 73–76. doi:10.1039/b302381h
46. Lai, S. M.; Martin-Aranda, R.; Yeung, K. L. *Chem. Commun.* **2003,** 218–219. doi:10.1039/b209297b
47. Mikami, K.; Yamanaka, M.; Islam, M. N.; Kudo, K.; Seino, N.; Shinoda, M. *Tetrahedron Lett.* **2003,** *44,* 7545–7548. doi:10.1016/S0040-4039(03)01835-5
48. Kobayashi, J.; Mori, Y.; Okamoto, K.; Akiyama, R.; Ueno, M.; Kitamori, T.; Kobayashi, S. *Science* **2004,** *304,* 1305–1308. doi:10.1126/science.1096956
49. Nagaki, A.; Kawamura, K.; Suga, S.; Ando, T.; Sawamoto, M.; Yoshida, J. *J. Am. Chem. Soc.* **2004,** *126,* 14702–14703. doi:10.1021/ja044879k
50. Lee, C.-C.; Sui, G.; Elizarov, A.; Shu, C. J.; Shin, Y.-S.; Dooley, A. N.; Huang, J.; Daridon, A.; Wyatt, P.; Stout, D.; Kolb, H. C.; Witte, O. N.; Satyamurthy, N.; Heath, J. R.; Phelps, M. E.; Quake, S. R.; Tseng, H.-R. *Science* **2005,** *310,* 1793–1796. doi:10.1126/science.1118919
51. Horcajada, R.; Okajima, M.; Suga, S.; Yoshida, J. *Chem. Commun.* **2005,** 1303–1305. doi:10.1039/b417388k
52. Kawaguchi, T.; Miyata, H.; Ataka, K.; Mae, K.; Yoshida, J. *Angew. Chem., Int. Ed.* **2005,** *44,* 2413–2416. doi:10.1002/anie.200462466
53. Ducry, L.; Roberge, D. M. *Angew. Chem., Int. Ed.* **2005,** *44,* 7972–7975. doi:10.1002/anie.200502387
54. Nagaki, A.; Togai, M.; Suga, S.; Aoki, N.; Mae, K.; Yoshida, J. *J. Am. Chem. Soc.* **2005,** *127,* 11666–11675. doi:10.1021/ja0527424
55. He, P.; Watts, P.; Marken, F.; Haswell, S. J. *Angew. Chem., Int. Ed.* **2006,** *45,* 4146–4149. doi:10.1002/anie.200600951
56. Uozumi, Y.; Yamada, Y.; Beppu, T.; Fukuyama, N.; Ueno, M.; Kitamori, T. *J. Am. Chem. Soc.* **2006,** *128,* 15994–15995. doi:10.1021/ja066697r
57. Tanaka, K.; Motomatsu, S.; Koyama, K.; Tanaka, S.; Fukase, K. *Org. Lett.* **2007,** *9,* 299–302. doi:10.1021/ol062777o
58. Sahoo, H. R.; Kralj, J. G.; Jensen, K. F. *Angew. Chem., Int. Ed.* **2007,** *46,* 5704–5708. doi:10.1002/anie.200701434
59. Hornung, C. H.; Mackley, M. R.; Baxendale, I. R.; Ley, S. V. *Org. Process Res. Dev.* **2007,** *11,* 399–405. doi:10.1021/op700015f
60. Iwasaki, T.; Nagaki, A.; Yoshida, J. *Chem. Commun.* **2007,** 1263–1265. doi:10.1039/b615159k
61. Nagaki, A.; Iwasaki, T.; Kawamura, K.; Yamada, D.; Suga, S.; Ando, T.; Sawamoto, M.; Yoshida, J. *Chem.–Asian J.* **2008,** *3,* 1558–1567. doi:10.1002/asia.200800081
62. Nagaki, A.; Tomida, Y.; Yoshida, J. *Macromolecules* **2008,** *41,* 6322–6330. doi:10.1021/ma800769n
63. Fukuyama, T.; Kobayashi, M.; Rahman, M. T.; Kamata, N.; Ryu, I. *Org. Lett.* **2008,** *10,* 533–536. doi:10.1021/ol702718z

64. Nagaki, A.; Tomida, Y.; Miyazaki, A.; Yoshida, J. *Macromolecules* **2009,** *42,* 4384–4387. doi:10.1021/ma900551a
65. Tricotet, T.; O'Shea, D. F. *Chem.–Eur. J.* **2010,** *16,* 6678–6686. doi:10.1002/chem.200903284
66. Greenway, G. M. S.; Haswell, J.; Morgan, D. O.; Skelton, V.; Styring, P. *Sens. Actuators, B* **2000,** *63,* 153–158. doi:10.1016/S0925-4005(00)00352-X
67. Haswell, S. J.; O'Sullivan, B.; Styring, P. *Lab Chip* **2001,** *1,* 164–166. doi:10.1039/b104035a
68. Niwa, S.; Eswaramoorthy, M.; Nair, J.; Raj, A.; Itoh, N.; Shoji, H.; Namba, T.; Mizukami, F. *Science* **2002,** *295,* 105–107. doi:10.1126/science.1066527
69. Jas, G.; Kirschning, A. *Chem.–Eur. J.* **2003,** *9,* 5708–5723. doi:10.1002/chem.200305212
70. Basheer, C.; Hussain, F. S. J.; Lee, H. K.; Valiyaveettil, S. *Tetrahedron Lett.* **2004,** *45,* 7297–7300. doi:10.1016/j.tetlet.2004.08.017
71. Liu, S.; Fukuyama, T.; Sato, M.; Ryu, I. *Org. Process Res. Dev.* **2004,** *8,* 477–481. doi:10.1021/op034200h
72. Kunz, U.; Schönfeld, H.; Solodenko, W.; Jas, G.; Kirschning, A. *Ind. Eng. Chem. Res.* **2005,** *44,* 8458–8467. doi:10.1021/ie048891x
73. Comer, E.; Organ, M. G. *J. Am. Chem. Soc.* **2005,** *127,* 8160–8167. doi:10.1021/ja0512069
74. Lee, C. K. Y.; Holmes, A. B.; Ley, S. V.; McConvey, I. F.; Al-Duri, B.; Leeke, G. A.; Santos, R. C. D.; Sevilled, J. P. K. *Chem. Commun.* **2005,** 2175–2177. doi:10.1039/b418669a
75. Mauger, C.; Buisine, O.; Caravieilhes, S.; Mignani, G. *J. Organomet. Chem.* **2005,** *690,* 3627–3629. doi:10.1016/j.jorganchem.2005.03.071
76. Kirschning, A.; Solodenko, W.; Mennecke, K. *Chem.–Eur. J.* **2006,** *12,* 5972–5990. doi:10.1002/chem.200600236
77. Shore, G.; Morin, S.; Organ, M. G. *Angew. Chem., Int. Ed.* **2006,** *45,* 2761–2766. doi:10.1002/anie.200503600
78. Shi, G.; Hong, F.; Liang, Q.; Fang, H.; Nelson, S.; Weber, S. G. *Anal. Chem.* **2006,** *78,* 1972–1979. doi:10.1021/ac051844+
79. Rahman, M. T.; Fukuyama, T.; Kamata, N.; Sato, M.; Ryu, I. *Chem. Commun.* **2006,** 2236–2238. doi:10.1039/b600970k
80. Murphy, E. R.; Martinelli, J. R.; Zaborenko, N.; Buchwald, S. L.; Jensen, K. F. *Angew. Chem., Int. Ed.* **2007,** *46,* 1734–1737. doi:10.1002/anie.200604175
81. Kawanami, H.; Matsushima, K.; Sato, M.; Ikushima, Y. *Angew. Chem., Int. Ed.* **2007,** *46,* 5129–5132. doi:10.1002/anie.200700611
82. Yamada, Y. M. A.; Watanabe, T.; Torii, K.; Uozumi, Y. *Chem. Commun.* **2009,** 5594–5596. doi:10.1039/b912696a
83. Jin, J.; Cai, M.-M.; Li, J. *Synlett* **2009,** 2534–2538. doi:10.1055/s-0029-1217730
84. Ahmed-Omer, B.; Barrow, D. A.; Wirth, T. *Tetrahedron Lett.* **2009,** *50,* 3352–3355. doi:10.1016/j.tetlet.2009.02.133
85. McMullen, J. P.; Stone, M. T.; Buchwald, S. L.; Jensen, K. F. *Angew. Chem., Int. Ed.* **2010,** *49,* 7076–7080. doi:10.1002/anie.201002590
86. Usutani, H.; Tomida, Y.; Nagaki, A.; Okamoto, H.; Nokami, T.; Yoshida, J. *J. Am. Chem. Soc.* **2007,** *129,* 3046–3047. doi:10.1021/ja068330s
87. Nagaki, A.; Tomida, Y.; Usutani, H.; Kim, H.; Takabayashi, N.; Nokami, T.; Okamoto, H.; Yoshida, J. *Chem.–Asian J.* **2007,** *2,* 1513–1523. doi:10.1002/asia.200700231
88. Nagaki, A.; Takabayashi, N.; Tomida, Y.; Yoshida, J. *Org. Lett.* **2008,** *10,* 3937–3940. doi:10.1021/ol8015572
89. Nagaki, A.; Kim, H.; Yoshida, J. *Angew. Chem., Int. Ed.* **2008,** *47,* 7833–7836. doi:10.1002/anie.200803205
90. Nagaki, A.; Takizawa, E.; Yoshida, J. *J. Am. Chem. Soc.* **2009,** *131,* 1654–1655. doi:10.1021/ja809325a
91. Nagaki, A.; Takabayashi, N.; Tomida, Y.; Yoshida, J. *Beilstein J. Org. Chem.* **2009,** *5,* No. 16. doi:10.3762/bjoc.5.16
92. Tomida, Y.; Nagaki, A.; Yoshida, J. *Org. Lett.* **2009,** *11,* 3614–3617. doi:10.1021/ol901352t
93. Nagaki, A.; Kim, H.; Yoshida, J. *Angew. Chem., Int. Ed.* **2009,** *48,* 8063–8065. doi:10.1002/anie.200904316
94. Nagaki, A.; Takizawa, E.; Yoshida, J. *Chem.–Eur. J.* **2010,** *16,* 14149–14158. doi:10.1002/chem.201000815
95. Nagaki, A.; Kim, H.; Moriwaki, Y.; Matsuo, C.; Yoshida, J. *Chem.–Eur. J.* **2010,** *16,* 11167–11177. doi:10.1002/chem.201000876
96. Nagaki, A.; Kim, H.; Matsuo, C.; Yoshida, J. *Org. Biomol. Chem.* **2010,** *8,* 1212–1217. doi:10.1039/b919325c
97. Tomida, Y.; Nagaki, A.; Yoshida, J. *J. Am. Chem. Soc.* **2011,** *133,* 3744–3747. doi:10.1021/ja110898s
98. Kim, H.; Nagaki, A.; Yoshida, J. *Nat. Commun.* **2011,** *2,* No. 264. doi:10.1038/ncomms1264
99. Suga, S.; Yamada, D.; Yoshida, J. *Chem. Lett.* **2010,** *39,* 404–406. doi:10.1246/cl.2010.404
100. Nagaki, A.; Kenmoku, A.; Moriwaki, Y.; Hayashi, A.; Yoshida, J. *Angew. Chem., Int. Ed.* **2010,** *49,* 7543–7547. doi:10.1002/anie.201002763

License and Terms

Beilstein Journal of Organic Chemistry

A practical microreactor for electrochemistry in flow

Kevin Watts[1], William Gattrell[2] and Thomas Wirth[*1]

Full Research Paper

Open Access

Address:
[1]Cardiff University, School of Chemistry, Park Place, Cardiff CF10 3AT, UK and [2]Prosidion Ltd, Watlington Road, Oxford OX4 6LT, UK

Email:
Thomas Wirth[*] - wirth@cf.ac.uk

* Corresponding author

Keywords:
diaryliodonium compounds; electrochemistry; flow chemistry; microreactor

Beilstein J. Org. Chem. **2011,** *7,* 1108–1114.
doi:10.3762/bjoc.7.127

Received: 06 June 2011
Accepted: 21 July 2011
Published: 15 August 2011

This article is part of the Thematic Series "Chemistry in flow systems II".

Guest Editor: A. Kirschning

Abstract

A microreactor for electrochemical synthesis has been designed and fabricated. It has been shown that different reactions can be carried out successfully using simple protocols.

Introduction

Electrochemical reactions offer a clean route to the formation of anion and cation radical species from neutral organic molecules. Electrons can be added or removed from the substrates under mild conditions without the need for chemical oxidizing or reducing reagents which might complicate the reaction sequence [1]. A major advantage of electrochemical methods is the reduced formation of side products, as no chemical reagents are necessary. Electrochemical methods therefore provide a better environment for subsequent reactions involving the electrochemically generated reactive species [2]. Traditional electrochemical batch methods can suffer from several drawbacks. The electrical field in the cell is heterogeneous and often supporting electrolytes have to be used, which must be removed after the reaction. As a result, only a few electrochemical processes for the production of organic compounds have been commercialized [3]. In microreactors, the distances between electrodes can be very small such that the two diffusion layers of the electrodes overlap or become "coupled". This allows ions to be electrogenerated and play the role of the supporting electrolyte.

Different microreactor systems have already been developed for chemistry in this area and have been successfully employed in the conduction of electrochemical reactions without any added electrolyte [4,5]. Atobe et al. constructed a thin layer flow cell from platinum and/or glassy carbon plates (3 × 3 cm), separated by adhesive tape (80 μm), with a space left in between to act as the channel, and the devices were sealed with epoxy resin [6]. They reported the self-supported, paired electrosynthesis of 2,5-dimethoxy-2,5-dihydrofuran from furan with excellent yields and flow rates of up to 0.5 $mL \cdot min^{-1}$. A microflow system where the current flow and liquid flow are parallel was reported by Yoshida et al. [7]. Two carbon fibre electrodes were separated by a hydrophobic porous PTFE membrane (75 μm

thickness). The substrate solution was fed into the anodic chamber and flowed through the membrane into the cathodic chamber, where it would leave as products. The carbon fibre electrodes used in this design allow for a much greater surface area than the empty space between electrodes in the setup reported by Atobe. The anodic methoxylation of 4-methoxytoluene was carried out in the electrochemical cell under a constant current of 11 mA with a flow rate of 2 $mL \cdot h^{-1}$ resulting in a 90% conversion. A simpler configuration of electrodes was reported by Haswell et al. [8]. Two platinum electrodes with a surface area of 45 mm^2 were positioned with an inter-electrode gap of either 160 µm or 320 µm, and C–C bond forming reactions based on the electro-reductive coupling of activated olefins and benzyl bromide derivatives were reported. The best result obtained was a 98% formation of the product at a flow rate of 10–15 $\mu L \cdot min^{-1}$ with a current of 0.6 mA.

Yoshida reported a method of producing carbocations such as **1** in the absence of a suitable nucleophile (the "cation pool" method). This is an unconventional method because the ions generated are unstable and usually need to be trapped immediately after generation. In the "cation flow" method, a carbocation is generated continuously in a flow system by low temperature electrolysis. The generation of the cation can be monitored by a FTIR spectrometer in the flow system. The electrochemically generated *N*-acyliminium ions can then be used in different subsequent reactions (Scheme 1).

The first reaction studied was a Friedel–Crafts reaction of aromatic compounds. In comparison with the "cation pool" method, the "cation flow" method was far more successful for this reaction, producing the monoalkylated product **2** in 92% yield in contrast to the batch method, which led to a 1:1 mixture of mono- and dialkylation products [9]. The reaction in flow is complete within seconds, and the extremely fast 1:1 mixing in a micromixer, together with efficient heat transfer in the microsystem, seems to be responsible for the dramatic increase in the product selectivity. Cycloadditions using the *N*-acyliminium ions as heterodienes with a variety of dienophiles, such as alkenes and alkynes, give the corresponding [4 + 2] cycloaddition products in high yields [10]. The same authors also reported a successful polymer synthesis using the same technique by adding a monomer to the initiator (*N*-acyliminium ions) followed by micromixing and the addition of the terminator (diisopropylamine) in a subsequent micromixer. This was considered to be a superior technique to the batch method as the molecular weight distribution of the polymer **3** decreased in the flow system [11].

Yoshida et al. also reported the electrochemical iodination of aromatic compounds by elemental iodine followed by a subsequent reaction with aromatic compounds. This sequential method has one main advantage over the batch method, in that the polyiodination problem for highly reactive aromatic compounds, based on disguised chemical selectivity, can be avoided by the micromixing of a solution of preformed iodine cations (I^+) and a solution of an aromatic compound, increasing the yield of mono iodination product from 38% to 85% [12]. Nishiyama et al. reported the synthesis of hypervalent iodine compounds using electrochemistry [13]. Electrochemical microreactors for investigations of laminar flow have also been reported recently [14,15].

Results and Discussion

The target of this research is to develop a simple and practical microreactor in which to carry out electrochemical reactions in flow. A small gap between the electrodes, to avoid the necessity of electrolytes, and a simple and robust setup, were the

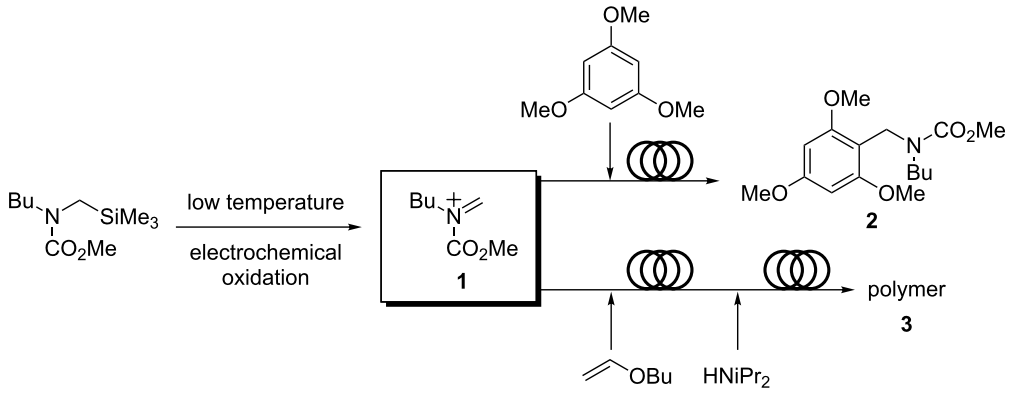

Scheme 1: Electrochemically generated *N*-acyliminium ions **1** and subsequent reactions.

leading principles in the design of the reactor. Herein we describe the construction of such a simple microreactor, some initial test reactions and the novel application to the continuous synthesis of diaryliodonium compounds. A microflow electrochemical reactor made out of two aluminium bodies (50 mm diameter, 25 mm height) was manufactured. The electrodes are constructed of two PTFE plates (35 mm diameter, 4 mm height) onto which 0.1 mm platinum foil electrodes [16] are mounted. The wires for connection to the potentiostat are fixed into the PFTE plate under the platinum. The electrodes are held apart by a FEP (fluorinated ethylene propylene) foil of variable thickness, into which a rectangular reaction channel is cut (3 × 30 mm) giving an overall channel volume of 23 µL (FEP foil 254 µm thick), and the whole device is held together by steel screws and wing nuts. The opened device is shown in Figure 1.

Known electrochemical reactions were used as test reactions for the electrochemical microreactor. The oxidative methoxylation of furan **4** in methanol (Scheme 2) is a very clean reaction with no extra reagents necessary. The product **5**, obtained in an approximate 1:1 *syn*:*anti* ratio, was identified by ^{1}H NMR and GC/MS and showed that our system functioned satisfactorily for electrochemical reactions. A yield for this reaction was not determined, but full conversion was achieved as established by GC/MS. The reaction shown in Scheme 2 has previously been performed in batch electrolysis leading to product **5** in 78% yield [17].

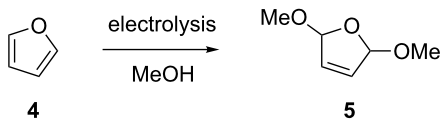

4 **5**

Scheme 2: Electrolysis of furan.

In addition, Kolbe-type reactions were investigated in flow. 2-Phenylacetic acid (**6a**) was used as a substrate and yields of up to 40% of 1,2-diphenylethane (**7a**) were obtained with the device depicted in Figure 1; the reactions are shown in Scheme 3. The Kolbe reaction did not seem to be a very suitable reaction for a flow reactor due to the large amount of carbon dioxide and hydrogen that is formed at the anode during the decarboxylation reaction. This was partially overcome by neutralising the solution with triethylamine as base, hence carbon dioxide gas was not liberated during the reaction [18]. The reactions were carried out in acetonitrile instead of methanol to reduce the amount of side-products that could be formed due to the reduction of methanol at the cathode. The Kolbe electrolysis of **6a** has also been described as a batch reaction, with a solid base, providing the product **7a** in 44% yield [19]. This means that the reaction conditions in the electrochemical microreactor were comparable to batch synthesis. The reaction conditions described for **6a** were also successful for 2,2-diphenylacetic acid (**6b**) and even an asymmetric reaction

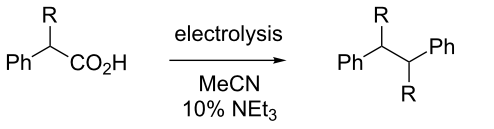

6a R = H
6b R = Ph

7a R = H (40%)
7b R = Ph (31%)

Scheme 3: Kolbe electrolysis of phenylacetic acids **6** in flow.

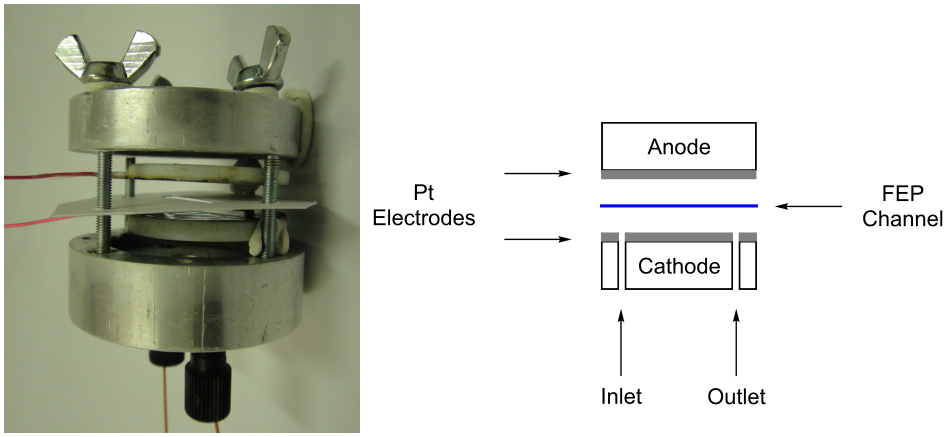

Figure 1: Electrochemical microreactor.

product could be formed through a mixture of phenylacetic acid (**6a**) and diphenylacetic acid (**6b**), although in smaller yield.

Hypervalent iodine compounds can be used in organic syntheses as mild, non-toxic and highly selective reagents. Iodine(III) reagents with two carbon ligands are known as iodonium salts. These salts are attractive alternatives to oxidants and catalysts based on heavy metals, as they have similar properties to those of heavy metal complexes and can, therefore, be used in similar reaction pathways, and are beneficial for organic synthesis due to their low toxicity and cost [20].

Iodonium salts are currently being used in three main types of reactions, namely ligand exchange, reductive elimination and ligand coupling. This is due to their highly electron deficient nature and high dissociation rates that make them excellent leaving groups. Symmetric salts are usually more desirable than asymmetric compounds purely for the reason that this avoids problems that can occur with selectivity in aryl-transfers. If a diaryliodonium salt is asymmetric it is usually the more electron deficient ligand that is transferred [21].

The formation of these compounds usually follows a two-step procedure. The first step is the oxidation of an iodoarene, which can then take part in an acid-catalyzed coupling reaction with another aryl compound. However, there are now more one-pot procedures to diaryliodonium salts known that involve both oxidation and ligand exchange directly from the aryl and iodoarene starting materials. The electrochemical oxidation of an iodoarene in the presence of another arene provides a quite general and simple one-step approach to the synthesis of diaryliodonium salts [22].

We describe herein a simple procedure for the flow synthesis of diaryliodonium salts using the electrochemical microreactor device described above. The products were obtained in good yields and only minimal work-up was required after the reaction. The reaction takes place with an iodoarene that is oxidized at the anode. The radical cation then undergoes a reaction with the other arene to form an intermediate, followed by the loss of a second electron [23]. The solvent system consisted of acetonitrile, sulfuric acid (2 M) and acetic anhydride, which was reported to increase the selectivity of the coupling reaction [21]. The sulfuric acid acts both as a counter reaction to the oxidation at the anode, with proton reduction, and simultaneously provides a counter ion for the positively charged iodonium salt. It also acts as an electrolyte in the reaction described above. A general procedure for the synthesis of both, symmetric and asymmetric iodonium salts, was developed, as shown in Scheme 4, and yields of up to 72% were obtained.

Initially, the conditions of the reaction were optimized with iodotoluene **8a** (R^1 = 4-Me) and toluene (**9a**) (R^2 = Me). A current of 30 mA led to a yield of 72%, whereas with higher currents (35, 40, or 45 mA) the yield dropped to 50% for identical flow rates. The increased formation of (diacetoxyiodo) arene derivatives as side products was observed in these cases. In Table 1 the results of the experiments using different combinations of iodoarenes **8** and arenes **9** are summarized.

Various yields were obtained in these experiments and not all reaction conditions were optimized. In some reactions the conversion was not complete and longer reaction times would have been necessary to achieve higher yields. Depending on the nature of the iodoarene **8**, traces of the corresponding diacetoxyiodo compounds were also observed as side products. After the reaction, treatment of the reaction mixture with potassium iodide was required, as the resulting diaryliodonium iodides **11** are insoluble in the reaction mixture (in contrast to the diaryliodonium hydrogensulfates **10**) and can thus be easily separated and purified by filtration and washing.

Conclusion

The successful development of a microreactor for different types of electrochemical reactions is described. The device has the advantage of being very easily dismantled, allowing cleaning when reactions cause a blockage in the channel. It is also possible to change the internal volume of the channel quickly by changing the channel height through the foil thicknesses.

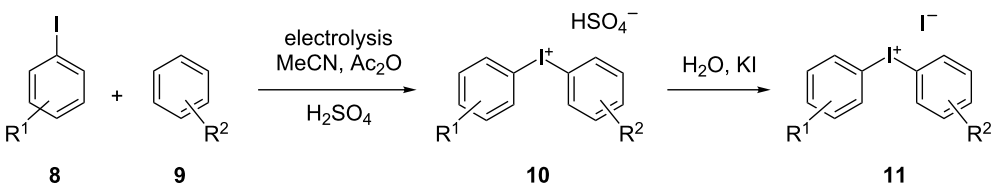

Scheme 4: Synthesis of diaryliodonium salts **11** in flow.

Table 1: Products and yields in the electrochemical generation of diaryliodonium compounds performed in an electrochemical microreactor (30 mA) at a flow rate of 80 µL/min (residence time: 17 s) at 25 °C.

Entry	R^1	R^2	Product	Yield [%]
1	4-Me	Me	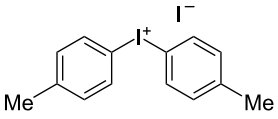 **11a**	72
2	4-Me	Et	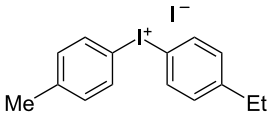 **11b**	51
3	4-Me	iPr	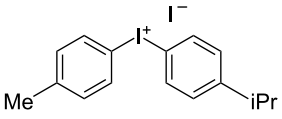 **11c**	60
4	H	Me	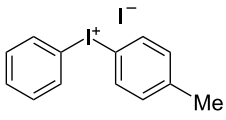 **11d**	44
5	H	Et	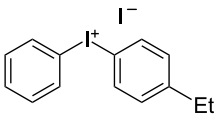 **11e**	39
6	H	iPr	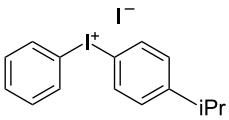 **11f**	19
7	H	*t*-Bu	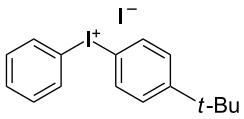 **11g**	64
8	3-Me	Me	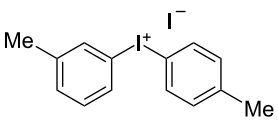 **11h**	36
9	3-Me	Et	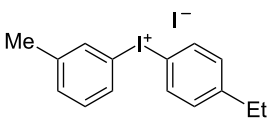 **11i**	25
10	3-Me	iPr	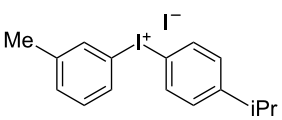 **11j**	18

Experimental

General: Melting points were obtained in open capillary tubes and are uncorrected. ^{1}H NMR and ^{13}C NMR spectra were recorded on a AV-400 Bruker spectrometer, in the solvents indicated, at 400 and 100 MHz, respectively. Mass spectra (*m*/*z*) and HRMS were recorded under the conditions of electron impact (EI). All reactions were monitored by thin-layer chromatography which was performed on precoated sheets of silica gel 60. The galvanostatic reactions were performed with a HEKA 510 galvanostat/potentiostat. The electrodes were cleaned with acetone after each reaction; no polishing was required. However, with earlier reactions using KF as an electrolyte in solution the electrodes did need polishing as they were slightly blackened. Methanol and acetonitrile were dried over 4 Å molecular sieves. All other chemicals were used as purchased without further purification.

Furan oxidation

A 0.05 M solution of furan (34 mg, 0.5 mmol) in methanol (10 mL) was introduced into the electrochemical device (channel dimensions: 3 mm × 30 mm × 100 µm, volume 9 µL) through a syringe pump (flow rate 80 µL/min; residence time: 7 s) with an applied current of 2 mA (current density: 1.11 mA/cm^2) and collected at the outlet to give **5** after removal of the solvent. The product was identified by GC/MS *m*/*z* (EI): M^+ 129.1.

Kolbe electrolysis

A 0.1 M solution of 2-phenylacetic acid (**6a**) (136 mg, 1 mmol) in acetonitrile (10 mL), with 10 mol % triethylamine (13 µL) was introduced into the electrochemical device (channel dimensions: 3 mm × 30 mm × 127 µm, volume 11 µL) through a syringe pump (flow rate 40 µL/min; residence time: 17 s) with an applied current of 4 mA (current density: 2.22 mA/cm^2) and collected at the outlet to give **7a** with 40% yield (72 mg, 0.4 mmol). The product was identified by GC/MS *m*/*z* (EI): M^+ 183.3.

General procedure for the synthesis of iodonium salts 11

A solution of aryl iodide **8** (0.1 M) and aryl compound **9** (0.3 M) was prepared in 2 M H_2SO_4/acetonitrile with 25% acetic anhydride and introduced into the electrochemical device (channel dimensions: 3 mm × 30 mm × 254 µm, volume 23 µl) through syringe pumps (flow rate 80 µL/min; residence time: 17 s) with an applied current of 30 mA (current density: 16.67 mA/cm^2) and collected at the outlet. The solvent was then removed, water was added (3 mL) and the iodide was precipitated by addition of KI (166 mg, 1 mmol) to give the diaryliodonium salts **11**.

Di-*p*-tolyliodonium iodide (11a) [24]

Collection of 3 mL, yield: 100 mg (72%); colourless solid; mp 162–164 °C; ^{1}H NMR (400 MHz, $CDCl_3$) δ 2.27 (s, 6H), 7.08 (d, *J* = 8 Hz, 4H), 7.74 (d, *J* = 8.3 Hz, 4H); HRMS–EI (*m*/*z*): $[M - I]^+$ calcd for $C_{14}H_{14}I$, 309.0135; found, 309.0130.

(4-Ethylphenyl)(*p*-tolyl)iodonium iodide (11b) [25]

Collection of 5 mL, yield: 114 mg (51%); colourless solid; mp 156–158 °C; ^{1}H NMR (400 MHz, $CDCl_3$) δ 1.13 (t, *J* = 7.6 Hz, 3H), 2.27 (s, 3H), 2.56 (q, *J* = 7.6 Hz, 2H), 7.09 (m, 4H), 7.77 (m, 4H); HRMS–EI (*m*/*z*): $[M - I]^+$ calcd for $C_{15}H_{16}I$, 323.0291; found, 323.0297.

(4-Isopropylphenyl)(*p*-tolyl)iodonium iodide (11c) [24]

Collection of 5 mL, yield: 139 mg (60%); colourless solid; mp 154–157 °C; ^{1}H NMR (400 MHz, $CDCl_3$) δ 1.14 (d, *J* = 6.9 Hz, 6H), 2.28 (s, 3H), 2.81 (td, *J* = 7.0, 13.9 Hz, 1H), 7.11 (m, 4H), 7.76 (m, 4H); HRMS–EI (*m*/*z*): $[M - I]^+$ calcd for $C_{16}H_{18}I$, 337.0448; found, 337.0440.

Phenyl(*p*-tolyl)iodonium iodide (11d) [24]

Collection of 5 mL, yield: 93 mg (44%); colourless solid; mp 135–139 °C; ^{1}H NMR (400 MHz, $CDCl_3$) δ 2.27 (s, 3H), 7.12 (d, *J* = 8.1 Hz, 2H), 7.30 (m, 2H), 7.48 (t, *J* = 7.4 Hz, 1H), 7.77 (dd, *J* = 2.0, 8.7 Hz, 2H), 7.88 (dd, *J* = 1.0, 8.3 Hz, 2H); HRMS–EI (*m*/*z*): $[M - I]^+$ calcd for $C_{13}H_{12}I$, 294.9978; found, 294.9973.

(4-Ethylphenyl)(phenyl)iodonium iodide (11e)

Collection of 5 mL, yield: 82 mg (39%); colourless solid; mp 159–161 °C; ^{1}H NMR (400 MHz, $CDCl_3$) δ 1.14 (t, *J* = 7.6 Hz, 3H), 2.57 (q, *J* = 7.7 Hz, 2H), 7.12 (d, *J* = 8.4 Hz, 2H), 7.29 (t, *J* = 7.7 Hz, 2H), 7.44 (t, *J* = 7.4 Hz, 1H), 7.79 (d, *J* = 8.3 Hz, 2H), 7.88 (d, *J* = 7.5 Hz, 2H); ^{13}C NMR (100 MHz, $CDCl_3$) δ 14.9, 28.6, 117.5, 121.1, 131.1, 131.2 (2C), 131.5 (2C), 134.5 (2C), 134.8 (2C), 148.1; HRMS–EI (*m*/*z*): $[M - I]^+$ calcd for $C_{14}H_{14}I$, 309.0140; found, 309.0130.

(4-Isopropylphenyl)(phenyl)iodonium iodide (11f)

Collection of 5 mL, yield: 88 mg (19%); colourless solid; mp 146–148 °C; ^{1}H NMR (400 MHz, $CDCl_3$) δ 1.15 (d, *J* = 6.9 Hz, 1H), 2.82 (td, *J* = 6.9, 13.8 Hz, 1H), 7.14 (d, *J* = 8.4 Hz, 2H), 7.30 (t, *J* = 7.8 Hz, 1H), 7.44 (t, *J* = 4.4 Hz, 1H), 7.79 (d, *J* = 8.4 Hz, 2H), 7.89 (d, *J* = 7.6 Hz, 2H); ^{13}C NMR (126 MHz, $CDCl_3$) δ 23.6 (2C), 34.0, 117.4, 121.2, 129.9 (2C), 131.1, 131.5 (2C), 134.6 (2C), 134.7 (2C), 152.7 ppm; HRMS–EI (*m*/*z*): $[M - I]^+$ calcd for $C_{15}H_{16}I$, 323.0291; found, 323.0298.

(4-(*tert*-Butyl)phenyl)(phenyl)iodonium iodide (11g)

Collection of 5 mL, yield: 148 mg (64%); colourless solid; mp 162–164 °C; ^{1}H NMR (400 MHz, $CDCl_3$) δ 1.23 (s, 9H), 7.34 (m, 4H), 7.48 (t, *J* = 7.4 Hz, 1H), 7.83 (m, 2H), 7.92 (td, *J* = 1.7, 2.9 Hz, 2H); ^{13}C NMR (100 MHz, $CDCl_3$) δ 30.0 (3C), 34.1, 116.5, 120.4, 127.8 (2C), 130.0, 130.4 (2C), 133.4 (2C), 133.7 (2C), 153.7; HRMS–EI (*m*/*z*): $[M - I]^+$ calcd for $C_{16}H_{18}I$, 337.0448; found, 337.0451.

m-Tolyl(*p*-tolyl)iodonium iodide (11h) [24]

Collection of 5 mL, yield: 78 mg (36%); colourless solid; mp 85–89 °C; ^{1}H NMR (400 MHz, $CDCl_3$) δ 2.27 (s, 6H), 7.09 (d, *J* = 8.1 Hz, 2H), 7.19 (m, 2H), 7.65 (d, *J* = 7.9 Hz, 1H), 7.72 (s, 1H), 7.79 (d, *J* = 8.8 Hz, 2H); HRMS–EI (*m*/*z*): $[M - I]^+$ calcd for $C_{14}H_{14}I$, 309.0135; found, 309.0141.

(4-Ethylphenyl)(*m*-tolyl)iodonium iodide (11i)

Collection of 5 mL, yield: 57 mg (25%); colourless solid; mp 124–127 °C; ^{1}H NMR (400 MHz, $CDCl_3$) δ 1.14 (t, *J* = 7.6 Hz, 3H), 2.28 (s, 3H), 2.57 (q, *J* = 7.6 Hz, 2H), 7.12 (d, *J* = 8.5 Hz, 2H), 7.21 (m, 2H), 7.67 (d, *J* = 7.9 Hz, 1H), 7.74 (s, 1H), 7.80 (d, *J* = 8.4 Hz, 2H); ^{13}C NMR (100 MHz, $CDCl_3$) δ 13.9, 20.4, 27.6, 116.1, 119.7, 130.2, 130.3 (2C), 130.6, 131.2, 133.6 (2C), 133.9, 141.1, 147.1; HRMS–EI (*m*/*z*): $[M - I]^+$ calcd for $C_{15}H_{16}I$, 323.0291; found, 323.0298.

(4-Isopropylphenyl)(*m*-tolyl)iodonium iodide (11j)

Collection of 5 mL, yield: 43 mg (18%); colourless solid; mp 152–155 °C; ^{1}H NMR (400 MHz, $CDCl_3$) δ 1.14 (d, *J* = 6.9 Hz, 2H), 2.27 (s, 3H), 2.81 (td, *J* = 6.9, 13.8 Hz, 1H), 7.13 (d, *J* = 8.4 Hz, 2H), 7.20 (m, 2H), 7.68 (d, *J* = 8.0 Hz, 1H), 7.75 (s, 1H), 7.80 (d, *J* = 8.4 Hz, 2H); ^{13}C NMR (100 MHz, $CDCl_3$) δ 20.4, 22.6 (2C), 32.9, 116.0, 119.6, 128.8 (2C), 130.1, 130.7, 131.0, 133.6 (2C), 134.0, 140.9, 151.4; HRMS–EI (*m*/*z*): $[M - I]^+$ calcd for $C_{16}H_{18}I$, 337.0448; found, 337.0444.

Acknowledgements

We thank Prosidion Ltd and Chemistry Innovation/EPSRC for generous support and the EPSRC National Mass Spectrometry Service Centre, Swansea, for mass spectrometry data.

References

1. Yoshida, J.; Kataoka, K.; Horcajada, R.; Nagaki, A. *Chem. Rev.* **2008,** *108,* 2265–2299. doi:10.1021/cr0680843
2. Yoshida, J. *Electrochem. Soc. Interface* **2009,** *18,* 40–45.
3. For example, the large scale production of adipodinitrile (BASF) or 4-*tert*-butylbenzaldehyde (Givaudan) and also some smaller scale productions (<100 t/year) such as 1,4-dihydronaphthalene (Rhone-Poulenc) or isonicotinic acid (Reilly Tarr).
4. Wirth, T., Ed. *Microreactors in Organic Synthesis and Catalysis;* Wiley-VCH: Weinheim, Germany, 2008.
5. Yoshida, J. *Flash Chemistry;* John Wiley & Sons: Chichester, 2008.
6. Horii, D.; Atobe, M.; Fuchigami, T.; Marken, F. *Electrochem. Commun.* **2005,** *7,* 35–39. doi:10.1016/j.elecom.2004.10.012
7. Horcajada, R.; Okajima, M.; Suga, S.; Yoshida, J. *Chem. Commun.* **2005,** 1303–1305. doi:10.1039/B417388K
8. He, P.; Watts, P.; Marken, F.; Haswell, S. J. *Angew. Chem., Int. Ed.* **2006,** *45,* 4146–4149. doi:10.1002/anie.200600951
9. Nagaki, A.; Togai, M.; Suga, S.; Aoki, N.; Mae, K.; Yoshida, J. *J. Am. Chem. Soc.* **2005,** *127,* 11666–11675. doi:10.1021/ja0527424
10. Suga, S.; Nagaki, A.; Tsutsui, Y.; Yoshida, J. *Org. Lett.* **2003,** *5,* 945–947. doi:10.1021/ol0341243
11. Yoshida, J. *Chem. Commun.* **2005,** 4509–4516. doi:10.1039/B508341A
12. Kataoka, K.; Hagiwara, Y.; Midorikawa, K.; Suga, S.; Yoshida, J. *Org. Process Res. Dev.* **2008,** *12,* 1130–1136. doi:10.1021/op800155m
13. Kajiyama, D.; Inoue, K.; Ishikawa, Y.; Nishiyama, S. *Tetrahedron* **2010,** *66,* 9779–9784. doi:10.1016/j.tet.2010.11.015
14. Simms, R.; Dubinsky, S.; Yudin, A.; Kumacheva, E. *Lab Chip* **2009,** *9,* 2395–2397. doi:10.1039/b904962b
15. Amemiya, F.; Matsumoto, H.; Fuse, K.; Kashiwagi, T.; Kuroda, C.; Fuchigami, T.; Atobe, M. *Org. Biomol. Chem.* **2011,** *9,* 4256–4265. doi:10.1039/c1ob05174a
16. Pt electrodes made from Pt foil 99.95%, thickness 0.1 mm (Goodfellow Cambridge Ltd).
17. Tajima, T.; Fuchigami, T. *Chem.–Eur. J.* **2005,** *11,* 6192–6196. doi:10.1002/chem.200500340
18. Beck, F.; Haufe, J.; Nohe, H. Electrolytic condensation of carboxylic acids. U.S. Patent 3,787,299, Jan 22, 1974.
19. Kurihara, H.; Fuchigami, T.; Tajima, T. *J. Org. Chem.* **2008,** *73,* 6888–6890. doi:10.1021/jo801016f
20. Wirth, T. *Angew. Chem., Int. Ed.* **2005,** *44,* 3656–3665. doi:10.1002/anie.200500115
21. Merritt, E. A.; Olofsson, B. *Angew. Chem., Int. Ed.* **2009,** *48,* 9052–9070. doi:10.1002/anie.200904689
22. Peacock, M. J.; Pletcher, D. *Tetrahedron Lett.* **2000,** *41,* 8995–8998. doi:10.1016/S0040-4039(00)01620-8
23. Hoffelner, H.; Lorch, H. W.; Wendt, H. *J. Electroanal. Chem.* **1975,** *66,* 183–194. doi:10.1016/S0022-0728(75)80002-7
24. Katritzky, A. R.; Gallos, J. K.; Durst, H. D. *Magn. Reson. Chem.* **1989,** *27,* 815–822. doi:10.1002/mrc.1260270902
25. Peacock, M. J.; Pletcher, D. *J. Electrochem. Soc.* **2001,** *148,* D37–D42. doi:10.1149/1.1353574

License and Terms

Beilstein Journal of Organic Chemistry

Continuous flow photolysis of aryl azides: Preparation of 3*H*-azepinones

Farhan R. Bou-Hamdan‡, François Lévesque‡, Alexander G. O'Brien‡ and Peter H. Seeberger*

Letter

Open Access

Address:
Max Planck Institute of Colloids and Interfaces, Department of Biomolecular Systems, Am Mühlenberg 1, 14476 Potsdam, Germany and Freie Universität Berlin, Institute for Chemistry and Biochemistry, Arnimallee 22, 14195 Berlin, Germany

Email:
Peter H. Seeberger* - peter.seeberger@mpikg.mpg.de

* Corresponding author ‡ Equal contributors

Keywords:
azepinones; azides; continuous flow; nitrenes; photochemistry

Beilstein J. Org. Chem. **2011,** *7,* 1124–1129.
doi:10.3762/bjoc.7.129

Received: 31 May 2011
Accepted: 02 August 2011
Published: 17 August 2011

This article is part of the Thematic Series "Chemistry in flow systems II".

Guest Editor: A. Kirschning

Abstract

Photolysis of aryl azides to give nitrenes, and their subsequent rearrangement in the presence of water to give 3*H*-azepinones, is performed in continuous flow in a photoreactor constructed of fluorinated ethylene polymer (FEP) tubing. Fine tuning of the reaction conditions using the flow reactor allowed minimization of secondary photochemical reactions.

Findings

Although photochemical rearrangements are an important class of reactions for heterocycle synthesis [1,2], their use is often hindered by technical difficulties, both in research laboratories and in industry, particularly when large quantities of material are required [3,4]. In response, there has been a recent growth in the application of continuous flow techniques [5-7] for the deployment of photochemical reactions [8-13]. As, from the Beer–Lambert law, the intensity of light decreases exponentially with increasing distance from the light source, minimization of the path length in a continuous flow photoreactor ensures efficient and uniform irradiation of the sample [14], and scaling up is simple to achieve by running the reactor over an extended period. Additionally, the precise control of the reaction conditions and the continuous removal of products inherent in flow systems can offer improved yields and selectivities [8,15].

Nitrenes generated by aryl azide photolysis are important tools, both for preparative heterocycle synthesis [16,17] and for photoaffinity labeling of proteins [18-20]. The photolysis of aryl azide **1** [21], a well-studied and widely used reaction [22-30], generates the singlet aryl nitrene intermediate ^{1}**2** (Scheme 1). Ring expansion of ^{1}**2**, via 2*H*-azirine **3**, affords didehydroazepine **4**, which can be trapped by variety of nucleophiles to provide the corresponding azepine **5**. Alternatively, intersystem crossing (ISC) of ^{1}**2** gives rise to ^{3}**2**, which can

dimerize to form diazo compound **6**. Performing the reaction in the presence of water typically affords 3*H*-azepinone **7** [31-34], a moiety present in natural products [35,36] and in azepinone-derived pharmaceuticals [37,38]. Despite the importance of these 7-membered nitrogen-containing heterocycles, there remain few methods for their preparation [39-44]. Overall, aryl azides, which are simple to prepare from the corresponding aniline derivative, are convenient precursors for the synthesis of azepine derivatives. However, the utility of the process is offset by the long reaction times required and by the low yields arising from poor selectivity and decomposition of the reaction mixture. We report herein the development of a continuous flow variant of the process and show how the reaction can be further optimized using a flow system [45,46].

For this study a 14 mL photoreactor was used, constructed from fluorinated ethylene polymer (FEP) tubing, wrapped around a 450 W medium pressure Hg lamp, surrounded by a cooling jacket and Pyrex filter (see Supporting Information File 1). Continuous flow photochemical reactors based upon FEP tubing are simple to construct and are seeing increasing use in photochemical synthesis [47-49]. A recirculating cryostat maintained an apparatus temperature of 25 °C for all experiments, and a back pressure regulator (6.9 bar) was used to suppress the formation of a separate gaseous phase from the evolved nitrogen. THF and water were pumped simultaneously into the reactor at the specified rates through a commercially available Vapourtec R2 pump, [50] and mixed by a PTFE T-mixer.

Aryl azide **8a** bearing a *p*-methyl ester substituent, prepared by treatment of the corresponding aniline with $NaNO_2$/HCl–NaN_3, was selected for initial optimization of the reaction (Scheme 2). During preliminary experiments under the conditions reported by Smalley (0.05 M in THF/H_2O, 1:1) [31], blockage of the tubing was observed, which was attributed to the poor solubility of the substrate in water. Running the reaction with a reduced water content (THF/H_2O, 4:3) obviated this problem and resulted in a 62% conversion of the starting azide to 3*H*-azepinone **9a**, after a residence time of 30 min (Table 1, entry 2). Further reduction in the water content had a detrimental effect on the conversion. An inverse dependence of the conversion on substrate concentration was observed (Table 1). Although the highest conversion was observed at 0.015 M, higher productivity was obtained at 0.030 M (0.38 mmol h^{-1}). Representing the best balance between conversion and productivity, 0.030 M was selected as the optimum concentration for further optimization. The use of other polar, aprotic, water-miscible solvents for the reaction was explored. Maintaining a residence time of 30 min, no significant change in conversion was observed upon replacing THF with DME or 1,4-dioxane; decreased conversion (22%) was observed with acetonitrile as the organic solvent.

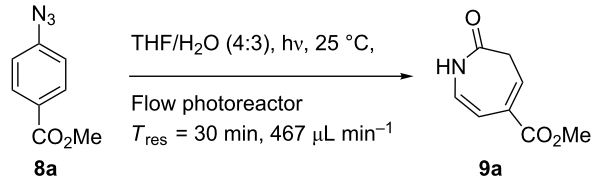

Scheme 2: Optimisation of the photolysis of aryl azide **8a**.

Increasing the residence time improved the conversion of **8a** (Figure 1), although this was accompanied by increased concomitant formation of the byproduct **10**. Lactam **10** was obtained upon re-exposure of purified **9a** to the reaction conditions and is believed to result from photochemical disrotatory electrocyclization of the 3*H*-azepinone diene moiety [51-54]

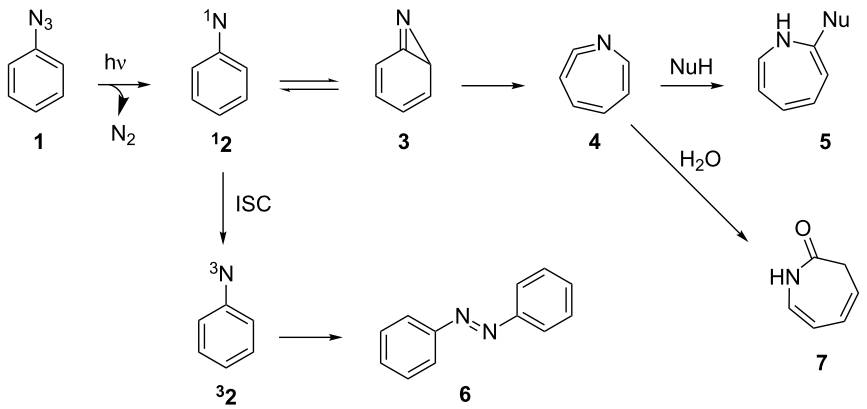

Scheme 1: Products of aryl azide photolysis.

Table 1: Effect of aryl azide concentration on conversion.

Entry	[**8a**] (M)	Conversion (%)[a]	Isolated Yield (%)
1	0.100	39	29
2	0.050	62	35
3	0.030	78	45
4	0.015	90	48

[a]By ^{1}H NMR analysis of the crude product mixture after a residence time of 30 min.

(Scheme 3). Instead of making a direct comparison between reaction progress in batch and flow, the effects of longer residence times reported for batch photolysis were evaluated in a stopped-flow experiment by irradiating a solution of **8a** for 3.5 h in the same FEP photoreactor (Figure 1). Analysis of the composition of the crude mixture showed significantly increased conversion of **9a** to **10** accompanied by a slight increase in the proportion of the starting material **8a**, which likely reflects decomposition of both of the reaction products. Overall, a residence time of 30 min was selected for a 0.030 M solution of **8a** in THF/H_2O 4:3, giving analytically pure **9a** in 45% yield. Only traces of the diazo product were observed in the NMR spectrum of the crude mixture.

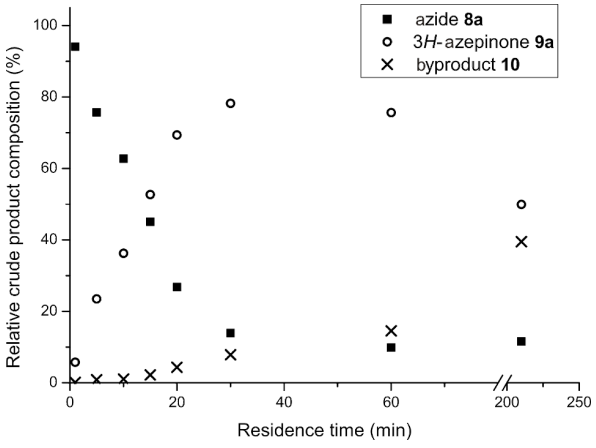

Figure 1: Relationship between residence time and relative composition of the crude reaction mixture.

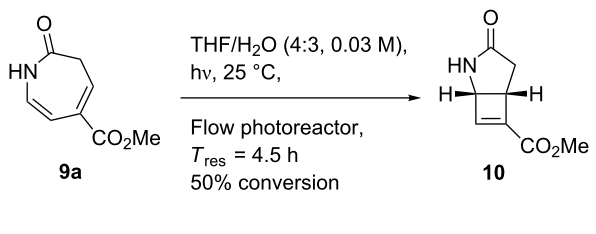

Scheme 3: Preparation of side product **10**.

A variety of other 3*H*-azepinones was prepared in moderate to good yields under the optimized reaction conditions (Scheme 4, Table 2). Residual starting material was easily recovered by silica column chromatography. Rearrangements of aryl azides bearing electron withdrawing substituents are better represented in the literature than their electron donating congeners [31], and this was reflected in our compound selection. Methyl 2-azidobenzoate (**8b**), the corresponding acid **8c** and dimethyl 2-azidoterephthalate (**8d**) each reacted favorably compared to the model substrate **8a**. We were particularly interested in the preparation of 5-aryl-3*H*-azepinones **9e–g**, examples of which have seen recent interest as γ-secretase inhibitors for the treatment of Alzheimer's disease [37]. Photolysis of methyl 2-azido-5-phenylbenzoate **8e** under the optimized conditions afforded a complex mixture of products. Upon shortening the residence time to 15 min, 3-methoxycarbonyl-5-phenyl-3*H*-azepinone (**9e**) was obtained in 35% yield. While both the corresponding acid **8f** and 4-azidobiphenyl **8g** decomposed upon photolysis, **8h** gave the corresponding 5-chloro-3*H*-azepinone **9h**, bearing a handle for further functionalization. To explore the preparation of bicyclic products, we studied the photolysis of 3-azidoquinoline (**8i**) to give the corresponding benzodiazepinone. Although the substrate decomposed under the original optimized conditions, reaction of **8i** in NaOMe–MeOH [55,56] afforded **9i** in good yield. Although yields were similar to those reported for batch processes [31,34,56], performing the reaction in continuous flow allows simple scaleup.

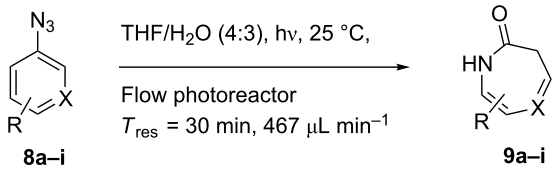

Scheme 4: General conditions for the photolysis of aryl azides in continuous flow.

In summary, the photochemical syntheses of 3*H*-azepinones and related azepines were performed and optimized in continuous flow through a photoreactor made from FEP tubing. Secondary photochemical reactions were minimized through careful control of the residence time. Although isolated yields were variable, a variety of aryl azides bearing electron withdrawing substituents underwent photolysis in good yield. Modification of the procedure allowed the preparation of benzodiazepine **9i**.

Table 2: 3*H*-azepinone derivatives prepared by photolysis of aryl azides in continuous flow.

Entry	Substrate		Product		Yield (%)[a]
1	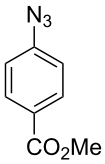	**8a**	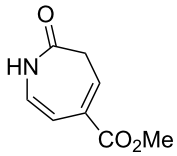	**9a**	45 (51)
2	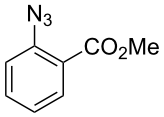	**8b**	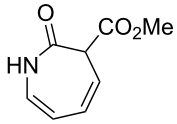	**9b**	75 (77)
3	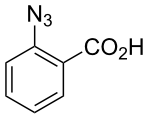	**8c**	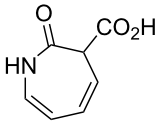	**9c**	50 (62)
4	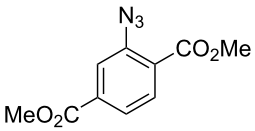	**8d**	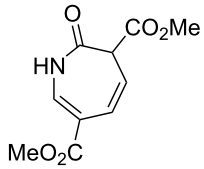	**9d**	74 (80)
5[b]	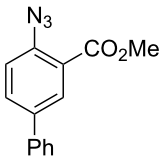	**8e**	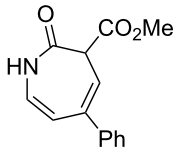	**9e**	35 (47)
6	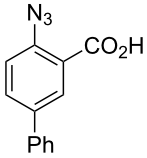	**8f**	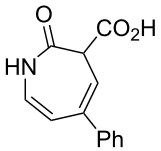	**9f**	0
7	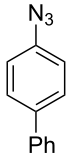	**8g**	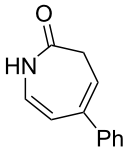	**9g**	0
8	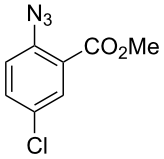	**8h**	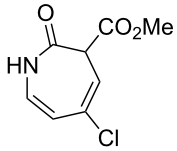	**9h**	70
9[c]	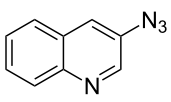	**8i**	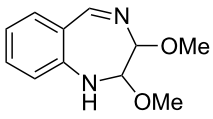	**9i**	44[d]

[a]Yields in parentheses are based on recovered starting material. [b]The residence time was reduced to 15 min. [c]The photolysis was performed with a 0.030 M solution of **8i** in 1.0 M NaOMe–MeOH. [d]Determined by ^{1}H NMR of the crude mixture.

Supporting Information

Supporting Information File 1

Description of the flow reactor setup, experimental procedures and spectroscopic data of all compounds.
[http://www.beilstein-journals.org/bjoc/content/supplementary/1860-5397-7-129-S1.pdf]

Acknowledgements

We gratefully thank the Max Planck Society, AstraZeneca R&D, Macclesfield, UK and Fonds de Recherche sur la Nature et les Technologies, Québec (postdoctoral scholarship to F. L.) for generous funding.

References

1. Hoffmann, N. *Chem. Rev.* **2008,** *108,* 1052. doi:10.1021/cr0680336
2. Bach, T.; Hehn, J. P. *Angew. Chem., Int. Ed.* **2011,** *50,* 1000. doi:10.1002/anie.201002845
3. André, J.-C.; Viriot, M.-L.; Villermaux, J. *Pure Appl. Chem.* **1986,** *58,* 907. doi:10.1351/pac198658060907
4. Pfoertner, K. H. *J. Photochem. Photobiol., A: Chem.* **1990,** *51,* 81.
5. Wirth, T., Ed. *Microreactors in Organic Synthesis and Catalysis;* Wiley-VCH: Weinheim, Germany, 2008.
6. Ehrfeld, W.; Hessel, V.; Löwe, H. *Microreactors: New Technology for Modern Chemistry;* Wiley-VCH: Weinheim, Germany, 2000.
7. Yoshida, J.-i., Ed. *Flash Chemistry: Fast Organic Synthesis in Microsystems;* John Wiley & Sons: Chichester, U.K., 2008.
8. Coyle, E. E.; Oelgemöller, M. *Photochem. Photobiol. Sci.* **2008,** *7,* 1313. doi:10.1039/b808778d
9. Bourne, R. A.; Han, X.; Poliakoff, M.; George, M. W. *Angew. Chem., Int. Ed.* **2009,** *48,* 5322. doi:10.1002/anie.200901731
10. Vasudevan, A.; Villamil, C.; Trumbull, J.; Olson, J.; Sutherland, D.; Pan, J.; Djuric, S. *Tetrahedron Lett.* **2010,** *51,* 4007. doi:10.1016/j.tetlet.2010.05.119
11. Fuse, S.; Tanabe, N.; Yoshida, M.; Yoshida, H.; Doi, T.; Takahashi, T. *Chem. Commun.* **2010,** *46,* 8722. doi:10.1039/c0cc02239j
12. Mimieux Vaske, Y. S.; Mahoney, M. E.; Konopelski, J. P.; Rogow, D. L.; McDonald, W. J. *J. Am. Chem. Soc.* **2010,** *132,* 11379. doi:10.1021/ja1050023
13. Wegner, J.; Ceylan, S.; Kirschning, A. *Chem. Commun.* **2011,** *47,* 4583. doi:10.1039/c0cc05060a
14. Shvydkiv, O.; Gallagher, S.; Nolan, K.; Oelgemöller, M. *Org. Lett.* **2010,** *12,* 5170. doi:10.1021/ol102184u
15. Maeda, H.; Mukae, H.; Mizuno, K. *Chem. Lett.* **2005,** *34,* 66. doi:10.1246/cl.2005.66
16. Bräse, S.; Gil, C.; Knepper, K.; Zimmermann, V. *Angew. Chem., Int. Ed.* **2005,** *44,* 5188. doi:10.1002/anie.200400657
17. Iddon, B.; Meth-Cohn, O.; Scriven, E. F. V.; Suschitzky, H.; Gallagher, P. T. *Angew. Chem., Int. Ed. Engl.* **1979,** *18,* 900. doi:10.1002/anie.197909001
18. Kotzyba-Hibert, F.; Kapfer, I.; Goeldner, M. *Angew. Chem., Int. Ed. Engl.* **1995,** *34,* 1296. doi:10.1002/anie.199512961
19. Sydnes, M. O.; Doi, I.; Ohishi, A.; Kuse, M.; Isobe, M. *Chem.–Asian J.* **2008,** *3,* 102. doi:10.1002/asia.200700211
20. Nielsen, P. E.; Buchardt, O. *Photochem. Photobiol.* **1982,** *35,* 317. doi:10.1111/j.1751-1097.1982.tb02568.x
21. Reiser, A.; Bowes, G.; Horne, R. J. *Trans. Faraday Soc.* **1966,** *62,* 3162. doi:10.1039/tf9666203162
22. von E. Doering, W.; Odum, R. A. *Tetrahedron* **1966,** *22,* 81. doi:10.1016/0040-4020(66)80104-7
23. DeGraff, B. A.; Gillespie, D. W.; Sundberg, R. J. *J. Am. Chem. Soc.* **1974,** *96,* 7491. doi:10.1021/ja00831a017
24. Borden, W. T.; Gritsan, N. P.; Hadad, C. M.; Karney, W. L.; Kemnitz, C. R., II; Platz, M. S. *Acc. Chem. Res.* **2000,** *33,* 765. doi:10.1021/ar990030a
25. Gritsan, N. P.; Platz, M. S. *Chem. Rev.* **2006,** *106,* 3844. doi:10.1021/cr040055+
26. Tsao, M.-L.; Platz, M. S. *J. Am. Chem. Soc.* **2003,** *125,* 12014. doi:10.1021/ja035833e
27. Li, Y. Z.; Kirby, J. P.; George, M. W.; Poliakoff, M.; Schuster, G. B. *J. Am. Chem. Soc.* **1988,** *110,* 8092. doi:10.1021/ja00232a022
28. Sundberg, R. J.; Sloan, K. B. *J. Org. Chem.* **1973,** *38,* 2052. doi:10.1021/jo00951a018
29. Budyka, M. F.; Kantor, M. M.; Alfimov, M. V. *Russ. Chem. Rev.* **1992,** *61,* 25. doi:10.1070/RC1992v061n01ABEH000929
30. Gritsan, N. P.; Pritchina, E. A. *Russ. Chem. Rev.* **1992,** *61,* 500. doi:10.1070/RC1992v061n05ABEH000959
31. Lamara, K.; Smalley, R. K. *Tetrahedron* **1991,** *47,* 2277. doi:10.1016/S0040-4020(01)96138-1
32. Lamara, K.; Redhouse, A. D.; Smalley, R. K.; Thompson, J. R. *Tetrahedron* **1994,** *50,* 5515. doi:10.1016/S0040-4020(01)80706-7
33. Koyama, K.; Takeuchi, H. *J. Chem. Soc., Perkin Trans. 1* **1982,** 1269.
34. Purvis, R.; Smalley, R. K.; Suschitzky, H.; Alkhader, M. A. *J. Chem. Soc., Perkin Trans. 1* **1984,** 249.
35. O'Hagan, D. *Nat. Prod. Rep.* **1997,** *14,* 637. doi:10.1039/np9971400637
36. Evans, P. A.; Holmes, B. *Tetrahedron* **1991,** *47,* 9131. doi:10.1016/S0040-4020(01)96203-9
37. Miller, M.; Hope, J.; Porter, W. J.; Reel, J. K.; Rubio-Esteban, A. Azepine derivatives as gamma-secretase inhibitors. U.S. Patent Appl. 2010/0197660 Aug 5, 2010.
38. Robl, J. A.; Sulsky, R.; Sieber-McMaster, E.; Ryono, D. E.; Cimarusti, M. P.; Simpkins, L. M.; Karanewsky, D. S.; Chao, S.; Asaad, M. M.; Seymour, A. A.; Fox, M.; Smith, P. L.; Trippodo, N. C. *J. Med. Chem.* **1999,** *42,* 305. doi:10.1021/jm980542f
39. Knobloch, K.; Eberbach, W. *Org. Lett.* **2000,** *2,* 1117. doi:10.1021/ol0056832
40. Knobloch, K.; Koch, J.; Keller, M.; Eberbach, W. *Eur. J. Org. Chem.* **2005,** 2715. doi:10.1002/ejoc.200400922
41. Masaki, M.; Fukui, K.; Kita, J. *Bull. Chem. Soc. Jpn.* **1977,** *50,* 2013. doi:10.1246/bcsj.50.2013
42. Atherton, F. R.; Lambert, R. W. *J. Chem. Soc., Perkin Trans. 1* **1973,** 1079.
43. Endo, Y.; Kataoko, K.-i.; Haga, N.; Shudo, K. *Tetrahedron Lett.* **1992,** *33,* 3339. doi:10.1016/S0040-4039(00)92083-5
44. Reissig, H.-U.; Böttcher, G.; Zimmer, R. *Can. J. Chem.* **2004,** *82,* 166. doi:10.1139/v03-186
45. O'Brien, A. G.; Lévesque, F.; Seeberger, P. H. *Chem. Commun.* **2011,** *47,* 2688. doi:10.1039/c0cc04481d
46. O'Brien, A. G.; Lévesque, F.; Suzuki, Y.; Seeberger, P. H. *Chim. Oggi* **2011,** *29,* 57.
47. Hook, B. D. A.; Dohle, W.; Hirst, P. R.; Pickworth, M.; Berry, M. B.; Booker-Milburn, K. I. *J. Org. Chem.* **2005,** *70,* 7558. doi:10.1021/jo050705p

48. Lainchbury, M. D.; Medley, M. I.; Taylor, P. M.; Hirst, P.; Dohle, W.; Booker-Milburn, K. I. *J. Org. Chem.* **2008,** *73,* 6497. doi:10.1021/jo801108h
49. Aggarwal, V. K.; Fang, G.; Kokotos, C. G.; Richardson, J.; Unthank, M. G. *Tetrahedron* **2006,** *62,* 11297. doi:10.1016/j.tet.2006.06.044
50. http://www.vapourtec.co.uk. (accessed July 15, 2011).
51. Odum, R. A.; Schmall, B. *Chem. Commun.* **1969,** 1299.
52. Odum, R. A.; Schmall, B. *J. Chem. Res., Synop.* **1997,** 276. doi:10.1039/a702465g
53. Chapman, O. L.; Hoganson, E. D. *J. Am. Chem. Soc.* **1964,** *86,* 498. doi:10.1021/ja01057a042
54. Paquette, L. A. 2-azabicyclo[3.2.0]hep-6-en-3-ones. U.S. Patent 3,285,934 Nov 15, 1966.
55. Sashida, H.; Fujii, A.; Tsuchiya, T. *Chem. Pharm. Bull.* **1987,** *35,* 4110.
56. Hollywood, F.; Khan, Z. U.; Scriven, E. V. F.; Smalley, R. K.; Suschitzky, H.; Thomas, D. R.; Hull, R. *J. Chem. Soc., Perkin Trans. 1* **1982,** 431.

License and Terms

Beilstein Journal of Organic Chemistry

Evaluation of a commercial packed bed flow hydrogenator for reaction screening, optimization, and synthesis

Marian C. Bryan[1], David Wernick[2], Christopher D. Hein[1], James V. Petersen[3], John W. Eschelbach[2] and Elizabeth M. Doherty[*1]

Full Research Paper

Open Access

Address:
[1]Medicinal Chemistry Research Technology, Department of Chemistry Research and Discovery, Amgen, Inc., One Amgen Center Drive, Thousand Oaks, CA 91320, USA, [2]Discovery Analytical Sciences, Department of Chemistry Research and Discovery, Amgen, Inc., One Amgen Center Drive, Thousand Oaks, CA 91320, USA and [3]Research Automation Technology, Department of Chemistry Research and Discovery, Amgen, Inc., One Amgen Center Drive, Thousand Oaks, CA 91320, USA

Email:
Elizabeth M. Doherty[*] - edoherty@amgen.com

* Corresponding author

Keywords:
catalyst leaching; CatCart®; H-Cube®; packed bed flow hydrogenation

Beilstein J. Org. Chem. **2011,** *7,* 1141–1149.
doi:10.3762/bjoc.7.132

Received: 26 May 2011
Accepted: 27 July 2011
Published: 22 August 2011

This article is part of the Thematic Series "Chemistry in flow systems II".

Guest Editor: A. Kirschning

Abstract

The performance of the ThalesNano H-Cube®, a commercial packed bed flow hydrogenator, was evaluated in the context of small scale reaction screening and optimization. A model reaction, the reduction of styrene to ethylbenzene through a 10% Pd/C catalyst bed, was used to examine performance at various pressure settings, over sequential runs, and with commercial catalyst cartridges. In addition, the consistency of the hydrogen flow was indirectly measured by in-line UV spectroscopy. Finally, system contamination due to catalyst leaching, and the resolution of this issue, is described. The impact of these factors on the run-to-run reproducibility of the H-Cube® reactor for screening and reaction optimization is discussed.

Introduction

The potential advantages of heterogeneous catalytic flow hydrogenation over traditional batch reactor processes are many and significant [1]. In particular, flow hydrogenation promises strict control of reaction parameters and, therefore, high reproducibility in reaction outcome. Additional advantages include: (1) greater safety due to the containment of the pyrophoric cata-

lyst in a cartridge, column, or microfluidic device; (2) simple product isolation, with no separate catalyst filtration step required; and (3) convenient screening of the reaction conditions and rapid sequential transformations facilitated by automation of the liquid handling.

There have been several reports published on custom flow hydrogenators, such as a Pd-immobilized 200 micron glass channel [2], a simple Pd/C packed bed bubble column reactor [3] and, more recently, a unique glass column packed bed system that introduces hydrogen across a Teflon-AF membrane [4]. In 2004, ThalesNano Inc. [5] was the first manufacturer to commercialize a convenient bench-top hydrogen flow reactor, the H-Cube®, designed for smaller-scale use in academic and drug discovery labs [6]. The reactor features a built-in hydrogen generator that functions by the electrolysis of water. Disposable pre-packed catalyst cartridges (CatCart®) are also available from ThalesNano. These cartridges consist of a solid catalyst contained within stainless steel tubes fitted with thin 8 micron frits. The manufacturer also demonstrated that high-throughput synthesis can be facilitated on the H-Cube® using a Tecan liquid handler for automated sample injection and collection of the product fractions [7]. Gilson automated liquid handling was similarly added to the H-Cube® by Ley and Ladlow [8], with the system controlled by software custom written at Aitken Scientific [9]. A similar system using a Bhodan robot and Visual Basic software was developed at Abbott Labs [10]. Subsequently, ThalesNano commercialized the system developed by Ley and Ladlow. More recently, ThalesNano has introduced a CatCart Changer® (CCC) attachment with six CatCart® port positions and a column switcher to increase throughput and facilitate screening through multiple catalysts. These ThalesNano H-Cube® systems have been used successfully for a variety of reductions; some of the more notable applications including *O*-debenzylation, CBz-hydrogenolysis, aromatic ring saturation, imine reduction, and enantioselective carbonyl reductions [8,10-13].

In our hands, the ThalesNano H-Cube® and the H-Cube® with CCC systems had previously produced experimental results that were difficult to explain. For example, we were unable to reproduce the reduction of ethyl pyridine-3-carboxylate by following the conditions reported by Kappe [11], although we were able to achieve similar results under modified conditions [14]. One of the most dramatic results we observed was the complete loss of selectivity in the reduction of an azido group in the presence of an aromatic nitrile (Scheme 1). Initially, the chemoselective reduction of azido nitrile **1** was successfully performed with a 30 mm 10% Pt/C CatCart® to afford amino nitrile **2** in 91% isolated yield. Reproduction of the same conditions on a different occasion, however, resulted in 100% conversion to the fully reduced product **3**. These unexpected results prompted us to seek a better understanding of the parameters affecting reproducibility in flow hydrogenations on the H-Cube®.

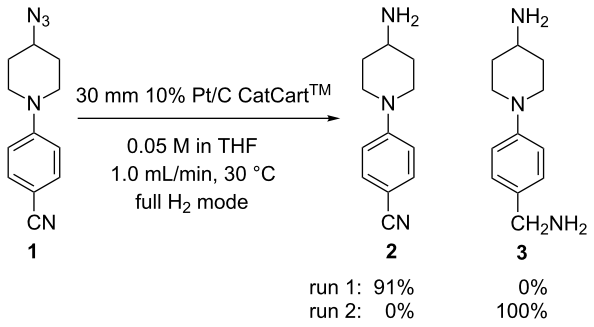

Scheme 1: Reduction of 4-(4-azidopiperidin-1-yl)benzonitrile on the H-Cube®.

Surprisingly, to date there have been few reports in the literature characterizing the influence of the H-Cube® system configuration and reaction parameters on the performance and reproducibility. Jones reported consistency in conversion over a series of nitroindole reductions [6] and in the reduction of a library of nitro-group containing molecules through the H-Cube® with the Tecan liquid handler [7]. Ley discussed the effect of temperature on the catalyst activity [8]. Kappe and co-workers showed a correlation between conversion, flow rate, and temperature [11]. But to the best of our knowledge, a systematic investigation identifying the most significant parameters affecting reproducibility and performance of the H-Cube® reactor, particularly during routine use, has not been published.

By incorporating an in-line UV detector, we previously characterized dispersion in the H-Cube® and the effect of that dispersion on the reaction outcome [15]. As a result of that study, we generated a predictive correlation between non-steady state and continuous flow scale-up conditions for simple reductions. In this report, using the reduction of styrene to ethylbenzene over 10% Pd/C as a model, we examine the H-Cube® reactor performance: (1) across different pressure settings, (2) over a series of sequential reactions, and (3) using different commercial CatCart® cartridges. For these studies, two reactor configurations were employed. In the first, a "stand-alone" H-Cube® (SAH^3) was equipped with a manual injector port and in-line UV detector (Figure 1). The second system ($AutoH^3$) consisted of an H-Cube® with CCC, equipped with a Gilson 215 liquid handler and programmed using the ThalesNano auto sampler software.

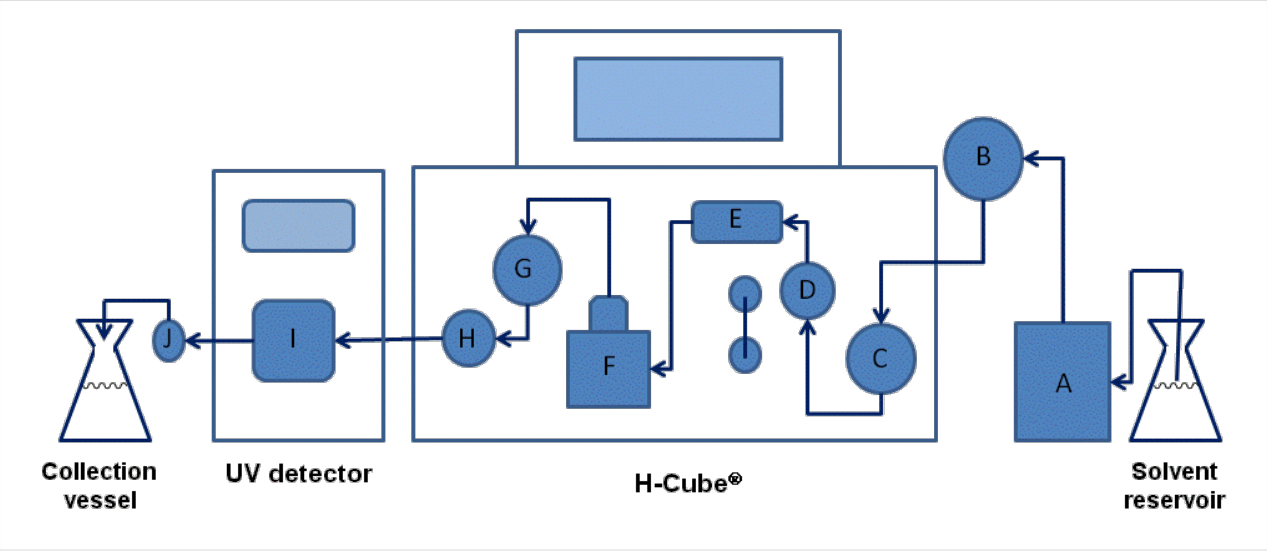

Figure 1: SAH[3] schematic with injector port and UV detector. Components: (A) pump; (B) six-position manual injector port; (C) inlet pressure sensor; (D) gas–liquid mixing chamber; (E) bubble detector; (F) CatCart® holder; (G) outlet pressure sensor; (H) back pressure regulator; (I) UV flow cell; (J) 10 bar fixed in-line back pressure regulator. Arrows indicate the flow direction.

Results and Discussion

Hydrogen variability

The H-Cube® introduces hydrogen to the reactant stream in one of two different modes: "Full H_2" and "controlled". In the full H_2 mode, the maximum amount of hydrogen that can be produced by the electrolytic cell (25 mL/min [16]) is delivered into the gas mixing chamber (D, Figure 1) with no back pressure at the outlet of the system (G, Figure 1). When running in full H_2 mode, the resultant system pressure is reported on the touch screen panel as 0–1 bar. In comparison to full H_2 mode, the flow rate of hydrogen in the controlled mode is dependent upon the liquid back pressure. The controlled mode settings (10 bar to 100 bar) are used to set the total back pressure (G, Figure 1) while the system maintains a roughly constant pressure differential between the hydrogen inlet pressure (internal sensor) and the liquid inlet pressure (C, Figure 1). As a consequence of this engineering design, setting the system to the controlled mode introduces less hydrogen into the reactant stream than in the full H_2 mode setting.

As an indirect measure of the availability of hydrogen during the course of a reaction in the controlled mode setting, the reduction of styrene to ethylbenzene was monitored by in-line UV using the SAH[3] system. The extinction coefficient of styrene, and the related absorbance at 265 nm, is significantly greater than that of the reduced product ethylbenzene. When the reaction is performed under hydrogen-limited conditions (high substrate concentration, excess catalyst), any increases in absorption observed over the course of the reaction correlate with a decrease in the available hydrogen. Six sequential 2 mL injections of styrene solutions in MeOH, alternating between 0.2 M and 0.4 M concentration, were made and the course of the reductions (80 bar in controlled mode, 1 mL/min, 35 °C) was followed by UV spectroscopy (Figure 2). UV traces from runs 3 and 5 represent uninterrupted, full conversion to ethylbenzene, with short spikes in the curve corresponding to bubbles passing through the flow cell. In four out of six of the reactions (runs 1, 2, 4, and 6), peaks corresponding to unreacted styrene were observed. As expected, the effect of fluctuations in hydrogen availability was more pronounced at higher styrene concentrations (runs 2, 4, and 6). While the system was running, the release of gas from the eluent stream (observed as "sputtering") would cease intermittently, which was another indicator of fluctuations in hydrogen availability. Whether these fluctuations are due to inconsistent production of hydrogen by the electrolytic cell, or are consequences of the design of the hydrogen flow controlling system, is not clear. This behavior was observed on each of the three unique H-Cube® reactors tested (including an instrument loaned by ThalesNano) and so appears to be associated with the design of the system and is not an isolated mechanical issue.

A series of experiments were then performed at different pressure settings with the AutoH[3] system. In these experiments the full H_2 mode was compared to the controlled mode at pressure settings of 10, 30, 60, 80 and 100 bar. Final conversion of styrene to ethylbenzene was monitored by GC–MS with decane as an internal standard. The results are shown in Figure 3. At a concentration of 0.5 M styrene, the reactions conducted at 1 bar in the full H_2 mode afforded the highest average conversion (100%, $n = 5$ experiments). In the controlled mode, the conversion was lower for all settings, with a progressive increase in

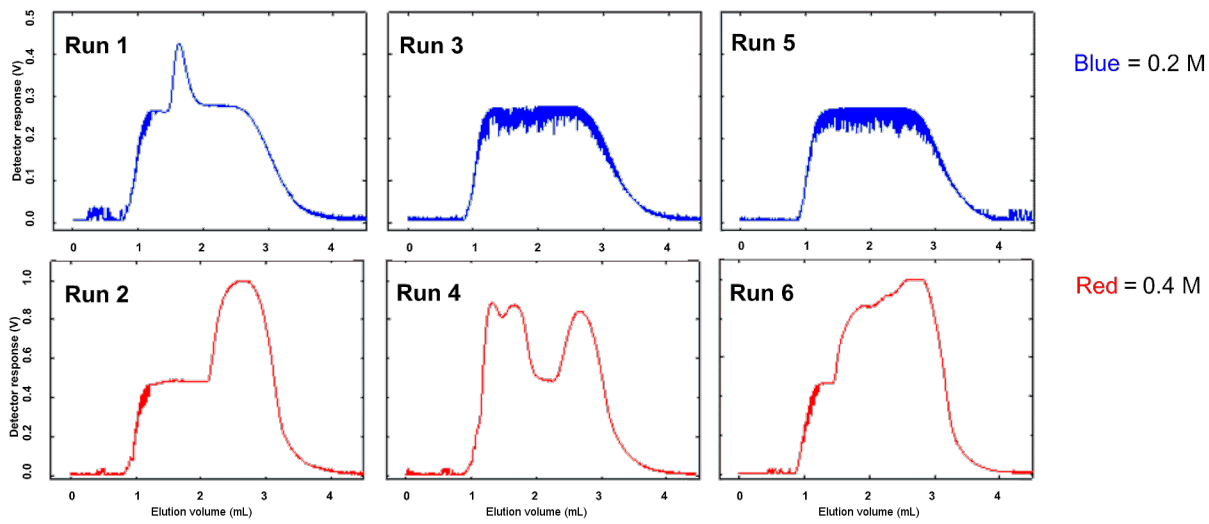

Figure 2: Variation in UV absorbance during the reduction of styrene to ethylbenzene, in the controlled mode on SAH[3], demonstrating variable hydrogen availability. Reactions were carried out through a 10% Pd/C 30 mm CatCart®, at pressure setting 80 bar, MeOH, with flow rate 1.0 mL/min, and temperature 35 °C, and were monitored at 265 nm.

the conversion correlating with increasing pressure. Significantly, the variability in the conversion increased with increasing pressure, with the largest ranges observed at 60 bar (68.8–81.6%), 80 bar (67.5–84.7%), and 100 bar (80.3–95.2%). This variability was not observed at lower styrene concentrations (0.05 M, Figure 3 results in red), where at both 10 bar and at 80 bar 100% conversion to ethylbenzene was observed. It should be noted that 0.05 to 0.10 M is the working concentration range recommended by the manufacturer. Nevertheless, the results suggest that data must be interpreted with caution when controlled mode settings are used.

In the case of the experiments at 80 bar and 100 bar in Figure 3, several of the reactions were accompanied by a warning in the software results panel: "Collected with Error (instability detected)". According to ThalesNano, this warning indicates that during some part of the run no hydrogen was detected by the bubble detector (E, Figure 1). The results from these reactions were excluded from statistical analysis, however, the observation prompted us to examine the frequency with which such errors occur during the routine use of the H-Cube®. Table 1 shows the accumulated results from 586 experiments recorded in the 13 months after installation of the AutoH[3] system and software. There were no instabilities detected in any of the 535 experiments run in the full H_2 mode setting. In comparison, instability was detected in 20% (10 out of 51) of the experiments run in a controlled mode setting. Instability occurred more frequently at higher pressure settings or when a controlled mode experiment came directly after an experimental run at a lower pressure setting (see Supporting Information File 1, Appendix A).

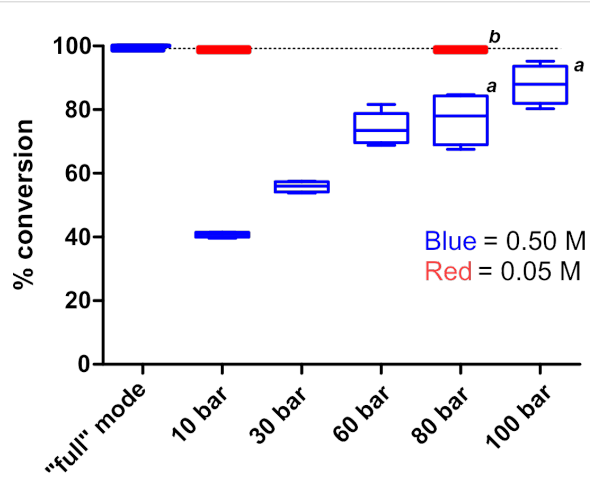

Figure 3: Box plot of data showing the percent conversion of styrene to ethylbenzene as a function of pressure. All reactions were performed using a 10% Pd/C 30 mm CatCart®, MeOH, flow rate 1.0 mL/min, at 30 °C, with 1.9 mL per injection and 10 mL product solution collected. The conversion was determined by GC–MS analysis with decane as an internal standard; n = 5 unless otherwise indicated. Data represented in blue correspond to 0.50 M styrene in MeOH. Data represented in red correspond to 0.050 M styrene in MeOH. [a]n = 4. [b]n = 1.

Catalyst cartridge variability

The performance of the ThalesNano CatCart® cartridges was examined by measuring the conversion of styrene to ethylbenzene in MeOH over 10% Pd/C. Based on our previous observations, the full H_2 mode was used to afford the greatest consistency in hydrogen availability. The reactions were run at a high concentration (2.0 M) in order to achieve an incomplete reduction and hence observe any variability in the conversion. The

Table 1: The number of experiments during which an "instability" was detected and automatically recorded by the AutoH^3 system. Experiments were conducted at flow rates in the range of 0.5 to 2.0 mL/min.

Pressure setting	Total # experiments	Instability detected
Full H_2 mode	535	0
Controlled mode 10 bar	10	1
Controlled mode 30 bar	6	0
Controlled mode 60 bar	20	3
Controlled mode 80 bar	10	5
Controlled mode 100 bar	5	1

first series of experiments shows the conversion over 20 reactions in sequence through a single CatCart® (Figure 4). The range of variation was low (56.4–60.2%) and the average conversion did not diminish over time, indicating that no activity was lost due to catalyst poisoning or leaching of metal from the catalyst bed.

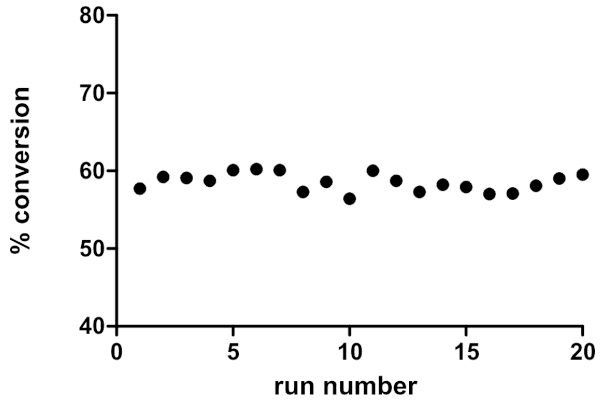

Figure 4: Conversion of styrene to ethylbenzene over 20 reactions in sequence through a single 30 mm 10% Pd/C CatCart®. All reactions were carried out with a 10% Pd/C 30 mm CatCart®, with 2.0 M in MeOH, at a flow rate of 1.0 mL/min, at 30 °C, with 1.9 mL per injection, and 10 mL product solution collected. The conversion was determined by GC–MS analysis with decane as an internal standard.

In the next series of experiments, commercial 30 mm 10 % Pd/C CatCart® cartridges were selected at random from two different lots and were used to examine differences in performance from lot to lot and from cartridge to cartridge. Each cartridge was placed in port position 1 on the AutoH^3 system, three styrene reductions were performed, and then the cartridge was replaced. In all examples, the catalyst was prereduced under the full H_2 mode and prewashed with MeOH. The results for six CatCart® cartridges (Figure 5) show a significant variation in the individual cartridge performance (38.5–100% conversion), but with minimal run-to-run variability for any given cartridge over three sequential experiments.

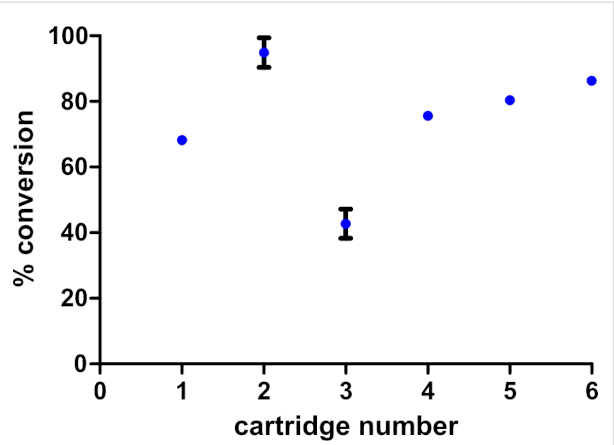

Figure 5: Cartridge-to-cartridge variability of the substrate conversion based on the reduction of styrene to ethylbenzene. All reactions were carried out at 2.0 M in MeOH, at a flow rate of 1.0 mL/min, at 30 °C, with 1.9 mL per injection, and 10 mL product solution collected; n = 3 experiments for each cartridge. The conversion was determined by GC–MS analysis with decane as an internal standard. Commercial 10% Pd/C 30 mm CatCart® cartridges were used; numbers 1, 2, and 3 from lot #02946; numbers 4, 5, and 6 from lot #02938.

The observed variations in cartridge performance may be attributed to a number of causes such as lot-to-lot variations in the catalyst, variability in mass loading, channeling effects, and column packing technique [17,18]. For example, Makkee and coworkers conducted a thorough investigation of the challenges associated with the scaling down of a "trickle bed" flow hydrogenator [19] and showed that both particle size homogeneity and column packing technique [18,20] have an impact on the conversion and the reproducibility. Whatever the causes, it appears that for any given cartridge the relative loading can be calibrated against a known reaction (such as styrene reduction). As long as that reaction does not reduce the catalytic activity of the cartridge, the subsequent behavior of the cartridge may be predicted with some level of confidence.

Cross-contamination

Catalyst cross-contamination from run to run has a profound effect on the results of the catalyst screening. To investigate cross-contamination in a typical catalyst screening experiment with the AutoH^3 system, we performed the styrene reduction sequentially through all six CCC port positions, alternating the cartridge between 30 mm 10% Pd/C CatCart® cartridges (ports 1, 3, and 5) and 30 mm quartz CatCart® cartridges (ports 2, 4, and 6). For each reaction, 1.0 mL of 0.5 M styrene in MeOH was injected and the reactions conducted at 30 °C, at a flow rate of 1.0 mL/min, in the full H_2 mode. The sequence of reactions was conducted in order, from port 1 through to port 6 (Figure 6). The results clearly demonstrate that the active catalyst was leached from the 10% Pd/C CatCart® cartridges and contaminated the subsequent experiments. The reaction

sequence was repeated an additional six times, with the same cartridges in positions 1 through 6, for a total of 42 reactions in sequence (see Supporting Information File 1, Appendix B). At the end of the sequence of experiments, the conversion due to background contamination had reduced to 15%, which is still a significant value. The conversion due to background contamination was subsequently reduced to 0–5%, at 0.5 M concentration of styrene, after the system was washed by injections of acetic acid, dimethylformamide, and MeOH, in that order [21].

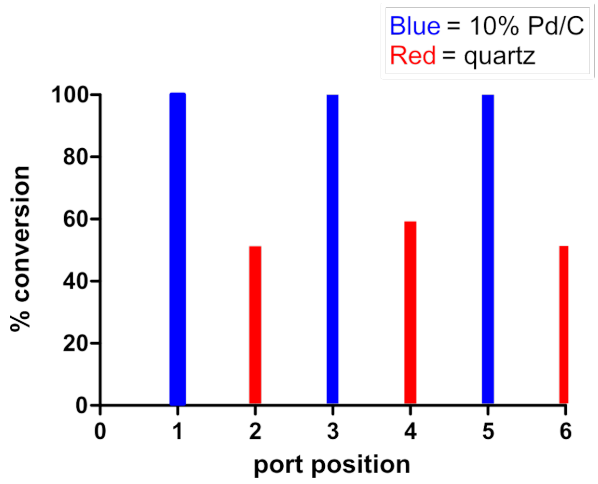

Figure 6: Conversion of styrene to ethylbenzene in a sequence of reactions alternating between 10% Pd/C and quartz-loaded CatCart® cartridges on the AutoH^3 system. All reactions were carried out at a flow rate of 1.0 mL/min, at 30 °C, with 0.5 M styrene in MeOH, with 1 mL injection per reaction, and run in order from 1 through to 6. The conversion was determined by GC–MS analysis with decane as an internal standard. Data represented in blue correspond to reactions performed through a 30 mm 10% Pd/C CatCart®. Data represented in red correspond to reactions performed through 30 mm quartz CatCart®.

The results of these experiments prompted us also to examine the SAH^3 system for residual system contamination. Prior to this examination, the SAH^3 had been utilized for a variety of applications requiring the Pd, Pt, Rh and Raney Ni-containing CatCart® cartridges. Two experiments were run with 2 mL injections of 0.5 M styrene in MeOH (30 mm quartz CatCart®, 1.0 mL/min, full H_2 mode) resulting in 22.5% and 23.6% conversion due to background contamination (Table 2, entry 1). After washing with AcOH, DMF, and MeOH [22], the background reduction was reduced to 14.0–16.4% (Table 2, entry 2). To reduce the contamination further, the accessible parts of the system were removed and sonicated in 5 N HCl followed by MeOH. The stainless steel CatCart® holder was contaminated with a dark residue that did not yield to cleaning by sonication or other mechanical means, so the holder was replaced. The Teflon membrane in the back-pressure regulator was replaced, as was the stainless steel mixing frit in the gas–liquid mixing chamber. After re-assembly and priming with MeOH, the level of conversion due to background contamination at 0.5 M styrene concentration was reduced to 2.2–3.2% (Table 2, entry 3), however, when the reaction was repeated at lower concentration (0.05 M styrene, manufacturer recommended), 6.1% and 11.5% conversion was observed (Table 2, entry 4).

Table 2: Background reduction of styrene to ethylbenzene caused by catalyst contamination on the SAH^3 system.[a]

Entry	Details	[Styrene]	Conversion[b]
1	Prior to system wash	0.5 M	22.5, 23.6%
2	After system wash with AcOH, DMF, MeOH	0.5 M	14.6, 14.0, 16.4%
3	After system wash, disassembly and cleaning, test run 1	0.5 M	2.2, 3.0, 3.2%
4	After system wash, disassembly and cleaning, test run 2	0.05 M	6.1, 11.5%

[a]All reactions were performed in MeOH using a 30 mm quartz CatCart® at a flow rate of 1.0 mL/min, full H_2 mode, 30 °C, 2 mL injection per reaction, 10 mL volume collected. [b]Conversion determined by GC–MS analysis with decane as an internal standard. Individual results from multiple experiments are shown.

The location of the remaining contamination was deduced through a series of bypass experiments (Table 3). The reduction was performed at 0.05 M styrene concentration with modifications to the reactor configuration as follows: (1) product was collected directly after passing through the CatCart® by disconnection of the tubing from the outlet pressure sensor (Figure 1, G), and 0% conversion was observed (Table 3, entry 1); (2) tubing was re-routed directly from the CatCart® holder to the back pressure regulator (Figure 1, H), thus bypassing the outlet pressure sensor, and resulting again in 0% conversion (Table 3, entry 2); finally, (3) tubing was disconnected from the back pressure regulator and product was collected after passing through the outlet pressure sensor, resulting in 5.5% and 8.8% conversions (Table 3, entry 3). Thus the remaining catalyst contamination was isolated to the outlet pressure sensor. Back-flushing the sensor with MeOH, 10% HNO_3, water, and DMF failed to remove this contamination [23]. The problem was resolved by replacement of the sensor.

These results led us to suspect that solid catalyst particles were escaping from the catalyst cartridge and becoming trapped in the pressure sensor. To measure the amount of Pd washed from a CatCart®, we re-configured the SAH^3 system to collect eluent directly downstream of the CatCart® holder. A series of 10 mL aliquots of MeOH were collected sequentially from a previously unused 30 mm 10% Pd/C CatCart® and the aliquots were

Table 3: Background reduction bypass experiments.[a]

Entry	Details	[Styrene]	Conversion[b]
1	Post-wash, back pressure regulator (H) and pressure sensor (G) bypassed	0.05 M	0%
2	Post-wash, pressure sensor (G) bypassed	0.05 M	0%
3	Post-wash, back pressure regulator (H) bypassed	0.05 M	5.5, 8.8%

[a]All reactions were performed in MeOH through a 30 mm quartz CatCart® at a flow rate of 1.0 mL/min, full H_2 mode, 30 °C, 2 mL injection per reaction, 10 mL volume collected. [b]Conversion determined by GC–MS analysis with decane as an internal standard. Individual results from multiple experiments are shown.

analyzed for Pd content by ICP–MS. The washing process was conducted in the full H_2 mode, at a flow rate of 2.0 mL/min, at 30 °C, to simulate a typical experiment. In the first 10 mL aliquot, 1.9 ppm of Pd was detected, corresponding to 19 μg Pd metal. In the subsequent three 10 mL aliquots, less than 1 ppm Pd was detected. When the wash samples were allowed to stand, a fine black free-flowing precipitate settled at the bottom of the first collection vial, whereas in the subsequent aliquot none was observed (Figure 7). It should be noted that Kappe observed a "Pd mirror" due to soluble Pd leaching from a CatCart® during a continuous flow Mizorki–Heck reaction [24]. In comparison, the fine black precipitate seen in our wash experiment is more consistent with solid Pd/C catalyst. The experiment was repeated with a new 30 mm 10% Pd/C CatCart® (from the same lot) to give 16 μg of Pd in the first 10 mL wash solvent. While this mass accounts for only ~0.1% of the average 150 mg catalyst loading per cartridge, the particle size is apparently very small and thus the relative catalytic activity is enhanced [25]. In addition, the contamination appears to accumulate through continued use of the reactor, presenting a signficant challenge with regard to performance stability. It should be noted that after thorough decontamination of the reactor we were able to reproduce the high chemoselectivity observed in the azide reduction in Scheme 1.

These observations, coupled with the previously discussed cartridge-to-cartridge performance variability, suggest that the best routine practice in handling commercial CatCart® cartridges is to wash with MeOH first, followed by calibration against a known reaction, prior to use. We are currently evaluating the effectiveness of this protocol, in combination with the use of inline filters, on a larger sample of cartridges.

Conclusion

We have shown that, for packed bed heterogeneous flow hydrogenation using the H-Cube® reactor, (1) inconsistencies in the delivery of hydrogen in the controlled mode, (2) variable performance of the catalyst cartridges, and (3) system contamination can all result in significant variability of the reaction outcome, particularly at high substrate concentrations. It is important to reiterate that the manufacturer recommends a maximum working concentration of 0.1 M in order to mitigate the issues observed under hydrogen-limited conditions. Based on our improved understanding of the scope and limitations of the H-Cube® reactor, we have applied the system to a variety of transformations and have achieved reproducible results. These results will be the subject of future reports.

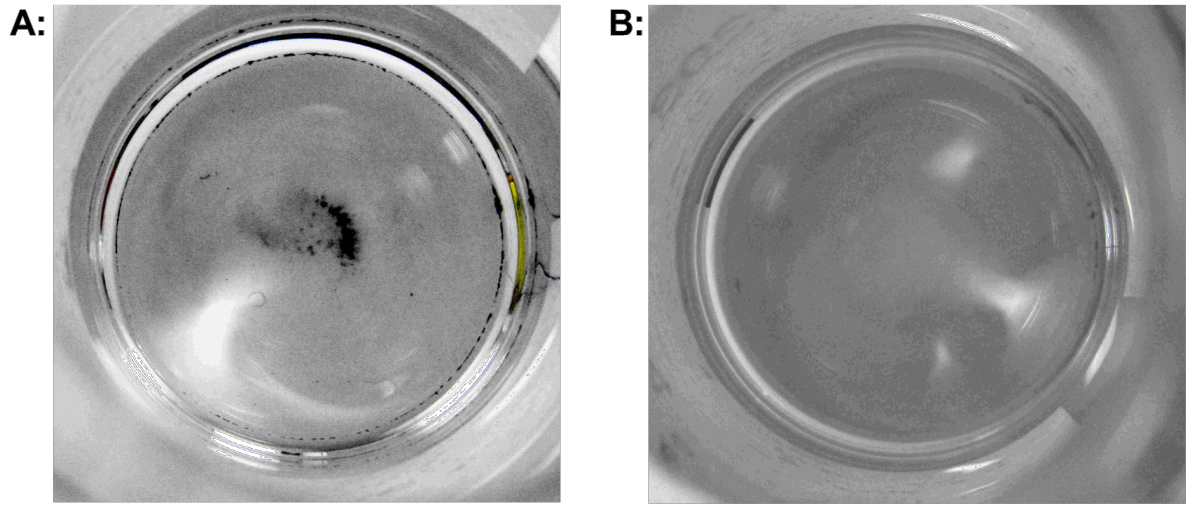

Figure 7: Leached catalyst from 30 mm 10% Pd/C CatCart®. First 10 mL wash aliquot (A) compared to second 10 mL wash aliquot (B). Photographs were taken from above, with the samples in 20 mL scintillation vials.

Experimental

Instrument set up

SAH^3 reactor configuration. A standard H-Cube® hydrogenation flow reactor (ThalesNano Technology, Inc., Budapest, Hungary) was adapted to allow for fixed-loop injections and real-time monitoring by UV. The schematic is shown in Figure 1. The injector was a 6-port manual injector (Model C2-2006, Valco Instruments, Houston, TX) and the injection loop was obtained from Valco with a fixed volume of 2 mL. An LC-10A UV–vis detector (Shimadzu Corp., Columbia, MD) with a prep flow cell (0.1 mm path length) was connected downstream of the H-Cube®. Backpressure in the system was maintained at a minimum of 10 bar by an Upchurch back pressure regulator (Model M-410, Idex HS, Oak Harbor, WA) with an internal volume of 6 μL. Connection tubing between the HPLC pump and H-Cube® was 0.020" i.d. stainless steel with 1/16" Valco HPLC fittings and lengths as short as possible to accommodate the unit in a standard bench top configuration. The tubing leaving the H-Cube® was 0.007" i.d. stainless steel (as part of the flow cell) and PEEK (as part of the Upchurch back pressure regulator).

AutoH^3 reactor configuration. A standard H-Cube® with CatCart Changer® (ThalesNano Technology, Inc., Budapest, Hungary) was connected to a Gilson 215 liquid handler (Gilson Inc., Middleton, WI). The liquid handler bed was configured to hold 20 mL conical-bottom glass vials in a 14-vial Gilson rack (rack code 24) for sample injections. The bed was also configured to hold 14-vial Gilson racks containing 20 mL, septa capped, scintillation vials for product collection. The liquid handler was equipped with a 5 mL sample loop. Reaction sequences were programmed through the ThalesNano H-Cube® auto sampler software.

Reaction protocols

Solutions of styrene (ReagentPlus®, ≥99% purity) in MeOH (Chromasolv®, HPLC grade, ≥99.9%) were prepared in volumetric flasks, with 0.5 equiv anhydrous decane (≥99% purity) included as an internal standard for quantification by GC. All reagents were purchased from Sigma-Aldrich and used as received. The CatCart® cartridges were purchased from ThalesNano Technology, Inc. and, unless otherwise indicated, were washed with MeOH in the full H_2 mode, at a flow rate of 1.0 mL/min, at 30 °C, for 10 minutes prior to use.

For reactions on the SAH^3 system, the 2 mL injection loop was filled by injection of a 1.5 fold excess of the loop volume before each injection by a standard syringe with Luer-lock tip. During each filling, ~0.1 mL volume was left in the syringe to ensure that no air bubbles were introduced into the loop. Volumetric flow rate, system pressure, and temperature were controlled using the H-Cube® front panel.

For reactions on the AutoH^3 system, reagent solutions were charged to 20 mL conical vials and sealed with septa screw caps. Reaction conditions were programmed using the ThalesNano H-Cube® sampler software. Unless otherwise noted, for each reaction a 1.9 mL injection was made and 10 mL product volume was collected in a 20 mL septa-capped scintillation vial.

Analytical methods

The UV signal was monitored at a fixed wavelength of 265 nm with a LabJack U3 DAQ (Lakewood, CO) used to acquire the analog output from the in-line UV detector, at an acquisition rate of 20 Hz. Raw data was processed in Microsoft Excel and SigmaPlot (Systat Software, San Jose, CA).

Product mixtures were analyzed by GC–MS with a Hewlett Packard HP 6890 series GC equipped with a CTC analytics-MSPAL auto injector and a HP 5973 mass selective detector [transmission quadrupole mass spectrometer, electron ionization (EI)]. An Agilent J&W DB-XLB 30 m × 0.25 mm i.d. capillary column, with a 0.5 micron film, was used in combination with the following oven temperature program: An initial temperature of 70 °C held for 5.0 min, then a 50 °C/min ramp to the final temperature of 200 °C, held for 1.0 min. The injector temperature was set to 250 °C and the ion source temperature was set to 230 °C. Helium (grade 5.0 purity, 100%) was used as the carrier gas with a gas flow of 37 cm/s average linear velocity and at a pressure of 8.90 psi. Either a split method (50:1 split ratio, 50 mL/min split flow) or a splitless method was used, depending upon sample concentration. Samples were diluted to 0.04 M when the split method was used, or to 0.004 M when the splitless method was used. Mass data was acquired after a 3.00 min solvent delay, and scan parameters covered the range of 15.0–550.0 amu. Data analysis was performed using Agilent GC/MSD Chemstation software.

Supporting Information

Supporting information features experimental queues for which an "instability detected" status was recorded by the auto sampler software during the run, and a full data set for the alternating Pd/quartz experiment.

Supporting Information File 1

Experimental queues and alternating Pd/quartz results.
[http://www.beilstein-journals.org/bjoc/content/supplementary/1860-5397-7-132-S1.pdf]

Acknowledgements

The authors thank Richard V. Jones, Paul Whittles and Alan Boyle of ThalesNano Technology for helpful discussions and technical support. We also thank our Amgen colleagues Alan Allgeier, Alex Mladenovic, Craig Schulz, and particularly Peter Grandsard for supporting these efforts. Thanks also to Chris Scardino for the ICP–MS analysis.

References

1. Frost, C. G.; Mutton, L. *Green Chem.* **2010,** *12,* 1687–1703. doi:10.1039/c0gc00133c
2. Kobayashi, J.; Mori, Y.; Okamoto, K.; Akiyama, R.; Ueno, M.; Kitamori, T.; Kobayashi, S. *Science* **2004,** *304,* 1305–1308. doi:10.1126/science.1096956
3. Yoswathananont, N.; Nitta, K.; Nishiuchi, Y.; Sato, M. *Chem. Commun.* **2005,** 40–42. doi:10.1039/b410014j
4. O'Brien, M.; Taylor, N.; Polyzos, A.; Baxendale, I. R.; Ley, S. V. *Chem. Sci.* **2011,** *2,* 1250–1257. doi:10.1039/c1sc00055a
5. ThalesNano Nanotechnology Inc., Graphisoft Park, H-1031 Budapest, Zahony u.7., Hungary. http://www.ThalesNano.com.
6. Jones, R. V.; Godorhazy, L.; Varga, N.; Szalay, D.; Urge, L.; Darvas, F. *J. Comb. Chem.* **2006,** *8,* 110–116. doi:10.1021/cc050107o
7. Jones, R.; Gödörházy, L.; Szalay, D.; Gerencsér, J.; Dormán, G.; Ürge, L.; Darvas, F. *QSAR Comb. Sci.* **2005,** *24,* 722–727. doi:10.1002/qsar.200540006
8. Knudsen, K. R.; Holden, J.; Ley, S. V.; Ladlow, M. *Adv. Synth. Catal.* **2007,** *349,* 535–538. doi:10.1002/adsc.200600558
9. Aitken Scientific Ltd, Sanderum House, Oakley Road, Chinnor, Oxfordshire, OX39 4TW, UK, http://www.aitken-sci.com.
10. Clapham, B.; Wilson, N. S.; Michmerhuizen, M. J.; Blanchard, D. P.; Dingle, D. M.; Nemcek, T. A.; Pan, J. Y.; Sauer, D. R. *J. Comb. Chem.* **2008,** *10,* 88–93. doi:10.1021/cc700178a
11. Irfan, M.; Petricci, E.; Glasnov, T. N.; Taddei, M.; Kappe, C. O. *Eur. J. Org. Chem.* **2009,** 1327–1334. doi:10.1002/ejoc.200801131
12. Saaby, S.; Knudsen, K. R.; Ladlow, M.; Ley, S. V. *Chem. Commun.* **2005,** 2909–2911. doi:10.1039/b504854k
13. Cserényi, S.; Szőllősi, G.; Szőri, K.; Fülöp, F.; Bartók, M. *Catal. Commun.* **2010,** *12,* 14–19. doi:10.1016/j.catcom.2010.08.008
14. Kappe reported a 92% yield of ethyl piperidine-3-carboxylate from ethyl pyridine-3-carboxylate, using the H-Cube®, with substrate concentration 0.05 M in AcOH, Pt/C, at 100 bar, H_2 controlled mode setting, at 100 °C, and 0.5 mL/min flow rate. We were unable to reproduce those conditions due to stabilization issues. By changing the solvent to 0.5 M AcOH in EtOH, we achieved 100% conversion in the full mode (0.05 M substrate, 10% Pt/C, 100 °C, 0.5 mL/min). Repeating our modified conditions at 100 bar in the H_2 controlled mode reduced the conversion to 78%.
15. Eschelbach, J. W. *manuscript in progress.*
16. Personal communication with Richard V. Jones of ThalesNano.
17. Fogler, H. S. *Elements of Chemical Reaction Engineering,* 4th ed.; Prentice Hall: New Jersey, 2005.
18. van Herk, D.; Castaño, P.; Quaglia, M.; Kreutzer, M. T.; Makkee, M.; Moulijn, J. A. *Appl. Catal., A* **2009,** *365,* 110–121. doi:10.1016/j.apcata.2009.06.003
19. van Herk, D.; Kreutzer, M. T.; Makkee, M.; Moulijn, J. A. *Catal. Today* **2005,** *106,* 227–232. doi:10.1016/j.cattod.2005.07.180
20. van Herk, D.; Castaño, P.; Makkee, M.; Moulijn, J. A.; Kreutzer, M. T. *Appl. Catal., A* **2009,** *365,* 199–206. doi:10.1016/j.apcata.2009.06.010
21. The AutoH^3 system was washed by replacing the solvent reservoirs (at both the Gilson and the Knauer pump) with wash solvent, then injecting 1.9 mL wash solvent through each CatCart Changer™ port position (quartz CatCart® cartridges), sequentially, and collecting 10 mL of wash solvent per injection.
22. The SAH^3 system was washed by replacing the solvent reservoir with wash solvent and installing a 30 mm quartz CatCart® in the holder. Wash solvent was pumped at a rate of 1.0 mL/min for 10–40 min per solvent, with the system set to the full H_2 mode at 30 °C.
23. Back-flushing was performed by plumbing directly from the Knauer pump to the outlet pressure sensor, with flow direction reversed, and disconnecting the remaining plumbing. The sensor was flushed with MeOH (15 mL, 3 mL/min), 10% HNO_3 (100 mL, 2 mL/min), water (100 mL, 2 mL/min), and DMF (10 mL by syringe).
24. Glasnov, T. N.; Findenig, S.; Kappe, C. O. *Chem.–Eur. J.* **2009,** *15,* 1001–1010. doi:10.1002/chem.200802200
25. Auer, E.; Freund, A.; Pietsch, J.; Tacke, T. *Appl. Catal., A* **1998,** *173,* 259–271. doi:10.1016/S0926-860X(98)00184-7

Beilstein Journal of Organic Chemistry

Scaling up of continuous-flow, microwave-assisted, organic reactions by varying the size of Pd-functionalized catalytic monoliths

Ping He[1], Stephen J. Haswell[*1], Paul D. I. Fletcher[1], Stephen M. Kelly[1] and Andrew Mansfield[2]

Full Research Paper

Open Access

Address:
[1]Department of Chemistry, University of Hull, Hull HU6 7RX, UK and [2]Pfizer Global Research & Development, Sandwich, Kent CT13 9NJ, UK

Email:
Stephen J. Haswell[*] - s.j.haswell@hull.ac.uk

* Corresponding author

Keywords:
continuous flow; microwave heating; monolith; scaling-up; Suzuki–Miyaura reaction

Beilstein J. Org. Chem. **2011,** *7,* 1150–1157.
doi:10.3762/bjoc.7.133

Received: 17 May 2011
Accepted: 02 August 2011
Published: 23 August 2011

This article is part of the Thematic Series "Chemistry in flow systems II".

Guest Editor: A. Kirschning

Abstract

A product-scalable, catalytically mediated flow system has been developed to perform Suzuki–Miyaura reactions under a microwave heating regime, in which the volumetric throughput of a Pd-supported silica monolith can be used to increase the quantity of the product without changing the optimal operating conditions. Two silica monoliths (both 3 cm long), with comparable pore diameters and surface areas, were fabricated with diameters of 3.2 and 6.4 mm to give volumetric capacities of 0.205 and 0.790 mL, respectively. The two monoliths were functionalized with a loading of 4.5 wt % Pd and then sealed in heat-shrinkable Teflon® tubing to form a monolithic flow reactor. The Pd-supported silica monolith flow reactor was then placed into the microwave cavity and connected to an HPLC pump and a backpressure regulator to minimize the formation of gas bubbles. The flow rate and microwave power were varied to optimize the reactant contact time and temperature, respectively. Under optimal reaction conditions the quantity of product could be increased from 31 mg per hour to 340 mg per hour simply by changing the volumetric capacity of the monolith.

Introduction

Interest in flow based reaction chemistry has grown over recent years with the realization that such systems can offer greater control over reaction conditions, such as catalyst and heating contact time, which in turn lead to improved product selectivity and yield when compared to batch based methods [1-7]. Much of this work has focused on continuous-flow microreactor methodology for laboratory based organic synthesis, and has featured the development of inorganic and organic polymer based functionalized monolithic reactors that can operate at elevated temperatures and under high pressure [8,9]. Recently, application of magnetic nanoparticles as media that can be heated in an electromagnetic field, was reported to be ideal for

use inside microfluidic fixed-bed reactors for chemical synthesis [10]. A new concept to build the catalytic membrane inside a microchannel reactor was demonstrated by Uozumi et al. [11], where carbon–carbon bond forming reactions of aryl halides and arylboronic acids under microflow conditions can be achieved quantitatively within 4 s residence time. However, the stability of the catalytic membrane was not discussed. Monolith based devices have shown good flow characteristics when coupled with the highly controlled surface properties associated with the formation of nano-, micro- and mesoporous structures, and they therefore represent ideal supports for reagents and catalysts where contact time and temperature can be spatially and temporally mediated [12,13]. To this end, the use of microwave heating in conjunction with microporous monolithic reactors has attracted some interest for small-scale synthesis under continuous-flow conditions [14-16]. One obvious problem, however, when using microwaves to heat solvents/reagents and surface-functionalized monoliths in a flow microreactor, is the achievement of an efficient coupling of the microwave energy, which will be a function of both the absorbing species present and of the penetration depth of microwave irradiation into the reaction zone [17]. This is especially important in flow systems where the reactants are present in the irradiation chamber for a short period of time [18,19]. Therefore, the application of microwave chemistry to scalable, continuous-flow processes, with commercially available microwave equipment and suitable flow instrumentation, is becoming increasingly important [7,20]. Finally, the high surface-to-volume ratio and spatial and temporal control over the reactants and products, without the need for additional optimization, is of considerable interest [7,21-23] as these factors promise to increase the quantity of product to desirable levels whilst maintaining the intrinsic benefits of the reaction geometry offered when using microreactor methodology.

In this work we report a simple and effective approach for achieving volumetric scalability in a flow reaction system through the use of Pd-supported silica-based monolithic reactors coupled with microwave heating. The practicality of this approach will be demonstrated using Suzuki–Miyaura reactions in which the Pd-supported silica-monolith catalysts exhibit excellent activities and the doubling of the monolith diameter, thus operating at four times the volumetric flow rate, increases product output without any observable change in the reaction conversion.

Results and Discussion

Synthesis of silica monolith and Pd-supported silica monolith catalyst

The reaction parameters, such as polymer concentration, acid strength, water content, amount of silicon alkoxide, reaction temperature and reaction time, all have an important impact on the physical properties of the silica monoliths prepared. Silica monoliths used as catalyst supports require not only a high surface area to maximize their catalytic activity, but also a high permeability to achieve good flow characteristics and enable fast mass transfer from the flowing reaction solutions to the catalytic surface. In addition, they must be mechanically strong enough to withstand the pressures required to drive fluid through the monolithic structure at the required flow rate. Silica monoliths were synthesized from PEO, tetraethoxysilane and nitric acid as supports for the Pd catalyst, as based on the results of previous studies [24]. Silica monoliths, i.e., monolith-3.2 and monolith-6.4 (diameters of 3.2 mm and 6.4 mm respectively), with two different diameters were synthesized using the same procedure, leading to structures with comparable surface characteristics but with different volumes for the solution-accessible connected pores. Characterization of these monoliths indicated that a 2-fold increase in the monolith diameter had little influence on the physical characteristics of the monoliths (see Table 1, entries 1 and 3, 2 and 4), except the total volume that was increased by a factor of almost four, as expected. In addition, the loading of metal particles within monoliths had no effect on either the nm-scale or μm-scale pore structures (see Table 1, entries 1 and 2, 3 and 4, also see Supporting Information File 1, Figure S1).

Table 1: The main characteristics of monoliths characterized by N_2 adsorption at 77 K.[a]

Entry	Monolith	D_{N2} (nm)	S_{BET} ($m^2\ g^{-1}$)	V_{N2} ($cm^3\ g^{-1}$)	V_{water} (mL)	φ_t
1	monolith-3.2	16.0	164	0.70	0.205	0.85
2	Pd-monolith-3.2	15.9	169	0.67	0.202	0.84
3	monolith-6.4	16.1	161	0.73	0.791	0.82
4	Pd-monolith-6.4	16.0	166	0.67	0.790	0.82

[a]D_{N2}, S_{BET} and V_{N2} are the pore diameter, specific surface area and pore volume, respectively, as determined by N_2 adsorption at 77 K. V_{water} is the total volume of the monoliths as measured by the adsorption of water at room temperature. φ_t is the total porosity as determined by equation $(W_M - W_T)/dlr^2\pi$, here W_T and W_M are the weights of the dry and water filled monolith respectively, d is the density of water and l and r are the overall length and radius of the cylindrical monoliths. The palladium loading for entries 2 and 4 was ca. 4.5 wt %.

According to IUPAC [24] the measurements obtained from N_2 adsorption and desorption isotherms indicate a type H2 hysteresis, which is consistent with the disordered mesoporous structure seen in the micrograph shown in Figure 1 (also see Supporting Information File 1, Figure S2)

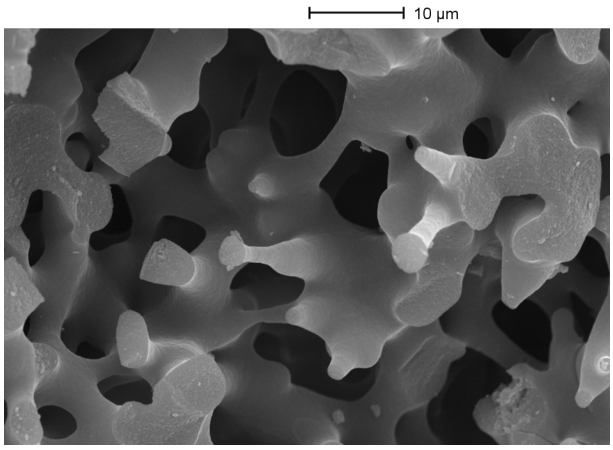

Figure 1: SEM image of silica monolith.

Effect of Pd precursor on the activity of the Pd-monolith catalyst

The Suzuki–Miyaura reaction is a widely used method in organic synthesis for the selective formation of aryl–aryl carbon–carbon bonds in the synthesis of high-value fine chemicals and intermediates in the pharmaceutical industry. This reaction requires a metal catalyst, such as palladium, in both homogeneous and heterogeneous reactions. In this study, the Suzuki–Miyaura reaction of bromobenzene with phenylboronic acid (Scheme 1) was initially used as a model heterogeneously catalyzed reaction for the evaluation of Pd-monolith activity under continuous flow conditions with microwave heating.

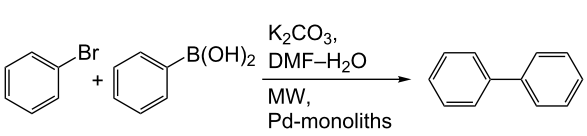

Scheme 1: Suzuki–Miyaura reaction of bromobenzene with phenylboronic acid.

The silica monoliths were impregnated with a range of Pd precursors, namely Na_2PdCl_4, $Pd(OAc)_2$, $Pd(dba)_2$ and $Pd(NO_3)_2$, by a standard method described previously for the preparation of Pd-monoliths. The Pd-monolith-3.2 catalysts were evaluated using the previously optimized solvent and basic reaction conditions [3,4]. The results of this study (Table 2, entries 1–4) indicate that, whilst all the Pd-monolith catalysts contain the same amount of palladium (around 4.5 wt %), their catalytic activity differs significantly even for similar reaction temperatures and contact times, showing a significant effect of the palladium precursor on the catalyst activity. The Pd-monolith catalyst that was synthesized from a Na_2PdCl_4 precursor showed the best activity and was therefore used as the Pd precursor for the preparation of a Pd-monolith catalyst to be employed in further investigations. As expected, reducing the reaction temperature and decreasing the catalyst contact time (see Table 2, entries 4–7) resulted in a corresponding reduction of the product yield.

Comparison of activity between Pd-monolith-3.2 and Pd-monolith-6.4

The main aim of this work is to develop a methodology to scale up the rate of product formation without a loss in the intrinsic reaction performance, by using a continuous-flow, microwave-assisted, Pd-supported silica-monolith reactor. The Pd-monolith-3.2 and Pd-monolith-6.4 (both with the same length of 3 cm) were used to perform the model reaction (1) to demonstrate this methodology. The total pore volume accessible to the

Table 2: Reactivity of Pd-monolith-3.2 synthesized using different Pd precursors in the Suzuki–Miyaura reaction between bromobenzene and phenylboronic acid under continuous flow conditions.[a]

Entry	Pd precursor	MW power (W)	Temperature (°C)	Flow rate (µL min^{-1})	Contact time (min)	Conversion (%)
1	$Pd(OAc)_2$	8	123	20	10	72
2	$Pd(dba)_2$	8	123	20	10	55
3	$Pd(NO_3)_2$	15	123	20	10	28
4	Na_2PdCl_4	5	123	20	10	97
5	Na_2PdCl_4	3	99	20	10	70
6	Na_2PdCl_4	10	116	40	5	66
7	Na_2PdCl_4	5	109	40	5	45

[a]All Pd-monolith catalysts have a Pd-loading of ca. 4.5 wt %. Conversions were determined using GC–MS versus internal standard. The main byproducts (1–3%) were formed by the debromination of halide reactants.

solution, determined by adsorption of water, was 0.20 mL for Pd-monolith-3.2 and 0.79 mL for Pd-monolith-6.4, which represents an almost 4-fold volume increase for the larger Pd-monolith-6.4. The activities of both monoliths for the Suzuki–Miyaura reaction (Scheme 1) are shown in Figure 2. It can be seen that Pd-monolith-6.4 produces a very similar percentage yield of product to that obtained using the Pd-monolith-3.2 under four times the flow rate to keep the same catalyst contact time. This observation is suggestive of virtually identical intrinsic properties for both monoliths in terms of flow rate and reaction conversion.

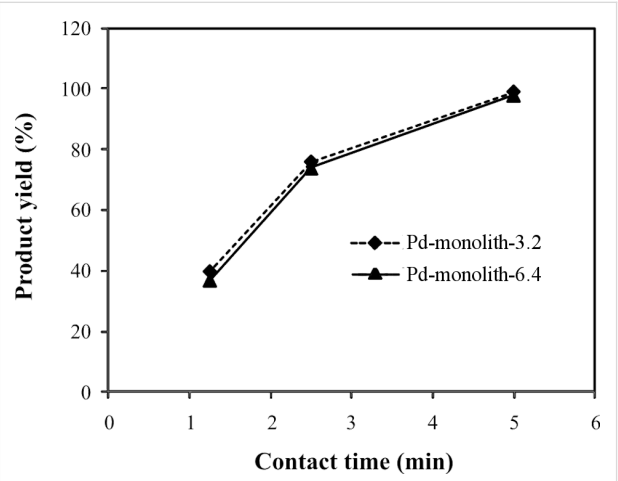

Figure 2: Reactivity of the Pd-monolith-3.2 and Pd-monolith-6.4 for the Suzuki–Miyaura reaction between bromobenzene (0.1 M) and phenylboronic acid (0.12 M): The relationship of product yield with contact time.

It can also be seen (Figure 3) that the rate of product formation scales up as expected, i.e., the larger catalyst monolith produces four times as much product compared to the smaller catalyst monolith under equivalent reaction conditions. However, it is also evident from the data that whilst shorter catalyst contact times (corresponding to higher solution flow rates) produce an increase in the rate of product formation, this increased rate of product formation is at the expense of reduced reagent conversion.

This methodology was also used to test Suzuki–Miyaura reactions with a variety of substrates, as shown in Table 3. It can be seen that this scale-up strategy also works very well, with the amount of product obtained with the Pd-monolith-6.4 being four times greater than that obtained with the Pd-monolith-3.2, under these conditions. Most reagents generated an excellent reaction conversion of the desired coupling product (see Supporting Information File 1, Figures S3, S4 and S5), even in the case of chlorobenzene, which is a notably poor substrate for the Suzuki–Miyaura reaction (entries 6 and 12). The

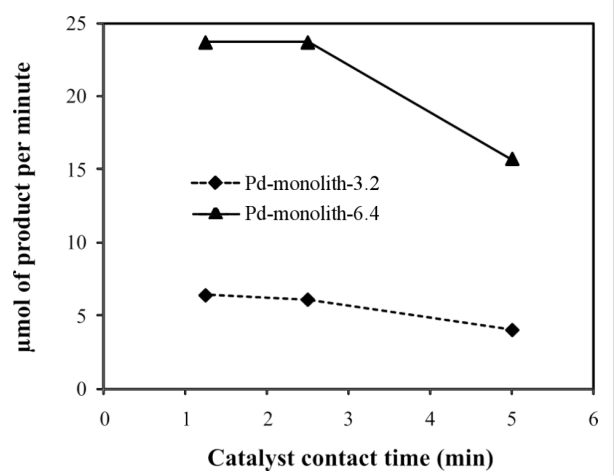

Figure 3: Reactivity of the Pd-monolith-3.2 and Pd-monolith-6.4 for the Suzuki–Miyaura reaction between bromobenzene (0.1 M) and phenylboronic acid (0.12 M): The dependence of micromoles of product obtained on contact time.

Suzuki–Miyaura reaction between bromobenzene and 4-bromobenzaldehyde with a higher concentration of reactants, i.e., 0.3 M, was also performed with the Pd-monolith-6.4 catalyst to evaluate the conversion ability. The reaction conversion was found to be high, i.e., 87–89 %, under these modified conditions.

The high catalytic activity of the Pd-monolith catalysts in Suzuki–Miyaura reactions can be attributed to the following three factors. First is the high dispersion of small Pd particles over the substrate surface within the monolith mesopores. The TEM image (Figure 4) shows that the catalyst sample incorporates metal particles, distributed over the substrate surface, with two different sizes: Small crystallites with dimensions of less than 2 nm (majority), and large crystallites with diameters of

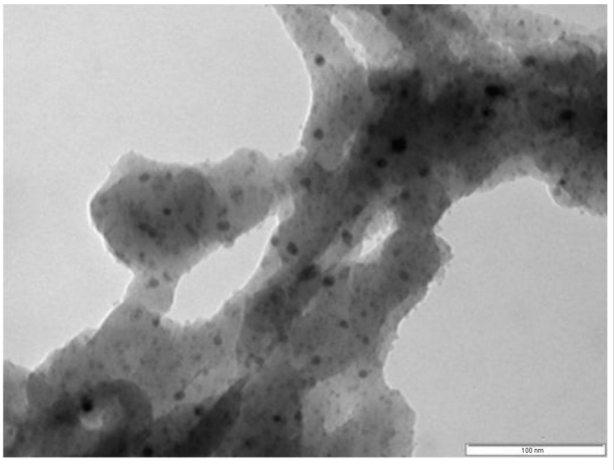

Figure 4: TEM image of Pd-monolith catalyst (scale bar: 100 nm).

Table 3: Reactivity of Pd-monoliths with different diameters, in the Suzuki–Miyaura reaction between various reactants under continuous-flow conditions.[a]

Entry	Catalyst	Flow rate (μL min^{-1})	Halide	Boronic acid	Product	Conversion (%)
1	Pd-monolith-3.2	40	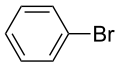	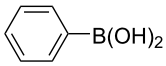	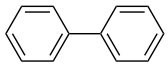	99
2	Pd-monolith-3.2	20	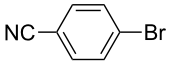	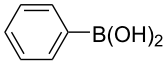	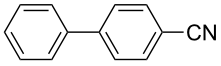	100
3	Pd-monolith-3.2	30	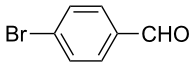	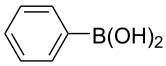	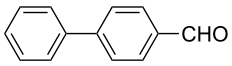	95
4	Pd-monolith-3.2	20	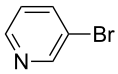	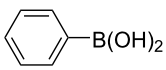	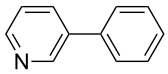	65
5	Pd-monolith-3.2	20	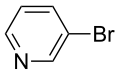	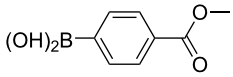	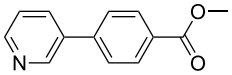	60
6	Pd-monolith-3.2	20	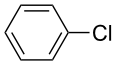	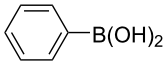	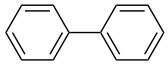	99
7	Pd-monolith-6.4	160	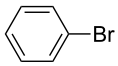	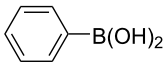	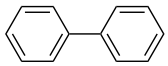	99
8	Pd-monolith-6.4	80	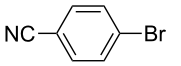	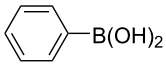	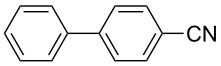	99
9	Pd-monolith-6.4	120	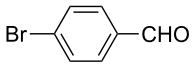	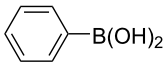	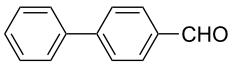	95
10	Pd-monolith-6.4	80	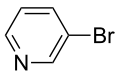	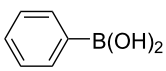	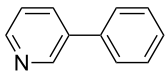	65
11	Pd-monolith-6.4	80	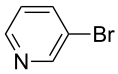	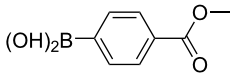	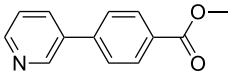	59
12	Pd-monolith-6.4	80	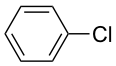	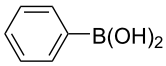	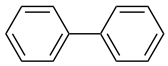	98

[a]MW power used was 5–10 W for Pd-monolith-3.2 and 1–2 W for Pd-monolith-6.4 to a maintain reaction temperature of 125–130 °C. The backpressure valve was set up 75 psi for Pd-monolith-3.2 and 45 psi for Pd-monolith-6.4, respectively. The reaction conversion was determined by GC–MS with an internal standard and the main byproduct (1–3%) was formed by debromination of halide reactants.

around 10 nm. Second is the large surface-to-volume ratio of the monoliths. The values of the surface-area-to-volume ratio for the microchannels typically range from 10,000 to 50,000 m^2/m^3, as a consequence of their decreased size. Based on BET characterization, the surface-area-to-volume ratio generated within the Pd-monolith-3.2 reactor was estimated to be 2.5×10^8 m^2/m^3, which contributed greatly to the promotion of the reaction. The final factor relates to the combination of microwave heating and palladium nanoparticles. Kappe et al. found that smaller particles are more active in traditional heating whereas bigger particles perform better in microwave heating [25]. The monolithic structure used in this work takes advantage of both these characteristics by having more reactive, nano-sized, Pd particles located within a strongly microwave-absorbing, meso-size, silica structure. Because it was difficult to measure the temperature inside the monolith, the outlet temperature measured by fiber probe was used, which gave a difference of at least 20 °C between the outlet temperature and the temperature of the outer surface of the monolith, as measured using the installed IR sensor. It was found that reaction conversion was only 40–50% with oil bath heating.

With supported Pd catalysts, leaching of palladium is always an issue of concern in terms of catalyst performance, cost and

recovery. Recent papers have shown that leaching from palladium catalysts is in the order of 1 to several tens of ppm [6,10,19,25] and that recovery of this palladium could be achieved with a scavenger column [6]. The tendency for leaching of palladium metal from the Pd-monoliths was measured through an ICP–OES analysis to determine the Pd concentration in the washing liquid, which immediately followed the first flow reaction experiment. This was achieved by pumping DMF/H_2O (3:1) solvent through the Pd-monolith at 0.1 mL/min for 20 min. For the Na_2PdCl_4 based monolithic catalyst, the amount of palladium present in the washing liquid was found to be as little as 74 ppb (Pd-monolith-3.2), corresponding to a loss of only 0.000011% of the initial amount of palladium added to the monoliths. The amount of palladium present in the final reaction sample was found still to be less than 100 ppb. This finding suggests that there is a highly specific and strong interaction between the impregnated metal nanoparticles and the monolith support surface, possibly through a combination of hydrogen bonding, ionic interactions and substitution of Cl by silanol groups present on the monolith surface, resulting in highly stable nanoparticle fixation [26,27]. The presence of a strong specific metal/support interaction is also supported by observations made during the impregnation process, where $PdCl_4^{2-}$ uptake in the silica monolith body was seen to be fast, with the monolith turning a stable dark brown color after several hours. In contrast, the $Pd(NO_3)_2$ salt gave the monolith a lighter coloration, much more slowly, and was easily washed away. The $PdCl_4^{2-}$ based Pd-monolith catalyst was in fact used for several runs (i.e., 6 runs representing 15–20 hours) with no deactivation being observed when the catalyst was washed with DMF, water or DMF/H_2O (3:1) after completion of each run.

Conclusion

It has been demonstrated that the combination of Pd-functionalized silica monolithic reactors with microwave heating results in a high percentage yield of the desired reaction products for Suzuki–Miyaura reactions under flow conditions. Yields can be scaled-up by increasing the diameter of the catalytic monolith used. The cylindrical catalyst monoliths were of a constant length, but of variable diameter and were produced to give the same intrinsic monolith activity and permeability properties, when operating under the same conditions of temperature and catalyst contact time. In this way the product formation rate scales quantitatively with the square of the catalyst monolith diameter. However, at least one alternative approach can be envisaged, i.e., changing the monolith length for scaling up whilst maintaining the required intrinsic properties. It is worth considering the relative advantages and disadvantages of these two possible approaches in light of the work presented. Increasing the diameter of a fixed length monolith, the scale-up method as used here, offers the advantage that the pressure drop required to produce a certain flow rate decreases with increasing diameter. However, as microwave penetration is necessary to obtain reliable heating characteristics, there will come a point at which the monolith diameter will become larger than the penetration depth of the microwaves (estimated to be 4 cm), which will lead to an unheated, cold "core". In addition for disc-shaped monoliths, where diameters are larger than the length, there will also come a point where the mechanical strength of the monolith will be a limitation with respect to the pressure drop required for flow. On the other hand, increasing the length of a fixed diameter monolith in order to achieve this scale-up offers the advantage that uniform microwave penetration/heating can be maintained. In addition, the catalyst contact time could be extended by increasing the length. The disadvantage, however, to this approach is related to the pressure drop required to produce the required flow rate, which will increase proportionally with the length. Hence, the mechanical strength of the monolith structure, i.e., the strength to resist collapse of the pores and/or the monolith casing material, ultimately limits the maximum length achievable.

Experimental

Materials

The reagents and solvents bromobenzene (99%), 4-bromobenzonitrile (99%), 4-bromobenzaldehyde (99%), 3-bromopyridine (99%), chlorobenzene (99%), phenylboronic acid (97%), 4-carboxyphenylboronic acid (97%), poly(ethylene oxide) (PEO) with average relative molar mass of 100 kDa, tetraethoxysilane (TEOS), *N,N*-dimethylformamide (99%, DMF), dichloromethane (99%, DCM), ammonium hydroxide (5 N) and nitric acid aqueous solutions (1 N) were purchased from Aldrich. All reagents were used as obtained, without further purification. Heat shrinkable Teflon® tubes (wall thickness 0.1 and 0.3 mm before and after shrinkage) with a shrinkage ratio of 2:1 were purchased from Adtech Polymer Engineering Ltd. (UK).

Synthesis of silica monolith supports

Silica based monoliths were prepared using a sol–gel process described in the literature [24]. The desired amount of PEO was added to an aqueous solution of nitric acid and the resultant mixture was cooled in an ice bath and stirred until a homogeneous solution formed. TEOS was then added to the reaction mixture, which was stirred vigorously in the ice bath for 30 min to form a transparent solution. Subsequently, the solution was poured into a plastic mould (diameter 4.8 mm and length 6 cm for monolith-3.2; and diameter 8.2 mm and length 5 cm for monolith-6.4). Both ends of the plastic mould were then closed and the sealed tube was incubated in an oven at 40 °C for 3 days, during which time a wet, semi-solid, gel monolith was

formed. Approximately 20% shrinkage occurred during this gel formation, which allowed easy removal of the wet gel monoliths from the plastic tube moulds. The wet gel monoliths were washed with copious amounts of water to remove any residues and then transferred to a 10 times larger volume of 0.5 M NH_4OH aqueous solution in an autoclave, where it was incubated at 80 °C for 24 h. The monoliths were again washed with copious amounts of water before drying in an oven at 90 °C for 24 h. Finally, the monoliths were calcined at 550 °C for 3 h (heating rate: 2 °C/min) in an air flow to remove the remaining PEO and form white silica-monolith rods (diameters 3.2 and 6.4 mm respectively) that were then cut to 3 cm long monoliths.

Preparation of Pd-supported silica-monolith catalyst (Pd-monolith)

An aqueous solution of 200 μL containing 0.017 g Na_2PdCl_4 (theoretical Pd loading 5.0 wt %) was adsorbed onto the monoliths, dried at 90 °C and calcined at 550 °C for 3 h (temperature ramp: 2 °C min^{-1}) under a flow of air, followed by reduction in a H_2 (10%)/N_2 stream at 340 °C for 3 h (heating rate: 2 °C) to produce a black Pd-monolith rod with Pd loading of approximately 4.5 wt % as determined by ICP–OES (Perkin Elmer Optima 5300DV). The Pd-monolith rod obtained was then clad in a heat-shrinkable Teflon® tube with a glass connector at each end. The assembly was heated in a furnace up to 330 °C until the monolith was sealed within the Teflon® tube to form a flow Pd-monolith reactor system.

Sample characterization

Scanning electron microscopy (SEM) images were obtained by means of a Cambridge S360 scanning electron microscope operated at 20 kV. Each sample was sputter coated with a thin layer of gold–platinum (thickness approximately 2 nm) by a SEMPREP 2 Sputter Coater (Nanotech Ltd.). Transmission electron microscopy (TEM) was carried out on a JEOL-2010 operating at 200 kV. The BET surface area and nm-scale pore-size distribution were obtained by measuring N_2 adsorption and desorption isotherms at 77 K by means of a Micromeritics Surface Area and Porosity Analyzer. The pore volume and pore size distributions of the nm-scale pores within the monoliths were evaluated from the isotherms within the BJH (Barrett-Joyner-Halenda) model. The palladium content in the monoliths and washing liquid was determined by ICP–OES. Determination of the μm-scale porosity φ_t (which determines the monolith permeability) was determined from the equation $(W_M - W_T)/dlr^2\pi$, where W_T and W_M were the weights of the dry and water filled monolith respectively, d was the density of water, l and r were the overall length and radius of the cylindrical monolith. The μm-scale pore size was determined from SEM measurements.

Activity measurements

The experimental setup is shown schematically in Supporting Information File 1, Figure S6. The 30 mm long Pd-monolith reactor with a diameter of either 3.2 mm (Pd-monolith-3.2) or 6.4 mm (Pd-monolith-6.4) was positioned in the cavity of a Discover microwave system (CEM Ltd.) with the capability of delivering 0–300 W of microwave power at 2.45 GHz with mono-mode operation. The microwave cavity was fitted with an infrared sensor to monitor the temperature of the external surface of the monolith catalyst. A reactant solution containing an aryl halide (0.1 M), arylboronic acid (0.12 M), K_2CO_3 (0.3 M) in DMF/H_2O (3:1) solvent was pumped through the reactor with an HPLC pump, and a backpressure valve (45–75 psi) was used to minimize the formation of gas bubbles (see Supporting Information File 1, Figure S6). The residence times of the reactants within the catalytic monoliths were determined based on the known monolith and pore volume and from the different flow rates. Product samples were collected at defined flow periods during a reaction run, weighed and a known amount of dodecane was added to the individual samples as an internal standard. Samples were treated with 1 M aqueous NaOH to remove unreacted arylboronic acid and extracted with DCM. The remaining organic material was then washed three times with distilled water, collected and dried over $MgSO_4$. Individual samples were analyzed using GC–MS (Varian 2000) as described in literature [3,4].

Supporting Information

The Supporting Information File contains six parts, Figure S1: SEM image of Pd-monolith; Figure S2: BET characterization; Figure S3: GC–MS chromatogram for Suzuki–Miyaura reaction of bromobenzene and phenylboronic acid; Figure S4: GC–MS chromatogram for Suzuki–Miyaura reaction of 4-bromobenzaldehyde and phenylboronic acid; Figure S5: GC–MS chromatogram for Suzuki–Miyaura reaction of 4-bromobenzonitrile and phenylboronic acid; Figure S6: Schematic diagram of the setup for continuous-flow, microwave-assisted Suzuki–Miyaura reactions.

Supporting Information File 1

Additional material.
[http://www.beilstein-journals.org/bjoc/content/supplementary/1860-5397-7-133-S1.pdf]

References

1. Vankayala, B. K.; Löb, P.; Hessel, V.; Menges, G.; Hoffmann, C.; Metzke, D.; Krtschil, U.; Kost, H.-J. *Int. J. Chem. React. Eng.* **2007,** *5,* A91. doi:10.2202/1542-6580.1463

2. de Mas, N.; Günther, A.; Kraus, T.; Schmidt, M. A.; Jensen, K. F. *Ind. Eng. Chem. Res.* **2005,** *44,* 8997. doi:10.1021/ie050472s
3. He, P.; Haswell, S. J.; Fletcher, P. D. I. *Lab Chip* **2004,** *4,* 38. doi:10.1039/b313057f
4. He, P.; Haswell, S. J.; Fletcher, P. D. I. *Appl. Catal., A* **2004,** *274,* 111. doi:10.1016/j.apcata.2004.05.042
5. Glasnov, T. N.; Kappe, C. O. *Adv. Synth. Catal.* **2010,** *352,* 3089. doi:10.1002/adsc.201000646
6. Mennecke, K.; Kirschning, A. *Beilstein J. Org. Chem.* **2009,** *5,* No. 21. doi:10.3762/bjoc.5.21
7. Razzaq, T.; Kappe, C. O. *Chem.–Asian J.* **2010,** *5,* 1274. doi:10.1002/asia.201000010
8. Comer, E.; Organ, M. G. *Chem.–Eur. J.* **2005,** *11,* 7223. doi:10.1002/chem.200500820
9. Gömann, A.; Deverell, J. A.; Munting, K. F.; Jones, R. C.; Rodemann, T.; Canty, A. J.; Smith, J. A.; Guijt, R. M. *Tetrahedron* **2009,** *65,* 1450. doi:10.1016/j.tet.2008.12.007
10. Ceylan, S.; Friese, C.; Lammel, C.; Mazac, K.; Kirschning, A. *Angew. Chem., Int. Ed.* **2008,** *47,* 8950. doi:10.1002/anie.200801474
11. Uozumi, Y.; Yamada, Y. M. A.; Beppu, T.; Fukuyama, N.; Ueno, M.; Kitamori, T. *J. Am. Chem. Soc.* **2006,** *128,* 15994. doi:10.1021/ja066697r
12. Svec, F.; Huber, C. G. *Anal. Chem.* **2006,** *78,* 2100. doi:10.1021/ac069383v
13. Preinerstorfer, B.; Bicker, W.; Lindner, W.; Lämmerhofer, M. *J. Chromatogr., A* **2004,** *1044,* 187. doi:10.1016/j.chroma.2004.04.078
14. Smith, C. J.; Smith, C. D.; Nikbin, N.; Ley, S. V.; Baxendale, I. R. *Org. Biomol. Chem.* **2011,** *9,* 1927. doi:10.1039/c0ob00813c
15. Kunz, U.; Kirschning, A.; Wen, H.-L.; Solodenko, W.; Cecilia, R.; Kappe, C. O.; Turek, T. *Catal. Today* **2005,** *105,* 318. doi:10.1016/j.cattod.2005.06.046
16. Nikbin, N.; Ladlow, M.; Ley, S. V. *Org. Process Res. Dev.* **2007,** *11,* 458. doi:10.1021/op7000436
17. Kappe, C. O.; Dallinger, D.; Murphree, S. S. *Practical Microwave Synthesis for Organic Chemists – Strategies, Instruments, and Protocols;* Wiley-VCH: Weinheim, Germany, 2009; pp 138–160.
18. Comer, E.; Organ, M. G. *J. Am. Chem. Soc.* **2005,** *127,* 8160. doi:10.1021/ja0512069
19. Shore, G.; Morin, S.; Organ, M. G. *Angew. Chem., Int. Ed.* **2006,** *45,* 2761. doi:10.1002/anie.200503600
20. Singh, B. K.; Kaval, N.; Tomar, S.; Van der Eycken, E.; Parmar, V. S. *Org. Process Res. Dev.* **2008,** *12,* 468. doi:10.1021/op800047f
21. Glasnov, T. N.; Kappe, C. O. *Macromol. Rapid Commun.* **2007,** *28,* 395. doi:10.1002/marc.200600665
22. Mason, B. P.; Price, K. E.; Steinbacher, J. L.; Bogdan, A. R.; McQuade, D. T. *Chem. Rev.* **2007,** *107,* 2300. doi:10.1021/cr050944c
23. Pennemann, H.; Watts, P.; Haswell, S. J.; Hessel, V.; Löwe, H. *Org. Process Res. Dev.* **2004,** *8,* 422. doi:10.1021/op0341770
24. Fletcher, P. D. I.; Haswell, S. J.; He, P.; Kelly, S. M.; Mansfield, A. J. *Porous Mater.* **2010,** *18,* 501. doi:10.1007/s10934-010-9403-3
25. Mennecke, K.; Cecilia, R.; Glasnov, T. N.; Gruhl, S.; Vogt, C.; Feldhoff, A.; Vargas, M. A. L.; Kappe, C. O.; Kunz, U.; Kirschning, A. *Adv. Synth. Catal.* **2008,** *350,* 717. doi:10.1002/adsc.200700510
26. Bronstein, L. M.; Polarz, S.; Smarsly, B.; Antonietti, M. *Adv. Mater.* **2001,** *13,* 1333. doi:10.1002/1521-4095(200109)13:17<1333::AID-ADMA1333>3.0.CO;2-P
27. Kosslick, H.; Mönnich, I.; Paetzold, E.; Fuhrmann, H.; Fricke, R.; Müller, D.; Oehme, G. *Micro. Meso. Mater.* **2001,** *44-45,* 537. doi:10.1016/S1387-1811(01)00232-3

License and Terms

Beilstein Journal of Organic Chemistry

Triple-channel microreactor for biphasic gas–liquid reactions: Photosensitized oxygenations

Ram Awatar Maurya[1], Chan Pil Park[1] and Dong-Pyo Kim[*1,2]

Letter

Open Access

Address:
[1]National Creative Research Center of Applied Microfluidic Chemistry, Chungnam National University, Daejeon, 305-764, South Korea, www.camc.re.kr and [2]Graduate School of Analytical Science and Technology, Chungnam National University, Daejeon, 305-764, South Korea, Fax: (+82)-42-823-6665

Email:
Ram Awatar Maurya - ram.cdri@gmail.com; Chan Pil Park - chan2seul@hanmail.net; Dong-Pyo Kim* - dpkim@cnu.ac.kr

* Corresponding author

Keywords:
gas–liquid reaction; microreactor; photosensitization; singlet oxygen

Beilstein J. Org. Chem. **2011,** *7,* 1158–1163.
doi:10.3762/bjoc.7.134

Received: 18 May 2011
Accepted: 04 August 2011
Published: 24 August 2011

This article is part of the Thematic Series "Chemistry in flow systems II".

Guest Editor: A. Kirschning

Abstract

A triple-channel microreactor fabricated by means of a soft-lithography technique was devised for efficient biphasic gas–liquid reactions. The excellent performance of the microreactor was demonstrated by carrying out photosensitized oxygenations of α-terpinene, citronellol, and allyl alcohols.

Introduction

Microreactors have recently attracted much interest among the scientific community for performing laboratory operations on small scales [1-23]. One of the major driving forces for the development of these devices is their unique characteristics compared to those of classical reaction vessels, such as large surface-to-volume ratio, diffusion dominated mass transfer, fast and efficient heat dissipation, and the capability of spatial and temporal control of the reagents or products. These advantages have been exploited for various purposes such as performing selective reactions with highly unstable intermediates [24,25], improving heterogeneous catalysis [26-29], multi-step synthesis [30,31], process safety [32-34], photo-reactions [35-39], gas-liquid reactions [40-43], etc.

In a biphasic gas–liquid reaction, mass transfer from the gas phase to the liquid phase proceeds through the interfacial area. In traditional batch reactors, the interfacial area between the gas and liquid phases is quite small and the ratio of the interfacial area to the volume further decreases with the volume of the reaction mixture. Thus, in scale-up batch reactors the rate of reaction is significantly decreased due to the considerably reduced interfacial-area-to-volume ratio. Therefore, vigorous stirring, ultrasonic agitation, high pressure or supercritical conditions are typically applied to enhance mass transfer in batch reactors for gas–liquid biphasic reactions. Recently, we reported a dual-channel microreactor that dramatically improved the reaction rate of biphasic gas–liquid reaction by

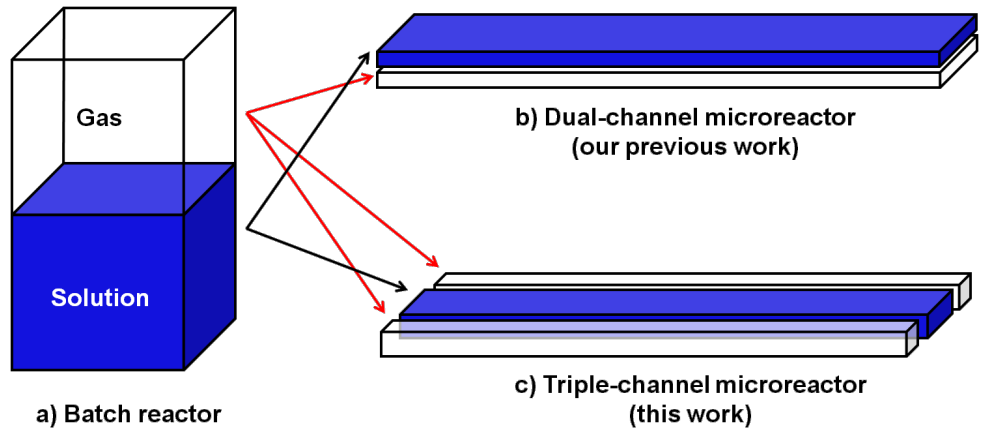

Figure 1: Schematic the for contacting modes of biphasic gas–liquid in (a) batch reactor, (b) dual-channel, and (c) triple-channel microreactors.

enhancing the effective interfacial area [44,45]. In the dual-channel microreactor, in which the top and bottom channels were separated by a thin polydimethylsiloxane (PDMS) membrane, gas from the bottom channel diffused into the solution of the top channel. Thus, only one face of the solution channel was exposed to the gas. Herein, we present an advanced version of the dual-channel microreactor in the form of a triple-channel microreactor where the reaction channel is exposed to gas from two sides, which further increases the effective interfacial area (Figure 1). More importantly, the process of fabrication of the triple-channel microreactor is simpler than for the dual-channel.

Results and Discussion

PDMS was used to fabricate the triple-channel microreactor for biphasic gas–liquid reactions. It is the most commonly used material for microfluidic devices due to the ease of fabrication and its optical transparency. Although microfluidic devices made of PDMS suffered from swelling problems caused by nonpolar organic solvents [46], we found that organic reactions can conveniently be performed in polar organic solvents such as DMF, DMSO, acetonitrile, etc., without any noticeable problems. The dimension of the middle channel of the fabricated triple-channel microreactor was 33 cm × 250 μm × 40 μm (volume = 3.3 μL). The outer parallel channels were 250 μm in width and 40 μm in depth. The membrane separating the parallel channels was 100 μm thick (for details of the fabrication, see the Supporting Information File 1); an optical image of the fabricated microreactor is shown in Figure 2.

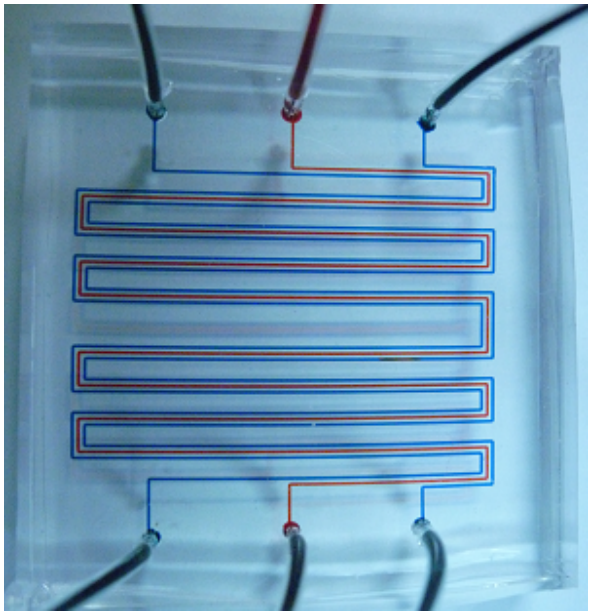

Figure 2: Optical image of the triple-channel microreactor (for demonstration purposes, the inner channel for reaction is filled with red solution and outer channels for gas with blue solution).

Photosensitized oxygenation was chosen as a biphasic gas–liquid reaction to study the efficiency of the triple-channel microreactor. Photooxygenations in classical reaction vessels suffer from long reaction times due to restricted spatial illumination. In addition, the short lifetime of singlet oxygen in solutions, the low interfacial area between the oxygen and the reaction solution, and the long molecular diffusion distances significantly reduce the reaction efficiency. In this context triple-channel microreactors could be quite useful as they comprise all the required elements for photosensitized oxygenations, namely continuous-flow processing, large gas–liquid interfacial area, short molecular diffusion distances, and very high surface illumination homogeneity.

The middle channel was used for the flow of the reaction solution containing the reactant and a photosensitizer, whereas the

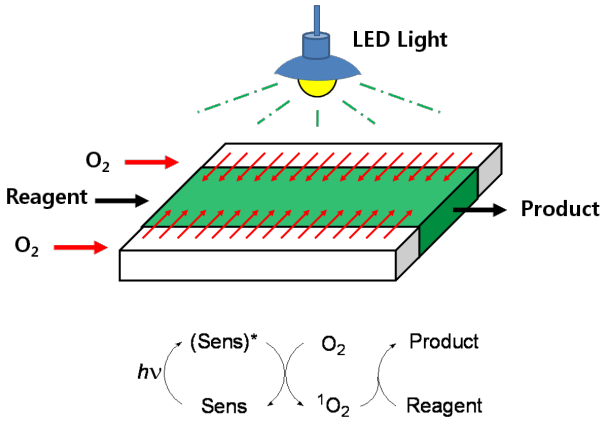

Figure 3: Photosensitized oxygenation in the triple-channel microreactor.

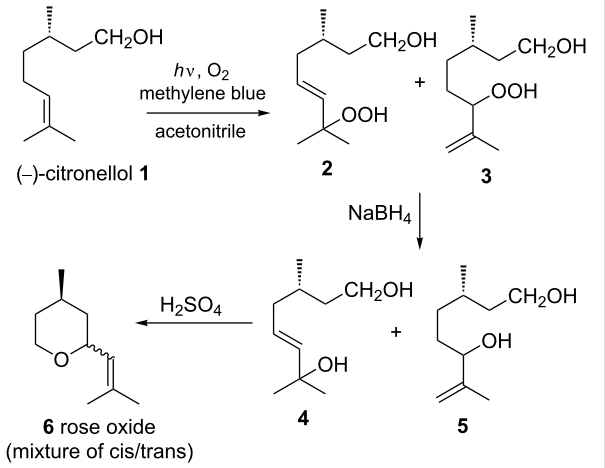

Scheme 1: Photosensitized oxygenation of citronellol (a key step in the synthesis of rose oxide).

outer two channels were used for oxygen supply (Figure 3). Efficient oxygen supply to the reaction mixture was achieved by adjustment of the pressure in the outer channels. The overpressure of oxygen in the outer channels results in the generation of bubbles in the middle channel, which affects the control of reagent flow by disturbing the flow rates. Therefore, the pressure of oxygen in the outer channels should be controlled in order to avoid bubble generation in the middle channel and to prevent diffusion of solvents from the middle channel to the outer channels. Thus, only oxygen diffuses into the solution and not the opposite way around. The efficiency of the triple-channel microreactor was studied by carrying out photosensitized oxygenation of citronellol, allyl alcohols, and α-terpinene.

Photosensitized oxygenation of (−)-citronellol

The photosensitized oxygenation of citronellol is an industrially important synthetic transformation [47] as it is used for bulk production of a fragrance, rose oxide (Scheme 1). The reaction was performed with methylene blue as a sensitizer in acetonitrile.

Table 1 represents the technical data for a typical batch reactor (50 mL round bottom flask), dual channel and triple channel microreactors. Since the illuminated area/volume and gas–liquid interfacial area/volume were highest in the case of triple-channel microreactor, much improved results were expected with the new triple-channel microreactor.

The microreactor was irradiated with a 16 W white LED light source (FAWOO-Tech. Korea, LH16-AFE39S-White) kept in close contact. The reaction mixture (a solution of citronellol and methylene blue in acetonitrile) was pumped into the middle channel without any presaturation with O_2. The outer channels were closed from one end and oxygen was pumped at a flow rate that was 10 times higher than that of the solution in the middle channel. The batch reaction was performed in a 50 mL round bottom flask and irradiated with the same light source.

Table 1: Technical data for the batch reactor and triple-channel microreactor.[a]

	batch reactor	dual[b]	triple[c]
volume	50 mL	38.9 μL	3.3 μL
illuminated area	15.2 cm^2	1.98 cm^2	0.825 cm^2
illuminated volume	20 mL	38.9 μL	3.3 μL
illuminated area/volume	0.76 cm^{-1}	50.9 cm^{-1}	250 cm^{-1}
gas–liquid interfacial area/volume	0.76 cm^{-1}	50.9 cm^{-1}	80 cm^{-1}

[a]For calculations see Supporting Information File 1. [b]Dual-channel microreactor, for details of the fabrication and the results of photosensitized oxygenation in the dual-channel microreactor, see reference [45]. [c]Triple-channel microreactor.

In the microreactor the reaction was completed within a few minutes whereas it took several hours to complete in the flask. The results are attributed to very high gas–liquid contact area and illumination area-to-volume ratio for the microreactor compared to that of the round bottom flask. In addition, high illumination homogeniety of the microreactor also plays an important role. These factors make the triple-channel microreactor quite promising for photosensitized oxygenation reactions. The ratio of hydroperoxides **2** and **3** were found to be identical (1:1.5 as determined by ^{1}H NMR) in both the microreactor and the batch reactor. It was particularly noticeable that reactions carried out under higher reactant concentration in the triple-channel microreactor took almost the same time to reach completion as at lower concentration, whereas in the batch reaction conversion was incomplete even after several hours (Table 2).

To compare the productivity for scale-up synthesis, the space–time yield of the triple-channel microreactor and that of the round bottom flask was calculated at various times during the course of the reaction. The space–time yield data reveals that triple-channel microreactors are quite promising for performing efficient photosensitized oxygenation of citronellol in condensed solutions that would minimize the waste of solvents.

Photosensitized oxygenation of allylic alcohols

The photosensitized oxygenation of allylic alcohols was taken as a second model reaction to illustrate the efficiency of the triple-channel microreactor. The product of this reaction is an allyl hydroperoxide alcohol that is used in the synthesis of artemisinin-derived antimalarial 1,2,4-trioxanes [48]. The reaction in the triple-channel and in batch was carried out as aforementioned with methylene blue as sensitizer. The results from the triple-channel microreactor and the batch reaction presented in Table 3 clearly indicate the efficiency of the former.

Photosensitized oxygenation of α-terpinene

The photosensitized oxygenation of α-terpinene is a Diels–Alder type [4 + 2] cycloaddition reaction. The product of the reaction is ascaridole, which is widely used as an

Table 2: Photosensitized oxygenation of (−)-citronellol.

			conversion (%)[a]		STY (mmol L^{-1} min^{-1})[b]	
entry	conc.	time	microreactor	batch	microreactor	batch
1	0.1 M	2 min	99	5	49.5	2.5
2	0.1 M	6 h	—	93	—	0.28
3	0.2 M	2 min	99	—	99	—
4	0.3 M	2 min	91	—	136.5	—
5	0.3 M	6 h	—	63	—	0.53

[a]Conversions were determined by ^{1}H NMR using an internal standard. [b]Space–time yield (STY) = mmol of products/(reactor volume × time).

Table 3: Photosensitized oxygenation of allyl alcohols.

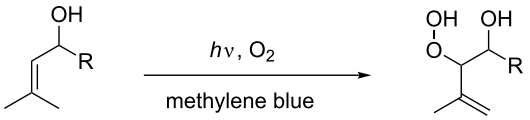

4 **5**

				conversion (%)[a]		STY (mmol L^{-1} min^{-1})[b]	
entry	conc.	time	R	microreactor	batch	microreactor	batch
1	0.2 M	2 min	H	98	6	49	3
2	0.2 M	2 min	Me[c]	97	—	97	—
3	0.3 M	2 min	H	95	—	142.5	—
4	0.3 M	6 h	H	—	62	—	0.52

[a]Conversions were determined by ^{1}H NMR using an internal standard. [b]Space–time yield (STY) = mmol of products/(Reactor volume × time).
[c]Syn/anti ratio = 75:25 as determined by ^{1}H NMR.

Table 4: Photosensitized oxygenation of α-terpinene.

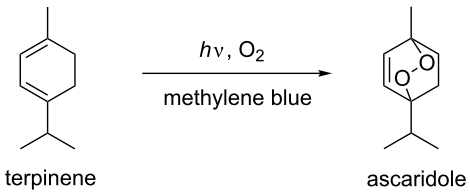

			conversion (%)[a]		STY (mmol L^{-1} min^{-1})[b]	
entry	conc.	time	microreactor	batch	microreactor	batch
1	0.1 M	1 min	99	7	99	7
2	0.1 M	6 h	—	91	—	0.25
3	0.2 M	1 min	96	—	192	—
4	0.2 M	6 h	—	57	—	0.32

[a]Conversions were determined by ^{1}H NMR using an internal standard. [b]Space time yield (STY) = mmol of products/(Reactor volume × time).

anthelmintic drug, in tonic drinks and in food flavoring [49]. The reaction was successfully carried out in the triple-channel microreactor with methylene blue as a sensitizer, as above. Significant reduction in the reaction time was again observed when compared to the batch reaction (Table 4). Very high space–time yield of the triple-channel microreactor in comparison to the batch reactor indicates that the microreactor is quite suitable for scaled-up production of the ascaridole.

Conclusion

In conclusion, we developed a triple-channel microreactor for biphasic gas–liquid reactions. In this microreactor, oxygen gas in two outer channels efficiently diffused into the liquid reactants in the middle channel through an extremely large effective interfacial area (area-to-volume ratio). The chemical synthetic efficiency was demonstrated by performing photosensitized oxygenation of α-terpinene, citronellol and allyl alcohols. As a result of the increased illumination as well as the increased gas–liquid contact area per unit volume, the triple-channel microreactor exhibited better performance in the oxygenations of citronellol, allyl alcohols and α-terpinene compared to the batch reactor, or even compared to a typical dual-channel microreactor [44].

Supporting Information

Supporting Information File 1

Experimental section, analytical data and fabrication of the triple-channel microreactor.
[http://www.beilstein-journals.org/bjoc/content/supplementary/1860-5397-7-134-S1.pdf]

Acknowledgements

This work was supported by the National Research Foundation of Korea (NRF) grant funded by the Korea government (MEST) (No. 2008-0061983).

References

1. Whitesides, G. M. *Nature* **2006,** *442,* 368–373. doi:10.1038/nature05058
2. Hartman, R. L.; Jensen, K. F. *Lab Chip* **2009,** *9,* 2495–2507. doi:10.1039/b906343a
3. Tanaka, K.; Fukase, K. *Beilstein J. Org. Chem.* **2009,** *5,* No. 40. doi:10.3762/bjoc.5.40
4. Wiles, C.; Watts, P.; Haswell, S. J. *Lab Chip* **2007,** *7,* 322–330. doi:10.1039/b615069a
5. Zhao, C.-X.; He, L.; Qiao, S. Z.; Middelberg, A. P. J. *Chem. Eng. Sci.* **2011,** *66,* 1463–1479. doi:10.1016/j.ces.2010.08.039
6. Hornung, C. H.; Mackley, M. R.; Baxendale, I. R.; Ley, S. V. *Org. Process Res. Dev.* **2007,** *11,* 399–405. doi:10.1021/op700015f
7. Kobayashi, J.; Mori, Y.; Okamoto, K.; Akiyama, R.; Ueno, M.; Kitamori, T.; Kobayashi, S. *Science* **2004,** *304,* 1305–1308. doi:10.1126/science.1096956
8. Wiles, C.; Watts, P. *Adv. Chem. Eng.* **2010,** *38,* 103–194. doi:10.1016/S0065-2377(10)38003-3
9. Wang, N.; Matsumoto, T.; Ueno, M.; Miyamura, H.; Kobayashi, S. *Angew. Chem., Int. Ed.* **2009,** *48,* 4744–4746. doi:10.1002/anie.200900565
10. Miller, P. W.; Long, N. J.; de Mello, A. J.; Vilar, R.; Audrain, H.; Bender, D.; Passchier, J.; Gee, A. *Angew. Chem., Int. Ed.* **2007,** *46,* 2875–2878. doi:10.1002/anie.200604541
11. Mak, X. Y.; Laurino, P.; Seeberger, P. H. *Beilstein J. Org. Chem.* **2009,** *5,* No. 19. doi:10.3762/bjoc.5.19
12. Rahman, M. T.; Fukuyama, T.; Kamata, N.; Sato, M.; Ryu, I. *Chem. Commun.* **2006,** 2236–2238. doi:10.1039/b600970k
13. Rebrov, E. V.; Klinger, E. A.; Berenguer-Murcia, A.; Sulman, E. M.; Schouten, J. C. *Org. Process Res. Dev.* **2009,** *13,* 991–998. doi:10.1021/op900085b

14. Lemke, E. A.; Gambin, Y.; Vandelinder, V.; Brustad, E. M.; Liu, H.-W.; Schultz, P. G.; Groisman, A.; Deniz, A. A. *J. Am. Chem. Soc.* **2009,** *131,* 13610–13612. doi:10.1021/ja9027023
15. Aota, A.; Nonaka, M.; Hibara, A.; Kitamori, T. *Angew. Chem., Int. Ed.* **2007,** *46,* 878–880. doi:10.1002/anie.200600122
16. Razzaq, T.; Kappe, C. O. *Chem.–Asian J.* **2010,** *5,* 1274–1289. doi:10.1002/asia.201000010
17. Park, C. P.; Van Wingerden, M. M.; Han, S.-Y.; Kim, D.-P.; Grubbs, R. H. *Org. Lett.* **2011,** *13,* 2398–2401. doi:10.1021/ol200634y
18. Park, C. P.; Kim, D.-P. *Angew. Chem., Int. Ed.* **2010,** *49,* 6825–6829. doi:10.1002/anie.201002490
19. Rasheed, M.; Wirth, T. *Angew. Chem., Int. Ed.* **2011,** *50,* 357–358. doi:10.1002/anie.201006107
20. Brivio, M.; Verboom, W.; Reinhoudt, D. N. *Lab Chip* **2006,** *6,* 329–344. doi:10.1039/b510856j
21. Mason, B. P.; Price, K. E.; Steinbacher, J. L.; Bogdan, A. R.; McQuade, D. T. *Chem. Rev.* **2007,** *107,* 2300–2318. doi:10.1021/cr050944c
22. He, P.; Watts, P.; Marken, F.; Haswell, S. J. *Angew. Chem., Int. Ed.* **2006,** *45,* 4146–4149. doi:10.1002/anie.200600951
23. Wegner, J.; Ceylan, S.; Kirschning, A. *Chem. Commun.* **2011,** *47,* 4583–4592. doi:10.1039/c0cc05060a
24. Nagaki, A.; Takabayashi, N.; Tomida, Y.; Yoshida, J.-i. *Beilstein J. Org. Chem.* **2009,** *5,* No. 16. doi:10.3762/bjoc.5.16
25. Tomida, Y.; Nagaki, A.; Yoshida, J.-i. *J. Am. Chem. Soc.* **2011,** *133,* 3744–3747. doi:10.1021/ja110898s
26. Frost, C. G.; Mutton, L. *Green Chem.* **2010,** *12,* 1687–1703. doi:10.1039/c0gc00133c
27. Mennecke, K.; Kirschning, A. *Beilstein J. Org. Chem.* **2009,** *5,* No. 21. doi:10.3762/bjoc.5.21
28. Shore, G.; Tsimerman, M.; Organ, M. G. *Beilstein J. Org. Chem.* **2009,** *5,* No. 35. doi:10.3762/bjoc.5.35
29. Massi, A.; Cavazzini, A.; Del Zoppo, L.; Pandoli, O.; Costa, V.; Pasti, L.; Giovannini, P. P. *Tetrahedron Lett.* **2011,** *52,* 619–622. doi:10.1016/j.tetlet.2010.11.157
30. Tricotet, T.; O'Shea, D. F. *Chem.–Eur. J.* **2010,** *16,* 6678–6686. doi:10.1002/chem.200903284
31. Bogdan, A. R.; Poe, S. L.; Kubis, D. C.; Broadwater, S. J.; McQuade, D. T. *Angew. Chem., Int. Ed.* **2009,** *48,* 8547–8550. doi:10.1002/anie.200903055
32. Palde, P. B.; Jamison, T. F. *Angew. Chem., Int. Ed.* **2011,** *50,* 3525–3528. doi:10.1002/anie.201006272
33. Brandt, J. C.; Wirth, T. *Beilstein J. Org. Chem.* **2009,** *5,* No. 30. doi:10.3762/bjoc.5.30
34. Gutmann, B.; Roduit, J.-P.; Roberge, D.; Kappe, C. O. *Angew. Chem., Int. Ed.* **2010,** *49,* 7101–7105. doi:10.1002/anie.201003733
35. Carofiglio, T.; Donnola, P.; Maggini, M.; Rossetto, M.; Rossi, E. *Adv. Synth. Catal.* **2008,** *350,* 2815–2822. doi:10.1002/adsc.200800459
36. Meyer, S.; Tietze, D.; Rau, S.; Schäfer, B.; Kreisel, G. *J. Photochem. Photobiol., A: Chem.* **2007,** *186,* 248–253. doi:10.1016/j.jphotochem.2006.08.014
37. Jähnisch, K.; Dingerdissen, U. *Chem. Eng. Technol.* **2005,** *28,* 426–427. doi:10.1002/ceat.200407139
38. Bourne, R. A.; Han, X.; Poliakoff, M.; George, M. W. *Angew. Chem., Int. Ed.* **2009,** *48,* 5322–5325. doi:10.1002/anie.200901731
39. Wootton, R. C. R.; Fortt, R.; de Mello, A. J. *Org. Process Res. Dev.* **2002,** *6,* 187–189. doi:10.1021/op0155155
40. O'Brien, M.; Taylor, N.; Polyzos, A.; Baxendale, I. R.; Ley, S. V. *Chem. Sci.* **2011,** *2,* 1250–1257. doi:10.1039/c1sc00055a
41. Polyzos, A.; O'Brien, M.; Petersen, T. P.; Baxendale, I. R.; Ley, S. V. *Angew. Chem., Int. Ed.* **2011,** *50,* 1190–1193. doi:10.1002/anie.201006618
42. Chambers, R. D.; Holling, D.; Spink, R. C. H.; Sandford, G. *Lab Chip* **2001,** *1,* 132–137. doi:10.1039/b108841f
43. Chambers, R. D.; Fox, M. A.; Holling, D.; Nakano, T.; Okazoe, T.; Sandford, G. *Lab Chip* **2005,** *5,* 191–198. doi:10.1039/b416400h
44. Park, C. P.; Kim, D.-P. *J. Am. Chem. Soc.* **2010,** *132,* 10102–10106. doi:10.1021/ja102666y
45. Park, C. P.; Maurya, R. A.; Lee, J. H.; Kim, D.-P. *Lab Chip* **2011,** *11,* 1941–1945. doi:10.1039/c1lc20071b
46. Lee, J. N.; Park, C.; Whitesides, G. M. *Anal. Chem.* **2003,** *75,* 6544–6554. doi:10.1021/ac0346712
47. Monnerie, N.; Ortner, J. J. *Sol. Energy Eng.* **2001,** *123,* 171–174. doi:10.1115/1.1354996
48. Griesbeck, A. G.; El-Idreesy, T. T.; Lex, J. *Tetrahedron* **2006,** *62,* 10615–10622. doi:10.1016/j.tet.2006.05.093
49. Bezerra, D. P.; Marinho Filho, J. D. B.; Alves, A. P. N. N.; Pessoa, C.; de Moraes, M. O.; Pessoa, O. D. L.; Torres, M. C. M.; Silveira, E. R.; Viana, F. A.; Costa-Lotufo, L. V. *Chem. Biodiversity* **2009,** *6,* 1224–1231. doi:10.1002/cbdv.200800253

License and Terms

Beilstein Journal of Organic Chemistry

The Eschenmoser coupling reaction under continuous-flow conditions

Sukhdeep Singh, J. Michael Köhler, Andreas Schober and G. Alexander Groß*

Full Research Paper

Open Access

Address:
Institute for Chemistry and Biotechnology, Technische Universität Ilmenau, Weimarerstr. 32, D-98693-Ilmenau

Email:
G. Alexander Groß* - alexander.gross@tu-ilmenau.de

* Corresponding author

Keywords:
activation energy; episulfide; flow chemistry; keto imine; kinetics; S-alkylation; sulfide contraction; triisopropyl phosphite

Beilstein J. Org. Chem. **2011,** *7,* 1164–1172.
doi:10.3762/bjoc.7.135

Received: 31 May 2011
Accepted: 28 July 2011
Published: 25 August 2011

This article is part of the Thematic Series "Chemistry in flow systems II".

Guest Editor: A. Kirschning

Abstract

The Eschenmoser coupling is a useful carbon–carbon bond forming reaction which has been used in various different synthesis strategies. The reaction proceeds smoothly if S-alkylated ternary thioamides or thiolactames are used. In the case of S-alkylated secondary thioamides or thiolactames, the Eschenmoser coupling needs prolonged reaction times and elevated temperatures to deliver valuable yields. We have used a flow chemistry system to promote the Eschenmoser coupling under enhanced reaction conditions in order to convert the demanding precursors such as S-alkylated secondary thioamides and thiolactames in an efficient way. Under pressurized reaction conditions at about 220 °C, the desired Eschenmoser coupling products were obtained within 70 s residence time. The reaction kinetics was investigated and 15 examples of different building block combinations are given.

Introduction

The Eschenmoser coupling [1,2] is a reaction method that yields β-enaminocarbonyl derivatives of type **4** by the elimination of sulfur (sulfide contraction) from an episulfide intermediate (Scheme 1). The reaction was described for the first time by Knott in 1955 [3] and became prominent later on when it was applied to the total synthesis of vitamin B12 by Eschenmoser [4]. Since these early days the Eschenmoser coupling has been applied many times as a useful reaction step in a variety of synthesis strategies. Different natural products, such as diplodialid macrolactone- [5], sedamine alkaloid- [6], sparteine- [7], mersicarpine- [8], batzelladine- [9], fuligocandin- [10] and vitamin B12-derivatives [11] were prepared with the aid of sulfide contraction steps. Pharmaceutically important substances, such as methylphenidat [12] or the marine neurotoxin hemibreve-

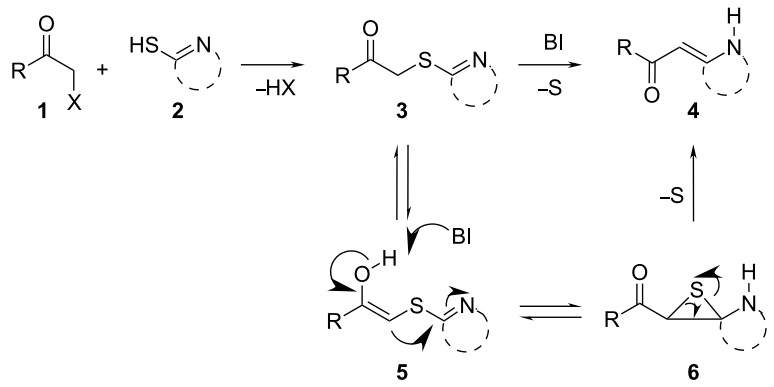

Scheme 1: Eschenmoser coupling reaction with secondary S-alkylated thioamide derivatives of type **3**.

toxin [13], were prepared by utilization of the Eschenmoser coupling reaction. Recently, we explored the Eschenmoser coupling in order to produce Biginelli type dihydropyrimidine (DHPM) derivatives as screening candidates for pharmaceutical and crop science research [14]. Moreover, the Eschenmoser coupling is quite a valuable, metal free, carbon–carbon bond forming reaction.

The necessary starting materials of type **3** can be prepared by S-alkylation of secondary thioamide or thiolactame building blocks of type **2** with α-bromoketones **1** (X = Br). The carbon–carbon coupling occurs between these building blocks as shown in Scheme 1. Due to the ease of accessibility of the building blocks and the usually high-yielding S-alkylation step, the Eschenmoser coupling is an interesting reaction for diversity-oriented combinatorial synthesis [15-17].

The new carbon–carbon bond formation occurs during the construction of the episulfide intermediate **6**, which requires base catalysis (Bl). The sulfur extraction from the episulfides **6** or **8** yields the desired β-enaminocarbonyl derivative **4** or **9**. However, the detailed reaction mechanism for the sulfur extraction step has not yet been fully proven and obviously depends on the applied reaction conditions. Experimental observations show that the reaction can take place without the addition of a thiophilic agent or base. This is a strong hint that the sulfide extraction is of an intramolecular pericylic nature, as proposed in Scheme 1. In the presence of a thiophilic agent, the mechanism of extraction via intermediate ionic states also seems plausible. Nevertheless, the Eschenmoser coupling reaction requires the addition of a base and a thiophilic agent in the most cases. Here, triphenylphosphine- or trialkyl-phosphite-derivatives are usually employed to promote the sulfide contraction with valuable yield and selectivity. Eschenmoser himself made use of bi-functional reagents with dual thiophile and basic properties in one molecule [2]. With regards to experimental considerations, the thiophilic reagent must be carefully chosen in order to overcome the difficulties in the separation of the desired product from phosphine sulfide byproducts.

S-Alkylated ternary thioamides of type **7** usually undergo the episulfide formation and subsequent sulfide contraction smoothly (Scheme 2). This is due to the strong electron accepting nature of the thioiminium intermediate **8**. Unfortunately, the S-alkylation is sometimes difficult in these cases [6]. In the case of secondary thiolactames of type **5**, sulfide contraction takes place as well, but prolonged reaction time and increased reaction temperature are necessary in most cases. In contrast to this, secondary thioamide derivatives of type **5** undergo the S-alkylation with α-bromoketones more readily than ternary thioamides. However, the specific reactivity of both reaction steps obviously depends on the building blocks used and their specific reactivity. For the present work we chose only commercially available α-bromoketone building blocks and secondary thiolactame and thioamide derivatives. To improve the long reaction times we investigated the Eschenmoser coupling under process intensification conditions. Therefore, reaction temperatures far beyond the solvent boiling point were applied under pressurized flow conditions for a minimum residence time. For small scale synthesis flow chemistry is of great advantage to realize these conditions on the laboratory bench safely [18].

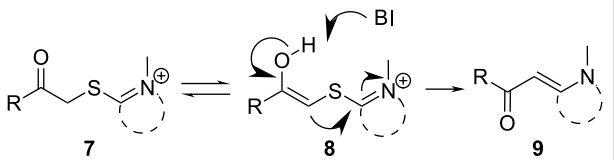

Scheme 2: Eschenmoser coupling sequence of S-alkylated ternary thioamides of type **7**.

Results and Discussion

For the reaction optimization we have focused on a straightforward procedure that finally prevents the isolation of the S-alkylated intermediates **3** and avoids a change of the reaction solvent for the subsequent step. To establish the best conditions we investigated the reaction of 2-bromo-1-phenylethanone (**1a**) with 2-mercapto-6-methyl-pyrimidin-4-ol (**2a**) in detail. Therefore, **2a** was dissolved in different solvents and 2 equiv NEt_3 were added. After 10 min, the dissolved α-bromoketone **1a** was added dropwise. A concentration of about 0.1 mol/L was achieved in this way. The reaction solutions were sonicated for about 1/2 h. Subsequently, the $HNEt_3Br$ precipitates were filtered off. The precipitation and filtration was done with care to prevent malfunctions of the feeding pumps. In the case of chloroform as solvent no precipitation took place, but the LC–MS analysis indicated the S-alkylation clearly, with a purity of about 89%. To all filtered solutions 1.25 equiv of triisopropylphosphite (TIP) were added as thiophilic agent before the reaction solutions were fed through the flow chemistry setup. A flow rate of 1000 µL/min (RT: 55 s) was adjusted and the reaction temperature was increased stepwise from 120 to 240 °C. The backpressure regulator was set for all experiments to about 100 bar. The received reaction products were collected and analyzed by LC–MS analysis. In the case of THF as solvent, precipitation took place in the capillary and the backpressure regulator became blocked. In case of chloroform, the reaction solution turned black, and oily polymeric products were formed when the reaction temperature exceeded 150 °C. As a result, only traces of the desired product **4aa** were observed by LC–MS analysis, along with multiple side products. The side products were not investigated in greater detail because of the complexity of the mixture. In the case of ethanol as solvent, the solubility of the starting materials and S-alkylated intermediate **3aa** was poor and the solutes tended to precipitate. However, anhydrous 1,4-dioxane was found to be the best solvent for both reaction steps. Conversions, with anhydrous 1,4-dioxane as solvent, are shown in Figure 1. Only poor conversion was observed up to 160 °C. The maximum conversion of about 98% was observed at 220 °C, with a flow rate of 250 µL/min. At reaction temperatures beyond 220 °C the selectivity of the reaction decreased dramatically and some unidentified decomposition products appeared. Nevertheless, the increase of the flow rate, to about 500 or 750 µL/min at 230 °C, led to comparable good yields and high reaction selectivities. In the case of higher flow rate, of 1000 µL/min and beyond, and the corresponding shorter reaction time, a decreased conversion was observed due to the slow reaction kinetics (Figure 1).

The flow chemistry technique allows the determination of reaction kinetics data in a fast and efficient way, even under pressurized process-identifying conditions. We investigated the kinetics of the sulfide contraction of **3aa** to **4aa** in detail. For this purpose, a 0.1 mol/L reaction solution was fed through the reaction system at different flow rates and reaction tempera-

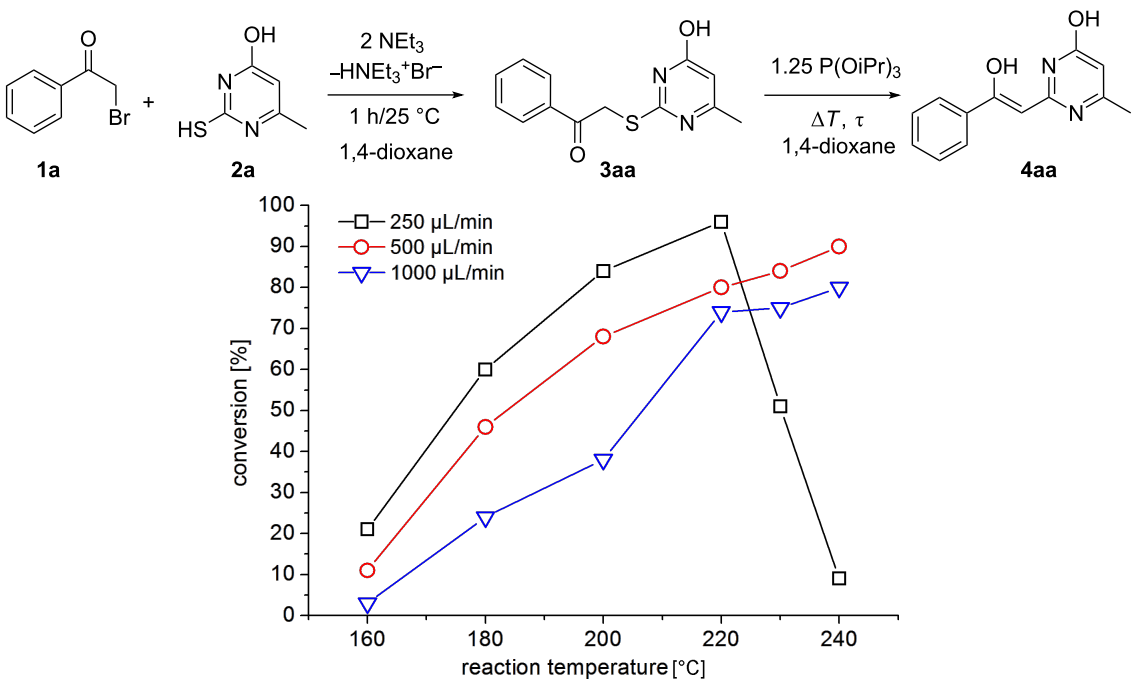

Figure 1: Conversion of **3aa** to **4aa** under different flow conditions.

tures. After each change in the reaction parameters the reaction system was allowed to reach a steady state before a sample was taken. After a change of the flow rate, samples were taken only after a minimum waiting period of about three times the residence time to achieve system equilibration.

In order to compare the reaction performance of the flow reaction with the conventional technique, the same reaction was carried out under batch conditions. The resulting product solutions were analyzed by LC–MS and isolated by the standard precipitation/recrystallization procedure. No conversion was observed in the batch reaction at ambient temperature within 48 h. Even heating up to the boiling point of 1,4-dioxane (101 °C) for about 1 h did not furnish the desired product in any significant amount. However, after refluxing overnight a yield of at least 43% **4aa** was isolated.

The investigated Eschenmoser coupling under flow conditions was found to be a first order reaction. Rate constants were calculated using the first order kinetic Equation 1, where c [mol/L] is the concentration of the product **4aa** at the reaction temperature T [K] after the reaction solution was passed through the heater with the residence time τ [s]. The resulting kinetic plot is shown in Figure 2 (left). The determined rate constants were used to prepare an Arrhenius plot and for calculation of the activation energy from Equation 2. The resulting Arrhenius plot is shown in Figure 2 (right). An activation energy E_A of about 91 kJ/mol, and a frequency factor A of about 3.73×10^9 s^{-1}, were found. This activation energy is obviously the reason for the slow reaction kinetics at moderate temperature. Hence, the application of pressurized high temperature conditions should lead to significant reaction intensification.

$$\ln\left(\frac{c}{c_0}\right) = -k(T)\cdot\tau \quad (1)$$

$$k(T) = A\cdot e^{-\frac{E_a}{R\cdot T}} \quad (2)$$

For the analysis of the reaction kinetics the following workflow was necessary: 1) Variation of the reaction parameters, 2) probe sampling, 3) HPLC analysis and 4) reaction kinetics calculations for six different temperatures at five different flow rates. The determination of the complete reaction kinetics data was complete within 6 h. A comparable analysis by a sequential batch technique would take approximately 1 week. Hence, flow chemistry is well suited to efficiently determine the kinetics for reactions under unconventional reaction conditions.

To explore the scope of the sulfide-contraction reaction we varied both building blocks in a systematic manner under the following reaction conditions: 0.1 M reaction solution in anhydrous 1,4-dioxane, 2 equiv NEt_3, 1.25 equiv TIP at 220 °C and 250–750 µL/min flow rate. First, we varied the thiolactame building blocks **2** and kept the α-bromoketone **1a** constant. In Table 1, the investigated building blocks **2a**–**2i** and the isolated yields are shown. For the product workup, 100% volume of water and 1% 1 M HCl were added to the product solution. If precipitation took place after addition, the residues were filtered. If no precipitation took place, then the reaction solution was extracted with ethyl acetate. The organic phase was separated and dried over $MgSO_4$ and the ethyl acetate was subsequently removed by evaporation. The resulting extracts or precipitates were recrystallized from a solvent mixture of hot methanol/dichloromethane. However, the crystallization process

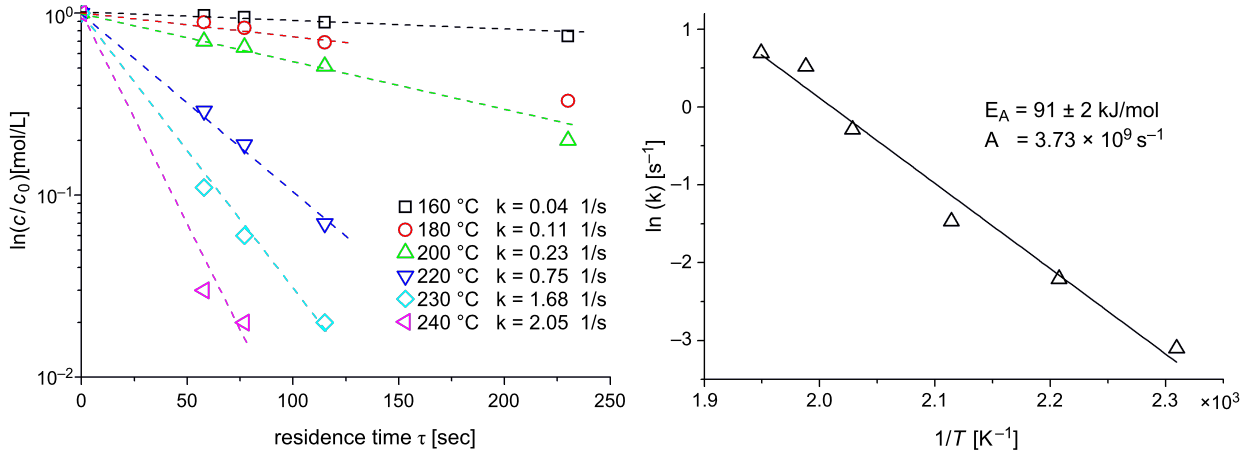

Figure 2: Reaction kinetics analysis. Left: Rate constants with 0.1 M reaction solution. Right: Arrhenius-plot for the determined rate constants.

Table 1: Product and yields received for different thio-substrates **2**.

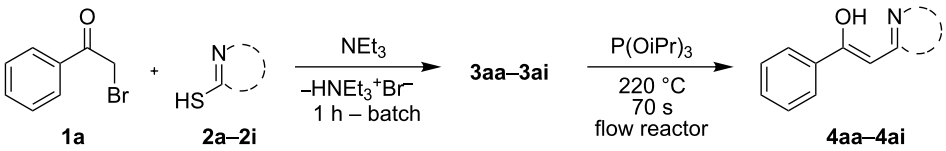

Structure of **2**		Product **4**		Yield[a]
2a	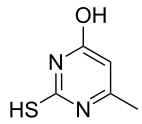	**4aa**	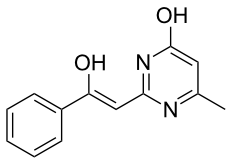	48
2b	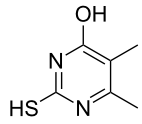	**4ab**	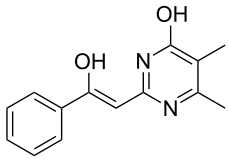	55
2c	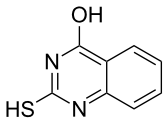	**4ac**	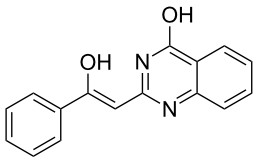	78
2d	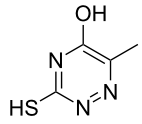	**4ad**	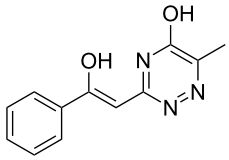	–[b]
2e	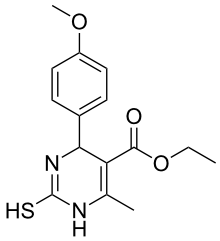	**4ae**	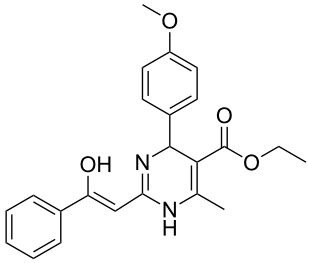	82
2f	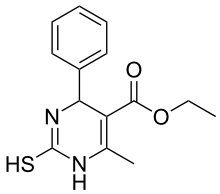	**4af**	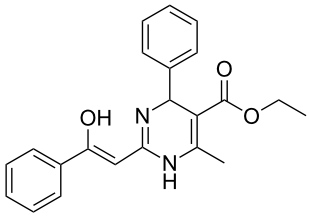	69
2g	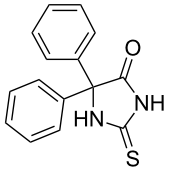	**4ag**	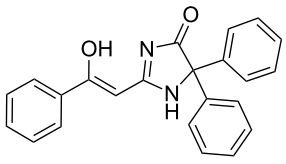	92

Table 1: Product and yields received for different thio-substrates **2**. (continued)

2h	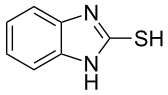	**4ah**	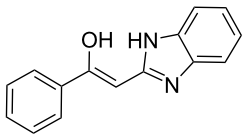	5[c]
2i	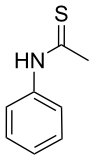	**4ai**	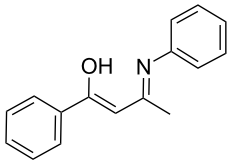	58

[a]Isolated yields; [b]Decomposition during sulfide contraction; [c]No product precipitation or extraction of **4ah** was possible; only **3ah** was isolated in smaller amount.

was not optimized and there is scope to increase yields further. The desired products **3** were received in synthetically useful yields in almost all cases. The NMR spectra of the resulting products **4** mainly comprise two sets of signals with varying intensities (details can be found in the Supporting Information File 1). This is due to the two different possibilities for the intramolecular H-bond formation caused by the keto–enol tautomerism of **4**. In this scheme, the reaction of 2-mercaptopyrimidin-4-ol derivatives **2a**, **2b** and **2c** proceeded smoothly with high yields. 6-Aza-2-thiothymine (**2d**) was quantitatively S-alkylated but decomposed during the sulfide-contraction step and subsequent workup. Therefore, we could not isolate the desired product **4ad**. The reaction of dihydropyrimidine substrates **2e** and **2f** proceeded in a facile way, and the desired products **3ae** and **3af** were isolated in good yields. Even the mercapto hydantoin derivative **2g** underwent the two step reaction smoothly and yielded the desired product **4ag** in good quantity. In case of the 1*H*-benzoimidazole-2-thiol (**2h**), the selective S-alkylation failed. The utilized alkylation conditions favor the bis-alkylation, and hence the S-alkylated product was produced in less than 10% yield (HPLC-peak area). LC–MS analysis after the sulfide contraction of this mixture showed that the bis-S-alkylated intermediate was only partially converted. Unfortunately, we could not isolate the product from the complex reaction mixture by the standard precipitation and extraction/crystallization processes. The 2-thiobenzimidazol (**2h**) underwent the S-alkylation as well as the sulfide contraction smoothly and showed good conversion to the desired product **3ah**. However, the applied precipitation technique yielded only a trace amount of the unconverted intermediate **3ah**. *N*-Phenylthioacetamide (**2i**) was additionally chosen as a noncyclic secondary thioamide example. The desired product **4ai** was received in excellent yield.

Various α-bromoketone building blocks, as shown in Table 2, were investigated in combination with the thiolactame **2a**. We choose only aromatic bromoketones because of their known good reactivity and selectivity for the sulfide contraction [1]. Recently, we investigated the reaction of dihydropyrimidine derivatives of type **11** with different aliphatic ketones **10** under batch conditions. In that case the S-alkylated substrates **12** did not undergo the sulfide contraction but rather the thiazole formation to **13** took place exclusively (Scheme 3) [19]. The thiazol formation by condensation is a well known side reaction of the sulfide contraction. Nevertheless, and in contrast to the batch reaction, no thiazole formation was observed under the investigated flow conditions.

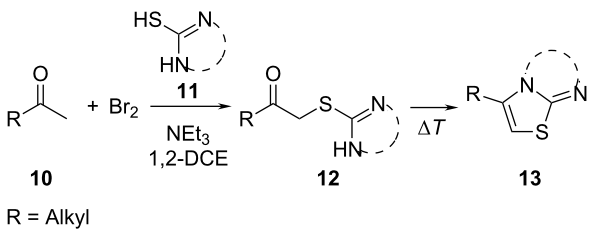

Scheme 3: Exclusive formation of thiazol **13** with dihydropyrimidine derivatives **11** take place in the case of aliphatic ketones **10** [19].

The influence of the bromoketone building blocks **1a**–**1g** on the flow reaction performance was investigated (Table 2). 2-Mercapto-6-methylpyrimidin-4-ol (**2a**) was chosen as the reaction partner for all bromoketones **1a**–**1g**. High yields and reaction selectivities were observed in all cases at the investigated temperature of 220 °C. The influence of the different aromatic bromoketones on the reaction seems to be negligible. The electron accepting nature of the thio-substrate seems to have the dominating effect on the reaction performance. However, all investigated combinations of the building blocks furnished the desired products in good yields within residence times of about 70 s.

Table 2: Product and yields for various α-bromoketones **1**.

1a–1g **2a** **4aa–4ga**

	Structure of **1**		Product **4**	Yield[a]
1a	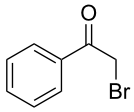	**4aa**	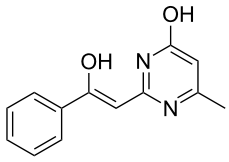	48
1b	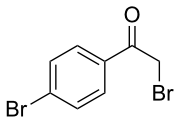	**4ba**	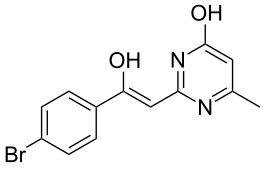	66
1c	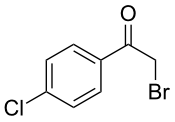	**4ca**	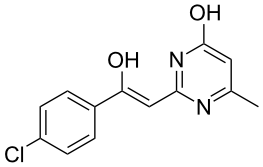	61
1d	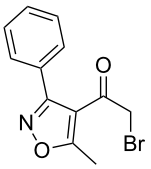	**4da**	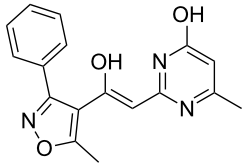	67
1e	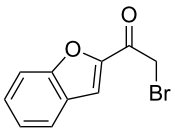	**4ea**	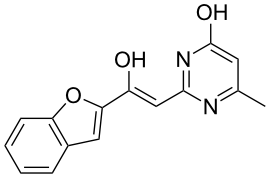	72
1f	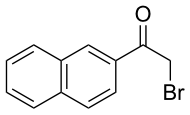	**4fa**	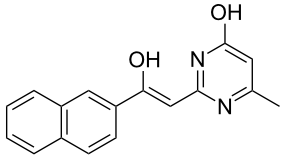	61
1g	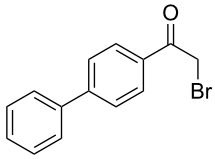	**4ga**	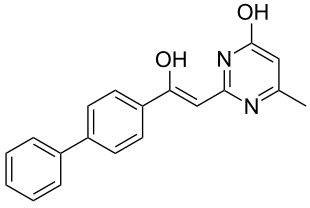	73

[a]Isolated yields.

Conclusion

We found that Eschenmoser coupling can be performed at a reaction temperature of 220 °C with residence times of about 70 s. 1,4-Dioxane was found to be the most effective solvent. The reaction kinetics was determined in a fast and efficient way for 0.1 M reaction concentration. As a result, the flow chemistry technique enabled the significant intensification of the reaction kinetics, by application of enhanced process conditions on the laboratory bench, in a safe and efficient way. The intensification potential was investigated for demanding secondary thiolactames of type **5**, and exemplary combinations of building blocks, as shown in Table 1 and Table 2, were examined. In almost all investigated cases the desired products were received in synthetically useful yields.

Experimental

Flow chemistry system

A flow chemistry assembly consisting of two feeding pumps, a capillary reactor, a heat controller and a backpressure regulator was used, as shown in Figure 3. The capillary reactor consists of a 2.1 m long steel capillary with 0.75 mm inner diameter (~930 µL), which was wrapped around a brass cylinder with an integrated heat-rod (hotset, HHP 200 W, 8 × 80 mm) and jacketed by a thermally isolated brass cover (Figure 4). Thermal control was achieved by using a commercial process controller (EMKO process controller ESM-4450) with adapted PT-100 temperature sensor. For pressure control a manual needle valve (micro splitter, Upchurch) was integrated at the capillary outlet. About 20 cm of the capillary between the heating cylinder and the backpressure regulator was tempered by a water chiller to ambient temperature. Feeds were delivered by the help of two double piston HPLC-pumps (Shimadzu LC-9A, double inlet check valves). The first pump was used to feed the reaction solutions and the second pump was used to feed pure solvent for purging and dilution. The maximum operational parameters for the complete flow chemistry setup were proven up to 250 °C and 200 bar. Residence times (τ) between 40 min and 60 s were achieved by adjusting the flow rate from 20 to 2000 µL/min.

Figure 4: Capillary reactor with jacketed cover removed, and the process controller.

Supporting Information

Supporting Information File 1

General procedures, analytical and spectral data.
[http://www.beilstein-journals.org/bjoc/content/supplementary/1860-5397-7-135-S1.pdf]

Acknowledgments

The support from K. Risch and S. Günther for compound analysis is gratefully acknowledged. The authors thank

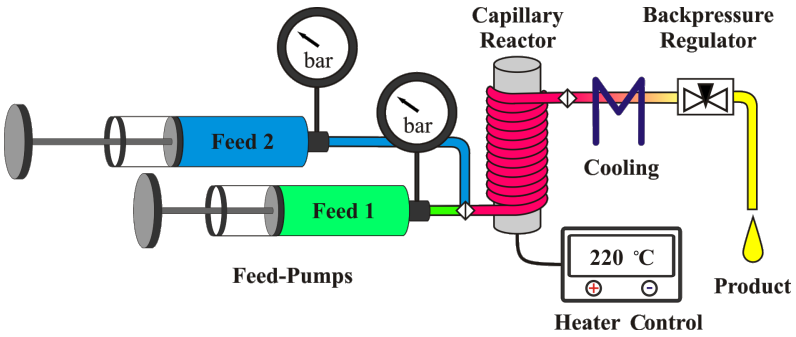

Figure 3: Flow chemistry setup scheme.

S. Schneider for the support during the development of the reaction setup. This work was partially supported by different BMBF projects: OPTIMI (FKZ: 16SV3701), BioMepSens (FKZ: 03ZIK062) and Mikrokunststoffformen (FKZ: 03ZIK465).

References

1. Shiosaki, K. The Eschenmoser Coupling Reaction. In *Comprehensive Organic Synthesis;* Trost, B. M., Ed.; Pergamon Press: Oxford, 1991; Vol. 2, pp 865–892. doi:10.1016/B978-0-08-052349-1.00051-2
2. Roth, M.; Dubs, P.; Götschi, E.; Eschenmoser, A. *Helv. Chim. Acta* **1971,** *54,* 710–734. doi:10.1002/hlca.19710540229
3. Knott, E. B. *J. Chem. Soc.* **1955,** 916–927. doi:10.1039/JR9550000916
4. Eschenmoser, A.; Wintner, C. E. *Science* **1977,** *196,* 1410–1426. doi:10.1126/science.867037
5. Ireland, R. E.; Brown, F. R., Jr. *J. Org. Chem.* **1980,** *45,* 1868–1880. doi:10.1021/jo01298a022
6. Neto, B. A. D.; Lapis, A. A. M.; Bernd, A. B.; Russowsky, D. *Tetrahedron* **2009,** *65,* 2484–2496. doi:10.1016/j.tet.2009.01.081
7. Wlodarczak, J.; Wysocka, W.; Katrusiak, A. *J. Mol. Struct.* **2010,** *971,* 12–17. doi:10.1016/j.molstruc.2010.02.050
8. Nakajima, R.; Ogino, T.; Yokoshima, S.; Fukuyama, T. *J. Am. Chem. Soc.* **2010,** *132,* 1236–1237. doi:10.1021/ja9103233
9. Elliott, M. C.; Long, M. S. *Org. Biomol. Chem.* **2004,** *2,* 2003–2011. doi:10.1039/b404679j
10. Pettersson, B.; Hasimbegovic, V.; Bergman, J. *J. Org. Chem.* **2011,** *76,* 1554–1561. doi:10.1021/jo101864n
11. Mulzer, J.; List, B.; Bats, J. W. *J. Am. Chem. Soc.* **1997,** *119,* 5512–5518. doi:10.1021/ja9700515
12. Russowsky, D.; da Silveira Neto, B. A. *Tetrahedron Lett.* **2003,** *44,* 2923–2926. doi:10.1016/s0040-4039(03)00420-9
13. Nicolaou, K. C.; Reddy, K. R.; Skokotas, G.; Sato, F.; Xiao, X. Y.; Hwang, C. K. *J. Am. Chem. Soc.* **1993,** *115,* 3558–3575. doi:10.1021/ja00062a021
14. Singh, S.; Schober, A.; Gebinoga, M.; Groß, G. A. *Tetrahedron Lett.* **2009,** *50,* 1838–1843. doi:10.1016/j.tetlet.2009.02.027
15. Groß, G. A.; Wurziger, H.; Schlingloff, G.; Schober, A. *QSAR & Comb. Sci. (Special Issue: Array Synthesis)* **2006,** *25,* 1055–1062. doi:10.1002/qsar.200640120
16. Groß, G. A.; Mayer, G.; Albert, J.; Riester, D.; Osterodt, J.; Wurziger, H.; Schober, A. *Angew. Chem., Int. Ed.* **2006,** *118,* 3174–3178. doi:10.1002/ange.200503041
17. Gebinoga, M.; Groß, G. A.; Albrecht, A.; Lübeck, T.; Henkel, T.; Hoffmann, P.; Klemm, U.; Schlingloff, G.; Frank, T.; Schober, A. *QSAR & Comb. Sci. (Special Issue: Array Synthesis)* **2006,** *25,* 1063–1068. doi:10.1002/qsar.200640113
18. Wegner, J.; Ceylan, S.; Kirschning, A. *Chem. Commun.* **2011,** *47,* 4583–4592. doi:10.1039/c0cc05060a
19. Singh, S.; Schober, A.; Gebinoga, M.; Groß, G. A. *Tetrahedron Lett.* **2011,** *52,* 3814–3817. doi:10.1016/j.tetlet.2011.05.067

License and Terms

Beilstein Journal of Organic Chemistry

Koch–Haaf reaction of adamantanols in an acid-tolerant hastelloy-made microreactor

Takahide Fukuyama*, Yu Mukai and Ilhyong Ryu*

Letter

Open Access

Address:
Department of Chemistry, Graduate School of Science, Osaka Prefecture University, Sakai, Osaka 599-8531, Japan

Email:
Takahide Fukuyama* - fukuyama@c.s.osakafu-u.ac.jp; Yu Mukai - y_mukai@c.s.osakafu-u.ac.jp; Ilhyong Ryu* - ryu@c.s.osakafu-u.ac.jp

* Corresponding author

Keywords:
continuous flow system; hastelloy; Koch–Haaf reaction; microreactor

Beilstein J. Org. Chem. **2011,** *7,* 1288–1293.
doi:10.3762/bjoc.7.149

Received: 16 June 2011
Accepted: 16 August 2011
Published: 15 September 2011

This article is part of the Thematic Series "Chemistry in flow systems II".

Guest Editor: A. Kirschning

Abstract

The Koch–Haaf reaction of adamantanols was successfully carried out in a microflow system at room temperature. By combining an acid-tolerant hastelloy-made micromixer, a PTFE tube, and a hastelloy-made microextraction unit, a packaged reaction-to-workup system was developed. By means of the present system, the multigram scale synthesis of 1-adamantanecarboxylic acid was achieved in ca. one hour operation.

Introduction

The recent evolution of microreactor technology has allowed synthetic chemists to use this precisely sophisticated reaction apparatus in place of the well-established glassware batch flask [1-10]. Microreactors are expected to have a significant impact on chemical synthesis and production because of their many advantageous characteristics, such as highly efficient mixing, efficient heat transfer ability, precise control over the residence time, and high operational safety. We have studied and developed practical organic syntheses using flow microreactors, and we have reported thus far examples of Pd-catalyzed coupling reactions [11-13], radical reactions [14-16], and photoreactions [17-21].

Carbonylation reactions are a powerful tool for the introduction of carbon monoxide into organic molecules, and we also reported that Pd-catalyzed carbonylation [13] and radical carbonylation [16] could be successfully carried out in a continuous microflow system with higher efficiency than in a batch autoclave system. In this study, we focused on the carbonylation of carbocation intermediates carried out in a continuous microflow system [22-24]. The Koch–Haaf reaction [25], that is the carbonylation of alcohols or olefins with formic acid in the presence of a strong acid, is an important reaction for the preparation of carboxylic acids, which are widely used in organic synthesis [26-31]. Since the Koch–Haaf reaction is

highly exothermic, the reaction is typically carried out at controlled temperature by means of a cooling bath, such as an ice bath, and with carefully controlled slow addition of reagents through an addition funnel. The temperature control causes a serious problem especially for large scale synthesis. Herein, we report that the Koch–Haaf reaction in a microflow reactor can be carried out at room temperature without any cooling equipment. The employed hastelloy-made microreactor system was compatible with corrosive (strongly acidic) conditions and confirmed for gram scale (7.1 g) synthesis of 1-adamantanecarboxylic acid in ca. 1 h operation.

Results and Discussion

The carbonylation reaction of 1-adamantanol (**1a**) was investigated in a microflow system as a model reaction. Since the Koch–Haaf reaction requires the use of concentrated sulfuric acid, an acid-tolerant system is essential. For this study, we employed a combination of a hastelloy-made micromixer (MiChS, β-150H) having 150 μm reactant inlet holes and 200 μm × 300 μm channels (Figure 1), and a PTFE tube (1.0 mm i.d. × 3 m, inner volume: 2.36 mL) as a residence time unit. To this reactor system, a hastelloy-made microextraction unit (a flow-workup system) was attached (Figure 2 and Figure 3). The microextraction unit has three inlets and one outlet (channel size: 1 mm i.d. × 14 cm). The reaction mixture was mixed at T-shaped junctions with Et_2O and water, and a biphasic mixture was collected from the outlet.

Figure 1: Hastelloy-made micromixer (MiChS β-150H).

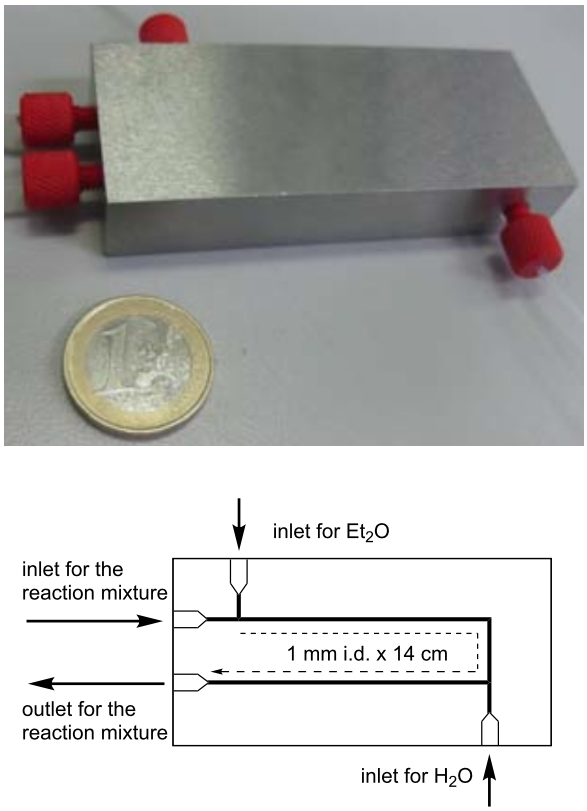

Figure 2: Hastelloy-made microextraction unit.

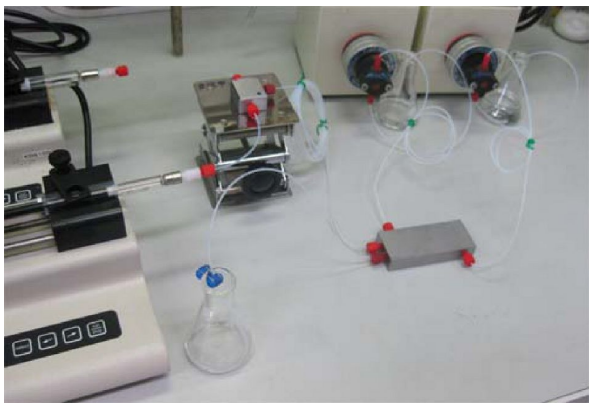

Figure 3: Acid-tolerant microflow system used for the Koch–Haaf reaction.

1-Adamantanol (**1a**) dissolved in HCOOH (flow rate: 0.30 mL/min) and 98% H_2SO_4 (flow rate: 0.88 mL/min) were mixed in the micromixer at room temperature, and the resulting reaction mixture was fed into the PTFE tube and then into the extraction unit, in which Et_2O (flow rate: 2.5 mL/min) and water (2 mL/min) were introduced to extract the carbonylation product and remove excess acids (Scheme 1). The biphasic mixture was collected in a flask and the ether layer was concentrated in vacuo. 1-Adamantanecarboxylic acid (**2a**) was obtained in 89% isolated yield after purification by silica gel column chromatography. While the residence time was a priori expected to be 2 min based on the total flow rate of the reagents and inner volume of the residence time unit, the observed

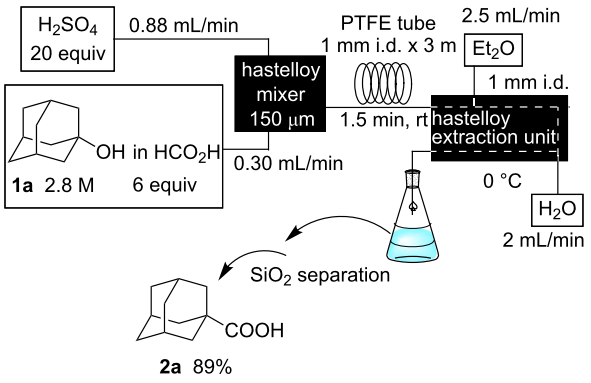

Scheme 1: Synthesis of 1-adamantanecarboxylic acid (**2a**) in a microflow system.

residence time was 1.5 min due to a plug flow by the CO gas generated.

For comparison, we also carried out the batch reaction in a 50 mL glass flask on 4 mmol scale to give **2a** in 92% yield. In the batch reaction, the careful addition of a solution of **1a** in formic acid over a period of 5 min and cooling in an ice bath were necessary to achieve good results. Indeed, without a cooling bath, we observed that the temperature of the reaction mixture rose up to 50–60 °C. It is therefore remarkable that the reaction in the microflow system can be performed successfully at room temperature without any cooling unit.

We then investigated the reaction of some other adamantanols, such as that of 2-adamantanol (**1b**) and 2-methyl-2-adamantanol (**1c**) (Scheme 2). The reaction of **1b** in a microflow system gave a mixture of 2-adamantanecarboxylic acid (**2b**) and 1-adamantanecarboxylic acid (**2a**) (82% total yield, **2b**:**2a** = 58:42), in which the latter compound originated from the isomerized tertiary cation, which derived from the initially formed secondary cation. The batch reaction gave a mixture of **2b** and **2a** in 65% total yield with a greater proportion of the rearranged product (**2b**:**2a** = 14:86). The reaction of 2-methyl-2-adamantanol (**1c**) resulted in a mixture of the carboxylated products, **2c**, **2c'**, and **2c''** in 97% total yield (**2c**:**2c'**:**2c''** = 23:53:24). The batch reaction resulted in an inferior yield with more of the rearranged products (83% yield, **2c**:**2c'**:**2c''** = 19:62:19). All results are summarized in Table 1.

Multigram scale synthesis of **2a** from **1a** was carried out in a continuous flow reaction. When the reaction of **1a** (45 mmol) was performed for 55 min, 7.1 g of **2a** was obtained in 88% yield, demonstrating that the present microflow system can be used for multigram scale synthesis without any problems (Scheme 3).

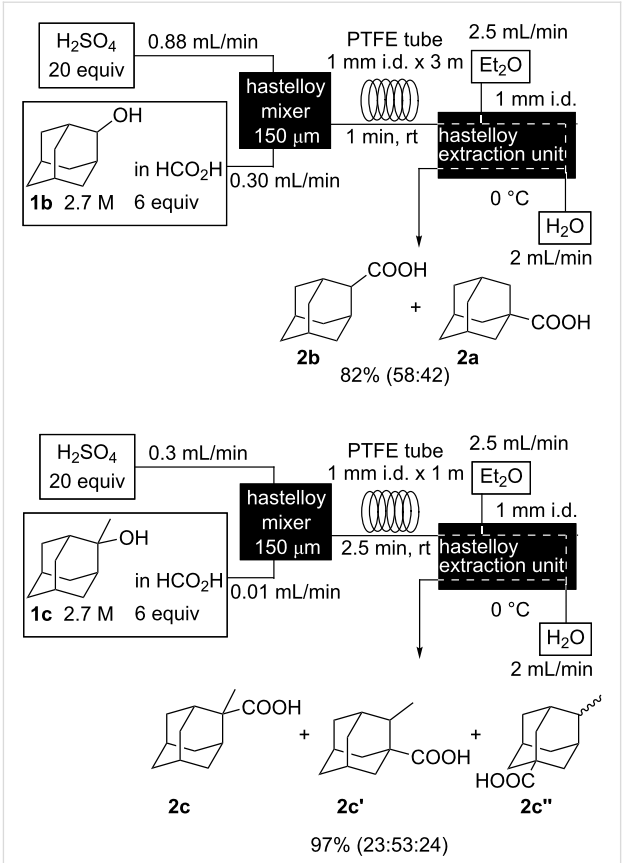

Scheme 2: Koch–Haaf reaction of **1b** and **1c** in a microflow system.

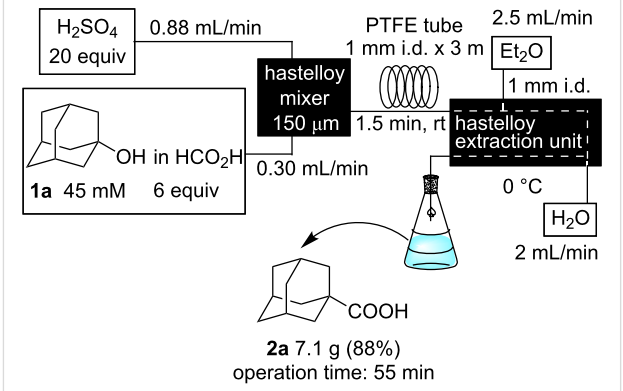

Scheme 3: Multigram scale flow synthesis of 1-adamantanecarboxylic acid (**2a**).

Conclusion

In this work, we demonstrated that the Koch–Haaf reaction of adamantanols was successfully carried out in an acid-tolerant microflow system comprising a hastelloy-made micromixer, a PTFE tube, and a hastelloy-made microextraction unit. Unlike in the batch system, the reaction could be carried out at room temperature without any cooling equipment. The employed reaction-to-workup system was useful for the multigram scale

Table 1: Koch–Haaf reactions of adamantanols.[a]

Entry	1	Reactor	Conditions	Product (yield)[b]
1	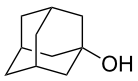 **1a**	microflow	*T*: 20 °C flow rate (**1a**/HCO_2H): 0.30 mL/min flow rate (H_2SO_4): 0.88 mL/min residence time: 2 min[c] residence time: 1.5 min[d]	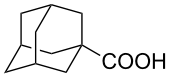 **2a** 89%
2	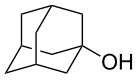 **1a**	batch	*T*: 15–20 °C addition time: 5 min reaction time: 2 min	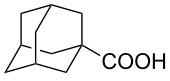 **2a** 92%
3	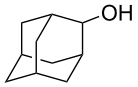 **1b**	microflow	*T*: 20 °C flow rate (**1b**/HCO_2H): 0.30 mL/min flow rate (H_2SO_4): 0.88 mL/min residence time: 2 min[c] residence time: 1 min[d]	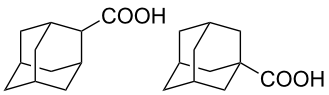 **2b** **2a** 82% (58:42)
4	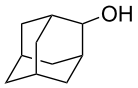 **1b**	batch	*T*: 17–20 °C addition time 5 min reaction time 1 min	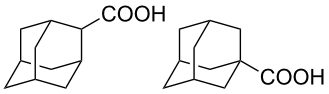 **2b** **2a** 65% (14:86)
5	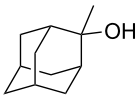 **1c**	microflow	*T*: 20 °C flow rate (**1c**/HCO_2H): 0.01 mL/min flow rate (H_2SO_4): 0.3 mL/min residence time: 20 min[c] residence time: 2.5 min[d]	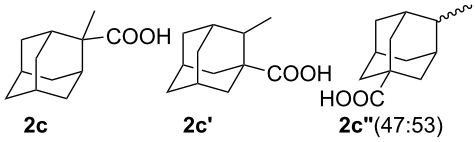 **2c** **2c'** **2c"**(47:53) 97% (23:53:24)
6	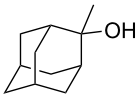 **1c**	batch	*T*: 17–20 °C addition time: 3 min reaction time: 10 min	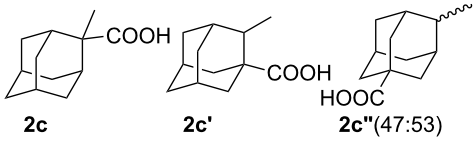 **2c** **2c'** **2c"**(47:53) 83% (19:62:19)

[a]**1** (4 mmol), HCOOH (6 equiv), H_2SO_4 (20 equiv); [b]isolated yield after column chromatography on SiO_2; [c]calculated; [d]observed.

synthesis of 1-adamantanecarboxylic acid (**2a**). We are now expanding the system to other cationic systems and the results will be published in due course.

Experimental

Typical procedure for Koch–Haaf reaction in a microflow system. Multigram scale synthesis of 1-adamantanecarboxylic acid (2a). 1-Adamantanol (**1a**, 60 mmol, 9.2 g) was dissolved in 96% HCOOH (360 mmol, 16.6 g), and the solution was placed in a 50 mL syringe (22.3 mL), which was then attached to a syringe pump. Concentrated H_2SO_4 (99%) (1.2 mol, 64 mL) was placed in 100 mL syringe. These liquids were mixed in the hastelloy micromixer (150 μm) (flow rate: **1a** in HCOOH = 0.3 mL/min, H_2SO_4 = 0.88 mL/min). The resulting reaction mixture was then fed into the residence time unit (PTFE tube, 1 mm i.d. × 3 m). The residence time was observed to be 1.5 min. The mixture of products was fed into the hastelloy-made extraction unit, which was cooled by an ice/water bath. Et_2O (2.5 mL/min) and water (2 mL/min) were fed into the extraction unit. The mixture that was eluted during the first 5 min was discarded and the portion that followed was collected for 55 min (**1a**: 45 mmol). The ethereal layer was separated, and washed with 1.4 N KOH aq. The aqueous layer was acidified with 1 N HCl and extracted with Et_2O. The organic layer was dried over $MgSO_4$, filtered, and evaporated. 1-Adamantanecarboxylic acid (**2a**) was obtained in 88% yield as a white solid (7.1 g, mp 171–172 °C). The obtained product was identified by comparison of the ^1H NMR and ^{13}C NMR spectra with those of commercially available authentic samples. All other products, **2b**, **2c**, **2c'**, and **2c''** were identified by means of NMR spectroscopy by comparison with literature data [32,33].

Typical procedure for Koch–Haaf reaction in a batch reaction system

In a 50 mL two-necked round bottom flask, 99% H_2SO_4 (80 mmol, 7.85 g) was placed. A solution of 1-adamantanol (**1a**, 4 mmol, 613 mg) in 96% HCOOH (24 mmol, 1.01 g) was added through a dropping funnel over a period of 5 min, while the temperature of the reaction mixture was maintained at 15–20 °C in an ice/water bath. The reaction mixture was stirred at 15–20 °C for an additional 2 min, poured into ice/water and extracted with Et_2O. The ethereal layer was washed with 1.4 N KOH aq, and the aqueous layer was acidified with 1 N HCl and extracted with Et_2O. The organic layer was dried over $MgSO_4$, evaporated and purified by column chromatography on SiO_2. Compound **2a** was obtained in 92% yield (667 mg). The reaction of **1b** and **1c** was carried out by a similar procedure.

Acknowledgements

The authors thank MCPT and NEDO for financial support of this work. IR acknowledges the Grant-in-Aid for Scientific Research on Innovative Areas (No. 2105) from the MEXT Japan for funding.

References

1. Wirth, T., Ed. *Microreactors in Organic Synthesis and Catalysis;* Wiley-VCH: Weinheim, Germany, 2008. doi:10.1002/9783527622856
2. Hessel, V.; Renken, A.; Schouten, J. C.; Yoshida, J. *Micro Process Engineering;* Wiley-VCH: Weinheim, Germany, 2009.
3. Mason, B. P.; Price, K. E.; Steinbacher, J. L.; Bogdan, A. R.; McQuade, D. T. *Chem. Rev.* **2007,** *107,* 2300–2318. doi:10.1021/cr050944c
4. Yoshida, J.; Nagaki, A.; Yamada, T. *Chem.–Eur. J.* **2008,** *14,* 7450–7459. doi:10.1002/chem.200800582
5. Lin, W.-Y.; Wang, Y.; Wang, S.; Tseng, H.-R. *Nano Today* **2009,** *4,* 470–481. doi:10.1016/j.nantod.2009.10.007
6. McMullen, J. P.; Jensen, K. F. *Annu. Rev. Anal. Chem.* **2010,** *3,* 19–42. doi:10.1146/annurev.anchem.111808.073718
7. Webb, D.; Jamison, T. F. *Chem. Sci.* **2010,** *1,* 675–680. doi:10.1039/C0SC00381F
8. Yoshida, J. *Chem. Rec.* **2010,** *10,* 332–341. doi:10.1002/tcr.201000020
9. Wegner, J.; Ceylan, S.; Kirschning, A. *Chem. Commun.* **2011,** *47,* 4583–4592. doi:10.1039/c0cc05060a
10. Fukuyama, T.; Rahman, M. T.; Sato, M.; Ryu, I. *Synlett* **2008,** 151–163. doi:10.1055/s-2007-1000884
11. Fukuyama, T.; Shinmen, M.; Nishitani, S.; Sato, M.; Ryu, I. *Org. Lett.* **2002,** *4,* 1691–1694. doi:10.1021/ol0257732
12. Liu, S.; Fukuyama, T.; Sato, M.; Ryu, I. *Org. Process Res. Dev.* **2004,** *8,* 477–481. doi:10.1021/op034200h
13. Rahman, M. T.; Fukuyama, T.; Kamata, N.; Sato, M.; Ryu, I. *Chem. Commun.* **2006,** 2236–2238. doi:10.1039/B600970K
14. Fukuyama, T.; Kobayashi, M.; Rahman, M. T.; Kamata, N.; Ryu, I. *Org. Lett.* **2008,** *10,* 533–536. doi:10.1021/ol702718z
15. Wienhöfer, I. C.; Studer, A.; Rahman, M. T.; Fukuyama, T.; Ryu, I. *Org. Lett.* **2009,** *11,* 2457–2460. doi:10.1021/ol900713d
16. Fukuyama, T.; Rahman, M. T.; Kamata, N.; Ryu, I. *Beilstein J. Org. Chem.* **2009,** *5,* No. 34. doi:10.3762/bjoc.5.34
17. Fukuyama, T.; Hino, Y.; Kamata, N.; Ryu, I. *Chem. Lett.* **2004,** *33,* 1430–1431. doi:10.1246/cl.2004.1430
18. Sugimoto, A.; Sumino, Y.; Takagi, M.; Fukuyama, T.; Ryu, I. *Tetrahedron Lett.* **2006,** *47,* 6197–6200. doi:10.1016/j.tetlet.2006.06.153
19. Sugimoto, A.; Fukuyama, T.; Sumino, Y.; Takagi, M.; Ryu, I. *Tetrahedron* **2009,** *65,* 1593–1598. doi:10.1016/j.tet.2008.12.063
20. Matsubara, H.; Hino, Y.; Tokizane, M.; Ryu, I. *Chem. Eng. J.* **2011,** *167,* 567–571. doi:10.1016/j.cej.2010.08.086
21. Tsutsumi, K.; Terao, K.; Yamaguchi, H.; Yoshimura, S.; Morimoto, T.; Kakiuchi, K.; Fukuyama, T.; Ryu, I. *Chem. Lett.* **2010,** *39,* 828–829. doi:10.1246/cl.2010.828
22. Suga, S.; Nagaki, A.; Yoshida, J. *Chem. Commun.* **2003,** 354–355. doi:10.1039/B211433J
    For Friedel–Crafts alkylation with carbocation intermediates using a microreator.
23. Tanaka, K.; Motomatsu, S.; Koyama, K.; Tanaka, S.; Fukase, K. *Org. Lett.* **2007,** *9,* 299–302. doi:10.1021/ol062777o
    For acid-catalyzed dehydration of alcohols via carbocation intermediates in a mircoflow system.
24. Brandt, J. C.; Elmore, S. C.; Robinson, R. I.; Wirth, T. *Synlett* **2010,** 3099–3103. doi:10.1055/s-0030-1259075
    For Ritter reaction in a microflow system.
25. Koch, H.; Haaf, W. *Justus Liebigs Ann. Chem.* **1958,** *618,* 251–266. doi:10.1002/jlac.19586180127
26. Hoffmann-Emery, F.; Hilpert, H.; Scalone, M.; Waldmeier, P. *J. Org. Chem.* **2006,** *71,* 2000–2008. doi:10.1021/jo0523666
27. Sorensen, B.; Rohde, J.; Wang, J.; Fung, S.; Monzon, K.; Chiou, W.; Pan, L.; Deng, X.; Stolarik, D.; Frevert, E. U.; Jacobson, P.; Link, J. T. *Bioorg. Med. Chem. Lett.* **2006,** *16,* 5958–5962. doi:10.1016/j.bmcl.2006.08.129
28. Becker, C. L.; Engstrom, K. M.; Kerdesky, F. A.; Tolle, J. C.; Wagaw, S. H.; Wang, W. *Org. Process Res. Dev.* **2008,** *12,* 1114–1118. doi:10.1021/op800065q
29. Wan, Z.; Laine, D. I.; Yan, H.; Zhu, C.; Widdowson, K. L.; Buckley, P. T.; Burman, M.; Foley, J. J.; Sarau, H. M.; Schmidt, D. B.; Webb, E. F.; Belmonte, K. E.; Palovich, M. *Bioorg. Med. Chem. Lett.* **2009,** *19,* 4560–4562. doi:10.1016/j.bmcl.2009.07.006
30. Barton, V.; Ward, S. A.; Chadwick, J.; Hill, A.; O'Neill, P. M. *J. Med. Chem.* **2010,** *53,* 4555–4559. doi:10.1021/jm100201j
31. Shmailov, A.; Alimbarova, L.; Shokova, E.; Tafeenko, V.; Vatsouro, I.; Kovalev, V. *Tetrahedron* **2010,** *66,* 3058–3064. doi:10.1016/j.tet.2010.02.043
32. Mukherjee, A.; Wu, Q.; le Noble, W. J. *J. Org. Chem.* **1994,** *59,* 3270–3274. doi:10.1021/jo00091a010
33. Alford, J. R.; Cuddy, B. D.; Grant, D.; McKervey, M. A. *J. Chem. Soc., Perkin Trans. 1* **1972,** 2707–2713. doi:10.1039/P19720002707

Beilstein Journal of Organic Chemistry

Efficient and selective chemical transformations under flow conditions: The combination of supported catalysts and supercritical fluids

M. Isabel Burguete, Eduardo García-Verdugo and Santiago V. Luis*

Review

Open Access

Address:
Department of Inorganic and Organic Chemistry, University Jaume I, Avda. Sos Baynat s/n, 12071-Castellón, Spain

Email:
M. Isabel Burguete - burguete@qio.uji.es;
Eduardo García-Verdugo - eduardo.garcia-verdugo@qio.uji.es;
Santiago V. Luis* - luiss@qio.uji.es

* Corresponding author

Keywords:
biphasic systems; continuous flow processes; enantioselective catalysis; immobilized catalysts; polymer-supported systems; supercritical fluids

Beilstein J. Org. Chem. **2011,** *7,* 1347–1359.
doi:10.3762/bjoc.7.159

Received: 30 June 2011
Accepted: 12 September 2011
Published: 30 September 2011

This article is part of the Thematic Series "Chemistry in flow systems II".

Guest Editor: A. Kirschning

Abstract

This paper reviews the current trends in the combined use of supported catalytic systems, either on solid supports or in liquid phases and supercritical fluids (scFs), to develop selective and enantioselective chemical transformations under continuous and semi-continuous flow conditions. The results presented have been selected to highlight how the combined use of those two elements can contribute to: (i) Significant improvements in productivity as a result of the enhanced diffusion of substrates and reagents through the interfaces favored by the scF phase; (ii) the long term stability of the catalytic systems, which also contributes to the improvement of the final productivity, as the use of an appropriate immobilization strategy facilitates catalyst isolation and reuse; (iii) the development of highly efficient selective or, when applicable, enantioselective chemical transformations. Although the examples reported in the literature and considered in this review are currently confined to a limited number of fields, a significant development in this area can be envisaged for the near future due to the clear advantages of these systems over the conventional ones.

Review

Introduction

An ideal synthetic process, combining the concepts of classical synthetic chemistry and those of the more recently developed green chemistry, would be one that provides complete conversions of the substrates and that would give place to high (ideally complete) selectivities, with the concomitant generation of only minor (ideally none) amounts of waste and the consumption of the lowest possible amount of energy. This, of course, needs to be associated with the production of relatively large amounts

of the desired product with high chemical and economic efficiency and in short time frames [1]. The use of flow systems clearly offers a simple approach towards addressing these last few issues. The main advantages of continuous flow systems using conventional or neoteric solvents have been highlighted in different books and reviews [2-7]. On the other hand, the use of catalytic approaches helps fulfill the other conditions and is always favored from the point of view of green chemistry [8,9]. To facilitate the recovery and reuse of the corresponding catalysts and, simultaneously, to avoid cross-contamination of the products with the catalyst, the use of immobilized systems is clearly preferred [10]. Besides, this is often associated with an increase in the long-term stability of the corresponding catalytic system [11]. For this purpose, immobilization was carried out on different supports. The most usual approach involved the anchoring of the catalytic subunit on a solid support that was either organic (polymeric) [12] or inorganic (zeolites, clays, silicas, etc.) [13]. Nevertheless, other possibilities have been also assayed. These include the use of soluble supports such as dendrimers [14,15], nanoparticles [16], soluble polymers and oligomers [17,18], etc., and the use of liquid phases as the immobilizing media [19-21]. A second method to improve the environmental friendliness of the chemical processes is through the use of neoteric solvents, allowing a reduction, or even elimination, of the use of toxic and environmentally risky organic solvents. In particular, scFs are very well suited for this purpose and, besides, they greatly facilitate the work-up for the isolation of reaction substrates and/or products, for instance by simple expansion of the reaction mixture [22]. Additionally, their tuneable properties provide simple tools for a rapid optimization of reaction parameters and facilitate the development of efficient flow processes [23-25]. Neoteric solvents (scFs, ionic liquids, PEG, etc.) have been considered as "green" alternative solvents due to their properties. However, in order to consider a given process as being more environmentally friendly than the corresponding one run in an organic solvent, the whole process should be evaluated ("cradle-to-grave" evaluation), including an assessment of the energy consumption. Such studies are out of the scope of this paper but they should be kept in mind for their possible implementation.

Supercritical fluids exhibit unique properties that offer the opportunity to manipulate, as required, the parameters of the reaction environment, such as density, viscosity, diffusivity or surface tension, continuously from gaslike to liquid-like properties through the control of pressure and temperature. Thus, for example, varying the temperature and pressure allows manipulation of the density of CO_2, which determines much of its power as a solvent. At its critical point (31 °C, 74 bar) CO_2 has a density of 0.46 $g \cdot mL^{-1}$, which, when compared to conventional solvents, may be expected to be associated with relatively weak solvent ability. Increasing pressure increases the density of the CO_2 for a given temperature. Thus, at pressures of, for example, 120 bar and 40 °C, densities of around 0.7 $g \cdot mL^{-1}$ are typical. The reaction rate and the product selectivity in homogeneous scFs media can be altered by changing these parameters [26,27]. Selected examples of phase equilibrium-controlled chemical reaction kinetics in high pressure CO_2 have been reviewed elsewhere [28].

Nevertheless, examples exploiting the great potential of the combined use of immobilized catalysts with scFs under continuous flow conditions for chemo- or enantioselective transformations are still limited. The reactions based on the combination of immobilized catalysts and scFs are usually performed under batch conditions [29,30]. The main aim of this paper is to highlight the advantages of the combined use of immobilized catalytic systems and supercritical fluids to develop efficient chemical transformations under flow conditions. This combination not only provides a way to obtain high yields and simple work-up, it can also be used in some cases to implement the selectivity and, when appropriate, the enantioselectivity of the corresponding transformations, although this last aspect is less frequently implemented. The illustrative examples selected for this review have been classified according to four different categories as a function of the reaction type. Our goal is not to present a comprehensive summary of all reactions having been reported for every category of processes but to present some selected and significant cases highlighting the main advantages of this approach.

1. Hydrogenation processes

The use of continuous flow hydrogenation protocols employing immobilized metal catalysts has increased significantly over the past few years [31]. Different approaches to the immobilization of catalysts in order to design flow processes in scFs can be mentioned:

a) Solid heterogeneous catalysts:

Hydrogenation processes, in particular those based on solid heterogeneous catalysts derived from Ni, Pd, Pt and other noble metals, are of fundamental importance for the industry, and therefore a great effort has been devoted to the detailed study of this kind of processe and to the development of practical protocols for industrial application [32,33].

The use of continuous flow operation conditions in this field has proved to increase the overall efficiency of the studied reactions when compared to the related batch processes [31,34]. One of the main advantages of the scFs is their complete miscibility with gases such as hydrogen. Bringing all reactants into the same phase eliminates the resistance of mass transport

across the gas–liquid (or solid) interface. This, in principle, should lead to higher reaction rates. However, the elimination of the gas–liquid mass transport limitation is not the only prerequisite for achieving high global reaction rates. Indeed, for some hydrogenations the reaction occurred faster in two-phase systems (dense solvent and expanded liquid (substrate)) [28]. The reaction rate of the hydrogenation in the presence of scFs is determined, to a great extent, by the phase behavior of the system. On the other hand, supercritical solvents, owing to the reduction of viscosity, can accelerate the adsorption and desorption steps of reactants and products in the catalytic sites. Thereby, a shift from adsorption- or desorption-controlled surface processes to surface-reaction-controlled processes can take place [23,35-37]. Besides, the solvent properties can be easily tuned by a proper selection of pressure and temperature parameters leading to a controlled variation of polarity, dissolution power, etc. All these factors offer good opportunities to perform hydrogenation reactions in $scCO_2$ and supercritical hydrocarbons, leading to improved activity and, in some cases, enhanced selectivity.

Some classical examples are provided by the work of Baiker [38,39]. Thus, initial studies focused on the enantioselective hydrogenation of ethyl pyruvate to (*R*)-ethyl lactate over cinchonidine (CD) modified Pt/Al_2O_3. The results obtained showed that a dramatic increase in both conversion and enantioselectivity were produced upon changing the solvent from $scCO_2$ to scC_2H_6 working at 30 °C and 10 MPa, in a flow reactor at 4.3 mmol·min^{-1} (Scheme 1). The poor performance of $scCO_2$ was related to the partial catalyst poisoning due to the formation of CO through a water-shift reaction. The use of scC_2H_6 was by far superior to the conventional toluene solvent, providing not only an easier separation of products, but also resulting in much higher reaction rates, with an eightfold increase in the resulting turnover frequency (TOF) values.

The conversion (20–60%) and the enantioselectivity (55–75%) were easily tuned by adjusting the H_2/substrate ratio and the working pressure. The effect of the temperature on the reaction rate was relatively moderate, although, as could be expected, the enantioselectivity significantly decreased with increasing temperatures.

A second example was provided by the group of Poliakoff [40,41]. In this case, the reaction studied was the hydrogenation of dimethyl itaconate over a chiral Rh catalyst on an inorganic support (Al_2O_3) with a phosphotungsten acid linker (Scheme 2). It is important to take into consideration a direct comparison with the work of Baiker, in as much as the catalytic system studied by Baiker is a heterogeneous multiple site system very different from the single site catalyst considered here. In this case, both conversion and enantioselectivity strongly depended on the temperature, the best results being obtained at 60 °C (10 MPa, 1.25 mL·min^{-1}, H_2/substrate ratio = 4). TON values ranged from a minimum of 250 to a maximum of 4600 [moles product]/[moles Rh]. The highest values were obtained at 60 °C and 10 MPa and this corresponds to a TOF of 560 [moles product]·[moles Rh]$^{-1}$·h^{-1} for an eight hour run.

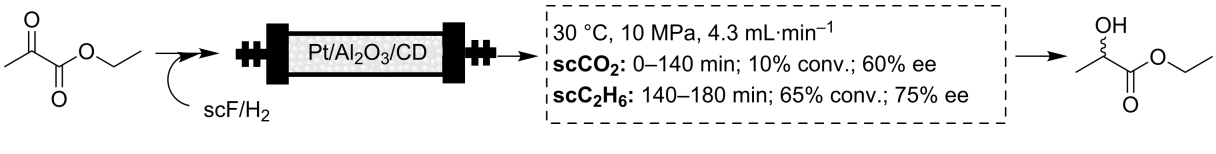

Scheme 1: Hydrogenation of ethyl pyruvate.

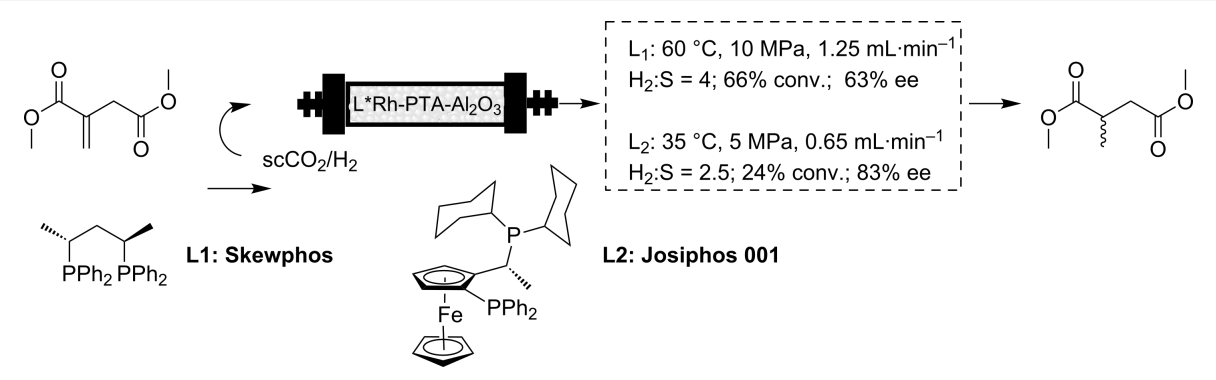

Scheme 2: Hydrogenation of dimethyl itaconate.

Importantly, neither conversion nor enantiomeric excess were observed to degrade over time, under steady-state conditions. Furthermore, with the initial ligand tested (Skewphos) the enantioselectivity achieved was similar to that obtained in conventional solvents (66% ee). Nevertheless, a further screening of a battery of ligands allowed the authors to obtain a system based on the ligand Josiphos, providing a higher enantioselectivity (83% ee at 55 °C) than the corresponding homogeneous system dissolved in $scCO_2$ [42].

b) Catalysts immobilized in ionic liquids (ILs)

The immobilization of a catalyst in an IL phase has been reported to afford a series of advantages over the use of solid supports: (a) first of all, no modification of the homogeneous catalyst is required for the immobilization, which is a factor that often affects the efficiency of solid-supported systems; (b) the presence of the counter anion can contribute to the activation of the catalyst; (c) the large variety of available ILs can be used for fine-tuning of the overall efficiency of the catalytic system through straightforward modifications in the structure of the IL (anion and cation nature, aliphatic chains, presence of additional functional groups, etc.); (d) finally, the IL phase can significantly contribute to the stabilization of the catalyst [43]. In this case, involving an ILs–$scCO_2$ multiphasic system, the CO_2 phase is intended to favor the delivery of substrates and H_2 to the IL phase and to facilitate the separation of the final products and the recycling of the IL phase containing the catalyst [44]. The IL–$scCO_2$ system shows a specific phase behavior where CO_2 can dissolve significantly into the IL phase, but no ionic liquid dissolves in the $scCO_2$. Thus, the phase behavior of IL–$scCO_2$ systems, including the partitioning of organic compounds between both solvents, is essential for developing this type of process, because it determines the contact conditions between $scCO_2$ and the solute, as well as the conditions for reducing the viscosity of the IL phase, thus enhancing the mass transfer rate of any catalytic system [45].

The use of this approach is illustrated by the enantioselective hydrogenation of *N*-(1-phenylethylidene)aniline with an Ir catalyst (Scheme 3a) [46,47]. The use of an IL such as [EMIM][NTf_2] (EMIM = 1-ethyl-3-methylimidazolium) in the absence of $scCO_2$ required high H_2 pressures (10 MPa) to obtain significant conversions (40 °C, 97% conv., 58% ee). In constrast, a quantitative hydrogenation was observed, in the presence of CO_2, under much milder conditions (40 °C, 3 MPa, >99% conv., 56% ee). As this transformation requires long

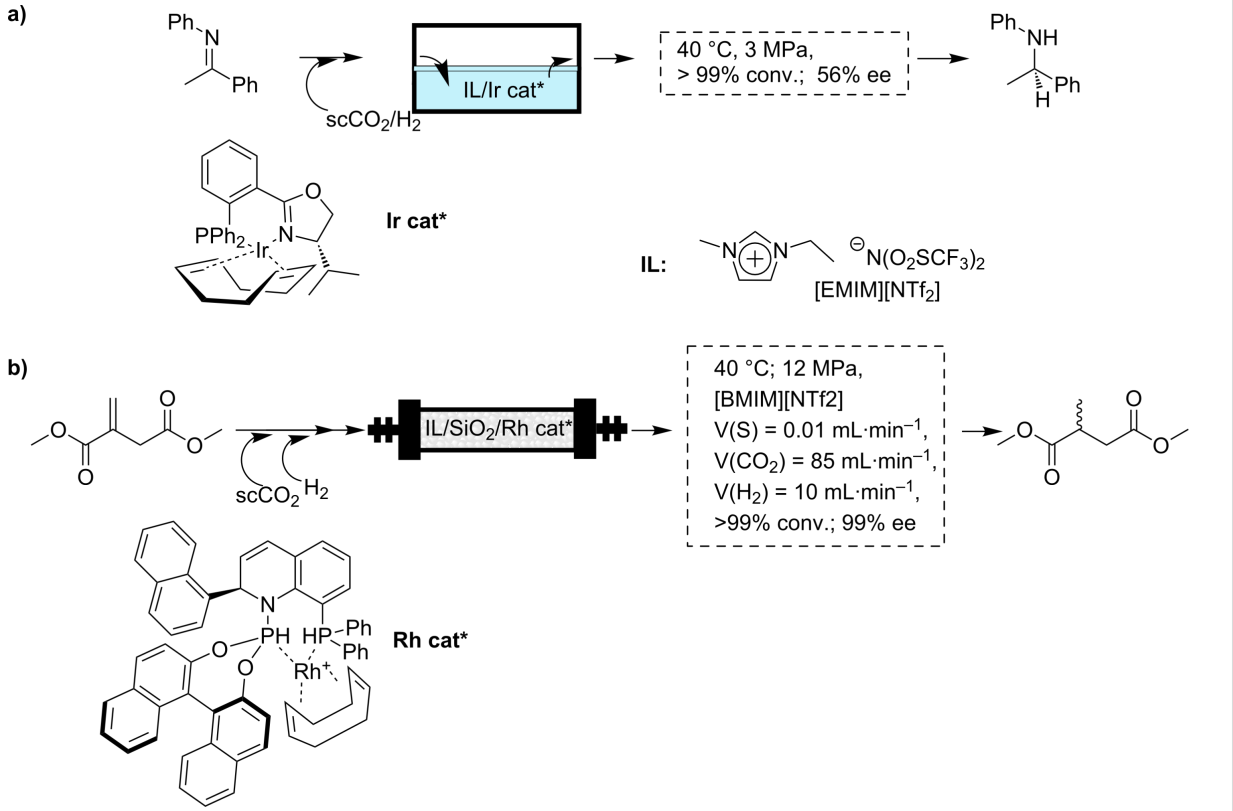

Scheme 3: a) Enantioselective hydrogenation of *N*-(1-phenylethylidene)aniline in IL–CO_2; b) Enantioselective hydrogenation of dimethyl itaconate in SILP–$scCO_2$.

reaction times (several hours), the initial setup reported by Leitner and coworkers can be described as a repetitive batch system based on successive reaction–extraction cycles (3 h each). This allowed the use of the system for at least seven cycles without any loss in conversion or enantioselectivity. Although this system worked in successive batch cycles, it fully illustrates the potential of biphasic ILs–$scCO_2$ systems. Indeed, this system was further implemented by the same authors to obtain a fully continuous process [20].

In this context, a simple approach to implement biphasic ILs–$scCO_2$ systems into continuous flow processes is to absorb the ILs on a porous support material (supported IL phase: SILP) [48-51]. This methodology allows simultaneously exploiting the full advantages of a homogeneous biphasic ILs–$scCO_2$ system together with those provided by catalysts immobilized onto an insoluble support. In this way, continuous flow catalytic transformations with scFs as a mobile phase to deliver the reactants to the IL phase and to extract the products from there can be easily designed. This approach has been recently used to carry out the asymmetric hydrogenation of dimethyl itaconate. A chiral organometallic catalyst was immobilized on a IL phase absorbed onto a commercial inorganic support, allowing mild reaction conditions and making the use of organic solvents or additional purification steps unnecessary (Scheme 3b). Thus, the commercially available (S_a,R_c)-1-naphthyl-QUINAPHOS in the ionic liquid [EMIM][NTf_2] gave the best results for the SILP-catalyst system leading to an active catalytic system, stable for 65 h of continuous operation. However, the enantioselectivity could not be kept stable over the entire reaction time. An almost enantiomerically pure product (>99% ee) was obtained for periods of up to 10 h on stream, corresponding to approximately 20,000 catalytic turnovers. A high catalytic efficiency was achieved with this system, reaching a TON value over 100,000 for the chiral transition metal complex, and a productivity of >150 kg product/g of Rh. The system operated with a space time yield (STY) of 0.3 kg·L^{-1} × h. Besides, the catalyst leaching was below the detection limit of 1 ppm [52].

c) Catalysts immobilized in other liquid phases

Other unconventional solvents such as fluorous solvents, polyethyleneglycol (PEG) or water were also used in a manner similar to that described above for ILs [19]. An example is the hydrogenation of itaconic acid or acetamido acrylate by means of a chiral Rh catalyst based on a fluorous BINAPHOS ligand. In this case, the substrate and the product are dissolved in water while the liphophilic catalyst is maintained in a $scCO_2$ phase, in a so-called inverted biphasic system [53,54]. A regime based on repetitive batch experiments was operated to afford a stable system for five consecutive runs. For this approach, the CO_2 phase was never depressurized and quantitative yields and excellent enantioselectivities (98.4% ee on average) were achieved (9 cycles, TOF > 200 h^{-1}).

2. Hydroformylation processes

Hydroformylation is also a reaction of high industrial importance, being one of the main routes to the production of aldehydes [55,56]. In this case, one important factor determining the efficiency of the process, besides the reaction rate, is the control of the selectivity, as either linear or branched aldehydes can be obtained (l/b selectivity). In general, the linear aldehydes are the desired final products for industrial applications. On the other hand, dimerization products can also be obtained along with the desired aldehydes (aldehyde selectivity).

a) Solid heterogeneous catalysts

An initial example was provided by Poliakoff and van Leeuwen [57]. A diphosphine ligand immobilized on silica was prepared by a sol–gel approach from *N*-[3-(tri-methoxysilyl)-*n*-propyl]-4,5-bis(diphenylphosphino)phenoxazine (Scheme 4). One remarkable result was that the hydroformylation rate, under flow conditions with $scCO_2$ as the carrier phase, was faster than for the batch reaction in toluene, although it was half the rate of the homogeneous system under comparable conditions. This was attributed to the enhanced mass transport properties and the lower viscosity of the medium caused by the presence of $scCO_2$. The residual 1-octene was easily separated by control-

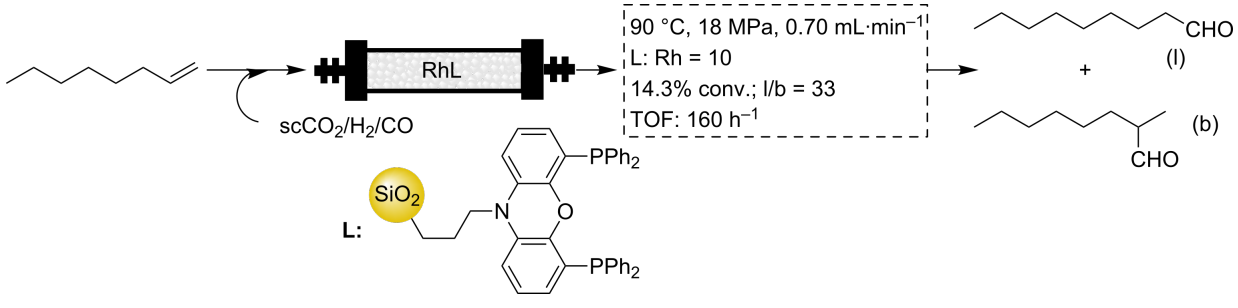

Scheme 4: Selective hydroformylation with a silica supported Rh catalyst.

ling the depressurization step and the catalyst performed constantly for 30 h, for six nonconsecutive days.

The same authors further explored a variety of different supported ligands for the same reaction, but the results did not improve significantly [58]. The reaction can also be driven towards the branched aldehyde. In this case, the resulting compound has a stereogenic center and an enantioselective process can be developed using a chiral catalyst. An example was reported by Shibahara et al. [59]. For this purpose, a chiral catalyst based on polystyrene-supported (PS) BINAPHOS was employed to form the corresponding Rh catalyst. For volatile alkenes, a direct flow system was used, while for nonvolatile substrates $scCO_2$ was used as the carrier phase. Thus, for styrene a ca. 50% conversion was achieved with an 80:20 b/l ratio and 85% ee (Scheme 5).

b) Catalysts immobilized in ionic liquids (ILs)

The immobilization of a Rh hydroformylation catalyst in [BMIM][PF_6] has been reported by Cole-Hamilton to produce a significant decrease in the aldehyde selectivity, relative to toluene, while retaining the conversion and the l/b selectivity [60,61]. Changing to a $scCO_2$–IL biphasic system produced a decrease in the conversion but the aldehyde selectivity was recovered and, more importantly, the l/b selectivity experienced a threefold increase. It has been considered that the main role of $scCO_2$ is to reduce the residence time of the product aldehyde in the catalyst solution and to protect it from further reaction. This can be associated with the rapid diffusion of the product from the IL phase to the $scCO_2$ phase. A comparison with Co-based commercial catalysts clearly favors the new system in terms of productivity, although other factors such as robustness, long-term productivity and operational costs should be also considered and have not yet been analyzed. The system has been further improved through the use of different Xantphos-related ligands containing imidazolium subunits to favor the solubility in the IL phase [62]. A system involving the immobilization of the catalyst in a film of an IL supported on silica (SILP) has also been described with either $scCO_2$ [63] or in the gas phase [64]. The results obtained for the hydroformylation in SILP–$scCO_2$ revealed the achievement of higher rates, as compared with the bulk-IL–$scCO_2$ system, reaching TOF values of 800 h^{-1} and more than threefold improved STYs. Statistical methods and a thorough study of the phase behavior were used to optimize the system. Optimum conditions were located just below the critical point of the mixture in an expanded liquid phase regime. High reaction rates corresponding to TOF values of 500–800 h^{-1} could be maintained for at least 40 h of continuous flow operation (TON > 20000) with low catalytic leaching [65].

3. Miscellaneous chemocatalytic processes

Reactions catalyzed by heterogeneous acids in supercritical fluids have been widely studied under flow conditions [66-68]. This approach is attractive because it combines acid heterogeneous catalysts, as an environmentally and economically acceptable alternative to conventional homogeneous catalysts such as H_2SO_4 and HF, with the advantages of scFs. Thus, simple fixed-bed reactors can be developed for carrying out continuous flow processes. Furthermore, the catalyst lifetime can, in many cases, be dramatically improved under supercritical conditions, owing to reduced coking [69,70].

The selective monoprotection of 1,*n*-terminal diols is a characteristic example of how mono-substituted ethers can be selectively prepared versus the bis-substituted ones [71]. The use of

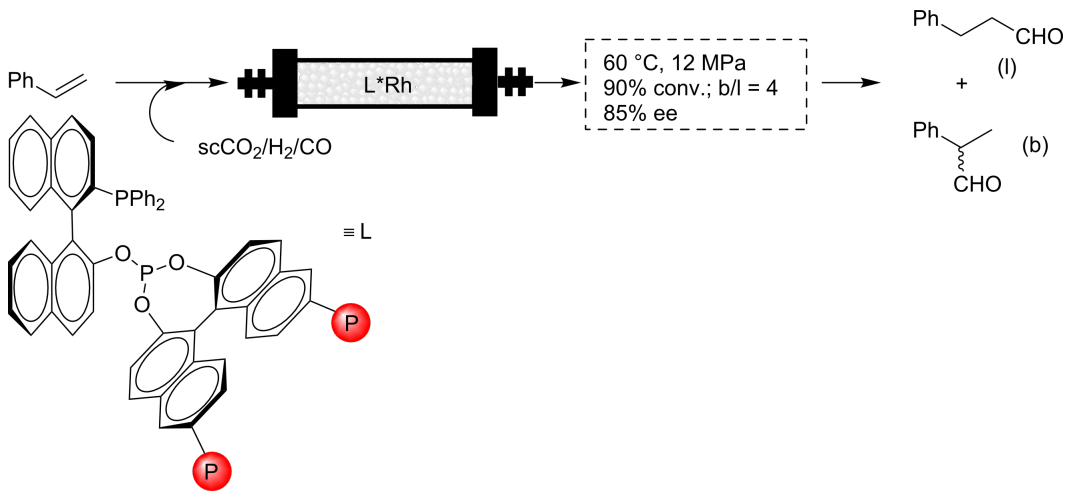

Scheme 5: Enantioselective hydroformylation of styrene.

an acid catalyst (Amberlyst 15) allows the formation of the corresponding mono-ethers by reaction of 1,6-hexanediol and other diols with simple alcohols under flow conditions ($scCO_2$, 150 °C, 20 MPa, 1.15 mL·min^{-1}). One of the most interesting results found was the observation that, at 150 °C, the selectivity of the reaction can be switched by a proper adjustment of the pressure. Thus, at 5 MPa the bis-ether predominates over the mono-ether by a factor of 20, while the reverse selectivity is achieved at 20 MPa (mono-/bis-ether = 9). This was shown to be related to the phase state of the reaction mixture. Thus, those results confirmed that it is possible to control the alkylation selectivity by a simple tuning of the properties of the supercritical fluid.

A second example involves the hydrovinylation of styrene using the Wilke's catalyst immobilized on an IL (Scheme 6) [72]. The work under continuous flow conditions with $scCO_2$ afforded good conversions and selectivities (25 °C, 8 MPa, 100% conversion, 64% yield, 89–84% ee). The presence of the IL phase facilitated the activation of the organometallic catalyst, while the combination with $scCO_2$ allowed a significant decrease in the viscosity of the IL solution, improving the mass transfer. Finally, the work under continuous flow conditions avoided the deactivation of this sensitive catalyst, as observed during its recycling in the batch mode. The increased long-term stability of the catalyst was associated with the low stability of the active species in the absence of the substrate and this could be avoided or minimized by continuous operation in a flow reactor. Thus, more than 60 h of operation time could be achieved moving from batch to continuous flow.

Finally, the remaining examples concern our own work on the enantioselective cyclopropanation with supported copper–bis-oxazoline (Cu–BOX) or copper-pyridineoxazoline (Cu–PyOX) complexes and related systems. The oxazoline ligands can be introduced in polystyrene–divinylbenzene (PS–DVB) matrices

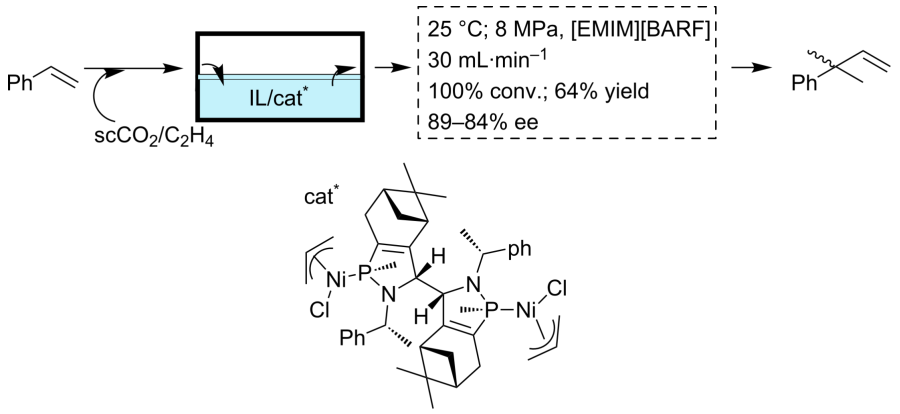

Scheme 6: Enantioselective hydrovinylation of styrene.

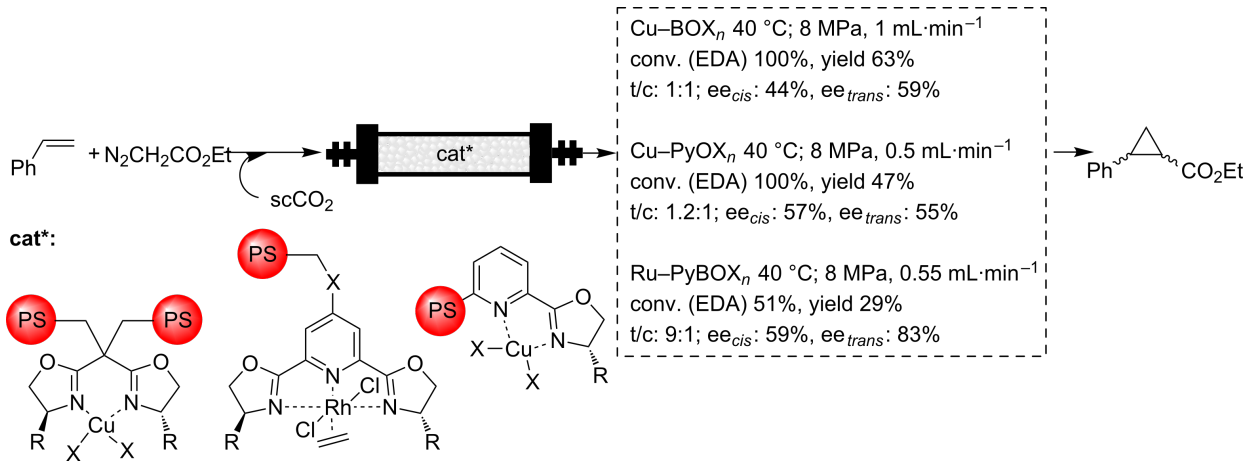

Scheme 7: Enantioselective cyclopropanation of styrene catalyzed by supported Cu–BOX, Cu–PyOX and Rh–PyBOX catalysts.

either by grafting, by reaction with chloromethyl groups of preformed resins, or by polymerization of the corresponding bisoxazolines or pyridineoxazolines containing polymerizable vinylic fragments [73,74]. The transformation of those BOX or PyOX moieties into the corresponding Cu complexes allows their use as catalysts for the enantioselective cyclopropanation of styrene (Scheme 7). Similar approaches allow the preparation of polymers containing PyBOX subunits, from which the corresponding Rh complexes can be formed and studied for the same reaction [75]. The preparation of this kind of catalyst in the form of monolithic polymers inside stainless steel columns is very well suited to work under flow conditions [76,77]. Both catalysts were studied in flow conditions with $scCO_2$ (40 °C, 8 MPa), with conventional solvents and under solvent-free conditions [74,78,79]. One of the main outcomes of the results obtained was the observation of a significant improvement in the productivity when going from conventional to supercritical conditions within the same reactor. Thus, for instance, when considering the total production per volume for a given time, the value obtained, working in continuous flow and using the Cu–PyOX system as the catalyst, was higher for $scCO_2$ than that achieved for methylene chloride (DCM) (1402 $g{\cdot}L^{-1}$ versus 836 $g{\cdot}L^{-1}$). It is noteworthy that this higher volumetric productivity was obtained in a shorter time, 165 min for $scCO_2$ compared with 540 min for DCM. Hence, in $scCO_2$ up to 1.5 mmol of cyclopropanes per hour can be obtained, whereas lower values, around 0.13–0.21 $mmol{\cdot}h^{-1}$, were achieved in DCM. More interestingly, in all cases the conversion, chemoselectivity, selectivity and enantioselectivity were comparable or slightly superior to those found for the work under batch conditions with the same catalysts. The results obtained also revealed that one additional advantage of the work under flow conditions with scFs is the easy and fast optimization of the system through a proper control of reaction parameters, such as pressure, temperature and flow.

4. Biocatalytic processes

The proper use of catalytic [8] and engineering [80] methodologies can improve significantly the energetic and synthetic efficiencies, as well as reaction selectivity, while reducing the production of concomitants. In this regard, biocatalysis-based transformations have an enormous potential, since they are able to increase stereo-, chemo- and regioselectivities for a vast number of chemical transformations [81,82]. Besides, a great variety (more than 13,000) of enzyme-catalyzed reactions have been successfully demonstrated at the laboratory scale, offering clear advantages for the synthesis of enantiopure fine chemicals over any other kind of catalysts [83,84]. As a result, the chemical industry is currently exploring the great potential of biocatalysis to manufacture both bulk and fine chemicals [85,86]. Although many of the reported examples involve the use of batch conditions, different examples of continuous biocatalytic processes have been described with conventional solvents [87]. The use of biocatalytic flow processes under unconventional conditions presents additional advantages [88]. Indeed, flow systems operating above atmospheric pressure enable the possibility of using fluids above their boiling point just by including a retention valve at the exit of the reactor. This facilitates the practical use of this kind of reactor in superheated solvents [89] or with supercritical fluids, either in $scCO_2$ [90,91] or also in non-$scCO_2$ supercritical fluids [92].

a) Solid supported biocatalysts

Nowadays many enzymes are commercially available immobilized on different solid supports and have found to be compatible with supercritical conditions [88]. In general, most of the examples are related to the preparation of nonchiral products, but the use of biocatalysts is even more interesting when the synthesis of chiral compounds is involved. Different examples can be found, in this regard, in the literature. The most common transformations are the kinetic resolution (KR) of secondary alcohols. For example, Matsuda has reported the use of the commercially available supported lipase Novozym 435 for the kinetic resolution of aromatic and nonaromatic substrates using $scCO_2$ (42 °C, 13 MPa) [93]. The space time yield was improved by a factor of 400 under flow conditions as compared to that of the corresponding batch processes. The enantioselectivity of the process was excellent and enantiomeric ratio values (E) larger than 1800 were obtained. The system maintained its activity and selectivity over at least three days of continuous use, allowing the resolution of 221 g of (±)-1-phenylethanol to the (*S*)-1-phenylethanol (99% ee) and the corresponding (*R*)-acetate (99% ee) with just 1.73 g of supported enzyme. An interesting flow system is that reported

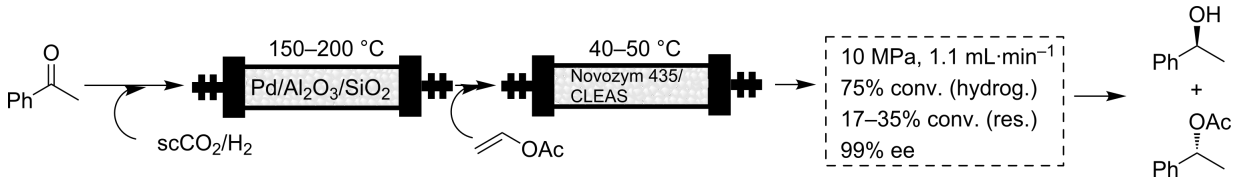

Scheme 8: Continuous hydrogenation of acetophenone coupled with the kinetic resolution of the product.

by Poliakoff and Sheldon involving two sequential reactions (Scheme 8) [94]. In that case, the first step was the continuous hydrogenation of acetophenone to afford the racemic phenylethanol with Pd supported on SiO_2/Al_2O_3 as the catalyst and $scCO_2$ as the reaction medium (150–200 °C, 10 MPa, 1.1 mL·min^{-1}, H_2:substrate ratio = 4). The racemic alcohol (75% conversion for the first step) was directly fed to a second catalytic reactor containing the supported biocatalyst to carry out the kinetic resolution (40–50 °C, Novozym 435 or CLEAS as the immobilized enzyme). Although only moderate conversions were achieved for the second step (17–35%) the corresponding acetate was obtained in high enantiomeric purity (ca. 99%).

b) Biocatalysts immobilized in ionic liquids (ILs)

The discovery of the possibility to immobilize biocatalysts in ionic-liquid phases has been a recent breakthrough that can be compared with the progress made by the use of enzymes in organic solvents [95,96]. One of the main advantages reported for the enzyme–IL system is the enhanced stability found for the biocatalysts especially in water-immiscible ILs [88,97]. The observed stabilization of enzymes in water-immiscible ILs was attributed to their inclusion in hydrophilic gaps of the network, where they are surrounded by a strong ionic net. The extremely ordered supramolecular structure of the ILs in the liquid phase may be able to act as a "mould", maintaining the active 3D structure of the enzyme and avoiding unfolding [88]. The combination of supporting the biocatalyst in an IL (either dissolved or suspended) with the use of a scF for delivering the substrates to the IL phase and to extract the final products from there, allows one to take full advantage of the above mentioned benefits and to develop continuous flow biocatalytic systems in which the IL phase acts as the stationary phase and the scF becomes the mobile phase [98]. Pioneering work in this field was carried out by the groups of Lozano and Leitner and Reetz [99,100]. Both groups studied the kinetic resolution of phenylethanol with *Candida Antarctica lipase B* (CALB) as the biocatalyst (Scheme 9). In the case of the work by Leitner and Reetz, the CALB enzyme was suspended in a bulk IL phase. At 45 °C and 10.5 MPa and using a substrate:donor ratio of 0.5 they achieved conversions of 43–50% with 99% ee values for the acetate. In a further improvement of the system, the same authors reported the coupling of the resolution step with the continuous separation of the two products formed based on their different solubilities in the $scCO_2$ phase [101]. Reetz et al. also extended this methodology to a biphasic polyethyleneglycol (PEG)/$scCO_2$ system [102]. An excellent conversion was maintained for at least 25 h. After a short induction period, the amount of product was almost identical to the amount of substrate and the system operated with a constant high activity of 5700 mmol·min^{-1}·g^{-1} corresponding to a space time yield of 0.1 kg·L^{-1}·h^{-1}. Since an excess of vinyl acetate was used, all of the PEG 1500 was also acylated.

A different approach was developed by Lozano et al. In their case, a thin layer of an IL phase containing the enzyme was created on the surface of silica and the resulting material was used in a packed-bed reactor, using vinyl propionate as the acyl donor (50 °C, 15 MPa, substrate:donor ratio 0.5, conversion >35%, 99% ee for the product). It is worth mentioning that, in the last case, the enzyme maintained an excellent activity and a reasonable stability even at 150 °C [103], which reveals the important stabilization associated with the combination of the biocatalyst with the IL phase [99]. These authors studied in detail the influence of the support and the IL used, as well as the effect of the previous adsorption of the enzyme onto a modified silica surface [104]. A partly related approach is the immobilization of the lipase onto a covalently supported ionic liquid-like phase (SILLP) [105,106]. Those SILLPs are prepared by functionalization of PS–DVB surfaces with IL-like (imidazolium)

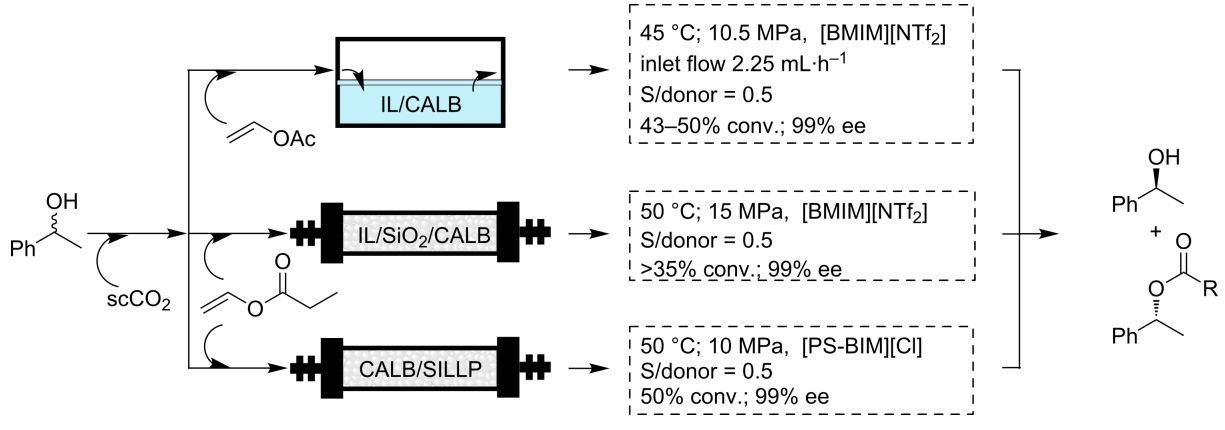

Scheme 9: Kinetic resolution of phenylethanol using CALB immobilized in ILs and supported ILs.

moieties [107,108]. Experimental results have shown that the resulting surfaces have similar physico-chemical properties to those of the corresponding bulk ILs [109]. CALB supported on those SILLPs was shown to be an efficient and very stable catalyst for the continuous flow synthesis of citronellyl propionate in $scCO_2$. The presence of a high IL/enzyme ratio is reflected in a high stabilization of the CALB in those systems. Thus, the process was carried out at 80 °C with yields of 93% for more than 10 h without any appreciable deactivation of the enzyme. Considering enantioselective transformations, the dynamic kinetic resolution (DKR) of phenylethanol was studied under continuous flow in $scCO_2$. This was easily achieved by the combination of a supported enzyme (Novozym 435) and a supported acid catalyst, both covered by a thin layer of an IL. This has allowed the development of the continuous chemoenzymatic dynamic kinetic resolution of the corresponding racemic alcohols with yields of up to 80% and enantioselectivities of about 91–98% [110,111]. Essentially enantiopure products with at least 80% yields were obtained with supported CALB as the biocatalyst.

Similarly, the synthesis of DKR phenylethanol can be performed by the combination of the two catalysts in a "one pot" single columnar minireactor. This was packed with a mixture of zeolite CP811E-150 as the acid catalyst for the racemization and CALB supported on a SILLP based on bead-type PS-DVB resins [106]. Good results were obtained when the zeolite catalyst was coated with a small amount of an IL. This follows the same trend observed in the case of SILPs. Nevertheless, contrary to the observations obtained with the use of commercial immobilized CALB (Novozym 435), no additional IL coating of the biocatalyst was required for the stabilization of the enzyme in the case of CALB–SILLPs. This clearly highlights how SILLPs are able to efficiently stabilize CALB against deactivation by $scCO_2$ or the presence of acidic catalysts. The best results were obtained by an appropriate control of the flow rate, and the DKR of *rac*-phenylethanol could be carried out with excellent yields and enantioselectivities (92%, >99.9% ee for the *R*-ester). The systems based on SILLPs have shown a remarkable stability, with consistent results for at least 17 days of continuous operation.

Conclusion

The development of flow processes using scFs in combination with catalysts supported either on solid or liquid phases (ILs, PEG, fluorous phases, etc.) presents a large potential for enantioselective reactions. In the examples shown, the activity, selectivity and enantioselectivity of the processes was modulated through the proper adjustment of the reaction parameters, such as pressure, temperature, flow, and the nature of the scF, etc., allowing for a rapid optimization of the process. An adequate design of the support (the nature of the solid matrix or the chemical nature of the IL for instance) was used advantageously to improve the overall efficiency of the system. A significant improvement in productivity was obtained, in general, under flow conditions. One of the reasons for such improvement is the increase in mass transfer provided by the scF and associated with the enhanced diffusion of substrates and reagents through the interfaces favored by the scFs. The long-term stability of the catalysts achieved under those conditions was also an additional factor to increase the final productivity. This last factor has often been related to the removal of the work-up steps associated with the recovery of the catalyst, which are frequently sensitive to humidity, air, or changes in temperature/pressure under batch conditions.

Up to now, the examples reported in the literature for enantioselective processes under flow conditions with scFs are confined to a limited number of fields, but considering the clear advantages of the use of these methodologies over the conventional ones, one should expect a significant development in this area for the near future, including the development of industrial applications.

Acknowledgements

Financial support by the Spanish Ministerio de Ciencia e Innovación (MICINN CTQ2008-04412) and UJI-BANCAIXA (P1-1B-2009-58) is acknowledged.

References

1. Anastas, P. T., Ed. *Handbook of Green Chemistry;* Wiley-VCH: Weinheim, Germany, 2009.
2. Luis, S. V.; Garcia-Verdugo, E., Eds. *Chemical Reactions and Processes Under Flow Conditions;* RSC Publishing: Cambridge and London, 2009. doi:10.1039/9781847559739
3. Wegner, J.; Ceylan, S.; Kirschning, A. *Chem. Commun.* **2011,** *47,* 4583–4592. doi:10.1039/c0cc05060a
4. Kirschning, A. *Beilstein J. Org. Chem.* **2009,** *5,* No. 15. doi:10.3762/bjoc.5.15
5. Hessel, V. *Chem. Eng. Technol.* **2009,** *32,* 1655–1681. doi:10.1002/ceat.200900474
6. Wiles, C.; Watts, P. *Chem. Commun.* **2011,** *47,* 6512–6535. doi:10.1039/c1cc00089f
7. Hintermair, U.; Franciò, G.; Leitner, W. *Chem. Commun.* **2011,** *47,* 3691–3701. doi:10.1039/c0cc04958a
8. Sheldon, R. A.; Arends, I. W. C. E.; Hanefeld, U. *Green Chemistry and Catalysis;* Wiley-VCH Verlag GmbH & Co. KGaA: Weinheim, 2007. doi:10.1002/9783527611003.indsub
9. Rothenberg, G. *Catalysis, Concepts and Green Applications;* Wiley-VCH Verlag GmbH: Weinheim, 2008. doi:10.1002/9783527621866
10. Cornils, B.; Herrmann, W. A.; Horváth, I. T.; Leitner, W.; Mecking, S.; Olivier-Bourbigou, H.; Vogt, D., Eds. *Multiphase Homogeneous Catalysis;* Wiley-VCH: Weinheim, 2005. doi:10.1002/9783527619597

11. Lu, J.; Toy, P. H. *Chem. Rev.* **2009,** *109,* 815–838. doi:10.1021/cr8004444
12. Albericio, F.; Tulla-Puche, J., Eds. *The Power of Functional Resins in Organic Synthesis;* Wiley-VCH Verlag GmbH & Co. KGaA: Weinheim, Germany, 2008.
13. Clark, J. H.; Rhodes, C. N. *Clean Synthesis Using Porous Inorganic Solid Catalysts and Supported Reagents*. In *RSC Clean Technology Monographs;* Clark, J. H., Ed.; Royal Society of Chemistry, 2000.
14. Helms, B.; Fréchet, J. M. J. *Adv. Synth. Catal.* **2006,** *348,* 1125–1148. doi:10.1002/adsc.200606095
15. Kehat, T.; Goren, K.; Portnoy, M. *New J. Chem.* **2007,** *31,* 1218–1242. doi:10.1039/b617855n
16. Roy, S.; Pericàs, M. A. *Org. Biomol. Chem.* **2009,** *7,* 2669–2677. doi:10.1039/b903921j
17. Dickerson, T. J.; Reed, N. N.; Janda, K. D. *Chem. Rev.* **2002,** *102,* 3325–3344. doi:10.1021/cr010335e
18. Bergbreiter, D. E.; Tian, J.; Hongfa, C. *Chem. Rev.* **2009,** *109,* 530–582. doi:10.1021/cr8004235
19. Sheldon, R. A. *Green Chem.* **2005,** *7,* 267–278. doi:10.1039/b418069k
20. Langanke, J.; Leitner, W. Regulated Systems for Catalyst Immobilisation Based on Supercritical Carbon Dioxide. In *Regulated Systems for Multiphase Catalysis;* Leitner, W.; Hölscher, M., Eds.; Topics in Organometallic Chemistry, Vol. 23; Springer: Berlin, Heidelberg, 2008; pp 91–108. doi:10.1007/3418_2008_069
21. Arai, M.; Fujitaa, S.-i.; Shirai, M. *J. Supercrit. Fluids* **2009,** *47,* 351–356. doi:10.1016/j.supflu.2008.08.012
22. Harwardt, T.; Franciò, G.; Leitner, W. *Chem. Commun.* **2010,** *46,* 6669–6671. doi:10.1039/c0cc02251a
23. Jessop, P. G.; Leitner, W. *Chemical Synthesis Using Supercritical Fluids;* Wiley-VCH: Weinheim, Germany, 1999. doi:10.1002/9783527613687
24. Beckman, E. J. *J. Supercrit. Fluids* **2004,** *28,* 121–191. doi:10.1016/S0896-8446(03)00029-9
25. Hintermair, U.; Leitner, W.; Jessop, P. G. Expanded Liquid Phases in Catalysis: Gas-expanded Liquids and Liquid–Supercritical Fluid Biphasic Systems. In *Supercritical Solvents;* Leitner, W.; Jessop, P. G., Eds.; Handbook of Green Chemistry, Vol. 4; Wiley-VCH: Weinheim, 2010; pp 103–187. doi:10.1002/9783527628698.hgc037
26. Rayner, C. M. *Org. Process Res. Dev.* **2007,** *11,* 121–132. doi:10.1021/op060165d
27. Nunes da Ponte, M. *J. Supercrit. Fluids* **2009,** *47,* 344–350. doi:10.1016/j.supflu.2008.10.007
28. Cole-Hamilton, D. J. *Adv. Synth. Catal.* **2006,** *348,* 1341–1351. doi:10.1002/adsc.200606167
29. Jessop, P. G. *J. Supercrit. Fluids* **2006,** *38,* 211–231. doi:10.1016/j.supflu.2005.11.025
30. Irfan, M.; Glasnov, T. N.; Kappe, C. O. *ChemSusChem* **2011,** *4,* 300–316. doi:10.1002/cssc.201000354
31. Nishimura, S. *Handbook of Heterogeneous Catalytic Hydrogenation for Organic Synthesis;* Wiley: Weinheim, Germany, 2001.
32. Klabunovskii, E.; Smith, G. V.; Zsigmond, A. *Heterogeneous Enantioselective Hydrogenations: Theory and Practice*. In *Catalysis by Metal Complexes;* James, B. M.; Piet, W. N. M., Eds.; Springer: Berlin, 2006; Vol. 31. doi:10.1007/978-1-4020-4296-6
33. Künzle, N.; Solèr, J. W.; Baiker, A. *Catal. Today* **2003,** *79–80,* 503–509. doi:10.1016/S0920-5861(03)00075-0
34. Baiker, A. *Chem. Rev.* **1999,** *99,* 453–474. doi:10.1021/cr970090z
35. Ciriminna, R.; Carraro, M. L.; Campestrini, S.; Pagliaro, M. *Adv. Synth. Catal.* **2008,** *350,* 221–226. doi:10.1002/adsc.200700255
36. Seki, T.; Grunwaldt, J. D.; Baiker, A. *Ind. Eng. Chem. Res.* **2008,** *47,* 4561–4585. doi:10.1021/ie071649g
37. Wandeler, R.; Künzle, N.; Schneider, M. S.; Mallat, T.; Baiker, A. *Chem. Commun.* **2001,** 673–674. doi:10.1039/b100511l
38. Wandeler, R.; Künzle, N.; Schneider, M. S.; Mallat, T.; Baiker, A. *J. Catal.* **2001,** *200,* 377–388. doi:10.1006/jcat.2001.3222
39. Stephenson, P.; Licence, P.; Ross, S. K.; Poliakoff, M. *Green Chem.* **2004,** *6,* 521–523. doi:10.1039/b411955j
40. Stephenson, P.; Kondor, B.; Licence, P.; Scovell, K.; Ross, S. K.; Poliakoff, M. *Adv. Synth. Catal.* **2006,** *348,* 1605–1610. doi:10.1002/adsc.200606172
41. Lange, S.; Brinkmann, A.; Trautner, P.; Woelk, K.; Bargon, J.; Leitner, W. *Chirality* **2000,** *12,* 450–457. doi:10.1002/(SICI)1520-636X(2000)12:5/6<450::AID-CHIR26>3.0.CO;2-H
42. Jutz, F.; Andanson, J.-M.; Baiker, A. *Chem. Rev.* **2011,** *111,* 322–353. doi:10.1021/cr100194q
43. Keskin, S.; Kayrak-Talay, D.; Akman, U.; Hortaçsu, Ö. *J. Supercrit. Fluids* **2007,** *43,* 150–180. doi:10.1016/j.supflu.2007.05.013
44. Jutz, F.; Andanson, J.-M.; Baiker, A. *Chem. Rev.* **2011,** *111,* 322–353. doi:10.1021/cr100194q
45. Kainz, S.; Brinkmann, A.; Leitner, W.; Pfaltz, A. *J. Am. Chem. Soc.* **1999,** *121,* 6421–6429. doi:10.1021/ja984309i
46. Solinas, M.; Pfaltz, A.; Cozzi, P. G.; Leitner, W. *J. Am. Chem. Soc.* **2004,** *126,* 16142–16147. doi:10.1021/ja046129g
47. Mehnert, C. P. *Chem.–Eur. J.* **2004,** *11,* 50–56. doi:10.1002/chem.200400683
48. Riisager, A.; Fehrmann, R.; Haumann, M.; Wasserscheid, P. *Top. Catal.* **2006,** *40,* 91–102. doi:10.1007/s11244-006-0111-9
49. Gu, Y.; Li, G. *Adv. Synth. Catal.* **2009,** *351,* 817–847. doi:10.1002/adsc.200900043
50. Van Doorslaer, C.; Wahlen, J.; Mertens, P.; Binnemans, K.; De Vos, D. *Dalton Trans.* **2010,** *39,* 8377–8390. doi:10.1039/c001285h
51. Hintermair, U.; Höfener, T.; Pullmann, T.; Franciò, G.; Leitner, W. *ChemCatChem* **2010,** *2,* 150–154. doi:10.1002/cctc.200900261
52. Burgemeister, K.; Franciò, G.; Hugl, H.; Leitner, W. *Chem. Commun.* **2005,** 6026–6028. doi:10.1039/b512110h
53. Burgemeister, K.; Franciò, G.; Gego, V. H.; Greiner, L.; Hugl, H.; Leitner, W. *Chem.–Eur. J.* **2007,** *13,* 2798–2804. doi:10.1002/chem.200601717
54. Van Leeuwen, P. W. N. M.; Claver, C., Eds. *Rhodium Catalysed Hydroformylation;* Kluwer Academic Press: Dordrecht, 2000.
55. Frohning, C. D.; Kohlpaintner, C. W.; Gauß, M.; Seidel, A.; Torrence, P.; Heymanns, P.; Höhn, A.; Beller, M.; Knifton, J. F.; Klausener, A.; Jentsch, J.-D.; Tafesh, A. M. Carbon Monoxide and Synthesis Gas Chemistry: Hydroformylation (Oxo Synthesis, Roelen Reaction). In *Applied Homogeneous Catalysis with Organometallic Compounds: A Comprehensive Handbook in Two Volumes;* Cornils, B.; Herrmann, W. A., Eds.; Wiley-VCH Verlag GmbH: Weinheim, 1996; Vol. 1, pp 27–104. doi:10.1002/9783527619351.ch2a
56. Meehan, N. J.; Sandee, A. J.; Reek, J. N. H.; Kamer, P. C. J.; Van Leeuwen, P. W. N. M.; Poliakoff, M. *Chem. Commun.* **2000,** 1497–1498. doi:10.1039/b002526g

57. Bronger, R. P. J.; Bermon, J. P.; Reek, J. N. H.; Kamer, P. C. J.; Van Leeuwen, P. W. N. M.; Carter, D. N.; Licence, P.; Poliakoff, M. *J. Mol. Catal. A: Chem.* **2004,** *224,* 145–152. doi:10.1016/j.molcata.2004.07.030
58. Shibahara, F.; Nozaki, K.; Hiyama, T. *J. Am. Chem. Soc.* **2003,** *125,* 8555–8560. doi:10.1021/ja034447u
59. Webb, P. B.; Sellin, M. F.; Kunene, T. E.; Williamson, S.; Slawin, A. M. Z.; Cole-Hamilton, D. J. *J. Am. Chem. Soc.* **2003,** *125,* 15577–15588. doi:10.1021/ja035967s
60. Webb, P. B.; Cole-Hamilton, D. J. *Chem. Commun.* **2004,** 612–613. doi:10.1039/b316311c
61. Webb, P. B.; Kunene, T. E.; Cole-Hamilton, D. J. *Green Chem.* **2005,** *7,* 373–379. doi:10.1039/b416713a
62. Hintermair, U.; Zhao, G.; Santini, C. C.; Muldoon, M. J.; Cole-Hamilton, D. J. *Chem. Commun.* **2007,** 1462–1464. doi:10.1039/b616186c
63. Jakuttis, M.; Schönweiz, A.; Werner, S.; Franke, R.; Wiese, K.-D.; Haumann, M.; Wasserscheid, P. *Angew. Chem., Int. Ed.* **2011,** *50,* 4492–4495. doi:10.1002/anie.201007164
64. Hintermair, U.; Gong, Z.; Serbanovic, A.; Muldoon, M. J.; Santini, C. C.; Cole-Hamilton, D. J. *Dalton Trans.* **2010,** *39,* 8501–8510. doi:10.1039/c000687d
65. Ginosar, D. M.; Thompson, D. N.; Coates, K.; Zalewski, D. J. *Ind. Eng. Chem. Res.* **2002,** *41,* 2864–2873. doi:10.1021/ie0106938
66. Gray, W. K.; Smail, F. R.; Hitzler, M. G.; Ross, S. K.; Poliakoff, M. *J. Am. Chem. Soc.* **1999,** *121,* 10711–10718. doi:10.1021/ja991562p
67. Petkovic, L. M.; Ginosar, D. M.; Thompson, D. N.; Burch, K. C. Application of Supercritical Fluids to Solid Acid Catalyst Alkylation and Regeneration. In *Ultraclean Transportation Fuels;* Ogunsola, O. I.; Gamwo, I. K., Eds.; ACS Symposium Series, Vol. 959; American Chemical Society, 2007; pp 169–179. doi:10.1021/bk-2007-0959.ch013
68. Baptist-Nguyen, S.; Subramaniam, B. *AIChE J.* **1992,** *38,* 1027–1037. doi:10.1002/aic.690380706
69. Madras, G.; Erkey, C.; Akgerman, A. *Ind. Eng. Chem. Res.* **1993,** *32,* 1163–1168. doi:10.1021/ie00018a022
70. Licence, P.; Gray, W. K.; Sokolova, M.; Poliakoff, M. *J. Am. Chem. Soc.* **2005,** *127,* 293–298. doi:10.1021/ja044814h
71. Bösmann, A.; Franciò, G.; Janssen, E.; Solinas, M.; Leitner, W.; Wasserscheid, P. *Angew. Chem., Int. Ed.* **2001,** *40,* 2697–2699. doi:10.1002/1521-3773(20010716)40:14<2697::AID-ANIE2697>3.0.CO;2-W
72. Burguete, M. I.; Fraile, J. M.; García-Verdugo, E.; Luis, S. V.; Martínez-Merino, V.; Mayoral, J. A. *Ind. Eng. Chem. Res.* **2005,** *44,* 8580–8587. doi:10.1021/ie0488288
73. Aranda, C.; Cornejo, A.; Fraile, J. M.; García-Verdugo, E.; Gil, M. J.; Luis, S. V.; Mayoral, J.; Martinez-Merino, V.; Ochoa, Z. *Green Chem.* **2011,** *13,* 983–990. doi:10.1039/c0gc00775g
74. Cornejo, A.; Fraile, J. M.; García, J. I.; Gil, M. J.; Luis, S. V.; Martínez-Merino, V.; Mayoral, J. A. *J. Org. Chem.* **2005,** *70,* 5536–5544. doi:10.1021/jo050504l
75. Altava, B.; Burguete, M. I.; Fraile, J. M.; García, J. I.; Luis, S. V.; Mayoral, J. A.; Vicent, M. J. *Angew. Chem., Int. Ed.* **2000,** *39,* 1503–1506. doi:10.1002/(SICI)1521-3773(20000417)39:8<1503::AID-ANIE1503>3.0.CO;2-B
76. Altava, B.; Burguete, M. I.; García-Verdugo, E.; Luis, S. V.; Vicent, M. J. *Green Chem.* **2006,** *8,* 717–726. doi:10.1039/b603494b
77. Burguete, M. I.; Cornejo, A.; García-Verdugo, E.; Gil, M. J.; Luis, S. V.; Mayoral, J. A.; Martínez-Merino, V.; Sokolova, M. *J. Org. Chem.* **2007,** *72,* 4344–4350. doi:10.1021/jo070119r
78. Burguete, M. I.; Cornejo, A.; García-Verdugo, E.; García, J.; Gil, M. J.; Luis, S. V.; Martínez-Merino, V.; Mayoral, J. A.; Sokolova, M. *Green Chem.* **2007,** *9,* 1091–1096. doi:10.1039/b704465h
79. Lankey, R. L.; Anastas, P. T. Sustainability Through Green Chemistry and Engineering. In *Advancing Sustainability Through Green Chemistry and Engineering;* Lankey, R. L.; Anastas, P. T., Eds.; ACS Symposium Series, Vol. 823; American Chemical Society, 2002; pp 1–11. doi:10.1021/bk-2002-0823.ch001
80. Silverman, R. B. *The Organic Chemistry of Enzyme-Catalyzed Reactions;* Academic Press: New York, 2002.
81. Anastas, P. T.; Crabtree, R., Eds. *Green Catalysis – Volume 3: Biocatalysis;* Handbook of Green Chemistry; Wiley-VCH Verlag GmbH: New York, 2009.
82. Gotor, V.; Alfonso, I.; García-Urdiales, E., Eds. *Asymmetric Organic Synthesis with Enzymes;* Wiley-VCH Verlag GmbH & Co. KGaA: Weinheim, 2008.
83. Hudlicky, T.; Reed, J. W. *Chem. Soc. Rev.* **2009,** *38,* 3117–3132. doi:10.1039/b901172m
84. Roberts, S. M.; Casy, G.; Nielson, M.-B.; Phythian, S.; Todd, C.; Wiggins, K. *Biocatalysts for Fine Chemicals Synthesis;* J. Wiley & Sons, 1999.
85. Liese, A.; Seelbach, K.; Wandrey, C., Eds. *Industrial Biotransformations – A Comprehensive Handbook,* 2nd ed.; Wiley-VCH: Weinheim, 2006. doi:10.1002/3527608184
86. Rao, N. N.; Lütz, S.; Würges, K.; Minör, D. *Org. Process Res. Dev.* **2009,** *13,* 607–616. doi:10.1021/op800314f
87. Lozano, P. *Green Chem.* **2010,** *12,* 555–569. doi:10.1039/b919088k
88. Razzaq, T.; Glasnov, T. N.; Kappe, C. O. *Eur. J. Org. Chem.* **2009,** *9,* 1321–1325. doi:10.1002/ejoc.200900077
89. Hobbs, H. R.; Thomas, N. R. *Chem. Rev.* **2007,** *107,* 2786–2820. doi:10.1021/cr0683820
90. Knez, Ž. *J. Supercrit. Fluids* **2009,** *47,* 357–372. doi:10.1016/j.supflu.2008.11.012
91. Karmee, S. K.; Casiraghi, L.; Greiner, L. *Biotechnol. J.* **2008,** *3,* 104–111. doi:10.1002/biot.200700199
92. Matsuda, T.; Watanabe, K.; Harada, T.; Nakamura, K.; Arita, Y.; Misumi, Y.; Ichikawa, S.; Ikariya, T. *Chem. Commun.* **2004,** 2286–2287. doi:10.1039/b406882c
93. Hobbs, H. R.; Kondor, B.; Stephenson, P.; Sheldon, R. A.; Thomas, N. R.; Poliakoff, M. *Green Chem.* **2006,** *8,* 816–821. doi:10.1039/b604738f
94. van Rantwijk, F.; Sheldon, R. A. *Chem. Rev.* **2007,** *107,* 2757–2785. doi:10.1021/cr050946x
95. Roosen, C.; Müller, P.; Greiner, L. *Appl. Microbiol. Biotechnol.* **2008,** *81,* 607–614. doi:10.1007/s00253-008-1730-9
96. Cantone, S.; Hanefeld, U.; Basso, A. *Green Chem.* **2007,** *9,* 954–971. doi:10.1039/b618893a
97. Lozano, P.; de Diego, T.; Gmouh, S.; Vaultier, M.; Iborra, J. L. *Biotechnol. Prog.* **2004,** *20,* 661–669. doi:10.1021/bp0342497
98. Lozano, P.; de Diego, T.; Carrie, D.; Vaultier, M.; Iborra, J. L. *Chem. Commun.* **2002,** 692–693. doi:10.1039/B200055E
99. Reetz, M. T.; Wiesenhöfer, W.; Franciò, G.; Leitner, W. *Chem. Commun.* **2002,** 992–993. doi:10.1039/b202322a
100. Reetz, M. T.; Wiesenhöfer, W.; Franciò, G.; Leitner, W. *Adv. Synth. Catal.* **2003,** *345,* 1221–1228. doi:10.1002/adsc.200303109

101. Reetz, M. T.; Wiesenhöfer, W. *Chem. Commun.* **2004,** 2750–2751. doi:10.1039/B412049C
102. Lozano, P.; de Diego, T.; Carrié, D.; Vaultier, M.; Iborra, J. L. *Biotechnol. Prog.* **2003,** *19,* 380–382. doi:10.1021/bp025759o
103. Lozano, P.; De Diego, T.; Sauer, T.; Vaultier, M.; Gmouh, S.; Iborra, J. L. *J. Supercrit. Fluids* **2007,** *40,* 93–100. doi:10.1016/j.supflu.2006.03.025
104. Lozano, P.; García-Verdugo, E.; Piamtongkam, R.; Karbass, N.; De Diego, T.; Burguete, M. I.; Luis, S. V.; Iborra, J. L. *Adv. Synth. Catal.* **2007,** *349,* 1077–1084. doi:10.1002/adsc.200600554
105. Lozano, P.; García-Verdugo, E.; Karbass, N.; Montague, K.; De Diego, T.; Burguete, M. I.; Luis, S. V. *Green Chem.* **2010,** *12,* 1803–1810. doi:10.1039/c0gc00076k
106. Karbass, N.; Sans, V.; Garcia-Verdugo, E.; Burguete, M. I.; Luis, S. V. *Chem. Commun.* **2006,** *29,* 3095–3097. doi:10.1039/b603224a
107. Sans, V.; Gelat, F.; Karbass, N.; Burguete, M. I.; García-Verdugo, E.; Luis, S. V. *Adv. Synth. Catal.* **2010,** *352,* 3013–3021. doi:10.1002/adsc.201000528
108. Sans, V.; Karbass, N.; Burguete, M. I.; Compañ, V.; García-Verdugo, E.; Luis, S. V.; Pawlak, M. *Chem.–Eur. J.* **2011,** *17,* 1894–1906. doi:10.1002/chem.201001873
109. Lozano, P.; De Diego, T.; Larnicol, M.; Vaultier, M.; Iborra, J. L. *Biotechnol. Lett.* **2006,** *28,* 1559–1565. doi:10.1007/s10529-006-9130-7
110. Lozano, P.; De Diego, T.; Mira, C.; Montague, K.; Vaultier, M.; Iborra, J. L. *Green Chem.* **2009,** *11,* 538–542. doi:10.1039/b821623a
111. Pitter, S.; Dinjus, E.; Ionescu, C.; Maniut, C.; Makarczyk, P.; Patcas, F. Evaluation of Supercritical Carbon Dioxide as a Tuneable Reaction Medium for Homogeneous Catalysis. In *Regulated Systems for Multiphase Catalysis;* Leitner, W.; Hölscher, M., Eds.; Topics in Organometallic Chemistry, Vol. 23; Springer: Berlin, Heidelberg, 2008; pp 109–147. doi:10.1007/3418_041

License and Terms

Beilstein Journal of Organic Chemistry

Translation of microwave methodology to continuous flow for the efficient synthesis of diaryl ethers via a base-mediated S_NAr reaction

Charlotte Wiles*[1] and Paul Watts[2]

Full Research Paper

Open Access

Address:
[1]Chemtrix BV, Burgemeester Lemmensstraat 358, 6163 JT, Geleen, The Netherlands and [2]Department of Chemistry, The University of Hull, Cottingham Road, Hull, HU6 7RX, UK

Email:
Charlotte Wiles* - c.wiles@chemtrix.com

* Corresponding author

Keywords:
automated synthesis; continuous flow; microreactor; microwave; nucleophilic substitution; organic bases

Beilstein J. Org. Chem. **2011,** *7,* 1360–1371.
doi:10.3762/bjoc.7.160

Received: 31 May 2011
Accepted: 13 September 2011
Published: 04 October 2011

This article is part of the Thematic Series "Chemistry in flow systems II".

Guest Editor: A. Kirschning

Abstract

Whilst microwave heating has been widely demonstrated as a synthetically useful tool for rapid reaction screening, a microwave-absorbing solvent is often required in order to achieve efficient reactant heating. In comparison, microreactors can be readily heated and pressurised in order to "super-heat" the reaction mixture, meaning that microwave-transparent solvents can also be employed. To demonstrate the advantages associated with microreaction technology a series of S_NAr reactions were performed under continuous flow by following previously developed microwave protocols as a starting point for the investigation. By this approach, an automated microreaction platform (Labtrix® S1) was employed for the continuous flow synthesis of diaryl ethers at 195 °C and 25 bar, affording a reduction in reaction time from tens of minutes to 60 s when compared with a stopped-flow microwave reactor.

Introduction

Diaryl ethers are a synthetically interesting subunit [1], with examples found in a series of medicinally significant natural products, such as (−)-K-13 (**1**) [2], riccardin C (**2**) [3] and combretastatins [4], along with synthetic herbicides, such as RH6201 (**3**) [5] (Figure 1). Installation of the diaryl ether can, however, be synthetically challenging, and this is illustrated by the wide number of techniques developed, which include Ullmann ether synthesis [6], Pummerer-type rearrangements [7], Buchwald–Hartwig couplings [8], phenolic additions to amines [9], fluoride mediated couplings [10,11], and the use of solid supports [12].

Until recently, the nucleophilic substitution of aromatic halides to phenolic substrates has been largely overlooked, with Ueno

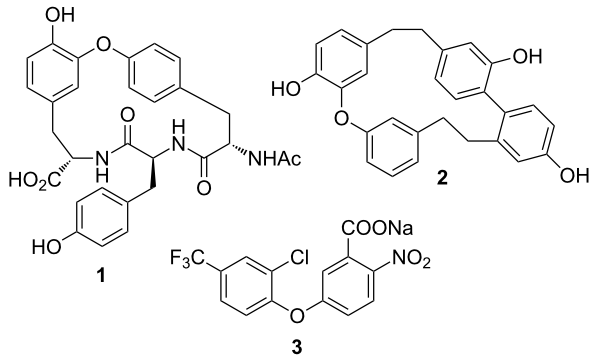

Figure 1: Illustration of synthetically interesting diaryl ethers.

and coworkers [13] reporting the use of triethylsilane and a phosphazene "super base", Holmes [14] describing the use of $scCO_2$, and Moseley et al. [15] employing microwave irradiation as a means of efficiently heating the reaction mixture in order to significantly reduce reaction times (Scheme 1). Although microwaves have found widespread application in the research laboratory, their implementation at a large scale, whilst increasing, is not as well established, largely due to the challenges associated with the uniform irradiation of large reactor vessels [16].

In a critical assessment of microwave-assisted organic synthesis, Moseley and Kappe [17] recently concluded that on a small scale (1 to 50 mL) any energy savings made as a result of using microwave irradiation were attributable to the reduction in reaction time achieved through the use of sealed vessels, and not because microwave irradition is a more energy efficient method of heating. When considering large-scale reactors [18], multimode microwave reactors have been found to be more energy efficient than small single-mode systems, but not more efficient than conventional heating, due to their minimal penetration depth [19]. Coupled with the fact that microwave heating is eight times more expensive than conventional heating [20], techniques for efficient heat transfer are required if costs are to be reduced, particularly at the production level.

Looking towards another emerging technology, that of continuous-flow methodology, Kappe and coworkers [21] and Ryu et al. [22] demonstrated that the "microwave effect" can be mimicked in high-temperature flow reactors, which can be scaled to increase production volume without changing the reaction conditions employed [23-25], resulting in a reduction in energy usage per mole. With this in mind, we report herein the translation, and further development, of a microwave method for the S_NAr reaction of chloroarenes to a series of *para*-substituted phenols to afford a general and efficient route to the diaryl ether subunit.

Results and Discussion

With the optimised conditions from Marafie and Moseley's [15] stopped-flow investigation taken as a starting point, the synthesis of diaryl ethers (Scheme 2) was investigated under continuous-flow conditions. As the continuous-flow reactor enables the reaction chamber to be maintained at the reaction temperature (once the steady state is reached) time is not wasted for heating and cooling of the stopped-flow "batches". Consequently, the system has the potential to be more efficient. The quantity of material generated can therefore be determined by the length of continuous operation and not by the number of "batches" performed.

To perform the flow reactions, the microreactor development apparatus Labtrix® S1 (Chemtrix BV, NL), illustrated in Figure 2, was employed. The heart of the system is a glass microreactor that is positioned on a thermally regulated stage, which enables reactions to be performed between −15 and

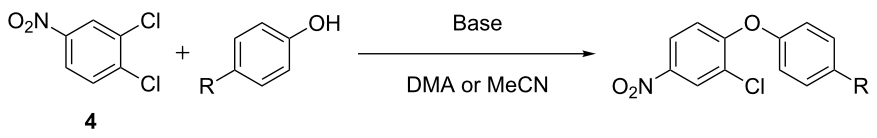

Scheme 1: Illustration of the model reaction used to compare the enabling technologies of microwave and microreactor synthesis.

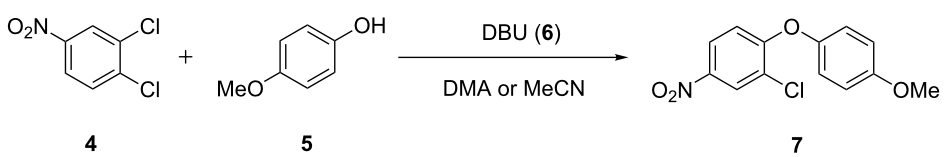

Scheme 2: Illustration of the model reaction used to benchmark Labtrix S1 against batch and stopped-flow microwave reactors.

195 °C. Reagent solutions are delivered to the reactor through a series of syringe pumps (0.1 to 25 µL·min^{-1}) and the system is maintained under a back pressure of 25 bar, which enables reactants and solvents to be heated above their atmospheric boiling point whilst staying in the liquid phase. The reactant flow rates, reactor temperature and sample collection point is automated and the system has an in-line pressure sensor that monitors the system pressure throughout the course of an investigation. The software enables the effect of reaction time, temperature and reactant stoichiometry to be investigated in an automated manner whilst the system is operated, unattended, within a fume cupboard.

Figure 2: Photograph illustrating Labtrix® S1, the automated microreactor development apparatus from Chemtrix BV (NL), used for the evaluation described herein.

The glass microreactors employed herein have a footprint of 44 mm × 22 mm and contain etched microfluidic channels (300 µm (wide) × 120 µm (deep)) in which the reactions take place. By varying the channel length a series of reactor volumes can be accessed (3221 (1 µL), 3222 (5 µL), 3223 (10 µL) and 3227 (19.5 µL)). In order to increase the efficiency of thermal and mass transport on the microscale, the devices contain preheating channels, which bring reagents to the reaction temperature ahead of mixing, and static micromixers (staggered oriented ridge (SOR-2)) [26] are incorporated where any two reagent streams meet in order to increase the efficiency of mixing ($T_{mix} \leq 0.3$ s), compared with T-mixers, and to increase the remaining channel volume available for reaction (Figure 3).

Employing a two-feed system, Figure 4, where one stock solution contained 3,4-dichloronitrobenzene (**4**, DCNB) and 4-methoxyphenol (**5**, 1.3 M and 1.56 M respectively) in dimethylacetamide (DMA) and the second 1,8-diazabicycloundec-7-ene (DBU, **6**, 1.95 M) in DMA, we investigated the nucleophilic substitution reaction under flow conditions. By using a reaction time of 10 min, achieved by setting a total flow rate of 1 µL·min^{-1}, the effect of reactor temperature on the synthesis of 2-chloro-1-(4-methoxyphenoxy)-4-nitrobenzene (**7**) was investigated. Reactions were initially performed in the absence of a base, in order to monitor the background reaction by means of offline GC-FID analysis. After a reaction time of 10 min at a reactant temperature of 195 °C, analysis of the reaction products by GC-FID confirmed no background reaction had occurred, with DCNB (**4**) and 4-methoxyphenol (**5**) recovered without reaction or degradation. Introducing DBU (**6**) into the reactor produced comparable results in the glass microreactor to those reported by Moseley et al. [15] (Figure 5).

Effect of reaction time: Satisfied by this result, we looked at increasing the efficiency of the reaction, and thus we subsequently investigated the effect of reaction time at 195 °C with a view to increasing the space yield time. This approach was successful and revealed that the reaction did not require a 10 min reaction time, with quantitative conversion of DCNB (**4**) to the diaryl ether **7** achieved in 60 s. It is important to note that

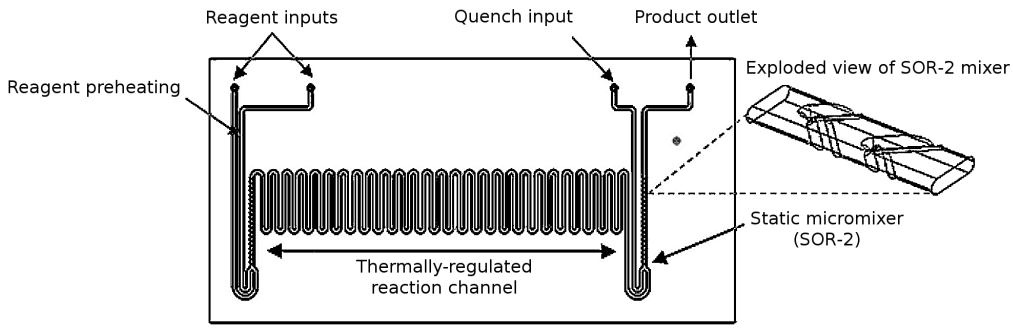

Figure 3: Schematic illustrating the 10 µL reactor manifold used for the S_NAr reactions described herein (3223; Chemtrix BV, NL), with the important features highlighted.

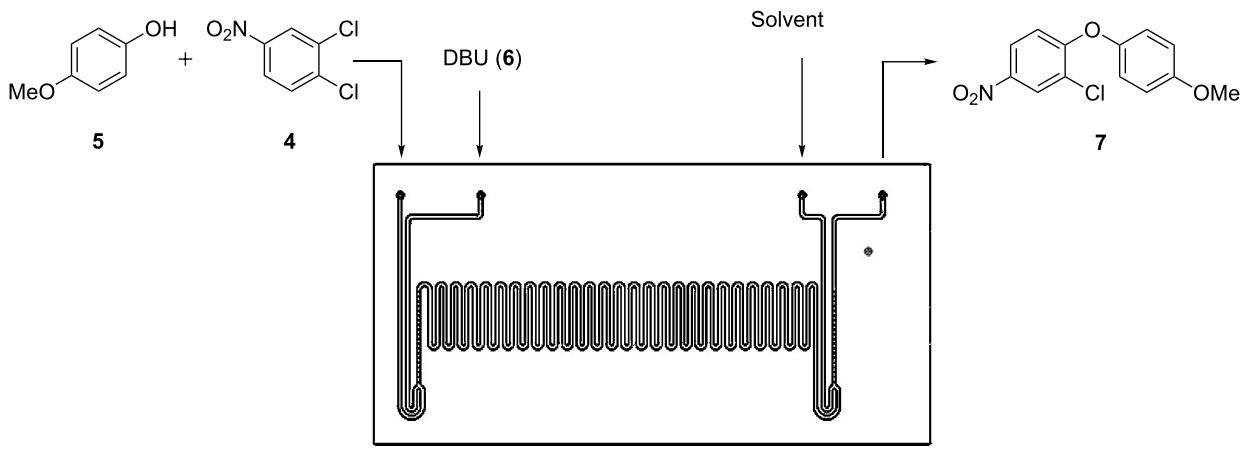

Figure 4: Schematic illustration of the reactor manifold used to evaluate the continuous-flow synthesis of 2-chloro-1-(4-methoxyphenoxy)-4-nitrobenzene (**7**) in the presence of DBU (**6**).

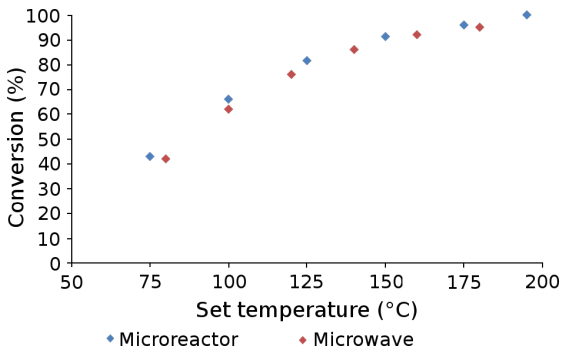

Figure 5: Comparison of the results obtained in Labtrix® S1 with reported data generated in a microwave synthesiser.

no degradation of the diaryl ether **7** was observed when extended reaction times of up to 45 min were employed. The ability to decrease the reaction time required in flow when compared to the microwave methodology can be rationalised if you think that part of the reaction time for a microwave reaction involves the heating up and cooling down of the system, and it is this increase in processing time that is removed by a flow reactor once it has reached steady state.

Effect of reaction solvent: When performing reactions under microwave irradiation, it is important to select a solvent that is not transparent to microwave radiation in order to ensure efficient heating of the reaction mixture. With this in mind, the method reported in the literature employed DMA, but the high boiling point of the solvent (164–166 °C) makes it difficult to isolate the diaryl ethers when reactions are performed on a small scale. Consequently, the reaction was investigated in a series of solvents with low boiling points. The microreactions were performed under 25 bar of back pressure, which means that solvents such as acetonitrile (MeCN) can be readily employed at temperatures exceeding their atmospheric boiling point (81–82 °C), and upon replication of the investigation summarised in Figure 5, comparable results were obtained, illustrating that MeCN is a suitable alternative to DMA.

Screening of organic bases: With one of the salient features of microreaction technology being the speed of reaction optimisation, due to the low system hold-up volume, we subsequently investigated the effect of base type and stoichiometry on the reaction in MeCN. Whilst this would conventionally be performed by preparing a series of solutions with different base concentrations, the control software for Labtrix® S1 enables facile programming of reactant stoichiometries from a single stock solution. Figure 6 illustrates the use of a 1.0 M DCNB (**4**) 4-methoxyphenol (**5**) solution (reactant A), a 1.0 M base solution (reactant B) and MeCN as the diluent (added through the quench input (Figure 4)). At this stage, it was also decided that the 4-methoxyphenol (**5**) equivalents would be reduced from 1.2 to 1.0 equiv in order to reduce the post reaction purification required in order to isolate the diaryl ether **7** in high purity.

Using this approach, we investigated stoichiometries from 0.01 to 2.00 equiv for 10 additional organic bases (Table 1), with 1.0 M stock solutions prepared owing to the variable miscibility of the selected bases with the reaction solvent, MeCN. In order to gauge the effect of the base, reactions were performed under the suboptimal conditions of 30 s at 195 °C, with each screen taking only 14 min to generate the samples for analysis.

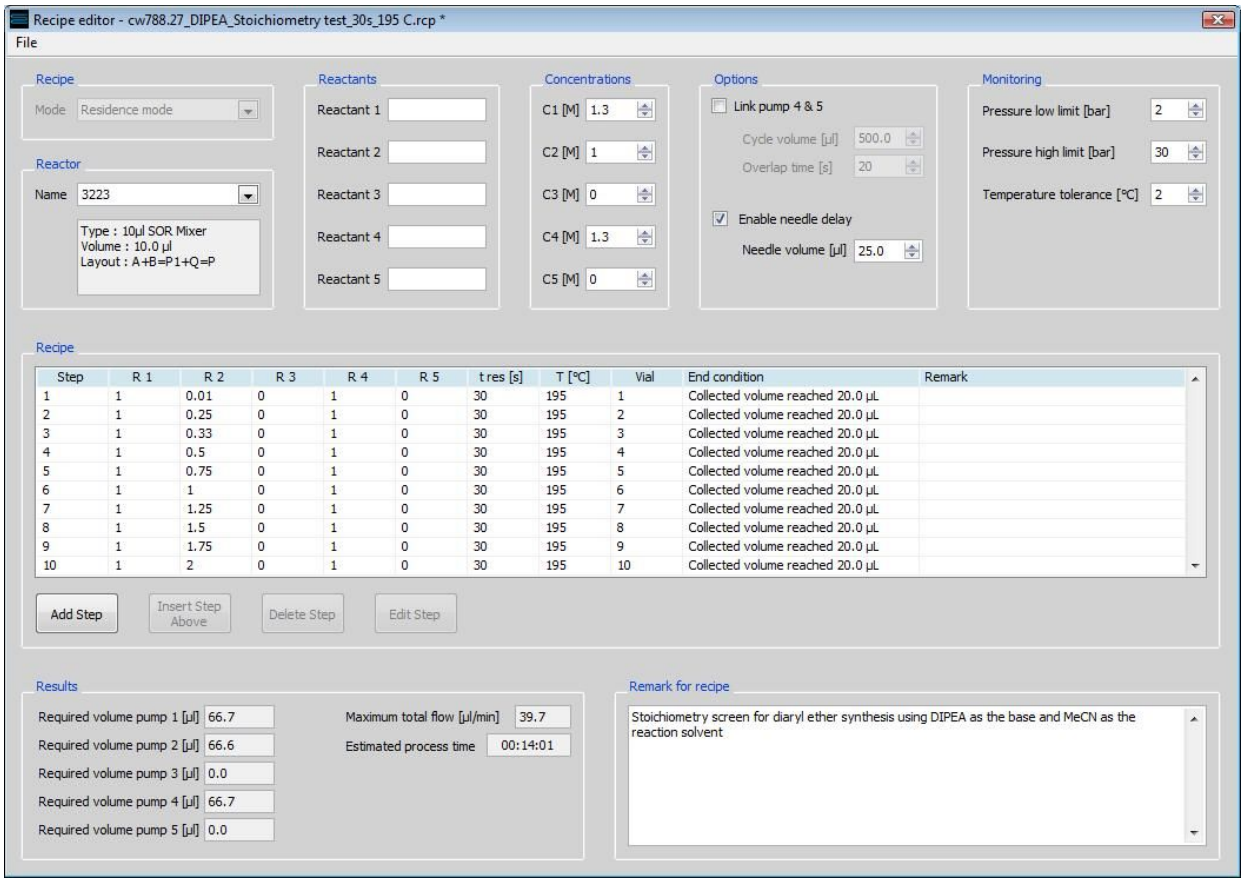

Figure 6: Screen shot from the Labtrix® S1 control software illustrating the system file that enables the user to readily program a stoichiometry screen; this example varies the base stoichiometry at a fixed reaction time and temperature, however, the user can alter all 3 variables at any point.

As Figure 7 illustrates, a wide range of reactivities was obtained, with pyridine, *N*-methylpiperidine, tetramethylpiperidine, lutidine, tetramethylethylenediamine (TMEDA) and triethylamine affording negligible conversions of DCNB (**4**) to 2-chloro-1-(4-methoxyphenoxy)-4-nitrobenzene (**7**). In comparison, DBU (**6**), 1,5-diazabicyclo(4.3.0)non-5-ene (DBN) and 1,1,3,3-tetramethylguanidine (TMG) afforded 55.5, 56.3 and 55.1% conversions (at 1 equiv), respectively. If we compare the results obtained with the dissociation constant of the bases employed (Table 1), a clear link can be seen. Importantly, in all

Table 1: Illustration of the organic bases investigated, ranked in order of increasing basicity and the conversion to diaryl ether **7** obtained when 1 equiv of base was used (residence time = 30 s; reactor temperature = 195 °C).

Entry	Organic base (1 equiv)	p*K*a	Conversion (%)
1	Pyridine	5.20	3.00
2	1,4-Diazabicyclo[2.2.2]octane (DABCO)	5.60	5.01
3	Lutidine	6.75	0.00
4	Tetramethylethylenediamine (TMEDA)	8.97	0.00
5	*N*-Methylpiperidine	10.08	1.62
6	Diisopropylethylamine (DIPEA)	10.50	25.27
7	Triethylamine	10.70	0.85
8	Tetramethylpiperidine (TMP)	11.07	0.00
9	1,8-Diazabicycloundec-7-ene (**6**, DBU)	12.00	55.54
10	1,5-Diazabicyclo(4.3.0)non-5-ene (DBN)	12.80	56.27
11	1,1,3,3-Tetramethylguanidine (TMG)	13.60	55.10

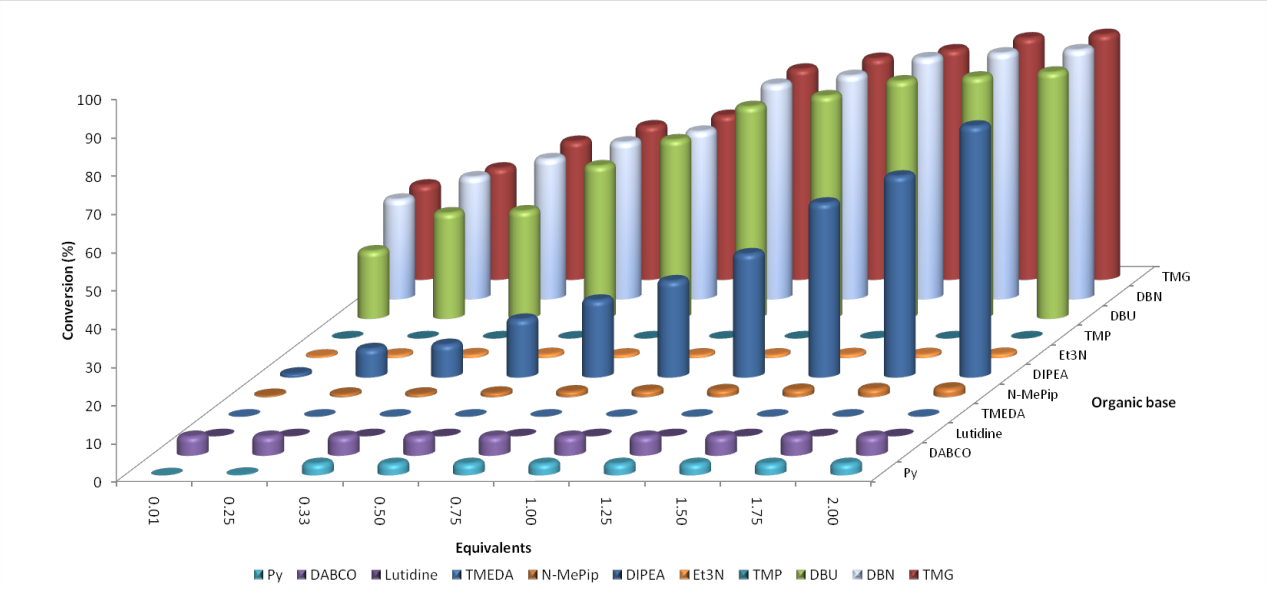

Figure 7: Summary of the results obtained for the organic base screen towards the S_NAr reaction between DCNB (**4**) and 4-methoxyphenol (**5**) (residence time = 30 s; reactor temperature = 195 °C).

cases the hydrochloride salt of the base, formed as a byproduct in the reaction, remained in solution.

With this information in hand, we retained DBU (**6**) as the base (1.5 equiv) and 2-chloro-1-(4-methoxyphenoxy)-4-nitrobenzene (**7**) was synthesised in 99.7% yield with a reaction time of 60 s at 195 °C, affording a throughput of **7** of 108.5 mg·h^{-1} with a 1:1 ratio of 4-methoxyphenol (**5**) and DCNB (**4**).

Effect of phenol substitution. Having optimised the reaction for the synthesis of 2-chloro-1-(4-methoxyphenoxy)-4-nitrobenzene (**7**), the next step in the investigation was to evaluate the effect of the *para*-substituent on the phenolic derivative. To do this a series of commercially available phenols were evaluated; 4-nitrophenol (**8**), 4-cyanophenol (**9**), 4-bromophenol (**10**) and 4-fluorophenol (**11**). Again after a reaction time of 30 s and a reactor temperature of 195 °C, the reactivities of the four phenols were compared before each reaction was optimised for diaryl ether isolation. As expected, Figure 8 illustrates that those phenol derivatives bearing an electron-donating substituent were found to be more reactive.

For each *para*-substituted phenol, the reaction time was optimised and, as Table 2 illustrates, this enabled the synthesis of five diaryl ethers in high yield and excellent purity as verified by MS and NMR spectroscopy. Compared to the work of Moseley [15], the use of a flow reactor meant that it was possible to optimise the reaction of 4-cyanophenol (**9**) to obtain 2-chloro-1-(4-cyanophenoxy)-4-nitrobenzene (**13**) in >99% yield, compared with 42% in the microwave reactor.

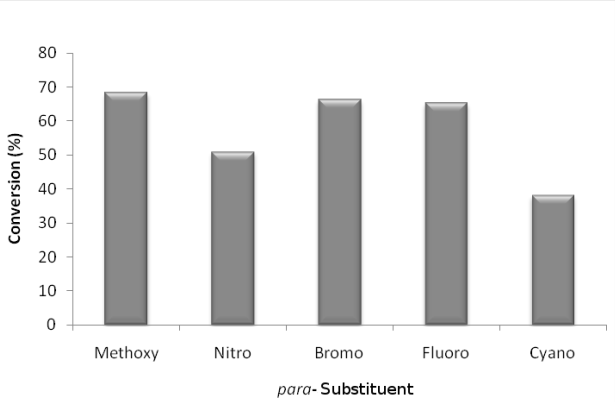

Figure 8: Illustration of the substituent effect on the synthesis of diaryl ethers under continuous flow (residence time = 30 s; reactor temperature = 195 °C).

Use of inorganic bases: Whilst the use of organic bases enabled a comparison of microwave and microreactor technologies to be performed, the use of organic bases can be viewed as disadvantageous due to their relatively high cost compared with inorganic bases [27]. In addition, standard "batch" conditions afforded slurries and were identified by Moseley [15] as being disadvantageous for the stopped-flow microwave reactor. Herein, we employed an aqueous solution of K_2CO_3, which resulted in a biphasic microreaction system. In batch this approach would prove disadvantageous as it would result in a biphasic system in which poor mass transport between the organic and aqueous layers would reduce the reaction rate.

Table 2: Summary of the reaction conditions employed for the DBU (**6**) mediated S_NAr reaction under continuous flow.

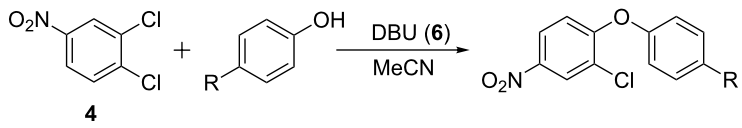

4

Phenol		Residence time (min)	Conversion (%)	Yield (%)
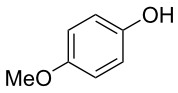	**5**	1	quant.	99.69
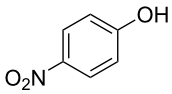	**8**	5	quant.	99.84
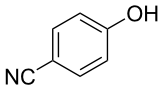	**9**	10	quant.	99.72
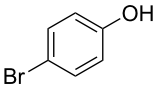	**10**	1	quant.	99.86
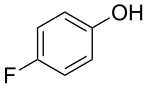	**11**	2	quant.	99.79

In a microfluidic channel, reproducible droplets can be formed within a continuous phase, giving rise to a high interfacial surface area, with mixing further promoted by internal circulation within the droplets (Figure 9). With this in mind the use of aqueous K_2CO_3 as the base was investigated as a means of simplifying postreaction processing and reducing the costs associated with the synthetic methodology developed.

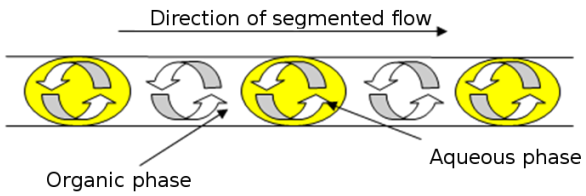

Figure 9: Schematic illustrating the mixing of immiscible reagent streams in a microfluidic channel, whereby the continuous phase composition depends on the ratio of organic and aqueous reactants employed.

Using this approach, we investigated the effect of K_2CO_3 stoichiometry at 195 °C with a reaction time of 30 s, and, as Figure 10 illustrates, comparable results to those obtained for DBU (**6**) were recorded.

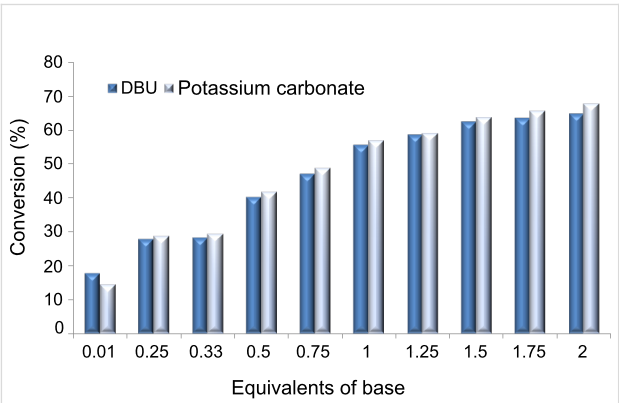

Figure 10: Comparison of base effect on the synthesis of 2-chloro-1-(4-methoxyphenoxy)-4-nitrobenzene (**7**) (residence time = 30 s; reactor temperature = 195 °C).

Under the optimal conditions, the target compound **7** would be obtained in a throughput of 109 mg·h^{-1} however this can be increased by using a more concentrated base solution and therefore reducing the proportion of the second solution within the reaction channel. Increasing the K_2CO_3 concentration to 4.5 M enabled the throughput to be increased to 152 mg·h^{-1} whilst maintaining a 1:1:1.5 reactants-to-base ratio.

Conclusion

Employing a microreactor with a small hold-up volume enabled us to screen a large number of reaction conditions using only mg quantities of substrate. Using this approach, we were able to build on the methodology developed by Moseley and coworkers [15]; by replacing the high-boiling-point reaction solvent DMA with MeCN and simultaneously reducing the proportion of phenol derivative employed, product isolation was more facile. Furthermore, in the case of 4-methoxyphenol (**5**) it was possible to reduce the reaction time from tens of minutes to 60 s at a reactor temperature of 195 °C; a time saving which can be attributed to the efficient heat transfer obtained within the microreactor, and the fact that in a microwave reactor the time to heat up and cool down the system can significantly increase the reaction time.

In addition, compared to previously reported microwave methodologies, employing a microreactor enabled us to investigate the use of a biphasic reaction system, reducing the costs associated with the transformation through the use of an inorganic base, to afford the target diaryl ethers in high yield and purity, after a simple offline aqueous extraction.

Whilst it can be seen from the data described herein that microreaction technology can be utilised for the rapid generation of reaction information and small quantities of isolated materials, the production volume of such units is inherently small. With efficient heat and mass transfer key to the success of microreactors, it is important that these features are retained when flow-reactor volume is increased. If this is not the case then the same issues arise as observed in batch when a process fails to scale either from a changing product-quality or safety perspective.

Experimental

Materials. In all cases, materials were used as received from Acros Organics, with reaction solvents purchased as "Extra Dry" and stored over molecular sieves and analytical grade solvents purchased for use in aqueous extractions.

Instrumentation. Unless otherwise stated, nuclear magnetic resonance (NMR) spectra were obtained at room temperature from solutions in deuterated chloroform ($CDCl_3$ 0.01% TMS) by means of a Jeol GX400 spectrometer; in the case of known compounds, all spectra obtained were consistent with the literature. The following abbreviations are used to report NMR spectroscopic data; s = singlet, d = doublet, t = triplet, br s = broad singlet, q = quartet, dd = double doublet, dt = doublet of triplets, m = multiplet and C_0 = quaternary carbon. Analysis of samples by gas chromatography-flame ionisation detection (GC-FID) were performed on a Varian GC (430) with a CP-Sil 8 (30 m) column (Phenomenex, UK) and ultrahigh purity helium (99.9999%, Energas, UK) as the carrier gas. Reaction products were analysed by the following method; injector temperature 200 °C, carrier-gas flow rate 1.60 mL·min^{-1}, oven temperature 50 °C for 0.1 min then ramped to 300 °C at 60 °C·min^{-1} and held at 300 °C for 1.0 min (Table 3). Mass spectrometry data was obtained by means of a Shimadzu QP5050A instrument with an EI ionisation source.

Microreactor setup: Microreactions were performed in the Labtrix® S1 (Chemtrix BV, NL), illustrated in Figure 2, fitted with a glass microreactor (3223, reactor volume = 10 μL) containing an SOR-2 static micromixer. Reactant solutions were introduced into the reactor through three 1 mL gas-tight syringes (SGE, UK) capable of delivering three solutions at flow rates between 0.1 and 100 μL·min^{-1}. The system was

Table 3: Summary of the retention times obtained for the key starting materials and products employed herein.

Analyte	Retention time (min)	Purity (%)
3,4-Dichloronitrobenzene (**4**)	3.20	99.0
4-Methoxyphenol (**5**)	3.36	98.0
4-Nitrophenol (**8**)	3.47	99.0
4-Cyanophenol (**9**)	3.22	99.0
4-Bromophenol (**10**)	2.92	97.0
4-Fluorophenol (**11**)	2.23	99.0
2-Chloro-1-(4-methoxyphenoxy)-4-nitrobenzene (**7**)	5.10	99.99[a]
2-Chloro-1-(4-nitrophenoxy)-4-nitrobenzene (**12**)	5.50	99.98[a]
2-Chloro-1-(4-cyanophenoxy)-4-nitrobenzene (**13**)	6.81	99.99[a]
2-Chloro-1-(4-bromophenoxy)-4-nitrobenzene (**14**)	5.07	99.99[a]
2-Chloro-1-(4-fluorophenoxy)-4-nitrobenzene (**15**)	4.37	99.98[a]

[a]As determined by GC-FID analysis.

maintained at 25 bar of back pressure by means of a preset ultralow dead-volume back-pressure regulator (Upchurch Scientific, USA), in order to prevent boiling of the reactants and solvent system when temperatures above the atmospheric boiling point were employed. The system was controlled through the Labtrix® S1 software, which enables control of reactant flow rate (total flow rate ≤80 μL·min^{-1}, reactant residence time (7.5 s to 50 min (for a 10 μL reactor)), reactor temperature (−15 to 195 °C), equilibration time and sample collection into one of twenty-nine 2 mL sample vials. The software also archives system parameters such as the set and actual temperature, system pressure, reactor type, and flow rates programmed, along with the sample collection time and vessel, for review both during and after the experiment (Figure 11).

General procedure for temperature and base screening. By using the Labtrix® S1, fitted with a glass microreactor (3223, reactor volume = 10 μL) and a back-pressure regulator set to 25 bar, thermostatted to 25 °C, a solution of 3,4-dichloronitrobenzene (**4**) and phenol derivative (1.3 M respectively) was pumped into the reactor from inlet 1, a solution of base (1.00 M or 1.95 M) was introduced from inlet 2 and the solvent system under investigation was introduced as a diluent from inlet 3. After the system volume had passed through the reactor three times the reaction was at steady state and a sample then collected and analysed offline by GC-FID (Table 3). The reactor temperature was then increased by 25 °C and the system allowed to equilibrate before a sample was taken for analysis in order to quantify the proportion of diaryl ether synthesised; this procedure was repeated up to the T_{max} (195 °C) of the system.

General procedure for diaryl ether synthesis with DBU (6). By using the Labtrix® S1, fitted with a glass microreactor (3223, reactor volume = 10 μL) and a back-pressure regulator set to 25 bar, a solution of 3,4-dichloronitrobenzene (**4**) and phenol derivative (1.3 M respectively) was pumped into the reactor from inlet 1 and a solution of 1,8-diazabicyclo[5.4.0]undec-7-ene (**6**, 1.95 M) was introduced from inlet 2. After a reactant residence time of 1 to 10 min (Table 2), a 500 μL aliquot of the reaction product was collected in a round-bottomed flask and concentrated in vacuo to remove the reaction solvent prior to aqueous extraction. The organic residue was dissolved in DCM (25 mL) and then washed with an aqueous solution of saturated ammonium chloride (3 × 25 mL) to remove the organic base. The organic layer was then dried with $MgSO_4$, filtered under suction and the filtrate concentrated in vacuo to afford the target diaryl ether. The reaction product was then analysed by mass spectrometry and $^1H/^{13}C$ NMR spectroscopy in order to characterise the ether and determine the product purity.

2-Chloro-1-(4-methoxyphenoxy)-4-nitrobenzene (7). A solution of DCNB (**4**) and 4-methoxyphenol (**5**, 0.2496 g and 0.1614 g·mL^{-1}, 1.3 M) in MeCN was introduced into the micro-

Figure 11: Graphical representation of an automated flow reaction for equilibration and screening of reactor temperature effects.

reactor at a flow rate of 5 μL·min^{-1} and a solution of DBU (**6**, 0.2968 mL·mL^{-1}, 1.95 M) in MeCN was introduced at a flow rate of 5 μL·min^{-1}. The microreactor was heated to 195 °C (in 25 °C stages) and, after an equilibration time of 3 min, 500 μL of reaction product was collected into a round-bottomed flask (10 mL) and concentrated in vacuo to remove the reaction solvent prior to aqueous extraction. The organic residue was dissolved in DCM (25 mL) and then washed with an aqueous solution of saturated ammonium chloride (3 × 25 mL) to remove the organic base. The organic layer was then dried with $MgSO_4$, filtered under suction and the filtrate concentrated in vacuo to afford the target diaryl ether, affording 2-chloro-1-(4-methoxyphenoxy)-4-nitrobenzene (**7**) as a pale yellow solid (90.4 mg, 99.7%); ^{1}H NMR (400 MHz, $CDCl_3$) δ 3.87 (3H, s, OCH_3), 6.80 (1H, dd, *J* = 3.0 and 9.2, 1 × ArH), 6.96 (2H, d, *J* = 9.0, 2 × 1 ArH), 7.04 (2H, d, *J* = 9.0, 2 × ArH), 8.01 (1H, dd, *J* = 3.0 and 9.2, 1 × ArH) and 8.35 (1H, d, *J* = 3.0, 1 × ArH); ^{13}C NMR (100 MHz, $CDCl_3$) δ 55.6 (OCH_3), 115.3 (2 × CH), 115.5 (CH), 121.6 (2 × CH), 123.5 (CH), 123.8 (C_0), 126.4 (CH), 142.1 (C_0NO_2), 147.4 (C_0), 157.3 (C_0) and 159.8 (C_0); *m*/*z* (EI) 280 (M^+ + 1, 25%), 279 (100), 264 (20), 233 (10), 198 (7), 183 (5), 123 (5), 108 (2) and 76 (5). The spectroscopic data obtained were consistent with those reported in the literature [15].

2-Chloro-1-(4-methoxyphenoxy)-4-nitrobenzene (7). A solution of DCNB (**4**) and 4-methoxyphenol (**5**, 0.2496 g and 0.1614 g·mL^{-1}, 1.3 M) in MeCN was introduced to the microreactor at a flow rate of 7 μL·min^{-1} and a solution of K_2CO_3 (4.5 M) in MeCN was introduced at a flow rate of 3 μL·min^{-1}. The microreactor was heated to 195 °C (in 25 °C stages) and, after an equilibration time of 3 min, 500 μL of reaction product was collected in a round-bottomed flask (10 mL) and concentrated in vacuo to remove the reaction solvent prior to aqueous extraction. The organic residue was dissolved in DCM (25 mL) and then washed with an aqueous solution of saturated ammonium chloride (3 × 25 mL) to remove the organic base. The organic layer was then dried with $MgSO_4$, filtered under suction and the filtrate concentrated in vacuo to afford the target diaryl ether, affording 2-chloro-1-(4-methoxyphenoxy)-4-nitrobenzene (**7**) as a pale yellow solid (152.0 mg, 99.8%); spectroscopic data obtained were consistent with those reported above and in the literature [15].

2-Chloro-1-(4-nitrophenoxy)-4-nitrobenzene (12): A solution of DCNB (**4**) and 4-nitrophenol (**8**, 0.2496 g and 0.1899 g·mL^{-1}, 1.3 M) in MeCN was introduced to the microreactor at a flow rate of 1 μL·min^{-1} and a solution of DBU (**6**, 0.2968 mL·mL^{-1}, 1.95 M) in MeCN was introduced at a flow rate of 1 μL·min^{-1}. The microreactor was heated to 195 °C (in 25 °C stages) and, after an equilibration time of 15 min, 500 μL of reaction product was collected in a round-bottomed flask (10 mL) and concentrated in vacuo to remove the reaction solvent prior to aqueous extraction. The organic residue was dissolved in DCM (25 mL) and then washed with an aqueous solution of saturated ammonium chloride (3 × 25 mL) to remove the organic base. The organic layer was then dried with $MgSO_4$, filtered under suction and the filtrate concentrated in vacuo to afford the target diaryl ether, affording 2-chloro-1-(4-nitrophenoxy)-4-nitrobenzene (**12**) as a yellow solid (95.4 mg, 99.8%); ^{1}H NMR (400 MHz, $CDCl_3$) δ 7.12 (2H, d, *J* = 9.1, 2 × ArH), 7.21 (1H, d, *J* = 9.0, 1 × ArH), 8.21 (1H, dd, *J* = 2.8 and 9.0, 1 × ArH), 8.30 (2H, d, *J* = 9.1, 2 × ArH) and 8.42 (1H, d, *J* = 2.8, 1 × ArH); ^{13}C NMR (100 MHz, $CDCl_3$) δ 118.2 (2 × CH), 120.7 (CH), 123.9 (CH), 126.2 (2 × CH), 126.8 (CH), 127.0 (C_0Cl), 144.1 (C_0NO_2), 144.5 (C_0NO_2), 160.4 (C_0O) and 160.6 (C_0O); *m*/*z* (EI) 297 (M^+ + 1, 25%) 296 (65), 295 (55), 294 (50), 282 (45), 267 (25), 265 (45), 264 (100), 251 (7), 249 (20), 167 (10), 91 (15) and 76 (10). The spectroscopic data obtained were consistent with those reported in the literature [15].

2-Chloro-1-(4-cyanophenoxy)-4-nitrobenzene (13): A solution of DCNB (**4**) and 4-cyanophenol (**9**) (0.2496 g and 0.1548 g·mL^{-1}, 1.3 M) in MeCN was introduced to the microreactor at a flow rate of 0.5 μL·min^{-1} and a solution of DBU (**6**, 0.2968 mL·mL^{-1}, 1.95 M) in MeCN was introduced at a flow rate of 0.5 μL·min^{-1}. The microreactor was heated to 195 °C (in 25 °C stages) and, after an equilibration time of 30 min, 500 μL of reaction product was collected in a round-bottomed flask (10 mL) and concentrated in vacuo to remove the reaction solvent prior to aqueous extraction. The organic residue was dissolved in DCM (25 mL) and then washed with an aqueous solution of saturated ammonium chloride (3 × 25 mL) to remove the organic base. The organic layer was then dried with $MgSO_4$, filtered under suction and the filtrate concentrated in vacuo to afford the target diaryl ether, affording 2-chloro-1-(4-cyanophenoxy)-4-nitrobenzene (**13**) as a pale yellow solid (88.8 mg, 99.72%); ^{1}H NMR (400 MHz, $CDCl_3$) δ 7.10 (2H, d, *J* = 8.8, 2 × ArH), 7.14 (1H, d, *J* = 9.1, 1 × ArH), 7.27 (2H, d, *J* = 8.8, 2 × ArH), 8.16 (1H, dd, *J* = 2.8 and 9.1, 1 × ArH) and 8.42 (1H, d, *J* = 2.8, 1 × ArH); ^{13}C NMR (100 MHz, $CDCl_3$) δ 108.4 (C_0CN), 118.1 (CN), 119.0 (2 × CH), 120.3 (CH), 123.8 (CH), 126.8 (C_0Cl), 126.9 (CH), 134.6 (2 × CH), 144.4 (C_0NO_2), 156.3 (C_0O) and 158.8 (C_0O); *m*/*z* (EI) 277 (M^+ + 1, 15%), 276 (30), 275 (17), 274 (100), 267 (10), 245 (15), 243 (12), 198 (35), 181 (20), 167 (5), 92 (10) and 76 (15). The spectroscopic data obtained were consistent with those reported in the literature [15].

2-Chloro-1-(4-bromophenoxy)-4-nitrobenzene (14): A solution of DCNB (**4**) and 4-bromophenol (**10**, 0.2496 g and

0.2249 g·mL^{-1}, 1.3 M) in MeCN was introduced to the microreactor at a flow rate of 5 μL·min^{-1}, a solution of DBU (**6**, 0.2968 mL·mL^{-1}, 1.95 M) in MeCN was introduced at a flow rate of 5 μL·min^{-1} and acetone was introduced at a flow rate of 10 μL·min^{-1} (to prevent crystallisation of the product in the outlet tube). The microreactor was heated to 195 °C (in 25 °C stages) and, after an equilibration time of 3 min, 500 μL of reaction product was collected into a round-bottomed flask (10 mL) and concentrated in vacuo to remove the reaction solvent prior to aqueous extraction. The organic residue was dissolved in DCM (25 mL) and then washed with an aqueous solution of saturated ammonium chloride (3 × 25 mL) to remove the organic base. The organic layer was then dried with $MgSO_4$, filtered under suction and the filtrate concentrated in vacuo to afford the target diaryl ether, affording 2-chloro-1-(4-bromophenoxy)-4-nitrobenzene (**14**) as a yellow solid (106.1 mg, 99.86%); ^{1}H NMR (400 MHz, $CDCl_3$) δ 6.90 (1H, d, J = 9.1, 1 × ArH), 6.97 (2H, d, J = 6.9, 2 × ArH), 7.54 (1H, d, J = 6.9, 2 × ArH), 8.06 (1H, dd, J = 2.8 and 9.1, 1 × ArH) and 8.37 (1H, d, J = 2.8, 1 × ArH); ^{13}C NMR (100 MHz, $CDCl_3$) δ 117.2 (CH), 118.4 (C_0Br), 121.6 (2 × CH), 123.6 (CH), 125.0 (C_0Cl), 126.6 (CH), 133.4 (2 × CH), 143.0 (C_0NO_2), 153.7 (C_0O) and 158.3 (C_0O); *m*/*z* (EI) 330 (M^+ + 1, 4%), 329 (100), 328 (3), 327 (75), 313 (3), 297 (5), 283 (5), 203 (20), 171 (10), 139 (25), 108 (5) and 76 (5). The spectroscopic data obtained were consistent with those reported in the literature [15].

2-Chloro-1-(4-fluorophenoxy)-4-nitrobenzene (15): A solution of DCNB (**4**) and 4-fluorophenol (**11**, 0.2496 g and 0.1457 g·mL^{-1}, 1.3 M) in MeCN was introduced to the microreactor at a flow rate of 2.5 μL·min^{-1}, a solution of DBU (**6**, 0.2968 mL·mL^{-1}, 1.95 M) in MeCN was introduced at a flow rate of 2.5 μL·min^{-1} and acetone was introduced at a flow rate of 10 μL·min^{-1} (to prevent product crystallisation in the outlet tube). The microreactor was heated to 195 °C (in 25 °C stages) and, after an equilibration time of 8 min, 500 μL of reaction product was collected into a round-bottomed flask (10 mL) and concentrated in vacuo to remove the reaction solvent prior to aqueous extraction. The organic residue was dissolved in DCM (25 mL) and then washed with an aqueous solution of saturated ammonium chloride (3 × 25 mL) to remove the organic base. The organic layer was then dried with $MgSO_4$, filtered under suction and the filtrate concentrated in vacuo to afford the target diaryl ether affording 2-chloro-1-(4-fluorophenoxy)-4-nitrobenzene (**15**) as a cream-coloured solid (86.6 mg, 99.79%); ^{1}H NMR (400 MHz, $CDCl_3$) δ 6.83 (1H, d, J = 9.1, 1 × ArH), 7.08–7.15 (4H, m, 4 × ArH), 8.06 (1H, dd, J = 2.8 and 9.1, 1 × ArH) and 8.38 (1H, d, J = 2.8, 1 × ArH); ^{13}C NMR (100 MHz, $CDCl_3$) δ 116.3 (CH), 117.1 (2 × CH, d, J = 23.7), 121.8 (2 × CH, d, J = 8.4), 123.6 (CH), 124.5 (C_0Cl), 126.6 (CH), 142.7 (C_0NO_2), 150.2 (C_0O, d, J = 3.0), 160.1 (C_0F, d, J = 243.9) and 161.3 (C_0O); *m*/*z* (EI) 269 (M^+ + 1, 35%), 268 (19), 267 (100), 249 (10), 222 (15), 186 (40), 157 (30), 139 (10), 112 (5), 107 (5) and 76 (7). The spectroscopic data obtained were consistent with those reported in the literature [15].

References

1. Frlan, R.; Kikelj, D. *Synthesis* **2006,** *14,* 2271–2285. doi:10.1055/s-2006-942440
2. Boger, D. L.; Yohannes, D. *J. Org. Chem.* **1989,** *54,* 2498–2502. doi:10.1021/jo00272a003
3. Gottsegen, Á.; Nógrádi, M.; Vermes, B.; Kajtár-peredy, M.; Bihátsi-karsai, É. *Tetrahedron Lett.* **1988,** *29,* 5039–5040. doi:10.1016/S0040-4039(00)80674-7
4. Cirla, A.; Mann, J. *Nat. Prod. Rep.* **2003,** *20,* 558–564. doi:10.1039/b306797c
5. Johnson, W. O.; Kollman, G. E.; Swithenbank, C.; Yih, R. Y. *J. Agric. Food Chem.* **1978,** *26,* 285–286. doi:10.1021/jf60215a027
6. Chan, D. M. T.; Monaco, K. L.; Wang, R.-P.; Winters, M. P. *Tetrahedron Lett.* **1998,** *39,* 2933–2936. doi:10.1016/S0040-4039(98)00503-6
7. Jung, M. E.; Jachiet, D.; Khan, S. I.; Kim, C. *Tetrahedron Lett.* **1995,** *36,* 361–364. doi:10.1016/0040-4039(94)02270-L
8. Burgos, C. H.; Barder, T. E.; Huang, X.; Buchwald, S. L. *Angew. Chem., Int. Ed.* **2006,** *45,* 4321–4326. doi:10.1002/anie.200601253
9. Kulagowski, J. J.; Rees, C. W. *Synthesis* **1980,** 215–216. doi:10.1055/s-1980-28968
10. Sawyer, J. S.; Schmittling, E. A.; Palkowitz, J. A.; Smith, W. J., III. *J. Org. Chem.* **1998,** *63,* 6338–6343. doi:10.1021/jo980800g
11. Zhao, J. K.; Wang, Y. G. *Chin. Chem. Lett.* **2003,** *14,* 1012–1014.
12. Jung, N.; Bräse, S. *J. Comb. Chem.* **2009,** *11,* 47–71. doi:10.1021/cc800032q
13. Ueno, M.; Yonemoto, M.; Hashimoto, M.; Wheatley, A. E. H.; Naka, H.; Kondo, Y. *Chem. Commun.* **2007,** 2264–2266. doi:10.1039/b700140a
14. Lee, J.-K.; Fuchter, M. J.; Williamson, R. M.; Leeke, G. A.; Bush, E. J.; McConvey, I. F.; Saubern, S.; Ryan, J. H.; Holmes, A. B. *Chem. Commun.* **2008,** 4780–4782. doi:10.1039/b808374f
15. Marafie, J. A.; Moseley, J. D. *Org. Biomol. Chem.* **2010,** *8,* 2219–2227. doi:10.1039/b926537f
16. Moseley, J. D.; Woodman, E. K. *Energy Fuels* **2009,** *23,* 5438–5447. doi:10.1021/ef900598m
17. Moseley, J. D.; Kappe, C. O. *Green Chem.* **2011,** *13,* 794–806. doi:10.1039/c0gc00823k
18. Iannelli, M.; Bergamelli, F.; Kormos, C. M.; Paravisi, S.; Leadbeater, N. E. *Org. Process Res. Dev.* **2009,** *13,* 634–637. doi:10.1021/op800296d
19. Razzaq, T.; Kappe, C. O. *ChemSusChem* **2008,** *1,* 123–132. doi:10.1002/cssc.200700036
20. Dressen, M. H. C. L.; van de Kruijs, B. H. P.; Meuldijk, J.; Vekemans, J. A. J. M.; Hulshof, L. A. *Org. Process Res. Dev.* **2010,** *14,* 351–361. doi:10.1021/op900257f
21. Damm, M.; Glasnov, T.; Kappe, C. O. *Org. Process Res. Dev.* **2010,** *14,* 215–224. doi:10.1021/op900297e
22. Wienhöfer, I. C.; Studer, A.; Rahman, M. T.; Fukuyama, T.; Ryu, I. *Org. Lett.* **2009,** *11,* 2457–2460. doi:10.1021/ol900713d
23. Wiles, C.; Watts, P. In *Micro reactors in organic synthesis*; CRC-Press, 2011.
24. Wiles, C.; Watts, P. *Chem. Commun.* **2011,** 6512–6535. doi:10.1039/c1cc00089f

25. Luis, S. V.; Garcia-Verdugo, E. In *Chemical reactions and processes under flow conditions;* Royal Society of Chemistry, 2010.
26. Fu, X.; Liu, S.; Ruan, X.; Yang, H. *Sens. Actuators, B* **2006,** *114,* 618–624. doi:10.1016/j.snb.2005.06.023
27. DBU (**6**) = £51.80/100g compared with £7.50/100 g for K_2CO_3 (www.sigmaaldrich.com (21/05/11)).

Beilstein Journal of Organic Chemistry

Continuous preparation of carbon-nanotube-supported platinum catalysts in a flow reactor directly heated by electric current

Alicja Schlange*, Antonio Rodolfo dos Santos, Ulrich Kunz and Thomas Turek

Full Research Paper

Open Access

Address:
Institute of Chemical Process Engineering, Clausthal University of Technology, Leibnizstr.17, D-38678 Clausthal-Zellerfeld, Germany

Email:
Alicja Schlange* - schlange@icvt.tu-clausthal.de;
Antonio Rodolfo dos Santos - arsantos@icvt.tu-clausthal.de;
Ulrich Kunz - kunz@icvt.tu-clausthal.de; Thomas Turek - turek@icvt.tu-clausthal.de

* Corresponding author

Keywords:
carbon nanotubes; continuous catalyst synthesis; direct electrical heating; flow reactors; fuel cell platinum catalyst

Beilstein J. Org. Chem. **2011,** *7,* 1412–1420.
doi:10.3762/bjoc.7.165

Received: 01 June 2011
Accepted: 12 September 2011
Published: 14 October 2011

This article is part of the Thematic Series "Chemistry in flow systems II".

Guest Editor: A. Kirschning

Abstract

In this contribution we present for the first time a continuous process for the production of highly active Pt catalysts supported by carbon nanotubes by use of an electrically heated tubular reactor. The synthesized catalysts show a high degree of dispersion and narrow distributions of cluster sizes. In comparison to catalysts synthesized by the conventional oil-bath method a significantly higher electrocatalytic activity was reached, which can be attributed to the higher metal loading and smaller and more uniformly distributed Pt particles on the carbon support. Our approach introduces a simple, time-saving and cost-efficient method for fuel cell catalyst preparation in a flow reactor which could be used at a large scale.

Introduction

Batch processes represent the state of the art in catalyst preparation. One reason for employing this operation mode is that the yearly production rates can be rather small, comparable to pharmaceutical or fine chemical synthesis. With the advent of microreactors or minireactors continuous preparation methods have entered the organic chemist's laboratory. This makes the small-scale preparation of products in a continuous operation mode attractive. On the one hand numerous organic reactions

have been described in the flow mode [1-11]. On the other hand the preparation of catalysts in a continuously operated flow reactor is still a research field with only a few published results. Most of the work is concerned with the precipitation of hydroxides, oxides or other hardly soluble metal compounds [12].

Platinum nanoparticles supported on conductive carbon materials such as carbon black or carbon nanotubes (CNTs) are commonly used as oxygen reduction reaction (ORR) catalysts for direct methanol fuel cells (DMFCs). This kind of fuel cell has attracted great attention during recent years as a future power source for portable and stationary applications [13-15]. One of the advantages of methanol as fuel is its high energy density. Additionally it offers easy storage and transportation in comparison to hydrogen. At present, factors such as low power densities and high material costs, especially of the electrode, are the main challenges in widespread commercialization of DMFCs. Several research groups have shown that there is a clear correlation between the morphology of a carbon supported Pt catalyst and its electrochemical activities [16-18]. To overcome this challenge, further research on electrocatalyst development is a necessity. Generally, high metal content, small platinum cluster size, and uniform particle distribution over the support material are needed to enhance the electrochemical activity, resulting in higher power density values. It is known that the catalyst preparation method strongly influences the noble metal cluster size and its dispersion on the carbon and therefore the electrocatalytic activity [19].

DMFC electrocatalysts are mostly prepared in batch processes where an oil bath or heat exchangers act as the heat source. While using these traditional methods, hot spots can occur, mostly when a large volume of reaction mixture is used, hindering homogenous nucleation of platinum particles. Moreover, when using these preparation methods a longer time is needed to reduce the noble metal particles [20], resulting in an increase of the production costs. Additionally the cluster size and their distribution cannot be well controlled [21]. Furthermore, the amount of products is limited by the volume and size of the used reaction vessels.

In this contribution we demonstrate, for the first time, a simple and cost-effective method for the preparation of carbon-nanotube-supported Pt catalysts by using a continuously operated tubular flow reactor. The heating concept was realized by passing electrical current directly through the reactor wall. The experimental setup is not cost intensive, because all components used for the construction are standard laboratory equipment. Using the continuously operated tubular reactor, heating rates comparable to a microwave oven were achieved. Furthermore, the preparation technique is supposed to have a great potential also for the production of other metal/carbon supported catalysts.

Electrocatalyst preparation methods

In recent years, different methods for the synthesis of carbon-supported Pt catalysts have been studied. Among these, three methods were mainly used:

1. **impregnation method**, based on the impregnation of platinum precursor salt on carbon support material followed by the reduction with a proper reducing agent ($NaBH_4$, N_2H_4) or under a gaseous reducing environment (H_2),
2. **microemulsion method**, based on a water–oil system where surfactant molecules are used for stabilization of nanoparticles, and
3. **colloidal method**, based on adsorption of platinum colloid on the surface of the carbon support material followed by the chemical reduction step.

The main advantage of the impregnation method is its simplicity in execution [22,23]. Nevertheless, catalysts prepared by impregnation show a broad cluster-size distribution and a large average cluster size resulting in lower electrocatalytic activity, as reported by [21]. The microemulsion method allows for better control of the nanoparticle size and distribution in comparison to the impregnation method. Disadvantages of this method are the high cost of the used surfactants and their time-consuming removal at the completion of the process [21], hindering the use of this method in a large-scale production. Therefore in recent years the colloidal method was often employed as the standard preparation technique for Pt deposition on carbon support. In this process (polyol reduction) ethylene glycol (EG) acts as both reducing agent and solvent for the Pt precursor. During the reduction step the solution of EG and Pt precursor salt is heated to 120–170 °C [24]. During this step EG is decomposed and generates the reducing species (CH_3CHO, Equation 1). This species reduces the Pt ions to metallic Pt particles, as shown in Equation 2:

$$CH_2OHCH_2OH \rightarrow CH_3CHO + H_2O \quad (1)$$

$$2\,CH_3CHO + (PtCl_6)^{2-} + 6\,OH^- \rightarrow 2\,CH_3COO^- + Pt + 6\,Cl^- + 4\,H_2O \quad (2)$$

The main advantage of this polyol synthesis is that the acetate can also serve as a stabilizer for Pt colloids through the formation of chelate-type complexes through its carboxyl group [24]. The application of stabilization agents to protect Pt particles from agglomeration is not necessary. A precondition for a

homogenous formation of nuclei during the polyol synthesis is the choice of a proper heating method. Conventional heating strategies, such as oil baths or heat exchangers, usually exhibit a heterogeneous temperature distribution including the possibility of hot spots. This can lead to temperature gradients in the reacting solution, resulting in poor dispersion of Pt on the carbon support. For this reason, in the past few years heating by means of microwave ovens was introduced. The microwave-assisted polyol synthesis method has many advantages over the conventional heating process [25,26]. It offers a more uniform environment for the nucleation and growth of metal particles [27], due to a rapid, homogeneous and effective heating. Moreover, fast heating rates can accelerate the reduction of the Pt precursor ions and the nucleation of the metal particles [27]. In consequence, the preparation of carbon-supported catalysts with smaller noble metal sizes and narrow size distributions is possible [21]. Amongst others, this attractive synthesis method for the production of CNT or carbon-black-supported Pt catalysts was successfully applied by several researchers [27-31]. It was possible to obtain highly dispersed Pt particles on the carbon support, resulting in an enhanced catalytic activity towards ORR, as described in [24,32,33].

The proposed microwave-heated polyol synthesis method was applied as a batch process only. Using our experimental setup it is possible to produce a Pt/CNT catalyst in a continuous polyol process. Heating rates generated during the reaction are comparable to a microwave oven. The apparatus does not require expensive temperature sensors as used in microwave heating systems. The costs for the described experimental setup are low compared to other heating equipment. In building our setup we incurred the following costs:

- reactor tube 20 EUR/m,
- two temperature controllers (with integrated power supply) 250 EUR each, and
- power supply – here a standard computer power supply was used (5V, 120A) 250 EUR.

Altogether, including the high diameter copper wires, some electronic components (MOSFET), standard tube connectors and the standard thermocouples, the costs for the materials were less than 1000 EUR. As remarked earlier, the setup consists solely of typical laboratory equipment such as NiCr-Ni thermocouples, Swagelok elements and stainless steel tubes. We think the presented approach is a flexible setup for the laboratory. Tubes in the range of 1/16" to 1/4" diameter made of stainless steel are appropriate starting materials for the reactor tubes.

Let us assume a reactor length of 50 cm with an inner diameter of 0.595 cm and an outer diameter of 0.635 cm, which is a standard 1/4" tube. The specific measured resistance of the chosen stainless steel tube, made of 1.4404 (X2CrNiMo17-12-2), is 0.724 $\Omega \cdot mm^2 \cdot m^{-1}$ and thus the electrical resistance of this tube is 0.094 Ω. According to Ohm's law, with a 5 V power supply a current of 53.2 A will develop inside the tube. This corresponds to a heating power of 265 W. This is sufficient to heat liquid reaction mixtures to reaction temperatures well above 100 °C in a short time if volumetric flow rates in the mL/min range are applied. Additional information on this aspect can be found in our previous publication [1]. The limitation of this concept is the availability of power supplies for high current since with tubes of larger diameter or shorter lengths the heating currents may reach more than 100 A. Up to this current rating the power supplies are low in price (less than 300 EUR) because these are produced for the large computer market. If different reactor lengths and diameters are to be tested it is recommended to purchase an adjustable low voltage/high current power supply. These are much more expensive, with prices ranging well beyond 1000 EUR.

Results and Discussions

Experimental setup

For the continuous preparation of CNT-supported catalysts an experimental setup as depicted in Figure 1 and similar to that described in our previous publication [1] was used. As seen in Figure 1 the reaction mixture of platinum precursor, EG and carbon nanotubes was pumped from the reservoir through two 1/8" stainless steel tubes (3.18 mm × 0.56 mm) with a flow rate of 1 $mL \cdot min^{-1}$ by means of a peristaltic pump. In the first tube (length of 50 cm) the reaction mixture was preheated from room temperature up to a temperature of 140 °C within 90 s. Along the tube a linear temperature profile was established resulting in gentle preheating of the reaction mixture in a short time. In the second tube (length of 17 cm) this constant reaction temperature was maintained (residence time of 30 s). The connections between both tubes were made with Swagelok connectors.

The heating concept is based on passing of the electric current through the reactor wall, which was delivered by a low voltage/high current power supply (5 V, 120 A). The advantages of this technique are the uniform heating across the whole surface area of the reactor without the occurrence of hot spots. In a previous work the temperature profile was measured with an infrared camera. This was published at a conference on infrared technology [34]. The temperature profile is linear since each volume element of the electrically heated tube produces the same amount of heat, which is caused by the fact that the average current along the tube is constant for a set heating rate. Overheating in the middle of the tube cannot occur and was not observed in the infrared measurements. In addition, we measured the temperature profile with thermocouples attached

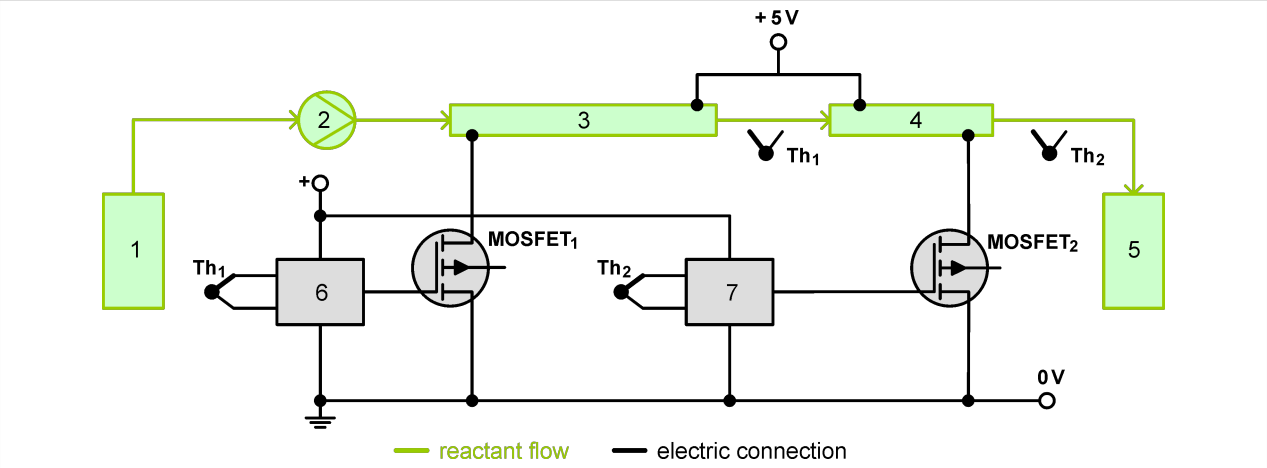

Figure 1: Experimental setup for catalyst synthesis in the tubular flow reactor; 1: Reaction mixture reservoir, 2: Peristaltic pump, 3: Preheating tube, 4: Heating tube, 5: Catalyst reservoir, 6: Temperature controller with thermocouple 1 (Th_1), 7: Temperature controller with thermocouple 2 (Th_2).

at different locations on the outer side of the reactor tubes. The measured axial temperature profile is depicted in Figure 2. This also demonstrates that the temperature profile is linear.

These reaction conditions promote the homogenous nucleation of platinum particles, resulting in a uniform metal distribution over the carbon support. For a precise temperature control NiCr–Ni thermocouples were installed at the outlets of both tubes. These were placed in the tube centre to adjust the temperature of the reaction mixture. All electrical connections within the heater supply lines were made of flexible, insulated 4 mm copper wires. At the outlet of the second tube the reaction mixture was continuously collected in a glass beaker and after cooling down and cleaning it was used for further cathode preparation. To investigate the reproducibility of the preparation method, three catalyst samples were taken at intervals of 25 min during the continuous reactor operation.

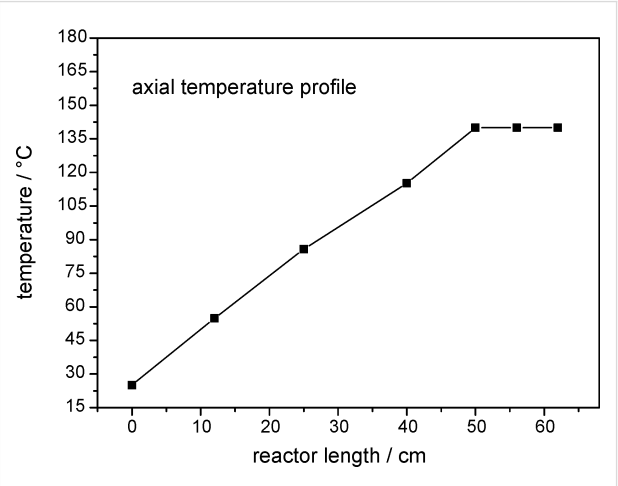

Figure 2: Measured temperature profile along the tubular reactor.

As a reference, an electrocatalyst was synthesized by a conventional method with traditional oil-bath heating. After preheating the oil bath to a temperature of 160 °C a 100 mL glass flask containing the reaction mixture was immersed. The temperature of the mixture was monitored during the chemical reduction with a Hg thermometer. A time of 10 min was needed to preheat the CNT/Pt-precursor/EG solution to the desired temperature of 140 °C. At this final temperature the reaction was performed for 3 h. Afterwards the product was cooled down to room temperature and cleaned several times with ethanol. Finally it was separated by means of a centrifuge at 4000 rpm and dried in an oven.

Catalysts and support material characterization

Thermogravimetric analysis (TGA) curves for pristine CNT, oxidized CNT, Pt/CNT oil bath and one of the Pt/CNT tubular reactor samples are given in Figure 3. Differences regarding the oxidation behavior for the different samples can be clearly seen. Pristine nanotubes are thermally stable up to a temperature of 450 °C. The residue of 2.3% can be attributed to impurities remaining in the sample after the production process. In comparison to this result the oxidized CNTs starts to decompose at lower temperature. The thermal degradation of HNO_3-treated CNTs in the temperature range between 150 to 350 °C is caused by the decomposition of the carboxylic groups attached to the surface during the nitric acid treatment. A weight loss of 4.69% in this temperature region reveals the successful functionalization of carbon nanotubes and formation of oxygen containing groups. For the electrocatalyst sample prepared in the tubular reactor a Pt loading of 31 wt % was estimated. In comparison, the reference catalyst synthesized by a conventional process exhibits a loading of 20 wt %. Differences in Pt amount between the calculated and the measured values after the chem-

ical reduction were also reported by others. The reason for metal loss could be the repeated filtering and washing process as described in [21]. The observation that platinum loading is higher in the tubular reactor samples than in the oil-bath-prepared samples was confirmed by several samples. An explanation for this phenomenon is so far not available. One reason might be that in the oil-bath method we work in a system with back mixing whereas the continuously operated tubular reactor has no back-mixing effect.

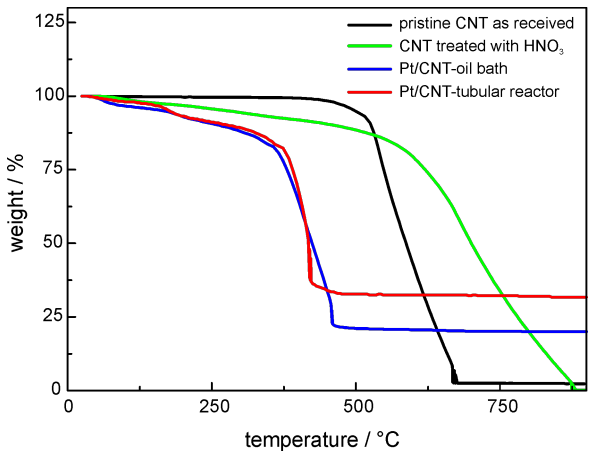

Figure 3: TGA weight loss curves for pristine CNT, HNO_3 oxidized CNT, Pt/CNT-oil bath and Pt/CNT-tubular reactor samples.

TEM micrographs of both catalyst samples are demonstrated in Figure 4. Cluster size histograms and the average cluster size are also shown. It can be clearly seen that for the catalyst prepared in the tubular reactor Pt particles are homogenously dispersed on carbon nanotubes. Particles range from 0.80 nm to 2.80 nm in diameter, with a mean value of 1.80 nm. In the case of the Pt/CNT catalyst synthesized in an oil bath the platinum particle sizes range from 1.00 nm to 4.75 nm resulting in an average size of 2.62 nm. For this catalyst sample some agglomeration of platinum particles was also observed as shown in Figure 4. The fact that some isolated platinum particles can be observed in the sample prepared in the tubular reactor can be attributed to the dispersion method employed during the TEM sample preparation.

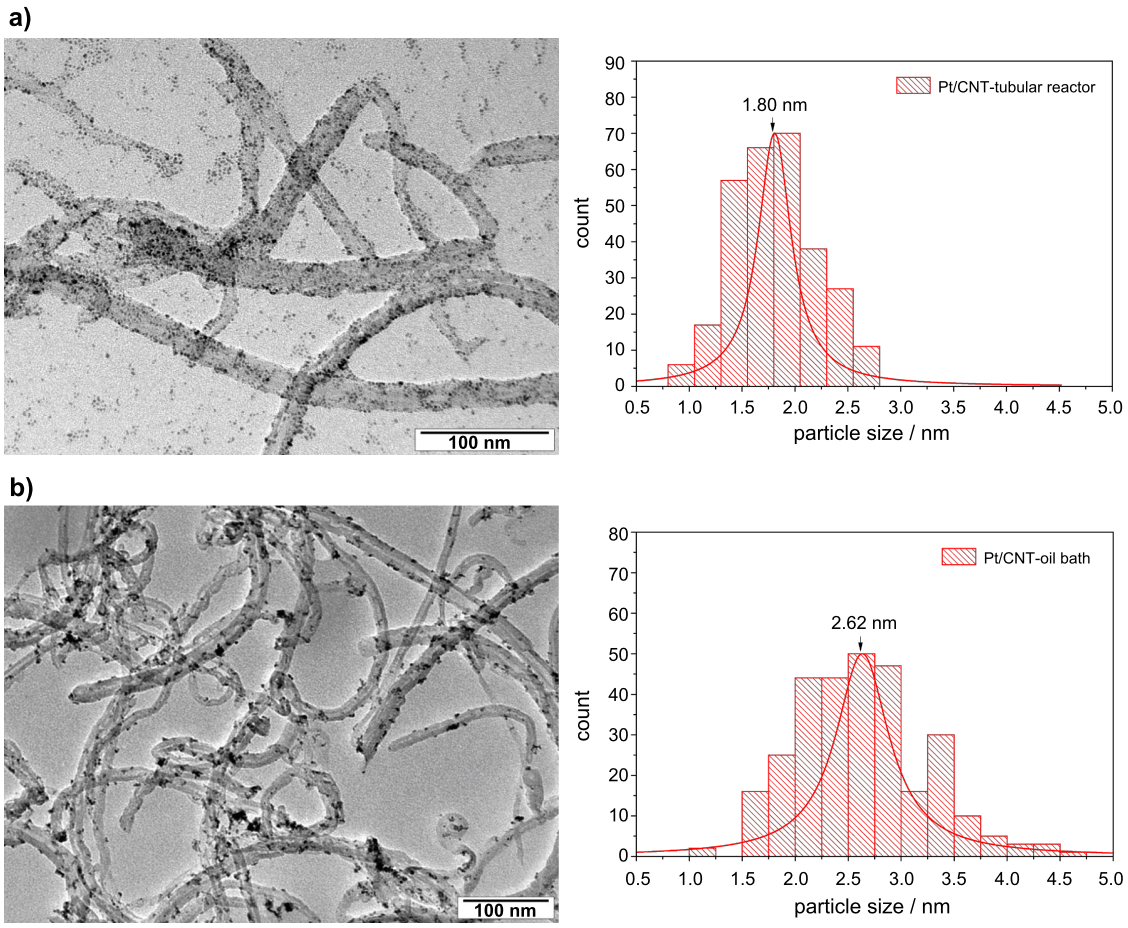

Figure 4: TEM micrographs of catalyst samples: a) Pt/CNT tubular reactor and b) Pt/CNT oil bath.

These results reveal that the catalyst preparation method strongly influences the metal cluster size and distribution. Uniform and rapid heat transfer offered by the resistively heated tubular reactor accelerates the reduction of Pt ions, which results in the formation of smaller metal particles.

Metal dispersion is one of the most fundamental properties of supported metal catalysts [35]. To estimate the degree of metal dispersion for both our electrocatalyst samples, CO pulse chemisorption measurements were performed. Pulse chemisorption is useful to quantify the amount of active components on the surface of the supported catalyst. As described in [35] the extent of metal dispersion is defined as the fraction of metallic atoms present on the surface and therefore determines the catalytic properties. Platinum dispersion can be calculated from the following equation [36,37]:

$$D_{\mathrm{Pt}} = \frac{V_{\mathrm{chem}}\, M_{\mathrm{Pt}}\, \nu_{\mathrm{Pt}}}{V_{\mathrm{M}}^{0}\, m_{\mathrm{sample}}\, x_{\mathrm{Pt}}} \qquad (3)$$

D_{Pt}	dispersion of Pt [%]
V_{chem}	amount of absorbed gas [L]
M_{Pt}	molar mass of Pt [g/mol]
ν_{Pt}	stoichiometric factor
V_{M}^{0}	molar volume of an ideal gas [L/mol]
m_{sample}	mass of the sample [g]
x_{Pt}	Pt-loading in the catalyst sample [%]

Using the CO chemisorption method a Pt dispersion of 16.49% for the Pt/CNT catalyst prepared in the tubular reactor was estimated compared to 12.65% for the reference catalyst. Dispersion values were measured for the same sample several times. In doing so the error of the method was found to be less than 5%. So the given values of 12.65 and 16.49% represent true differences between the two catalysts. As an additional reference, we have measured other catalyst samples indicating that the measuring method works accurately. We measured an industrial reference catalyst, 20 wt % Pt/C. The measured dispersion is 4.54%, which indicates that the sample prepared in the continuously operated tubular reactor has much higher dispersion.

Powder X-ray diffraction analysis was performed to investigate the crystalline structure of the prepared catalysts and the support material. XRD spectra are given in Figure 5. For pristine carbon nanotubes the diffraction peaks at 30.0° and 50.4° can be attributed to the (002) and (004) planes of the hexagonal graphite structure.

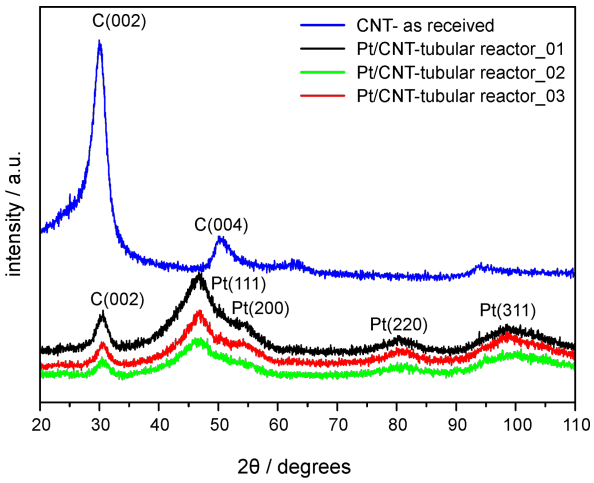

Figure 5: X-ray diffraction patterns for the as-received CNT and the three Pt/CNT samples taken at intervals of 25 min in the tubular reactor.

For Pt/CNT catalysts prepared with the tubular reactor four characteristic peaks at 46.6°, 54.7°, 80.6° and 98.7° were found, which correspond to (111), (200), (220) and (311) reflection planes of the face-centered cubic (fcc) platinum, respectively. For these samples the diffraction spectra are very broad indicating small noble metal cluster sizes. The average Pt cluster size can be calculated from Pt (220) reflections with the Scherrer equation [38]

$$D = \frac{0.9\lambda}{B\cos\theta} \qquad (4)$$

where λ is 0.178 and B is the full width at half maximum of the peak in radians. The Pt cluster sizes calculated for Pt/CNT catalysts prepared with the tubular reactor were measured as 1.77 nm, 1.74 nm and 1.77 nm. These results are in agreement with results determined by TEM analysis. For the reference Pt/CNT catalyst (not shown in Figure 5) the Pt cluster size calculated with the Scherrer equation was 2.31 nm.

Electrochemical activity of prepared catalysts

The single cell performances of the prepared Pt/CNT catalysts used as the cathode of a DMFC are shown in Figure 6. The measurements for both catalyst samples were performed under the same operating conditions (80 °C, 1 M MeOH at a flow rate of 5 mL·min^{-1}, oxygen at a flow rate of 200 mL·min^{-1}). In the fuel cell test the platinum loading in both experiments was the same. The differences of the Pt loading on the supports were taken into account. The higher loaded catalyst was applied in a smaller amount. Thus both electrodes had 1 mg Pt·cm^{-2}.

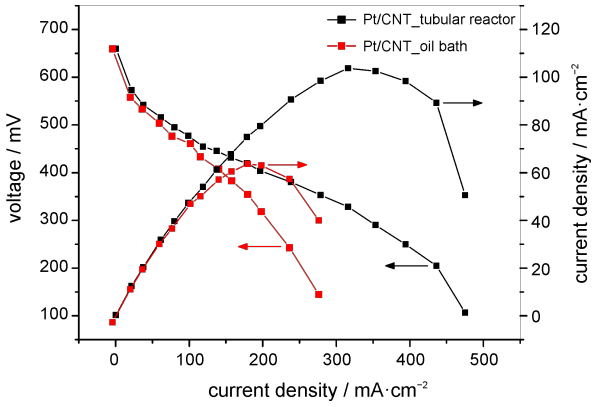

Figure 6: Comparison of performance in DMFC with Pt/CNT oil bath and Pt/CNT tubular reactor samples as cathode catalysts (Pt loading of 1 mg·cm^{-2} on each anode and cathode).

Both samples show a nearly equal open circuit voltage (OCV) of 660 mV. The current densities at 0.4 V were found to be 203 mA·cm^{-2} for Pt/CNT (tubular reactor) and 139 mA·cm^{-2} for Pt/CNT (oil bath). The cell containing the electrocatalyst synthesized in the continuous process exhibits a maximum power density of 103 mW·cm^{-2} at 320 mA·cm^{-2}. This means an increase in performance of 60% in comparison to the oil-bath sample (64 mW·cm^{-2} at 177 mA·cm^{-2}). This improvement can be explained by the higher catalyst dispersion and the smaller platinum particles.

Conclusion

The present work reveals that the preparation method is one of the most important factors determining the morphology and activity of Pt catalysts supported by carbon nanotubes. Short heating times and short reaction times are essential for the reduction of highly active platinum particles on nanotube supports. The proposed continuous preparation process offers simplicity in the production, a low cost experimental setup, and uniform reaction conditions due to a good temperature control. Therefore, the proposed preparation of Pt/CNT catalysts in a large-scale process is possible. In comparison to a reference catalyst prepared by a conventional method (oil bath) the samples synthesized in the tubular reactor show a more uniform distribution of the platinum cluster size (average particle size of 1.80 nm) without any agglomerates over the carbon support. The metal dispersion of the described catalyst (16.49%) is much higher than for the oil-bath sample (12.65%). DMFC performance tests reveal excellent catalytic activity of the catalyst prepared in the continuous process, resulting in a measured maximum power density of 103 mW·cm^{-2} in comparison to 64 mW·cm^{-2} for the reference sample. This improvement in fuel cell performance can be attributed to the smaller and homogenously dispersed Pt particles on the carbon nanotubes.

According to the obtained results, we can also state that the proposed continuous preparation technique by resistive heating may be very useful for the synthesis of other carbon-supported metal catalysts used in metal/air batteries or fuel cells, or even in other processes.

Experimental

Reagents

Carbon nanotubes (MWCNT, Baytubes®, C 150) with inner diameter of 2–6 nm and outer diameter of 5–20 nm were obtained from Bayer MaterialScience AG. Ethylene glycol (EG), HNO_3, HCl and NaOH were purchased from Sigma-Aldrich and used as received. The platinum precursor ($H_2PtCl_6{\cdot}6H_2O$) was purchased from Merck.

Pretreatment of carbon nanotubes

The pristine nanotubes are inert and therefore have to be modified to create the anchoring sites for the Pt precursor. For this purpose 40 g of carbon nanotubes were first treated with 37 wt % HCl at 100 °C for 5 h to remove any impurities remaining after the production process. In the next step the purified nanotubes were refluxed with 1 L of concentrated nitric acid (65 wt %) for 5 h under a nitrogen atmosphere. After each acid treatment the product was cooled down, filtered, washed several times with deionised water to a desired pH value of 7 and finally dried in an oven at 60 °C for 24 h.

Preparation of electrocatalysts

Carbon nanotube supported Pt catalysts were synthesized by the polyol synthesis method (ethylene glycol mediated reaction). The procedure was as follows: 160 mg HNO_3 treated carbon nanotubes were ultrasonically dispersed in 60 mL of ethylene glycole (EG). Then 265 mg of $H_2PtCl_6{\cdot}6H_2O$ were dissolved in 20 mL EG and added dropwise into the prepared suspension of the carbon nanotubes. In the following step the pH value was adjusted to be above 10 through the use of 1 M NaOH. The resulting reaction mixture was used for electrocatalyst preparation, which was performed in a tubular reactor or by use of an oil bath (reference sample) as the heating source. After the reaction was completed, the resulting catalyst was cooled down to room temperature, washed with ethanol, then separated by means of a centrifuge at 4000 rpm and finally dried in a furnace at 60 °C under air flow.

Characterization methods

The crystalline structures of the support material and electrocatalysts were analyzed by X-ray diffraction (XRD) with a Siemens D5000/Kristalloflex diffractometer using Co Kα radia-

tion (λ = 1.789 Å). The 2θ Bragg angles were scanned over a range from 20° to 110° with a step size of 0.02°. Transmission electron micrographs were obtained using a JEOL TEM 2100 with an accelerating voltage of 200 kV. Catalyst samples for TEM characterization were prepared by placing a drop of Pt/CNT suspension dispersed in ethanol on a carbon-coated copper (Cu) grid followed by drying at room temperature. The distribution of Pt particles over the carbon support was estimated with the LINCE 2.42e Software [39].

To investigate the thermal stability of nanotubes and to estimate the Pt loading of the catalyst samples, thermogravimetric analysis (TGA) was carried out. The measurements were performed with a Mettler TGA 860 thermo balance in air at a flow rate of 50 $cm^3 \cdot min^{-1}$ and a heating rate of 20 $K \cdot min^{-1}$ over a temperature range of 25–900 °C. The Pt loading in the sample was calculated from the last weight loss step at around 600 °C. The metal dispersion of the prepared electrocatalysts was estimated by means of a BELCAT-M (BEL Japan, Inc.) with 10 vol % CO/He gas at a flow rate of 15 $mL \cdot min^{-1}$.

Single cell test and electrode preparation

For electrocatalytic activity measurements a homemade DMFC test station equipped with high impedance potentiometer (Delta Elektronika SM3000) was used. The active area of the single cell with parallel flow field was 5 cm^2. The platinum loading for both electrodes, anode and cathode, was 1 $mg \cdot cm^{-2}$, respectively. The fuel cell performance tests were carried out at 80 °C with pure oxygen as an oxidant (200 $mL \cdot min^{-1}$). 1 M MeOH solution at a flow rate of 5 $mL \cdot min^{-1}$ was supplied to the anode. The cathode layer was prepared using synthesized Pt/CNT catalysts, while the anode was fabricated using commercial Pt/Ru catalyst from BASF (40 wt % Pt, 20 wt % Ru) supported on Vulcan® XC-72R carbon. Catalyst coated membranes (CCM) were fabricated by spraying catalyst ink (water:catalyst:Nafion® ionomer (15 wt %) at a weight ratio of 9:1:1.175) on the Nafion® 117 membrane. After application of catalyst ink the membrane was hot-pressed at 120 °C at a pressure of 14 MPa for 3 min. The diffusion layers were prepared by coating a carbon cloth from Ballard (AvCarb 1071HCB) with a layer of 85 wt % carbon black (Ketjen Black EC 300J) and 15 wt % PTFE. A single DMFC test cell was finally assembled from diffusion layers, catalyst coated membrane, bipolar plates (material BMA5 from Eisenhuth GmbH & Co. KG) and Teflon gaskets.

Acknowledgements

The authors thank the Energie-Forschungszentrum Niedersachsen (EFZN) for financial support of this work. We also thank Dr.-Ing. R. Weber from Bayer MaterialScience AG for kindly donating the used MWCNT.

References

1. Kunz, U.; Turek, T. *Beilstein J. Org. Chem.* **2009,** *5,* No. 70. doi:10.3762/bjoc.5.70
2. Wegner, J.; Ceylan, S.; Kirschning, A. *Chem. Commun.* **2011,** *47,* 4583–4592. doi:10.1039/c0cc05060a
3. McMullen, J. P.; Jensen, K. F. *Annu. Rev. Anal. Chem.* **2010,** *3,* 19–42. doi:10.1146/annurev.anchem.111808.073718
4. Tanaka, T.; Fukase, K. *Org. Process Res. Dev.* **2009,** *13,* 983–990. doi:10.1021/op900084f
5. Roberge, D. M.; Zimmermann, B.; Rainone, F.; Gottsponer, M.; Eyholzer, M.; Kockmann, N. *Org. Process Res. Dev.* **2008,** *12,* 905–910. doi:10.1021/op8001273
6. Hessel, V. *Chem. Eng. Technol.* **2009,** *32,* 1655–1681. doi:10.1002/ceat.200900474
7. Hartman, R. L.; Jensen, K. F. *Lab Chip* **2009,** *9,* 2495–2507. doi:10.1039/b906343a
8. Mak, X. Y.; Laurino, P.; Seeberger, P. H. *Beilstein J. Org. Chem.* **2009,** *5,* No. 19. doi:10.3762/bjoc.5.19
9. Wiles, C.; Watts, P. *Eur. J. Org. Chem.* **2008,** 1655–1671. doi:10.1002/ejoc.200701041
10. Fukuyama, T.; Rahman, M. T.; Sato, M.; Ryu, I. *Synlett* **2008,** 151–163. doi:10.1055/s-2007-1000884
11. Mason, B. P.; Price, K. E.; Steinbacher, J. L.; Bogdan, A. R.; McQuade, D. T. *Chem. Rev.* **2007,** *107,* 2300–2318. doi:10.1021/cr050944c
12. Song, Y.; Hormes, J.; Kumar, C. S. S. R. *Small* **2008,** *4,* 698–711. doi:10.1002/smll.200701029
13. Ren, X.; Zelenay, P.; Thomas, S.; Davey, J.; Gottesfeld, S. *J. Power Sources* **2000,** *86,* 111–116. doi:10.1016/S0378-7753(99)00407-3
14. Thomas, S. C.; Ren, X.; Gottesfeld, S.; Zelenay, P. *Electrochim. Acta* **2002,** *47,* 3741–3748. doi:10.1016/S0013-4686(02)00344-4
15. Chang, H.; Joo, S. H.; Pak, C. *J. Mater. Chem.* **2007,** *17,* 3078–3088. doi:10.1039/b700389g
16. Ahmadi, T. S.; Wang, Z. L.; Green, T. C.; Henglein, A.; El-Sayed, M. A. *Science* **1996,** *272,* 1924–1925. doi:10.1126/science.272.5270.1924
17. Aricò, A. S.; Srinivasan, S.; Antonucci, V. *Fuel Cells* **2001,** *1,* 133–161. doi:10.1002/1615-6854(200107)1:2<133::AID-FUCE133>3.0.CO;2-5
18. Zhang, J.; Wang, X.; Wu, C.; Wang, H.; Yi, B.; Zhang, H. *React. Kinet. Catal. Lett.* **2004,** *83,* 229–236. doi:10.1023/B:REAC.0000046081.96554.ae
19. Tang, Z.; Ng, H. Y.; Lin, J.; Wee, A. T. S.; Chua, D. H. C. *J. Electrochem. Soc.* **2010,** *157,* B245–B250. doi:10.1149/1.3266933
20. Huang, M.; Li, L.; Guo, Y. *Electrochim. Acta* **2009,** *54,* 3303–3310. doi:10.1016/j.electacta.2008.12.047
21. Liu, H.; Zhang, J. *Electrocatalysis of Direct Methanol Fuel Cells;* Wiley-VCH: Weinheim, Germany, 2009.
22. Ramkumar, R.; Dheenadayalan, S.; Pattabiraman, R. *J. Power Sources* **1997,** *69,* 75–80. doi:10.1016/S0378-7753(97)02572-X
23. Goodenough, J. B.; Hamnet, A.; Kennedy, B. J.; Manoharan, R.; Weeks, S. A. *Electrochim. Acta* **1990,** *35,* 199–207. doi:10.1016/0013-4686(90)85059-V
24. Lee, K.; Zhang, J.; Wang, H.; Wilkinson, D. P. *J. Appl. Electrochem.* **2006,** *36,* 507–522. doi:10.1007/s10800-006-9120-4
25. Chen, X. W.; Lee, J. Y.; Liu, Z. *Chem. Commun.* **2002,** 2588–2589. doi:10.1039/b208600j
26. Liu, Z.; Lee, J. Y.; Chen, W.; Han, M.; Gan, L. M. *Langmuir* **2004,** *20,* 181–187. doi:10.1021/la035204i

27. Sakthivel, M.; Schlange, A.; Kunz, U.; Turek, T. *J. Power Sources* **2010,** *195,* 7083–7089. doi:10.1016/j.jpowsour.2010.05.002
28. Tsuji, M.; Kubokawa, M.; Yano, R.; Miyamae, N.; Tsuji, T.; Jun, M.-S.; Hong, S.; Lim, S.; Yoon, S. H.; Mochida, I. *Langmuir* **2007,** *23,* 387–390. doi:10.1021/la062223u
29. Li, X.; Chen, W. X.; Zhao, J.; Xing, W.; Xu, Z. D. *Carbon* **2005,** *43,* 2168–2174. doi:10.1016/j.carbon.2005.03.030
30. Guo, Z. P.; Han, D. M.; Wexler, D.; Zeng, R.; Liu, H. K. *Electrochim. Acta* **2008,** *53,* 6410–6416. doi:10.1016/j.electacta.2008.04.050
31. Han, D. M.; Guo, Z. P.; Zhao, Z. W.; Zeng, R.; Meng, Y. Z.; Shu, D.; Liu, H. K. *J. Power Sources* **2008,** *184,* 361–369. doi:10.1016/j.jpowsour.2008.03.051
32. Liu, Z.; Gan, L. M.; Hong, L.; Chen, W.; Lee, J. Y. *J. Power Sources* **2005,** *139,* 73–78. doi:10.1016/j.jpowsour.2004.07.012
33. Chen, W.; Zhao, J.; Lee, J. Y.; Liu, Z. *Mater. Chem. Phys.* **2005,** *91,* 124–129. doi:10.1016/j.matchemphys.2004.11.003
34. Wittenhorst, S.; Feuerriegel, U.; Kunz, U. Infrared imaging and simulation of temperature profiles in directly electrically-heated tubular reactors. Lecture held at infraR&D 2009 – 5th International Infrared Forum, Fulda, Germany.
35. Perrichon, V.; Retailleau, L.; Bazin, P.; Daturi, M.; Lavalley, J. C. *Appl. Catal., A* **2004,** *260,* 1–8. doi:10.1016/j.apcata.2003.09.031
36. Brodzi´nski, A.; Bonarowska, M. *Langmuir* **1997,** *13,* 5613–5620. doi:10.1021/la962103u
37. Scholten, J. J. F.; Pijpers, A. P.; Hustings, A. M. L. *Catal. Rev. - Sci. Eng.* **1985,** *27,* 151–206.
38. Scherrer, P. *Nachr. Ges. Wiss. Goettingen, Math.-Phys. Kl.* **1918,** *26,* 98–100.
39. *LINCE,* 2.4.2e; Department of Materials Science, Darmstadt University of Technology: Darmstadt, 1998.

License and Terms

Beilstein Journal of Organic Chemistry

Multistep flow synthesis of vinyl azides and their use in the copper-catalyzed Huisgen-type cycloaddition under inductive-heating conditions

Lukas Kupracz, Jan Hartwig, Jens Wegner, Sascha Ceylan and Andreas Kirschning*

Full Research Paper

Open Access

Address:
Institute of Organic Chemistry, Leibniz University Hannover, Schneiderberg 1b, 30167 Hannover, Germany

Email:
Lukas Kupracz - lukas.kupracz@oci.uni-hannover.de; Jan Hartwig - jan.hartwig@oci.uni-hannover.de; Jens Wegner - jens.wegner@oci.uni-hannover.de; Andreas Kirschning* - andreas.kirschning@oci.uni-hannover.de

* Corresponding author

Keywords:
flow reactor; inductive heating; iodine azide; polymer-supported reagents; vinyl azides

Beilstein J. Org. Chem. **2011,** *7,* 1441–1448.
doi:10.3762/bjoc.7.168

Received: 21 August 2011
Accepted: 07 October 2011
Published: 20 October 2011

This article is part of the Thematic Series "Chemistry in flow systems II".

Associate Editor: J. Murphy

Abstract

The multistep flow synthesis of vinyl azides and their application in the synthesis of vinyltriazoles is reported. The synthesis relies on a stable polymer-bound equivalent of iodine azide that serves to carry out 1,2-functionalization of alkenes in a telescope flow protocol. The intermediate 2-iodo azides are subjected to a DBU-mediated polymer-supported elimination step yielding vinyl azides in good yield. The third step involves the formation of vinyl triazoles by a copper-catalyzed Huisgen-"click" cycloaddition. The required heat is generated by electromagnetic induction based on copper. Copper serves both as heatable as well as catalytically active packed-bed material inside the flow reactor.

Introduction

Azides are highly versatile organic functional groups and their preparation and their reactivity are well explored [1]. In contrast, the synthesis of vinyl azides is far away from being well established despite the fact that an even richer chemistry than that which has lately been developed for azides can be envisaged as vinyl azides bear the additional alkene moiety. One of the first synthetic studies on vinyl azides was disclosed by L'Abbé as early as 1975 [1]. Surprisingly, only a very few applications based on these potentially very useful functional groups have been reported to date. Lately, Yu et al. [2] disclosed the synthesis of pyrazoles, while Chiba et al. employed vinyl azides for the Mn(III)-mediated synthesis of different azaheterocycles [3,4]. Furthermore, vinyl azides can be converted into the corresponding 2*H*-azirines by thermolysis or alternatively by photolysis [5]. The highly reactive azirines can further react as dipolarophiles, dienophiles, electrophiles or

nucleophiles [6] thereby accessing oxazoles and isoxazoles [7]. In addition, 2*H*-azirines were also used in the Hemetsberger reaction, which yields indoles [8]. However, straightforward and safe methods for the preparation of vinyl azides are still scarce. In fact, in most cases the synthesis involves the generation of toxic and explosive azido intermediates. The most frequently used batch process for the generation of vinyl azides **4** is the two-step protocol developed by Hassner et al. [9] through the in situ reaction of sodium azide with iodine chloride in dichloromethane or another polar solvent (Scheme 1). Thus, it includes the generation of hazardous and highly explosive iodine azide (IN_3, **1**).

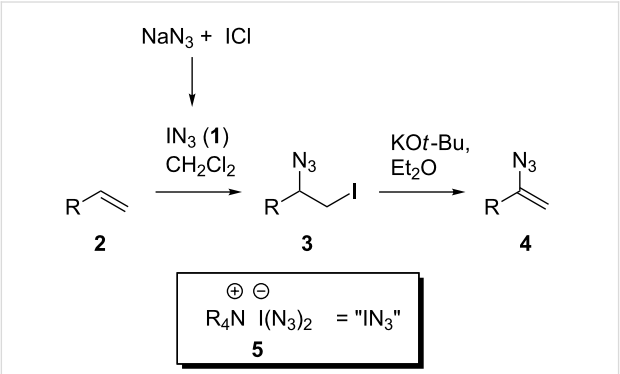

Scheme 1: Hassner's synthesis of vinyl azides and a stable, nonexplosive analogue **5** of iodine azide (**1**).

In their synthesis of carbamates Wirth and coworkers [10] recently showed that some of the practical problems associated with iodine azide can be circumvented or minimized by generating and immediately consuming iodine azide under flow conditions. Because of low yields, this ingenious process requires further optimization. This and other examples [11-13] principally demonstrate that flow chemistry is an ideal enabling technology [14] for generating and utilizing hazardous azido reagents because only small amounts are generated at a time and are subsequently consumed in situ. The other benefits of flow chemistry, when working with highly reactive reagents, are the better heat-transfer characteristics due to a larger surface-to-volume ratio, as well as the increased mixing efficiency [15-24]. To practically eliminate the generation of explosive iodine azide we developed the iodine azide transfer reagent **5** based on ammonium iodate(I) complexes [25]. As depicted in Scheme 2 the reagent can be prepared in three steps without the generation of free iodine azide (**1**). Importantly, this reagent can easily be prepared as an ion-exchange resin based on Amberlyst A-26 [26]. Chemically, this reagent behaves like iodine azide (**1**), but in contrast it is not explosive and is storable for weeks without a substantial loss of activity [27].

In this report, we disclose the first two-step flow synthesis of vinyl azides based on functionalized polymers **5** and **8**. The protocol starts from alkenes, which are transformed by a 1,2-addition of iodine azide and then to the corresponding vinyl azides. Furthermore, for the first time we present the copper-mediated Huisgen-type "click" cycloaddition of vinyl azides with alkynes to yield vinyl triazoles under inductive-heating conditions.

Results and Discussion

Synthesis of vinyl azides

Our study commenced with the preparation and utilization of polymer-bound iodate(I) complex **5** as packed-bed material in a flow device. Here, the polymer served as an electrophilic reagent for the mild 1,2-azidoiodination of alkenes under flow conditions. A solution of the alkene dissolved in dichloromethane (0.2 M) was passed, at room temperature, through a glass reactor (12 cm length and 8.5 mm internal diameter) filled with polymer **5** (5 g; theoretical loading = 3.5 mmol/g) that had been prepared as reported before [26]. Reaction conditions listed in Table 1 are optimized with respect to loading, flow rates and temperature. Higher temperatures and solvents other than dichloromethane were not beneficial due to degradation of the functionalized polymer **5** or the generation of byproducts. The resulting β-iodo azides **3** were isolated in moderate to very good yields. In two cases, the flow procedure was compared with the corresponding batch experiment. Yields were comparable but reaction times were shorter for the flow process. The dead volume of the polymer-filled reactor is about 4.5 mL and thus the theoretical residence times in the reactor at the given flow rates are between 1.5 h to 3.5 h.

Mechanistically the good regioselectivity is based on the generation of the more stable carbenium ion after electrophilic attack of the iodonium species on the olefinic double bond. In cases of

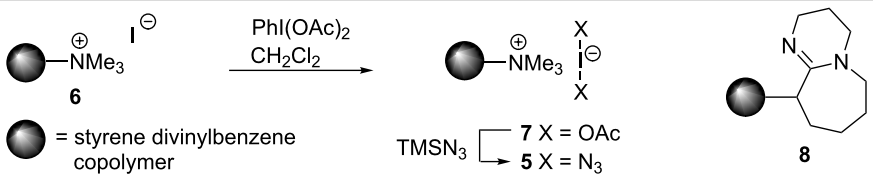

Scheme 2: Preparation of polymer-bound bisazido iodate(I) **5** and polymer-bound 1,8-diaza-[5.4.0]bicyclo-7-undecene **8**.

Table 1: Azido iodination of alkenes **2a–f** under flow conditions with polymer-bound bisazido iodate(I) complex **5**.

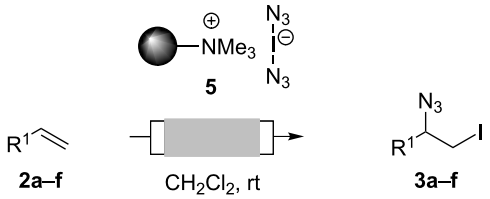

entry	substrate	flow rate [mL/min]	equiv **5**[a]	product (racemic)	yield flow[b]	*t*, (yield) batch[b]
1	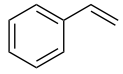 **2a**	0.05	5	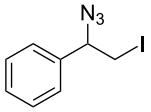 **3a**	98%	15 h (97%)
2	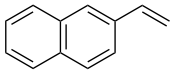 **2b**	0.04	5	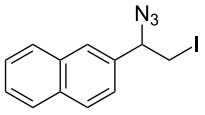 **3b**	91%	20 h (95%)
3	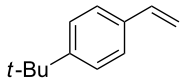 **2c**	0.03	5	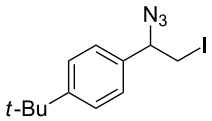 **3c**	61%	
4	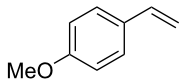 **2d**	0.02	5	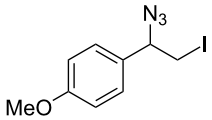 **3d**	75%	
5	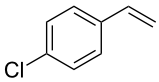 **2e**	0.02	6	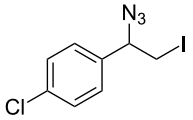 **3e**	78%[c]	
6	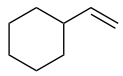 **2f**	0.02	7	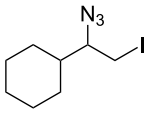 **3f**	70%[d]	

[a]Equiv of **5** refers to the theoretical loading based on polymer-bound ammonium groups of Amberlyst A-26; [b]Isolated yields of pure products after evaporation of the solvent and in some cases followed by chromatographic purification; [c]Contains about 12% starting material; [d]Contains 15% of bisazido product.

aliphatic alkenes without aryl substituents, prolonged reaction times were observed, which could be shortened by use of more equivalents of the functionalized polymer **5**. However, when a larger excess of reagent **5** was applied we observed the formation of the diazido byproducts, which are likely formed after a second nucleophilic-substitution step of the azide anion onto the intermediate iodo azide.

Next, we studied the elimination step that should yield the target vinyl azides. Hassner et al. [9] relied on potassium *tert*-butoxide as a base, which indeed worked well in diethyl ether as the solvent in our initial batch experiments (Table 2, entry 1). However, as the first flow step was performed in dichloromethane, we tested this solvent for the elimination in order to achieve a telescope process. Unfortunately, we encountered decomposition of the starting material (Table 2, entry 2) so that, again, an optimized protocol had to be found.

The best results in dichloromethane were achieved when 1,8-diazabicyclo[5.4.0]undec-7-ene (DBU, **8**) was employed as a

Table 2: Optimization of the elimination protocol and formation of vinyl azide **4a** under batch conditions (entries 1–7) and as a flow protocol (entry 8).

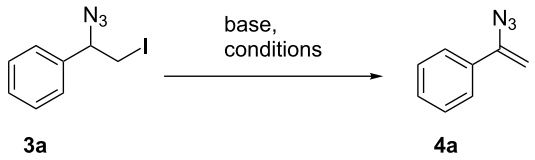

3a **4a**

entry	base	solvent	*T* [°C]	*t* [h]	yield[a]
1	1.5 equiv KO*t*-Bu	Et_2O	rt	2	95%
2	1.5 equiv KO*t*-Bu	CH_2Cl_2	rt	2	decomposition
3	5 equiv K_2CO_3	CH_2Cl_2	rt	18	5%
4[b]	5 equiv K_2CO_3	CH_2Cl_2	60	18	23%
5	2.5 equiv DIPEA[c]	DMF	60	2	92%
6	2 equiv DBU	CH_2Cl_2	rt	1.5	92%
7	2 equiv PS–DBU[d]	CH_2Cl_2	rt	1.5	93%
8[e]	2 equiv PS–DBU	CH_2Cl_2	rt	0.04 mL/min	complete transformation

[a]Isolated yields; [b]Reaction was carried out in a microwave-compatible tube heated in an oil bath, [c]DIPEA = diisopropylethyl amine; [d]PS–DBU = polystyrene-bound 1,8-diaza-[5.4.0]bicyclo-7-undecene (**8**); [e]Flow process: Glass reactor (12 cm length and 8.5 mm internal diameter) filled with polymer **8** (0.5 g; theoretical loading = 1.15 mmol/g).

base (Table 2, entry 6). The polymer-bound variant of DBU (PS–DBU) also gave excellent results (Table 2, entry 7) such that these conditions could directly be used for the flow process (Table 2, entry 8).

Finally, both flow reactors were telescoped, which allowed us to prepare vinyl azides **4a–e** and **4g–i** in one flow process starting from alkenes **2a–e** and **2g–i** (Scheme 3). Advantageously, isolation and purification of intermediate iodo azides **3**

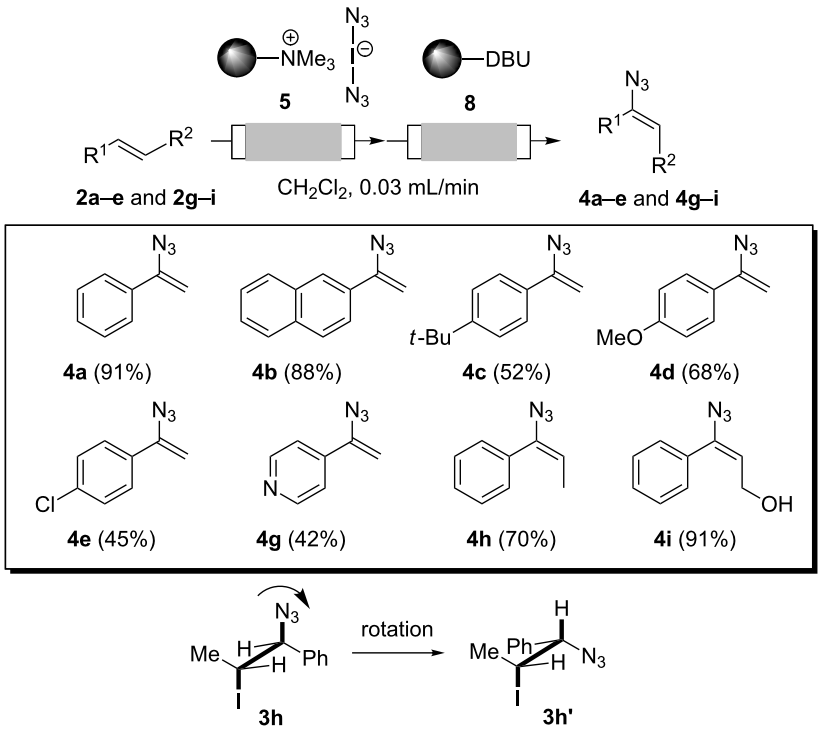

Scheme 3: Two-step protocol for the preparation of vinyl azides **4a–e** and **4g–i** under flow conditions.

was avoided. As a consequence we achieved improved yields compared to those obtained for individual steps. When starting from (*E*)-configured alkenes **2h** and **2i**, configurationally pure vinyl azides **4h** and **4i** with *syn*-orientation for both alkyl substituents were formed, as judged by nuclear Overhauser effect (NOE) experiments (Supporting Information File 1). The stereochemical outcome of this addition–elimination process may be rationalized by assuming an *anti*-addition of iodine azide onto the π-bond. After rotation along the C–C σ-bond (**3h** to **3h'**) *anti*-orientation of the proton and iodine allows for facile base-mediated elimination. This results in trisubstituted alkenes **4h** and **4i** owing to the observed stereochemistry.

Both of the functionalized polymers **5** and **8** are ideally suited for regeneration of the active species by employing simple flushing protocols without having to change the principal setup. Thus, azide-loaded ion-exchange resin **9**, which is supposed to be the main species after azido iodination, was regenerated by first ion exchange to the iodide form **2**. Next, oxidation to the bisacetoxy iodate(I)-complex **7** was achieved by treatment with diacetoxyiodo benzene. Finally, pumping of a solution of trimethylsilyl azide ($TMSN_3$) in dichloromethane afforded the functionalized polymer **5**, which could be used for 1,2-functionalization of alkenes with the same efficiency as described in Table 1. In addition the protonated form of PS–DBU **10** was regenerated to PS–DBU **8** by rinsing the reactor with a 1 M solution of DBU (Scheme 4).

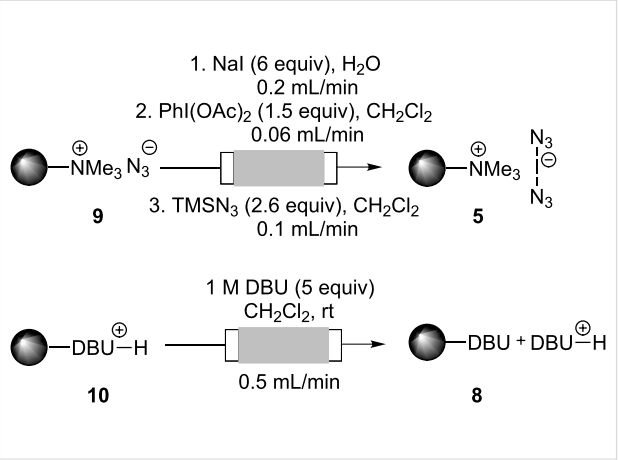

Scheme 4: Regeneration of functionalized polymers **5** and **8**.

Copper-catalyzed Huisgen-type cycloadditions

The copper-catalyzed Huisgen-type cycloaddition (CuAAC) is a general and useful method for the synthesis of 1,4-disubstituted-1,2,3-triazoles and is based on the 1,3-dipolar cycloaddition of alkynes and azides [28]. Besides Cu(I) sources also Cu(0) sources, such as copper wire [29] or copper-on-charcoal (Cu/C) [30], can serve as a catalytic source that promotes the CuAAC. Bogdan et al. combined this observation with flow technology by using a custom-made heated copper flow reactor [31]. We successfully implemented the CuAAC by inductively heating copper wire inside a flow microreactor [32]. A key benefit of this technology is that the copper metal is directly and instantaneously heated inside the reactor, which results in a higher reactivity than with conventionally heated elemental copper [32]. These results prompted us to investigate the reaction of vinyl azides **4** in the copper-catalyzed Huisgen-type cycloaddition. Importantly, this cycloaddition has not been reported for vinyl azides so far.

Therefore, a series of experiments had to be conducted in order to find the best conditions for achieving triazole formation. The temperature was measured on the reactor surface by means of an IR pyrometer. We chose 2-(1-azidovinyl)naphthalene (**4b**) and phenylacetylene (**11a**) as reaction partners for optimization. First, we had to find the best copper source (Table 3). We found that Cu-turnings gave complete conversion and a good isolated yield (Table 3, entry 2) for which the larger surface area can be held responsible. Flow rates of 0.05 mL/min or higher led to very low or zero conversion. Increasing the temperature led to decomposition of the reactants (Table 3, entries 4 and 5) as noted above. Employing DMF as the solvent gave the best results (Table 3, entries 6 and 7). Addition of a base or $CuSO_4$ in order to create more of the active copper species did not turn out to be beneficial for this transformation (Table 3, entries 8 and 9).

However, with the optimized flow protocol in hand, alkyl and aryl substituted triazoles **12 a**–**l** were prepared (Scheme 5)

It can be envisaged that this three step sequence can be alternatively arranged in a different order. Thus, after the azido iodination, first the cycloaddition is conducted, followed by the elimination step. In fact, we tested this route but experienced substantial difficulties. First, we were unable to achieve the cycloaddition in dichloromethane, and second, this transformation only proceeded in poor yields.

Conclusion

In summary, we developed the first telescope protocol for preparing vinyl azides starting from the corresponding alkenes, which was conducted in the flow mode. This two-step protocol was achieved by employing two functionalized polymers that served as a packed-bed material inside the reactor. Additionally, we showed that copper-catalyzed vinyl triazole formation of these vinyl azides in the presence of alkynes is possible by using elemental copper as an inductively heatable material. The method avoids the use of explosive and hazardous iodine azide.

Table 3: Optimization of the reaction of vinyl azide **4b** in the inductively heated (IH) copper-catalyzed Huisgen-type cycloaddition.

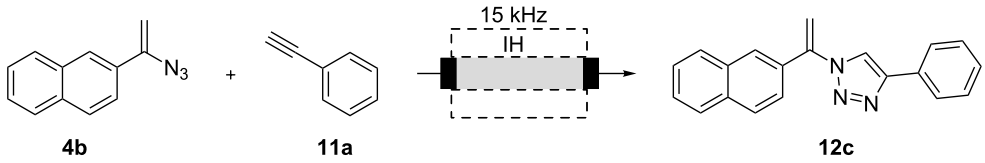

4b **11a** **12c**

entry	catalyst	solvent	flow rate [mL/min]	*T* [°C]	yield [%]
1	Cu-wire	DMF	0.04	70	32
2	**Cu-turnings**	**DMF**	**0.04**	**80**	**72**
3	Cu-turnings	DMF	0.07	80	44
4	Cu-turnings	DMF	0.04	100	23
5	Cu-turnings	DMF	0.04	110	10
6	Cu-turnings	acetone	0.04	80	59
7	Cu-turnings	dioxane	0.04	80	55
8	Cu-turnings/0.2 equiv $CuSO_4$	DMF/H_2O 1:1	0.04	80	58
9	Cu-turnings/1 equiv DIPEA	DMF	0.04	80	68

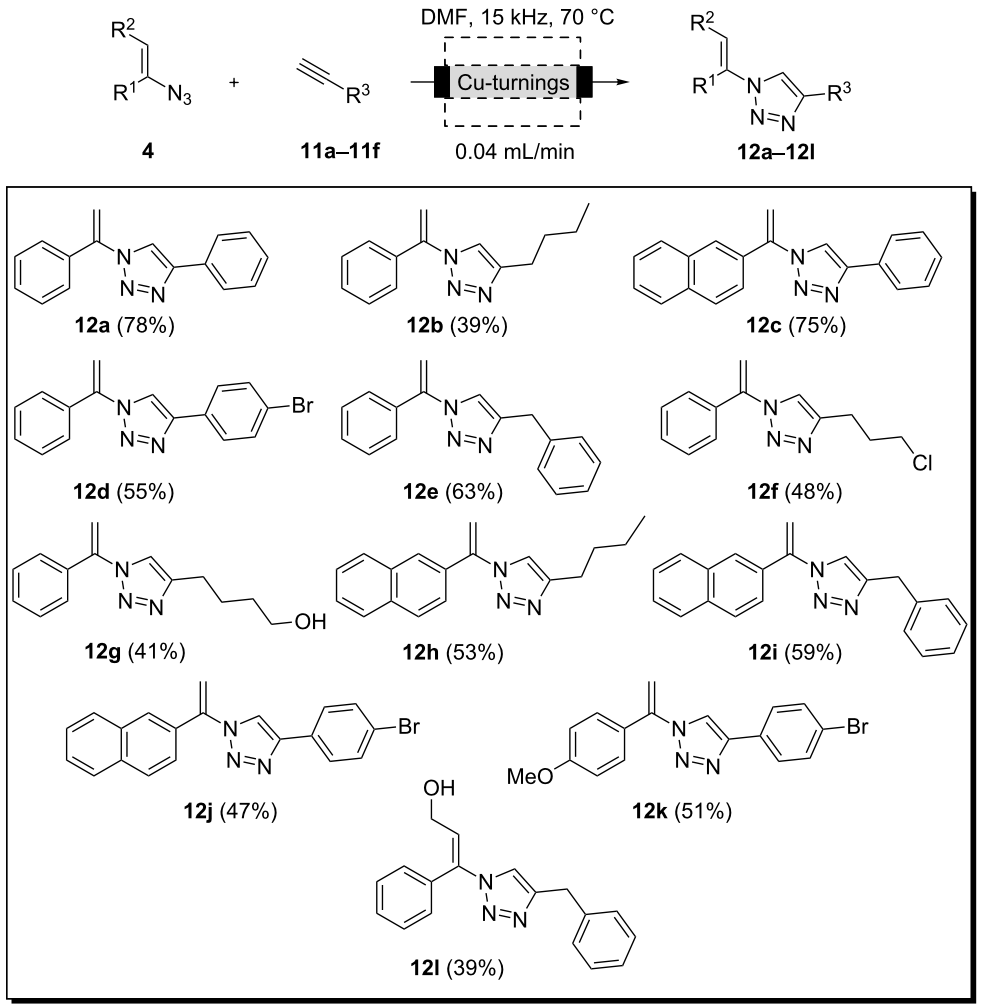

Scheme 5: Preparation of triazoles **12a–l** by using inductively heated copper turnings as a packed-bed material inside flow reactors.

Experimental

General procedure for azido iodination of alkenes **2** under flow conditions

A glass reactor (12 cm length and 8.5 mm internal diameter) was filled with polymer-bound iodate(I) complex **5** (5 g; theoretical loading = 3.5 mmol/g) and protected from light with aluminum foil. The reactor (void volume: 4.5 mL) was connected to the pump and, at the outlet side, to a collection flask. The system was first flushed with dry CH_2Cl_2 (8 mL, 0.5 mL/min). Then, a solution of styrene (**2a**) (364 mg, 3.5 mmol) in dry CH_2Cl_2 (17.5 mL) was pumped through the reactor at a flow rate of 0.04 mL/min. Then, 10 mL of CH_2Cl_2 was used to wash the reactor (5 mL, 0.04 mL/min + 5 mL, 0.5 mL/min). Product **3a** (936 mg, 3.4 mmol, 98%) was directly obtained after evaporation of the combined organic phases.

General procedure for the two-step preparation of vinyl azides **4** under flow conditions

A glass reactor (12 cm length and 8.5 mm internal diameter) filled with polymer-bound iodate(I) complex **5** (5 g; theoretical loading = 3.5 mmol/g) and a second identical flow reactor, which was filled with a slurry of polystyrene-bound 1,8-diaza-[5.4.0]bicyclo-7-undecene (**8**) (4 g; theoretical loading = 1.15 mmol/g) in dry CH_2Cl_2 (5 mL), were telescoped and protected from light with aluminum foil. The system was connected to the pump and, at the outlet side, to a collection flask. After priming with CH_2Cl_2 (10 ml), a solution of styrene (**2a**) (364 mg, 3.5 mmol) in dry CH_2Cl_2 (17.5 mL) was flushed at 0.04 mL/min. Then, 10 mL more of CH_2Cl_2 was pumped through the reactor (5 mL, 0.04 mL/min + 5 mL, 0.5 mL/min). The crude product **4a** (462 mg, 3.2 mmol, 91%) was isolated after evaporation of the solvent. If necessary (see Supporting Information File 1), the crude product was purified by column chromatography (petroleum ether/ethyl acetate).

Regeneration of functionalized polymer-bound iodate(I) complex **5** under flow conditions

The reactor with azide-loaded ion-exchange resin **9** (5 g; theoretical loading = 3.5 mmol/g) was connected to the pump and, at the outlet side, to a collection flask. The system was first flushed with water (10 mL, 0.5 mL/min). A solution of NaI (15.7 g, 105 mmol) in water (20 mL) was pumped through the reactor at flow rate of 0.15 mL/min. Then the reactor was successfully washed with 10mL each of water, acetone and finally with CH_2Cl_2 at a flow rate of 0.5 mL/min.

In the second step the system was flushed with a solution of $PhI(OAc)_2$ (8.5 g, 26.3 mmol) in 60 mL of dry CH_2Cl_2 at a flow rate of 0.06 mL/min. Then, the reactor was washed with 20 mL of CH_2Cl_2 at a flow rate of 0.5 mL/min.

In the third step, a solution of $TMSN_3$ (6.0 mL, 45.5 mmol) in 20 mL of dry CH_2Cl_2 was pumped through the reactor at a flow rate of 0.10 mL/min. Finally, the reactor was washed with 20 mL of CH_2Cl_2 at a flow rate of 0.5 mL/min.

General procedure for the copper-catalyzed Huisgen-type cycloaddition under flow conditions

A glass reactor (12 cm length and 8.5 mm internal diameter) packed with copper turnings (12 g) was encased within the inductor. The reactor was connected to the pump and, at the outlet side, to a collection flask. The system was flushed with DMF (flow rate 0.04 mL/min), and the temperature was adjusted to 70 °C regulating the PMW (pulse-width modulation). A sample loop was filled with a solution of vinyl azides **4** (0.3 mmol, 1 equiv) and alkynes **11** (0.45 mmol, 1.5 equiv) in DMF (0.5 mL). After the flow and temperature values reached a steady state, the solution was pumped through the system. Washing was continued until no product was detected at the outlet as judged by TLC. The resulting solution was diluted with 50 mL of ethyl acetate and washed with water and brine (3 × 60 mL). The organic layers were dried over anhydrous $MgSO_4$ and evaporated under vacuum. The crude product was then purified by flash chromatography (petroleum ether/ethyl acetate) to yield the pure products **12**.

Supporting Information

The Supporting Information provides details on individual reactions and analytical data.

Supporting Information File 1

Details on individual reactions and analytical data.
[http://www.beilstein-journals.org/bjoc/content/supplementary/1860-5397-7-168-S1.pdf]

Acknowledgements

This work was supported by the Fonds der Chemischen Industrie. We thank Henkel AG & Co. KGaA (Düsseldorf, Germany), Evonik Degussa GmbH (Essen, Germany) and IFF GmbH (München, Germany) for financial or technical support. We thank Fabien Coudray and Victor Olmos for experimental support.

References

1. L'Abbé, G. *Angew. Chem.* **1975,** *87,* 831–838. doi:10.1002/ange.19750872304
Angew. Chem., Int. Ed. Engl. **1975,** *14*, 775–782. doi:10.1002/anie.197507751
2. Zou, H.; Zhu, H.; Shao, J.; Wu, J.; Chen, W.; Giulianotti, M. A.; Yu, Y. *Tetrahedron* **2011,** *67,* 4887–4891. doi:10.1016/j.tet.2011.04.103

3. Wang, Y.-F.; Toh, K. K.; Ng, E. P. J.; Chiba, S. *J. Am. Chem. Soc.* **2011,** *133,* 6411–6421. doi:10.1021/ja200879w
4. Ng, E. P. J.; Wang, Y.-F.; Chiba, S. *Synlett* **2011,** 783–786. doi:10.1055/s-0030-1259920
5. Sjöholm Timén, Å.; Risberg, E.; Somfai, P. *Tetrahedron Lett.* **2003,** *44,* 5339–5341. doi:10.1016/S0040-4039(03)01205-X
6. Palacios, F.; Ocjoa de Retana, A. M.; Martínez de Marigorta, E.; de los Santos, J. M. *Eur. J. Org. Chem.* **2001,** 2401–2414. doi:10.1002/1099-0690(200107)2001:13<2401::AID-EJOC2401>3.0.CO;2-U
7. Brahma, S.; Ray, J. K. *J. Heterocycl. Chem.* **2008,** *45,* 311–317. doi:10.1002/jhet.5570450203
8. Gilchrist, T. L. *Aldrichimica Acta* **2001,** *34,* 51–55.
9. Hassner, A.; Fowler, F. W. *J. Org. Chem.* **1968,** *33,* 2686–2691. doi:10.1021/jo01271a016
10. Brandt, J. C.; Wirth, T. *Beilstein J. Org. Chem.* **2009,** *5,* No. 30. doi:10.3762/bjoc.5.30
11. Smith, C. J.; Smith, C. D.; Nikbin, N.; Ley, S. V.; Baxendale, I. R. *Org. Biomol. Chem.* **2011,** *9,* 1927–1937. doi:10.1039/c0ob00813c
12. Smith, C. J.; Nikbin, N.; Ley, S. V.; Lange, H.; Baxendale, I. R. *Org. Biomol. Chem.* **2011,** *9,* 1938–1947. doi:10.1039/c0ob00815j
13. Delville, M. M. E.; Nieuwland, P. J.; Janssen, P.; Koch, K.; van Hest, J. C. M.; Rutjes, F. P. J. T. *Chem. Eng. J.* **2011,** *167,* 556–559. doi:10.1016/j.cej.2010.08.087
14. Kirschning, A.; Solodenko, W.; Mennecke, K. *Chem.–Eur. J.* **2006,** *12,* 5972–5990. doi:10.1002/chem.200600236
15. Wegner, J.; Ceylan, S.; Kirschning, A. *Chem. Commun.* **2011,** *47,* 4583–4592. doi:10.1039/c0cc05060a
16. McMullen, J. P.; Jensen, K. F. *Annu. Rev. Anal. Chem.* **2010,** *3,* 19–42. doi:10.1146/annurev.anchem.111808.073718
17. Tanaka, T.; Fukase, K. *Org. Process Res. Dev.* **2009,** *13,* 983–990. doi:10.1021/op900084f
18. Roberge, D. M.; Zimmermann, B.; Rainone, F.; Gottsponer, M.; Eyholzer, M.; Kockmann, N. *Org. Process Res. Dev.* **2008,** *12,* 905–910. doi:10.1021/op8001273
19. Hessel, V. *Chem. Eng. Technol.* **2009,** *32,* 1655–1681. doi:10.1002/ceat.200900474
20. Hartman, R. L.; Jensen, K. F. *Lab Chip* **2009,** *9,* 2495–2507. doi:10.1039/b906343a
21. Mak, X. Y.; Laurino, P.; Seeberger, P. H. *Beilstein J. Org. Chem.* **2009,** *5,* No. 19. doi:10.3762/bjoc.5.19
22. Wiles, C.; Watts, P. *Eur. J. Org. Chem.* **2008,** 1655–1671. doi:10.1002/ejoc.200701041
23. Fukuyama, T.; Rahman, M. T.; Sato, M.; Ryu, I. *Synlett* **2008,** 151–163. doi:10.1055/s-2007-1000884
24. Mason, B. P.; Price, K. E.; Steinbacher, J. L.; Bogdan, A. R.; McQuade, D. T. *Chem. Rev.* **2007,** *107,* 2300–2318. doi:10.1021/cr050944c
25. Kirschning, A.; Hashem, M. A.; Monenschein, H.; Rose, L.; Schöning, K.-U. *J. Org. Chem.* **1999,** *64,* 6522–6526. doi:10.1021/jo990478p
26. Kirschning, A.; Monenschein, H.; Schmeck, C. *Angew. Chem.* **1999,** *111,* 2720–2722. doi:10.1002/(SICI)1521-3757(19990903)111:17<2720::AID-ANGE2720>3.0.CO;2-W
Angew. Chem. Int. Ed. **1999**, *38*, 2594–2596. doi:10.1002/(SICI)1521-3773(19990903)38:17<2594::AID-ANIE2594>3.0.CO;2-U
27. In fact, for several years, the polymer-bound version of **5** was commercially available from Novabiochem GmbH, Bad Soden, Germany.
28. Meldal, M.; Tornøe, C. W. *Chem. Rev.* **2008,** *108,* 2952–3015. doi:10.1021/cr0783479
29. Rostovtsev, V. V.; Green, L. G.; Fokin, V. V.; Sharpless, K. B. *Angew. Chem.* **2002,** *114,* 2708–2711. doi:10.1002/1521-3757(20020715)114:14<2708::AID-ANGE2708>3.0.CO;2-0
Angew. Chem., Int. Ed. **2002**, 41, 2596–2599. doi:10.1002/1521-3773(20020715)41:14<2596::AID-ANIE2596>3.0.CO;2-4
30. Lipshutz, B. H.; Taft, B. R. *Angew. Chem.* **2006,** *118,* 8415–8418. doi:10.1002/ange.200603726
Angew. Chem., Int. Ed. **2006**, *45*, 8235–8238. doi:10.1002/anie.200603726
31. Bogdan, A. R.; Sach, N. W. *Adv. Synth. Catal.* **2009,** *351,* 849–854. doi:10.1002/adsc.200800758
32. Ceylan, S.; Klande, T.; Vogt, C.; Friese, C.; Kirschning, A. *Synlett* **2010,** 2009–2013. doi:10.1055/s-0030-1258487

License and Terms

Beilstein Journal of Organic Chemistry

Coupled chemo(enzymatic) reactions in continuous flow

Ruslan Yuryev, Simon Strompen and Andreas Liese*

Review

Open Access

Address:
Institute of Technical Biocatalysis, Hamburg University of Technology, Denickestr. 15, 21073, Hamburg, Germany

Email:
Ruslan Yuryev - ruslan.yuryev@tuhh.de; Simon Strompen - simon.strompen@tuhh.de; Andreas Liese* - liese@tuhh.de

* Corresponding author

Keywords:
biocatalysis; chemo-enzymatic reaction sequences; continuous flow; coupled reactions; reaction cascades

Beilstein J. Org. Chem. **2011,** *7,* 1449–1467.
doi:10.3762/bjoc.7.169

Received: 28 June 2011
Accepted: 22 September 2011
Published: 24 October 2011

This article is part of the Thematic Series "Chemistry in flow systems II".

Guest Editor: A. Kirschning

Abstract

This review highlights the state of the art in the field of coupled chemo(enzymatic) reactions in continuous flow. Three different approaches to such reaction systems are presented herein and discussed in view of their advantages and disadvantages as well as trends for their future development.

Introduction

For a long time, the living cell has been considered to be a perfect chemical factory, whose organizational principles can inspire every organic chemist and chemical engineer. The effectiveness, with which nutrients are converted into complex chemical building blocks required for the cell metabolism, is still a distant goal for any man-made chemical factory. Metabolic pathways, consisting of enzymatic sequential and coupled reactions (Figure 1), lie at the core of any living system and have been optimized by evolution over billions of years to create the phenomenon of life as we know it.

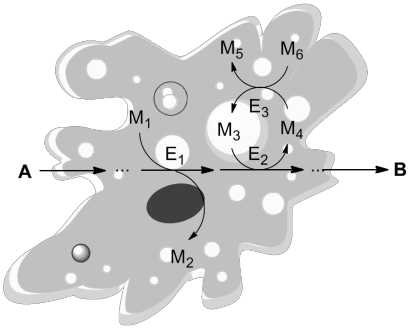

Figure 1: Metabolic pathways in a living cell as an example of efficient coupled-reaction processes. A: Substrate; B: Product; $E_{1–3}$: Enzymes; $M_{1–6}$: Metabolites.

In the field of applied biocatalysis, chemists are constantly trying to recognize the principles responsible for the efficiency of cell metabolism and to exploit them in organic synthesis

[1-3]. There are three biological principles whose implementation may be regarded as important milestones in this field and which can be used for the classification of existing biotransformations. One of these principles is that a single reaction step of a given metabolic pathway proceeds in a very specific manner due to the intrinsically high chemo-, regio- and stereoselectivity of the enzyme catalyzing this step. This principle is the soul of applied biocatalysis and has already been widely exploited in the chemical industry for decades in the production of chemicals by enzymatic processes [4-6]. Biotransformations solely based on this principle, i.e., "single-reaction–single-enzyme" systems, may be classified as first-generation enzymatic processes (Figure 2, I), which historically were the first to be applied in the chemical industry and till now remain the most abundant among industrial biotransformations.

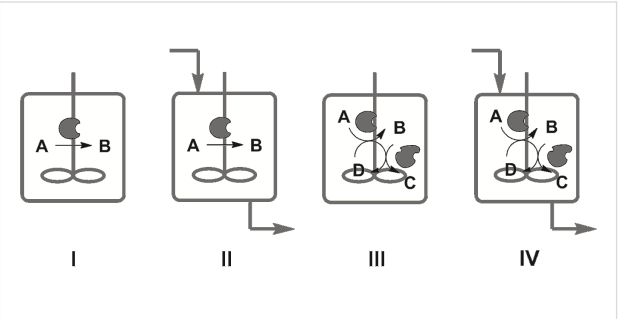

Figure 2: Four generations of biotransformations. I: Single-reaction processes; II: Single-reaction processes in continuous flow; III: Coupled-reaction processes; IV: Coupled-reaction processes in continuous flow.

The second biological principle states that cell metabolism is a continuous process. Every metabolically active living cell is an open system that requires a constant flux of nutrients in order to stay alive. The numerous continuous chemocatalytic processes implemented on laboratory and on industrial scales prove that this principle can be effectively transferred to technical systems as well [7-11]. Biotransformations, which combine both of the biological principles mentioned, may be regarded as "single-reaction–single-enzyme continuous-flow" systems and classified as second-generation enzymatic processes (Figure 2, II). Such biotransformations naturally evolve from the corresponding first-generation "single-reaction" batch processes and are often economically more attractive than their ancestors due to the higher productivity that they afford. Therefore, it is not surprising that the second-generation biotransformations have received much attention in recent years [12].

The third biological principle says that cell metabolism is a complex network of reactions coupled through common substrates and products: Multistep syntheses of metabolites are conducted in sequential reactions catalyzed by spatially aligned enzymatic complexes, while coupled parallel reactions are used to regenerate costly cofactors or to enable thermodynamically unfavorable steps. The practical realization of this principle is a dream for every organic chemist who wishes to perform a multistep organic synthesis of a desired compound in one pot, without isolation of the intermediates. And this dream has recently become reality: In the last few decades the concept of reaction cascades has become increasingly popular and has been proven to be a viable synthetic route to many classes of organic compounds [13-15]. Biotransformations consisting of coupled sequential and/or parallel reactions catalyzed by one or several enzymes may be regarded as third-generation enzymatic processes (Figure 2, III). The interest in such systems is prompted by their obvious economical potential: In situ regeneration of expensive cofactors and reduction of downstream processing steps decreases production costs and generation of waste [16,17]. Therefore such processes are generally expected to have a higher "green index" [18] and E-factor (kilograms of total waste produced per kilogram of product) [19]. One may also consider so-called chemo-enzymatic reaction sequences, that is multistep-reaction systems in which chemical and biocatalytic reaction steps are coupled, as third-generation biotransformations. These hybrid systems, in which the strengths of both chemical and biological approaches are combined, have proven to be powerful tools for organic synthesis and thus have nowadays become a hot topic in applied biocatalysis [20]. From a formal point of view, reactions such as the lipase-catalyzed hydrolysis of triglycerides to glycerol and fatty acids, or amylase-catalyzed hydrolysis of amylose to glucose should also be classified as multistep-reaction processes, because they proceed stepwise via a sequence of intermediates. However, such transformations differ from the third-generation multistep-reaction enzymatic processes in the sense that every reaction step is formally the same, i.e., it is catalyzed by the same enzyme under the same reaction conditions and the intermediates are of the same nature. Therefore, reaction cascades catalyzed by a single enzyme belong instead to the first-generation processes.

When following the logic of the chosen classification of enzymatic processes, the final or fourth-generation biotransformations would be defined as coupled chemo(enzymatic) reactions in continuous-flow systems based on all three of biological principles mentioned (Figure 2, IV). From a technical point of view, biotransformations of the last generation are the most sophisticated ones most closely resembling the metabolic activity of a living cell. At the same time, however, due to their complexity, these biotransformations are not as widespread as the enzymatic processes of earlier generations and their development is still in an early stage. Nevertheless, they can already be considered as a complementary technology to multistep

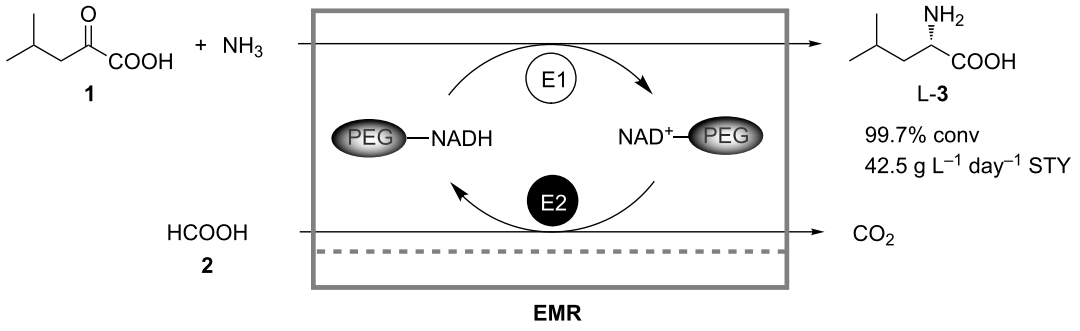

Scheme 1: Production of L-leucine (**3**) in a continuously operating enzyme membrane reactor (EMR). E1: L-Leucine dehydrogenase; E2: Formate dehydrogenase [22].

continuous-flow organic synthesis: A chemical technology that has recently emerged on the frontier of organic chemistry and chemical engineering [8,21]. In this work we present achievements and challenges of the fourth-generation biotransformations, and highlight existing trends in this field, which in the foreseeable future may lead to the next-generation enzymatic processes.

Review

1. Single-reactor processes in vitro

Certainly, the most elegant and technically the most attractive way to perform coupled (chemo)enzymatic reactions is to bring all reactants and catalysts in contact in one vessel filled with one reaction medium. In this case the requirements with respect to equipment are reduced to a minimum. The single-reactor or so-called "in-pot" [17] coupled-reaction processes in continuous flow were established as early as 1981, most probably for the first time by Wichmann and Wandrey for the continuous production of L-leucine (**3**) in an ultrafiltration membrane reactor using a coupled parallel enzymatic system [22]. Here, L-leucine dehydrogenase was used for the reductive amination of α-ketoisocaproate (**1**) to the amino acid **3**. The required cofactor NADH was regenerated in a coupled parallel reaction by oxidation of formate (**2**) catalyzed by formate dehydrogenase (Scheme 1). Retention of the cofactor was achieved by its covalent binding to polyethylene glycol (PEG) with a molecular weight of 10 kDa. The reactor was operated continuously for 48 days under sterile conditions. A maximal conversion of 99.7% and a space-time yield (STY) of 42.5 g L^{-1} day^{-1} were reached.

Hummel and coworkers similarly described the stereoselective conversion of benzoyl formate (**4**) to D-mandelic acid (**5**) by a D-(−)-mandelic acid dehydrogenase from *Lactobacillus curvatus* in a sterilized enzyme membrane reactor, which was operated continuously (Scheme 2) [23]. Again, formate dehy-

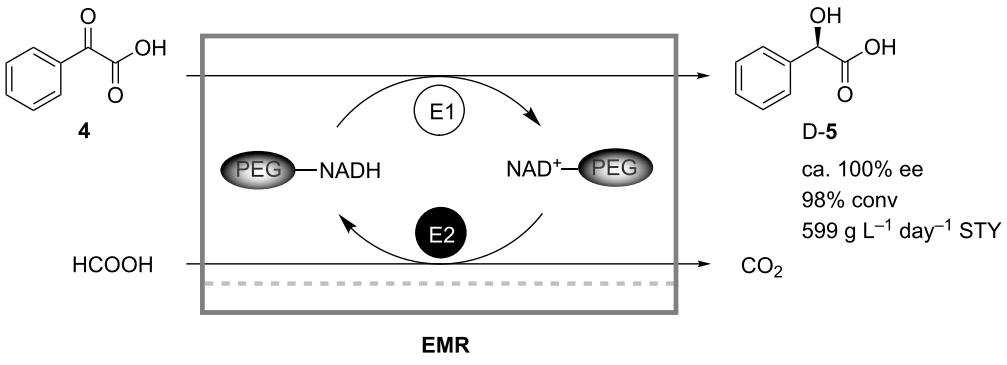

Scheme 2: Production of D-mandelic acid (**5**) in a continuously operating enzyme membrane reactor. E1: D-(−)-Mandelic acid dehydrogenase; E2: Formate dehydrogenase [23].

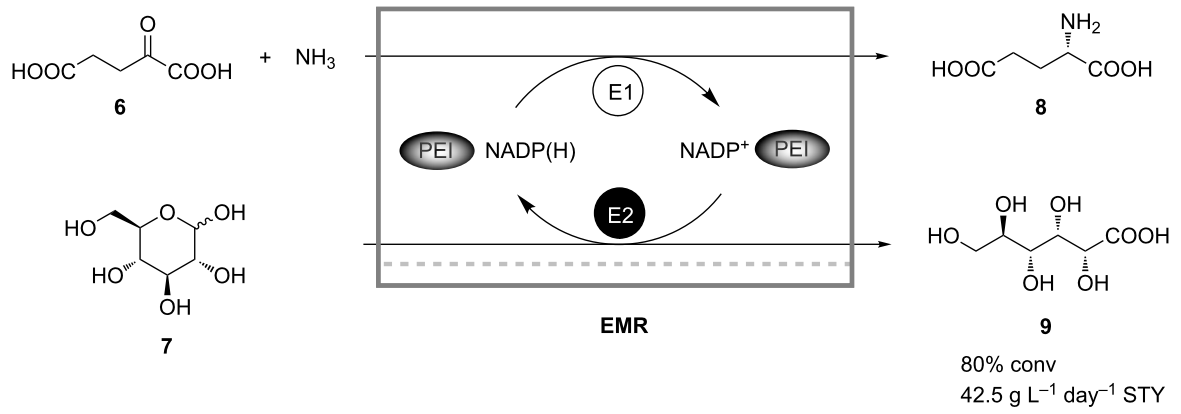

Scheme 3: Simultaneous synthesis of gluconic acid (**9**) and glutamic acid (**8**) in a continuously operated membrane reactor. E1: Glutamate dehydrogenase; E2: Glucose oxidase [24].

drogenase was used for cofactor regeneration, and immobilization of NADH on PEG prevented loss of the cofactor in the continuously operated reactor. Space-time yields of 700 g L^{-1} day^{-1} were achieved with the optimized reactor at 95% conversion. Deactivation of enzyme and PEG–NADH led to a decrease of conversion to 90%. However, by adjustment of the residence time a continuous operation for 20 days was demonstrated.

Covalent grafting of cofactors on soluble polymers for retention in continuously operating membrane reactors suffers from the disadvantage that enzymes often do not accept the cofactor derivatives. To overcome this problem Obón et al. proposed a new concept to retain native NADP(H) without chemical modification inside an enzyme membrane reactor by adding charged soluble polymers, such as polyethyleneimine (PEI), which bind the cofactor electrostatically [24]. The concept was successfully tested in the continuous simultaneous synthesis of gluconic acid (**9**) and glutamic acid (**8**) by coupling the $NADP^+$-dependent glucose (**7**) oxidation catalyzed by glucose oxidase with the reductive amination of α-ketoglutaric acid (**6**) catalyzed by glutamate dehydrogenase (Scheme 3). When the process was carried out in a continuously operated enzyme membrane reactor loaded with 1 mM PEI, 80% conversion and 7.8 g L^{-1} day^{-1} space-time yield with respect to **9** could be achieved at the retention time of 12 hours.

Seelbach and Kragl showed that the retention of NADH in a continuous synthesis can also be achieved without immobilization or addition of charged polymer, but by using nanofiltration membranes instead of ultrafiltration ones [25]. The reactor for the synthesis of L-*tert*-leucine (**11**) from trimethylpyruvate (**10**) catalyzed by leucine dehydrogenase (Scheme 4) was operated for 10 days with a total turnover number increased by a factor

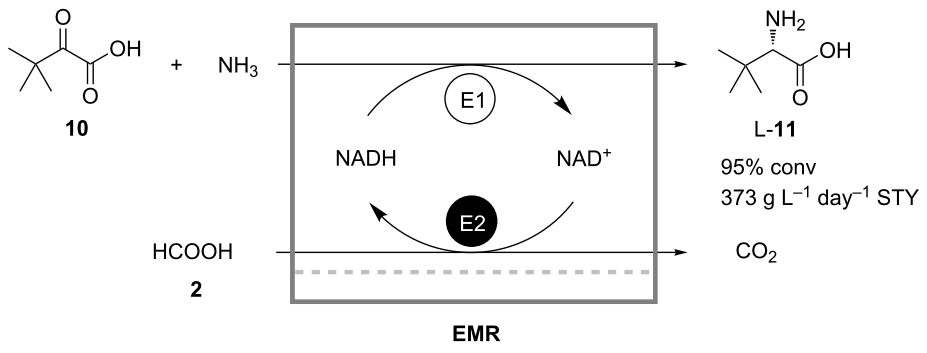

Scheme 4: Production of L-*tert*-leucine (**11**) in a continuously operated enzyme membrane reactor equipped with a nanofiltration membrane. E1: Leucine dehydrogenase; E2: Formate dehydrogenase [25].

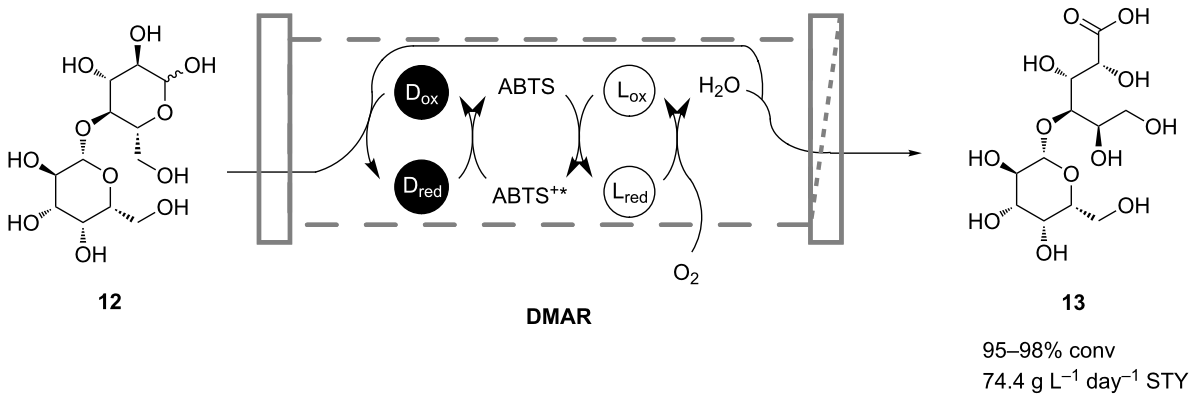

Scheme 5: Continuous oxidation of lactose (**12**) to lactobionic acid (**13**) in a dynamic membrane-aerated reactor (DMAR) catalyzed by cellobiose dehydrogenase (D) and laccase (L) [26].

of 3.4 compared to a reactor without cofactor retention. The regeneration of NADH was achieved in a coupled biocatalytic oxidation of formate (**2**).

Hecke and coworkers described the production of lactobionic acid (**13**) from lactose (**12**) in a coupled two-enzyme reaction both in discontinuous- and continuous-operation modes (Scheme 5) [26]. Cellobiose dehydrogenase was applied to catalyze the oxidation of **12**, while laccase was used as a regenerating enzyme coupled by the redox mediator 2,2-azino-bis(3-ethylbenzothiazoline-6-sulfonic acid) (ABTS). In continuous-flow experiments, the enzymes were retained by using an ultrafiltration membrane, whereas **12** and also ABTS were fed continuously. Reactions were carried out on a 20 L scale in a dynamic membrane-aeration reactor, which offered the advantage of bubble-free aeration and thus avoiding enzyme deactivation at a gas–liquid interface. The reactor was operated for 3 days and maintained ~80% of the initial enzyme activity. Only microbial contamination prevented a longer operation time of the process as it was carried out under nonsterile conditions. An overall space-time yield of 74.4 g L^{-1} day^{-1} was calculated with conversions in the range of 95–98%.

The continuous enzymatic synthesis of *N*-acetylneuraminic acid (**17**) from *N*-acetylglucosamine (GlcNAc, **14**) in an enzyme membrane reactor employing two enzymes was developed by Kragl and coworkers [27]. In their coupled-reaction system the first enzyme GlcNAc 2-epimerase catalyzed the epimerization of **14** yielding the epimer *N*-acetylmannosamine (**15**), which consequently was condensed by the second enzyme aldolase with pyruvic acid (**16**) to form the product **17** (Scheme 6). By appropriately adjusting the reaction parameters, such as pH, temperature and substrate concentrations, the authors minimized cross-inhibition effects, maintained high enzyme activities and shifted the chemical equilibrium towards the product side. A space-time yield of 109 g L^{-1} day^{-1} was obtained.

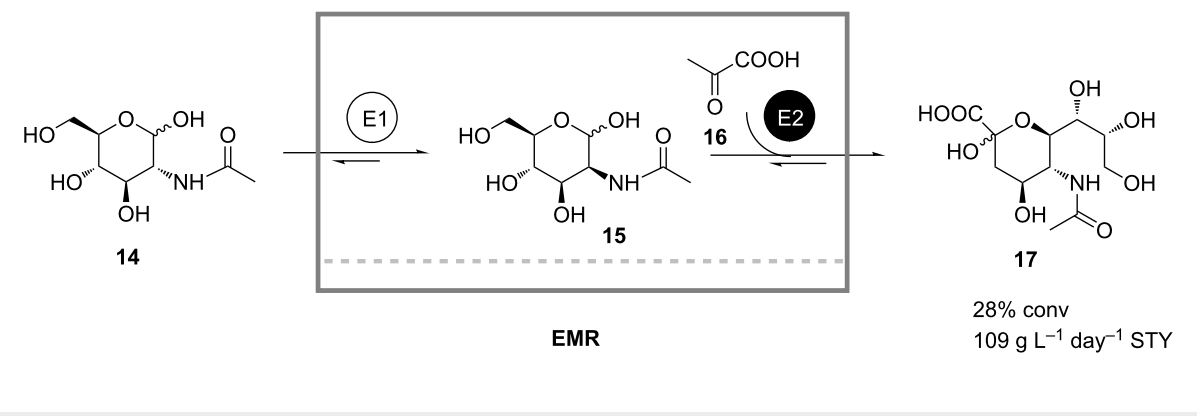

Scheme 6: Production of *N*-acetylneuraminic acid (**17**) in a continuously operated enzyme membrane reactor. E1: Epimerase; E2: Aldolase [27].

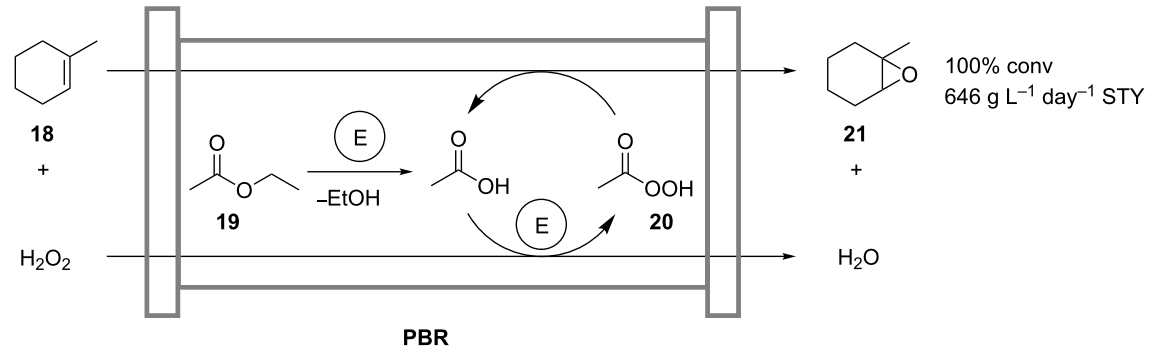

Scheme 7: Chemo-enzymatic epoxidation of 1-methylcyclohexene (**18**) in a packed-bed reactor (PBR) containing Novozym 435 (E) [28].

Wiles and coworkers transferred a coupled chemoenzymatic reaction for the oxidation of alkenes from batch operation to an efficient continuous-flow process (Scheme 7) [28]. The process involves the lipase-catalyzed in situ formation of peracetic acid (**20**) from hydrogen peroxide and ethyl acetate (**19**), which oxidizes the model substrate 1-methylcyclohexene (**18**) to form the product 1-methylcyclohexene oxide (**21**). The coupled reaction is carried out in a continuously operated packed-bed microreactor. As compared to the batch-mode experiments, higher concentrations of H_2O_2 were applied without detectable catalyst deactivation after 24 hours. At 100% conversion, a space-time yield of 646 g L^{-1} day^{-1} was obtained.

Lozano and coworkers reported on a continuous, chemoenzymatic dynamic kinetic resolution (DKR) process for the production of (*R*)-1-phenylethyl propionate (**24**) from (*rac*)-1-phenylethanol (**22**) and vinyl propionate (**23**) (Scheme 8) [29-31]. In a multiphase packed-bed reactor, commercially available immobilized *Candida antarctica* lipase B (Novozym 435) was used as a heterogeneous catalyst in the kinetic resolution of the alcohol **22** [30]. Racemization of the unreacted (*S*)-**22** was achieved with acidic zeolite catalysts. Both heterogenous catalysts were coated with ionic liquids for improved stability of the lipase in the presence of the acidic chemocatalysts and for reduction of zeolite-catalyzed side reactions [30,31]. The substrates and supercritical CO_2 were fed continuously, thus omitting the use of organic solvents for product extraction. An enantiomeric excess of 97% was achieved for the product (*R*)-**24** at 98% conversion and a space-time yield of 50 g L^{-1} day^{-1}. Operational stability was maintained over a period of 14 days. Previously applied *Candida antarctica* lipase B immobilized on modified C4-silica proved to be unstable upon combination with acidic chemocatalysts. Separation of the acidic chemocatalyst from the lipase by spatial separation in a single column [29] or in consecutive packed-bed reactors [31], however, similarly allowed the process to be efficiently run with high enantiomeric excesses of up to 99%, but with a reduced yield of 60%.

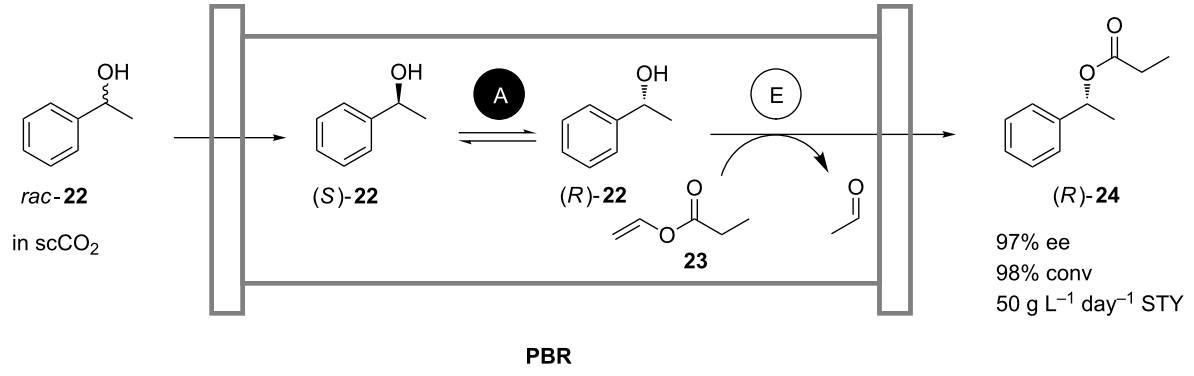

Scheme 8: Continuous production of (*R*)-1-phenylethyl propionate (**24**) by dynamic kinetic resolution of (*rac*)-1-phenylethanol (**22**) in supercritical CO_2 in a packed-bed reactor loaded with acidic zeolite (A) and Novozym 435 (E) [30].

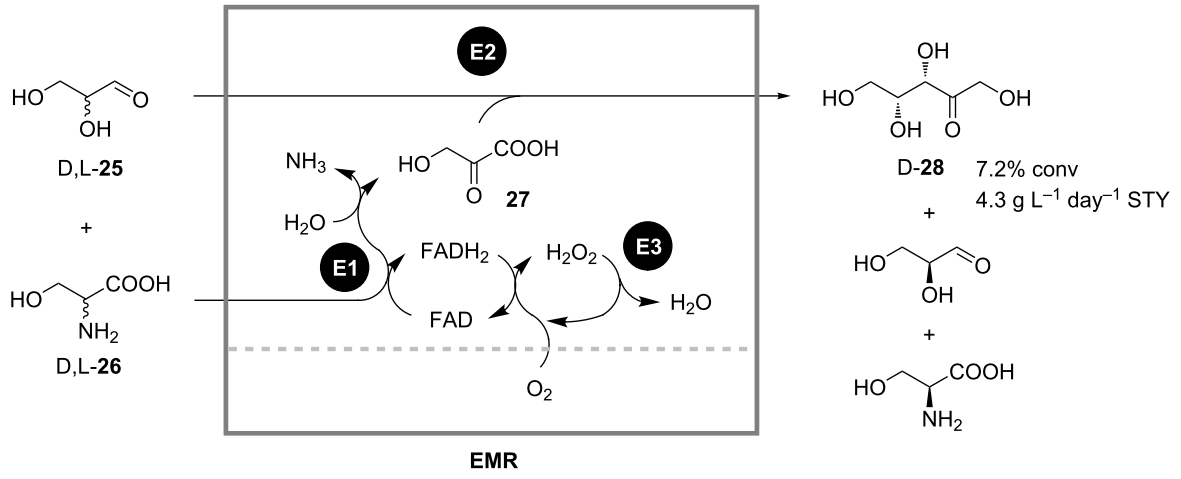

Scheme 9: Synthesis of D-xylulose (**28**) from D,L-serine (**26**) and D,L-glyceraldehyde (**25**) in a continuously operated enzyme membrane reactor. E1: D-Amino acid oxidase; E2: Transketolase; E3: Catalase [32].

A reaction sequence for the continuous synthesis of D-xylulose (**28**) from D,L-serine (**26**) and D,L-glyceraldehyde (**25**) involving three enzymes in a single continuously stirred tank reactor (CSTR) was presented by Bongs (Scheme 9) [32]. Here, a D-amino acid oxidase was used to form hydroxypyruvic acid (**27**) from D-**26**, which was subsequently converted to D-**28** by a transketolase-catalyzed reaction with added D,L-**25**. Catalase was used to regenerate the reduced cofactor FADH by oxidation with oxygen. In order to decrease enzyme deactivation caused by shear forces, a bubble-free aeration through a silicon membrane was implemented. A space-time yield of 4.3 g L^{-1} day^{-1} was achieved. However, further optimization of the process was not feasible due to the complexity of the system caused by possible cross-inhibition, deactivation, and reactant instabilities.

All of the single-reactor continuous (chemo)enzymatic processes mentioned, except for the one described by Bongs (Scheme 9), employed a maximum of two different catalysts. To the best of our knowledge, until now there is no established continuous (chemo)enzymatic process catalyzed by four or more isolated catalysts combined in one pot. Therefore, it seems that a simple single-reactor or "in-pot" approach would hardly cope with more complex multicatalyst systems. Even in the three-enzyme process Bongs already encountered problems preventing further optimization of the process. There are three reasons for this: (a) Different enzymes usually work best under different, sometimes even incompatible, reaction conditions, e.g., pH, temperature, ionic strength, or the presence of metal ions; (b) intermediates or mediators of certain steps can inhibit enzymes catalyzing other steps (cross-inhibition); (c) certain enzymes may act on the reactants involved in other steps, and thus catalyze undesirable side reactions. Nevertheless, it may be assumed that in the future continuous multistep (chemo)enzymatic processes involving more than three catalysts will be realized in a single reactor as well. For instance, Liu et al. developed a packed-bed reactor containing seven enzymes co-immobilized through hexahistidine tags on nickel–agarose beads ("super beads") [33]. These enzymes catalyze a complex network of sequential and coupled reactions, in which galactose, uridine monophosphate (UMP) and inorganic polyphosphate are converted to uridine diphospate galactose (UDP-Gal) in the presence of catalytic amounts of ATP and glucose 1-phosphate. When the reaction mixture containing starting materials and cofactors was circulated for 48 hours through the reactor, 50% of UMP was transformed to UDP-Gal. Although in their work the authors did not establish the continuous production of UDP-Gal, in principle such a reactor could be operated in continuous mode as well, if the immobilized enzymes were more active and stable enough.

2. Cascade-reactor processes in vitro

The drawbacks of single-reactor coupled-reaction enzymatic processes arising from incompatibility of individual reaction steps may be overcome in cascade-reactor systems in which the conflicting steps are spatially separated. This idea was recognized and realized already in 1982 by Jandel et al. in their continuous production of L-alanine (**31**) through two consecutive biotransformations conducted in a two-stage EMR cascade [34]. In the first reactor L-aspartic acid (**30**) is formed from fumaric acid (**29**) and ammonia through the action of a soluble aspartase isolated from *E. coli* (Scheme 10). Subsequently, in

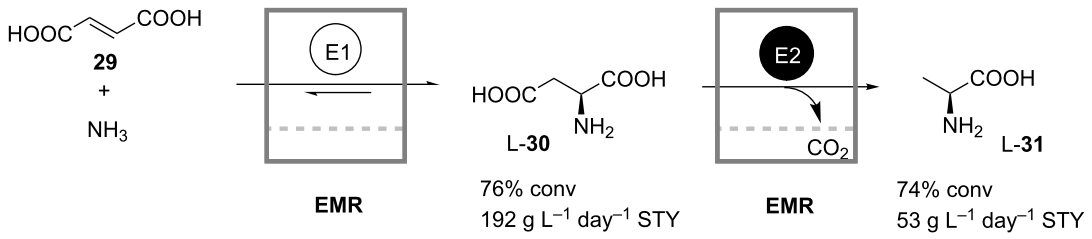

Scheme 10: Continuous production of L-alanine (**31**) from fumarate (**29**) in a two-stage enzyme membrane reactor. E1: Aspartase; E2: L-Aspartate-β-decarboxylase [34].

the second reactor L-**30** is irreversibly decarboxylated by L-aspartate-β-decarboxylase to produce L-**31** and CO_2. Both enzymes differ significantly in their pH and temperature optima, thus necessitating two separate consecutive reactors. During the operation of the reactor cascade the loss of productivity due to enzyme deactivation in both reactors was compensated by automated enzyme addition. The enzyme consumption required to maintain constant productivity was found to depend on the conversion level. It was also shown that the decarboxylase was deactivated much faster than the aspartase, probably due to the shear forces caused by the formation of CO_2 bubbles and by recirculating pumps. A space-time yield of approximately 53 g L^{-1} day^{-1} at 56% of overall conversion was achieved.

In the continuous sequential synthesis of *vic*-diols in a multicatalyst system described by Liese [2], the incompatible reaction steps were successfully separated in a cascade of two enzyme membrane reactors as well. The first reactor contained benzoyl formate decarboxylase (BFD) catalyzing the (*S*)-selective aldol condensation of benzaldehyde (**33**) and acetaldehyde (**32**) with formation of (*S*)-2-hydroxy-1-phenyl-propanone (**34**) (Scheme 11). In the second vessel the intermediate (*S*)-**34** was asymmetrically reduced by rec*Lb*-alcohol dehydrogenase (ADH) and the cofactor was regenerated by coupled formate (**2**) oxidation catalyzed by formate dehydrogenase (FDH). Due to the high K_M value of BFD for **32** an excessive concentration of this compound had to be applied in the first reactor in order to maximize the productivity. Since the aldehyde **32** is also a substrate for the ADH, it was removed inline by stripping with nitrogen in a membrane-based gas–liquid contactor installed before the second reactor. Such an experimental setup enabled continuous synthesis of 1-phenyl-(1*S*,2*S*)-propanediol (**35**) with 90% de and overall space-time yield of 32 g L^{-1} day^{-1}.

Similarly, Schwarz and Wandrey developed a cascade of two membrane reactors for the production of dipeptides [35]. In the first reactor carboxypeptidase Y (CPD-Y) catalyzes the conden-

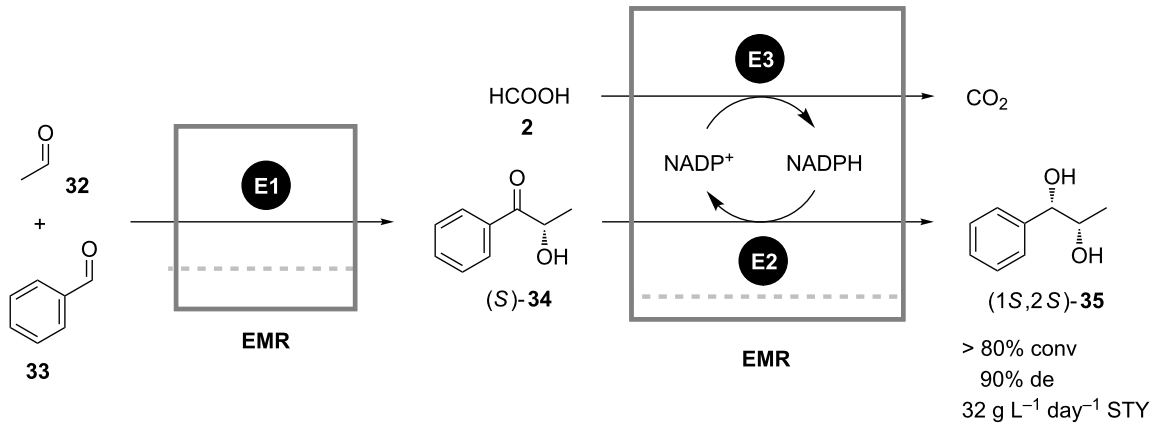

Scheme 11: Continuous synthesis of 1-phenyl-(1*S*,2*S*)-propanediol (**35**) in a cascade of two enzyme membrane reactors. E1: Benzoyl formate decarboxylase; E2: Rec*Lb*-alcohol dehydrogenase; E3: Formate dehydrogenase [2].

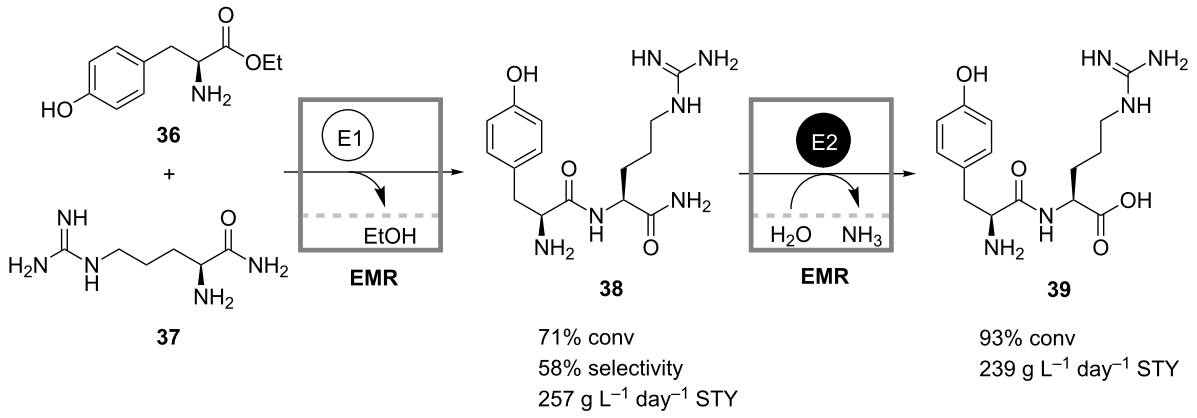

Scheme 12: Production of a dipeptide **39** in a cascade of two continuously operated membrane reactors. E1: Carboxypeptidase Y; E2: Peptide amidase [35].

sation between the ester **36** and the amide **37** of two amino acids (Scheme 12). Deamidation of the resulting dipeptide-amide **38** proceeds in the second reactor loaded with a selective peptide-amidase that does not react on dipeptide bonds. In a slow side reaction, however, CPD-Y hydrolyzes the final deamidated dipeptide **39**, whereas it does not act on the intermediate **38**. Separation of the two reactions was thus preferred in order to maximize yields.

The cascade-reactor approach may be useful not only in situations where incompatible reaction steps need to be spatially separated, but also in the case of coupled-reaction processes that, from a reaction-engineering point of view, should be conducted in CSTR series. For instance, when developing a continuous enzymatic production of GDP-mannose **43** from mannose 1-phosphate (**40**) using GDP-mannose pyrophosphorylase (Scheme 13), Fey and co-workers encountered a two-fold product inhibition of the enzyme by both products **43** and pyrophosphate **41**, which deteriorated production performance [36]. Inhibition by pyrophosphate was successfully circumvented by applying the second enzyme pyrophosphatase, which catalyzed the hydrolysis of **41** to the noninhibiting inorganic phosphate **42**. Strong product inhibition by the target product **43** was avoided by means of reaction engineering: The process was conducted in a cascade of two CSTRs, whose kinetic behavior approximates an optimum for this reaction system in a plug-flow reactor. In this way the authors were able to reach 95% conversion with a space-time yield of 28 g L^{-1} day^{-1} and an enzyme consumption of 0.9 U g^{-1}. The reactor cascade was stably operated for a period of 50 hours.

The potential of the cascade-reactor approach is also appreciated in continuous chemo-enzymatic sequences, where overcoming the intrinsic incompatibility of chemical and enzymat-

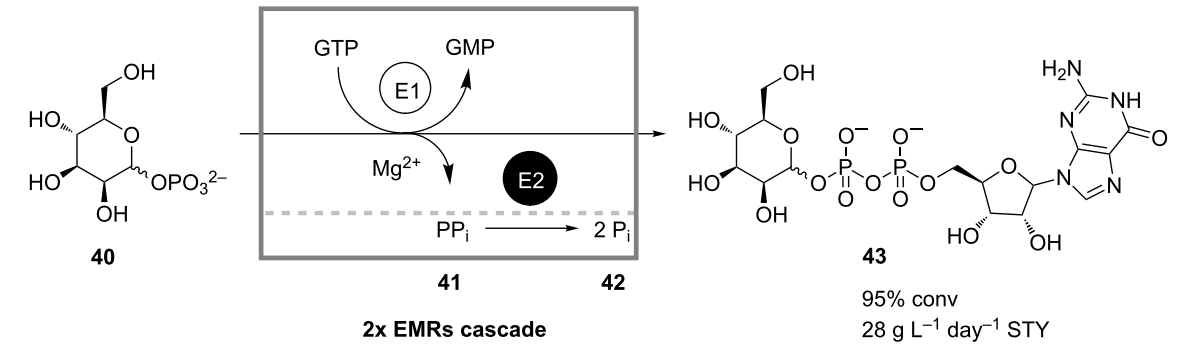

Scheme 13: Continuous production of GDP-mannose (**43**) from mannose 1-phosphate (**40**) in a cascade of two enzyme membrane reactors. E1: GDP-mannose pyrophosphorylase; E2: Pyrophosphatase [36].

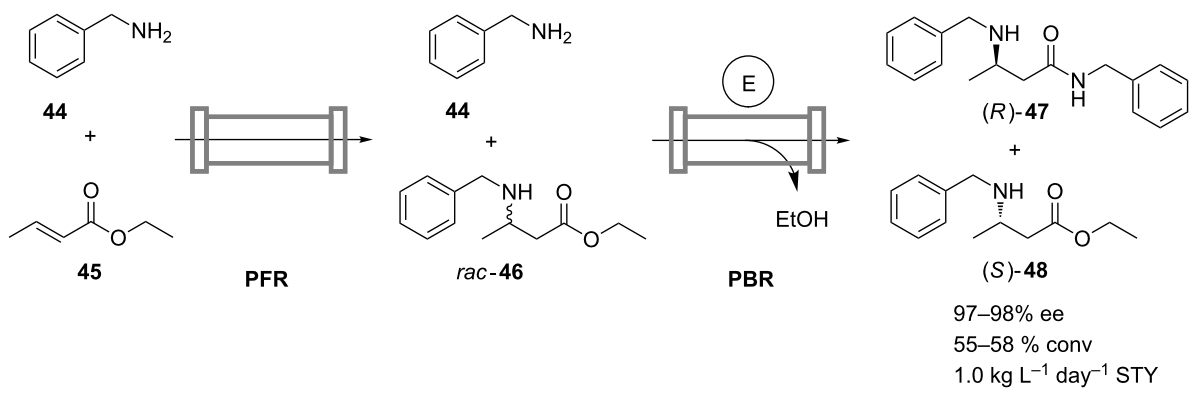

Scheme 14: Continuous solvent-free chemo-enzymatic synthesis of ethyl (*S*)-3-(benzylamino)butanoate (**48**) in a sequence of a plug-flow reactor (PFR) and a packed-bed reactor containing Novozym 435 (E) [38].

ical reaction steps is a common problem. Based on the one-pot batch process described by Weiß and Gröger [37], Strompen et al. developed a continuous chemo-enzymatic synthesis of ethyl (*S*)-3-(benzylamino)butanoate (**48**), which is a precursor to (*S*)-3-aminobutanoic acid. In contrast to the multistep enzymatic processes previously mentioned here, this transformation is carried out in a nonaqueous and solvent-free environment [38]. In the first noncatalyzed thermal aza-Michael addition performed at 80 °C, the racemic ester *rac*-**46** is formed from cheap starting materials benzylamine (**44**) and *trans*-ethylcrotonate (**45**) (Scheme 14). Subsequently, Novozym 435 is applied for the kinetic resolution of *rac*-**46** through aminolysis with the excess of the amine **44**. The resolution is conducted at 60 °C and yields the corresponding (*R*)-amide **47** and the remaining essentially enantiopure ester (*S*)-**48** as the products. Due to the advantage provided by entirely omitting the use of solvents, a high space-time yield of 1 kg L^{-1} day^{-1} was achieved. Apart from the difference in operation temperatures, separation of the two steps of this reaction sequence into individual reactors was also necessary as Novozym 435 is also able to catalyze the unwanted aminolysis of **45**.

Baxendale et al. [39] established a continuous synthesis of the neolignan natural product grossamide (**52**) by a two-step chemo-enzymatic reaction cascade starting from ferulic acid (**49**) and tyramine (**50**) (Scheme 15). The synthesis was

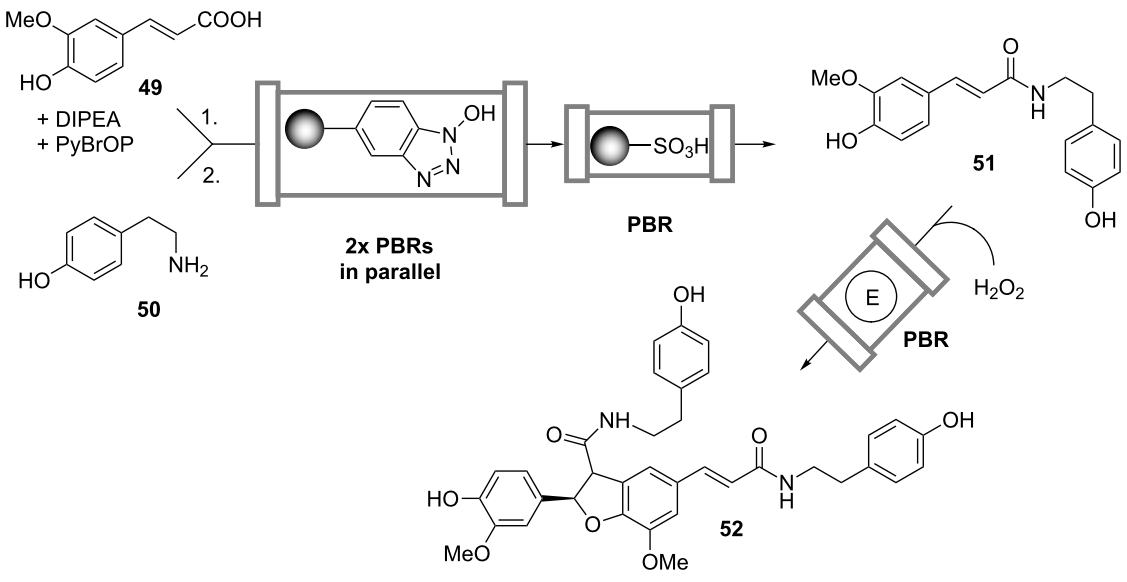

Scheme 15: Continuous chemo-enzymatic synthesis of grossamide (**52**) in a cascade of packed-bed reactors. E: Peroxidase [39].

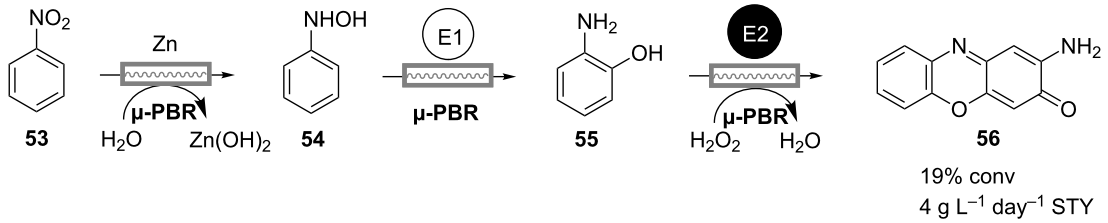

Scheme 16: Chemo-enzymatic synthesis of 2-aminophenoxazin-3-one (**56**) in a cascade of continuously operating packed-bed microreactors. E1: Hydroxyaminobenzene mutase; E2: Soybean peroxidase [40].

performed in a fully automated flow reactor consisting of three types of prepacked columns. The first two columns connected in parallel were filled with polymer-supported hydroxybenzotriazole, and during the process they worked either in loading or in elution mode. In the loading mode the columns were flushed with a solution of **49**, bromo-tris-pyrrolidino-phosphonium hexafluorophosphate (PyBrOP) and diisopropylethylamine (DIPEA), while in the elution mode a solution of **50** was pumped through. In this manner the acid **49** was first activated in the form of an ester, which then reacted with the amine **50** to yield the intermediate amide **51**. The unreacted **50** was removed from the reaction stream when passing through the scavenger column containing a sulfonic acid resin. The H_2O_2-mediated oxidative dimerization and intramolecular cyclization of **51** to the product **52** was catalyzed by an immobilized peroxidase enzyme packed into the last column. The authors validated the design of the flow reactor by synthesizing gram quantities of the compound and suggested that such a setup can be used for the continuous multistep synthesis of a much wider range of chemical substances.

A sequential chemo-enzymatic reaction in continuous flow was also developed by Luckarift and coworkers [40]. Their three-step process comprises reduction of nitrobenzene (**53**) by zinc to hydroxyaminobenzene (HAB, **54**), which in the second HAB-mutase-catalyzed step is rearranged intramolecularly to form 2-aminophenol (**55**) (Scheme 16). The final transformation involves the oxidation of **55** to 2-aminophenoxazin-3-one (**56**) by H_2O_2, catalyzed by soybean peroxidase. All reactions are carried out in an aqueous microfluidic system consisting of a cascade of three microreactors separately loaded with zinc powder and immobilized enzymes. The observed low conversion of 19% and space-time yield of 4 g L^{-1} day^{-1} imply the need for optimization, but demonstrate the feasibility and applicability of this process for the screening of nitroarene conversions.

The cascade-reactor approach is also powerful for the multistep enzymatic processes involving more than three reaction steps. An illustrative example is the continuous conversion of D-3-phosphoglycerate (**57**) into D-ribulose 1,5-bisphosphate (**58**) in a series of eleven packed-bed reactors containing immobilized enzymes (Scheme 17) [41]. The aim of the process is to continuously regenerate D-**58**, which is used as an acceptor for the biocatalytic fixation of CO_2 resulting in the formation of two molecules of D-**57**. The authors achieved 56% overall conversion at 0.3 g L^{-1} day^{-1} space-time yield and, thus, demonstrated the feasibility of carrying out such complex sequences in continuous flow. However, the observed overall conversion was significantly lower than the 90% predicted from enzyme performances in individual reaction steps. This discrepancy was explained by possible modulation of the kinetic properties of the enzymes by the residual intermediates, cofactors, and by-products from previous incomplete enzymatic conversions.

Although the cascade-reactor approach to continuous coupled (chemo)enzymatic reactions allows one in many cases to overcome the challenge of incompatible reaction steps, its practical usefulness is limited to the systems in which every reaction step itself proceeds efficiently. For example, if the conversion after each step in the reaction cascade is 80%, which is usually an excellent value for most single-reaction organic syntheses, after five consecutive steps the overall conversion of such a process will be dramatically decreased to only 33%. Moreover, the presence of the remaining nonconverted intermediates increases the chance of possible cross-inhibition and complicates the isolation of the target compound.

Certainly, one way to solve this problem is to find better catalysts for problematic steps or, by means of catalyst engineering, to improve the existing ones. Another plausible way to enhance the overall coupled-reaction process performance is “to polish” inefficient reaction steps with the aid of hybrid-reactor technology, which combines reaction and downstream processing steps in situ for the removal of undesired by-products. The work of Martinkova and coworkers, who observed the formation of isonicotinamide (**60**) as a by-product in the nitrilase-catalyzed conversion of 4-cyanopyridine (**59**) to isonicotinic acid (**61**), serves as an illustration of this method [42]. There, a cascade of two packed-bed reactors was set up with the second reactor

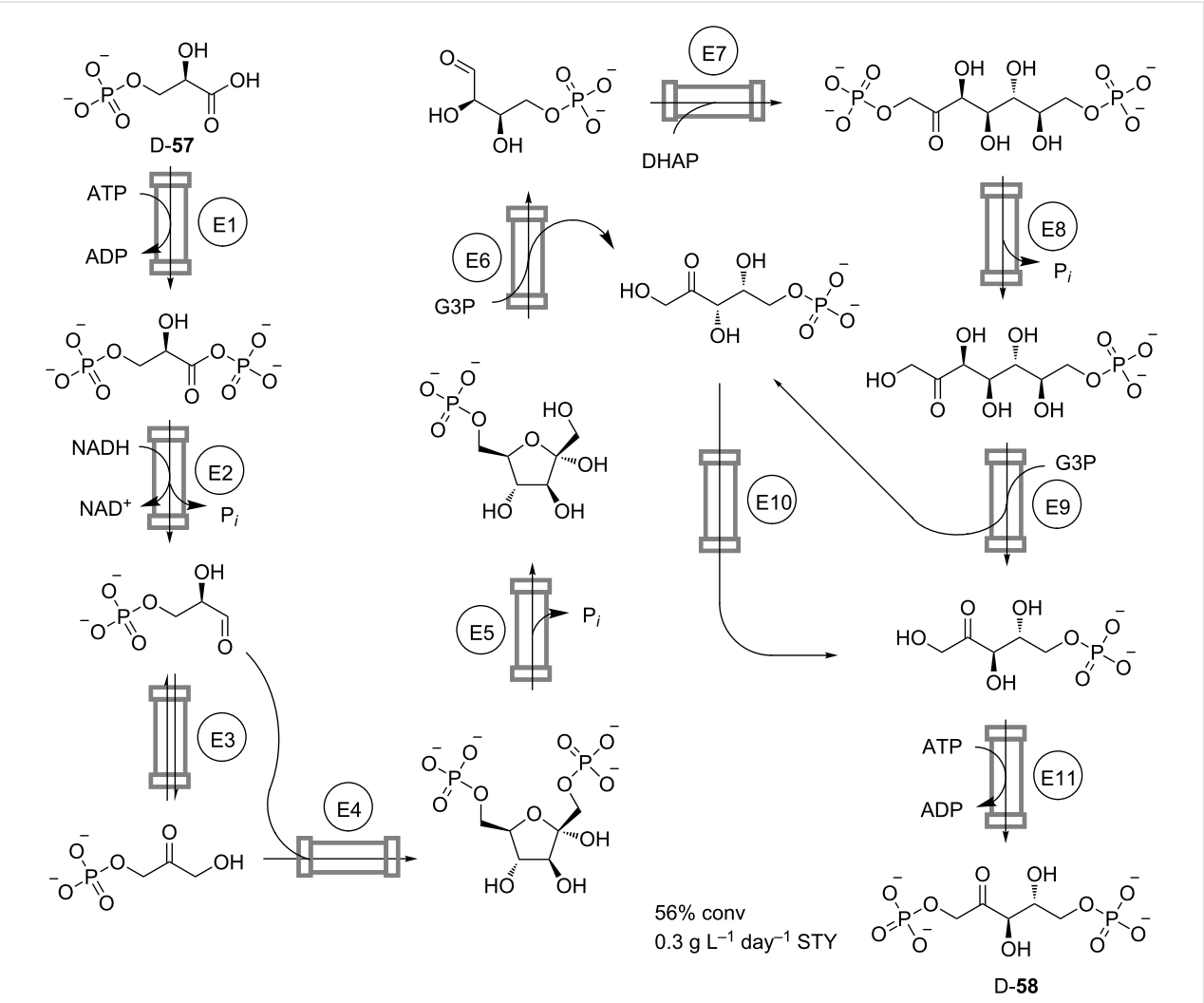

Scheme 17: Continuous conversion of 3-phospho-D-glycerate (**57**) into D-ribulose 1,5-bisphosphate (**58**) in a cascade of packed-bed reactors. E1: Phosphoglycerate kinase; E2: Glycerate phosphate dehydrogenase; E3: Triose phosphate isomerase; E4: Aldolase/FBP; E5: Phosphatase/FBPase; E6: Transketolase; E7: Aldolase/SuBP; E8: Phosphatase/SBPase; E9: Transketolase; E10: Epimerase; E11: Phosphoribulokinase [41].

loaded with an immobilized amidase, which catalyzed the hydrolysis of the residual amide **60** (Scheme 18). Both reactions were carried out in an aqueous system, while care was taken to find suitable buffer salts acceptable for both enzymes. A space-time yield of 2.1 kg L^{-1} day^{-1} was obtained at full conversion and 99.8% purity of the desired product. The same reaction sequence, but catalyzed by enzymes of a different origin, was realized by Malandra et al. in two enzyme membrane reactors operated in series [43].

3. Whole-cell processes in vivo

If living cells are the most efficient chemical factories known up to now, then why not let them do multistep organic synthesis for our benefit? This fact was already recognized before 6000 BC when the ancient Sumerians and Babylonians practiced the brewing of beer and winemaking [6]. Indeed, in vivo fermentation of sugars to ethanol by yeast is a complex process involving at least 12 enzymes and 2 cofactors, NAD^+ and ADP. Nowadays microbial biotransformations have become an indispensable part of industrial biotechnology, and are used in the production of a broad range of bulk and fine chemicals [6]. When a microbial multistep biotransformation is carried out in continuous flow it might formally also be considered as a fourth-generation enzymatic process according to the above-mentioned classification. However, in contrast to the in vitro multistep transformations already discussed, the whole-cell processes proceed in vivo, and, therefore, they are treated separately herein.

There are many continuous microbial biotransformations/fermentations described in the literature, for example fermentative production of ethanol, butanol, lactic acid, acetic acid/

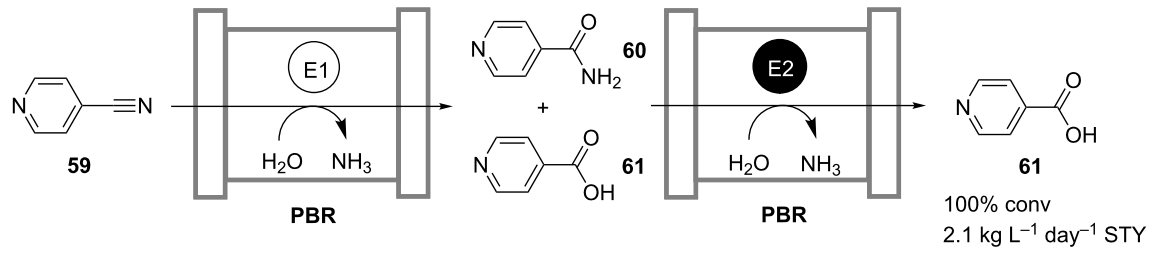

Scheme 18: Continuous hydrolysis of 4-cyanopyridine (**59**) to isonicotinic acid (**61**) in a cascade of two packed-bed reactors. E1: Nitrilase; E2: Amidase [42].

vinegar, succinic acid and fumaric acid in continuously operated biofilm reactors containing thick layers of microbial cells [44]. In this section only a few representative examples are reviewed, which illustrate the potential and the drawbacks of the whole-cell approach to continuous enzymatic coupled-reaction processes.

One of these examples is the continuous fermentative production of ethanol (**64**) developed by South et al. It is based on degradation of hardwood lignocellulose (**62**) by application of both free enzymes and whole cells as biocatalysts (Scheme 19) [45]. At the beginning the substrate **62** is pretreated with diluted acid in order to allow continuous feeding of the substrate suspension to a fermenter and to enhance conversion rates. In the fermenter the pretreated **62** is first hydrolyzed to cellobiose (**63**) by a cellulase from *Trichoderma reesi*. Then the second enzyme β-glucosidase breaks **63** down to form glucose (**7**), which is finally fermented by *Saccharomyces cerevisiae* to yield **64**. The side products formed during the acidic pretreatment of **62** cause only minor inhibition effects on the progress of the enzymatic saccharification and fermentation. A 60% conversion was obtained after a residence time of 2 days and with a space-time yield of 10 g L^{-1} day^{-1}. This process also demonstrates the applicability of continuous microbial biotransformations in biorefinery – the technology, which is aimed at generating energy from renewable resources and which is actively propagated presently in view of the forthcoming global energy crisis.

Another example of a biorefinery process is the production of hydrogen, i.e., the most environmentally friendly fuel. Oh and coworkers realized a continuous anaerobic fermentation of *Clostridium acetobutylicum* strains, which convert glucose (**7**) to hydrogen (Scheme 20) [46]. The reactor was initially operated in batch mode until the redox potential went below −200 mV. Afterwards, the reactor was continuously fed with a solution of **7**. During one week of continuous operation at 30 °C and retention time of 10 hours, approximately 2.4 mole of H_2 per mole of glucose were produced with a space-time yield of 0.6 g L^{-1} day^{-1}. Fermentation by-products comprised mainly butyrate and acetate as well as low amounts of ethanol and butanol.

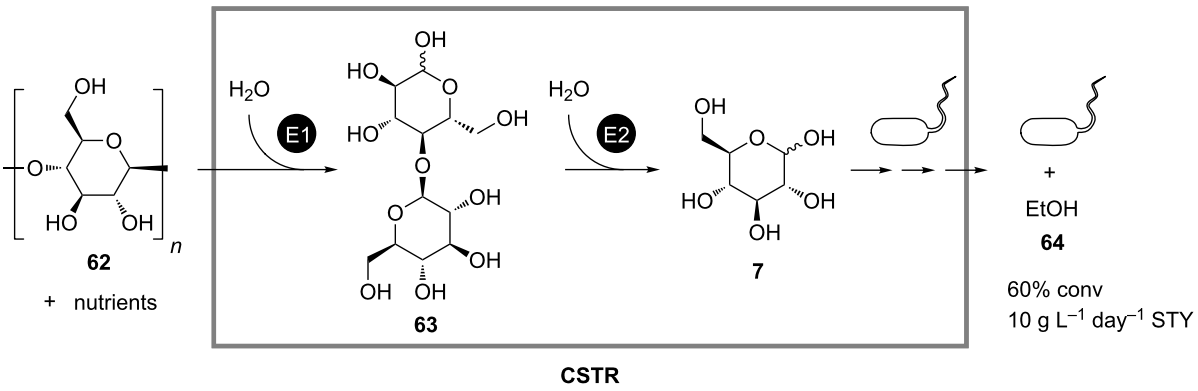

Scheme 19: Continuous fermentative production of ethanol (**64**) from hardwood lignocellulose (**62**) in a stirred-tank reactor (CSTR) containing yeast cells, cellulase (E1) and β-glucosidase (E2) [45].

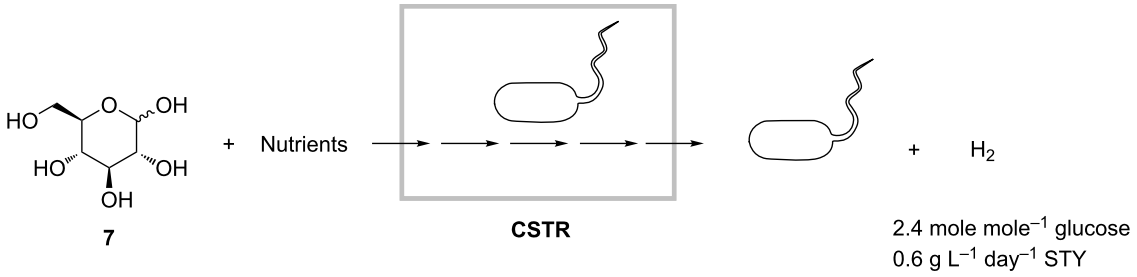

Scheme 20: Production of hydrogen by anaerobic fermentation of glucose (**7**) using *Clostridium acetobutylicum* cells in a continuously operating stirred-tank reactor [46].

Microbial biotransformations were also successfully exploited in the continuous multistep enzymatic synthesis of fine chemicals, where cofactor regeneration is required. In such cases the whole-cell in vivo approach is advantageous over in vitro approaches, because it is not necessary to use immobilization or nanofiltration membranes for the retention of small cofactor molecules when whole cells are applied as biocatalysts. Instead, the cofactors are kept in the cytoplasm by the cell membrane, which functions as a natural and efficient diffusion barrier. Moreover, the enzymes are usually more stable in their native environment inside a living cell than they are in buffer solutions or in immobilized forms.

Lactobacillus kefir whole cells were used by Haberland et al. for the continuous production of (2*R*,5*R*)-hexanediol (**67**) from 2,5-hexanedione (**65**) by in vivo reaction sequence in an ultrafiltration membrane reactor (Scheme 21) [47]. Native *L. kefir* alcohol dehydrogenases catalyzed the enantioselective and diastereoselective reduction of the ketone **65** while the reduction equivalents were supplied by the cosubstrate glucose. During the process the cells produced one mole of lactic acid (**66**) per mole of glucose (**7**) by fermentation. Therefore, NaOH was constantly added to the reactor to maintain the pH. The production facility also included an in-line product-separation unit consisting of a continuously operated counter-current extraction unit, and an online distillation unit for recycling of the organic solvent. The reaction product (2*R*,5*R*)-**67** was obtained at a space time yield of 63.8 g L^{-1} day^{-1} and a selectivity of 78%.

The biocatalytic reduction of **65** to (2*R*,5*R*)-**67** was also accomplished by Schroer and Luetz in a continuously operated double-membrane reactor loaded with recombinant *E. coli* cells overexpressing an alcohol dehydrogenase from *Lactobacillus brevis* [48]. In contrast to the work of Haberland [47], the consumed cofactor NADPH was regenerated by coupling the reduction of the ketone **65** with the oxidation of 2-propanol to acetone. The encountered thermodynamic limitation of the reaction system was overcome by continuous product removal of acetone by pervaporation (vaporization by permeation) through a polymethoxysiloxane membrane. To reach the highest space-time yields of >170 g L^{-1} day^{-1}, the reactor was constantly fed

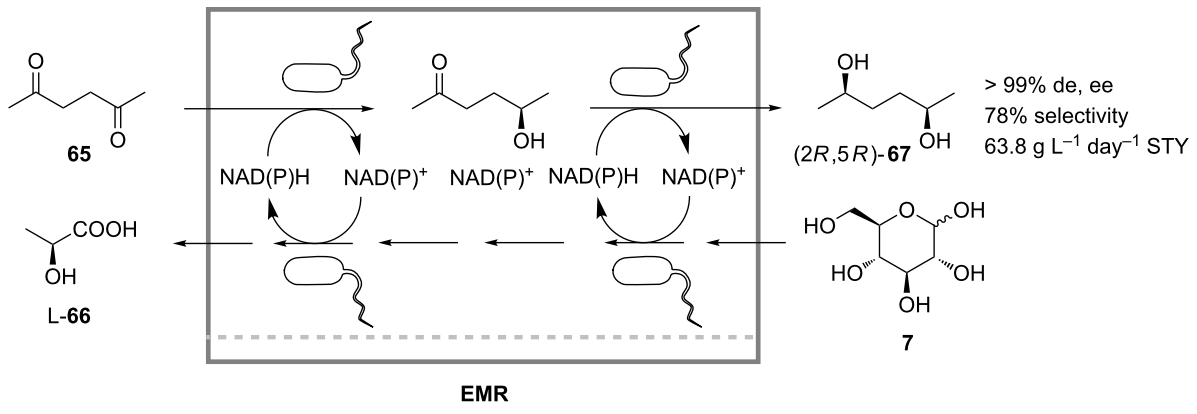

Scheme 21: Continuous production of (2*R*,5*R*)-hexanediol (**67**) in an enzyme membrane reactor containing whole cells of *Lactobacillus kefir* [47].

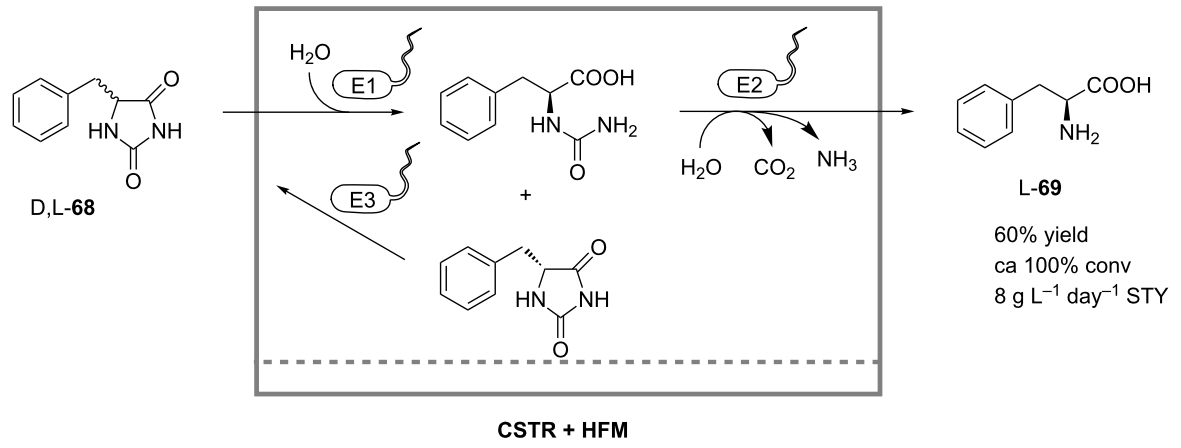

Scheme 22: Synthesis of L-phenylalanine (**69**) in a continuously stirred tank reactor equipped with a hollow-fiber module (HFM) for retention of *Arthrobacter aurescens* cells. E1: Hydantoine racemase; E2: L-Hydantoinase; E3: L-*N*-Carbamoylase [49].

with a 10 mM solution of NADP; although without addition of the cofactor the reactor also revealed high productivity and operational stability.

The multistep microbial biotransformations are also feasible for the continuous processes that do not require cofactor regeneration. Nöthe and coworkers developed a whole-cell membrane reactor operated in CSTR mode, with continuous product removal by ultrafiltration, for the microbial conversion of D,L-5-monosubstituted hydantoines [49]. Resting whole cells of *Arthrobacter aurescens* containing a hydantoine racemase, an L-hydantoinase and an L-*N*-carbamoylase were used to catalyze the synthesis of L-phenylalanine (**69**) from the model substrate D,L-benzylhydantoine (**68**) (Scheme 22) in 60% yield at almost 100% substrate conversion and a space-time yield of 8 g L^{-1} day^{-1}. Shear forces introduced by pumps were responsible for irreversibly damaging the cell walls, thus causing an increased enzyme deactivation rate, after an initial gain in activity from the improved permeability of substrates through the cell wall. Additionally, membrane fouling was identified as a problem for long-term operation. After several rounds of optimization, this multistep L-hydantoinase process was commercialized by DSM for industrial production of natural and non-natural L-amino acids [50].

A serious disadvantage of the whole-cell approach for continuous coupled-reaction processes is the sensitivity of living cells to high concentrations of organic substances, which are usually toxic. To overcome this challenge, Steinig and coworkers developed a special closed-gas-loop bioreactor and used it for the continuous epoxidation of 1,7-octadiene (**70**) to (*R*)-7-epoxyoctene (**72**) by a strain of *Pseudomonas oleovorans* growing on heptane (**71**) (Scheme 23) [51]. In a continuous operation, with regard to the aqueous phase, substrates for both growth and biotransformation were supplied in the gas phase from a reservoir and were dissolved in the liquid phase containing the whole cells and other nutrients required for the cell growth. The product was again removed in the gas phase and collected in a saturator/absorber module. By supplying and removing substrates and products by transfer to the gas phase, problems related to cell toxicity in the presence of organic phases or emulsified product streams were avoided. A space-time yield of approximately 2.5 g L^{-1} day^{-1} was achieved.

Another method to surmount substrate toxicity was used by Gross et al. in the oxidation of styrene (**73**) to (*S*)-styrene oxide (**74**) in a biofilm membrane reactor (Scheme 24) [52,53]. Cells of *Pseudomonas sp.* were grown in a biofilm attached to the inner surface of a silicon tube, through which a nutrient solution was constantly pumped. In a specially designed hermetic reaction compartment the tube was partially submerged into liquid **73**, which slowly diffused through the tube wall to the biofilm. Inside the tube **73** was enantioselectively oxidized to (*S*)-**74**, which in turn diffused back into the reaction compartment. The cofactor $FADH_2$ required for the oxidation was regenerated during metabolic activity of the cells. Due to diffusion limitations the substrate and the product concentrations in the biofilm were lower than their toxic levels, which allowed for continuous operation of the reactor for a period of more than 50 days, reaching maximally a space-time yield of 70 g L^{-1} day^{-1}.

Cheng and Tsai encountered the problem of substrate inhibition and low product yields during the reduction of estrone (**75**) to

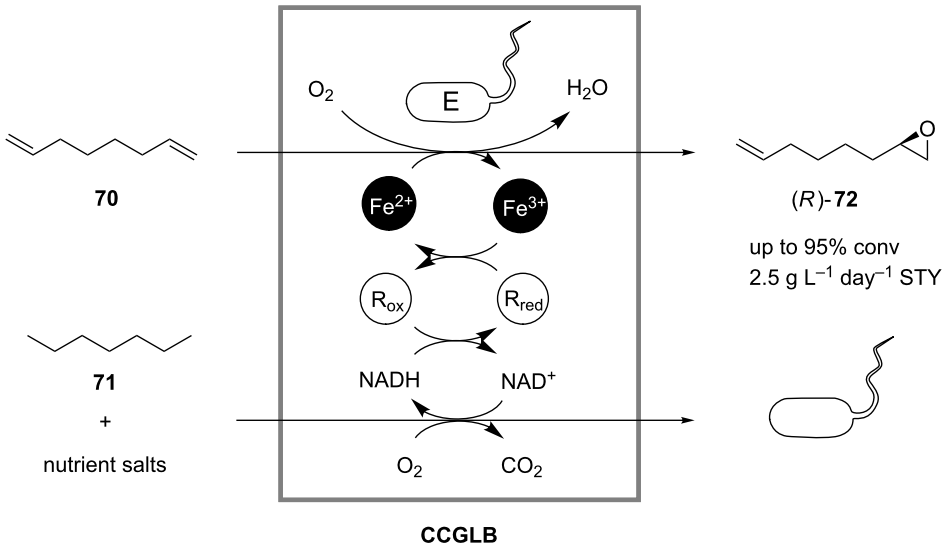

Scheme 23: Continuous epoxidation of 1,7-octadiene (**70**) to (*R*)-7-epoxyoctene (**72**) by a strain of *Pseudomonas oleovorans* in a closed-gas-loop bioreactor (CCGLB). R: Reductase; Fe: Rubredoxin [51].

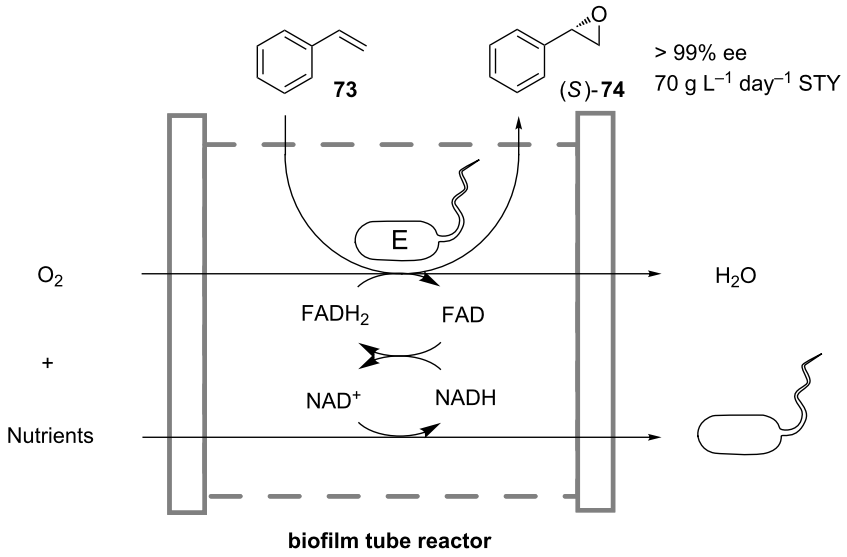

Scheme 24: Oxidation of styrene (**73**) to (*S*)-styrene oxide (**74**) in a continuously operated biofilm tube reactor containing cells of *Pseudomonas sp.* [53].

β-estradiol (**76**) in batch cell cultures of *Saccharomyces cerevisiae* expressing a native enzyme 17β-hydroxysteroid dehydrogenase. Therefore, in order to increase the productivity of cells, the authors proposed to perform the process continuously in a cascade of two stirred-tank reactors [54]. In the first reactor a continuous cell culture of the yeast was grown aerobically and continuously fed to the second reactor, in which reduction of **75** took place (Scheme 25). The constant flux of fresh active cells from the first reactor maintained the productivity of the second reactor at a constant level, which otherwise would drop down due to substrate-promoted cell inactivation and consequent cell wash-out. In the continuous process the productivity of yeast cells was improved compared to batch operation, giving a yield of 64.8% of the steroid **76**, and the overall product recovery was

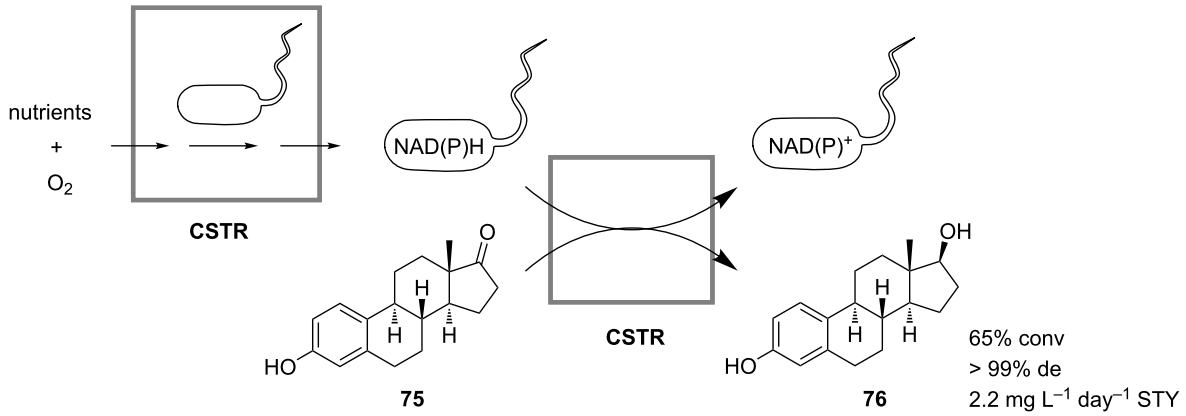

Scheme 25: Reduction of estrone (**75**) to β-estradiol (**76**) by *Saccharomyces cerevisiae* in a cascade of two stirred-tank reactors [54].

increased by a factor of about 4.3. A space-time yield of approximately 2.2 mg L^{-1} day^{-1} was achieved after three days of operation.

Conclusion

The examples of continuous coupled (chemo)enzymatic reactions reviewed herein demonstrate that such biotransformations can be considered as workable and competitive synthetic routes in the organic synthesis of fine and bulk chemicals. However, despite its obvious potential, this technology is presently in its infancy and the number of successful practical implementations is rather small; this number will certainly increase significantly in the future. There is no universal approach or recipe for how to build up a novel, efficient fourth-generation enzymatic process, but there are three different approaches, namely the single-reactor, cascade-reactor and whole-cell approach, the application of which in a particular coupled-reaction enzymatic system can be advantageous or disadvantageous (Table 1) depending on the process criteria under consideration. It is anticipated that in the future all three approaches will be further optimized in order to minimize their drawbacks and to maximize their positive sides. In this respect the exploitation of other biological principles could be of advantage and could lead to the next generation of enzymatic processes.

For instance, another biological principle states that the cell metabolism is compartmentalized, i.e., the interior of a living cell consists of compartments clustering the enzymes of a given metabolic pathway. Moreover, the clustered enzymes usually form supramolecular complexes enabling so-called “substrate

Table 1: Advantages and disadvantages of the three approaches to continuous coupled-reaction (chemo)enzymatic processes.[a]

Criterion	in vitro single reactor	in vitro cascade reactor	in vivo whole cell
Separation of incompatible steps	−	+	−
Incorporation of chemical steps	0	+	−
Optimization by reaction engineering	0	+	−
Modularization/incorporation of downstream processing units	−	+	−
Enzyme preparation/costs	−	−	+
Cofactor regeneration	0	−	+
Atomic efficiency	0	0	−

[a](+) advantage; (−) disadvantage; (0) no general comment possible, dependent on respective reaction system.

channeling", where intermediates of sequential metabolic steps are not released into the cytoplasm, but instead are "channeled" from one enzyme to another. This principle has been recently utilized in applied biocatalysis for the development of novel types of catalysts for multistep reaction cascades, i.e., metabolon catalysts [55], self-assembled fusion protein complexes [56] and polymerosomes [57]. It is very probable that application of these novel catalysts in continuous "in-pot" coupled-reaction processes will facilitate the separation of incompatible reaction steps, and thus can help to overcome the main disadvantage of a single-reactor approach.

A common drawback for both in vitro approaches is the stability of the enzyme preparations used, which is usually too low to make the long-term operation of the processes economically attractive. Furthermore, the activity and selectivity of enzymes in the non-natural environment is often deteriorated, which has a negative impact on the overall process performance. The enhancement of enzyme properties, or "fitting" them to a particular operation window by means of directed evolution or protein design [58], is a good way to make continuous coupled-reaction (chemo)enzymatic processes more appealing for practical purposes. And proceeding in this way would represent the realization of one more biological principle, namely that cell metabolism is steadily enhanced or adapted to the changing environment by natural evolution.

The main problem associated with the in vivo whole-cell approach is the complexity of metabolic networks, which is responsible for the comparably low yields and atomic efficiency of the multistep synthesis of target compounds, due to the dissipation of intermediates in numerous side reactions. The amendment of continuous in vivo coupled-reaction processes by metabolic engineering [59] is a promising technology, which brings into play another crucial biological principle, manifesting a control of the metabolic activity of a living cell through its genetic composition. The related and more advanced technology, which in the foreseeable future will revolutionize the field of whole-cell biotransformations, is that of genome engineering as pioneered by Craig Venter [60]. This technology is believed to be the main tool of synthetic biology, envisioning the creation of artificial cells with synthetic metabolic networks programmed to do a specific task, such as the treatment of diseases, the degradation of pollutants, or the synthesis of biofuels, and bulk and fine chemicals. Although there is still a long way to go to establish multistep continuous biotransformations catalyzed by artificial cells, there is no doubt, that when this goal is reached, chemists will be proud to say that they are on their way to being able to compete with nature in the virtuosity of organic synthesis.

References

1. Drauz, K.; Waldmann, H., Eds. *Enzyme Catalysis in Organic Synthesis;* Wiley-VCH: Weinheim, 2002.
2. Liese, A. *Biological Principles Applied to Technical Asymmetric Catalysis;* Verlag Forschungszentrum Jülich: Jülich, Germany, 2003. http://hdl.handle.net/2128/127
3. Faber, K. *Biotransformations in Organic Chemistry;* Springer: Berlin, Germany, 2011.
4. Schmid, A.; Dordick, J. S.; Hauer, B.; Kiener, A.; Wubbolts, M.; Witholt, B. *Nature* **2001,** *409,* 258–268. doi:10.1038/35051736
5. Hou, C. T. *Handbook of Industrial Biocatalysis;* CRC Press: Boca Raton, FL, 2005.
6. Liese, A.; Seelbach, K., Eds. *Industrial Biotransformations;* Wiley-VCH: Weinheim, Germany, 2006.
7. Kirschning, A.; Jas, G. *Top. Curr. Chem.* **2004,** *242,* 209–239. doi:10.1007/b96877
8. Mason, B. P.; Price, K. E.; Steinbacher, J. L.; Bogdan, A. R.; McQuade, D. T. *Chem. Rev.* **2007,** *107,* 2300–2318. doi:10.1021/cr050944c
9. Wiles, C.; Watts, P. *Eur. J. Org. Chem.* **2008,** *2008,* 1655–1671. doi:10.1002/ejoc.200701041
10. Mak, X. Y.; Laurino, P.; Seeberger, P. H. *Beilstein J. Org. Chem.* **2009,** *5,* No. 19. doi:10.3762/bjoc.5.19
11. Hessel, V. *Chem. Eng. Technol.* **2009,** *32,* 1655–1681. doi:10.1002/ceat.200900474
12. Rao, N. N.; Lütz, S.; Würges, K.; Minör, D. *Org. Process Res. Dev.* **2009,** *13,* 607–616. doi:10.1021/op800314f
13. Bruggink, A.; Schoevaart, R.; Kieboom, T. *Org. Process Res. Dev.* **2003,** *7,* 622–640. doi:10.1021/op0340311
14. Broadwater, S. J.; Roth, S. L.; Price, K. E.; Kobašlija, M.; McQuade, D. T. *Org. Biomol. Chem.* **2005,** *3,* 2899–2906. doi:10.1039/b506621m
15. Zhou, J. *Chem.–Asian J.* **2010,** *5,* 422–434. doi:10.1002/asia.200900458
16. Findrik, Z.; Vasić-Rački, Đ. *Chem. Biochem. Eng. Q.* **2009,** *23,* 545–553.
17. Santacoloma, P. A.; Sin, G.; Gernaey, K. V.; Woodley, J. M. *Org. Process Res. Dev.* **2011,** *15,* 203–212. doi:10.1021/op1002159
18. *The Application of Biotechnology to Industrial Sustainability;* OECD Publications: Paris, France, 2001. http://www.oecd.org/bookshop?pub=932001061P1
19. Sheldon, R. A. *Chem. Commun.* **2008,** 3352–3365. doi:10.1039/b803584a
20. Pàmies, O.; Bäckvall, J.-E. *Chem. Rev.* **2003,** *103,* 3247–3261. doi:10.1021/cr020029g
21. Webb, D.; Jamison, T. F. *Chem. Sci.* **2010,** *1,* 675–680. doi:10.1039/c0sc00381f
22. Wichmann, R.; Wandrey, C.; Bückmann, A. F.; Kula, M.-R. *Biotechnol. Bioeng.* **1981,** *23,* 2789–2802. doi:10.1002/bit.260231213
23. Hummel, W.; Schütte, H.; Kula, M.-R. *Appl. Microbiol. Biotechnol.* **1988,** *28,* 433–439. doi:10.1007/BF00268209
24. Obón, J. M.; Almagro, M. J.; Manjón, A.; Iborra, J. L. *J. Biotechnol.* **1996,** *50,* 27–36. doi:10.1016/0168-1656(96)01545-3
25. Seelbach, K.; Kragl, U. *Enzyme Microb. Technol.* **1997,** *20,* 389–392. doi:10.1016/S0141-0229(96)00166-4
26. van Hecke, W.; Haltrich, D.; Frahm, B.; Brod, H.; Dewulf, J.; van Langenhove, H.; Ludwig, R. *J. Mol. Catal. B: Enzym.* **2011,** *68,* 154–161. doi:10.1016/j.molcatb.2010.10.004

27. Kragl, U.; Gygax, D.; Ghisalba, O.; Wandrey, C. *Angew. Chem., Int. Ed. Engl.* **1991,** *30,* 827–828. doi:10.1002/anie.199108271
28. Wiles, C.; Hammond, M. J.; Watts, P. *Beilstein J. Org. Chem.* **2009,** *5,* No. 27. doi:10.3762/bjoc.5.27
29. Lozano, P.; De Diego, T.; Gmouh, S.; Vaultier, M.; Iborra, J. L. *Int. J. Chem. React. Eng.* **2007,** *5,* A53.
30. Lozano, P.; De Diego, T.; Mira, C.; Montague, K.; Vaultier, M.; Iborra, J. L. *Green Chem.* **2009,** *11,* 538–542. doi:10.1039/b821623a
31. Lozano, P.; García-Verdugo, E.; Karbass, N.; Montague, K.; De Diego, T.; Burguete, M. I.; Luis, S. V. *Green Chem.* **2010,** *12,* 1803–1810. doi:10.1039/c0gc00076k
32. Bongs, J. Reaktiostechnische Optimierung Transketolase - katalysierter Synthesen. Ph.D. Thesis, University of Bonn, Germany, 1997.
33. Liu, Z.; Zhang, J.; Chen, X.; Wang, P. G. *ChemBioChem* **2002,** *3,* 348–355. doi:10.1002/1439-7633(20020402)3:4<348::AID-CBIC348>3.0.CO;2-K
34. Jandel, A.-S.; Hustedt, H.; Wandrey, C. *Eur. J. Appl. Microbiol.* **1982,** *15,* 59–63. doi:10.1007/BF00499507
35. Schwarz, A.; Wandrey, C.; Steinke, D.; Kula, M. R. *Biotechnol. Bioeng.* **1992,** *39,* 132–140. doi:10.1002/bit.260390203
36. Fey, S.; Elling, L.; Kragl, U. *Carbohydr. Res.* **1997,** *305,* 475–481. doi:10.1016/S0008-6215(97)10095-7
37. Weiß, M.; Gröger, H. *Synlett* **2009,** *8,* 1251–1254. doi:10.1055/s-0029-1216721
38. Strompen, S.; Weiß, M.; Gröger, H.; Hilterhaus, L.; Liese, A. Unpublished results.
39. Baxendale, I. R.; Griffiths-Jones, C. M.; Ley, S. V.; Tranmer, G. K. *Synlett* **2006,** 427–430. doi:10.1055/s-2006-926244
40. Luckarift, H. R.; Ku, B. S.; Dordick, J. S.; Spain, J. C. *Biotechnol. Bioeng.* **2007,** *98,* 701–705. doi:10.1002/bit.21447
41. Bhattacharya, S.; Schiavone, M.; Gomes, J.; Bhattacharya, S. K. *J. Biotechnol.* **2004,** *111,* 203–217. doi:10.1016/j.jbiotec.2004.04.002
42. Vejvoda, V.; Kaplan, O.; Kubáč, D.; Křen, V.; Martínková, L. *Biocatal. Biotransform.* **2006,** *24,* 414–418. doi:10.1080/10242420601033910
43. Malandra, A.; Cantarella, M.; Kaplan, O.; Vejvoda, V.; Uhnáková, B.; Štěpánková, B.; Kubáč, D.; Martínková, L. *Appl. Microbiol. Biotechnol.* **2009,** *85,* 277–284. doi:10.1007/s00253-009-2073-x
44. Qureshi, N.; Annous, B. A.; Ezeji, T. C.; Karcher, P.; Maddox, I. S. *Microb. Cell Fact.* **2005,** *4,* 24. doi:10.1186/1475-2859-4-24
45. South, C. R.; Hogsett, D. A.; Lynd, L. R. *Appl. Biochem. Biotechnol.* **1993,** *39-40,* 587–600. doi:10.1007/BF02919020
46. Oh, S.-E.; Zuo, Y.; Zhang, Z.; Guiltinan, M. J.; Logan, B. E.; Regan, J. M. *Int. J. Hydrogen Energy* **2009,** *34,* 9347–9353. doi:10.1016/j.ijhydene.2009.09.084
47. Haberland, J.; Hummel, W.; Daussmann, T.; Liese, A. *Org. Process Res. Dev.* **2002,** *6,* 458–462. doi:10.1021/op020023t
48. Schroer, K.; Lütz, S. *Org. Process Res. Dev.* **2009,** *13,* 1202–1205. doi:10.1021/op9001643
49. Nöthe, C.; Syldatk, C.; Wagner, F.; Millies, M.; Mewes, D. *Chem. Ing. Tech.* **1993,** *65,* 1224–1228. doi:10.1002/cite.330651008
50. May, O.; Verseck, S.; Bommarius, A.; Drauz, K. *Org. Process Res. Dev.* **2002,** *6,* 452–457. doi:10.1021/op020009g
51. Steinig, G. H.; Livingston, A. G.; Stuckey, D. C. *Biotechnol. Bioeng.* **2000,** *70,* 553–563. doi:10.1002/1097-0290(20001205)70:5<553::AID-BIT10>3.0.CO;2-2
52. Gross, R.; Hauer, B.; Otto, K.; Schmid, A. *Biotechnol. Bioeng.* **2007,** *98,* 1123–1134. doi:10.1002/bit.21547
53. Gross, R.; Lang, K.; Bühler, K.; Schmid, A. *Biotechnol. Bioeng.* **2010,** *105,* 705–717. doi:10.1002/bit.22584
54. Cheng, C.; Tsai, H.-R. *J. Chem. Technol. Biotechnol.* **2011,** *86,* 601–607. doi:10.1002/jctb.2561
55. Moehlenbrock, M. J.; Toby, T. K.; Pelster, L. N.; Minteer, S. D. *ChemCatChem* **2011,** *3,* 561–570. doi:10.1002/cctc.201000384
56. Hirakawa, H.; Nagamune, T. *ChemBioChem* **2010,** *11,* 1517–1520. doi:10.1002/cbic.201000226
57. Tanner, P.; Onaca, O.; Balasubramanian, V.; Meier, W.; Pavilan, C. G. *Chem.–Eur. J.* **2011,** *17,* 4552–4560. doi:10.1002/chem.201002782
58. Dalby, P. A. *Recent Pat. Biotechnol.* **2007,** *1,* 1–9.
59. Yu, C.; Cao, Y.; Zou, H.; Xian, M. *Appl. Microbiol. Biotechnol.* **2011,** *89,* 573–583. doi:10.1007/s00253-010-2970-z
60. Gibson, D. G.; Glass, J. I.; Lartigue, C.; Noskov, V. N.; Chuang, R.-Y.; Algire, M. A.; Benders, G. A.; Montague, M. G.; Ma, L.; Moodie, M. M.; Merryman, C.; Vashee, S.; Krishnakumar, R.; Assad-Garcia, N.; Andrews-Pfannkoch, C.; Denisova, E. A.; Young, L.; Qi, Z.-Q.; Segall-Shapiro, T. H.; Calvey, C. H.; Parmar, P. P.; Hutchison, C. A., III; Smith, H. O.; Venter, J. C. *Science* **2010,** *329,* 52–56. doi:10.1126/science.1190719

License and Terms

Beilstein Journal of Organic Chemistry

Continuous-flow enantioselective α-aminoxylation of aldehydes catalyzed by a polystyrene-immobilized hydroxyproline

Xacobe C. Cambeiro[1], Rafael Martín-Rapún[1], Pedro O. Miranda[1], Sonia Sayalero[1], Esther Alza[1], Patricia Llanes[1] and Miquel A. Pericàs[*1,2]

Full Research Paper

Open Access

Address:
[1]Institute of Chemical Research of Catalonia (ICIQ). Avda. Països Catalans, 16. E-43007, Tarragona, Spain and [2]Departament de Química Orgànica, Universitat de Barcelona. Avda. Martí I Franqués, 1. E-08028, Barcelona, Spain

Email:
Miquel A. Pericàs[*] - mapericas@iciq.es

* Corresponding author

Keywords:
α-aminoxylation; continuous flow; packed-bed reactors; polystyrene-immobilized catalysts; proline

Beilstein J. Org. Chem. **2011,** *7,* 1486–1493.
doi:10.3762/bjoc.7.172

Received: 31 August 2011
Accepted: 17 October 2011
Published: 31 October 2011

This article is part of the Thematic Series "Chemistry in flow systems II".

Guest Editor: A. Kirschning

Abstract

The application of polystyrene-immobilized proline-based catalysts in packed-bed reactors for the continuous-flow, direct, enantioselective α-aminoxylation of aldehydes is described. The system allows the easy preparation of a series of β-aminoxy alcohols (after a reductive workup) with excellent optical purity and with an effective catalyst loading of ca. 2.5% (four-fold reduction compared to the batch process) working at residence times of ca. 5 min.

Introduction

Optically active α-hydroxycarbonyl moieties are highly versatile functional synthons and are present in a wide range of biologically active natural products [1,2]. Traditional strategies for the preparation of these kinds of synthons involves the oxidation of preformed enolates, both with the use of chiral auxiliaries (chiral, enantiopure enolates and achiral oxidizing agents, or achiral enolates and chiral, enantiopure oxidizing agents) [3-5] and by Mukaiyama-type catalytic processes involving preformed achiral enolate equivalents and achiral oxidants, with chiral enantiopure Lewis acids as catalysts [6-11].

Worth noting is the contribution made by Yamamoto et al., who introduced the use of nitrosobenzene as an electrophilic source of oxygen in the aminoxylation of preformed tin enolates catalyzed by a chiral, silver-based Lewis acid [12]. With this methodology an α-aminoxyketone was obtained that could be readily transformed into the corresponding α-hydroxyketone in the presence of catalytic amounts of $CuSO_4 \cdot 5H_2O$ in methanol.

This strategy was soon extrapolated to the field of organocatalysis, leading in 2003 [13] to the first organocatalytic

approaches to the direct enantioselective α-aminoxylation of carbonyl compounds and, shortly after, to the implementation of the α-aminoxylation of aldehydes with proline as catalyst [14,15] (Scheme 1). In 2004, the scope of the reaction was extended to ketones [16,17] and the reaction was subsequently applied to the synthesis of several biologically active compounds [18-20].

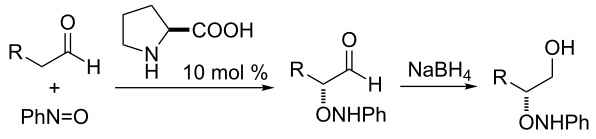

Scheme 1: Proline-catalyzed direct enantioselective α-aminoxylation of aldehydes.

Proline is the most frequently used catalyst in α-aminoxylation reactions, but other catalytic species have also been developed and used. Chiral secondary amines, such as substituted pyrrolidines other than proline [21], binaphthyl-derived amines [22-24], pyrrolidin-2-yl-tetrazoles [25-28], thiaproline [29], 2-aminomethylpyrrolidine sulfonamide [30] and sulfonylcarboxamide [31], have been successfully used to promote the reaction. As a matter of fact, the rapid development of the methodology for the asymmetric organocatalyzed α-aminoxylation of aldehydes and ketones experienced in the last few years has transformed it into a powerful, reliable and environmentally friendly method for the synthesis of α-hydroxyaldehydes and ketones [32-34].

Despite its extreme simplicity and very high enantiocontrol, organocatalysis has frequently been the subject of criticism for the relatively low catalytic activities, which hence require the use of catalyst loadings as high as 30 mol % [35,36] for the achievement of high conversions in reasonable reaction times. A very reliable and convenient strategy to overcome this limitation is the development of reusable immobilized catalysts, thus allowing important reductions of the "effective" catalyst loading (through recycling and repeated use). Different approaches have been used for the development of immobilized analogs of proline and other organic catalysts. Among them, a prominent position is occupied by catalysts covalently immobilized onto insoluble, cross-linked polymers [37-40]. An interesting development arising from this strategy is the polystyrene-immobilized 4-hydroxyproline **1a** (Figure 1), reported by our group as an extremely efficient and reusable catalyst for the direct enantioselective aldol [41] and Mannich reactions [42] as well as for the α-aminoxylation of carbonyl compounds under batch conditions [43]. Interestingly, the triazole linker between the polymer and the active unit, inherently resulting from the Cu(I)-catalyzed cycloaddition of azides and alkynes (CuAAC) used as the immobilization strategy [44-46], led to improved efficiency, both in terms of catalytic activity and asymmetric induction, and different behaviour of the resulting materials in terms of hydrophilicity or hydrophobicity [47-50].

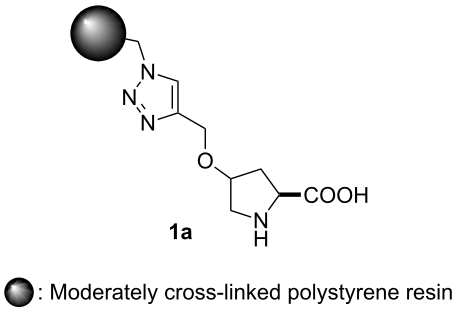

Figure 1: Polystyrene-immobilized hydroxyproline **1a**.

An even better alternative for improving the productivity of catalytic species results from the implementation of heterogenized catalysts in continuous-flow reactors. Flow chemistry has experienced a very important development in the last ten years as an emerging technology for organic synthesis [51-66]. It offers as its main advantages facile automation and excellent heat and mass transfer, rendering the scale-up of a process a trivial task, in contrast with the obstacles always met in the scale-up of batch processes [67-71].

The combination of flow chemistry with solid-supported catalysts allows the advantages inherent to both technologies to be added together. Thus, the physical immobilization of the catalyst in a packed-bed reactor allows it to be submitted constantly to the reaction conditions, avoiding possible degradation of the catalyst during operations other than the reaction itself (washing, drying, storage, etc.) [72]. This frequently leads to a significant extension of the catalyst's lifetime. In addition, any further processing for the separation of the catalyst from the reaction mixture is no longer needed. The combined effect of these factors is an improvement in the catalyst productivity, with a corresponding reduction in the cost of any given process [42,50,73-75].

Herein we present the implementation of a continuous-flow packed-bed reactor with heterogenized catalyst **1** for the fast, enantioselective, direct α-aminoxylation of aldehydes.

Results and Discussion

The preparation of the immobilized catalysts **1a** and **1b** was easily achieved by a modification of the reported procedure [41-43], with the tris(triazolyl)methyl copper complex **3** [76] as the

catalyst for the CuAAC reaction between azidomethylpolystyrene, prepared from a Merrifield resin, and propargyloxyproline derivative **2**, which was readily obtained in two steps from commercially available (2*S*,4*R*)-*N*-Boc-4-hydroxyproline (Scheme 2).

Based on previous experience, we considered that variations in the degree of cross-linking of the support resins could have an important effect on their mechanical stability [66], this resulting in differences in their performance. In order to assess this issue, we prepared two different immobilized catalysts, starting in one case (**1a**) from commercially available Merrifield resin containing 1% of 1,4,-divinylbenzene (DVB) as a cross-linking agent and in the other case (**1b**) from a home-made Merrifield resin with 8% DVB (prepared by radical copolymerization of styrene, 4-chloromethylstyrene and DVB, under previously reported conditions [77-79]).

It is well known that slightly cross-linked (1–2% DVB) polystyrene is microporous in nature and readily swells in a variety of solvents, leading to gel formation. For catalytic resins, this ensures contact of the reactants in solution with essentially all the catalytic sites and, accordingly, high activity. This positive characteristic, however, can be countered by a poor mechanical stability that can lead to structural collapse and deactivation under the pressure applied for flow operation. Polystyrene cross-linked with 8% DVB still shows significant swelling with a variety of solvents, such that its behaviour can be considered as being intermediate between those of microporous and macroporous resins. We accordingly expected that the catalyst immobilized on such a more heavily cross-linked resin, such as **1b**, would retain an important level of activity while having less of a tendency for structural collapse under the flow conditions, and that, as a consequence, the useful lifetime of the catalyst would be significantly improved.

After final deprotection, immobilized catalysts **1a** and **1b** were obtained with functionalizations (f) of 0.48 and 0.74 mmol·g^{-1}, respectively.

Both resins were evaluated as catalysts for the α-aminoxylation reaction of aldehydes with nitrosobenzene, with propanal as a benchmark substrate, under standard batch conditions [43]. In both cases the product, isolated in the form of its reduced β-aminoxy alcohol due to the intrinsic instability of α-aminoxy aldehydes, was obtained with good yields and enantioselectivities in short reaction times (Scheme 3). Although catalyst **1a** afforded better results both in terms of enantioselectivity and catalytic activity, we were pleased to observe that the more heavily cross-linked catalytic resin **1b** exhibited a catalytic activity almost identical to that of **1a**, with only a marginal decrease in enantioselectivity.

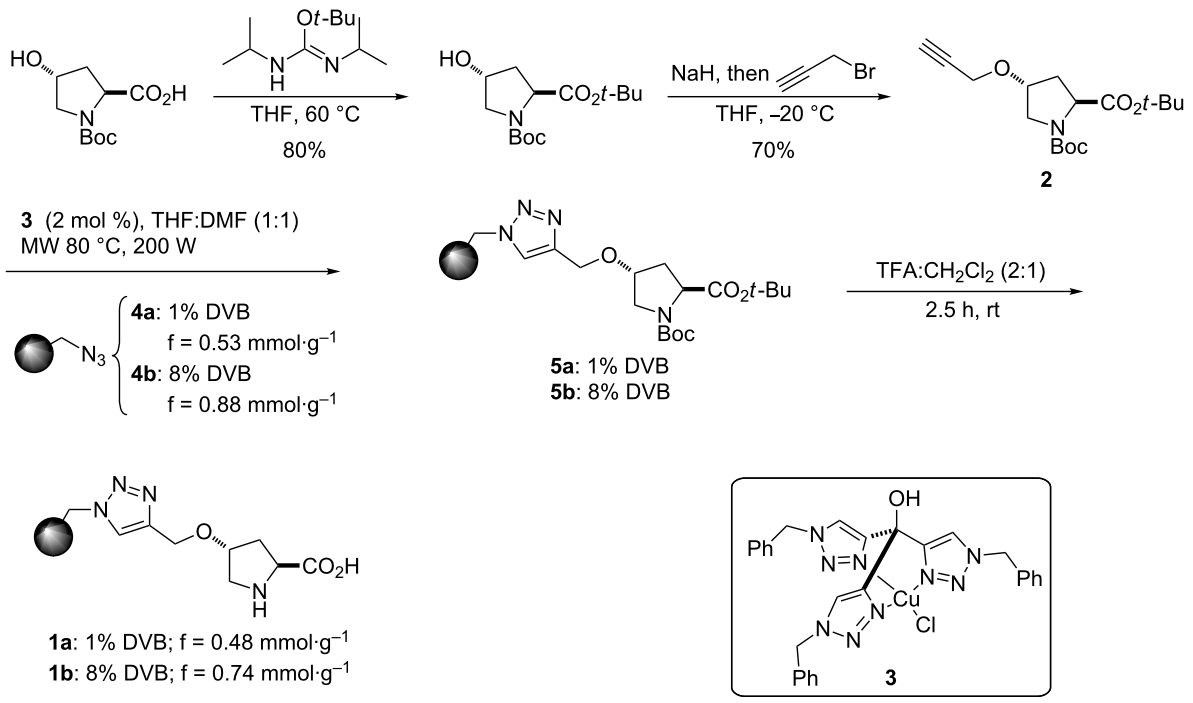

Scheme 2: Preparation of the immobilized catalysts **1a** and **1b**.

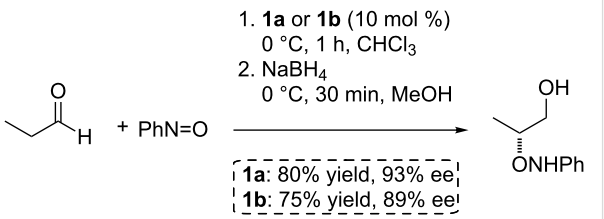

Scheme 3: Direct enantioselective α-aminoxylation of propanal catalyzed by resins **1a** and **1b**.

With these results in hand, we set up flow conditions for the two catalysts to study the scope and limitations of their use in the α-aminoxylation of aldehydes.

For the continuous-flow experiments, following our previous experience with similar systems, the instrumental setup shown in Figure 2 was used. The packed-bed reactor consisted of a vertically mounted, fritted and jacketed low-pressure Omnifit glass chromatography column (10 mm pore size and up to a maximal 70 mm of adjustable bed height) filled with 300 mg of swollen resin (ca. 17 mm bed height). Two separate piston pumps were connected to the reactor inlet through a T-shape connector placed right before the reactor, and which acted as a mixing chamber, and a collection flask was connected to the reactor outlet.

During operation, each of the pumps was connected to one of the feeding solutions **A** and **B**; solution **A** containing nitrosobenzene (0.24 M) and 1,1,2,2-tetrachloroethane (0.06 M, internal standard), and solution **B** containing propanal (0.72 M) in chloroform. Both solutions were pumped through the system at a rate of 0.12 mL·min^{-1} each.

Additionally, a supply of pure chloroform was connected to both pumps, for nonreaction operations such as swelling the resin and washing the tubing before and after the reaction. Isothermal operation was ensured by circulation of a cooling fluid at the desired operation temperature (0 °C) through the column jacket. Finally, the collection flask was set in a cold bath at −78 °C, in order to avoid degradation of the aminoxylated products after collection.

The conversion at any given moment was determined from the ^{1}H NMR spectra of samples periodically collected from the reactor output. At the end of the experiment the product was reduced with sodium borohydride.

After optimization of the parameters for the continuous-flow process, both catalysts **1a** and **1b** were tested with different substrates, with the results as shown in Table 1.

Both immobilized catalysts **1a** and **1b** provided equally excellent enantioselectivities, which remained completely stable throughout the reaction. On the other hand, regarding catalytic activity, resin **1a**, containing only 1% of the cross-linking agent DVB, exhibited consistently better productivities with the different substrates. It is also worth noting that in the case of catalyst **1a** the conversions registered for the different substrates were not dependent on the chain length (Table 1, entries 3–5) or

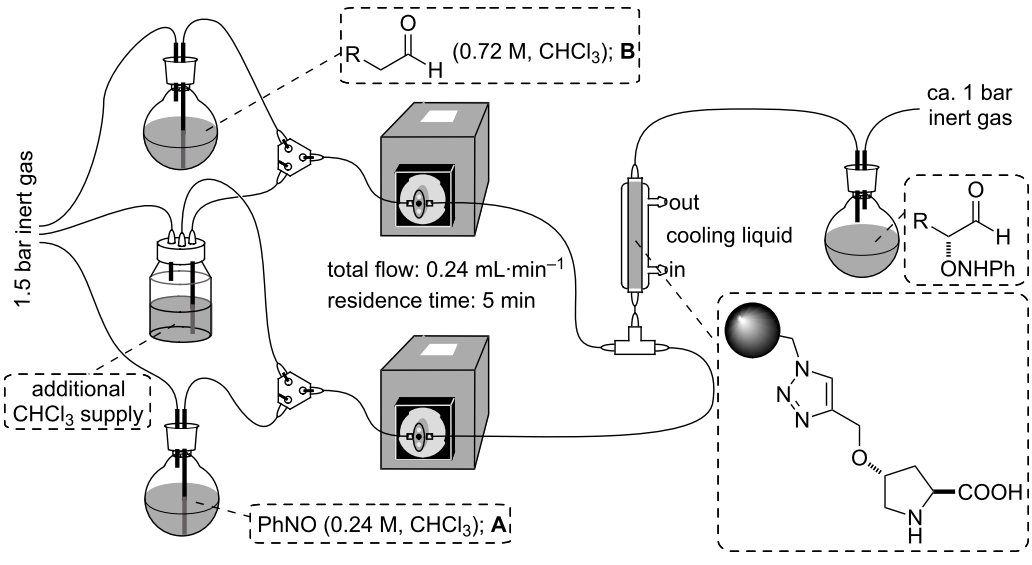

Figure 2: Experimental setup for the continuous-flow α-aminoxylation of aldehydes.

Table 1: Continuous-flow, direct, enantioselective α-aminoxylation of various aldehydes with immobilized catalysts **1a** and **1b**.[a]

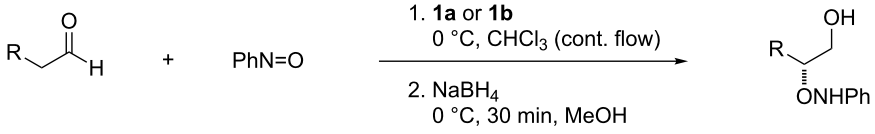

Entry	Aldehyde	Time (h)	Catalyst **1a** Conv[b] (%)	ee[c] (%)	Productivity[d]	Catalyst **1b** Conv[b] (%)	ee[c] (%)	Productivity[d]
1		1	75			94		
		2	69			90		
		3	67	95	27.3	88	96	16.1
		4	65			93		
		5	60			82		
2	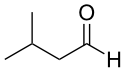	1	83			57		
		2	70			63		
		3	76	94	12.6	54	98	9.3
		4	82			70		
		5	65			49		
3	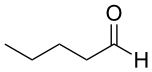	1	49			47		
		2	57			46		
		3	43	95	31.4	43	95	3.7
		4	48			72		
		5	49			–		
4	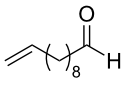	1	68			67		
		2	70			39		
		3	63	96	26.7	42	95	9.8
		4	55			36		
		5	54			43		
5	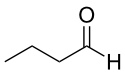	1	95			–		
		2	70			–		
		3	67	96	32.7	–	–	–
		4	69			–		
		5	67			–		

[a]Reactions were performed with 300 mg of resin (0.144 mmol for **1a** or 0.222 mmol for **1b**), 0.24 mL min^{-1} total flow rate (ca. 5 min residence time), 0.12 M concentration of nitrosobenzene and 0.36 M of the corresponding aldehyde. [b]Instant conversion, determined by ^1H NMR of samples without any workup. [c]Determined by HPLC analysis of the reduced ($NaBH_4$) product. [d]In mmol of pure isolated product per mmol of catalyst (accumulated throughout the process).

on the presence of branching in the β-position of the aldehyde (Table 1, entry 2). In the case of catalyst **1b**, lower catalytic activity was observed in all cases (note that the catalyst loading was 0.222 mmol for **1b** while it was 0.144 mmol for **1a**) and, intriguingly, it was strongly dependent on the chain length and branching. Propanal (Table 1, entry 1) gave place to a much higher conversion with resin **1b** than longer-chain (Table 1, entries 3–5) or branched (Table 1, entry 2) aldehydes did. A possible explanation for this behaviour could be the increased rigidity of the resin **1b**, which contains 8% of DVB, causing stable channels and pores of a rather small diameter to be present (macroporous behaviour), instead of the more geometrically tolerant gel in the case of the resin **1a** with 1% of DVB.

Finally, both immobilized catalysts showed only a moderate stability, a slow decrease in the conversion being observed with time in both cases. Contrary to our expectations based on the different degrees of cross-linking, no significant difference in stability was detected between resin **1a** and resin **1b** (the one with 8% DVB being only slightly more stable, as indicated by the conversion versus time data for propanal; see Table 1, entry 1). Although not conclusive, these data suggest that the deactiv-

ation process is of a chemical nature, possibly due to the formation of an oxazolidinone between proline and the aldehyde [80-82], rather than a physical denaturation of the polymer. With the most efficient resin (**1a**), ca. 30 mmol of product was isolated per mmol of resin for every flow experiment (5 h), thus meaning a four-fold improvement with respect to the batch process.

Conclusion

In summary, a packed-bed continuous-flow reactor was designed and implemented, based on polystyrene-immobilized 4-hydroxyproline, for the direct enantioselective α-aminoxylation of simple aldehydes. The system allowed for the first time the medium-scale preparation of a series of α-oxy-substituted aldehydes through a simple flow process involving short residence times. A lack of stability of the catalyst under the employed reaction conditions led to slow deactivation (15–20% in a five-hour reaction cycle), such that further work towards a practical solution of this problem is still required. Research aimed at understanding the principles determining the stability of immobilized catalysts in flow processes and, consequently, at the development of immobilized species with extended life cycle for α-aminoxylation and for other synthetically important reactions is currently underway in our laboratories.

Experimental

General procedure for the α-aminoxylation of aldehydes under continuous-flow conditions

Typical conditions for ca. five hours operation with pentanal: A solution (**A**) containing nitrosobenzene (1.29 g, 12 mmol) and 1,1,2,2-tetrachloroethane (317 μL, internal standard) in chloroform (50 mL, 0.24 M in nitrosobenzene) and another one (**B**) containing pentanal (3.8 mL, 36 mmol) in chloroform (50 mL, 0.72 M) were prepared. Both solutions were separately pumped at a rate of 0.12 mL·min^{-1} each through a glass column containing the immobilized catalyst **1a** (300 mg, 0.144 mmol), which had been previously swollen with chloroform. The effluent of the column was collected in a closed flask cooled down to –78 °C and the reaction was monitored by ^{1}H NMR of samples taken directly from the effluent.

After the feeding solutions were finished, chloroform was pumped at the same rate throughout the system for 1 h in order to rinse all the remaining materials. The product solution was diluted with 50 mL of methanol and, after the mixture was allowed to warm up to 0 °C, sodium borohydride (1.36 g, 36 mmol) was added in portions. The resulting slurry was vigorously stirred at 0 °C for 30 min and then water (100 mL) was added. The two layers were separated and the organic one was washed with brine (3 × 50 mL), dried with anhydrous sodium sulfate, filtered and concentrated under reduced pressure. The yellow oil obtained was purified by flash chromatography through silica gel with hexane-ethyl acetate mixtures to yield, after removal of the solvents, the β-aminoxy alcohol product as a colourless oil (910 mg, 96% ee).

Supporting Information

Supporting Information File 1

Detailed experimental procedures for the preparation of the catalysts and chromatographic methods for the determination of the enantiomeric excess of the products.
[http://www.beilstein-journals.org/bjoc/content/supplementary/1860-5397-7-172-S1.pdf]

Acknowledgements

This work was funded by MICINN (Grant CTQ2008-00947/BQU and Consolider Ingenio 2010 Grant CSD2006-0003), DIUE (Grant 2009SGR623), and ICIQ Foundation. P.O.M. and R. M.-R. thank MICINN for Juan de la Cierva fellowships.

References

1. Noyori, R. *Asymmetric Catalysis in Organic Synthesis;* John Wiley & Sons: New York, 1994.
2. Ojima, I., Ed. *Catalytic Asymmetric Synthesis, 3rd ed.;* John Wiley & Son: Hoboken, New Jersey, 2010.
3. Davis, F. A.; Chen, B.-C. In *Houben-Weyl: Methods of Organic Chemistry;* Helmchen, G.; Hoffmann, R. W.; Mulzer, J.; Schaumann, E., Eds.; Georg Thieme Verlag: Stuttgart, 1995; Vol. E 21, p 4497.
4. Zhou, P.; Chen, B.-C.; Davis, F. A. In *Asymmetric Oxidation Reactions;* Katsuki, T., Ed.; Oxford University Press: Oxford, 2001; p 128.
5. Davis, F. A.; Chen, B.-C. *Chem. Rev.* **1992,** *92,* 919–934. doi:10.1021/cr00013a008
6. Davis, F. A.; Haque, M. S. *J. Org. Chem.* **1986,** *51,* 4083–4085. doi:10.1021/jo00371a038
7. Chen, B.-C.; Weismiller, M. C.; Davis, F. A.; Boschelli, D.; Empfield, J. R.; Smith, A. B., III. *Tetrahedron* **1991,** *47,* 173–182. doi:10.1016/S0040-4020(01)80914-5
8. Davis, F. A.; Kumar, A. *J. Org. Chem.* **1992,** *57,* 3337–3339. doi:10.1021/jo00038a021
9. Davis, F. A.; Weismiller, M. C.; Murphy, C. K.; Reddy, R. T.; Chen, B.-C. *J. Org. Chem.* **1992,** *57,* 7274–7285. doi:10.1021/jo00052a050
10. Davis, F. A.; Kumar, A.; Reddy, R. E.; Chen, B.-C.; Wade, P. A.; Shah, S. W. *J. Org. Chem.* **1993,** *58,* 7591–7593. doi:10.1021/jo00078a049
11. Davis, F. A.; Clark, C.; Kumar, A.; Chen, B.-C. *J. Org. Chem.* **1994,** *59,* 1184–1190. doi:10.1021/jo00084a042
12. Momiyama, N.; Yamamoto, H. *J. Am. Chem. Soc.* **2003,** *125,* 6038–6039. doi:10.1021/ja0298702
13. Zhong, G. *Angew. Chem., Int. Ed.* **2003,** *42,* 4247–4250. doi:10.1002/anie.200352097
14. Brown, S. P.; Brochu, M. P.; Sinz, C. J.; MacMillan, D. W. C. *J. Am. Chem. Soc.* **2003,** *125,* 10808–10809. doi:10.1021/ja037096s

15. Hayashi, Y.; Yamaguchi, J.; Hibino, K.; Shoji, M. *Tetrahedron Lett.* **2003,** *44,* 8293–8296. doi:10.1016/j.tetlet.2003.09.057
16. Bøgevig, A.; Sundén, H.; Córdova, A. *Angew. Chem., Int. Ed.* **2004,** *43,* 1109–1112. doi:10.1002/anie.200353018
17. Hayashi, Y.; Yamaguchi, J.; Hibino, K.; Sumiya, T.; Urushima, T.; Shoji, M.; Hashizume, D.; Koshino, H. *Adv. Synth. Catal.* **2004,** *346,* 1435–1439. doi:10.1002/adsc.200404166
18. Shaikh, T. M.; Sudalai, A. *Eur. J. Org. Chem.* **2010,** 3437–3444. doi:10.1002/ejoc.201000169
19. Sabitha, G.; Chandrashekhar, G.; Yadagiri, K.; Yadav, J. S. *Tetrahedron Lett.* **2010,** *51,* 3824–3826. doi:10.1016/j.tetlet.2010.05.063
20. Rawat, V.; Chouthaiwale, P. V.; Chavan, V. B.; Suryavanshi, G.; Sudalai, A. *Tetrahedron Lett.* **2010,** *51,* 6565–6567. doi:10.1016/j.tetlet.2010.10.029
21. Córdova, A.; Sundén, H.; Bøgevig, A.; Johansson, M.; Himo, F. *Chem.–Eur. J.* **2004,** *10,* 3673–3684. doi:10.1002/chem.200400137
22. Kano, T.; Yamamoto, A.; Maruoka, K. *Tetrahedron Lett.* **2008,** *49,* 5369–5371. doi:10.1016/j.tetlet.2008.06.093
23. Kano, T.; Yamamoto, A.; Mii, H.; Takai, J.; Shirakawa, S.; Maruoka, K. *Chem. Lett.* **2008,** *37,* 250–251. doi:10.1246/cl.2008.250
24. Kano, T.; Mii, H.; Maruoka, K. *Angew. Chem., Int. Ed.* **2010,** *49,* 6638–6641. doi:10.1002/anie.201002965
25. Lu, M.; Zhu, D.; Lu, Y.; Hou, Y.; Tan, B.; Zhong, G. *Angew. Chem., Int. Ed.* **2008,** *47,* 10187–10191. doi:10.1002/anie.200803731
26. Kumarn, S.; Shaw, D. M.; Longbottom, D. A.; Ley, S. V. *Org. Lett.* **2005,** *7,* 4189–4191. doi:10.1021/ol051577u
27. Jiao, P.; Kawasaki, M.; Yamamoto, H. *Angew. Chem., Int. Ed.* **2009,** *48,* 3333–3336. doi:10.1002/anie.200900682
28. Ramachary, D. B.; Barbas, C. F., III. *Org. Lett.* **2005,** *7,* 1577–1580. doi:10.1021/ol050246e
29. Chua, P. J.; Tan, B.; Zhong, G. *Green Chem.* **2009,** *11,* 543–547. doi:10.1039/b817950f
30. Wang, W.; Wang, J.; Li, H.; Liao, L. *Tetrahedron Lett.* **2004,** *45,* 7235–7238. doi:10.1016/j.tetlet.2004.08.029
31. Sundén, H.; Dahlin, N.; Ibrahem, I.; Adolfsson, H.; Córdova, A. *Tetrahedron Lett.* **2005,** *46,* 3385–3389. doi:10.1016/j.tetlet.2005.03.085
32. Merino, P.; Tejero, T. *Angew. Chem., Int. Ed.* **2004,** *43,* 2995–2997. doi:10.1002/anie.200301760
33. Janey, J. M. *Angew. Chem., Int. Ed.* **2005,** *44,* 4292–4300. doi:10.1002/anie.200462314
34. Vilaivan, T.; Bhanthumnavin, W. *Molecules* **2010,** *15,* 917–958. doi:10.3390/molecules15020917
35. Ballini, R., Ed. *Eco-friendly synthesis of fine chemicals;* Royal Society of Chemistry: Cambridge, 2009.
36. Martín-Rapún, R.; Fan, X.; Sayalero, S.; Bahramnejad, M.; Cuevas, F.; Pericàs, M. A. *Chem.–Eur. J.* **2011,** *17,* 8780–8783. doi:10.1002/chem.201101513
37. De Vos, D. E.; Vankelecom, I. F. J.; Jacobs, P. A., Eds. *Chiral Catalyst Immobilzation and Recycling;* Wiley-VCH: Weinheim, 2000. doi:10.1002/9783527613144
38. Ding, K.; Uozumi, Y., Eds. *Handbook of Asymmetric Heterogeneous Catalysis;* Wiley-VCH: Weinheim, 2008.
39. Gruttadauria, M.; Giacalone, F.; Noto, R. *Chem. Soc. Rev.* **2008,** *37,* 1666–1688. doi:10.1039/b800704g
40. Jimeno, C.; Sayalero, S.; Pericàs, M. A. Covalent Heterogenization of Asymmetric Catalysts on Polymers and Nanoparticles. In *Heterogenized Homogeneous Catalysts for Fine Chemicals Production: Materials and Processes;* Barbaro, P.; Liguori, F., Eds.; Catalysis By Metal Complexes, Vol. 33; Springer Science: Berlin, 2010; pp 123–171. doi:10.1007/978-90-481-3696-4_4
41. Font, D.; Jimeno, C.; Pericàs, M. A. *Org. Lett.* **2006,** *8,* 4653–4655. doi:10.1021/ol061964j
42. Alza, E.; Rodríguez-Escrich, C.; Sayalero, S.; Bastero, A.; Pericàs, M. A. *Chem.–Eur. J.* **2009,** *15,* 10167–10172. doi:10.1002/chem.200901310
43. Font, D.; Bastero, A.; Sayalero, S.; Jimeno, C.; Pericàs, M. A. *Org. Lett.* **2007,** *9,* 1943–1946. doi:10.1021/ol070526p
44. Meldal, M.; Tornøe, C. W. *Chem. Rev.* **2008,** *108,* 2952–3015. doi:10.1021/cr0783479
45. Tornøe, C. W.; Christensen, C.; Meldal, M. *J. Org. Chem.* **2002,** *67,* 3057–3064. doi:10.1021/jo011148j
46. Rostovtsev, V. V.; Green, L. G.; Folkin, V. V.; Sharpless, K. B. *Angew. Chem., Int. Ed.* **2002,** *41,* 2596–2599. doi:10.1002/1521-3773(20020715)41:14<2596::AID-ANIE2596>3.0.CO;2-4
47. Font, D.; Sayalero, S.; Bastero, A.; Jimeno, C.; Pericàs, M. A. *Org. Lett.* **2008,** *10,* 337–340. doi:10.1021/ol100738h
48. Alza, E.; Pericàs, M. A. *Adv. Synth. Catal.* **2009,** *351,* 3051–3056. doi:10.1002/adsc.200900817
49. Alza, E.; Cambeiro, X. C.; Jimeno, C.; Pericàs, M. A. *Org. Lett.* **2007,** *9,* 3717–3720. doi:10.1021/ol071366k
50. Alza, E.; Sayalero, S.; Cambeiro, X. C.; Martín-Rapún, R.; Miranda, P. O.; Pericàs, M. A. *Synlett* **2011,** 464–468. doi:10.1055/s-0030-1259528
51. Baxendale, I. R.; Ley, S. V. Solid Supported Reagents in Multi-Step Flow Synthesis. In *New Avenues to Efficient Chemical Synthesis;* Seeberger, P. H.; Blume, T., Eds.; Ernst Schering Foundation Symposium Proceedings, Vol. 2006/3; Springer: Heidelberg, 2007; pp 151–185. doi:10.1007/2789_2007_033
52. Mason, B. P.; Price, K. E.; Steinbacher, J. L.; Bogdan, A. R.; McQuade, D. T. *Chem. Rev.* **2007,** *107,* 2300–2318. doi:10.1021/cr050944c
53. Wiles, C.; Watts, P. *Eur. J. Org. Chem.* **2008,** 1655–1671. doi:10.1002/ejoc.200701041
54. Kirschning, A. *Beilstein J. Org. Chem.* **2009,** *5,* No. 15. doi:10.3762/bjoc.5.15
55. Baxendale, I. R.; Deeley, J.; Griffiths-Jones, C. M.; Ley, S. V.; Saaby, S.; Tranmer, G. K. *Chem. Commun.* **2006,** *24,* 2566–2568. doi:10.1039/b600382f
56. Jasper, C.; Adibekian, A.; Busch, T.; Quitschalle, M.; Wittenberg, R.; Kirschning, A. *Chem.–Eur. J.* **2006,** *12,* 8719–8734. doi:10.1002/chem.200600082
57. Bogdan, A. R.; Mason, B. P.; Sylvester, K. T.; McQuade, D. T. *Angew. Chem., Int. Ed.* **2007,** *46,* 1698–1701. doi:10.1002/anie.200603854
58. Smith, C. D.; Baxendale, I. R.; Lanners, S.; Hayward, J. J.; Smith, S. C.; Ley, S. V. *Org. Biomol. Chem.* **2007,** *5,* 1559–1561. doi:10.1039/b702995k
59. Riva, E.; Rencurosi, A.; Gagliardi, S.; Passarella, D.; Martinelli, M. *Chem.–Eur. J.* **2011,** *17,* 6221–6226. doi:10.1002/chem.201100300
60. Kockmann, N.; Gottsponer, M.; Zimmermann, B.; Roberge, D. M. *Chem.–Eur. J.* **2008,** *14,* 7470–7477. doi:10.1002/chem.200800707
61. Carter, C. F.; Baxendale, I. R.; O'Brien, M.; Pavey, J. B. J.; Ley, S. V. *Org. Biomol. Chem.* **2009,** *7,* 4594–4597. doi:10.1039/b917289k

62. Palmieri, A.; Ley, S. V.; Hammond, K.; Polyzos, A.; Baxendale, I. R. *Tetrahedron Lett.* **2009,** *50,* 3287–3289. doi:10.1016/j.tetlet.2009.02.059
63. Patel, M. K.; Davis, B. G. *Org. Biomol. Chem.* **2010,** *8,* 4232–4235. doi:10.1039/c0ob00226g
64. Chandrasekhar, S.; Vijaykumar, B. V. D.; Chandra, B. M.; Reddy, C. R.; Naresh, P. *Tetrahedron Lett.* **2011,** *52,* 3865–3867. doi:10.1016/j.tetlet.2011.05.042
65. Tarleton, M.; McCluskey, A. *Tetrahedron Lett.* **2011,** *52,* 1583–1586. doi:10.1016/j.tetlet.2011.01.096
66. Massi, A.; Cavazzini, A.; Del Zoppo, L.; Pandoli, O.; Costa, V.; Pasti, L.; Giovannini, P. P. *Tetrahedron Lett.* **2011,** *52,* 619–622. doi:10.1016/j.tetlet.2010.11.157
67. Jas, G.; Kirschning, A. *Chem.–Eur. J.* **2003,** *9,* 5708–5723. doi:10.1002/chem.200305212
68. Kirschning, A.; Solodenko, W.; Mennecke, K. *Chem.–Eur. J.* **2006,** *12,* 5972–5990. doi:10.1002/chem.200600236
69. Hessel, V. *Chem. Eng. Technol.* **2009,** *32,* 1655–1681. doi:10.1002/ceat.200900474
70. Wegner, J.; Ceylan, S.; Kirschning, A. *Chem. Commun.* **2011,** *47,* 4583–4592. doi:10.1039/c0cc05060a
71. Geyer, K.; Codée, J. D. C.; Seeberger, P. H. *Chem.–Eur. J.* **2006,** *12,* 8434–8442. doi:10.1002/chem.200600596
72. Marcos, R.; Jimeno, C.; Pericàs, M. A. *Adv. Synth. Catal.* **2011,** *353,* 1345–1352. doi:10.1002/adsc.201000948
73. Pericàs, M. A.; Herrerías, C. I.; Solà, L. *Adv. Synth. Catal.* **2008,** *350,* 927–932. doi:10.1002/adsc.200800108
74. Popa, D.; Marcos, R.; Sayalero, S.; Vidal-Ferran, A.; Pericàs, M. A. *Adv. Synth. Catal.* **2009,** *351,* 1539–1556. doi:10.1002/adsc.200900163
75. Rolland, J.; Cambeiro, X. C.; Rodríguez-Escrich, C.; Pericàs, M. A. *Beilstein J. Org. Chem.* **2009,** *5,* No. 56. doi:10.3762/bjoc.5.56
76. Özçubukçu, S.; Ozkal, E.; Jimeno, C.; Pericàs, M. A. *Org. Lett.* **2009,** *11,* 4680–4683. doi:10.1021/ol9018776
77. Xu, H.; Hu, X.-Z. *J. Polym. Sci., Part A: Polym. Chem.* **1998,** *36,* 2151–2154. doi:10.1002/(SICI)1099-0518(19980915)36:12<2151::AID-POLA22>3.0.CO;2-4
78. Itsuno, S.; Watanabe, K.; El-Shehawy, A. A. *Adv. Synth. Catal.* **2001,** *343,* 89–94. doi:10.1002/1615-4169(20010129)343:1<89::AID-ADSC89>3.0.CO;2-6
79. Itsuno, S.; El-Shehawy, A. A. *Polym. Adv. Technol.* **2001,** *12,* 670–679. doi:10.1002/pat.87
80. Zotova, N.; Franzke, A.; Armstrong, A.; Blackmond, D. G. *J. Am. Chem. Soc.* **2007,** *129,* 15100–15101. doi:10.1021/ja0738881
81. Seebach, D.; Beck, A. K.; Badine, D. M.; Limbach, M.; Eschenmoser, A.; Treasurywala, A. M.; Hobi, R.; Prikoszovich, W.; Linder, B. *Helv. Chim. Acta* **2007,** *90,* 425–471. doi:10.1002/hlca.200790050
82. Nielsen, M.; Worgull, D.; Zweifel, T.; Gschwend, B.; Bertelsen, S.; Jørgensen, K. A. *Chem. Commun.* **2011,** *47,* 632–649. doi:10.1039/c0cc02417a

License and Terms

Beilstein Journal of Organic Chemistry

The application of a monolithic triphenylphosphine reagent for conducting Appel reactions in flow microreactors

Kimberley A. Roper[1], Heiko Lange[1], Anastasios Polyzos[1], Malcolm B. Berry[2], Ian R. Baxendale[1] and Steven V. Ley[*1]

Full Research Paper

Open Access

Address:
[1]Innovative Technology Centre, Department of Chemistry, University of Cambridge, Lensfield Road, Cambridge, Cambridgeshire, CB2 1EW, UK and [2]GlaxoSmithKline, Gunnels Wood Road, Stevenage, Hertfordshire, SG1 2NY, UK

Email:
Steven V. Ley[*] - svl1000@cam.ac.uk

* Corresponding author

Keywords:
Appel reaction; bromination; flow chemistry; solid-supported reagent; triphenylphosphine monolith

Beilstein J. Org. Chem. **2011,** *7,* 1648–1655.
doi:10.3762/bjoc.7.194

Received: 30 September 2011
Accepted: 16 November 2011
Published: 08 December 2011

This article is part of the Thematic Series "Chemistry in flow systems II".

Guest Editor: A. Kirschning

Abstract

Herein we describe the application of a monolithic triphenylphosphine reagent to the Appel reaction in flow-chemistry processing, to generate various brominated products with high purity and in excellent yields, and with no requirement for further off-line purification.

Introduction

Flow chemistry is well-established as a useful addition to the toolbox of the modern research chemist, with advantages accrued through increased efficiency, reproducibility and reaction safety [1-6]. Further benefits can be realised when flow processing techniques are combined with the use of solid-supported reagents and scavengers, which allow telescoping of reactions or in-line removal of byproducts to both increase the purity profile of the output product stream and to, ideally, negate the need for subsequent purification [7-12]. Reagents on macroporous or gel-type beads are commonly used; however, these can suffer from poor mass transfer as well as presenting practical problems caused by the swelling or compression characteristics of the beads related to the solvent employed. To circumvent some of the issues with bead-type supports, monoliths have been developed as replacements for use in continuous-flow synthesis. Monoliths are a single continuous piece of uniformly porous material prepared by precipitation polymerisation of a functionalised monomer [13-17]. They have been shown to have superior chemical efficiency over other bead-based materials, due to enhanced mass transfer governed

by convective flow rather than diffusion, as well as possessing lower void volumes [18]. Practically, their rigid structure is maintained over a wide range of solvents and under reasonable pressure due to the high degree of cross linking, making them easier to use in flow processes. Historically monoliths have traditionally been used to facilitate the isocratic separation of peptides [19]; however, our group and others have shown interest in using monolithic supports to facilitate key chemical transformations [20-31]. We recently reported on the development of a new monolithic triphenylphosphine reagent and its use in the Staudinger aza-Wittig reaction in flow [32,33]. Here we discuss the application of this monolith to the transformation of an alkyl alcohol into the corresponding alkyl bromide by using carbon tetrabromide in the Appel reaction.

In the 1960s Ramirez and co-workers reported the formation of a phosphine–methylene species when triphenylphosphine was mixed with carbon tetrabromide [34]. This was utilised by Appel in the mid 70s, who reported on the use of triphenylphosphine and carbon tetrachloride to convert an alcohol into the corresponding alkyl chloride [35]. The reaction produces byproducts, such as triphenylphosphine oxide, during the reaction that can be very difficult to remove, and extensive, time-consuming purification protocols are often needed in order to isolate the desired product in high purity. We envisioned that the use of an immobilised triphenylphosphine source in combination with continuous-flow technologies could circumvent this problem, allowing easy separation of the phosphine side products through its retention on the solid phase. Examination of the literature revealed that a variety of different bead supports have been used to facilitate this reaction to produce chloro-, bromo- and iodoalkanes from the corresponding alcohols [36-38]. However, the flow characteristics of beads make these techniques undesirable for application in a continuous-flow setup, and the relatively high cost of these reagents limits their widespread use in common laboratory practices. It is particularly interesting that these past investigations have noted an increase in the rate of the reaction on a solid-supported reagent, attributed to neighbouring group participation as a consequence of using a polymeric source of triphenylphosphine [39]. Mechanistically, the Appel reaction has been proposed to proceed via two complex and competing pathways (Scheme 1). In pathway A the reaction is thought to proceed through the simple ion pair **3** formed by the reaction of one equivalent of triphenylphosphine (**1**) and one equivalent of carbon tetrabromide (**2**). This can react with the alcohol substrate to form an oxy-phosphonium **4** along with bromoform (**5**), which is removed under reduced pressure at the end of the reaction along with the solvent. The oxy-phosphonium salt **4** then reacts with the bromide counterion to produce the substituted product **6** along with the triphenylphosphine oxide byproduct (**7**). However, **3** is in equilibrium with the inverted ion pair **8**, which can proceed via pathway B in which **8** reacts with a second equivalent of triphenylphosphine to form the dibromophosphorane **9** and phosphorane **10**. This dibromophosphorane **9** is then able to react with an alcohol to give intermediate **4**, which can proceed to the product, whereas **10** proceeds to a phosphonium salt intermediate **11**. This can then react again with another equivalent of triphenylphosphine and continue reacting in a similar manner until the methylphosphonium salt **15** is formed. This pathway, therefore, can use up to four equivalents of triphenylphosphine to give up to three brominated products. The rate determining step for both pathways has been proposed to be the formation of an active halogenating species **3** or **10** [40]. The increase in the rate of reaction with regards to the Appel reaction, with solid-supported triphenylphosphine compared to the solution-phase counterpart, is proposed to be a result of neighbouring-group participation assisting in the formation of the active species **9** and **10** in pathway B [39,41,42]. Analysis by gas chromatography of chloride Appel reactions indicated that the relative proportion of chloroform was a lot lower than would be expected if both pathways were followed equally in both the solution or solid-phase reactions (5% with solution-based triphenylphosphine and 18–29% with solid-supported triphenylphosphine), indicating that path B is the major pathway in either case [40,43].

Using a polystyrene-based triphenylphosphine monolith we hoped to benefit from the accelerated rate of reaction observed as well as to circumvent problems associated with the use of bead-based immobilised reagents in continuous flow.

Results and Discussion

Formation of the triphenylphosphine monolith

The triphenylphosphine monoliths were formed by precipitation polymerisation of the appropriate phosphine monomer with a cross-linking component and a porogen [32,33]. A stock solution of the functionalised monomer (diphenyl(4-vinylphenyl)phosphine), cross-linking material (divinylbenzene and styrene) and porogen (1-dodecanol) was heated to 50 °C until a homogeneous solution was obtained. The dibenzoyl peroxide was then added and the mixture maintained at elevated temperature (50 °C) until the initiator had dissolved (approximately 5 minutes). The mixture was decanted into a glass column and the ends were sealed with custom-made PTFE end pieces. The column was incubated at 92 °C [44,45] for 48 hours in a Vapourtec R4 heater to give a white polymeric solid, which filled the column. It was noted that the addition of styrene as part of the cross-linking component was necessary to increase the active loading of the monolith during the reactions. Dibenzoyl peroxide was chosen as a radical initiator as it was found to be soluble in the polymerisation mixture at the stock solution

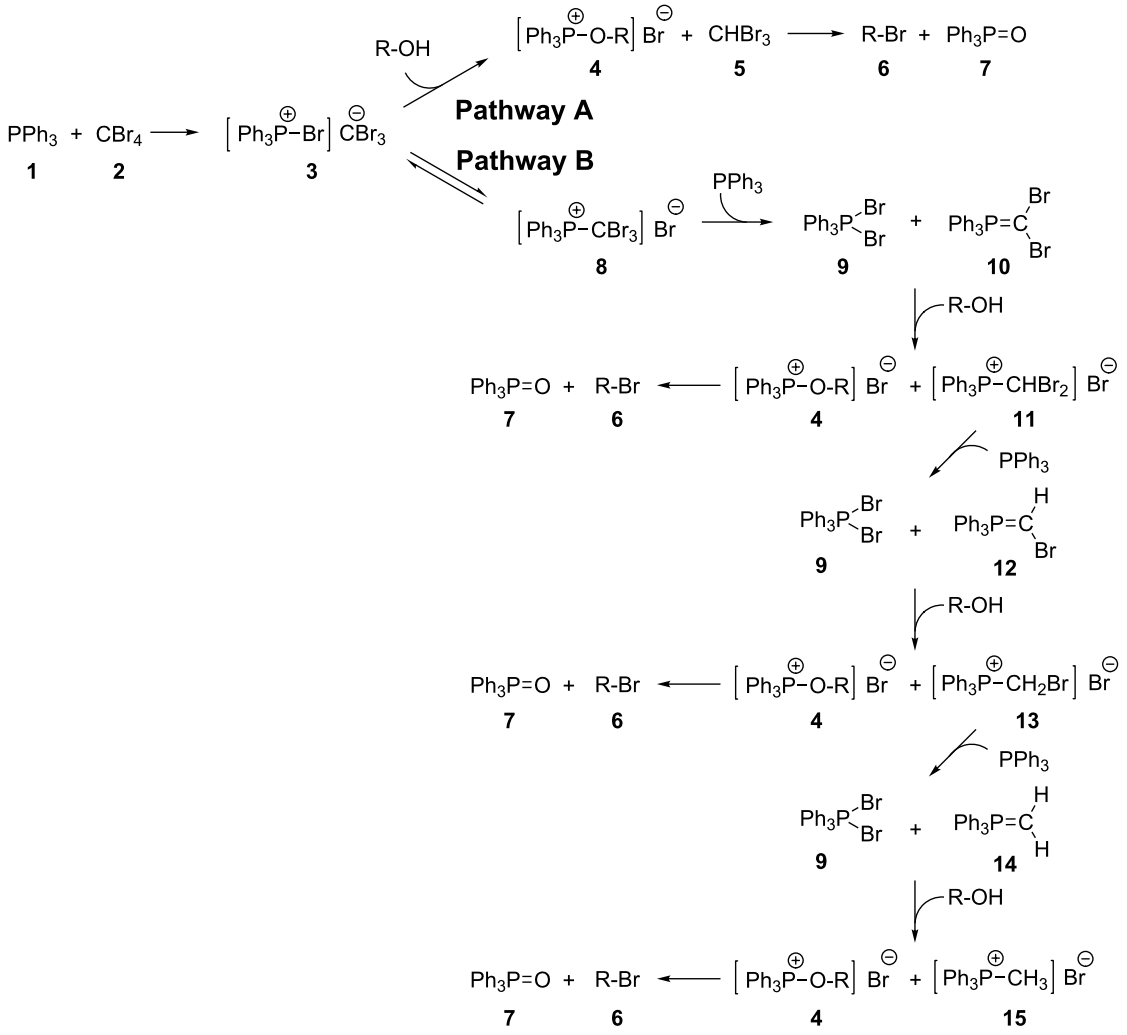

Scheme 1: The two proposed mechanistic pathways for the Appel reaction.

temperature of 50 °C, giving a homogeneous mixture. The slower initiation rate compared to azo-based initiators also ensured the entire polymerisation mixture was at the target temperature before precipitation of polymer chains occurred (approximately one hour after heating at 92 °C), ensuring a more homogeneous polymerisation. Following this polymerisation procedure, the monolith was cooled to room temperature and the end plugs were replaced with standard flow-through connectors. Dry dichloromethane was pumped through the column, which was heated to 60 °C, to elute the porogen and any unreacted monomer starting material. It was found that this polymerisation technique gave consistent, low pressure drops across the monolith, and these were consistent across multiple batches of monolith syntheses, making them ideal for use in a flow-chemistry setup. Elemental analysis showed an approximate loading of 1.87 mmol of phosphorus per gram, giving a calculated loading of 4.68 mmol of phosphorus per monolith, which is comparable to commercially available triphenylphosphine resins.

Loading the monolith

The monolith was then loaded with carbon tetrabromide to give the active species with which to perform the Appel bromination reaction. To achieve this, carbon tetrabromide in dichloromethane [46] was recirculated through the monolith for 16 hours at room temperature (Scheme 2), resulting in a colour change from white (a) to a light brown colour (b) (shown in Figure 1). Elemental analysis revealed that the monolith consisted of 27.6% bromine showing that the carbon tetrabromide had loaded onto the monolith and there was an average of less than one molecule of carbon tetrabromide per phosphorus atom. This suggests that a complex mixture of phosphorus species is present within the monolith. Triphenylphosphine oxide, from the starting material, and unreacted triphenyl-

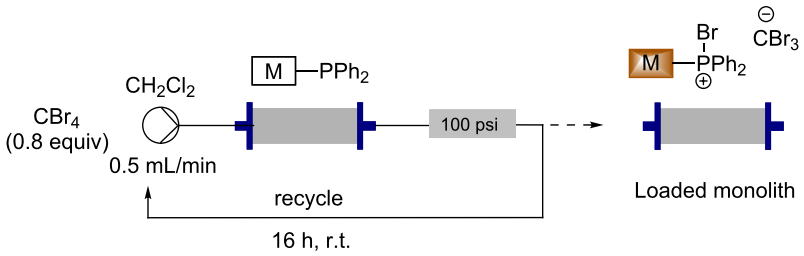

Scheme 2: Functionalisation of the triphenylphosphine monolith by using carbon tetrabromide in a recycling process.

phosphine, due to inaccessible sites within the monolith, are probably present along with potentially a complex combination of active brominating species. If the monolith reacts in the way reported in previous literature, then both mechanistic pathways are followed and therefore many different active brominating species are present (**3**, **8**, **9** and **10**). Although it is thought that a complex mixture is present, the loaded brominating monolith is represented as intermediate **3** for simplicity in the schemes that follow.

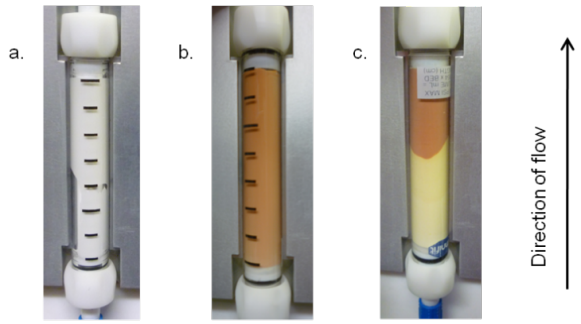

Figure 1: a. Unfunctionalised triphenylphosphine monolith; b. Monolith after fuctionalisation with carbon tetrabromide; c. Monolith after partial consumption of the active brominating agent.

Reaction of this monolith with an alcohol resulted in a further colour change from a brown monolith (b) to a depleted monolith (c) (Figure 1), with a pale yellow region corresponding to the triphenylphosphine oxide, or potentially later intermediates in pathway B, formed in the Appel reaction. This same colour change was initially observed during the loading protocol when approximately one-fifth of the coloured region of the monolith was transformed to the pale yellow colour. In this case, analysis of the recycled solvent suggested the presence of 1-bromododecane and that the dodecanol porogen was not being fully removed during the initial flushing procedure, but instead was being brominated during the subsequent loading process. Unfortunately attempts to adapt the solvent system to ensure complete dodecanol removal before loading were unsuccessful. Scavenging the dodecanol in the loading process by means of a column of polymer-supported tosyl chloride or by adding calcium chloride to the recycling carbon tetrabromide solution was also unsuccessful. Although the presence of dodecanol caused a partially depleted monolith during the loading process, these monoliths were still successfully used for the Appel reaction. No detrimental effect on the reaction products was observed, although obviously a lower active loading of the monolith was observed. In order to achieve the maximum active loading of 1.3 mmol for a monolith, a previously loaded monolith was placed in-line with the unloaded triphenylphosphine monolith in the recycling procedure with carbon tetrabromide.

Bromination reactions in flow with the loaded triphenylphosphine monolith

With the functionalised, active brominating monolith in hand, the transformation of an alcohol into the corresponding bromide in flow was investigated. By employing the commercially available Uniqsis FlowSyn, a 0.1 M solution of the alcohol in dry dichloromethane was prepared and loaded into the sample loop (2 mL). This solution was then switched in-line to be pumped through the monolith at a flow rate of 0.5 mL/min, the output stream was collected for 1 hour and the solvent removed (Scheme 3). For benzylic and sterically unhindered alcohols (Table 1, entries 1–6), complete conversion was achieved by a single pass of the alcohol through the monolith, requiring only solvent removal to yield the pure brominated product in high

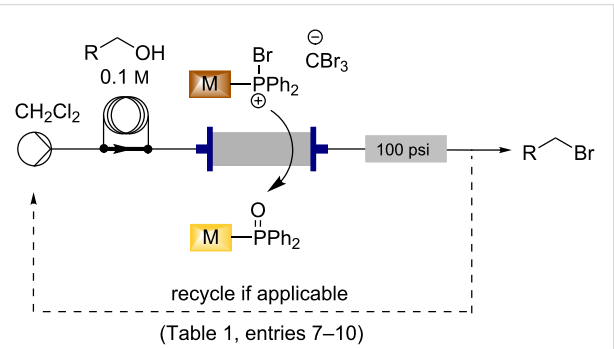

Scheme 3: Flow synthesis of bromides from alcohols by using the functionalised triphenylphosphine monolith.

Table 1: Bromides prepared from the corresponding alcohols by using the functionalised triphenylphosphine monolith.

Entry	Starting material	Product	Conversion after one pass (%)[a]	Time required for full conversion[b]	Isolated yield[c] (%)
1	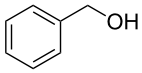	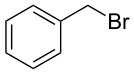	100	–	80[d]
2	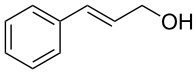	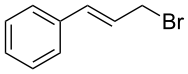	100	–	82
3	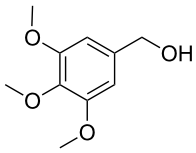	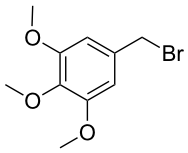	100	–	92
4	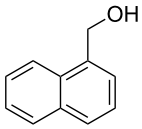	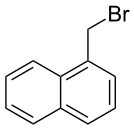	100	–	74
5	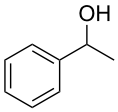	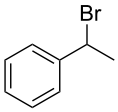	100	–	92
6	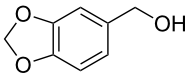	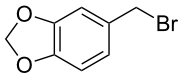	100	–	91
7	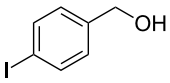	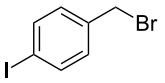	94	1 h 15 min	95
8	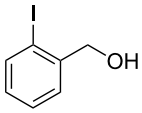	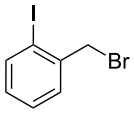	84	1 h 15 min	95
9	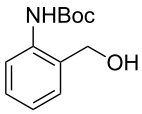	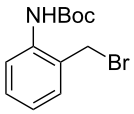	85	2 h 30 min	68[e]
10	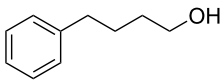	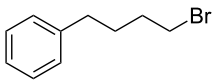	<0.5	14 h	77

[a]One pass through the monolith at 0.5 mL/min, percentage conversion determined by ^{1}H NMR analysis, [b]substrates recirculated through the monolith at 0.5 mL/min until full consumption of starting material indicated by TLC, [c]reactions performed on a 0.2 mmol scale, [d]volatile product, [e]corresponding solution-phase triphenylphosphine batch process yielded 52% pure product after chromatography.

yield. An analogous reaction with polymer-supported triphenylphosphine beads, loaded and reacted in an identical way, only gave 26% conversion to halogenated material, which was impure by ^{1}H NMR for cinnamyl bromide (Table 1, entry 2). For less-activated substrates, such as the iodo-substituted benzylic alcohols (Table 1, entries 7 and 8), a single pass gave incomplete conversion to the bromide, resulting in a mixture of the starting alcohol and the bromide product upon removal of the solvent. Conversion to the bromide could be increased by decreasing the flow rate; however, to obtain complete conversion it was found to be necessary to recycle the flow stream through the monolith. When a recycling protocol was employed, upon full consumption of the starting material by thin-layer chromatography the input was changed to a fresh solution of dichloromethane. The system was then flushed for a further 45 minutes at 0.5 mL/min to yield the pure bromide product following removal of the solvent. An investigation of the substrate scope revealed that starting materials containing unprotected amines could not be transformed into the corresponding bromides. Little or no mass return was observed

suggesting that an aminophosphonium species was formed on the monolith in accordance with similar reactions between triphenylphosphine, bromine and amines [47]. It was possible to brominate the monoprotected aniline (Table 1, entry 9) by using the triphenylphosphine monolith, but recycling for a longer time was required, and resulted in a lower isolated yield than most of the other substrates. For the nonactivated alkyl alcohol (Table 1, entry 10), recycling for 14 hours was found to be necessary to achieve complete conversion to the desired bromide. While in this work the benzylic brominated products were not used in subsequent flow reactions, such as alkylations, these processes have been reported by us [48] and others [49] using continuous-flow technologies.

A single monolith can be used for many different alcohols with no cross-contamination detected by ^{1}H NMR between substrates. It was found that the colour of the monolith can be used as an approximate indication of the degree of loading of active brominating species on the monolith, and the off-white, pale yellow region of triphenylphosphine oxide, or later stage intermediate, was formed in a proportional manner to the quantity of the substrate that was passed through the monolith (Figure 2). Elemental analysis revealed that the off-white region contained 19.8% bromine, implying that although bromine is consumed proportionally with the consumption of the dark-coloured areas of the monolith, there is nevertheless still bromine left on the monolith. This bromine could be present in hard-to-access active sites within the polymeric structure of the monolith, but could also be accounted for by some of the late intermediates in pathway B (**10**–**15** in Scheme 1). The conversion of a particular substrate did not decrease with continued use of the monolith until the monolith became completely pale yellow, at which point the activity of the monolith decreased sharply. Up to this point the conversion of a substrate was comparable at the beginning and at the end of the monolith use. After the brown colouration had been diminished through bromination reactions, the monolith activity reduced significantly, giving 19% conversion to halogenated product by using a previously readily converted substrate (Table 1, entry 6). Each monolith was found to convert 1.3 mmol of alcohol before the conversion dropped.

It was found that heating the monolith increased the rate of reaction and thus could be used to promote the reaction of the aniline substrate (Table 1, entry 9) in one pass, albeit with a lower isolated yield [50]. While investigating the feasibility of heating the monolith in order to drive the less activated 4-iodobenzyl alcohol (Table 1, entry 7) to completion, it was found that heating the monolith resulted in the production of an impurity, at 29.7% conversion by ^{1}H NMR (with 64.5% conversion to the bromide). This was identified as 1-(chloromethyl)-4-iodobenzene, i.e., the starting material underwent chlorination rather than bromination. The two halogenated products could not be separated by flash column chromatography. Interestingly this impurity was also observed in small amounts when a loaded monolith was stored for prolonged periods at room temperature in the presence of dichloromethane. The Appel reaction using 4-iodobenzyl alcohol (Table 1, entry 7) was repeated with a loaded monolith stored in dichloromethane at room temperature for 9 days and resulted in a conversion of less than 3% to the chloride by ^{1}H NMR. The conversion to the chloride was found to increase with increased flushing of dichloromethane through the monolith, implying that the source of the chloride was through exchange with the dichloromethane solvent. From our initial screens, dichloromethane was found to be the optimum solvent for monolith loading and the bromination reactions. As this impurity was only observed at elevated temperatures or with monoliths that had been stored over long periods of time, we feel that we have demonstrated that it is not a significant problem for the main

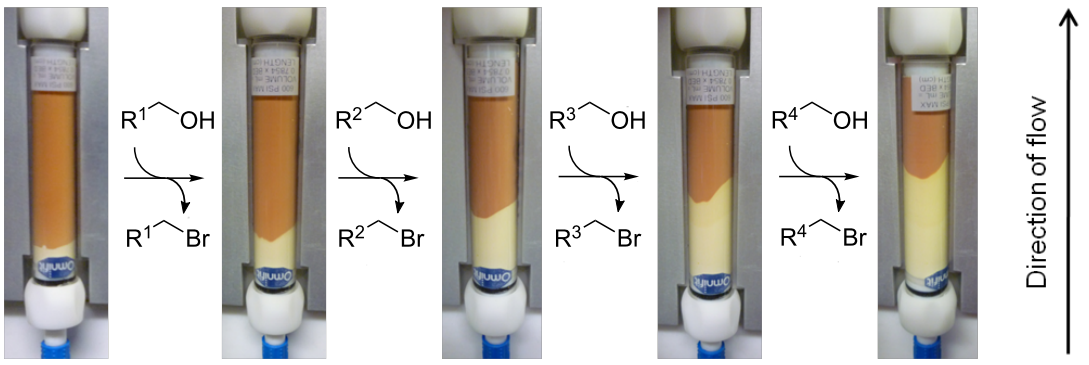

Figure 2: Linear decrease of the brown decolourisation.

aim of the reagent, which is to convert alcohols into bromides without the need for purification.

Conclusion

In summary, the monolithic triphenylphosphine reagent recently developed by our group [32,33] was also successfully applied to facilitate the Appel reaction. An active brominating species was formed readily by recirculating carbon tetrabromide through the monolith. This loaded monolith was then successfully applied to the Appel reaction, allowing the synthesis of the corresponding brominated product from an alcohol in high purity and yield, with only a simple removal of the solvent required. Activated benzylic alcohols were transformed to the desired bromide with a single pass, whereas sterically hindered or alkyl alcohols required a recycling process through the monolith to reach complete conversion to the brominated product. Heating the monolith in an attempt to accelerate the reaction was found to be unsuccessful due to the decomposition of the active brominating salt, resulting in the formation of an undesired chloride byproduct.

Supporting Information

Supporting information features full experimental details and data for the reactions performed above.

Supporting Information File 1

Experimental details.
[http://www.beilstein-journals.org/bjoc/content/supplementary/1860-5397-7-194-S1.pdf]

Acknowledgements

We thank GlaxoSmithKline (Stevenage) for studentship support (KAR), the Alexander von Humboldt Foundation (HL), the EPSRC (KAR & TP), the Royal Society University Research Fellowship (IRB) and the BP 1702 Fellowship (SVL) for financial support. We gratefully acknowledge Hokko Chemical Industry Co., Ltd. for their kind donation of diphenyl(4-vinylphenyl)phosphine).

References

1. Wenger, J.; Ceylan, S.; Kirschning, A. *Chem. Commun.* **2011,** *47,* 4583–4592. doi:10.1039/C0CC05060A
2. Webb, D.; Jamison, T. F. *Chem. Sci.* **2010,** *1,* 675–680. doi:10.1039/c0sc00381f
3. Baxendale, I. R.; Hayward, J. J.; Lanners, S.; Ley, S. V.; Smith, C. D. Heterogeneous Reactions. In *Microreactors in Organic Synthesis and Catalysis;* Wirth, T., Ed.; Wiley-VCH: Weinheim, Germany, 2008; pp 84–122.
4. Baumann, M.; Baxendale, I. R.; Ley, S. V. *Mol. Diversity* **2011,** *15,* 613–630. doi:10.1007/s11030-010-9282-1
5. Ahmed-Omer, B.; Brandt, J. C.; Wirth, T. *Org. Biomol. Chem.* **2007,** *5,* 733–740. doi:10.1039/b615072a
6. Baumann, M.; Baxendale, I. R.; Ley, S. V.; Smith, C. D.; Tranmer, G. K. *Org. Lett.* **2006,** *8,* 5231–5234. doi:10.1021/ol061975c
7. Baxendale, I. R.; Ley, S. V. Solid Supported Reagents in Multi-Step Flow Synthesis. In *New Avenues to Efficient Chemical Synthesis: Emerging Technologies. Ernst Schering Foundation Symposium Proceedings 06.3;* Seeberger, P. H.; Blume, T., Eds.; Springer-Verlag: Berlin, Heidelberg, Germany, 2007; pp 151–185.
8. Hodge, P. *Ind. Eng. Chem. Res.* **2005,** *44,* 8542–8553. doi:10.1021/ie040285e
9. Kirschning, A.; Solodenko, W.; Mennecke, K. *Chem.–Eur. J.* **2006,** *12,* 5972–5990. doi:10.1002/chem.200600236
10. Baxendale, I. R.; Deeley, J.; Griffiths-Jones, C. M.; Ley, S. V.; Saaby, S.; Tranmer, G. K. *Chem. Commun.* **2006,** 2566–2568. doi:10.1039/b600382f
11. Baxendale, I. R.; Griffiths-Jones, C. M.; Ley, S. V.; Tranmer, G. K. *Synlett* **2006,** *3,* 427–430. doi:10.1055/s-2006-926244
12. Ley, S. V.; Baxendale, I. R.; Bream, R. N.; Jackson, P. S.; Leach, A. G.; Longbottom, D. A.; Nesi, M.; Scott, J. S.; Storer, R. I.; Taylor, S. J. *J. Chem. Soc., Perkin Trans. 1* **2000,** 3815–4195. doi:10.1039/b006588i
13. Švec, F.; Tennikova, T. B. Historical Review. In *Monolithic Materials: Preparation, Properties and Applications;* Švec, F.; Tennikova, T. B.; Deyl, Z., Eds.; Journal of Chromatography Library, Vol. 67; Elsevier Science B. V.: Amsterdam, The Netherlands, 2003; pp 1–15.
14. Švec, F.; Fréchet, J. M. J. Rigid Macroporous Organic Polymer Monoliths Prepared by Free Radical Polymerization. In *Monolithic Materials: Preparation, Properties and Applications;* Švec, F.; Tennikova, T. B.; Deyl, Z., Eds.; Journal of Chromatography Library, Vol. 67; Elsevier Science B. V.: Amsterdam, The Netherlands, 2003; pp 19–50.
15. Buchmeiser, M. R. *Polymer* **2007,** *48,* 2187–2198. doi:10.1016/j.polymer.2007.02.045
16. Svec, F.; Fréchet, J. M. J. *Science* **1996,** *273,* 205–211. doi:10.1126/science.273.5272.205
17. Kunz, U.; Kirschning, A.; Wen, H.-L.; Solodenko, W.; Cecilia, R.; Kappe, C. O.; Turek, T. *Catal. Today* **2005,** *105,* 318–324. doi:10.1016/j.cattod.2005.06.046
18. Peters, E. C.; Svec, F.; Fréchet, J. M. J. *Adv. Mater.* **1999,** *11,* 1169–1181. doi:10.1002/(SICI)1521-4095(199910)11:14<1169::AID-ADMA1169>3.0.CO;2-6
19. Svec, F.; Fréchet, J. M. *J. Anal. Chem.* **1992,** *64,* 820–822. doi:10.1021/ac00031a022
20. Lange, H.; Capener, M. J.; Jones, A. X.; Smith, C. J.; Nikbin, N.; Baxendale, I. R.; Ley, S. V. *Synlett* **2011,** *6,* 869–873. doi:10.1055/s-0030-1259923
21. Baumann, M.; Baxendale, I. R.; Kirschning, A.; Ley, S. V.; Wegner, J. *Heterocycles* **2011,** *82,* 1297–1316. doi:10.3987/COM-10-S(E)77
22. Baumann, M.; Baxendale, I. R.; Martin, L. J.; Ley, S. V. *Tetrahedron* **2009,** *65,* 6611–6625. doi:10.1016/j.tet.2009.05.083
23. Mennecke, K.; Kirschning, A. *Beilstein J. Org. Chem.* **2009,** *5,* No. 21. doi:10.3762/bjoc.5.21
24. Baumann, M.; Baxendale, I. R.; Ley, S. V.; Nikbin, N.; Smith, C. D. *Org. Biomol. Chem.* **2008,** *6,* 1587–1593. doi:10.1039/b801634h
25. Nikbin, N.; Ladlow, M.; Ley, S. V. *Org. Process Res. Dev.* **2007,** *11,* 458–462. doi:10.1021/op7000436
26. Altava, B.; Burguete, M. I.; García-Verdugo, E.; Luis, S. V.; Vicent, M. J. *Green Chem.* **2006,** *8,* 717–726. doi:10.1039/b603494b

27. Kirschning, A.; Altwicker, C.; Dräger, G.; Harders, J.; Hoffmann, N.; Hoffmann, U.; Schönfeld, H.; Solodenko, W.; Kunz, U. *Angew. Chem., Int. Ed.* **2001,** *40,* 3995–3998. doi:10.1002/1521-3773(20011105)40:21<3995::AID-ANIE3995>3.0.CO;2-V
28. Solodenko, W.; Wen, H.; Leue, S.; Stuhlmann, F.; Sourkouni-Argirusi, G.; Jas, G.; Schönfeld, H.; Kunz, U.; Kirschning, A. *Eur. J. Org. Chem.* **2004,** 3601–3610. doi:10.1002/ejoc.200400194
29. Kunz, U.; Schönfeld, H.; Kirschning, A.; Solodenko, W. *J. Chromatogr., A* **2003,** *1006,* 241–249. doi:10.1016/S0021-9673(03)00556-9
30. Burguete, M. I.; García-Verdugo, E.; Vicent, M. J.; Luis, S. V.; Pennemann, H.; Graf von Keyserling, N.; Martens, J. *Org. Lett.* **2002,** *4,* 3947–3950. doi:10.1021/ol026805o
31. Tripp, J. A.; Stein, J. A.; Svec, F.; Fréchet, J. M. J. *Org. Lett.* **2000,** *2,* 195–198. doi:10.1021/ol9912837
32. Smith, C. J.; Smith, C. D.; Nikbin, N.; Ley, S. V.; Baxendale, I. R. *Org. Biomol. Chem.* **2011,** *9,* 1927–1937. doi:10.1039/c0ob00813c
33. Smith, C. J.; Nikbin, N.; Ley, S. V.; Lange, H.; Baxendale, I. R. *Org. Biomol. Chem.* **2011,** *9,* 1938–1947. doi:10.1039/c0ob00815j
34. Desai, N. B.; McKelvie, N.; Ramirez, F. *J. Am. Chem. Soc.* **1962,** *84,* 1745–1747. doi:10.1021/ja00868a057
35. Appel, R. *Angew. Chem., Int. Ed. Engl.* **1975,** *14,* 801–811. doi:10.1002/anie.197508011
36. Choi, M. K. W.; He, H. S.; Toy, P. H. *J. Org. Chem.* **2003,** *68,* 9831–9834. doi:10.1021/jo035226+
37. Anilkumar, G.; Nambu, H.; Kita, Y. *Org. Process Res. Dev.* **2002,** *6,* 190–191. doi:10.1021/op010094c
38. Årstad, E.; Barrett, A. G. M.; Hopkins, B. T.; Köbberling, J. *Org. Lett.* **2002,** *4,* 1975–1977. doi:10.1021/ol026008q
39. Harrison, C. R.; Hodge, P. *J. Chem. Soc., Chem. Commun.* **1978,** 813–815. doi:10.1039/C39780000813
40. Harrison, C. R.; Hodge, P.; Hunt, B. J.; Khoshdel, E.; Richardson, G. *J. Org. Chem.* **1983,** *48,* 3721–3728. doi:10.1021/jo00169a022
41. Hodge, P.; Khoshdel, E. *J. Chem. Soc., Perkin Trans. 1* **1984,** 195–198. doi:10.1039/P19840000195
42. Sherrington, D. C.; Craig, D. J.; Dagleish, J.; Domin, G.; Taylor, J.; Meehan, G. V. *Eur. Polym. J.* **1977,** *13,* 73–76. doi:10.1016/0014-3057(77)90140-9
43. Tömöskozi, I.; Gruber, L.; Radics, L. *Tetrahedron Lett.* **1975,** *16,* 2473–2476. doi:10.1016/0040-4039(75)80041-4
44. At 92 °C the half life of dibenzoyl peroxide is 1 hour, hence this temperature was used for a long initiation time.
45. Sanchez, J.; Myers, T. N. Peroxide Initiators (overview). In *Polymeric Materials Encyclopedia;* Salamone, J. C., Ed.; CRC Press Inc.: Boca Raton, USA, 1996; Vol. 7, pp 4927–4938. See for half-life information for dibenzyol peroxide.
46. 5 mmol carbon tetrabromide (1.5 g, 0.81 equivalents per mmol of triphenylphosphine equivalent incorporated into monolith) was dissolved in 40 mL dry dichloromethane (0.11 M). Approximately 2.3 mmol CBr_4 (0.75 g) was recovered by mass, indicating that approximately 2.3 mmol was consumed during the loading process.
47. de la Fuente, G. F.; Huheey, J. E. *Phosphorus, Sulfur Silicon Relat. Elem.* **1993,** *78,* 23–36. doi:10.1080/10426509308032419
48. Hornung, C. H.; Mackley, M. C.; Baxendale, I. R.; Ley, S. V. *Org. Process Res. Dev.* **2007,** *11,* 399–405. doi:10.1021/op700015f
49. He, P.; Haswell, S. J.; Fletcher, P. D. I. *Sens. Actuators, B* **2005,** *105,* 516–520. doi:10.1016/j.snb.2004.07.013
50. Heating the monolith to 50 °C gave full conversion of the amide with one pass through the monolith at a flow rate of 0.4 mL/min. This gave an isolated yield of 52%, equivalent to the solution-phase isolated yield.

License and Terms

Beilstein Journal of Organic Chemistry

Continuous proline catalysis via leaching of solid proline

Suzanne M. Opalka[1], Ashley R. Longstreet[2] and D. Tyler McQuade[*2]

Full Research Paper

Open Access

Address:
[1]Department of Chemistry and Chemical Biology, Cornell University, Ithaca, NY 14853 and [2]Department of Chemistry and Biochemistry, Florida State University, Tallahassee, FL 32306

Email:
D. Tyler McQuade[*] - mcquade@chem.fsu.edu

* Corresponding author

Keywords:
aminoxylation; flow chemistry; heterogeneous catalysis; packed-bed microreactor; proline/thiourea catalysis

Beilstein J. Org. Chem. **2011,** *7,* 1671–1679.
doi:10.3762/bjoc.7.197

Received: 09 September 2011
Accepted: 14 November 2011
Published: 14 December 2011

This article is part of the Thematic Series "Chemistry in flow systems II".

Guest Editor: A. Kirschning

Abstract

Herein, we demonstrate that a homogeneous catalyst can be prepared continuously via reaction with a packed-bed of a catalyst precursor. Specifically, we perform continuous proline catalyzed α-aminoxylations using a packed-bed of L-proline. The system relies on a multistep sequence in which an aldehyde and thiourea additive are passed through a column of solid proline, presumably forming a soluble oxazolidinone intermediate. This transports a catalytic amount of proline from the packed-bed into the reactor coil for subsequent combination with a solution of nitrosobenzene, affording the desired optically active α-aminooxy alcohol after reduction. To our knowledge, this is the first example in which a homogeneous catalyst is produced continuously using a packed-bed. We predict that the method will not only be useful for other L-proline catalyzed reactions, but we also foresee that it could be used to produce other catalytic species in flow.

Introduction

Continuous flow chemistry [1-3], performed in small dimension tubing or channels, differs from batch chemistry in that mixing and heat transfer are significantly faster and can be precisely controlled. In addition, continuous technology enables the generation and immediate use of unstable or hazardous intermediates [4-9] as well as the combination of many reactions in series to achieve multistep synthesis [9-13]. Despite the many favorable attributes of micro- and mesoflow reactors, the continuous use of solids remains challenging. The introduction of solids to a flow reactor is particularly difficult as most pumps function poorly with even small particulates, which in turn can result in channel clogging. Although the use of solids in flow has been the topic of a number of recent papers, they have focused on overcoming the challenges associated with the introduction and suspension of solid reagents and starting materials [14-18]. An area that has received less attention is the continuous use of solid catalysts (and catalyst precursors) that only partially or slowly dissolve into or react with the solution.

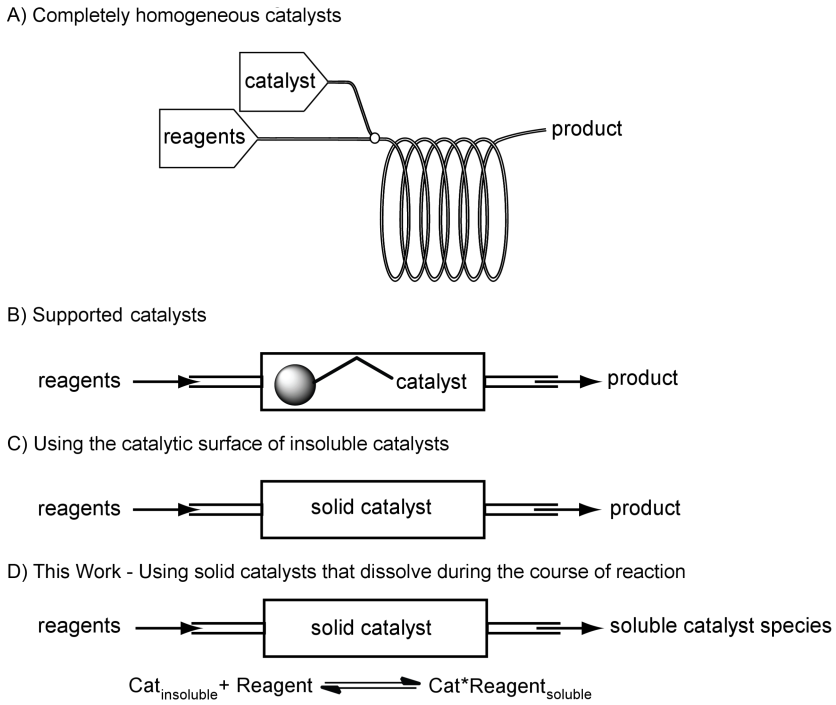

Figure 1: Methods for catalyst use in flow.

(See Figure 1 for a comparison of solid catalysts that are used in flow.) Proline is an example of such a catalyst [19] (others include zero-valent transition metals, many solid acid catalysts, and other secondary amine catalysts). Proline is often added to a reaction mixture as a solid, and only a few mole percent dissolves into solution at any given time. Since proline is fairly inexpensive, it is an attractive test catalyst for the design of new methods to utilize solid catalysts or catalyst precursors in flow.

Current strategies involving the use of catalysts with limited solubility in flow rely on them being supported on resins or polymers (Figure 1A and B). This can be an attractive method as the catalysts are often easily recycled [20-24]. Finding a suitable solid support for a reaction, however, can prove time-consuming and expensive. In addition, care must be taken to identify a support that provides both high activity for the catalyst and appropriate swelling properties to enable adequate mass transport (often the best solvent for the resin will not be the best for the reaction) [25-29]. With researchers becoming increasingly interested in developing continuous-flow processes, the rapid assessment of catalyst conditions necessary for potential synthetic routes requires a simple approach to deal with limited-solubility catalysts.

We have both a long-standing interest in the production, use and management of solids [30-33] and reactions [34,35] in flow as well as in proline catalysis [36,37]. This prompted us to consider new strategies for the implementation of proline in a continuous-flow system without resorting to proline analogues or tethered catalysts [38-40]. Achieving this goal would enable us and others to perform proline-catalyzed reactions, aldol [41-43] and Mannich [42] reactions as well as α-functionalizations (α-aminoxylation, α-amination or α-halogenations), continuously [44].

We hypothesized that the proline-catalyzed α-aminoxylation could be implemented in flow with reasonably short residence times using a urea additive. Many researchers, including us [36,37], have found that urea [45] additives increase the rate of various proline-catalyzed reactions [46-50]. The role that ureas play remains unclear, and a number of hypotheses have been suggested. Initially, researchers gathered ^{1}H NMR, UV, and fluorescence data to show that ureas enhance the solubility of proline through a host–guest interaction between the urea and proline carboxylate: A substrate-independent model [49,50]. However, it has been proposed that substrate–urea–proline interactions may also contribute to the rate enhancement [50]. Our group observed that a urea tethered to a tertiary amine increases the rate of a number of batch reactions, including the α-aminoxylation reaction [36,37]. For the α-aminoxylation reaction, we proposed that the urea promotes formation of the active enamine intermediate through breakdown of the putative oxazolidinone intermediate: A substrate-dependent model. Here, we

report that a packed-bed of solid proline can be used to create a homogeneous catalyst, and we use this system to perform continuous α-aminoxylations. Not only do we illustrate a unique use of catalysts in flow, but we provide additional insight into the role of additives in proline-catalyzed reactions.

Results and Discussion

In our previously published batch work, we found that the combination of L-proline and bifunctional urea **3a** greatly accelerated the rate of α-aminoxylation (Scheme 1). It was shown that a longer linker between the urea and amine functionality enhanced the rate of reaction (see Supporting Information of [37]). The rate enhancement enabled the reaction to be performed in greener solvents such as ethyl acetate instead of the more commonly used chloroform. We have a long standing interest in the conversion of the reaction into a continuous process, but recognized that the solubility of proline would hinder its use in flow. To circumvent this problem, we envisioned using a cartridge of solid proline as a precatalyst source, whereby the flow of a combination of solvents, reactants and cocatalysts through the packed-bed would produce the active, homogeneous, oxazolidinone catalyst.

To test our hypothesis, we used a Vapourtec R series reactor system [51] consisting of HPLC pumps for solvent and reagent inputs, a low-temperature tube reactor containing a glass column packed with 1 g of proline, and a low-temperature 10 mL PFA coil-tube reactor in which each reagent stream could be precooled prior to mixing (Figure 2). As we demonstrate below, the success of our experiments depended on the ability of the system to heat, or cool, the packed-bed and the reaction coil independently of one another.

Using this device configuration, experiments were performed to identify the conditions that favor the reaction between the aldehyde and the proline packed-bed in order to yield enough soluble oxazolidinone catalyst to support rapid α-aminoxylations. We were particularly interested to determine which substrate and additive components were necessary to dissolve the solid proline. Since the inherent solubility of proline in ethyl acetate is very low, we extrapolated that this solvent alone would be insufficient to dissolve enough catalytic proline [37,52]. Furthermore, we knew from our previous batch work that a urea additive would be beneficial to provide reaction rates suitable for use in flow [37].

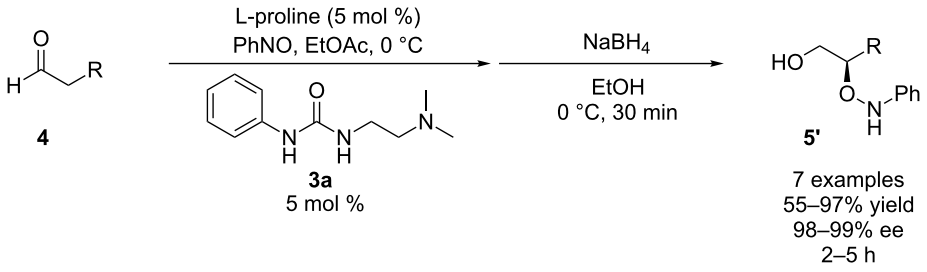

Scheme 1: Prior results for batch α-aminoxylation reaction.

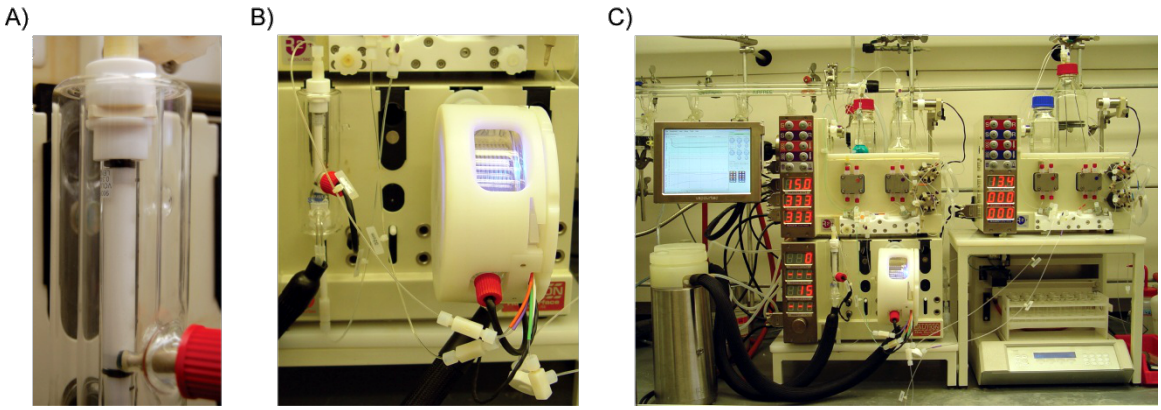

Figure 2: General reactor setup. A) A glass Omnifit column is packed with 1 g of proline. B) The column is then placed in-line with a 10 mL PFA coil-tube reactor. C) The components are connected to HPLC pumps for solvent and reagent inputs. The reactor is controlled by a computer in order to program the timing of the reagent and solvent inputs and fraction collection.

Therefore, various combinations of reagents and catalysts entering the packed proline column were investigated. For our initial experiments we selected a 15 min coil residence time and temperature of 0 °C for both the column and the coil, based on our prior knowledge of the reaction in batch. We began by determining the necessity of a urea cocatalyst. We were surprised to find that when hexanal alone was passed through the column and combined with nitrosobenzene in the coil, the desired product was not detected by crude ^{1}H NMR analysis (Table 1, entry 1). This indicates that, with this reactor setup, the reaction is too slow without a urea additive to be a viable method. Additionally, flowing thiourea **3b** (0.047 M in EtOAc) through the proline packed-bed prior to combination with the other reaction partners resulted in no detectable reaction (Table 1, entry 2). This shows that thiourea **3b** alone cannot solubilize enough proline to support the reaction. When hexanal alone, however, was passed through the column and combined with the remaining reagents in the coil (including thiourea **3b**) the reaction produced 27% yield and 99% ee (Table 1, entry 3). This indicates that the aldehyde alone can react with solid proline to produce a reactive homogeneous catalyst. However, when both thiourea **3b** and hexanal were used in the same stock solution and passed through the column the reaction attained 43% yield with 98% ee (Table 1, entry 4). This increase in yield, relative to when hexanal alone was passed through the column, suggests that the rate of proline leaching is enhanced by the addition of thiourea **3b**. Consequently, it appears that our observed rate enhancements with thiourea **3b** cannot be attributed to a model involving only urea–proline interactions resulting in enhanced solubility, and that substrate–urea–proline interactions are responsible for the observed reactivity when using this combination of thiourea, substrate and proline.

We were delighted to find that further increasing the residence time of the coil to 20 min with the same reagent configuration resulted in 69% yield (Table 2, entry 2). For further experiments, we therefore used a setup in which a thiourea/aldehyde stock solution was passed through the proline packed-bed before entering the coil and reacting with nitrosobenzene.

As all of the reactions performed in Table 1 had the same residence time and temperature, the yield can be used as a rough proxy for reaction rate. We conjecture, based on our prior work in this area, that the aldehyde slowly reacts with solid L-proline in the cartridge to form the soluble oxazolidinone intermediate (Figure 3, part C), leaching proline out of the column and into the coil for reaction with nitrosobenzene. The increased yield observed when both hexanal and thiourea **3b** were passed through the proline-bed suggests that more catalyst was drawn into the solution, resulting in a faster reaction rate. In our prior batch experiments, we proposed that the urea aided the breakdown of the oxazolidinone intermediate (Figure 3, part C) for

Table 1: Screening of the reactor setup.

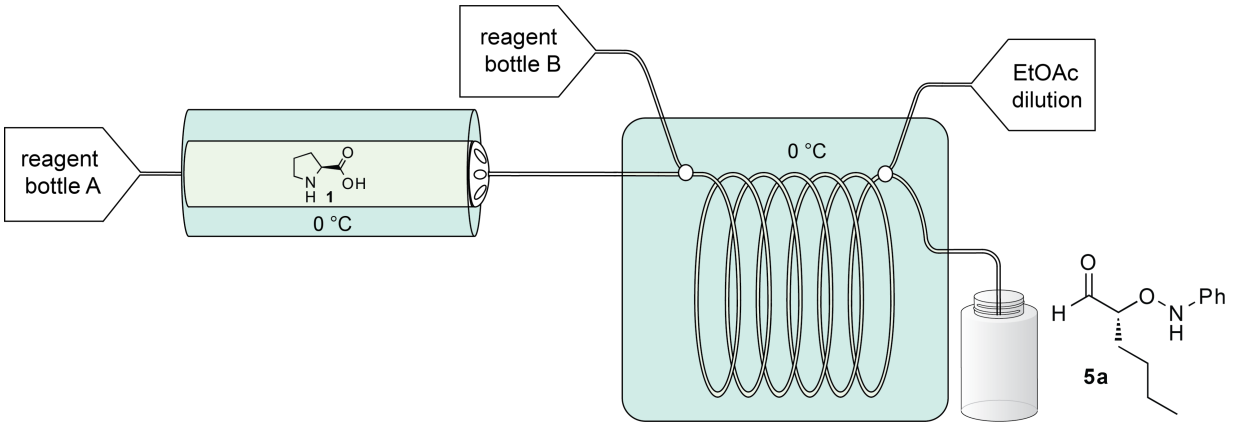

entry	reagent bottle A	reagent bottle B[a]	yield (%)	ee (%)[b]
1	hexanal	nitrosobenzene	nr[c]	na
2	thiourea **3b**	nitrosobenzene + hexanal	nr[c]	na
3	hexanal	nitrosobenzene + thiourea **3b**	27[d]	99
4	hexanal + thiourea **3b**	nitrosobenzene	43[d]	98

[a]Entry 4 also contained dodecane as an internal standard. [b]Determined by chiral HPLC. [c]nr = no reaction as determined by ^{1}H NMR analysis of the crude reaction mixture after reduction. [d]Isolated yield (due to instability of the aldehyde, products were reduced to their corresponding 2-aminooxy alcohols in batch, prior to isolation). na = not applicable. See Supporting Information File 1 for detailed reaction conditions.

Table 2: Screening of temperature and residence time.

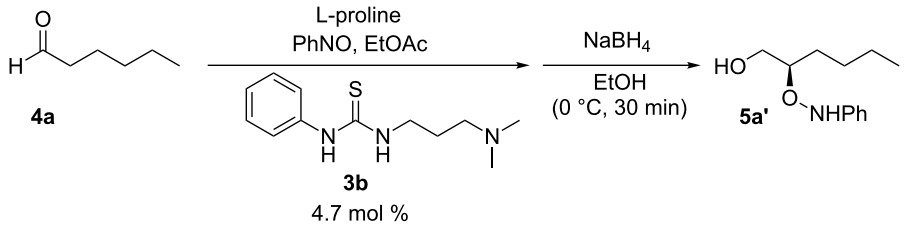

entry	column temperature (°C)	coil temperature (°C)	residence time (min)	yield (%)[a]	ee (%)[b]
1	0	0	15	43	98
2	0	0	20	69	98
3	0	15	15	82	98
4	0	15	20	85	98
5	0	15	10	61	98
6	0	10	20	84	98
7	0	5	20	86	98
8	0	5	25	81	98
9	−5	5	20	84	98
10	5	5	20	75	98
11	10	5	20	66	98
12	20	5	20	68	98

[a]Isolated yield (due to instability of the aldehyde, products were reduced to their corresponding 2-aminooxy alcohols in batch, prior to isolation).
[b]Determined by chiral HPLC. See Supporting Information File 1 for detailed reaction conditions.

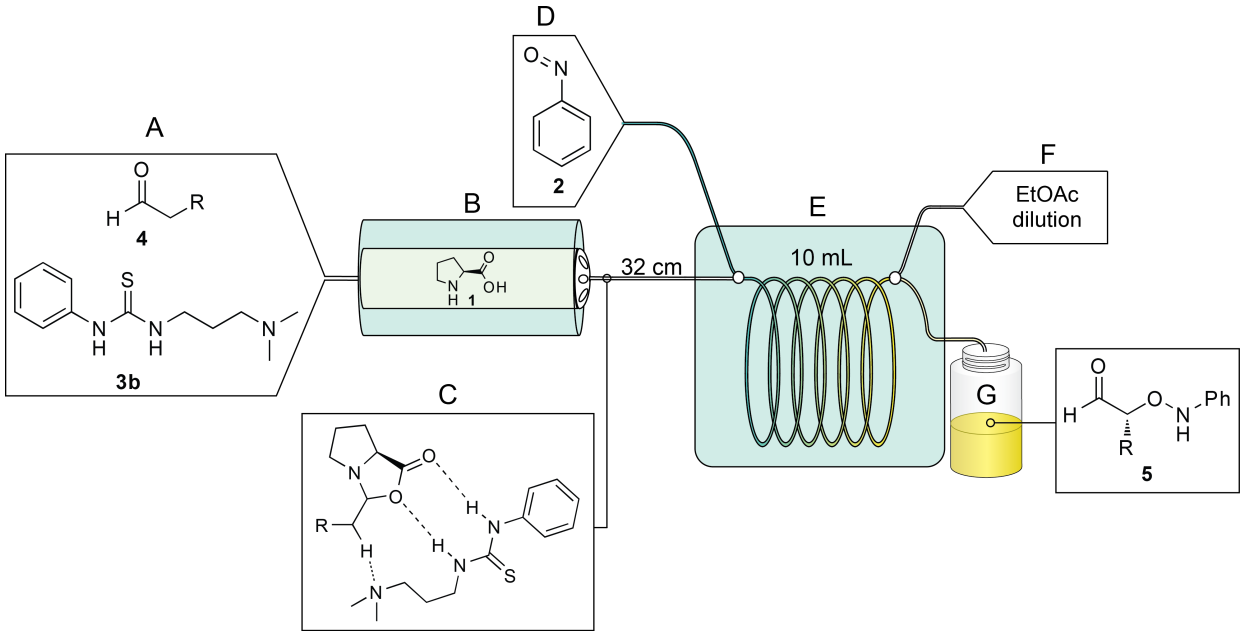

Figure 3: Schematic of the reactor setup. As the starting aldehyde and thiourea **3b** (A) enter the proline packed-bed (B) an oxazolidinone intermediate is formed, drawing the proline into the solution (C). Upon precooling in a reactor coil (E) the intermediate is mixed with nitrosobenzene (D). Prior to exiting, ethyl acetate is added to dilute the reaction (F) and product is collected into vials (G) for further reduction, work-up, and isolation.

rapid reaction with nitrosobenzene, and this thesis is supported by our observations reported herein.

With evidence for adequate proline transport into the coil, optimization experiments were performed. Based on previously published studies on the α-aminoxylation, we believed that careful control of the temperature would be necessary to avoid the formation of byproducts and to realize high enantioselectivity. The forced convection cooling system facilitated easy and precise temperature control of both the column and coil independently. Reported byproducts include the self-aldol product, the formation of azoxybenzene from the reaction of the desired product with nitrosobenzene, and finally azobenzene by product disproportionation [53-55]. Byproduct suppression is both solvent and temperature dependent. Hayashi reported that when the reaction is performed at room temperature in acetonitrile with 30 mol % proline, the reaction is complete in 10 min, but achieves only 29% yield [55]. MacMillan, however, found the reaction to be rapid in chloroform at room temperature with 78% yield, using 10 mol % proline [56]. In addition, our prior batch work with urea **3a** in ethyl acetate found that the α-aminoxylation of hexanal worked well at 0 °C with 5 mol % proline in 2 h. Therefore, we studied the impact of both the packed-bed and reaction-coil temperature on the enantioselectivity and product yield.

To begin with, we kept the column temperature at 0 °C and increased the *coil* temperature to 15 °C. Under these conditions a 15 min residence time provided 82% yield (Table 2, entry 3). Increasing the residence time to 20 min provided little gain in yield, while reducing the residence time to 10 min afforded only 61% yield (Table 2, entries 4 and 5). We found that as the coil temperature was decreased from 15 to 10 and then to 5 °C the yield corresponding to a 20 min residence time remained steady (Table 2, entries 4, 6, and 7). A further reduction to 0 °C, however, showed a decrease to 69% (Table 2, entry 2). At each of these temperatures the enantioselectivity remained high.

Next, the *packed-bed* temperature was varied to determine how temperature influenced the formation of the active catalyst species from hexanal, proline, and thiourea **3b**. We found that at column temperatures less than 0 °C the reaction performed well (Table 2, entries 7 and 9). As the temperature was increased to 5, 10, and 20 °C the yield dropped and was 68% at 20 °C (Table 2, entries 10, 11, and 12). Therefore, for further experiments we chose a column temperature of 0 °C and a coil temperature of 5 °C with a 20 min residence time. It is clear, however, from the parameters investigated, that when simple sterically unencumbered aldehydes are used this reaction works well under a variety of conditions.

To assess the long term stability and activity of the L-proline packed-bed, the system was run continuously for over 4 h. After the system reached equilibrium, 20 mL fractions of product were periodically collected, reduced and purified. The data shown in Figure 4 indicate that the reaction is stable over this period of use. During the ~5 h collection period, assuming an average yield of 78%, approximately 9.8 g was produced. Over the entire run 80 mL of hexanal/thiourea **3b** stock solution was passed through the column. Upon completion of this study it was determined that 82% of the proline was consumed (823.1 mg out of 1 g) (Figure 4).

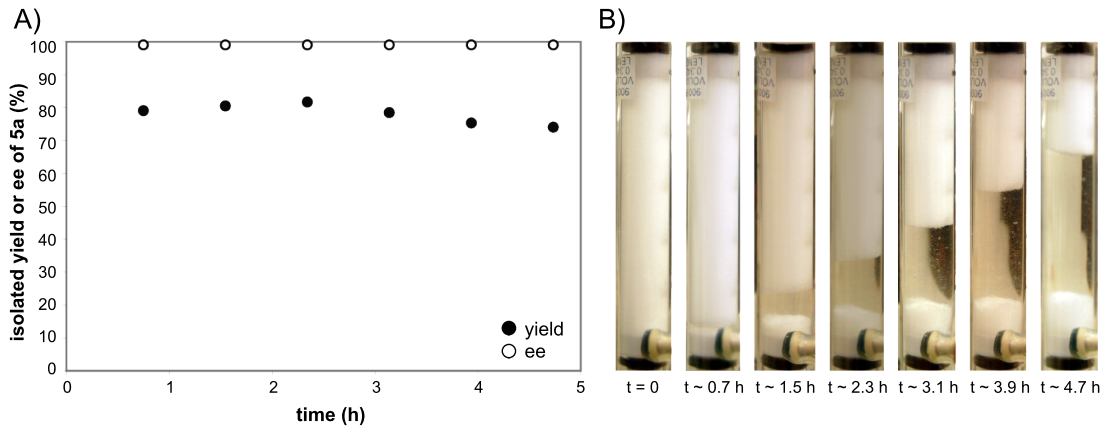

Figure 4: The long-term stability of a proline packed bed in the α-aminoxylation reaction of hexanal. A solution of hexanal (3 M in EtOAc) and thiourea **3b** (0.047 M in EtOAc) was passed through a packed-bed of proline (entering at the bottom of the column and exiting at the top) at 0 °C combined with a solution of nitrosobenzene (1 M in EtOAc) in a coil at 5 °C with a 20 min residence time in the coil, for over 4 h. A) 20 mL of product was periodically collected into vials, reduced in batch, and purified. The resulting yields and enantioselectivities were plotted as a function of time. B) Close up images of the proline column (see Figure 2A) showing the amount of proline consumed during the course of the reaction.

As further support that the direct use of solid catalysts in flow is a viable strategy, two additional substrates, 3-phenylpropionaldehyde and isovaleraldehyde, were selected because they have different properties compared to hexanal, and thus we predicted that they would require alterations to the system to maximize yield. As a starting point, the conditions optimized for hexanal were investigated. With 3-phenylpropionaldehyde, the use of a 0 °C column temperature, 5 °C coil temperature and a 20 min coil residence time led to rapid reaction (based upon color change in the coil) and subsequent reactor clogging. This led us to conclude that this aldehyde reacts rapidly with proline to yield an oxazolidinone with lower solubility than hexanal and that lowering the overall residence time would limit the amount of aldehyde reacting with proline. We confirmed that our assertion was reasonable by reducing the residence time to 10 min to provide the product in 76% yield and 99% ee (Scheme 2).

When isovaleraldehyde was investigated under the optimized hexanal conditions, i.e., 0 °C column temperature, 5 °C coil temperature and a 20 min coil residence time, there was little conversion as judged by GC analysis. We were not surprised by this observation, because increased steric hindrance about the aldehyde can suppress the rate of oxazolidinone formation. With limited proline (in the form of oxazolidinone) entering the system, the rate of α-aminoxylation decreases significantly. From our hexanal and 3-phenylpropionaldehyde experiments, we learned that by adjusting one of three parameters (residence time or the coil or packed-bed temperature) we could improve the amount of catalyst entering the system. In this particular case, we predicted that, unlike 3-phenylpropionaldehyde, the isovaleraldehyde would form the oxazolidinone slowly. Furthermore, we predicted that raising the packed-bed temperature would increase the rate of proline/isovaleraldehyde reaction resulting in more rapid formation of the soluble catalyst species. A quick survey of temperatures revealed that a 40 °C packed-bed temperature and a 20 °C coil temperature with a 25 min residence time provided 76% yield and 97% ee (Scheme 3). It is apparent from these results and our initial conditions that substrate-to-substrate optimization can be rapidly achieved by a quick survey of the three critical parameters. The data further highlight the value of running reactions continuously.

Conclusion

We have demonstrated that a packed-bed of proline can be used to continuously form a soluble catalyst through reaction with an aldehyde and cocatalytic urea. The formed soluble catalyst can support a variety of α-aminoxylation reactions with good yields and high enantioselectivities. The system is designed so that the first step involves the flow of aldehyde and urea solution through the proline packed-bed to generate the catalytic intermediate (presumably an oxazolidinone). This catalyst solution is then combined with a stream of nitrosobenenze, resulting in the α-aminoxylation. The most critical parameters that control the yield and selectivity were identified, and these parameters were varied in order to optimize the system for each substrate. We predict that this basic setup can be adapted to generate a

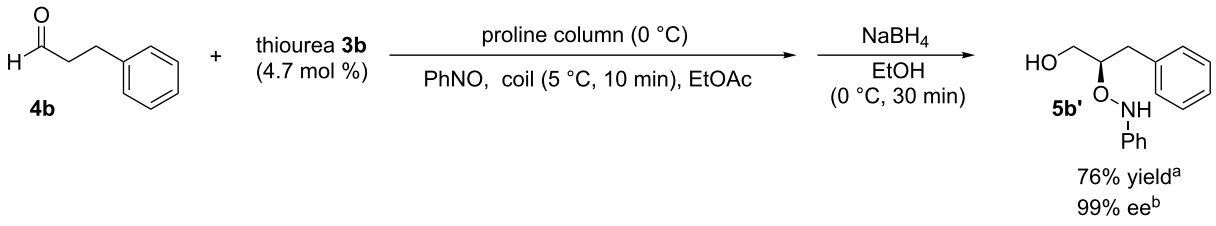

Scheme 2: Reaction with 3-phenylpropionaldehyde through reactor setup.
[a]Isolated yield, due to the instability of the aldehyde, the product was reduced in batch to the corresponding 2-aminoxy alcohol prior to isolation.
[b]Determined by chiral HPLC.

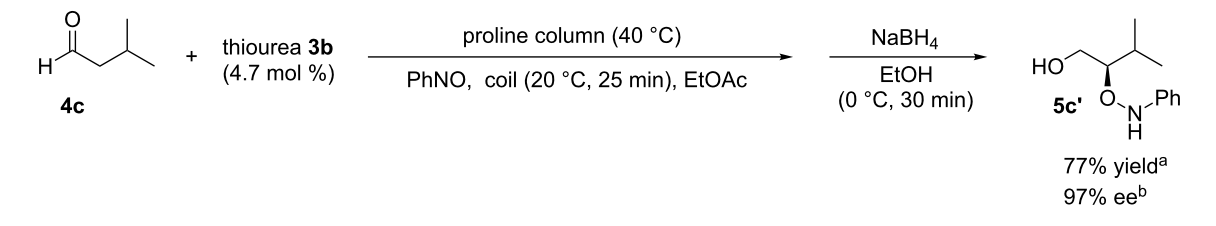

Scheme 3: Reaction with isovaleraldehyde through reactor setup.
[a]Isolated yield, due to the instability of the aldehyde, the product was reduced in batch to the corresponding 2-aminooxy alcohol prior to isolation.
[b]Determined by chiral HPLC.

wide range of other catalysts by replacing proline with another solid catalyst precursor. We are currently investigating the combination of ligands and solid metal salts to generate transition-metal catalysts continuously.

Supporting Information

The Experimental Section describes reactor setup and operational details, screening conditions, synthesis, purification and characterization data of all catalysts, and the starting materials and substances given in this article.

Supporting Information File 1

Experimental Section.
[http://www.beilstein-journals.org/bjoc/content/supplementary/1860-5397-7-197-S1.pdf]

Acknowledgements

The authors thank NSF (CHE-0809261), NDSEG (SMO), Corning Glass, Pfizer and FSU for financial support. Megan Frugoli and Jeffrey Fleming are thanked for solution preparation and urea synthesis. We also thank Duncan Guthrie, Chris Butters, David Griffin, Adrian Clarkson, and Lillian Auchincloss from Vapourtec Ltd. for their assistance throughout this project.

References

1. Wegner, J.; Ceylan, S.; Kirschning, A. *Chem. Commun.* **2011,** *47,* 4583–4592. doi:10.1039/c0cc05060a
2. Wiles, C.; Watts, P. *Chem. Commun.* **2011,** *47,* 6512–6535. doi:10.1039/c1cc00089f
3. Yoshida, J.-I. *Chem. Rec.* **2010,** *10,* 332–341. doi:10.1002/tcr.201000020
4. Bedore, M. W.; Zaborenko, N.; Jensen, K. F.; Jamison, T. F. *Org. Process Res. Dev.* **2010,** *14,* 432–440. doi:10.1021/op9003136
5. Grafton, M.; Mansfield, A. C.; Fray, M. J. *Tetrahedron Lett.* **2010,** *51,* 1026–1029. doi:10.1016/j.tetlet.2009.12.071
6. O'Brien, M.; Baxendale, I. R.; Ley, S. V. *Org. Lett.* **2010,** *12,* 1596–1598. doi:10.1021/ol100322t
7. Baxendale, I. R.; Ley, S. V.; Mansfield, A. C.; Smith, C. D. *Angew. Chem., Int. Ed.* **2009,** *48,* 4017–4021. doi:10.1002/anie.200900970
8. Kulkarni, A. A.; Kalyani, V. S.; Joshi, R. A.; Joshi, R. R. *Org. Process Res. Dev.* **2009,** *13,* 999–1002. doi:10.1021/op900129w
9. Mason, B. P.; Price, K. E.; Steinbacher, J. L.; Bogdan, A. R.; McQuade, D. T. *Chem. Rev.* **2007,** *107,* 2300–2318. doi:10.1021/cr050944c
10. Webb, D.; Jamison, T. F. *Chem. Sci.* **2010,** *1,* 675–680. doi:10.1039/c0sc00381f
11. Hartman, R. L.; Jensen, K. F. *Lab Chip* **2009,** *9,* 2495–2507. doi:10.1039/b906343a
12. Jas, G.; Kirschning, A. *Chem.–Eur. J.* **2003,** *9,* 5708–5723. doi:10.1002/chem.200305212
13. Ley, S. V.; Baxendale, I. R.; Bream, R. N.; Jackson, P. S.; Leach, A. G.; Longbottom, D. A.; Nesi, M.; Scott, J. S.; Storer, R. I.; Taylor, S. J. *J. Chem. Soc., Perkin Trans. 1* **2000,** 3815–4195. doi:10.1039/B006588I
14. Browne, D. L.; Deadman, B. J.; Ashe, R.; Baxendale, I. R.; Ley, S. V. *Org. Process Res. Dev.* **2011,** *15,* 693–697. doi:10.1021/op2000223
15. Kelly, C. B.; Lee, C.; Leadbeater, N. E. *Tetrahedron Lett.* **2011,** *52,* 263–265. doi:10.1016/j.tetlet.2010.11.027
16. Horie, T.; Sumino, M.; Tanaka, T.; Matsushita, Y.; Ichimura, T.; Yoshida, J.-I. *Org. Process Res. Dev.* **2010,** *14,* 405–410. doi:10.1021/op900306z
17. Sedelmeier, J.; Ley, S. V.; Baxendale, I. R.; Baumann, M. *Org. Lett.* **2010,** *12,* 3618–3621. doi:10.1021/ol101345z
18. Jongen, N.; Donnet, M.; Bowen, P.; Lemaître, J.; Hofmann, H.; Schenk, R.; Hofmann, C.; Aoun-Habbache, M.; Guillemet-Fritsch, S.; Sarrias, J.; Rousset, A.; Viviani, M.; Buscaglia, M. T.; Buscaglia, V.; Nanni, P.; Testino, A.; Herguijuela, J. R. *Chem. Eng. Technol.* **2003,** *26,* 303–305. doi:10.1002/ceat.200390046
19. Isart, C.; Burés, J.; Vilarrasa, J. *Tetrahedron Lett.* **2008,** *49,* 5414–5418. doi:10.1016/j.tetlet.2008.07.028
20. Mager, I.; Zeitler, K. *Org. Lett.* **2010,** *12,* 1480–1483. doi:10.1021/ol100166z
21. Kristensen, T. E.; Hansen, T. *Eur. J. Org. Chem.* **2010,** 3179–3204. doi:10.1002/ejoc.201000319
22. Gruttadauria, M.; Giacalone, F.; Noto, R. *Chem. Soc. Rev.* **2008,** *37,* 1666–1688. doi:10.1039/b800704g
23. Cozzi, F. *Adv. Synth. Catal.* **2006,** *348,* 1367–1390. doi:10.1002/adsc.200606096
24. Benaglia, M. *New J. Chem.* **2006,** *30,* 1525–1533. doi:10.1039/b610416a
25. Costantini, F.; Bula, W. P.; Salvio, R.; Huskens, J.; Gardeniers, H. J. G. E.; Reinhoudt, D. N.; Verboom, W. *J. Am. Chem. Soc.* **2009,** *131,* 1650–1651. doi:10.1021/ja807616z
26. ElKadib, A.; Chimenton, R.; Sachse, A.; Fajula, F.; Galarneau, A.; Coq, B. *Angew. Chem., Int. Ed.* **2009,** *48,* 4969–4972. doi:10.1002/anie.200805580
27. Bogdan, A. R.; Mason, B. P.; Sylvester, K. T.; McQuade, D. T. *Angew. Chem., Int. Ed.* **2007,** *46,* 1698–1701. doi:10.1002/anie.200603854
28. Nikbin, N.; Watts, P. *Org. Process Res. Dev.* **2004,** *8,* 942–944. doi:10.1021/op049857x
29. Svec, F.; Fréchet, J. M. J. *Science* **1996,** *273,* 205–211. doi:10.1126/science.273.5272.205
30. Poe, S. L.; Cummings, M. A.; Haaf, M. P.; McQuade, D. T. *Angew. Chem., Int. Ed.* **2006,** *45,* 1544–1548. doi:10.1002/anie.200503925
31. Steinbacher, J. L.; McQuade, D. T. *J. Polym. Sci., Part A: Polym. Chem.* **2006,** *44,* 6505–6533. doi:10.1002/pola.21630
32. Steinbacher, J. L.; Moy, R. W. Y.; Price, K. E.; Cummings, M. A.; Roychowdhury, C.; Buffy, J. J.; Olbricht, W. L.; Haaf, M.; McQuade, D. T. *J. Am. Chem. Soc.* **2006,** *128,* 9442–9447. doi:10.1021/ja0612403
33. Quevedo, E.; Steinbacher, J.; McQuade, D. T. *J. Am. Chem. Soc.* **2005,** *127,* 10498–10499. doi:10.1021/ja0529945
34. Bogdan, A.; McQuade, D. T. *Beilstein J. Org. Chem.* **2009,** *5,* No. 17. doi:10.3762/bjoc.5.17
35. Bogdan, A. R.; Poe, S. L.; Kubis, D. C.; Broadwater, S. J.; McQuade, D. T. *Angew. Chem., Int. Ed.* **2009,** *48,* 8547–8550. doi:10.1002/anie.200903055

36. Opalka, S. M.; Steinbacher, J. L.; Lambiris, B. A.; McQuade, D. T. *J. Org. Chem.* **2011,** *76,* 6503–6517. doi:10.1021/jo200838v
37. Poe, S. L.; Bogdan, A. R.; Mason, B. P.; Steinbacher, J. L.; Opalka, S. M.; McQuade, D. T. *J. Org. Chem.* **2009,** *74,* 1574–1580. doi:10.1021/jo802461w
38. Alza, E.; Sayalero, S.; Cambeiro, X. C.; Martin-Rapún, R.; Miranda, P. O.; Pericàs, M. A. *Synlett* **2011,** 464–468. doi:10.1055/s-0030-1259528
39. Massi, A.; Cavazzini, A.; Zoppo, L. D.; Pandoli, O.; Costa, V.; Pasti, L.; Giovannini, P. P. *Tetrahedron Lett.* **2011,** *52,* 619–622. doi:10.1016/j.tetlet.2010.11.157
40. Alza, E.; Rodríguez-Escrich, C.; Sayalero, S.; Bastero, A.; Pericàs, M. A. *Chem.–Eur. J.* **2009,** *15,* 10167–10172. doi:10.1002/chem.200901310
41. Trost, B. M.; Brindle, C. S. *Chem. Soc. Rev.* **2010,** *39,* 1600–1632. doi:10.1039/b923537j
42. Notz, W.; Tanaka, F.; Barbas, C. F., III. *Acc. Chem. Res.* **2004,** *37,* 580–591. doi:10.1021/ar0300468
43. List, B.; Lerner, R. A.; Barbas, C. F., III. *J. Am. Chem. Soc.* **2000,** *122,* 2395–2396. doi:10.1021/ja994280y
44. Guillena, G.; Ramón, D. J. *Tetrahedron: Asymmetry* **2006,** *17,* 1465–1492. doi:10.1016/j.tetasy.2006.05.020
45. The term urea will be used as a broad category to include thioureas as well as ureas unless we are explicitly examining the difference between the two.
46. El-Hamdouni, N.; Companyó, X.; Rios, R.; Moyano, A. *Chem.–Eur. J.* **2010,** *16,* 1142–1148. doi:10.1002/chem.200902678
47. Demir, A. S.; Eymur, S. *Tetrahedron: Asymmetry* **2010,** *21,* 405–409. doi:10.1016/j.tetasy.2010.02.009
48. Wang, W.-H.; Abe, T.; Wang, X.-B.; Kodama, K.; Hirose, T.; Zhang, G.-Y. *Tetrahedron: Asymmetry* **2010,** *21,* 2925–2933. doi:10.1016/j.tetasy.2010.11.025
49. Reis, Ö.; Eymur, S.; Reis, B.; Demir, A. S. *Chem. Commun.* **2009,** 1088–1090. doi:10.1039/b817474a
50. Companyó, X.; Valero, G.; Crovetto, L.; Moyano, A.; Rios, R. *Chem.–Eur. J.* **2009,** *15,* 6564–6568. doi:10.1002/chem.200900488
51. Vapourtec Flow Chemistry Equipment, UK. http://www.vapourtec.co.uk (accessed Oct 25, 2011).
52. Prior ^{1}H NMR studies found the concentration of proline alone in chloroform to be 0.0047 M. The addition of 1 equiv of a urea additive resulted in a proline concentration of 0.0044 M.
53. Font, D.; Bastero, A.; Sayalero, S.; Jimeno, C.; Pericàs, M. A. *Org. Lett.* **2007,** *9,* 1943–1946. doi:10.1021/ol070526p
54. Morales, M. R.; Momiyama, N.; Yamamoto, H. *Synlett* **2006,** 705–708. doi:10.1055/s-2006-933123
55. Hayashi, Y.; Yamaguchi, J.; Sumiya, T.; Hibino, K.; Shoji, M. *J. Org. Chem.* **2004,** *69,* 5966–5973. doi:10.1021/jo049338s
56. Brown, S. P.; Brochu, M. P.; Sinz, C. J.; MacMillan, D. W. C. *J. Am. Chem. Soc.* **2003,** *125,* 10808–10809. doi:10.1021/ja037096s

License and Terms

Beilstein Journal of Organic Chemistry

Continuous-flow hydration–condensation reaction: Synthesis of α,β-unsaturated ketones from alkynes and aldehydes by using a heterogeneous solid acid catalyst

Magnus Rueping*, Teerawut Bootwicha, Hannah Baars and Erli Sugiono

Full Research Paper

Open Access

Address:
Institute of Organic Chemistry, RWTH Aachen University, Landoltweg 1, D-52074 Aachen, Germany

Email:
Magnus Rueping* - magnus.rueping@rwth-aachen.de

* Corresponding author

Keywords:
chalcones; flow reactor; green chemistry; heterogeneous catalysis, microwave

Beilstein J. Org. Chem. **2011,** *7,* 1680–1687.
doi:10.3762/bjoc.7.198

Received: 18 September 2011
Accepted: 12 December 2011
Published: 15 December 2011

This article is part of the Thematic Series "Chemistry in flow systems II".

Guest Editor: A. Kirschning

Abstract

A simple, practical and efficient continuous-flow hydration–condensation protocol was developed for the synthesis of α,β-unsaturated ketones starting from alkynes and aldehydes by employing a heterogeneous catalyst in a flow microwave. The procedure presents a straightforward and convenient access to valuable differently substituted chalcones and can be applied on multigram scale.

Introduction

In recent years, the development of continuous-flow technologies has expanded considerably and has had a significant impact on modern organic synthetic chemistry. Continuous-flow processes offer advantages, such as operational simplicity, energy savings, reduced reagent consumption, and improved mixing quality as well as precise control of the reaction parameters, including pressure, temperature, residence time and heat transfer. The improved operational safety over classical batch reactions reduces the problems of working with hazardous chemicals [1-22]. Furthermore, continuous-flow technologies allow chemical processes to be easily and rapidly scaled up, either by changing the volume of the single reactor, by performing the reaction for an extended reaction time, or by running the reaction in multiple reactors in parallel. Moreover, the products may be collected continuously and formation of byproducts may be reduced by the immediate separation of the products from the reaction mixtures [23-34]. More recently, it has been shown that even asymmetric reactions can be conducted in a continuous-flow fashion [35-40]. Recently, the combination of flow processes and microwave technology has become an interesting endeavour in both academia and in industry. The combination of continuous-flow technology and

microwave heating offers advantages such as a cleaner reaction profile, reduction of reaction times, higher yields and better selectivity [41-54].

Results and Discussion

α,β-Unsaturated ketones are a common motif found in the principal core of a large number of important biologically active compounds. They show pharmacological properties such as antimalarial, antitumor, antiviral, and anti-inflammatory activities [55-60]. They are also well known to be key intermediates in the synthesis of flavones, flavonoids, isoflavonoids and other heterocyclic compounds [61-65]. Consequently, the development of an efficient synthesis to obtain these valuable compounds attracted our interest.

Thus, we decided to develop an efficient continuous-flow synthesis of α,β-unsaturated ketones starting from alkynes and aldehydes by employing a heterogeneous solid acid catalyst [66-84].

The continuous-flow apparatus for the experiment was set up according to Scheme 1. A 10 mL reaction vessel was charged with the heterogeneous solid acid catalyst (10 g) and inserted into the reactor. By means of a peristaltic pump the reagents were continuously pumped through the reaction vessel under microwave irradiation (50 W). The product solution was collected from the outlet tube, which was connected to a 250 psi backpressure regulator of the commercial flow microwave system.

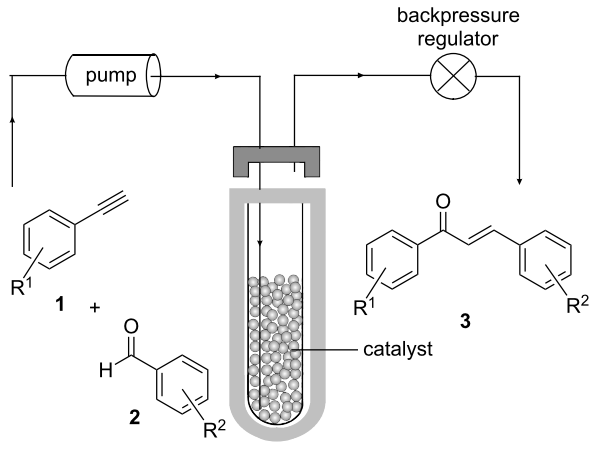

Scheme 1: The schematic arrangement of the continuous-flow system.

Our initial reaction development was focussed on finding the optimal conditions for the continuous-flow reaction of phenylacetylene (**1a**) with benzaldehyde (**2a**) applying the ion-exchange resin amberlyst-15 [85] as heterogeneous solid acid catalyst. The effects of the substrate concentration, the reaction temperature and the flow rate are summarized in Table 1. Performing the reaction at 80 °C afforded the α,β-unsaturated ketone in 70% yield (Table 1, entry 5). Running the reaction at higher temperature (90 °C) showed a noticeable impact on the conversion and the product was isolated in 84% (Table 1, entry 2). However, a further temperature increase did not result in improved yield (Table 1, entry 1). Next, we set out to probe the influence of the flow rate on the chemical yield. Performing the reaction at 90 °C and 0.5 mL min^{-1} gave the product in 84% yield (Table 1, entry 2). A significant drop in chemical yield was observed when the flow rate increased from 0.5 mL min^{-1} to 1.0 mL min^{-1} (Table 1, entry 2 versus entry 8), indicating that the flow rate should be 0.5 mL min^{-1}. Further reaction optimization was accomplished by varying the substrate concentration. While the chemical yields remained constant during an increase from 0.2 M to 0.3 M (Table 1, entries 2 and 7), performing the reaction at lower concentration (0.1 M) afforded the product in lower yield (Table 1, entry 6). A slightly better conversion was obtained when the reaction was performed in dry solvent (Table 1, entry 3). However, the best result was achieved when the reaction was conducted under solvent-free conditions (Table 1, entry 4).

To probe the influence of microwave heating on this transformation, we examined the same transformation under batch conditions and without microwave irradiation. As shown in Table 1, under classical batch conditions no product formation was observed when the reaction was performed at 35 °C (Table 1, entry 9). By increasing the reaction temperature to 80 °C using an oil bath, 17% of the product was isolated after 1 hour reaction time (Table 1, entry 10). Higher isolated yield (47%) was obtained with a longer reaction time (3 h) (Table 1, entry 11). Identical transformation under microwave conditions gave 70% isolated yield after 30 min reaction time (Table 1, entry 5).

Having established the optimal reaction conditions, we set out to investigate the scope and applicability of the procedure by employing various alkynes **1** and a range of substituted aromatic aldehydes **2** [86]. All the reactions were performed neat, except where the aldehydes were solid. In those cases the reactions were performed in dry DCE. The results are summarized in Table 2.

Generally, the reaction mixture of alkyne **1** and aldehyde **2** was constantly pumped into the flow cell, filled with the solid acid catalyst and solvent, at the flow rate of 0.5 mL min^{-1} under microwave irradiation. This was followed by a washing procedure with 100 mL of solvent and then the next substrate was introduced. Importantly, the same catalyst was maintained throughout the reactions.

Table 1: Optimization of hydration–condensation reactions.[a]

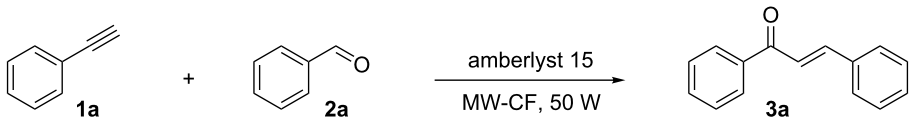

Entry	Flow rate [mL min^{-1}]	Conc. **1a** [M]	Heat Source	Temp. [°C]	Yield [%][b]
1	0.5	0.2	microwave	100	84
2	0.5	0.2	microwave	90	84
3	0.5	0.2	microwave	90	87[c]
4	0.5	–	microwave	90	91[d]
5	0.5	0.2	microwave	80	70
6	0.5	0.1	microwave	90	62
7	0.5	0.3	microwave	90	84
8	1.0	0.2	microwave	90	30
9[e]	–	0.1	–	35	n.r.
10[f]	–	0.2	oil bath	80	17
11[g]	–	0.2	oil bath	80	47

[a]Reaction conditions: Phenylacetylene (**1a**) (1.0 equiv), 0.2 M in 1,2-dichloroethane (DCE) and benzaldehyde (**2a**) (4.0 equiv), 50 W, 30 min. [b]Isolated yield after column chromatography. [c]Performed with dry 1,2-dichloroethane (DCE). [d]Performed under neat (solvent-free) conditions. [e]Performed in DCM under batch conditions for 24 h. [f]Performed in DCE under batch conditions for 1 h. [g]Performed in DCE under batch conditions for 3 h.

Table 2: Flow hydration–condensation of alkynes **1** and aldehydes **2**.[a]

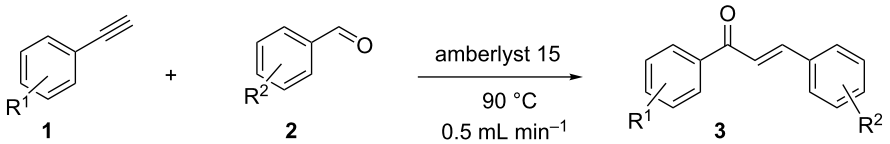

Entry	Alkyne **1**	Aldehyde **2**	Product **3**	Yield [%][b]
1	**1a**	**2a**	**3a**	87[c] 91
2[c]	**1a**	**2b**	**3b**	96
3[c]	**1a**	**2c**	**3c**	98
4	**1a**	**2d**	**3d**	87

Table 2: Flow hydration–condensation of alkynes **1** and aldehydes **2**.[a] (continued)

5	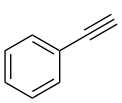 **1a**	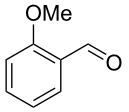 **2e**	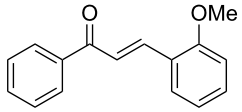 **3e**	85
6[c]	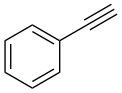 **1a**	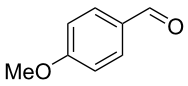 **2f**	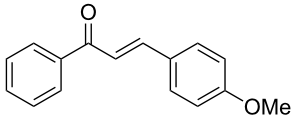 **3f**	89
7	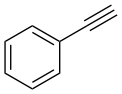 **1a**	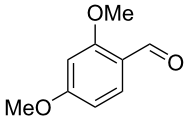 **2g**	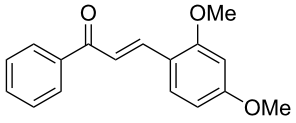 **3g**	88
8	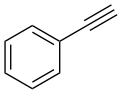 **1a**	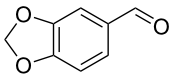 **2h**	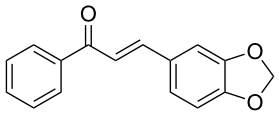 **3h**	95
9	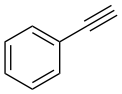 **1a**	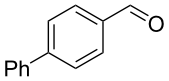 **2i**	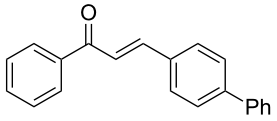 **3i**	86
10[c]	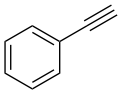 **1a**	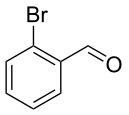 **2j**	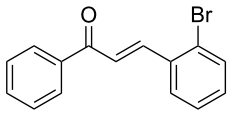 **3j**	82
11[c]	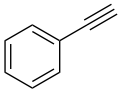 **1a**	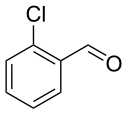 **2k**	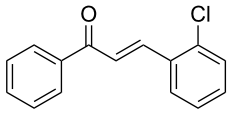 **3k**	77
12	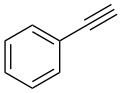 **1a**	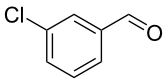 **2l**	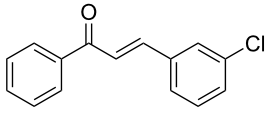 **3l**	68
13	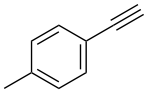 **1b**	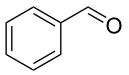 **2a**	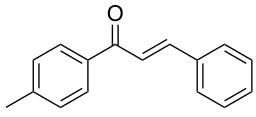 **3m**	98
14	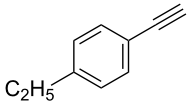 **1c**	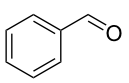 **2a**	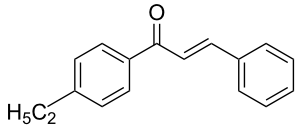 **3n**	97
15	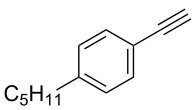 **1d**	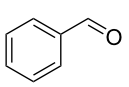 **2a**	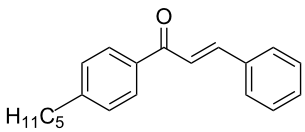 **3o**	83

Table 2: Flow hydration–condensation of alkynes **1** and aldehydes **2**.[a] (continued)

16	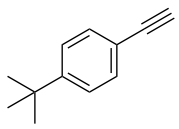 **1e**	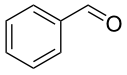 **2a**	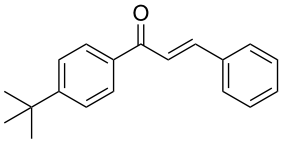 **3p**	91
17	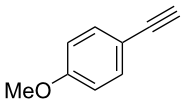 **1f**	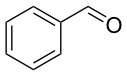 **2a**	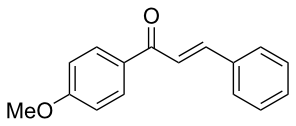 **3q**	73
18	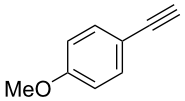 **1f**	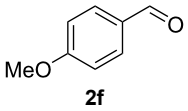 **2f**	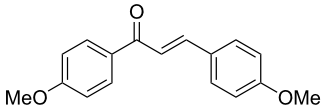 **3r**	79
19	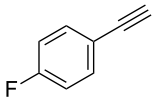 **1g**	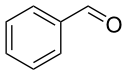 **2a**	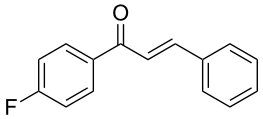 **3s**	70
20	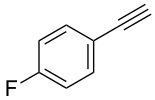 **1g**	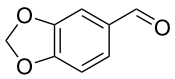 **2h**	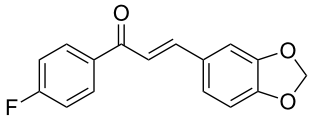 **3t**	77
21	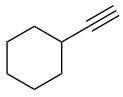 **1h**	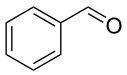 **2a**	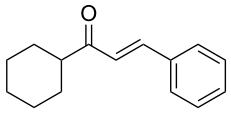 **3u**	74

[a]Reaction conditions: alkynes **1** (1 equiv), aldehydes **2** (4 equiv), solvent-free conditions, 50 W. [b]Isolated yield after column chromatography. [c]Performed in dry 1,2-dichloroethane (0.2 M).

In general, various aldehydes bearing electron-withdrawing or -donating groups, as well as different substitution patterns were suitable substrates in the reactions. The corresponding α,β-unsaturated ketones were obtained in good to excellent yields (Table 2, entries 1–12). Applying this procedure no formation of propargylic alcohols was observed and in general no amount of methyl ketone was detected.

Employing the above optimized reaction conditions, further experiments were conducted with a range of substituted alkynes **1** and aldehydes **2** (Table 2, entries 13–21). Again, both electron-rich and electron-poor substrates were well tolerated and the corresponding products were isolated in good yields.

Once the optimal reaction conditions were successfully established on a small scale, we evaluated the potential of this protocol by performing the reactions on a 20 and 49 mmol scale. The reactions of phenylacetylene (**1a**) with *p*-methyl substituted benzaldehyde **2b** proceeded smoothly providing the corresponding product in excellent isolated yields (Scheme 2).

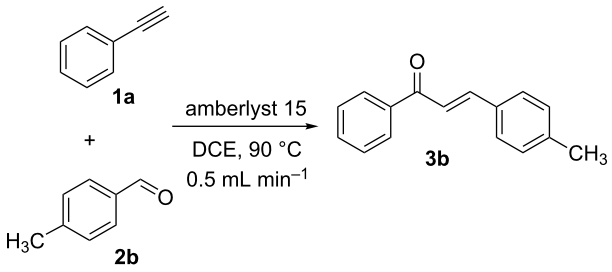

2.0 g (20 mmol) phenylacetylene **1a**; 4.2 g **3b** (97% yield)
5.0 g (49 mmol) phenylacetylene **1a**; 9.8 g **3b** (91% yield)

Scheme 2: Preparation of chalcone **3b** on larger scale.

Conclusion

In conclusion, we have developed a general protocol to access a series of valuable differently substituted chalcones. Starting from commercially available alkynes and aldehydes, a continuous-flow hydration–condensation protocol leads to the desired products in good to excellent yields. The reactions were sequentially introduced into the flow cell and performed several times without the heterogeneous catalyst needing to be changed, demonstrating the high robustness of this catalytic system. Additionally, this new method was readily applied for the preparation of chalcones in multigram quantities. The technology presented is advantageous over classical non-microwave batch reactions in particular with regard to the continuous harvesting of the product, the fast optimization of the reaction parameters, the simple operation and reliability, and the restriction of byproduct formation, especially the formation of methyl ketones and propargylic alcohols.

Experimental

General procedure for hydration–condensation reaction of phenylacetylene (**1a**) and benzaldehyde (**2a**). A solution of phenylacetylene (**1a**) (0.4 mmol) and benzaldehyde (**2a**) (1.6 mmol) was pumped through the flow cell filled with amberlyst-15 resin (16–50 mesh) (10.0 g) and dry 1,2-dichloroethane at a flow rate of 0.5 mL min^{-1}. During this period the reaction vessel in a microwave cavity was irradiated at 90 °C (50 W). Following the reaction, 100 mL solvent was pumped through the flow cell at the same flow rate in order to wash the system, and the combined solutions were evaporated in vacuo. The residue was purified by column chromatography (*n*-hexane/DCM [2:1 to 1:1]).

Supporting Information

Supporting Information File 1

Experimental procedures and characterization of compounds.
[http://www.beilstein-journals.org/bjoc/content/supplementary/1860-5397-7-198-S1.pdf]

Acknowledgements

The authors acknowledge the European Research Council for a starting grant.

References

1. Jas, G.; Kirschning, A. *Chem.–Eur. J.* **2003,** *9,* 5708–5723. doi:10.1002/chem.200305212
2. Kikutani, Y.; Kitamori, T. *Macromol. Rapid Commun.* **2004,** *25,* 158–168. doi:10.1002/marc.200300192
3. Kirschning, A.; Solodenko, W.; Mennecke, K. *Chem.–Eur. J.* **2006,** *12,* 5972–5990. doi:10.1002/chem.200600236
4. Watts, P.; Haswell, S. J. *Chem. Soc. Rev.* **2005,** *34,* 235–246. doi:10.1039/b313866f
5. Geyer, K.; Codée, J. D. C.; Seeberger, P. H. *Chem.–Eur. J.* **2006,** *12,* 8434–8442. doi:10.1002/chem.200600596
6. Mason, B. P.; Price, K. E.; Steinbacher, J. L.; Bogdan, A. R.; McQuade, D. T. *Chem. Rev.* **2007,** *107,* 2300–2318. doi:10.1021/cr050944c
7. Ahmed-Omer, B.; Brandt, J. C.; Wirth, T. *Org. Biomol. Chem.* **2007,** *5,* 733–740. doi:10.1039/b615072a
8. Wiles, C.; Watts, P. *Eur. J. Org. Chem.* **2008,** 1655–1671. doi:10.1002/ejoc.200701041
9. Yoshida, J-i.; Nagaki, A.; Yamada, T. *Chem.–Eur. J.* **2008,** *14,* 7450–7459. doi:10.1002/chem.200800582
10. Kirschning, A. *Beilstein J. Org. Chem.* **2009,** *5,* No. 15. doi:10.3762/bjoc.5.15
11. Jähnisch, K.; Hessel, V.; Löwe, H.; Baerns, M. *Angew. Chem., Int. Ed.* **2004,** *43,* 406–446. doi:10.1002/anie.200300577
12. Razzaq, T.; Kappe, C. O. *Chem.–Asian J.* **2010,** *5,* 1274–1289. doi:10.1002/asia.201000010
13. Wegner, J.; Ceylan, S.; Kirschning, A. *Chem. Commun.* **2011,** *47,* 4583–4592. doi:10.1039/c0cc05060a
14. Hartman, R. L.; McMullen, J. P.; Jensen, K. F. *Angew. Chem., Int. Ed.* **2011,** *50,* 7502–7519. doi:10.1002/anie.201004637
15. Yamada, Y. M. A.; Torii, K.; Uozumi, Y. *Beilstein J. Org. Chem.* **2009,** *5,* No. 18. doi:10.3762/bjoc.5.18
16. Brandt, J. C.; Wirth, T. *Beilstein J. Org. Chem.* **2009,** *5,* No. 30. doi:10.3762/bjoc.5.30
17. Rolland, J.; Cambeiro, X. C.; Rodríguez-Escrich, C.; Pericàs, M. A. *Beilstein J. Org. Chem.* **2009,** *5,* No. 56. doi:10.3762/bjoc.5.56
18. Kunz, U.; Turek, T. *Beilstein J. Org. Chem.* **2009,** *5,* No. 70. doi:10.3762/bjoc.5.70
19. Gutmann, B.; Glasnov, T. N.; Razzaq, T.; Goessler, W.; Roberge, D. M.; Kappe, C. O. *Beilstein J. Org. Chem.* **2011,** *7,* 503–517. doi:10.3762/bjoc.7.59
20. Wiles, C.; Hammond, M. J.; Watts, P. *Beilstein J. Org. Chem.* **2009,** *5,* No. 27. doi:10.3762/bjoc.5.27
21. Singh, S.; Köhler, J. M.; Schober, A.; Groß, G. A. *Beilstein J. Org. Chem.* **2011,** *7,* 1164–1172. doi:10.3762/bjoc.7.135
22. Fukuyama, T.; Mukai, Y.; Ryu, I. *Beilstein J. Org. Chem.* **2011,** *7,* 1288–1293. doi:10.3762/bjoc.7.149
23. Ley, S. V.; Baxendale, I. R. *Chimia* **2008,** *62,* 162–168. doi:10.2533/chimia.2008.162
24. Benito-López, F.; Egberink, R. J. M.; Reinhoudt, D. N.; Verboom, W. *Tetrahedron* **2008,** *64,* 10023–10040. doi:10.1016/j.tet.2008.07.108
25. Bowman, M. D.; Holcomb, J. L.; Kormos, C. M.; Leadbeater, N. E.; Williams, V. A. *Org. Process Res. Dev.* **2008,** *12,* 41–57. doi:10.1021/op700187w
26. Benali, O.; Deal, M.; Farrant, E.; Tapolczay, D.; Wheeler, R. *Org. Process Res. Dev.* **2008,** *12,* 1007–1011. doi:10.1021/op700225u
27. Strauss, C. R. *Org. Process Res. Dev.* **2009,** *13,* 915–923. doi:10.1021/op900194z
28. Styring, P.; Parracho, A. I. R. *Beilstein J. Org. Chem.* **2009,** *5,* No. 29. doi:10.3762/bjoc.5.29
29. Bogdan, A.; McQuade, D. T. *Beilstein J. Org. Chem.* **2009,** *5,* No. 17. doi:10.3762/bjoc.5.17
30. Mennecke, K.; Kirschning, A. *Beilstein J. Org. Chem.* **2009,** *5,* No. 21. doi:10.3762/bjoc.5.21

31. Palmieri, A.; Ley, S. V.; Polyzos, A.; Ladlow, M.; Baxendale, I. R. *Beilstein J. Org. Chem.* **2009,** *5,* No. 23. doi:10.3762/bjoc.5.23
32. Damm, M.; Glasnov, T. N.; Kappe, C. O. *Org. Process Res. Dev.* **2010,** *14,* 215–224. doi:10.1021/op900297e
33. Lehmann, H.; LaVecchia, L. *Org. Process Res. Dev.* **2010,** *14,* 650–656. doi:10.1021/op900269y
34. Lv, Y.; Yu, Z.; Su, W. *Org. Process Res. Dev.* **2011,** *15,* 471–475. doi:10.1021/op1003083
35. He, P.; Haswell, S. J.; Fletcher, P. D. I.; Kelly, S. M.; Mansfield, A. *Beilstein J. Org. Chem.* **2011,** *7,* 1150–1157. doi:10.3762/bjoc.7.133
36. Burguete, M. I.; García-Verdugo, E.; Luis, S. V. *Beilstein J. Org. Chem.* **2011,** *7,* 1347–1359. doi:10.3762/bjoc.7.159
37. Schlange, A.; dos Santos, A. R.; Kunz, U.; Turek, T. *Beilstein J. Org. Chem.* **2011,** *7,* 1412–1420. doi:10.3762/bjoc.7.165
38. Mak, X. Y.; Laurino, P.; Seeberger, P. H. *Beilstein J. Org. Chem.* **2009,** *5,* No. 19. doi:10.3762/bjoc.5.19
39. Cambeiro, X. C.; Martín-Rapún, R.; Miranda, P. O.; Sayalero, S.; Alza, E.; Llanes, P.; Pericàs, M. A. *Beilstein J. Org. Chem.* **2011,** *7,* 1486–1493. doi:10.3762/bjoc.7.172
40. Fritzsche, S.; Ohla, S.; Glaser, P.; Giera, D. S.; Sickert, M.; Schneider, C.; Belder, D. *Angew. Chem., Int. Ed.* **2011,** *50,* 9467–9470. doi:10.1002/anie.201102331
41. Kappe, C. O.; Dallinger, D.; Murphree, S. *Practical Microwave Synthesis for Organic Chemists;* Wiley-VCH: Weinheim, 2009.
42. Cablewski, T.; Faux, A. F.; Strauss, C. R. *J. Org. Chem.* **1994,** *59,* 3408–3412. doi:10.1021/jo00091a033
43. Bagley, M. C.; Jenkins, R. L.; Lubinu, M. C.; Mason, C.; Wood, R. *J. Org. Chem.* **2005,** *70,* 7003–7006. doi:10.1021/jo0510235
44. Baxendale, I. R.; Pitts, M. R. *Chim. Oggi* **2006,** *24,* 41–45.
45. Shore, G.; Morin, S.; Organ, M. G. *Angew. Chem., Int. Ed.* **2006,** *45,* 2761–2766. doi:10.1002/anie.200503600
46. Baxendale, I. R.; Griffiths-Jones, C. M.; Ley, S. V.; Tranmer, G. K. *Chem.–Eur. J.* **2006,** *12,* 4407–4416. doi:10.1002/chem.200501400
47. Glasnov, T. N.; Kappe, C. O. *Macromol. Rapid Commun.* **2007,** *28,* 395–410. doi:10.1002/marc.200600665
48. Baxendale, I. R.; Hayward, J. J.; Ley, S. V. *Comb. Chem. High Throughput Screening* **2007,** *10,* 802–836.
49. Shore, G.; Tsimerman, M.; Organ, M. G. *Beilstein J. Org. Chem.* **2009,** *5,* No. 35. doi:10.3762/bjoc.5.35
50. Shore, G.; Yoo, W.-J.; Li, C.-J.; Organ, M. G. *Chem.–Eur. J.* **2010,** *16,* 126–133. doi:10.1002/chem.200902396
51. Dressen, M. H. C. L.; van de Kruijs, B. H. P.; Meuldijk, J.; Vekemans, J. A. J. M.; Hulshof, L. A. *Org. Process Res. Dev.* **2010,** *14,* 351–361. doi:10.1021/op900257f
52. Bagley, M. C.; Fusillo, V.; Jenkins, R. L.; Lubinu, M. C.; Mason, C. *Org. Biomol. Chem.* **2010,** *8,* 2245–2251. doi:10.1039/b926387j
53. Rueping, M.; Bootwicha, T.; Sugiono, E. *Adv. Synth. Catal.* **2010,** *352,* 2961–2965. doi:10.1002/adsc.201000538
54. Wiles, C.; Watts, P. *Beilstein J. Org. Chem.* **2011,** *7,* 1360–1371. doi:10.3762/bjoc.7.160
55. Won, S.-J.; Liu, C.-T.; Tsao, L.-T.; Weng, J.-R.; Ko, H.-H.; Wang, J.-P.; Lin, C.-N. *Eur. J. Med. Chem.* **2005,** *40,* 103–112. doi:10.1016/j.ejmech.2004.09.006
56. Trivedi, J. C.; Bariwal, J. B.; Upadhyay, K. D.; Naliapara, Y. T.; Joshi, S. K.; Pannecouque, C. C.; De Clercq, E.; Shah, A. K. *Tetrahedron Lett.* **2007,** *48,* 8472–8474. doi:10.1016/j.tetlet.2007.09.175
57. Nowakowska, Z. *Eur. J. Med. Chem.* **2007,** *42,* 125–137. doi:10.1016/j.ejmech.2006.09.019
58. Aponte, J. C.; Verástegui, M.; Málaga, E.; Zimic, M.; Quiliano, M.; Vaisberg, A. J.; Gilman, R. H.; Hammond, G. B. *J. Med. Chem.* **2008,** *51,* 6230–6234. doi:10.1021/jm800812k
59. Nowakowska, Z.; Kędzia, B.; Schroeder, G. *Eur. J. Med. Chem.* **2008,** *43,* 707–713. doi:10.1016/j.ejmech.2007.05.006
60. Bhattacharya, A.; Mishra, L. C.; Sharma, M.; Awasthi, S. K.; Bhasin, V. K. *Eur. J. Med. Chem.* **2009,** *44,* 3388–3393. doi:10.1016/j.ejmech.2009.02.008
61. Wang, S.; Yu, G.; Lu, J.; Xiao, K.; Hu, Y.; Hu, H. *Synthesis* **2003,** 487–490. doi:10.1055/s-2003-37642
62. Bhat, B. A.; Dhar, K. L.; Puri, S. C.; Saxena, A. K.; Shanmugavel, M.; Qazi, G. N. *Bioorg. Med. Chem. Lett.* **2005,** *15,* 3177–3180. doi:10.1016/j.bmcl.2005.03.121
63. Schijlen, E. G. W. M.; de Vos, C. H. R.; Martens, S.; Jonker, H. H.; Rosin, F. M.; Molthoff, J. W.; Tikunov, Y. M.; Angenent, G. C.; van Tunen, A. J.; Bovy, A. G. *Plant Physiol.* **2007,** *144,* 1520–1530. doi:10.1104/pp.107.100305
64. Cabrera, M.; Simoens, M.; Falchi, G.; Lavaggi, M. L.; Piro, O. E.; Castellano, E. E.; Vidal, A.; Azqueta, A.; Monge, A.; de Ceráin, A. L.; Sagrera, G.; Seoane, G.; Cerecetto, H.; González, M. *Bioorg. Med. Chem.* **2007,** *15,* 3356–3367. doi:10.1016/j.bmc.2007.03.031
65. Siddiqui, Z. N.; Asad, M.; Praveen, S. *Med. Chem. Res.* **2008,** *17,* 318–325. doi:10.1007/s00044-007-9067-y
66. Hayashi, A.; Yamaguchi, M.; Hirama, M. *Synlett* **1995,** 195–196. doi:10.1055/s-1995-4909
67. Kokubo, K.; Matsumasa, K.; Miura, M.; Nomura, M. *J. Org. Chem.* **1997,** *62,* 4564–4565. doi:10.1021/jo9709458
68. Ishikawa, T.; Mizuta, T.; Hagiwara, K.; Aikawa, T.; Kudo, T.; Saito, S. *J. Org. Chem.* **2003,** *68,* 3702–3705. doi:10.1021/jo026592g
69. Curini, M.; Epifano, F.; Maltese, F.; Rosati, O. *Synlett* **2003,** 552–554. doi:10.1055/s-2003-37515
70. Xu, L.-W.; Li, L.; Xia, C.-G.; Zhao, P.-Q. *Helv. Chim. Acta* **2004,** *87,* 3080–3084. doi:10.1002/hlca.200490276
71. Viswanathan, G. S.; Li, C.-J. *Tetrahedron Lett.* **2002,** *43,* 1613–1615. doi:10.1016/S0040-4039(02)00082-5
72. Park, J. Y.; Ullapu, P. R.; Choo, H.; Lee, J. K.; Min, S.-J.; Pae, A. N.; Kim, Y.; Baek, D.-J.; Cho, Y. S. *Eur. J. Org. Chem.* **2008,** 5461–5469. doi:10.1002/ejoc.200800782
73. Yadav, J. S.; Subba Reddy, B. V.; Vishnumurthy, P. *Tetrahedron Lett.* **2008,** *49,* 4498–4500. doi:10.1016/j.tetlet.2008.05.056
74. Jia, H.-P.; Dreyer, D. R.; Bielawski, C. W. *Adv. Synth. Catal.* **2011,** *353,* 528–532. doi:10.1002/adsc.201000748
75. Frantz, D. E.; Fässler, R.; Carreira, E. M. *J. Am. Chem. Soc.* **2000,** *122,* 1806–1807. doi:10.1021/ja993838z
76. Anand, N. K.; Carreira, E. M. *J. Am. Chem. Soc.* **2001,** *123,* 9687–9688. doi:10.1021/ja016378u
77. Gao, G.; Moore, D.; Xie, R.-G.; Pu, L. *Org. Lett.* **2002,** *4,* 4143–4146. doi:10.1021/ol026921r
78. Liu, Q.-Z.; Xie, N.-S.; Luo, Z.-B.; Cui, X.; Cun, L.-F.; Gong, L.-Z.; Mi, A.-Q.; Jiang, Y.-Z. *J. Org. Chem.* **2003,** *68,* 7921–7924. doi:10.1021/jo034831+
79. Trost, B. M.; Weiss, A. H.; Jacobi von Wangelin, A. *J. Am. Chem. Soc.* **2006,** *128,* 8–9. doi:10.1021/ja054871q
80. Scarpi, D.; Galbo, F. L.; Guarna, A. *Tetrahedron: Asymmetry* **2006,** *17,* 1409–1414. doi:10.1016/j.tetasy.2006.04.010
81. Ramu, E.; Varala, R.; Sreelatha, N.; Adapa, S. R. *Tetrahedron Lett.* **2007,** *48,* 7184–7190. doi:10.1016/j.tetlet.2007.07.196
82. Yang, F.; Xi, P.; Yang, L.; Lan, J.; Xie, R.; You, J. *J. Org. Chem.* **2007,** *72,* 5457–5460. doi:10.1021/jo0707535

83. Krauzy-Dziedzic, K.; Ejfler, J.; Szafert, S.; Sobota, P. *Dalton Trans.* **2008,** 2620–2626. doi:10.1039/b715048b
84. Xu, Z.; Mao, J.; Zhang, Y. *Org. Biomol. Chem.* **2008,** *6,* 1288–1292. doi:10.1039/b719624e
85. Amberlyst-15 resin was purchased from Aldrich. Particle size: 16–50 mesh. Matrix: styrene-divinylbenzene (macroreticular).
86. Lower chemical yields were obtained with open-chain aliphatic aldehydes.

Beilstein Journal of Organic Chemistry

Continuous-flow catalytic asymmetric hydrogenations: Reaction optimization using FTIR inline analysis

Magnus Rueping*, Teerawut Bootwicha and Erli Sugiono

Full Research Paper

Open Access

Address:
Institute of Organic Chemistry, RWTH Aachen University, Landoltweg 1, D-52074 Aachen, Germany

Email:
Magnus Rueping* - magnus.rueping@rwth-aachen.de

* Corresponding author

Keywords:
asymmetric reduction; binolphosphoric acid; Brønsted acid; Hantzsch dihydropyridine; IR spectroscopy; real-time analysis

Beilstein J. Org. Chem. **2012,** *8,* 300–307.
doi:10.3762/bjoc.8.32

Received: 03 January 2012
Accepted: 13 February 2012
Published: 23 February 2012

This article is part of the Thematic Series "Chemistry in flow systems II".

Guest Editor: A. Kirschning

Abstract

The asymmetric organocatalytic hydrogenation of benzoxazines, quinolines, quinoxalines and 3*H*-indoles in continuous-flow microreactors has been developed. Reaction monitoring was achieved by using an inline ReactIR flow cell, which allows fast and convenient optimization of reaction parameters. The reductions proceeded well, and the desired products were isolated in high yields and with excellent enantioselectivities.

Introduction

In recent years, a growing interest in microreactor technology has been seen in the scientific community and the development of microfabricated reaction systems is actively pursued. Microreactor technology offers numerous advantages, including precise control of reaction variables, enhanced mixing quality, improved operational safety, reduced reagent consumption and ready scale-up of chemical processes. Due to the high surface-area-to-volume ratios of microstructured reactors, a high thermal rate and high portability of substrates can be achieved, which leads to improved product formation [1-42]. Furthermore, by incorporating inline analytical devices the progress of reactions can be monitored and analyzed in real time, allowing fast reaction screening and optimization [43-55].

Continuous flow microreactors have been applied to a number of standard transformations in organic synthesis [56-80]; however, examples regarding asymmetric reactions as well as organocatalytic reactions are scarce [81-96]. Herein, we present the first example of a continuous-flow organocatalytic asymmetric transfer hydrogenation performed in a microreactor. In this work a ReactIR flow cell was coupled with the microreactor and applied as an inline monitoring device for optimizing the reactions.

Results and Discussion

The continuous-flow microreactor system for the experiment was set up according to Scheme 1. The flow device was set up

either with a single reactor, or with multiple reactors when a prolonged residence time was needed. The reagents were introduced separately, by using a syringe pump, through two inlets connected to Y-shaped connectors. The internal reaction temperature was monitored with an internal thermal sensor. The ReactIR 45m microflow cell equipped with a DiComp ATR (diamond-composite attenuated total reflection) probe was attached to the microreactor at the end of the reaction stream and was used as an inline analytical tool to determine the optimum reaction conditions. The IR spectra were recorded at predefined intervals and the raw data were analysed with iC-IR analysis software.

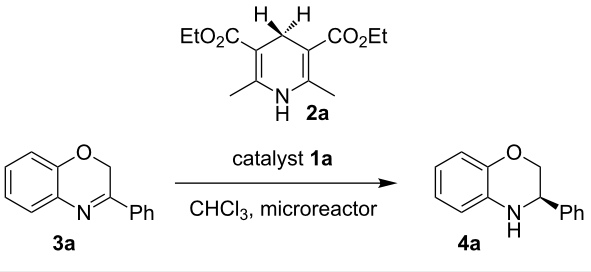

Scheme 2: Asymmetric hydrogenation of benzoxazines.

The first reaction examined the asymmetric organocatalytic transfer hydrogenation [97-101] of benzoxazine **3a** in the presence of Hantzsch dihydropyridine **2a** as hydrogen source and a catalytic amount of chiral Brønsted acid **1a** (Scheme 2) [102].

Initial experiments were carried out at 0.1 mL min^{-1} flow rate in a commercial glass microreactor, which was attached to the ReactIR flow cell for in situ reaction monitoring. In order to control the reaction and to determine the use of educts and formation of product, reference spectra of the starting materials, solvents and reagents were recorded. Figure 1b and Figure 1c show real time IR spectra of the reaction mixtures after the subtraction of solvent in the spectral region of 1440 and 1530 cm^{-1}. For direct inline analysis the signals at $\tilde{\nu}$ = 1479 cm^{-1} and $\tilde{\nu}$ = 1495 cm^{-1} were ideal as they could easily be assigned to benzoxazine **3a** and dihydrobenzoxazine **4a**. Thus, in continuous flow the substrate consumption and product formation could readily be determined.

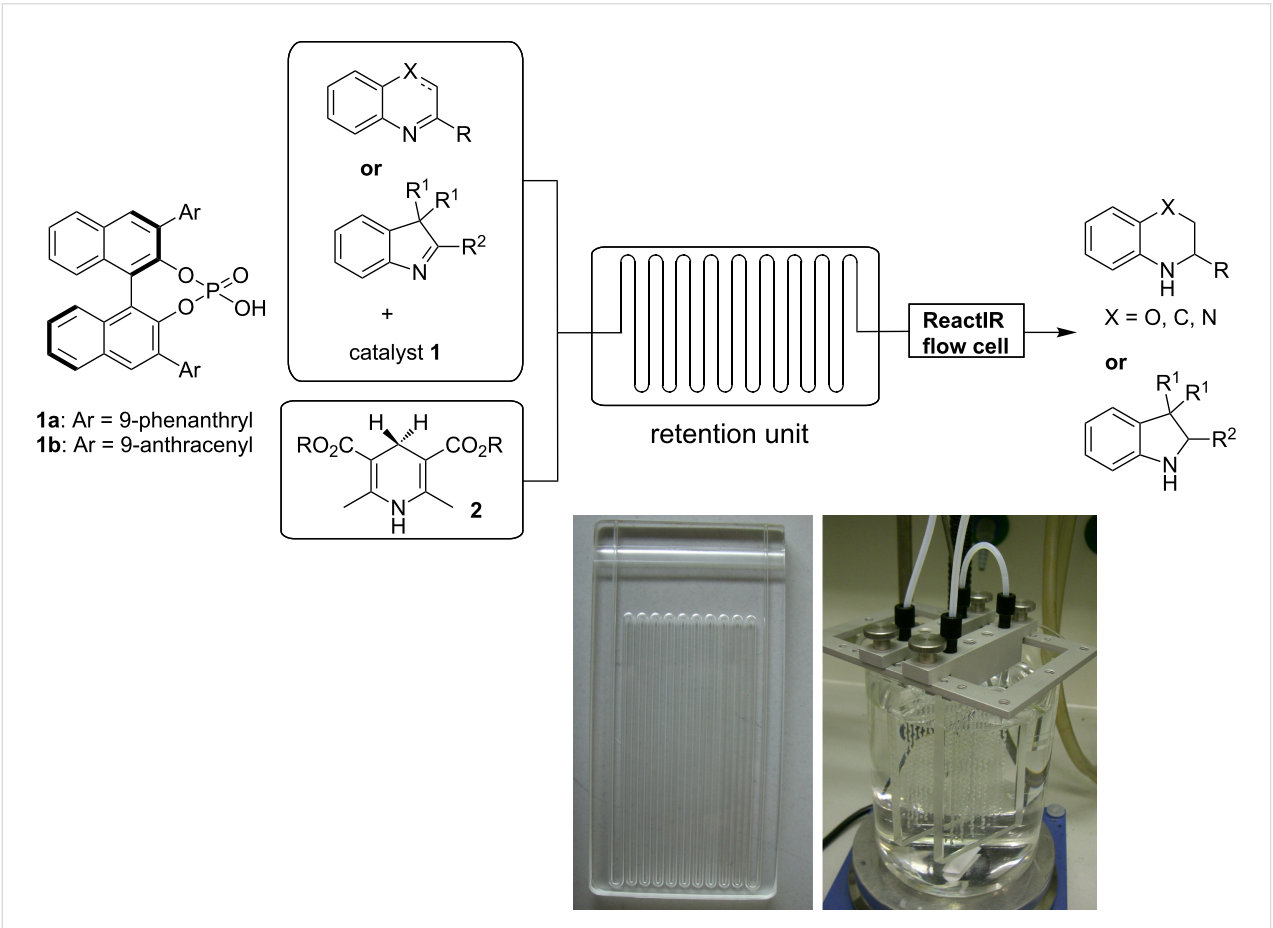

Scheme 1: Experimental setup for the asymmetric transfer hydrogenation.

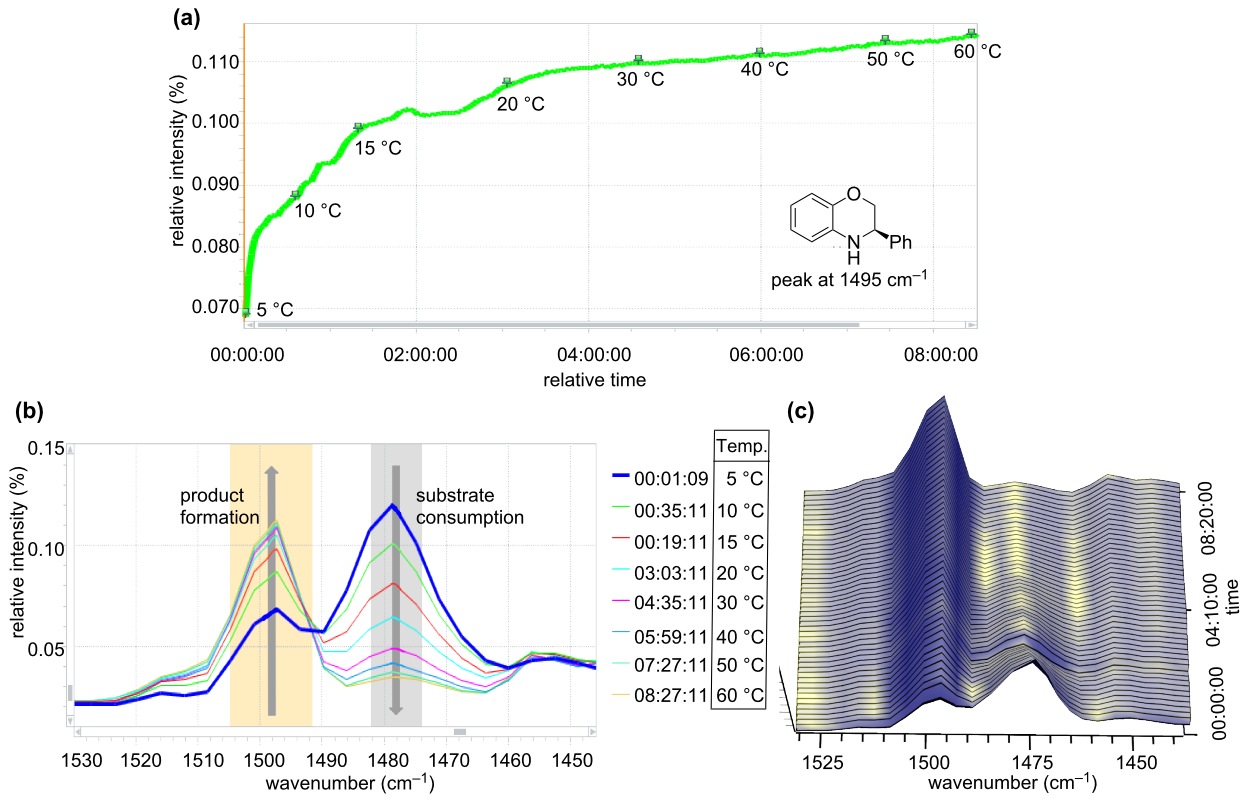

Figure 1: In situ ReactIR monitoring: (a) Trend curve of product formation at different temperatures. (b) Reaction spectra showing the consumption of the substrate and the formation of product at different temperatures. (c) Three-dimensional time-resolved spectral data.

In order to find the optimal temperature for the asymmetric continuous-flow reduction, a temperature profile was recorded. The reaction temperature was initially 5 °C and was increased to 60 °C over a period of 8 h, while the conversion was monitored by inline IR-spectroscopy. Figure 1a shows the real-time plot of the peak intensity versus reaction time for the 1495 cm^{-1} absorption band at different temperatures. The trend-curve analysis by peak-height integration of this absorption band shows increased product formation with increasing temperature. By monitoring the signal change in this spectral region over the time of the reaction, the product formation ($\tilde{\nu}$ = 1495 cm^{-1}) and substrate consumption ($\tilde{\nu}$ = 1479 cm^{-1}) can be determined in real time. Analysis of the spectra provided us with an optimal temperature of 60 °C for this reaction. In general the IR-flow-cell technology is a good tool for in situ monitoring and provides a fast read out of reaction progress as the intensity of substrate and product peaks can be directly related to the conversion. Thus, as exemplified above, applying the inline analysis to different reaction parameters provides a fast and convenient method for reaction optimization.

By using the optimized reaction temperature and flow rate of 0.1 mL min^{-1}, further experiments were conducted to examine the influence of the residence time on the conversion (Table 1). By performing the reaction with a residence time of 20 min, the product was isolated in 50% yield. With residence times of 40 min and 60 min, the product was isolated in 87% and 98% yields, respectively (Table 1).

Table 1: Optimization of the Brønsted acid catalyzed reduction of benzoxazines.[a]

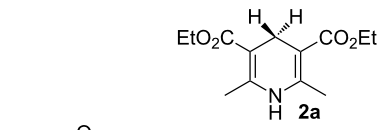

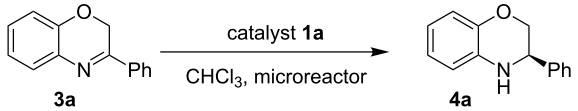

Entry	1a [mol %]	Residence time [min]	Flow rate [mL min^{-1}]	Yield [%][b]
1	2	20	0.1	50%
2	2	40	0.1	87%
3	2	60	0.1	98%

[a]Reaction conditions: **3a**, **2a** (1.2 equiv), **1a** in $CHCl_3$ (0.05 M) at 60 °C. [b]Isolated yields after column chromatography.

Having found the optimum reaction conditions, we next investigated the scope of the Brønsted acid catalyzed reduction of 3-aryl-substituted benzoxazines **3** (Table 2). In general, 3-aryl benzoxazines **3** bearing either electron-withdrawing or electron-donating groups can be reduced in a continuous fashion and the products **4** were isolated in good yields and with excellent enantioselectivities.

Encouraged by the results, we next studied the transfer hydrogenation of quinolines **5** [103-106]. The optimum reaction temperature was determined according to the experiment described above. The effects of catalyst loading and residence time on the conversion and the enantioselectivity are summarized in Table 3. Performing the reaction at 60 °C with 5 mol % of Brønsted acid **1a** and residence time of 20 min afforded the desired product in 88% yield and 94% enantioselectivity (Table 3, entry 1). When the catalyst loading was reduced from 5 mol % to 2 mol %, a residence time of 40 min was found to be optimal to achieve comparable results (Table 3, entry 1 versus entry 2). A slight improvement of the conversion was observed by increasing the residence time to 60 min (Table 3, entry 3 versus entry 2). The catalyst loading can be decreased to 0.5 mol % without loss of reactivity and selectivity; the desired tetrahydroquinoline was isolated in 96% yield with 94% enantiomeric excess (Table 3, entry 5). A further decrease of catalyst loading to 0.1 mol % resulted in a significant drop in chemical yield, affording the product in lower yield while enantioselectivity was maintained (Table 3, entry 6).

Although continuous-flow reactions provide many advantages, in certain cases it can be beneficial to conduct reactions under classical batch conditions. Therefore, we decided to carry out a direct comparison. Transferring the reaction conditions from continuous-flow to the batch showed a noticeable drop in conversion and the product was isolated only in 67% yield (Table 3, entry 5 vs entry 7). This observation is general, and typically lower reactivities were obtained. This can be explained by the better heat transfer in the microreactors as compared to the glass flask typically used in our batch reactions.

Table 2: Scope of the Brønsted acid catalyzed reduction of benzoxazines.[a]

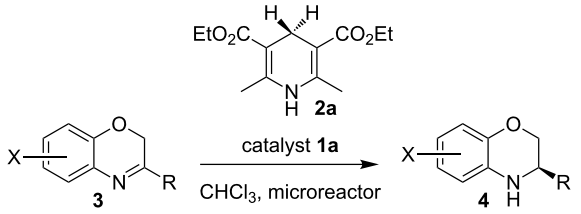

Entry	Product **4**	Yield [%][b]	ee [%][c]
1	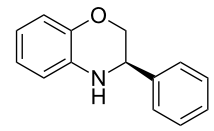 **4a**	98	98
2	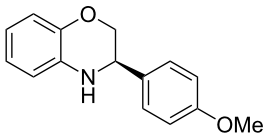 **4b**	96	97
3	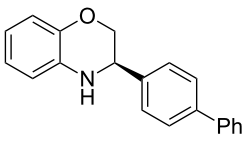 **4c**	98	98
4	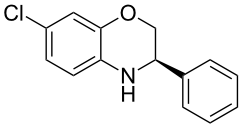 **4d**	81	97
5	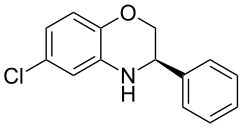 **4e**	85	99

[a]Reaction conditions: **3**, **2a** (1.2 equiv), 2 mol % **1a** in $CHCl_3$ (0.05 M) at 60 °C, flow rate 0.1 mL min^{-1}, residence time = 60 min. [b]Isolated yields after column chromatography. [c]Determined by chiral HPLC analysis.

Table 3: Optimization of the Brønsted acid catalyzed transfer hydrogenation of quinolines.[a]

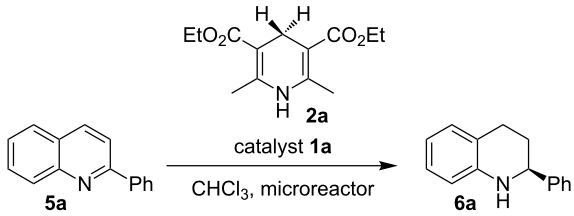

Entry	**1a** [mol %]	*t* [min]	Flow rate [mL min^{-1}]	Yield [%][b]	ee [%][c]
1	5	20	0.1	88	94
2	2	40	0.1	91	92
3	2	60	0.1	97	92
4	1	60	0.1	97	92
5	0.5	60	0.1	96	94
6	0.1	60	0.1	72	94
7[d]	0.5	60	batch	67	94

[a]Reaction conditions: **5a**, **2a** (2.4 equiv), **1a** in $CHCl_3$ (0,1 M) at 60 °C, flow rate 0.1 mL min^{-1}. [b]Isolated yields after column chromatography. [c]Determined by chiral HPLC analysis. [d]Performed under batch conditions.

The scope and applicability of the method was then tested on various 2-substituted quinolines (Table 4). In general the asymmetric continuous-flow transfer hydrogenation of 2-substituted quinolines **5** proceeded well and afforded tetrahydroquinolines **6a**–**e** with excellent yields and enantioselectivities (Table 4).

Having established a protocol for a general and highly enantioselective transfer hydrogenation of quinolines, we decided to extend its scope to the reduction of quinoxalines **7** (Table 5) [107]. The asymmetric reduction of quinoxalines is typically more difficult to achieve. Using the optimized conditions for the fast inline reaction, we found that the continuous-flow reduction could be performed using 10 mol % Brønsted acid **1b**, a flow rate of 0.1 mL min^{-1} and 60 min residence time (Table 5).

To broaden the scope of the asymmetric hydrogenations in continuous flow further, the reduction of 3*H*-indoles **9** was

Table 4: Scope of the Brønsted acid catalyzed transfer hydrogenation of quinolines.[a]

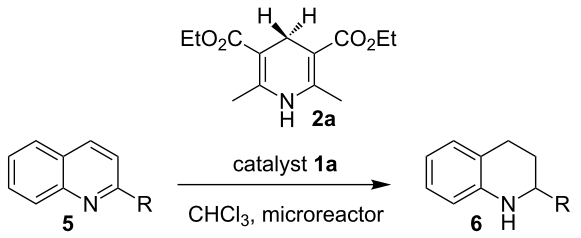

Entry	Product **6**	Yield [%][b]	ee [%][c]
1	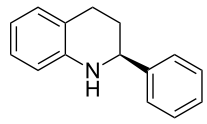 **6a**	96	94
2	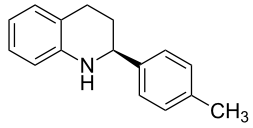 **6b**	91	96
3	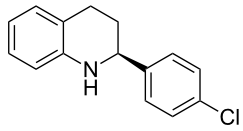 **6c**	94	99
4	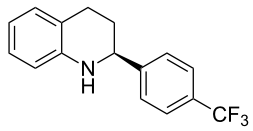 **6d**	91	99
5	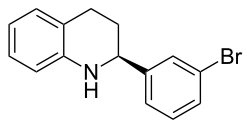 **6e**	97	96

[a]Reaction conditions: **5**, **2a** (2.4 equiv), 5 mol % **1a** in $CHCl_3$ (0.1 M) at 60 °C, flow rate 0.1 mL min^{-1}, residence time = 60 min. [b]Isolated yields after column chromatography. [c]Determined by chiral HPLC analysis.

Table 5: Scope of the Brønsted acid catalyzed transfer hydrogenation of quinoxalines.[a]

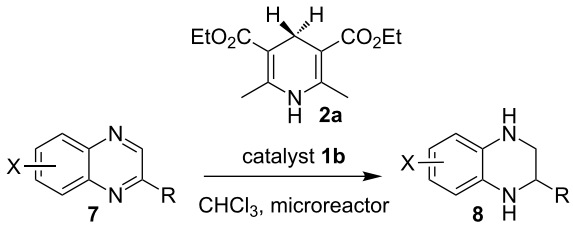

Entry	Product **8**	Yield [%][b]	ee [%][c]
1	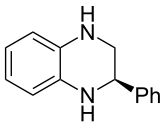 **8a**	77	90
2	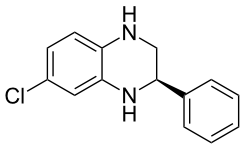 **8b**	68	84
3	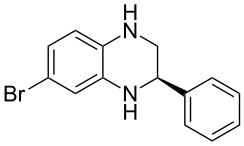 **8c**	53	86
4	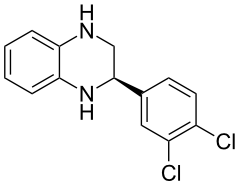 **8d**	86	94
5	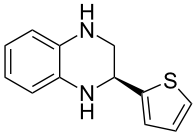 **8e**	41	76

[a]Reaction conditions: **7**, **2a** (2.4 equiv), 10 mol % **1b** in $CHCl_3$ (0.1 M) at 60 °C, flow rate 0.1 mL min^{-1}, residence time = 60 min. [b]Isolated yields after column chromatography. [c]Determined by chiral HPLC analysis.

Table 6: Scope of the Brønsted acid catalyzed transfer hydrogenation of 3*H*-indoles.[a]

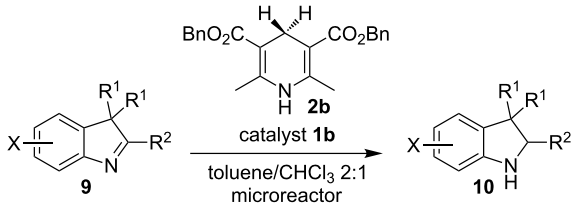

Entry	Product **10**	Yield [%][b]	ee [%][c]
1	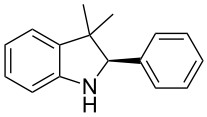 **10a**	95[d]	90
2	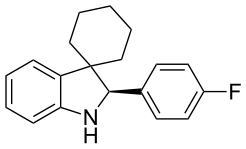 **10b**	88[d] 98	98 98
3	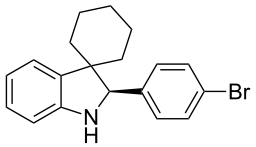 **10c**	60[d] 96	99 99
4	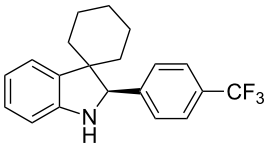 **10d**	78[d] 95	99 99
5	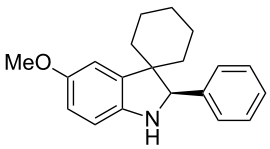 **10e**	94	97

[a]Reaction conditions: **9**, **2b** (1.3 equiv), 5 mol % **1b** in toluene/$CHCl_3$ (2:1) (0.1 M) at 30 °C, flow rate 0.1 mL min^{-1}, residence time = 20 min. [b]Isolated yields after column chromatography. [c]Determined by chiral HPLC analysis. [d]Retention time: 10 min.

studied (Table 6) [108]. Here the best reaction conditions turned out to be a temperature of 30 °C, a flow rate of 0.1 mL min^{-1}, and a residence time of 20 min. The desired indolines **10** were isolated in good to high yields and with excellent enantioselectivities.

Conclusion

In conclusion, we have demonstrated the potential of a microreactor setup coupled with FTIR inline analysis for monitoring asymmetric continuous-flow hydrogenations of benzoxazines, quinolines, quinoxalines and 3*H*-indoles. Following a real-time continuous-flow optimization, the corresponding products were obtained in good yields and with excellent enantioselectivities. By applying the FTIR inline monitoring, reaction parameters can be screened rapidly in a single reaction setup, and the optimal reaction conditions can be obtained much faster as compared to the classical sequence of conducting the reaction followed by analysis. Further work will include automated integration and feedback optimization of reaction parameters.

Acknowledgements

The authors acknowledge the funding by the Excellence Initiative of the German federal and state governments and the European Research Council for a starting grant.

References

1. Ehrfeld, W.; Hessel, V.; Löwe, H. *Microreactors: New Technology for Modern Chemistry;* Wiley-VCH: Weinheim, Germany, 2000.
2. Wirth, T., Ed. *Microreactors in Organic Synthesis and Catalysis;;* Wiley-VCH: Weinheim, Germany, 2008.
3. Jas, G.; Kirschning, A. *Chem.–Eur. J.* **2003,** *9,* 5708–5723. doi:10.1002/chem.200305212
4. Kikutani, Y.; Kitamori, T. *Macromol. Rapid Commun.* **2004,** *25,* 158–168. doi:10.1002/marc.200300192
5. Jähnisch, K.; Hessel, V.; Löwe, H.; Baerns, M. *Angew. Chem., Int. Ed.* **2004,** *43,* 406–446. doi:10.1002/anie.200300577
6. Doku, G. N.; Verboom, W.; Reinhoudt, D. N.; van den Berg, A. *Tetrahedron* **2005,** *61,* 2733–2742. doi:10.1016/j.tet.2005.01.028
7. Watts, P.; Haswell, S. J. *Chem. Soc. Rev.* **2005,** *34,* 235–246. doi:10.1039/b313866f
8. Geyer, K.; Codée, J. D. C.; Seeberger, P. H. *Chem.–Eur. J.* **2006,** *12,* 8434–8442. doi:10.1002/chem.200600596
9. deMello, A. J. *Nature* **2006,** *442,* 394–402. doi:10.1038/nature05062
10. Song, H.; Chen, D. L.; Ismagilov, R. F. *Angew. Chem., Int. Ed.* **2006,** *45,* 7336–7356. doi:10.1002/anie.200601554
11. Kobayashi, J.; Mori, Y.; Kobayashi, S. *Chem.–Asian J.* **2006,** *1,* 22–35. doi:10.1002/asia.200600058
12. Mason, B. P.; Price, K. E.; Steinbacher, J. L.; Bogdan, A. R.; McQuade, D. T. *Chem. Rev.* **2007,** *107,* 2300–2318. doi:10.1021/cr050944c
13. Watts, P.; Wiles, C. *Chem. Commun.* **2007,** 443–467. doi:10.1039/b609428g
14. Ahmed-Omer, B.; Brandt, J. C.; Wirth, T. *Org. Biomol. Chem.* **2007,** *5,* 733–740. doi:10.1039/b615072a
15. Fukuyama, T.; Rahman, M. T.; Sato, M.; Ryu, I. *Synlett* **2008,** 151–163. doi:10.1055/s-2007-1000884
16. Yoshida, J.-i.; Nagaki, A.; Yamada, T. *Chem.–Eur. J.* **2008,** *14,* 7450–7459. doi:10.1002/chem.200800582
17. Wiles, C.; Watts, P. *Eur. J. Org. Chem.* **2008,** 1655–1671. doi:10.1002/ejoc.200701041
18. Kirschning, A. *Beilstein J. Org. Chem.* **2009,** *5,* No. 15. doi:10.3762/bjoc.5.15
19. Geyer, K.; Gustafsson, T.; Seeberger, P. H. *Synlett* **2009,** 2382–2391. doi:10.1055/s-0029-1217828
20. Nagaki, A.; Takabayashi, N.; Tomida, Y.; Yoshida, J.-i. *Beilstein J. Org. Chem.* **2009,** *5,* No. 16. doi:10.3762/bjoc.5.16

21. Yamada, Y. M. A.; Torii, K.; Uozumi, Y. *Beilstein J. Org. Chem.* **2009,** *5,* No. 18. doi:10.3762/bjoc.5.18
22. Brandt, J. C.; Wirth, T. *Beilstein J. Org. Chem.* **2009,** *5,* No. 30. doi:10.3762/bjoc.5.30
23. Fukuyama, T.; Rahman, M. T.; Kamata, N.; Ryu, I. *Beilstein J. Org. Chem.* **2009,** *5,* No. 34. doi:10.3762/bjoc.5.34
24. Tanaka, K.; Fukase, K. *Beilstein J. Org. Chem.* **2009,** *5,* No. 40. doi:10.3762/bjoc.5.40
25. Kunz, U.; Turek, T. *Beilstein J. Org. Chem.* **2009,** *5,* No. 70. doi:10.3762/bjoc.5.70
26. Marre, S.; Jensen, K. F. *Chem. Soc. Rev.* **2010,** *39,* 1183–1202. doi:10.1039/b821324k
27. Yoshida, J-i.; Kim, H.; Nagaki, A. *ChemSusChem* **2011,** *4,* 331–340. doi:10.1002/cssc.201000271
28. Wegner, J.; Ceylan, S.; Kirschning, A. *Chem. Commun.* **2011,** *47,* 4583–4592. doi:10.1039/c0cc05060a
29. Min, K.-I.; Lee, T.-H.; Park, C. P.; Wu, Z.-Y.; Girault, H. H.; Ryu, I.; Fukuyama, T.; Mukai, Y.; Kim, D.-P. *Angew. Chem., Int. Ed.* **2010,** *49,* 7063–7067. doi:10.1002/anie.201002004
30. McMullen, J. P.; Stone, M. T.; Buchwald, S. L.; Jensen, K. F. *Angew. Chem., Int. Ed.* **2010,** *49,* 7076–7080. doi:10.1002/anie.201002590
31. McMullen, J. P.; Jensen, K. F. *Annu. Rev. Anal. Chem.* **2010,** *3,* 19–42. doi:10.1146/annurev.anchem.111808.073718
32. Hartman, R. L.; McMullen, J. P.; Jensen, K. F. *Angew. Chem., Int. Ed.* **2011,** *50,* 7502–7519. doi:10.1002/anie.201004637
33. Shvydkiv, O.; Nolan, K.; Oelgemöller, M. *Beilstein J. Org. Chem.* **2011,** *7,* 1055–1063. doi:10.3762/bjoc.7.121
34. Nagaki, A.; Uesugi, Y.; Tomida, Y.; Yoshida, J.-i. *Beilstein J. Org. Chem.* **2011,** *7,* 1064–1069. doi:10.3762/bjoc.7.122
35. Watts, K.; Gattrell, W.; Wirth, T. *Beilstein J. Org. Chem.* **2011,** *7,* 1108–1114. doi:10.3762/bjoc.7.127
36. Roper, K. A.; Lange, H.; Polyzos, A.; Berry, M. B.; Baxendale, I. R.; Ley, S. V. *Beilstein J. Org. Chem.* **2011,** *7,* 1648–1655. doi:10.3762/bjoc.7.194
37. Saito, K.; Ueoka, K.; Matsumoto, K.; Suga, S.; Nokami, T.; Yoshida, J-i. *Angew. Chem., Int. Ed.* **2011,** *50,* 5153–5156. doi:10.1002/anie.201100854
38. Wiles, C.; Watts, P. *Chem. Commun.* **2011,** *47,* 6512–6535. doi:10.1039/c1cc00089f
39. Yoshida, J-i.; Saito, K.; Nokami, T.; Nagaki, A. *Synlett* **2011,** 1189–1194. doi:10.1055/s-0030-1259946
40. Bogdan, A.; McQuade, D. T. *Beilstein J. Org. Chem.* **2009,** *5,* No. 17. doi:10.3762/bjoc.5.17
41. Wiles, C.; Watts, P. *Green Chem.* **2012,** *14,* 38–54. doi:10.1039/c1gc16022b
42. Wegner, J.; Ceylan, S.; Kirschning, A. *Adv. Synth. Catal.* **2012,** *354,* 17–57. doi:10.1002/adsc.201100584
43. Carter, C. F.; Baxendale, I. R.; O'Brien, M.; Pavey, J. B. J.; Ley, S. V. *Org. Biomol. Chem.* **2009,** *7,* 4594–4597. doi:10.1039/b917289k
44. Carter, C. F.; Lange, H.; Ley, S. V.; Baxendale, I. R.; Wittkamp, B.; Goode, J. G.; Gaunt, N. L. *Org. Process Res. Dev.* **2010,** *14,* 393–404. doi:10.1021/op900305v
45. Qian, Z.; Baxendale, I. R.; Ley, S. V. *Chem.–Eur. J.* **2010,** *16,* 12342–12348. doi:10.1002/chem.201002147
46. Carter, C. F.; Baxendale, I. R.; Pavey, J. B. J.; Ley, S. V. *Org. Biomol. Chem.* **2010,** *8,* 1588–1595. doi:10.1039/b924309g
47. Leadbeater, N. E. *Chem. Commun.* **2010,** *46,* 6693–6695. doi:10.1039/c0cc01921f
48. Malet-Sanz, L.; Madrzak, J.; Ley, S. V.; Baxendale, I. R. *Org. Biomol. Chem.* **2010,** *8,* 5324–5332. doi:10.1039/c0ob00450b
49. McMullen, J. P.; Jensen, K. F. *Org. Process Res. Dev.* **2010,** *14,* 1169–1176. doi:10.1021/op100123e
50. Foley, D. A.; Doecke, C. W.; Buser, J. Y.; Merritt, J. M.; Murphy, L.; Kissane, M.; Collins, S. G.; Maguire, A. R.; Kaerner, A. *J. Org. Chem.* **2011,** *76,* 9630–9640. doi:10.1021/jo201212p
51. Smith, C. J.; Nikbin, N.; Ley, S. V.; Lange, H.; Baxendale, I. R. *Org. Biomol. Chem.* **2011,** *9,* 1938–1947. doi:10.1039/c0ob00815j
52. Lange, H.; Carter, C. F.; Hopkin, M. D.; Burke, A.; Goode, J. G.; Baxendale, I. R.; Ley, S. V. *Chem. Sci.* **2011,** *2,* 765–769. doi:10.1039/c0sc00603c
53. Koos, P.; Gross, U.; Polyzos, A.; O'Brien, M.; Baxendale, I. R.; Ley, S. V. *Org. Biomol. Chem.* **2011,** *9,* 6903–6908. doi:10.1039/c1ob06017a
54. Keybl, J.; Jensen, K. F. *Ind. Eng. Chem. Res.* **2011,** *50,* 11013–11022. doi:10.1021/ie200936b
55. Brodmann, T.; Koos, P.; Metzger, A.; Knochel, P.; Ley, S. V. *Org. Process Res. Dev.* **2011**. doi:10.1021/op200275d
56. Hook, B. D. A.; Dohle, W.; Hirst, P. R.; Pickworth, M.; Berry, M. B.; Booker-Milburn, K. I. *J. Org. Chem.* **2005,** *70,* 7558–7564. doi:10.1021/jo050705p
57. Wiles, C.; Watts, P.; Haswell, S. J. *Tetrahedron Lett.* **2007,** *48,* 7362–7365. doi:10.1016/j.tetlet.2007.08.027
58. Griffiths-Jones, C. M.; Hopkin, M. D.; Jönsson, D.; Ley, S. V.; Tapolczay, D. J.; Vickerstaffe, E.; Ladlow, M. *J. Comb. Chem.* **2007,** *9,* 422–430. doi:10.1021/cc060152b
59. Mennecke, K.; Solodenko, W.; Kirschning, A. *Synthesis* **2008,** 1589–1599. doi:10.1055/s-2008-1072579
60. Mennecke, K.; Kirschning, A. *Synthesis* **2008,** 3267–3272. doi:10.1055/s-2008-1067274
61. Baxendale, I. R.; Ley, S. V.; Mansfield, A. C.; Smith, C. D. *Angew. Chem., Int. Ed.* **2009,** *48,* 4017–4021. doi:10.1002/anie.200900970
62. Wang, N.; Matsumoto, T.; Ueno, M.; Miyamura, H.; Kobayashi, S. *Angew. Chem., Int. Ed.* **2009,** *48,* 4744–4746. doi:10.1002/anie.200900565
63. Brasholz, M.; Macdonald, J. M.; Saubern, S.; Ryan, J. H.; Holmes, A. B. *Chem.–Eur. J.* **2010,** *16,* 11471–11480. doi:10.1002/chem.201001435
64. Costantini, F.; Benetti, E. M.; Tiggelaar, R. M.; Gardeniers, H. J. G. E.; Reinhoudt, D. N.; Huskens, J.; Vancso, G. J.; Verboom, W. *Chem.–Eur. J.* **2010,** *16,* 12406–12411. doi:10.1002/chem.201000948
65. Gutmann, B.; Roduit, J.-P.; Roberge, D.; Kappe, C. O. *Angew. Chem., Int. Ed.* **2010,** *49,* 7101–7105. doi:10.1002/anie.201003733
66. Wahab, B.; Ellames, G.; Passey, S.; Watts, P. *Tetrahedron* **2010,** *66,* 3861–3865. doi:10.1016/j.tet.2010.03.005
67. Fuse, S.; Tanabe, N.; Yoshida, M.; Yoshida, H.; Doi, T.; Takahashi, T. *Chem. Commun.* **2010,** *46,* 8722–8724. doi:10.1039/c0cc02239j
68. Venturoni, F.; Nikbin, N.; Ley, S. V.; Baxendale, I. R. *Org. Biomol. Chem.* **2010,** *8,* 1798–1806. doi:10.1039/b925327k
69. Webb, D.; Jamison, T. F. *Chem. Sci.* **2010,** *1,* 675–680. doi:10.1039/c0sc00381f
70. Gutmann, B.; Roduit, J.-P.; Roberge, D.; Kappe, C. O. *Chem.–Eur. J.* **2011,** *17,* 13146–13150. doi:10.1002/chem.201102772
71. Maurya, R. A.; Park, C. P.; Lee, J. H.; Kim, D.-P. *Angew. Chem., Int. Ed.* **2011,** *50,* 5952–5955. doi:10.1002/anie.201101977

72. Sniady, A.; Bedore, M. W.; Jamison, T. F. *Angew. Chem., Int. Ed.* **2011,** *50,* 2155–2158. doi:10.1002/anie.201006440
73. Li, P.; Buchwald, S. L. *Angew. Chem., Int. Ed.* **2011,** *50,* 6396–6400. doi:10.1002/anie.201102401
74. Noël, T.; Maimone, T. J.; Buchwald, S. L. *Angew. Chem., Int. Ed.* **2011,** *50,* 8900–8903. doi:10.1002/anie.201104652
75. Shu, W.; Pellegatti, L.; Oberli, M. A.; Buchwald, S. L. *Angew. Chem., Int. Ed.* **2011,** *50,* 10665–10669. doi:10.1002/anie.201105223
76. O'Brien, A. G.; Lévesque, F.; Seeberger, P. H. *Chem. Commun.* **2011,** *47,* 2688–2690. doi:10.1039/c0cc04481d
77. Noël, T.; Buchwald, S. L. *Chem. Soc. Rev.* **2011,** *40,* 5010–5029. doi:10.1039/c1cs15075h
78. Kim, H.; Nagaki, A.; Yoshida, J.-i. *Nat. Commun.* **2011,** 264. doi:10.1038/ncomms1264
79. Browne, D. L.; Baumann, M.; Harji, B. H.; Baxendale, I. R.; Ley, S. V. *Org. Lett.* **2011,** *13,* 3312–3315. doi:10.1021/ol2010006
80. Allian, A. D.; Richter, S. M.; Kallemeyn, J. M.; Robbins, T. A.; Kishore, V. *Org. Process Res. Dev.* **2011,** *15,* 91–97. doi:10.1021/op100249z
81. Wiles, C.; Wattts, P.; Haswell, S. J.; Pombo-Villar, E. *Lab Chip* **2004,** *4,* 171–173. doi:10.1039/b400280f
82. Jönsson, C.; Lundgren, S.; Haswell, S. J.; Moberg, C. *Tetrahedron* **2004,** *60,* 10515–10520. doi:10.1016/j.tet.2004.08.080
83. de Bellefon, C.; Lamouille, T.; Pestre, N.; Bornette, F.; Pennemann, H.; Neumann, F.; Hessel, V. *Catal. Today* **2005,** *110,* 179–187. doi:10.1016/j.cattod.2005.09.002
84. Hamberg, A.; Lundgren, S.; Wingstrand, E.; Moberg, C.; Hult, K. *Chem.–Eur. J.* **2007,** *13,* 4334–4341. doi:10.1002/chem.200601638
85. Sakeda, K.; Wakabayashi, K.; Matsushita, Y.; Ichimura, T.; Suzuki, T.; Wada, T.; Inoue, Y. *J. Photochem. Photobiol., A* **2007,** *192,* 166–171. doi:10.1016/j.jphotochem.2007.05.019
86. Mak, X. Y.; Laurino, P.; Seeberger, P. H. *Beilstein J. Org. Chem.* **2009,** *5,* No. 19. doi:10.3762/bjoc.5.19
87. Shi, L.; Wang, X.; Sandoval, C. A.; Wang, Z.; Li, H.; Wu, J.; Yu, L.; Ding, K. *Chem.–Eur. J.* **2009,** *15,* 9855–9867. doi:10.1002/chem.200900899
88. Rolland, J.; Cambeiro, X. C.; Rodríguez-Escrich, C.; Pericàs, M. A. *Beilstein J. Org. Chem.* **2009,** *5,* No. 56. doi:10.3762/bjoc.5.56
89. Alza, E.; Rodríguez-Escrich, C.; Sayalero, S.; Bastero, A.; Pericàs, M. A. *Chem.–Eur. J.* **2009,** *15,* 10167–10172. doi:10.1002/chem.200901310
90. Tomida, Y.; Nagaki, A.; Yoshida, J.-i. *J. Am. Chem. Soc.* **2011,** *133,* 3744–3747. doi:10.1021/ja110898s
91. Carter, C. F.; Lange, H.; Sakai, D.; Baxendale, I. R.; Ley, S. V. *Chem.–Eur. J.* **2011,** *17,* 3398–3405. doi:10.1002/chem.201003148
92. Massi, A.; Cavazzzini, A.; Del Zoppo, L.; Pandoli, O.; Costa, V.; Pasti, L.; Giovannini, P. P. *Tetrahedron Lett.* **2011,** *52,* 619–622. doi:10.1016/j.tetlet.2010.11.157
93. Takeda, K.; Oohara, T.; Shimada, N.; Nambu, H.; Hashimoto, S. *Chem.–Eur. J.* **2011,** *17,* 13992–13998. doi:10.1002/chem.201102733
94. Fritzsche, S.; Ohla, S.; Glaser, P.; Giera, D. S.; Sickert, M.; Schneider, C.; Belder, D. *Angew. Chem., Int. Ed.* **2011,** *50,* 9467–9470. doi:10.1002/anie.201102331
95. Cambeiro, X. C.; Martín-Rapún, R.; Miranda, P. O.; Sayalero, S.; Alza, E.; Llanes, P.; Pericàs, M. A. *Beilstein J. Org. Chem.* **2011,** *7,* 1486–1493. doi:10.3762/bjoc.7.172
96. Ayats, C.; Henseler, A. H.; Pericàs, M. A. *ChemSusChem* **2012,** *5,* 320–325. doi:10.1002/cssc.201100570
97. Rueping, M.; Sugiono, E.; Azap, C.; Theissmann, T.; Bolte, M. *Org. Lett.* **2005,** *7,* 3781–3783. doi:10.1021/ol0515964
98. Rueping, M.; Antonchick, A. P. *Angew. Chem., Int. Ed.* **2007,** *46,* 4562–4565. doi:10.1002/anie.200701158
99. Rueping, M.; Sugiono, E.; Schoepke, F. R. *Synlett* **2010,** 852–865. doi:10.1055/s-0029-1219528
100. Rueping, M.; Merino, E.; Koenigs, R. M. *Adv. Synth. Catal.* **2010,** *352,* 2629–2634. doi:10.1002/adsc.201000547
101. Rueping, M.; Dufour, J.; Schoepke, F. R. *Green Chem.* **2011,** *13,* 1084–1105. doi:10.1039/c1gc15027h
102. Rueping, M.; Antonchick, A. P.; Theissmann, T. *Angew. Chem., Int. Ed.* **2006,** *45,* 6751–6755. doi:10.1002/anie.200601832
103. Rueping, M.; Antonchick, A. P.; Theissmann, T. *Angew. Chem., Int. Ed.* **2006,** *45,* 3683–3686. doi:10.1002/anie.200600191
104. Rueping, M.; Theissmann, T.; Raja, S.; Bats, J. W. *Adv. Synth. Catal.* **2008,** *350,* 1001–1006. doi:10.1002/adsc.200800020
105. Rueping, M.; Stoeckel, M.; Sugiono, E.; Theissmann, T. *Tetrahedron* **2010,** *66,* 6565–6568. doi:10.1016/j.tet.2010.04.091
106. Rueping, M.; Theissmann, T.; Stoeckel, M.; Antonchick, A. P. *Org. Biomol. Chem.* **2011,** *9,* 6844–6850. doi:10.1039/c1ob05870c
107. Rueping, M.; Tato, F.; Schoepke, F. R. *Chem.–Eur. J.* **2010,** *16,* 2688–2691. doi:10.1002/chem.200902907
108. Rueping, M.; Brinkmann, C.; Antonchick, A. P.; Atodiresei, I. *Org. Lett.* **2010,** *12,* 4604–4607. doi:10.1021/ol1019234

License and Terms